This document was produced
by scanning the original publication.

Ce document est le produit d'une
numérisation par balayage
de la publication originale.

Geological Survey of Canada
Commission géologique du Canada

PAPER/ÉTUDE
89-1E

CURRENT RESEARCH PART E
CORDILLERA AND PACIFIC MARGIN

RECHERCHES EN COURS PARTIE E
CORDILLÈRE ET MARGE DU PACIFIQUE

Canada

1989

NOTICE TO LIBRARIANS AND INDEXERS

The Geological Survey's Current Research series contains many reports comparable in scope and subject matter to those appearing in scientific journals and other serials. Most contributions to Current Research include an abstract and bibliographic citation. It is hoped that these will assist you in cataloguing and indexing these reports and that this will result in a still wider dissemination of the results of the Geological Survey's research activities.

AVIS AUX BIBLIOTHÉCAIRES ET PRÉPARATEURS D'INDEX

La série Recherches en cours de la Commission géologique paraît une fois par année; elle contient plusieurs rapports dont la portée et la nature sont comparables à ceux qui paraissent dans les revues scientifiques et autres périodiques. La plupart des articles publiés dans Recherches en cours sont accompagnés d'un résumé et d'une bibliographie, ce qui vous permettra, nous l'espérons, de cataloguer et d'indexer ces rapports, d'ou une meilleure diffusion des résultats de recherche de la Commission géologique.

GEOLOGICAL SURVEY OF CANADA
COMMISSION GÉOLOGIQUE DU CANADA
PAPER/ÉTUDE 89-1E

CURRENT RESEARCH, PART E
CORDILLERA AND PACIFIC MARGIN

RECHERCHES EN COURS, PARTIE E
CORDILLÈRE ET MARGE DU PACIFIQUE

1989

Energy, Mines and Resources Canada

Énergie, Mines et Ressources Canada

© Minister of Supply and Services Canada 1989

Available in Canada through

authorized bookstore agents and other bookstores

or by mail from

Canadian Government Publishing Centre
Supply and Services Canada
Ottawa, Canada K1A 0S9

and from

Geological Survey of Canada offices:

601 Booth Street
Ottawa, Canada K1A 0E8

3303-33rd Street N.W
Calgary, Alberta T2L 2A7

100 West Pender Street
Vancouver, British Columbia V6B 1R8

A deposit copy of this publication is also available
for reference in public libraries across Canada

Cat. No. M44-89/1E
ISBN 0-660-54778-3

Cover description

Dissected Quaternary lava dome, Mount Cayley,
southwestern Coast Mountains, British Columbia.
Photo by J.G. Souther GSC 204796

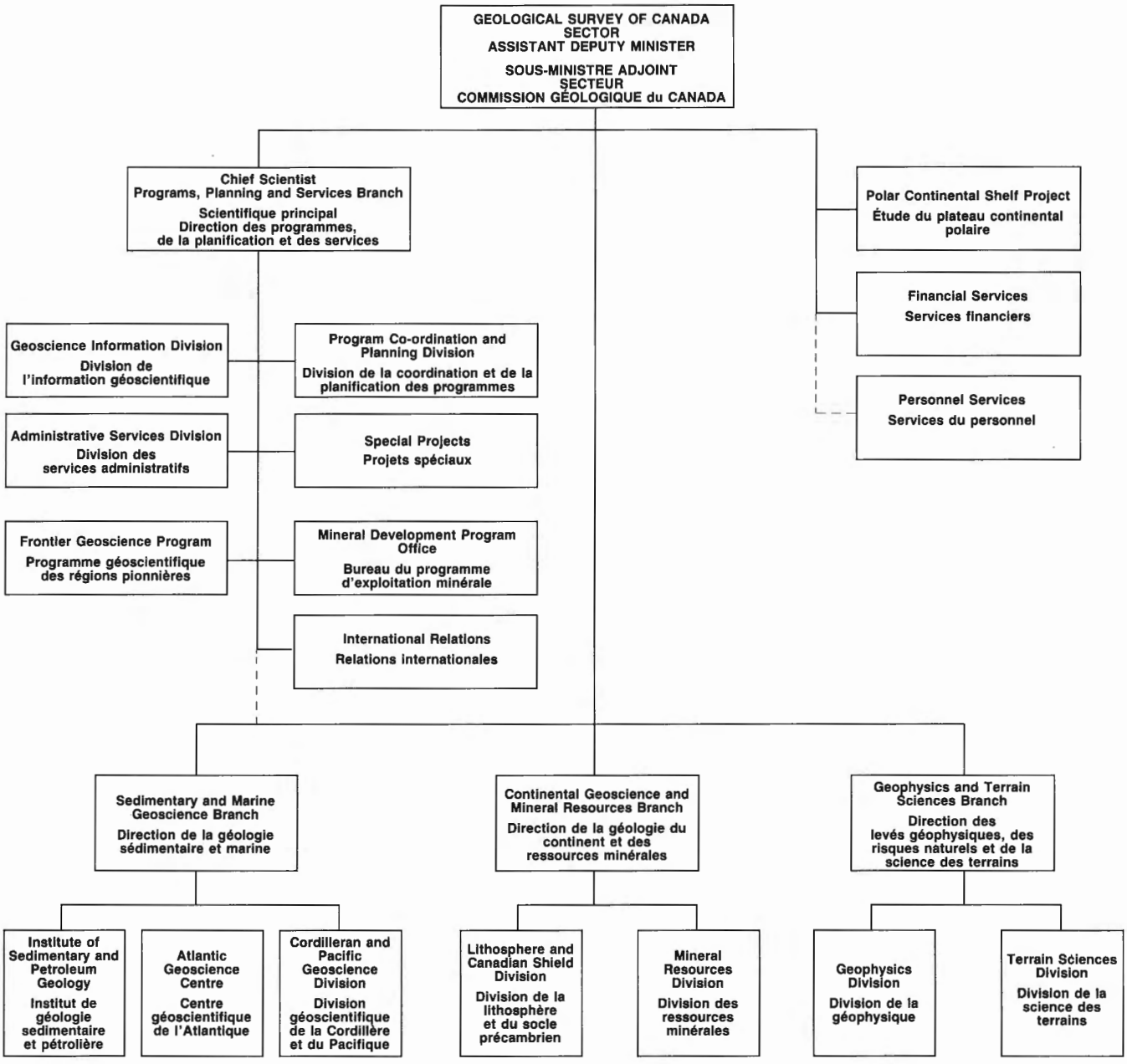
GEOLOGICAL SURVEY OF CANADA
SECTOR
ASSISTANT DEPUTY MINISTER
SOUS-MINISTRE ADJOINT
SECTEUR
COMMISSION GÉOLOGIQUE du CANADA
Chief Scientist
Programs, Planning and Services Branch
Scientifique principal
Direction des programmes,
de la planification et des services
Polar Continental Shelf Project
Étude du plateau continental
polaire
Financial Services
Services financiers
Personnel Services
Services du personnel
Geoscience Information Division
Division de
l'information géoscientifique
Program Co-ordination and
Planning Division
Division de la coordination et de la
planification des programmes
Administrative Services Division
Division des
services administratifs
Special Projects
Projets spéciaux
Frontier Geoscience Program
Programme géoscientifique
des régions pionnières
Mineral Development Program
Office
Bureau du programme
d'exploitation minérale
International Relations
Relations internationales
Sedimentary and Marine
Geoscience Branch
Direction de la géologie
sédimentaire et marine
Continental Geoscience and
Mineral Resources Branch
Direction de la géologie du
continent et des
ressources minérales
Geophysics and Terrain
Sciences Branch
Direction des
levés géophysiques, des
risques naturels et de la
science des terrains
Institute of
Sedimentary and
Petroleum
Geology
Institut de
géologie
sedimentaire
et pétrolière
Atlantic
Geoscience
Centre
Centre
géoscientifique
de l'Atlantique
Cordilleran and
Pacific
Geoscience
Division
Division
géoscientifique
de la Cordillère
et du Pacifique
Lithosphere and
Canadian Shield
Division
Division de la
lithosphère
et du socle
précambrien
Mineral
Resources
Division
Division des
ressources
minérales
Geophysics
Division
Division de la
géophysique
Terrain Sciences
Division
Division de la
science des
terrains

Separates

A limited number of separates of the papers that appear in this volume are available by direct request to the individual authors. The addresses of the Geological Survey of Canada offices follow:

601 Booth Street,
OTTAWA, Ontario
K1A 0E8

Institute of Sedimentary and Petroleum Geology,
3303-33rd Street N.W.,
CALGARY, Alberta
T2L 2A7

Cordilleran and Pacific Geoscience Division,
100 West Pender Street,
VANCOUVER, B.C.
V6B 1R8

Pacific Geoscience Centre
P.O. Box 6000,
9860 Saanich Road
SIDNEY, B.C.
V8L 4B2

Atlantic Geoscience Centre
Bedford Institute of Oceanography,
P.O. Box 1006,
DARTMOUTH, N.S.
B2Y 4A2

Geological Survey of Canada
Institut national de la recherche scientifique
complexe scientifique
2700, rue Einstein
C.P. 7500
STE-FOY, Quebec
G1V 4C7

When no location accompanies an author's name in the title of a paper, the Ottawa address should be used.

Tirés à part

On peut obtenir un nombre limité de «tirés à part» des articles qui paraissent dans cette publication en s'adressant directement à chaque auteur. Les adresses des différents bureaux de la Commission géologique du Canada sont les suivantes:

601, rue Booth
OTTAWA, Ontario
K1A 0E8

Institut de géologie sédimentaire et pétrolière
3303-33rd St. N.W.,
CALGARY, Alberta
T2L 2A7

Division géoscientifique de la Cordillère et du Pacifique
100 West Pender Street,
VANCOUVER, Colombie-Britannique
V6B 1R8

Centre géoscientifique du Pacifique
B.P. 6000,
9860 Saanich Road
SIDNEY, Colombie-Britannique
V8L 4B2

Centre géoscientifique de l'Atlantique
Institut océanographique de Bedford
B.P. 1006
DARTMOUTH, Nouvelle-Écosse
B2Y 4A2

Commission géologique du Canada
Institut national de la recherche scientifique
Complexe scientifique
2700, rue Einstein
C.P. 7500
STE-FOY, Québec
G1V 4C7

Lorsque l'adresse de l'auteur ne figure pas sous le titre d'un document, on doit alors utiliser l'adresse d'Ottawa.

CONTENTS

Introduction to Geological Survey of Canada activities in the Canadian Cordillera

D.J. Tempelman-Kluit
Director, Cordilleran and Pacific Geoscience Division

Canada's western margin is one of the world's exciting geological laboratories. It has two spectacular mountain chains next to an active ocean margin. Our eastern mountains that border the Great Plains are a giant fold and thrust belt. To build this chain, beds deposited at the continent margin in the Paleozoic and Mesozoic were stacked and duplicated during the Cretaceous. Our western mountain chain, right at the continent's edge, is an enormous plutonic welt which contains the roots of a Mesozoic plutonic arc. They became high mountains only during the late Tertiary and parts are rising rapidly even now. The upland plateau has the exotic terranes with their varied and distinctive histories expressed in unique stratigraphic sequences; fossil faunas and paleomagnetic signatures show that some of them originated far to the south. Directly west of our narrow continental shelf the last remnant of the Juan de Fuca Plate fights time. Even as it is consumed along the coast by sliding under the continent's west margin it grows on the opposite edge at the Juan de Fuca submarine ridge. Farther north along the Queen Charlotte transform fault the Pacific Plate slips northward next to the continent, periodically rocking the margin with large earthquakes similar to those of southern California.

We are fortunate to have more than a narrow cross-section of the system within Canada. In the 2000 km of strike length from southern B.C. to northern Yukon we can examine lateral changes: if the answer is not to be had in one place we can look elsewhere along the chain to find it.

Each geological element has unique mineral and hydrocarbon resource endowments; each has unique environmental hazards that impact on human activity. Each needs a full range of geoscience work to unlock the answers and understand the complexity.

Young volcanoes stand above the down-going Juan de Fuca Plate. Mount Garibaldi and Mount Baker are the two nearest Vancouver. At once they present a hazard and an opportunity: a hazard if they erupt or if their flanks are mobilized in debris flows, opportunity for their geothermal heat, a potential source of power.

Our mountainous country and extreme relief pose local rock slide hazards and, where combined with high runoff, can produce damaging debris flows. Communities along the Squamish Highway have experienced some of these first hand recently. Much of greater Vancouver is built on the delta of the Fraser River, a sequence of unconsolidated sediments built out into the Strait of Georgia during the last 10 000 years. Its stability under conditions of severe groundshaking such as might be expected during a large earthquake is a concern that needs investigation.

Introduction aux activités de la Commission géologique du Canada dans la Cordillère canadienne

D.J. Tempelman-Kluit
Directeur de la Division géoscientifique de la Cordillère et du Pacifique

La marge continentale occidentale du Canada est un des laboratoires géologiques les plus remarquables du monde. Elle comprend deux spectaculaires chaînes de montagnes à proximité de la marge océanique active. La chaîne orientale qui borde les Plaines intérieures constituent une immense zone de plis et nappes de charriage. Pour l'orogenèse de cette chaîne, les couches déposées sur la marge continentale au Paléozoïque et au Mésozoïque ont été empilées et repliées pendant le Crétacé. La chaîne occidentale, située immédiatement sur la bordure continentale, est un énorme bombement plutonique qui renferme les racines d'un arc plutonique mésozoïque. Ces deux chaînes ont donné des hautes montagnes à la fin du Tertiaire et certaines parties continuent à se soulever de nos jours. Les bas-plateaux renferment les terranes exotiques avec toute leur évolution variée et distincte qu'on retrouve dans des séquences stratigraphiques uniques; des faunes fossiles et des signatures paléomagnétiques montrent que certains de ces terranes sont venus loin du sud. Immédiatement à l'ouest de la plateforme continentale étroite, le dernier reste de la plaque Juan de Fuca essaie de survivre. Même si elle disparaît le long de la côte en glissant sous la marge occidentale du continent, cette plaque s'accroît du côté opposé, sur la crête sous-marine Juan de Fuca. Plus loin vers le nord, le long de la faille transformante de la Reine-Charlotte, la plaque du Pacifique glisse vers le nord à proximité du continent, secouant périodiquement la marge par des tremblements de terre importants similaires à ceux du sud de la Californie.

Heureusement, nous avons plus qu'une coupe géologique étroite du système à l'intérieur du Canada. Dans les 2000 km de longueur, suivant la direction, allant du sud de la C.-B. au nord du Yukon nous pouvons examiner des changements latéraux; si nous ne pouvons pas trouver de réponse en un endroit, nous pouvons chercher ailleurs, le long de la chaîne.

Chaque élément géologique possède naturellement des ressources uniques en minéraux et en hydrocarbures; chacun présente aussi des risques environnementaux uniques qui ont une influence sur l'activité humaine. La compréhension de chacun de ces éléments, dans toute sa complexité, nécessite toute une gamme de travaux géoscientifiques.

Des volcans récents dominent la plaque Juan de Fuca qui s'enfonce. Le mont Garibaldi et le mont Baker sont les plus proches de Vancouver. Ils sont à la fois source de danger et de richesse: de danger s'ils se mettent en éruption ou si leurs flancs s'éboulent, de richesse en raison de leur chaleur géothermique, convertible en énergie.

Le relief montagneux et extrêmement accidenté présente des risques de glissements de terrain locaux qui, en présence

To understand this region and to provide answers to the resource potential, environment and hazard questions, we conduct studies that run the gamut from the classical to those involving the newest technology. Our users are people concerned with resource search and environment quality. People who need geoscience data for planning and policy formulation also use our expertise and await our products. We are committed to providing, interpreting, disseminating and explaining up-to-date geoscience data about our region for society's expanding needs.

This volume and its companion (volume H) contain much new data and a number of creative ideas in preliminary reports of work carried out by GSC staff and by others supported by us. They record all GSC activities in the Cordillera and Pacific offshore. Most reports are by staff of the Cordilleran and Pacific Geoscience Division, but Cordilleran work by members of GSC's Calgary and Ottawa divisions and by university students and faculty supported by the GSC are also reported here.

de fortes eaux de ruissellement, peuvent produire des écoulements de débris dommageables. Des collectivités situées sur la route de Squamish ont été victimes, il n'y a pas longtemps, de tels écoulements de débris. Une bonne partie du grand Vancouver est construite sur le delta du Fraser, constitué d'une séquence de sédiments non consolidés qui s'est déposée dans le détroit de Géorgie pendant les 10 000 dernières années. Sa stabilité lors de secousses violentes du sol, comme pendant les grands tremblements de terre, est une préoccupation qui nécessite des recherches.

Afin de comprendre la région et de déterminer son potentiel, les éventuels problèmes environnementaux et les risques présents, nous effectuons des études faisant appel aussi bien aux techniques classiques que de pointe. Les usagers de la Division sont des personnes qui s'intéressent à la prospection des ressources et à la qualité de l'environnement. Ceux qui ont besoin de données géoscientifiques à des fins de planification et de formation des politiques ont aussi recours à notre expertise technique et attendent nos produits. Nous nous sommes engagés à fournir, à interpréter, à diffuser et à expliquer des données géoscientifiques à jour pour les besoins sans cesse croissants de la société.

Le présent volume et le volume d'accompagnement (volume H) comprennent beaucoup de nouvelles données ainsi qu'un certain nombre d'idées créatrices tirées de rapports préliminaires de travaux effectués par le personnel de la CGC et par d'autres qui reçoivent notre aide. Ces volumes donnent toutes les activités de la CGC effectuées dans la région de la Cordillère et au large dans le Pacifique. La plupart des rapports sont rédigés par le personnel de la Division géoscientifique de la Cordillère et du Pacifique, mais les travaux sur la Cordillère effectués par les chercheurs des divisions de Calgary et d'Ottawa de la CGC ainsi que par des étudiants et professeurs d'université qui reçoivent l'aide de la CGC, sont également signalés dans le présent volume.

Permian and Devonian plutonic rocks in the Sylvester Allochthon, Cry Lake and McDame map areas, northern British Columbia

H. Gabrielse and T.A. Harms[1]
Cordilleran and Pacific Geoscience Division, Vancouver

Gabrielse, H. and Harms, T.A., Permian and Devonian plutonic rocks in the Sylvester Allochton, Cry Lake and McDame map areas, northern British Columbia; in Current Research, Part E, Geological Survey of Canada, Paper 89-1E, p. 1-4, 1989.

Abstract

The "Four Mile batholith", formerly included in the Cassiar Suite of mid-Cretaceous granitic rocks, consists of four lithologically distinct bodies with compositions ranging from diorite to granite. Preliminary U-Pb zircon ages indicate that three of the granitoid rocks are Permian and one may be Late Devonian. They appear to occur in gently dipping structural sheets associated with lithologies typical of the oceanic Sylvester Allochthon.

Résumé

Le « batholite de Four Mile », autrefois inclus dans la série de Cassiar et composé de roches granitiques datant du Crétacé moyen, se compose de quatre corps lithologiquement distincts, dont la composition se situe entre celle d'une diorite et celle d'un granite. Les datations préliminaires par la méthode U-Pb appliquée au zircon indiquent que trois des corps granitoïdes sont d'âge permien, et que l'un d'eux date peut-être du Dénovien supérieur. Ils semblent se manifester dans des nappes structurales légèrement inclinées, associées à des roches caractéristiques de l'allochtone océanique de Sylvester.

[1] Department of Geology, Amherst College, Amherst, MA 01002, U.S.A.

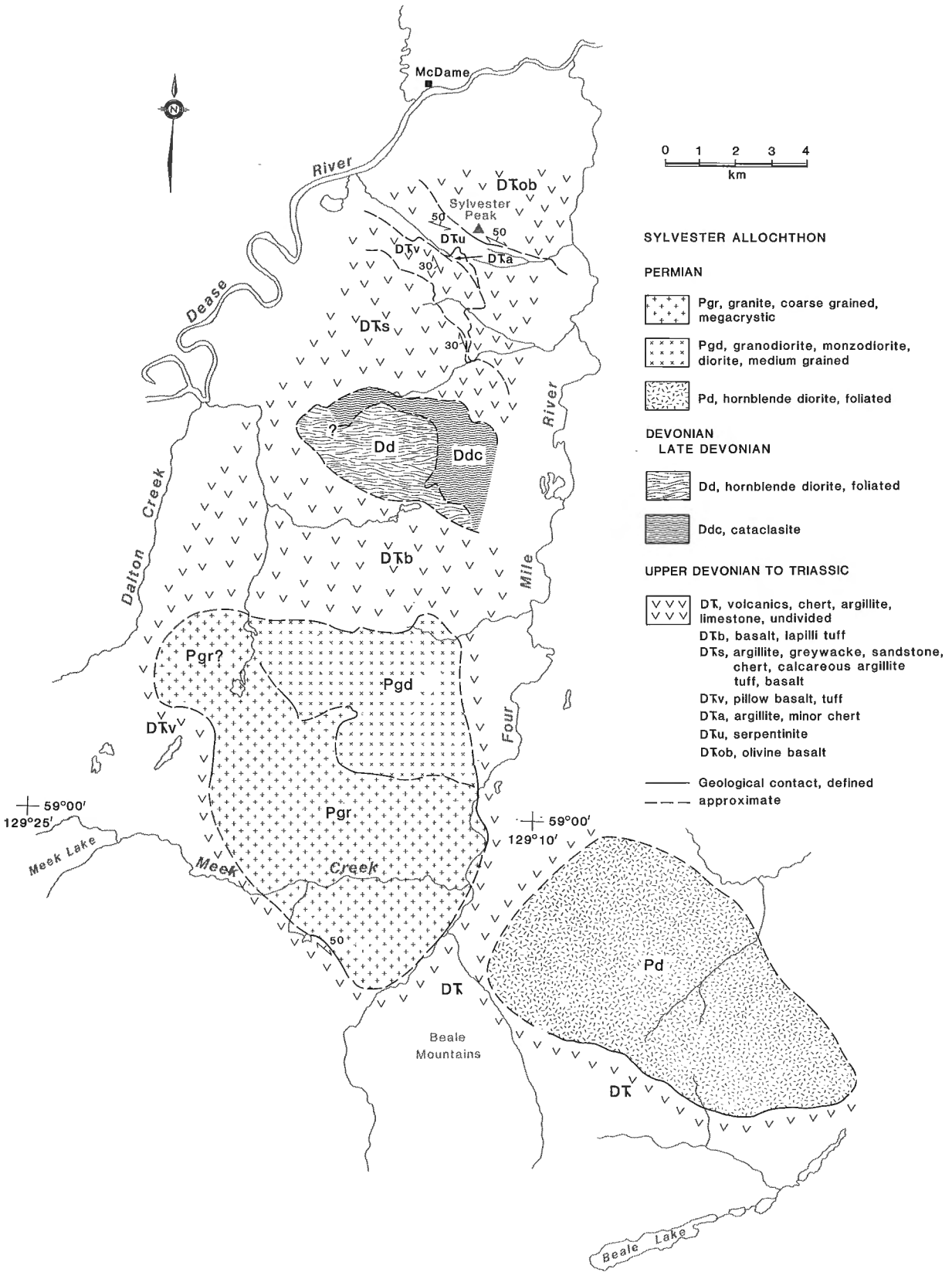

Figure 1. Geological map of the Four Mile River region in McDame and Cry Lake map areas.

INTRODUCTION

Reconnaissance mapping in north-central Cry Lake and south-central Dease Lake map areas has depicted the "Four Mile batholith" as a single body of granitic rock of variable composition extending from south of Sylvester Peak west of Four Mile River to near the Rapid River northeast of Beale Lake (Fig. 1; Hanson and McNaughton, 1936; Gabrielse, 1963; and Gabrielse et al., 1979). On the basis of lithologies noted in the area east of Meek Lake the rocks were included in the mid-Cretaceous "Cassiar Intrusions" (Gabrielse, 1963) now referred to as the Cassiar Plutonic Suite (Woodsworth et al., in press). Preliminary K-Ar and U-Pb zircon age determinations on various compositions of granitic rocks have shown, however, that Permian and Late Devonian lithologies are present (P. van der Heyden, R.R. Parrish and J.C. Roddick, pers. comm., 1986). Detailed studies during the 1988 field season were undertaken to determine the relationships between the different lithologies and to assess their structural setting within the bounding Sylvester Group.

REGIONAL SETTING

The granitic rocks occur in the axial part of the McDame synclinorium, the core of which is underlain by an oceanic assemblage of chert, shale, limestone, mafic volcanics, gabbro, metadiorite, ultramafic rocks and minor quartzose clastic rocks assigned to the Sylvester Group of Late Devonian(?) to Late Triassic age (Gabrielse, 1963; Harms, 1986). Structurally the allochthon consists of a nested stack of gently to moderately dipping, fault-bounded slices each with a distinctive association of lithologies. A planar, basal fault separates the Sylvester rocks from underlying miogeoclinal Devonian strata.

STRATIGRAPHY AND STRUCTURE

The north end of the Sylvester Peak massif is underlain by four lithotectonic structural slices bounded by faults. The lowest structural slice, underlying Sylvester Peak, consists of massive, grey to green, aphanitic, volcanic rocks with abundant chloritic veinlets. Olivine phenocrysts are present locally. These rocks are presumed to directly overlie the basal fault beneath the Sylvester Allochthon. Although most lithotectonic units and unit-bounding faults on the northeast side of the allochthon dip gently to the west, a northeast-dipping fault separates the Sylvester Peak volcanics from rocks to the southwest. This fault may be similar to other east-dipping faults on the extreme eastern flank of the Sylvester Allochthon in the Cry Lake map area to the south which mark a leading-edge triangle zone structure.

A conspicuous band of dark green, glossy, fish-scale serpentinite crosses the ridge directly south of Sylvester Peak and is structurally overlain by a wedge of recessive, strongly cleaved black argillite with minor interbedded black chert. The argillite is truncated by a fault at the base of a volcanic unit characterized by well developed pillow basalt. The basalt is aphanitic but locally contains small augite phenocrysts. Minor well bedded feldspar crystal tuff and olive green lapilli tuff are also present.

A predominantly sedimentary unit with a structural thickness of more than 2000 m overlies the volcanics. The structurally lowest part consists dominantly of black argillite, greywacke and fine grained quartz sandstone. Higher in the sequence black argillite and olive-green, banded chert includes four, brown weathering carbonate members. The upper half of the sedimentary unit contains volcanic sills or flows, and tuff interlayered with black argillite.

All units described above are interpreted to be bounded by moderately southwest-dipping, curviplanar subparallel faults. This conclusion is based on the development of penetrative cleavage or fractures along the base of each unit, the truncation of bedding or entire units along strike, and the absence of crosscutting feeders for volcanic units.

South of the foliated diorite body which forms the crest of the ridge about 6-7 km south of Sylvester Peak is a distinctive unit of predominantly green lapilli tuff with green aphanitic basalt more than 1000 m thick. Augite phenocrysts are present locally. Most lapilli are green aphanitic basalt fragments but red lapilli and crystal tuff occur sporadically.

Elsewhere, rocks of the Sylvester Group have not been subdivided. Southeast of Meek Lake and along Four Mile River volcanic rocks are prominent. In places, apple green chert and rusty weathering chert containing much pyrite form distinctive members. Several discontinuous limestone units south of Meek Creek shows that the succession there dips generally to the north.

PLUTONIC ROCKS

Diorite northeast of Beale Mountains

Medium grained, commonly foliated, hornblende diorite consisting of about 40 % hornblende and 60 % sodic andesine feldspar underlies an area of more than 50 km^2 southeast of Four Mile River and northeast of Beale Lake. Sills of the diorite occur in hornfelsed metasedimentary rocks of the Sylvester Group along the southern and southwestern contact which everywhere dips to the southwest. The diorite appears to be more strongly foliated near its margins than elsewhere. Inclusions of mafic-rich rocks are locally abundant.

Granite along Meek Creek and Four Mile River

Remarkably fresh, nonfoliated, coarse grained granite forms distinctive, bold, strongly jointed outcrops underlying an area of more than 35 km^2 along and near Meek Creek and along the Four Mile River. The rock is characterized by a high content of coarsely megacrystic K-feldspar (30 %) and quartz (25-30 %). Biotite is the only mafic mineral present. In places near its margins the granite contains numerous fine- to medium-grained dioritic inclusions with porphyroblasts of K-feldspar.

South of Meek Creek, limestone and argillaceous strata are strongly foliated and locally brecciated near contacts with the granite but show no evidence of contact metamorphism. Hence the granite is probably in fault contact with the sediments.

Contact relationships on the north side of the granite are equivocal. In a few places, the margins of the granite are finer grained and have more biotite than elsewhere. One outcrop shows a sharp, presumably intrusive contact with finer grained hornblende granodiorite to quartz monzodiorite exposed to the north. In the bordering granodiorite are fine grained, pink aplitic dykes of composition similar to the granite. Based on these criteria the granite is assumed to be intrusive along its northern contact.

Granodiorite and monzodiorite between Dalton Creek and Four Mile River

In this area medium grained, diorite hornblende granodiorite and monzodiorite underlies an area of about 35 km^2. Typical lithologies consist of 50 % or more andesine feldspar and about 15 % each of K-feldspar, quartz and hornblende. Plagioclase is generally much altered to sericite, and hornblende is in part altered to chlorite. An unusual feature is the presence of spectacular micrographic texture involving quartz and K-feldspar. In some localities the rock has a high content of hornblende, particularly in finer grained phases which have the composition of monzodiorite to diorite.

As mentioned above, the granodiorite appears to have been intruded by granite along its southern margin. Its relationship with massive green volcanic rocks to the north has not been determined.

Foliated diorite south of Sylvester Peak

Foliated diorite underlies an area of about 15 km^2 along the crest of the ridge about 6 km south of Sylvester Peak. The rock has been highly strained and consists of 75-80 % andesine feldspar and 10-15 % hornblende which is pleochroic from tan to olive green. Sphene is abundant. Preliminary U-Pb determinations on zircon suggest the diorite is of Late Devonian age with a strong early Middle Proterozoic inheritance.

Phases of the foliated diorite range from white weathering, leucocratic, medium grained rocks to finer grained rocks rich in hornblende. Underlying the body, at least on its north side, is a unit of biotite-bearing, quartzofeldspathic tectonite with minor carbonaceous layers. It consists of paper-thin subhorizontal laminae with well developed lineation. The tectonite has been intruded by the overlying plutonic rocks and in both lithologies a strong S-C mylonitic fabric has been superimposed in a zone about 500 m thick along the base of the lithotectonic slice. Very fine grained, dark grey diabasic(?) dykes and sills crosscut the mylonitic fabric along the base of the tectonite.

CONCLUSIONS

The Sylvester Allochthon in the region discussed in this report contains a remarkable record of late Paleozoic and Mesozoic volcanism, sedimentation, plutonism and structural development. Because the various packages of lithologies occur in lithotectonic slices their original relationships are essentially unknown. The compositions of the Meek Creek and Dalton Creek bodies strongly suggest derivation involving continental crust. The origin of zircons in foliated diorite associated with the tectonite unit is a problem. It is possible that the early Middle Proterozoic inheritance in the zircons reflects the age of the intruded tectonite. In any event Precambrian crust seems to have been involved. The diorite body northeast of Beale Mountains is more typical of the Permian plutons that occur elsewhere in the Sylvester Allochthon.

Pre-Late Devonian tectonism is suggested by the relationships of Late Devonian diorite and underlying tectonite. Elsewhere in the Cordillera Late Devonian granitic rocks are mainly assigned to the Kootenay Terrane. Data from the Cry Lake map area farther south indicate both pre-Permian and Mesozoic ages for the faults bounding lithotectonic slices.

ACKNOWLEDGMENTS

We thank Christine Davis for drafting the figure.

REFERENCES

Gabrielse, H.
1963: McDame map-area, Cassiar District, British Columbia; Geological Survey of Canada, Memoir 319, 138 p.

Gabrielse, H., Anderson, R.G., Leaming, S.F., Mansy, J.L., Monger, J.W.H., Thorstad, L.E., and Tipper, H.W.
1979: Geology of Cry Lake map-area (104I); Geological Survey of Canada, Open File 610.

Hanson, G. and McNaughton, D.A.
1936: Eagle – McDame area, Cassiar District, British Columbia; Geological Survey of Canada, Memoir 194, 16 p.

Harms, T.A.
1986: Structural and tectonic analysis of the Sylvester Allochthon, northern British Columbia: implications for paleogeography and accretion; unpublished Ph.D. thesis, University of Arizona, Tucson, 80 p.

Woodsworth, G.J., Anderson, R.G., and Armstrong, R.L.
— Chapter 15, Plutonic Regimes; *in* The Cordilleran Orogen: Canada, H. Gabrielse and C.J. Yorath (eds.), Geological Survey of Canada, no. 5. (also Geological Society of America, The Geology of North America, no. G-2). (in press).

Isotopic characteristics of the McDame gold-silver deposits, Cassiar District, British Columbia

B.E. Nesbitt[1], P.A. Cavell[1], and K. Muehlenbachs[1]

Nesbitt, B.E., Cavell, P.A., and Muehlenbachs, K., Isotopic characteristics of the McDame gold-silver deposits, Cassiar District, British Columbia; in Current Research, Part E, Geological Survey of Canada, Paper 89-1E, p. 5-11, 1989.

Abstract

$\delta^{18}O$ investigations of quartz veins from the Sylvester allochthon indicate that mineralized and unmineralized quartz veins have similar, ^{18}O-enriched values of +15 to +18‰. Late, crosscutting carbonate veins are depleted in ^{18}O with $\delta^{18}O$ values close to 0‰. δD data from fluid inclusions indicate that the quartz veins formed from meteoric water that had undergone extreme ^{18}O enrichment. The ^{18}O enrichment is believed to be a product of water/rock interaction between the meteoric water and metasedimentary rocks.

Sm-Nd and Rb-Sr studies have been unsuccessful in establishing an isochron for either system. However, results from both radiogenic systems indicate that the ore-forming fluids interacted with Paleozoic to Proterozoic metasedimentary rocks. The combined results of the isotopic studies document deep convection of meteoric water through the autochthonous sedimentary units underlying the Sylvester allochthon, subsequent ascent of the fluids and formation of the ores in the Sylvester allochthon.

Résumé

L'examen de $\delta^{18}O$ dans des filons de quartz provenant de l'allochtone de Sylvester indique que des filons de quartz minéralisés et non minéralisés présentent des valeurs similaires d'enrichissement en ^{18}O, comprises entre +15 et −18‰. Les filons carbonatés transversaux et tardifs sont épuisés en ^{18}O et se caractérisent par des valeurs $\delta^{18}O$ proches de 0‰. Les données δD obtenues sur des inclusions fluides indiquent que les filons de quartz se sont formés à partir d'eaux météoriques ayant subi un enrichissement extrême en ^{18}O. On croît que l'enrichissement en ^{18}O est un produit de l'interaction entre l'eau et la roche, en particulier entre les eaux météoriques et les roches métasédimentaires.

Les études de datation par les méthodes Sm-Nd et Rb-Sr n'ont pas permis d'établir un isochrone pour l'un et l'autre systèmes. Cependant, les résultats de l'étude des deux systèmes radiogéniques indiquent que les fluides minéralisants ont agi sur les roches métasédimentaires d'âge paléozoïque à protérozoïque. Les résultats combinés des études isotopiques fournissent des données sur la convection à grande profondeur des eaux météoriques à travers les unités sédimentaires autochtones sous-jacentes à l'allochtone de Sylvester, sur la montée ultérieure des fluides, et sur la formation des minerais dans l'allochtone de Sylvester.

[1] Department of Geology, University of Alberta, Edmonton, Alberta T6G 2E3

INTRODUCTION

Gold was first discovered in the Cassiar district in placer deposits on McDame Creek in 1874. Quartz veins carrying economic quantities of free gold were discovered in 1934 and production began in 1937. Mining was intermittent in the area until 1978 when Erickson Gold Mining Co. undertook a major development (Diakow and Panteleyev, 1981). The Erickson Gold Mining Co. has now consolidated the production from most of the vein systems into a 400-tonne/day operation. In addition, operations on the Taurus vein in the northern portion of the district are conducted by Taurus Resources Ltd.

The objectives of this contribution are 1) to summarize the results from an ongoing study of stable and radiogenic isotope systematics of mineralization and associated alteration, and 2) to present current interpretations of the genetic significance of these results.

REGIONAL AND DEPOSIT GEOLOGY

Au-bearing quartz veins of the Erickson and Taurus mines are hosted by Permian to Pennsylvanian basalts of the Sylvester Group in the Sylvester Allochthon (Fig. 1). The Sylvester Allochthon is composed of thrust slices of oceanic lithologies (basalts, ultramafics, cherts, and black shales), which have been thrust over autochthonous, continental shelf, sedimentary units of Proterozoic to Paleozoic age (Gordey et al., 1982). The age of thrusting is not well established, but is bracketed between Late Triassic and Middle Cretaceous (Gordey et al., 1982). The Cassiar Stock is situated on the western flank of the region and has been dated by K-Ar at 70-77 Ma (Sketchley et al., 1986). The Cassiar Batholith, which lies to the west of the Cassiar Stock, has been dated by K-Ar at 89-100 Ma and by Rb-Sr at 111 Ma. K-Ar dating of micas associated with the ore-bearing, quartz veins indicates a pre-intrusion age of 129 $\pm$ 4 Ma for the veins (Sketchley et al., 1986).

Mineralization in the Cassiar district consists of a series of east-west to northeast-southwest trending veins, which are roughly normal to a major, north-south lineament (Somerville, pers. comm., 1985). The quartz veins are generally steeply dipping and 0.5 to 1 m wide, should be "ten of metres" in the vertical dimension and can be over a 100 m long (Panteleyev and Diakow, 1982). The veins are composed of over 95 % quartz with the remainder consisting of pyrite, carbonate and graphite with minor tetrahedrite, chalcopyrite, sphalerite and galena. Layers of graphitic material in the veins often produce a banded or ribboned texture. Extensive carbonate alteration of the host basalts occurs adjacent to the veins. A listwanitic alteration assemblage, composed of fuchsite, carbonate and quartz, is also quite common (Dussel, 1986). Fluid inclusion data from the quartz veins (Dussel, 1986) and (Nesbitt, unpublished data) indicate temperatures of homogenization of 250 to 350°C, with variable salinities from 1 to 10 equivalent wt. % NaCl and CO_2 contents up to 15 mole per cent.

In many respects, Au mineralization in the McDame deposits closely resembles quartz vein systems in other parts of the North American Cordillera and Archean terranes (Hodgson et al., 1982; Colvine et al., 1984; Nesbitt et al., 1986; Bohlke and Kistler, 1986). Consequently, the results of this investigation of a relatively young Cordilleran system can be significant to the understanding of deposits as old as the Archean.

TECHNIQUES

Minerals for δ ^{18}O analyses were separated by chemical and hand-picking techniques. Extraction of fluids from fluid inclusions was done by decrepitation (Nesbitt et al., 1987 a, b). All of the samples were analyzed using conventional stable isotope techniques (McCrea, 1951; Clayton and Mayeda, 1963; Godfrey, 1962) and the data are given in the conventional δ-notation with respect to SMOW for oxygen

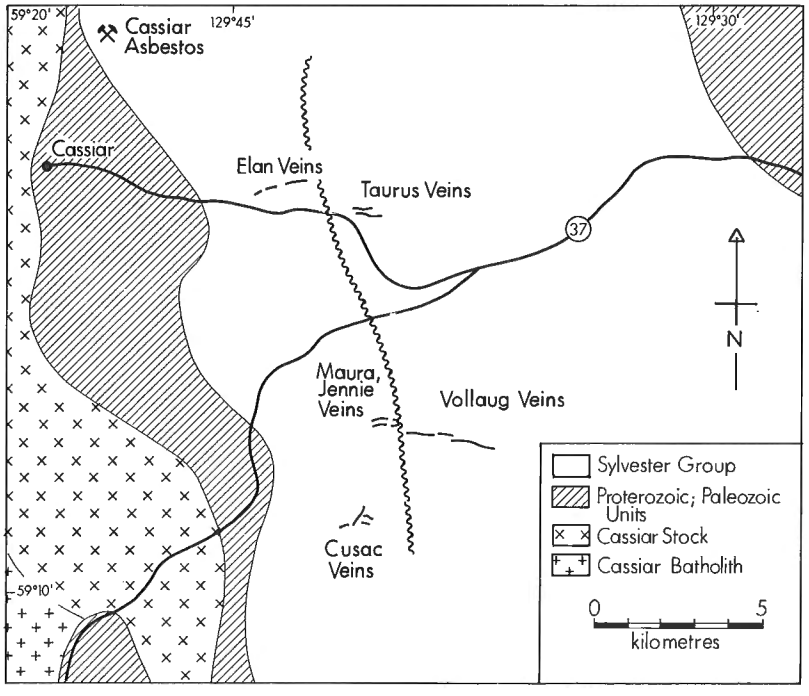

Figure 1. Distribution of principal Au-bearing veins in units of the Sylvester Group of the Sylvester Allochthon. After Sketchley et al. (1986) and unpublished maps of Erickson Gold Mines Ltd.

and hydrogen isotope ratios. Experimental uncertainties and details on precision are the same as given in Nesbitt et al. (1987 a, b).

RADIOGENIC ISOTOPES

In this preliminary study, Rb-Sr and Sm-Nd isotopic ratios were determined for minerals in a listwanite sample from the Erickson mine (EN-26 from the Vollaug vein). Formation of listwanite is inferred to be closely linked to mineralization (Dussel, 1986) and this rock type (carbonate+fuchsite ± quartz, carbon) can potentially provide minerals with widely different Sm/Nd and Rb/Sr ratios. Widely varying parent-daughter ratios may enable calculation of mineral isochrons, if the minerals were simultaneously isotopically homogenized. Whole rock powder, a fuchsite separate and a carbonate separate, split into two magnetic fractions, were analyzed.

A single sample of each of the three mineral separates and of whole rock powder was decomposed for determination of isotope ratios and concentrations of Rb, Sr, Sm and Nd. In addition, an aliquot of the less magnetic carbonate fraction was partially digested with 2 N HCl and the soluble portion was analyzed along with the other samples. Separate aliquots of each sample solution were used for determination of concentrations and of isotopic compositions. This procedure reduced errors which might result from inhomogeneity between aliquots of sample powder. Analyses for Sm and Nd utilized procedures reported in Cavell and Baadsgaard (1986) and for Rb and Sr the procedures in Baadsgaard et al. (1981) were used. Sr was separated by co-precipitation with $Ba(NO_3)_2$ and purified by ion exchange methods. Rb, Sm and Nd were isolated from the supernatant solution after $Ba(NO_3)_2$ precipitation. Sm and Nd were separated by cation exchange using 0.2 N methyllactic acid as eluant. Isotope analyses were carried out on VG MM30 and VG 354 mass spectrometers. For Nd and Sr determinations the sample/blank ratio was greater than 300:1 in all cases. Repeated runs of the NBS 987 SR standard gave a value of 0.71026 ± 5 (2σ). Five interspersed runs of the La Jolla Nd standard gave a value of 0.511857 ± 6 (2σ). Sm/Nd data were normalized to a value of 0.7219 for $^{146}Nd/^{144}Nd$.

RESULTS OF STABLE ISOTOPE ANALYSES

Analyses of oxygen and hydrogen isotopes were conducted on a variety of samples from the mines and regional exposures to obtain information on the origin, composition and evolution of hydrothermal fluids.

Oxygen isotope analyses of seven samples of quartz from ore-grade veins yielded an average $\delta^{18}O$ value of + 16.8 ± 1.4‰ over a range of +15.6 to +18.8‰ (Table 1). Isotopic analyses of quartz from seven, isolated, low-grade to unmineralized veins in greenstones yielded a range

Table 1. Stable isotope results

	Silicates		Carbonates	
Quartz from Ore Grade Veins	$\delta^{18}O$‰	δD‰	$\delta^{13}C$‰	$\delta^{18}O$‰
Vollaug Vein	+18.8			
Vollaug Vein	+18.7	−158		
Taurus Vein	+15.7			
Taurus Vein	+15.6	−125		
Elan Vein	+16.2			
Elan Vein	+16.3	−142		
Maura Vein	+16.3	−153		
Average	+16.8±1.4 (7)	−145±15 (4)		
Average for Regional Quartz Veins	+16.1±1.1 (7)			
Serpentinite Assoc. with Ore	+9.6±0.1(1)			
Average for Sylvester Basalts	+9.5+1.4 (5)			
Average for Altered Sylvester Basalts	+14.0±1.6 (7)			
Average for Post-Ore Carbonate Veins	−0.5±0.1(1)		−0.1±1.0 (2)	−3.6±1.1(2)
Carbonate Vein near Cassiar Pluton			−3.4±0.1(1)	−2.6±0.1(1)

Notes: ( ) number of samples in average; δD of fluids extracted by decrepitation of fluid inclusions in quartz

of $\delta^{18}O$ values of +14.3 to +17.8‰ with an average of +16.1 ± 1.1‰. This lack of a $\delta^{18}O$ contrast between ore grade and low grade or unmineralized veins suggests that all of the quartz veins were formed by the same or at least similar hydrothermal systems. This conclusion is further supported by similarities in textures, mineralogy and alteration between ore grade and low grade or unmineralized regional veins.

Exceptions to the general uniformity of $\delta^{18}O$ results are found in unmineralized carbonate (dolomite ± calcite) ± quartz veins, such as the McDame vein, which cut mineralized veins, and in minor carbonate veins near the Cassiar Stock. Carbonate and quartz (Table 1) from both of these units possess low $\delta^{18}O$ values. The low $\delta^{18}O$ values indicate a clear distinction between these veins and the more comon, mineralized and unmineralized quartz veins. In addition, the low $\delta^{18}O$ values indicate that the fluid which formed these later veins was composed dominantly of relatively pristine, meteoric water.

It is important to note that whole rock values for $\delta^{18}O$ of serpentinites average +8.2 ± 0.3‰ for the Cassiar asbestos deposits (Wenner and Taylor, 1974) and +9.6 ± 0.2‰ (this study) for a serpentinite which is closely associated with ore (Table 1). These values are substantially enriched in ^{18}O relative to other serpentinites in central and northern British Columbia, where typical $\delta^{18}O$ values are +2 to +3‰ (Wenner and Taylor, 1974).

Results of whole rock $\delta^{18}O$ analyses of the basaltic units, which host the ore, average +9.5 ± 1.4‰ (Table 1). These basalts are enriched in ^{18}O relative to pristine MORBs indicating ^{18}O enrichment by hydrothermal processes either on the seafloor or after accretion (Muehlenbachs, 1986). With increasing proximity to the quartz veins, the $\delta^{18}O$ values of the whole rock samples of the basalts increase, going from background $\delta^{18}O$ values of +9 to +10‰ to +13 to +15‰ at the vein margins over a distance of less than 10 m (Table 1).

Analyses of deuterium/hydrogen ratios were undertaken to better constrain the origin of the ore forming fluids. Six analyses of fluids, extracted from fluid inclusions in ore grade quartz veins, have an average δD value of 147 ± 12‰. Analyses by Wenner and Taylor (1974) of whole rock serpentinite samples from the Cassiar asbestos mine yielded an average value δD of -179 ± 14‰, which is similar to recent results on antigorite mineral separates from the Cassiar mine (T.K. Kyser, pers. comm.).

DISCUSSION OF THE RESULTS FROM THE STABLE ISOTOPE STUDIES

Using the average $\delta^{18}O$ value of +16.4‰ for vein quartz, a temperature of 300°C and equations of Matsuhisa et al. (1979), an average value of +9.5‰ was calculated for the ore forming fluid. This value is substantially enriched in ^{18}O relative to local meteoric water and could be indicative of magmatic, marine, metamorphic or isotopically evolved meteoric fluids (Sheppard, 1986). For similar deposits in Archean terranes of Ontario and Quebec, metamorphic or magmatic models for fluid origin are generally favored (Kerrich, 1987; Burrows et al., 1986). However, the ore forming fluids at Cassiar are extremely low in deuterium content, which indicates the involvement of a major component of meteoric water. Calculated values of $\delta^{18}O = +8.2$ and $\delta D = -151$ (calculated at 300°C with equations of Wenner and Taylor, 1974) for the Cassiar serpentinites are similar to the values estimated from the isotopic results for the quartz veins, suggesting that the serpentinites equilibrated isotopically with the mineralizing or similar solutions.

The degree to which a fluid isotopically evolves during migration through the subsurface is a function of three main variables: the temperature of water-rock interaction, water/rock ratios and the differences in the isotopic compositions between the rock and water (Taylor, 1979). Plotted in Figure 2 are different paths of isotopic evolution for a

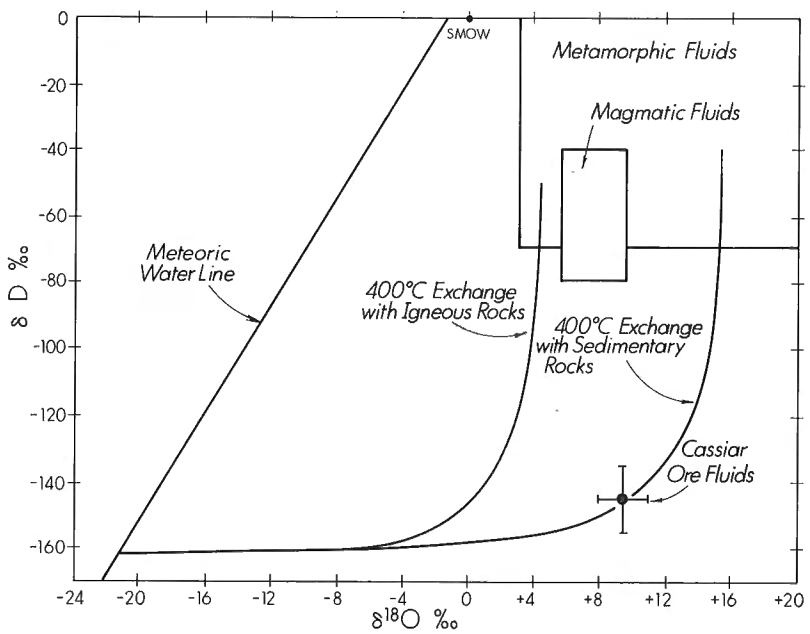

Figure 2. $\delta D/\delta^{18}O$ plot showing fluid evolution paths with varying water/rock ratios in different rock types (Taylor, 1979). High water/rock ratios plot near the meteoric water line; low water/rock ratios plot near the metamorphic field.

fluid as a function of rock type. The brittle/ductile transition at a temperature of approximately 400°C is believed to limit the depth of fluid of penetration in such systems (Nesbitt, in press). Consequently, a temperature of 400°C is used in the calculations. The calculations are based on equations in Field and Fifarek (1985) using initial $\delta^{18}O$ and δD values of +7 and -70 for igneous rocks (andesites to rhyolites), and +18 and -60 for sedimentary rocks (siliciclastic and carbonates). As is apparent from the diagram, it is not possible to generate the isotopic characteristics of the ore-forming fluid from fluid interactions with unaltered igneous rocks. The generation of the inferred isotopic composition of the ore forming fluid is possible only via the interaction of meteoric water with sedimentary units. Consequently, the fluids which formed the Cassiar deposits must have originated as meteoric water which circulated deep into the autochthonous Proterozoic-Paleozoic units below the Sylvester allochthon and rose through a fracture system in the Sylvester allochthon. This conclusion is further supported by the radiogenic isotope analyses, summarized in the following section.

RESULTS OF RADIOGENIC ISOTOPIC ANALYSES

Analytical results for the listwanite sample, EN-26, are presented in Table 2. Data for unaltered, host basalts are not yet available. Relative to an "average oceanic basalt" (Cohen et al., 1980), the listwanite has slightly lower Sm and Nd concentrations, a similar Sm/Nd ratio, much higher Rb concentration (about 100-fold), and a correspondingly high $^{87}Rb/^{86}Sr$ ratio. A corresponding high K content has been reported by Sketchley (1986). The high Rb content of listwanite is contained mainly in fuchsite. Variations in Rb content of the two carbonate separates and the leachable carbonate suggest that they contain fuchsite inclusions or intergrowths.

Data for neither the Rb-Sr nor Sm-Nd system yield an isochron. Major disturbances of the Rb-Sr system may have occurred through geological processes or may be, at least partially, a result of sample preparation techniques. Model initial $^{87}Sr/^{86}Sr$ ratios, calculated for an alteration age of 130 Ma (Sketchley et al., 1986) suggest both causes. The carbonates and whole rock powder show variations in initial ratios (outside of experimental error) inferred to be related to geological processes because no chemical treatment was used in preparation of these samples. The fuchsite has an extremely low model, initial $^{87}Sr^{86}Sr$ ratio. Either Rb has recently been added to the fuchsite or loosely bound radiogenic Sr has been removed by the acid leaching used to remove carbonate from the mica, prior to analysis (Machado et al., 1986), but to a lesser extent because of the geochemical similarity of parent and daughter elements. Separation of minerals by mechanical means only is in progress.

Table 2. Radiogenic isotope results

Sample	Nd (ppm)	Sm (ppm)	$\frac{^{147}Sm}{^{144}Nd}$ [a]	$\frac{^{143}Nd}{^{144}Nd}$ [a]	$\frac{^{143}Nd}{^{144}Nd}^{i}$ [b]
Carbonate:					
1. Magnetic fraction, total decomposition	3.6	1.89	0.3157	0.51238	0.51211
2. Non-magnetic fraction, total decomposition	3.74	1.97	0.3171	0.51238	0.51211
3. Non-magnetic fraction, acid soluble only	3.74	1.97	0.3156	0.51237	0.51210
Whole Rock	3.18	0.90	0.1705	0.51216	0.51202
Fuchsite	0.84	0.12	0.0842	0.51213	0.51205
	Sr (ppm)	Rb (ppm)	$\frac{^{87}Rb}{^{86}Sr}$	$\frac{^{87}Sr}{^{87}Sr}$ [c]	$\frac{^{87}Sr}{^{86}Sr}^{i}$ [b]
Carbonate:					
1. Magnetic fraction, total decomposition	1441.	11.403	0.0220	0.71336	0.71332
2. Non-magnetic fraction, total decomposition	1708.	6.040	0.0098	0.71252	0.71250
3. Non-magnetic fraction, acid soluble only	0.172	0.554	0.00089	0.71233	0.71233
Whole Rock	145.0	126.23	2.416	0.71644	0.71198
Fuchsite	4.73	311.41	182.60	0.9144	0.5772

(a) The uncertainty in the $^{147}Sm/^{144}Nd$ ratio is estimated at less than 0.1%, that of the $^{143}Nd/^{144}Nd$ ratio at less than 0.006%. A normalization factor of $^{146}Nd/^{144}Nd = 0.7219$ was applied to the measured $^{143}Nd/^{144}Nd$ ratios. $\lambda(^{147}Sm) = 6.54 \times 10^{-12} yr^{-1}$.
(b) Initial ratios are calculated for radiogenic decay of measured Rb or Sm since 130 Ma (Sketchley et al, 1986).
(c) The uncertainty on the Rb & Sr concentrations is estimated at 0.1%, that of the $^{87}Sr/^{86}Sr$ measurements at ±0.0001. $\lambda(^{87}Rb) = 1.42 \times 10^{-11}$ yr.$^{-1}$.

DISCUSSION OF RADIOISOTOPE RESULTS

Although the results do not yield an age for alteration and mineralization, they do present evidence about the source of the fluids from which the carbonate and mica crystallized. The fluids were apparently enriched in radiogenic Sr and depleted in radiogenic Nd, differing from values which would be expected in equilibrium with the host volcanic rocks. The host rocks are oceanic basalts of the Sylvester Group, which are Pennsylvanian to Permian in age (about 300 Ma maximum). If unaltered at 130 Ma, these basalts would have had a $^{87}Sr/^{86}Sr$ ratio between 0.702 and 0.703 and a $^{143}Nd/^{144}Nd$ in the range of 0.5124 to 0.5129. The initial $^{87}Sr/^{86}Sr \geq 0.7120$ is more radiogenic than would have been expected from equilibration with the Sylvester basalts. The initial $^{143}Nd/^{144}Nd$ obtained for the listwanite (≤ 0.5120) is less radiogenic than would have been expected. The Sr and Nd isotopic composition of the fluids which formed the listwanite must have been derived from passage through rocks, probably felsic crustal rocks, which had been more enriched in Rb and depleted in Sm than the host basalts prior to approximately 130 Ma. The Nd composition of the fluids (≤ 0.5120) further indicates that the crustal residence age (O'Nions et al., 1983) of the source rocks was at least 500 Ma, using the CHUR model (DePaolo and Wasserburg, 1976) and greater than 800 Ma using the depleted mantle (Goldstein et al., 1984). A probable source for such crustal residence ages and isotopic compositions are the autochthonous Proterozoic-Paleozoic units below the Sylvester Allochthon.

CONCLUSIONS

In summary the stable isotopic studies of the McDame gold deposits, Cassiar district have shown that: 1) the ore-forming fluids were highly evolved meteoric water which had reacted primarily with sedimentary material, and 2) late stage carbonate veins, present in the mineralized areas, are isotopically distinct from the ore-grade quartz veins and are probably related to the Cassiar intrusives.

Concurrent work on Sm-Nd and Rb-Sr radiogenic isotopes indicates that the ore-forming fluids reacted with metasedimentary rocks at least 500 Ma. Consequently, the results indicate that the ore-forming fluids of the McDame deposits were meteoric waters which had migrated deep into the autochthonous crust, evolved isotopically and chemically, and subsequently rose through the Sylvester allochthon forming the deposits.

ACKNOWLEDGMENTS

We would like to thank Drs. Baadsgaard and Gray for the use of their laboratories in the course of this work. The Erickson Gold Mining Company was generous with hospitality and assistance in sampling during the field work associated with the project. Funding for the project was provided by an EMR Research Agreement. A review of an early draft of the manuscript by P. Lhotka aided in clarification of the text. Careful reviews by F. Dudas and B. Taylor aided significantly in revisions of the text.

REFERENCES

Baadsgaard, H., Chaplin, C., and Griffin, W.L.
1981: Geochronology of the Gloserheia Pegmatite, Froland, Southern Norway; Norsk Geologisk Tidsskrift, v. 64, p. 111-119.

Bohlke, J.K. and Kistler, R.W.
1986: Rb-Sr, K-Ar, and stable isotope evidence for the ages and sources of fluid components of gold quartz veins in the northern Sierra Nevada foothills metamorphic belt, California; Economic Geology, v. 81, p. 296-322.

Burrows, D.R., Wood, P.C., and Spooner, E.T.C.
1986: Carbon isotope evidence for a magmatic origin for Archean gold-quartz vein deposits; Nature, v. 321 p. 851-854.

Cavell, P.A. and Baadsgaard, H.
1986: Geochronology of the Big Spruce Lake alkaline intrusion; Canadian Journal of Earth Sciences, v. 23, p. 1-10.

Clayton, R.N. and Mayeda, T.K.
1963: The use of bromine pentafluoride in the extraction of oxygen from oxides and silicates for isotopic analyses; Geochimica et Cosmochimica Acta, v. 27, p. 43-52.

Cohen, R.S., Evensen, N.M., Hamilton, P.J., and O'Nions, R.K.
1980: U-Pb, Sm-Nd and Rb-Sr systematics of mid-ocean ridge basalt glasses; Nature, v. 283, p. 149-153.

Colvine, A.C., Andrews, A.J., Cherry, M.E., Durocher, M.E., Fyon, A.J., Lavigne, M.J., Jr., Macdonald, A.J., Marmont, S., Poulsen, K.H., Springer, J.S., and Troop, D.G.
1984: An integrated model for the origin of Archean lode gold deposits; Ontario Geological Survey, Open-File Report 5524, 98 p.

Diakow, L.C. and Panteleyev, A.
1981: Cassiar gold deposits, McDame map-area; British Columbia Ministry of Energy, Mines and Petroleum Resources, Geological Division Paper 1981-1, p. 5562.

De Paolo, D.J. and Wasserburg, G.J.
1976: Nd isotope variation and petrogenetic models; Geophysical Research Letters, v. 3, p. 249-252.

Dussel, E.
1986: Listwanites and their relationship to gold mineralization at Erickson mine, British Columbia, Canada; M.Sc. thesis, Western Washington University, 90 p.

Field, C.W. and Fifarek, R.H.
1985: Light stable-isotope systematics in the epithermal environment; in Geology and Geochemistry of Epithermal Systems, edited by B.R. Berger and P.M. Bethke, Society of Economic Geologists, Reviews in Economic Geology, v. 2, p. 99-128.

Godfrey, J.D.
1962: The deuterium content of hydrous minerals from the East-Central Sierra Nevada and Yosemite National Park; Geochimica et Cosmochimica Acta, v. 26, p. 1215-1245.

Goldsteain, S.L., O'Nions, R.K., and Hamilton, P.J.
1984: A Sm-Nd isotopic study of atmospheric dusts and particulates from major river systems; Earth and Planetary Science Letters, v. 70, p. 221-236.

Gordey, S.P., Gabrielse, H., and Orchard, M.J.
1982: Stratigraphy and structure of the Sylvester Allochthon, southwest McDame map area, northern British Columbia; in Current Research, Part B. Geological Survey of Canada, Paper 82-1B, p. 101-106.

Hodgson, C.J., Chapman, R.S.G., and MacGeehan, P.J.
1982: Application of exploration criteria for gold deposits in the Superior Province of the Canadian Shield to gold exploration in the Cordillera; in Precious Metals in the Northern Cordillera: Vancouver, British Columbia, Association of Exploration Geochemists, p. 173-206.

Kerrich, R.
1987: The stable isotope geochemistry of Au-Ag vein deposits in metamorphic rocks; in Short Course in Stable Isotope Geochemistry of Low Temperature Fluids, edited by T.K. Kyser, Mineralogical Association of Canada, v. 13, p. 287-336.

Machado, N., Brooks, C., and Hart, S.R.
1986: Determination of inital $^{87}Sr/^{86}Sr$ and $^{143}Nd/^{144}Nd$ in primary minerals from mafic and ultramafic rocks: Experimental procedure and implications for the isotopic characteristics of the Archean mantle under the Abitibi greenstone belt, Canada; Geochimica et Cosmochimica Acta, v. 50, p. 2335-2348.

McCrea, J.M.
1951: On the isotope chemistry of carbonates and a paleotemperature scale; Journal of Chemistry and Physical v. 18, p. 849-857.
Matsuhisa, Y., Goldsmith, J.R., and Clayton, R.N.
1979: Oxygen isotope fractionation in the system quartz-albite-anorthite-water; Geochimica et Cosmochimica Acta, v. 43, p. 1131-1140.
Muehlenbachs, K.
1986: Alteration of the oceanic crust and the ^{18}O history of seawater; in Stable Isotopes in High Temperature Geological Processes; edited by J.W. Valley et al. Reviews in Mineralogy, Mineralogical Society of America, v. 16. p. 425-444.
Nesbitt, B.E.
—: The gold deposit continuum: A genetic model for the origin of gold deposits in the continental crust; Geology, (in press).
Nesbitt, B.E., Murowchick, J.B., and Muehlenbachs, K.
1986: Dual origins of lode gold deposits in the Canadian Cordillera; Geology, v. 14, p. 506-509.
Nesbitt, B.E., Muehlenbachs, K., and Murowchick, J.B.
1987a: Dual origins of lode gold deposits in the Canadian Cordillera: Reply to comment by W.J. Pickthorn, R.J. Goldfarb, and D.L. Leach; Geology, v. 15 p. 472-473.
Nesbitt, B.E., St. Louis, R.M., and Muehlenbachs, K.
1987b: Distribution of gold in altered basalts of DSDP hole 504B; Canadian Journal of Earth Sciences, v. 24, p. 201-209.
O'Nions, R.K., Hamilton, P.J., and Hooker, P.J.
1983: A Nd isotope investigation of sediments related to crustal development in the British Isles; Earth and Planetary Science Letters, v. 63, p. 229-240.
Panteleyev, A. and Diakow, L.J.
1982: Cassiar gold deposits McDame map-area; in Geological Fieldwork 1981: British Columbia Ministry of Energy, Mines and Petroleum Resources, Paper 1982-1, p. 156-161.
Sheppard, S.M.F.
1986: Characterization and isotopic variations in natural waters; in Stable Isotopes in High Temperatures Geological Processes; Mineralogical Society of America, Reviews in Mineralogy, v. 16, p. 165-183.
Sketchley, D.A.
1986: The nature of carbonate alteration in basalt at Erickson gold mine, Cassiar, north-central British Columbia; Ph.D. Thesis, University of British Columbia, Vancouver, B.C., 273 p.
Sketchley, D.A., Sinclair, A.J., and Godwin, C.I.
1986: Early Cretaceous gold-silver mineralization in the Sylvester Allochthon, near Cassiar, north-central British Columbia; Canadian Journal of Earth Sciences, v. 23, p. 1455-1458.
Taylor, H.P., Jr.
1979: Oxygen and hydrogen isotope relationships in hydrothermal mineral deposits; in Geochemistry of Hydrothermal Ore Deposits, 2nd ed., edited by H.L. Barnes, John Wiley and Sons, New York, p. 236-277.
Wenner, D.B. and Taylor, H.P., Jr.
1974: D/H and 18O/16O studies of serpentinization of ultramafic rocks; Geochimica et Cosmochimica Acta, v. 38, p. 1225-1286.

Conodont biostratigraphy and constraints on Upper Devonian mineral deposits in the Earn Group, northern British Columbia and Yukon

Steven E.B. Irwin[1] and M.J. Orchard
Cordilleran and Pacific Geoscience Division, Vancouver

Irwin, S.E.B. and Orchard, M.J., Conodont biostratigraphy and constraints on Upper Devonian mineral deposits in the Earn Group, northern British Columbia and Yukon; in Current Research, Part E, Geological Survey of Canada, Paper 89-1E, p. 13-19, 1989.

Abstract

In the Selwyn and Kechika basins, sedimentary exhalative barite-Pb-Zn-Ag deposits occur in sediments of the Earn Group. Conodont faunas from these deposits are commonly Late Devonian, and include zonal indices of the Polygnathus asymmetricus, Ancyrognathus triangularis, Palmatolepis rhenana, Pa. triangularis, Pa. crepida, *and* Pa. marginifera *zones.*

The oldest Earn group strata are found at Macmillan Pass where conodont faunas associated with stratiform mineral deposits range from Early Devonian to middle Famennian. At Gataga the Earn Group spans at least lower Frasnian to middle Famennian. At Midway, where the Earn Group rests unconformably on the McDame Group, the basal Earn strata is early to middle Famennian.

Late Devonian mineralizing events were not synchronous within the miogeocline. Sedimentary exhalative deposits at Macmillan Pass appear to be Frasnian, whereas those at Gataga are constrained by Famennian conodonts. This may have implications for Late Devonian tectonism and for exploration strategies.

Résumé

Dans les bassins de Selwyn et de Kechica, on trouve des gisements exhalatifs sédimentaires de barytine, plomb, zinc et argent dans les sédiments du groupe d'Earn. Les faunes de conodontes de ces gisements supérieurs remontent en général au Dévonien et renferment des indices zonaux des zones Polygnathus asymmetricus, Ancyrognathus triangularis, Palmatolepis rhenana, Pa. triangularis, Pa. crepida et Pa. marginifera.

Les couches du groupe d'Earn les plus anciennes se trouvent au col Macmillan où les faunes de conodontes associées à des gisements de minéraux stratiformes se situent entre le Dévonien inférieur et le Famennien moyen. À Gataga, le groupe d'Earn s'étend au moins du Frasnien inférieur au Famennien moyen. À Midway, où le groupe d'Earn repose en discordance sur le groupe de McDame, les couches basales d'Earn datent du Famennien inférieur à moyen.

Les minéralisations du Dévonien supérieur ne sont pas contemporaines au sein du miogéosynchinal. Les gisements exhalatifs sédimentaires au col Macmillan semblent remonter au Frasnien, tandis que ceux de Gataga et de Midway sont limités par des conodontes du Famennien. Cela pourrait avoir une incidence en ce qui a trait au tectonisme du Dévonien supérieur et les stratégies d'exploration.

[1] Department of Geological Sciences, University of British Columbia, 6339 Stores Road, Vancouver, B.C. V6T 2B4

INTRODUCTION

There is a significant belt of economically important Late Devonian syngenetic sedimentary exhalative lead-zinc-silver-barite deposits and stratiform barite deposits in western North America (Fig. 1). These syngenetic deposits, precipitated from metalliferous geothermal brines, are associated with fault zones in tectonically active environments. Because of their sedimentary nature, the timing of the specific tectonic event(s) that produced the mineralization can be determined by dating the associated sediments.

The Earn Group of Yukon Territory and northern British Columbia hosts several important Late Devonian sedimentary exhalative deposits. Late Devonian conodont biostratigraphy of the Earn Group is being currently investigated in order to provide age constraints on stratiform mineral deposits. Conodont collections from the Selwyn and Kechika basins (map areas 94F,K,L; 104I,P; 105 A,I,J,K,O,P) are being used in this study. The area of the Selwyn and Kechika basins refers to the Cordilleran miogeocline southwest of the Ogilvie and Mackenzie platforms (Fig. 2; Abbott et al., 1986). The present study is focused on three areas with mineral deposits: Macmillan Pass, Gataga, and Midway. Previously, only broad age constraints were available for these deposits. With tighter paleontological control, the absolute age, frequency, and duration of the Late Devonian sedimentary exhalative deposits can be determined and will lead to a fuller understanding of the tectonic history of the miogeocline.

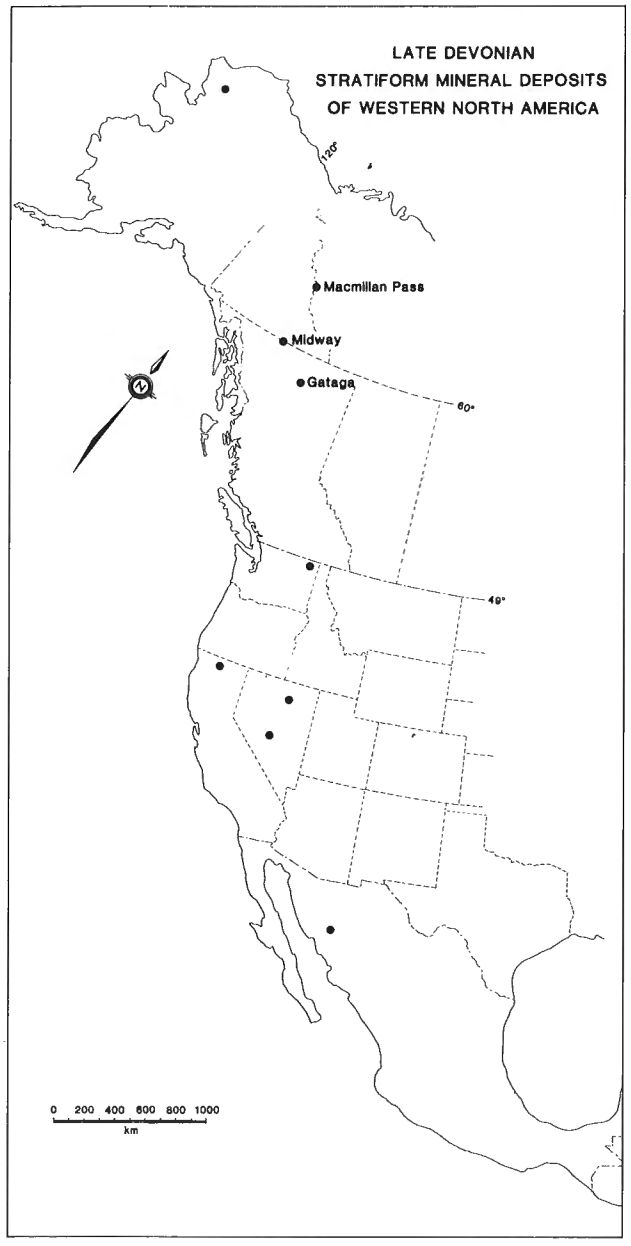

Figure 1. Location of Late Devonian stratiform mineral deposits within the North American Cordillera. Deposits include Pb-Zn-Ag-barite and barite mineralization.

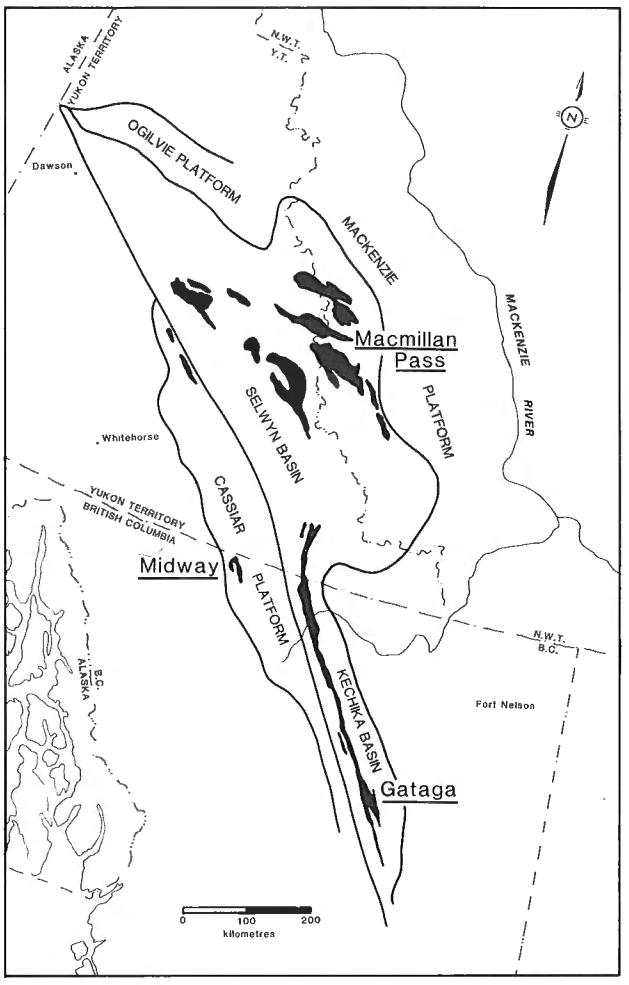

Figure 2. General geological area of the stratiform mineral deposits of Macmillan Pass, Midway, and Gataga after restoration of 450 km of sinistral movement on the Tintina Fault. Black areas show Earn Group outcrop after Wheeler and McFeely (1987).

REGIONAL GEOLOGY

Sediments of the Cordilleran miogeocline were deposited along the relatively stable margin of western North America from Late Proterozoic to Middle Jurassic. The sedimentary facies of the miogeocline have been divided into four broad sequences (Abbott et al., 1986). The Late Proterozoic Windermere Supergroup, a clastic-dominated sequence, is believed to have resulted from an early episode of continental rifting. From Early Cambrian through Middle Devonian time, a variety of shallow water clastics and platform carbonates were deposited in the inner portion of the miogeocline, while deeper water clastic sequences were deposited in the outer miogeocline. From Middle Devonian through Mississippian time, the transgressive, westerly and northerly derived Earn Group sequence of chert, shale and locally derived coarse clastics was deposited in the outer miogeocline (Gordey et al., 1987).

The Earn Group is distinguished by a complex stratigraphy with internal unconformities and abrupt changes in lithology, thickness and facies. Thick sequences of chert conglomerate and other coarse clastic sediments accumulated in fault-controlled troughs of the outer miogeocline (Gordey et al., 1982). This sequence is representative of a tensional regime involved in either continental rifting and separation, or extensional basins related to strike-slip faulting (Abbott et al., 1986). During these events the syngenetic sedimentary exhalative deposits at Macmillan Pass, Midway, and Gataga were formed in the Earn Group. The inner part of the miogeocline received the shale and siltstone limits of the transgressive wedge. Fine grained clastic sediment, limestone, and chert indicate that a relatively stable post-Earn Group marine shelf environment existed during the Mississippian through Triassic.

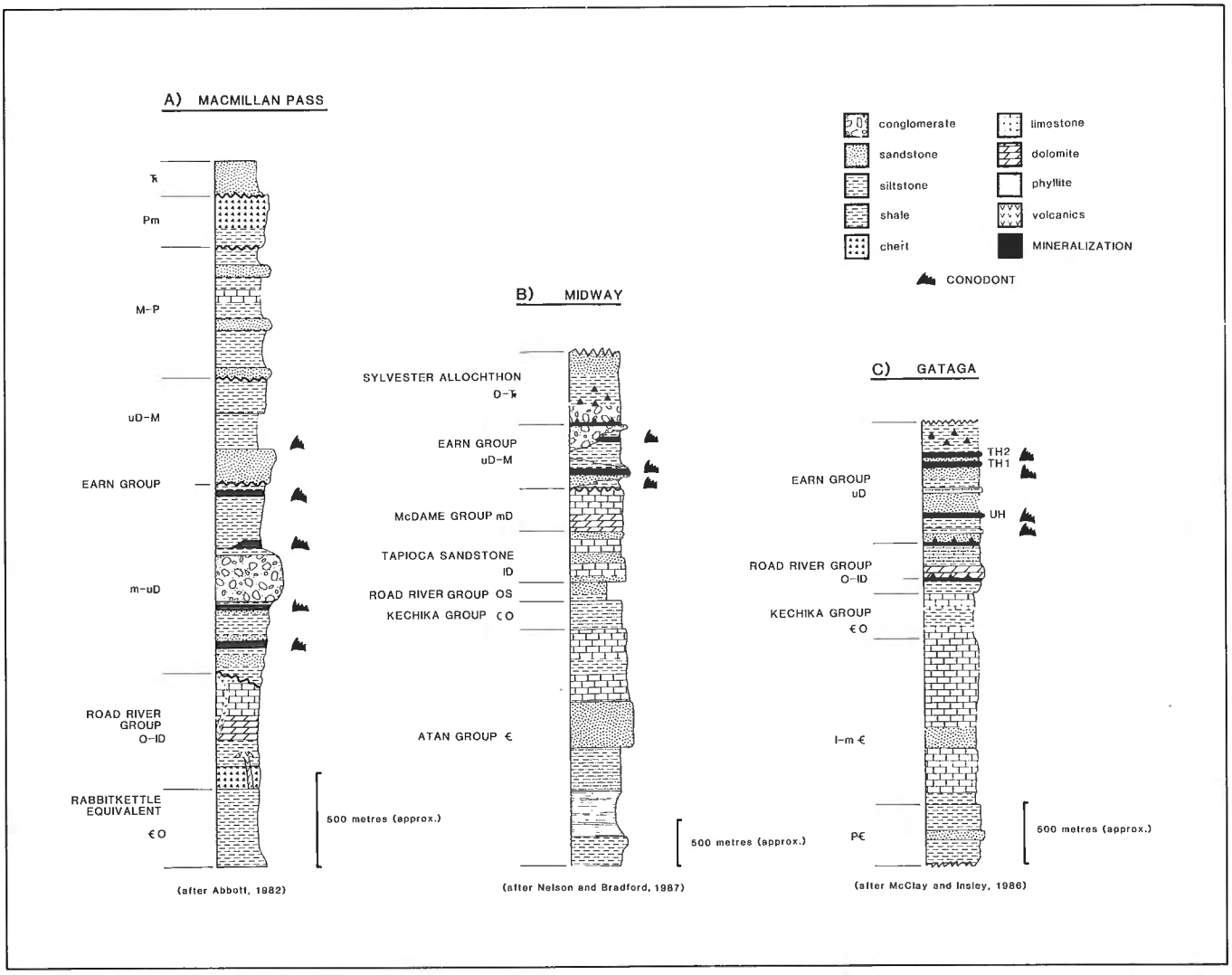

Figure 3. Simplified composite stratigraphic sections from Macmillan Pass (Abbott, 1982), Midway (Nelson and Bradford, 1987), and Gataga (McClay and Insley, 1986). Geology, age, and relative position of mineral horizons are based on previous regional geology work. The position of conodont faunas associated with the Earn Group stratiform mineral deposits is based on preliminary investigations and may be modified.

Macmillan Pass

There is a relatively complete stratigraphic section of Cambrian through Triassic strata at Macmillan Pass (Fig. 3a). Pre-Earn strata includes: Late Proterozoic "Grit" unit: Cambro-Ordovician shale and siltstone equivalent to the Rabbitkettle Formation: and Ordovician through Lower Devonian chert, shale, carbonate, and local volcanics of the Road River Group (Abbott, 1982). The base of the Earn Group (Fig. 3a) is diachronous and regionally unconformable with the Road River Group (Gordey et al., 1982). The Earn Group typically is a diverse turbiditic sequence of clastic sediments. There is at least one unconformity within the Earn Group that separates it into lower and upper parts. Mississippian through Triassic quartz arenite, shale, and chert rest unconformably above the Earn Group (Gordey et al., 1982).

Midway

The oldest strata seen near Midway correlates with the Lower Cambrian Atan Group which includes quartzite, phyllite, shale and limestone. Strata above the Atan Group (Fig. 3b) include Cambro-Ordovician Kechika Group siltstone, Ordovician and Silurian Road River Group siltstone and carbonate, Lower Devonian Tapioca Sandstone carbonate and quartzite, and Middle Devonian McDame Group carbonate (Nelson and Bradford, 1987). The Earn Group rests unconformably on a significant karst horizon within the upper McDame Group carbonates (Orchard and Irwin, 1988). Nelson and Bradford (1987) reported up to 200 m of relief at the McDame-Earn contact. Here also the Earn Group is a diverse sequence of clastic sediments. The upper contact of the Earn Group is a poorly defined thrust at the base of a complexly thrusted sequence of possibly allochthonous strata known as the Sylvester Allochthon. The strata of the Sylvester Allochthon include chert, shale, limestone, volcanic and plutonic rocks of latest Devonian to Triassic age (Nelson and Bradford, 1987).

Gataga

The Gataga area is directly east of the Northern Rocky Mountain Trench-Kechika strike-slip fault system (Gabrielse, 1985). Strata of Late Proterozoic through Mississippian age are exposed within a complex fold-thrust belt (McClay et al., 1988). The Late Proterozoic strata includes a thick sequence of slate, sandstone, and phyllite (Fig. 3c). A thick sequence of Lower-Middle Cambrian carbonates and sandstones is conformably overlain by the Cambro-Ordovician dolomite and phyllite of the Kechika Group. Ordovician through Lower Devonian Road River Group black shale, chert, and limestone rest conformably above the Kechika Group. The Earn Group, unconformably overlying the Kechika Group, is the uppermost unit. The base of the Earn Group is strongly folded and thrusted (McClay et al., 1988). As in other areas, the Earn Group at Gataga is a complex assemblage of turbiditic marine clastic sediments.

CONODONT BIOSTRATIGRAPHY

Prior to the use of conodonts, it was difficult to date the complex and rapidly changing stratigraphy of the Earn Group. Diagnostic macrofossils are rare due to the both the unfavourable depositional environment and the high

SERIES	STAGE	STANDARD CONODONT ZONATION (PELAGIC BIOFACIES)		DEFINITION OF LOWER LIMIT BY APPEARANCE OF:
UPPER DEVONIAN	FAMMENIAN	*praesulcata*	U	*Pr. kockeli*
			M	poorly defined
			L	*S. praesulcata*
		expansa	U	*B. ultimus*
			M	*B. aculeatus*
			L	*Pa.gracilis expansa*
		postera	U	*Pa. gracilis manca*
			L	*Pa. perlobata postera*
		trachytera	U	*Ps. granulosus*
			L	*Pa. rugosa trachytera*
		marginifera	Um	*Sc. velifer velifer*
			U	*Pa. marginifera utahensis*
			L	*Pa. m. marginifera*
		rhomboidea	U	*Pa. rhomboidea*
			L	*Pa. poolei*
		crepida	U	*Pa. glabra glabra*
			M	*Pa. termini*
			L	*Pa. crepida*
		triangularis	U	*Pa. tenuipunctata*
			M	*Pa. deicatula clarki*
			L	*Pa. triangularis*
	FRASNIAN	*linguiformis*		*Pa. linguiformis*
		gigas	U	*An. asymmetricus*
			L	*Pa. gigas*
		An. triangularis		*An. triangularis*
		asymmetricus	U	*A. curvata*
			M	*Pa. punctata*
			L	*A. rotundilobata*

Figure 4. Conodont zonations for the Upper Devonian Series, incorporating pelagic (basinal) biofacies. Based on Ziegler (1962), Ziegler and Sandberg (1984), and Sandberg et al. (1988). For *gigas* Zone read *rhenana* Zone (Klapper & Foster, 1988). Key to Genera; An. = *Ancyrognathus*, A. = *Ancyrodella*, B. = *Bispathodus*, Pa. = *Palmatolepis*, Pr. = *Protognathodus*, Ps. = *Pseudopolygnathus*, S. = *Siphonodella*, and Sc. = *Scaphignathus*.

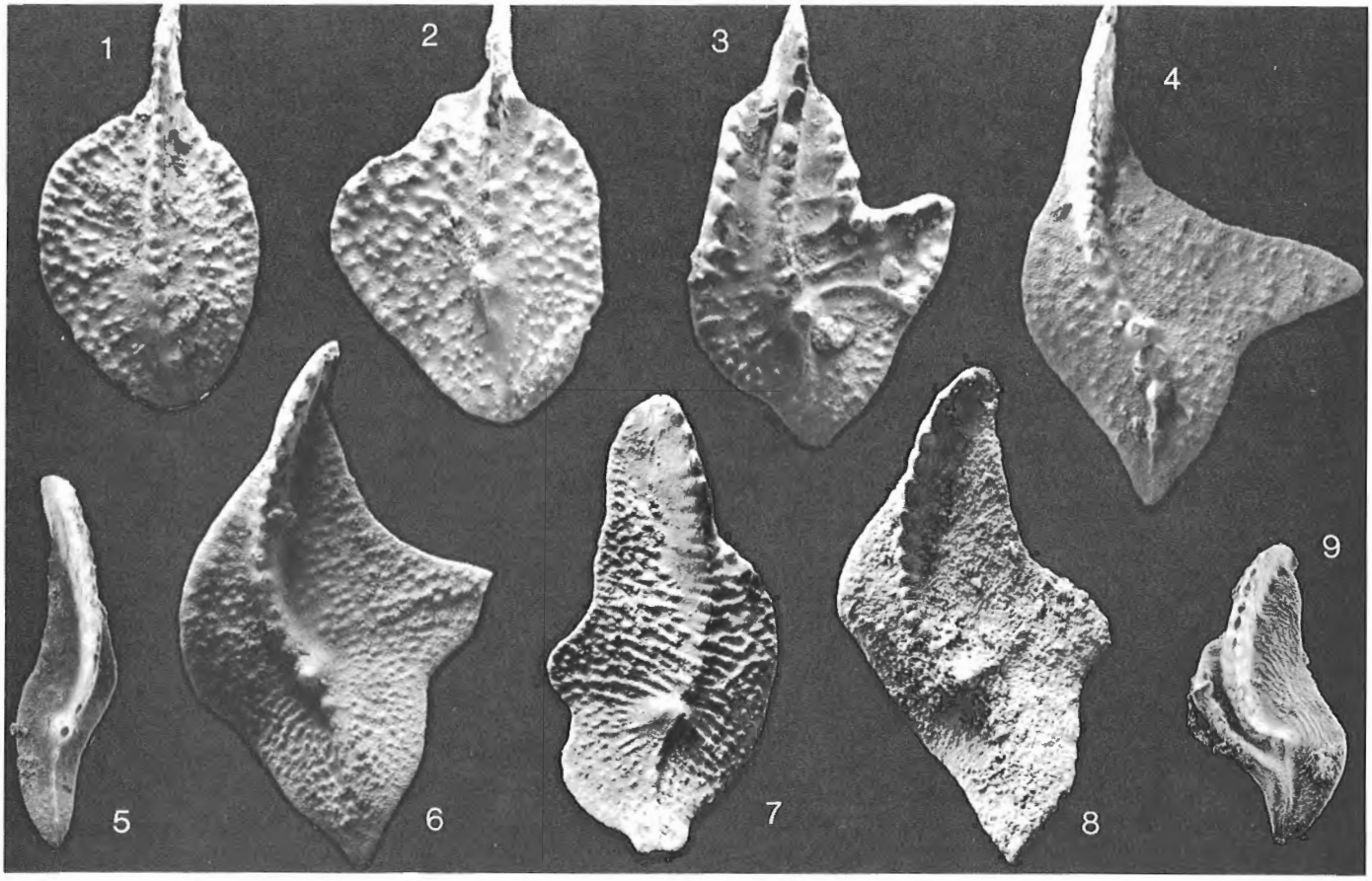

Table 1. Locality registry

GSC Loc. No. C-102891. Sample no. M81-032, Ware map area (94F/11), 57°40′32″, 125°03′33″. Limestone bed in section of black cherty argillites in Earn Group. Fauna includes *Palmatolepis punctata* (Hinde) and *Pa. transitans* Muller.

GSC Loc. No. C-102874. Sample no. M81-005, Ware map area (94F/10), 57°40′48″, 124°53′08″. Crinoidal limestone unit overlain by black cherty argillite and underlain by quartz wacke, Earn Group. Fauna includes *Polygnathus asymmetricus* Bischoff & Ziegler, *Po. dengleri* Bischoff & Ziegler, *Palmatolepis disparalvea* Orr & Klapper.

GSC Loc. No. C-118032. Sample no. 84-MJO-MM3, Niddery Lake map area (105O/8), 63°28′, 130°14′. Unit 3B above Tom outcrop, Earn Group. Fauna includes *Palmatolepis rhenana* Bischoff and *Ancyrognathus* sp.

GSC Loc. No. C-087558. Sample no. 81-GGA-36-A2, Sekwi Mountain map area (105P/12), 63°36.6′, 129°39.4′. Limy interval within bedded barite, Earn Group. Fauna includes *Palmatolepis surecta* Miller & Youngquist and *Ancyrodella* sp.

GSC Loc. No. C-108159. Sample no. 83-TOA-15-2, Niddery Lake map area (105O/1), 63°15.5′, 130°28.0′. Within silver weathering shale of the lower Earn Group. Fauna includes *Palmatolepis glabra pectinata* Ziegler, *Pa. g. distorta* Branson & Mehl, and *Pa. perlobata* Ulrich & Bassler.

GSC Loc. No. C-118892. Sample no. 85-OF-M70, Tuchodi Lakes map area (94K/4), 58°02.0′, 125°55.0′. Driftpile Creek, Mount Waldemar ridge, Earn Group. Fauna includes *Palmatolepis quadrantinodosalobata* Sannemann, *Pa. minuta* Branson & Mehl, *Pa. subperlobata* Branson & Mehl.

GSC Loc. No. C-087561. Sample no. GGA-81-31A-0m, Niddery Lake map area (105O/9), 63°38.4′, 130°02.8′. Shale unit near base of section J1, section 19, Earn Group. Fauna includes *Palmatolepis subperlobata* Branson & Mehl and *Pa.* cf. *Pa. minuta* Branson & Mehl.

Plate 1.
(Localities are described in Table 1).

Figure 1. *Polygnathus asymmetricus ovalis* Ziegler & Klapper. GSC 81212, x50. GSC Loc. No. C-102891.
Figure 2. *Palmatolepis disparilis* Ziegler, Klapper, & Johnson. GSC 81213, x45. GSC Loc. No. C-102874.
Figure 3. *Palmatolepis proversa* Ziegler. GSC 81214, x60. GSC Loc. No. C-118032.
Figure 4. *Palmatolepis rhenana* Bischoff. GSC 81215, x50. GSC Loc. No. C-087558.
Figure 5. *Palmatolepis glabra lepta* Ziegler & Huddle. GSC 81216, x60. GSC Loc. No. C-108159.
Figure 6. *Palmatolepis triangularis* Sannemann. GSC 81217, x 40. GSC Loc. No. C-118892.
Figure 7. *Palmatolepis crepida* Sannemann. GSC 81218, x40. GSC Loc. No. C-118892.
Figure 8. *Palmatolepis tenuipunctata* Sannemann. GSC 81219, x50. GSC Loc. No. C-087561.
Figure 9. *Palmatolepis marginifera marginifera* Helms. GSC 812120, x60. GSC Loc. No. C-108159.

regional metamorphic overprint. In contrast, 42 Frasnian conodont samples and 53 Famennian conodont samples are now known from the Earn Group. Over fifty different conodont species have been identified in the several thousand separate conodont elements collected. Precise time constraints are possible through the application of the standard Upper Devonian conodont zonation (Fig. 4), developed by Ziegler (1962) and later modified by Ziegler and Sandberg (1984) and Sandberg et al. (1988).

Macmillan Pass

Conodont species of early Frasnian to middle Famennian age have been collected from the Earn Group at Macmillan Pass. They are all relatively well preserved and have C.A.I. values of about five. Frasnian fauna, associated with several Pb-Zn horizons (Fig. 3a), include the nominal conodont zonal indices of the *Polygnathus asymmetricus, Ancyrognathus triangularis*, the *Palmatolepis rhenana* (see Klapper and Foster, 1986, p. 1222) and the *Pa. triangularis* zones (Fig. 4). Middle to late Frasnian conodonts are also associated with the Pete, GHMS, and Jeff stratiform barite deposits at Macmillan Pass (Dawson and Orchard, 1982; Gordey et al., 1982; Orchard, in press). Fauna including the conodonts indicative of the early to middle Famennian *Pa. marginifera* Zone (Fig. 4) have been collected from the Earn Group above the main Pb-Zn horizons. Some of these fauna correlate with Fauna II (Orchard and Irwin, 1988) found at Midway and Gataga.

Midway

Early to middle Famennian conodont fauna (Fauna II, Orchard and Irwin, 1988), collected from siliceous pyritic Pb-Zn exhalative horizons within the basal Earn Group (Fig. 3b) at Midway, are dominated by subspecies of *Palmatolepis* ex. gr. *glabra* Ulrich & Bassler accompanied by *Pa. minuta* Branson & Mehl, *Pa. subperlobata* Branson & Mehl, *Pa.* cf. *Pa. regularis* Cooper, *Pa. quadrantinodosalobata* Sannemann, and *Pa. triangularis* Sannemann. This fauna represents the early to middle Famennian Upper *Pa. crepida* or *Pa. rhomboidea* zones (Fig. 4) Orchard and Irwin, 1988). The mineralized horizons at the Ewen and Perry barites, higher up in the Earn Group (Fig. 3b), contain early Mississippian conodonts dominated by *Siphonodella* Branson and Mehl (Fauna III, Orchard and Irwin, 1988). These early Mississippian conodonts correlate with those at the Tea barite deposit in the Yukon Territory (Dawson and Orchard, 1982).

Gataga

Conodonts of early Frasnian through middle Famennian age have been recognized at Gataga (Orchard, in McClay et al., 1988). Within the Earn Group at Gataga, key index species for the Frasnian *Polygnathus asymmetricus* zone include the nominal species, as well as *Palmatolepis transitans* Muller and *Pa. disparalvea* Orr & Klapper; in addition, *Pa. subrecta* Miller & Youngquist, *Pa. punctata* (Hinde), and *Pa. proversa* Ziegler have also been collected. In drillcore, middle Famennian conodonts representing the *Pa. marginifera* Zone (Fig. 4), are found about 60 m below the lowest stratiform barite-Fe-Zn-Pb horizon (Fig. 3c; UH after McClay and Insley, 1986) and from both above and below a second barite-Fe-Zn-Pb horizon (Fig. 3c; TH1). Early and middle Famennian conodont fauna including the zonal indicators *Pa. triangularis* and *Pa. crepida* have been collected at Gataga. Some conodonts recognized in Fauna II (Orchard and Irwin, 1988) also occur at Gataga. Conodonts have not yet been found above the highest mineralized horizon (Fig. 3c; TH2).

CONCLUSIONS

1) Stratiform Pb-Zn-Ag deposits at Macmillan Pass are Frasnian in age. Middle Famennian conodonts occur well above the stratiform mineral deposits.

2) Siliceous pyritic Pb-Zn horizons at Midway are early to middle Famennian, indicating a younger mineralization event than at Macmillan Pass.

3) Gataga stratiform barite-Fe-Zn-Pb horizons are bracketed with Famennian conodonts. Frasnian conodonts have been collected only from below the mineralized horizons.

4) Mississippian stratiform barite deposits are recognized at Midway and Macmillan Pass.

5) Fauna representing the nominal conodont zonal indices of the *Polygnathus asymmetricus, Ancyrognathus triangularis, Palmatolepis rhenana, Pa. triangularis, Pa. crepida*, and *Pa. marginifera* zones are recognized within the Earn Group.

In summary, events that produced stratiform mineral deposits in different areas of the Cordillera are not coeval, but are developed at different levels within the Earn Group. Stratiform mineralizing events may be synchronous locally, but conodont dating suggests Late Devonian events in the north preceded those to the south. This may reflect the southward progression of a single tectonic event, or more than one geographically and temporally separated event.

ACKNOWLEDGMENTS

This project is partly supported by a Canada/British Columbia Mineral Development Agreement grant from the British Columbia Ministry of Energy, Mines and Petroleum Resources, and by an NSERC operating grant, no. 581450. The authors wish to thank the many geologists who have collected Earn Group conodont samples including J.G. Abbott, K.M. Dawson, S.P. Gordey, M.W. Insley, W. Jakubowski, K.R. McClay, D. MacIntyre, and J. Nelson.

REFERENCES

Abbott, J.G.
1982: Structure and stratigraphy of the Macmillan Fold Belt: evidence for Devonian faulting; *in* Yukon Geology and Exploration 1981, Department of Indian Affairs and Northern Development (Canada), Open File Report, 16 p.

Abbott, J.G., Gordey, S.P., and Tempelman-Kluit, D.J.
1986: Setting of stratiform, sediment-hosted lead-zinc deposits in Yukon and northeastern British Columbia; *in* Mineral Deposits of Northern Canadian Cordillera, edited by J.A. Morin, Canadian Institute of Mining and Metallurgy, Special Volume 37, p. 1-18.

Dawson, K.M. and Orchard, M.J.
1982: Regional metallogeny of the northern Cordillera: biostratigraphy, correlation and metallogenic significance of bedded barite occurrences in eastern Yukon and western District of Mackenzie; *in* Current Research, Part C, Geological Survey of Canada, Paper 82-1C, p. 31-38.

Gabrielse, H.
1985: Major dextral displacements along Northern Rocky Mountain Trench and related lineaments in north-central British Columbia; Geological Society of America Bulletin, v. 96, p. 1-14.

Gordey, S.P., Abbott, J.G., and Orchard, M.J.
1982: Devono-Mississippian (Earn Group) and younger strata in east-central Yukon; *in* Current Research, Part B, Geological Survey of Canada, Paper 82-1B, p. 93-100.

Gordey, S.P., Abbott, J.G., Tempelman-Kluit, D.J., and Gabrielse, H.
1987: "Antler" clastics in the Canadian Cordillera; Geology, v. 15, p. 103-107.

Klapper, G.R. and Foster, C.T., Jr.
1986: Quantification of outlines in Frasnian (Upper Devonian) platform conodonts, Canadian Journal of Earth Sciences, v. 23, p. 1214-1222.

McClay, K.R. and Bidwell, G.E.
1986: Geology of the Tom deposit, Macmillan Pass, Yukon; *in* Mineral Deposits of Northern Canadian Cordillera, edited by J.A. Morin, Canadian Institute of Mining and Metallurgy, Special Volume 37, p. 100-114.

McClay, K.R. and Insley, M.W.
1986: Structure and stratigraphy of the Gataga fold and thrust belt, northeastern British Columbia; *in* Current Research, Part A, Geological Survey of Canada, Paper 86-1A, p. 259-264.

McClay, K.R., Insley, M.W., Way, N.A., and Anderton, R.
1988: Tectonics and mineralization of the Kechika Trough, Gataga area, northeastern British Columbia; *in* Current Research, Part E, Geological Survey of Canada, Paper 88-1E, p. 1-12.

Nelson, J. and Bradford, J.
1987: Geology of the area around the Midway deposit, northern British Columbia (104O/16); *in* Geological Fieldwork 1986, British Columbia Ministry of Energy, Mines and Petroleum Resources, Paper 1987-1, p. 181-192.

Orchard, M.J.
— Conodonts from the Frasnian-Famennian boundary interval in western Canada; *in* Devonian of the World, Proceedings of the Second International Symposium on the Devonian System, edited by N.J. Macmillan et al., Canadian Society of Petroleum Geologists, Memoir 14. (in press).

Orchard, M.J. and Irwin, S.E.B.
1988: Conodont biostratigraphy, Midway property, northern British Columbia; *in* Geological Fieldwork 1986, British Columbia Ministry of Energy, Mines and Petroleum Resources, Paper 1987-1, p. 249-253.

Sandberg, C.A., Ziegler, W., Dreesen, R., and Butler, J.L.
1988: Late Frasnian mass extinction: conodont event stratigraphy, global changes, and possible causes; *in* 1st International Senckenberg Conference and 5th European Conodont Symposium (ECOS V) Contributions 1, edited by W. Ziegler, Courier Forschungsinstitut Senckenberg 102, p. 263-307.

Wheeler, J.O. and McFeely, P.
1987: Tectonic assemblage map of the Canadian Cordillera and adjacent parts of the United States of America; Geological Survey of Canada, Open File 1565.

Ziegler, W.
1962: Taxionomie und Phylogenie Oberdevonischer Conodonten und ihre stratigraphische Bedeutung; Hessisches Landesamt Bodenforschung, Abhandlungen 38, 166 p.

Ziegler, W. and Sandberg, C.A.
1984: Palmatolepis-based revision of upper part of standard Late Devonian conodont zonation; *in* Conodont Biofacies and Provincialism, edited by D.L. Clark, Geological Society of America, Special Paper 196, p. 179-194.

Isotopic geochemistry of the Jason stratiform sediment-hosted zinc-lead deposit, Macmillan Pass, Yukon

Robert J.W. Turner, Wayne D. Goodfellow[1], and Bruce E. Taylor[1]
Cordilleran and Pacific Geoscience Division, Vancouver

Turner, R.J.W., Goodfellow, W.D., and Taylor, B.E., Isotopic geochemistry of the Jason stratiform sediment-hosted zinc-lead deposit, Macmillan Pass, Yukon; in Current Research, Part E, Geological Survey of Canada, Paper 89-1E, p. 21-30, 1989.

Abstract

A fossil seafloor hydrothermal vent complex partially replaces widespread laminated barite, chert and Zn-Pb sulphides at the Jason deposit. Study of the sulphur, carbon, oxygen, hydrogen and strontium isotope geochemistry of this fossil exhalative system is in progress to address (1) the source of reduced sulphur; (2) the sources and mixing sites of the hydrothermal fluids; and (3) the genetic relationship between extensive ferroan carbonate alteration and stratiform Zn-Pb ores.

Résumé

Un complexe fossile de cheminées hydrothermales formées sur le fond marin remplace partiellement dans le gisement de Jason de grandes étendues de barytine, de chert et de sulfures de Zn et Pb à structure rubanée. Les études en cours portent sur la géochimie du soufre, du carbone, de l'oxygène, de l'hydrogène et des isotopes du strontium dans ce système exhalatif fossile pour examiner 1) la source du soufre réduit; 2) les sources et les lieux de mélange des fluides hydrothermaux, et; 3) la relation génétique existant entre l'altération à grande échelle des carbonates ferreux et la présence de minerais stratiformes de Zn et Pb.

[1] Mineral Resources Division, Ottawa.

INTRODUCTION

The Jason deposits at Macmillan Pass, Yukon provide an opportunity to study a fossil sub-seafloor hydrothermal vent complex and associated laminated barite, sulphide, and chert (Turner, 1986). Vent complexes are not commonly associated with sediment-hosted stratiform Zn-Pb deposits; study of the vent system at Jason gives insights into the character of the metal-bearing hydrothermal fluids prior to and during mixing with seawater. This paper describes the geological and isotopic data that are the basis for the current stable isotope (S, C, O, and H) and strontium isotope study of this fossil submarine exhalative system. This study will address: (1) the source of the reduced sulphur; (2) the sources and mixing sites of the hydrothermal fluids; and (3) the genetic relationship between extensive ferroan carbonate alteration and stratiform Zn-Pb ores. The following discussion of the geological setting is based on Turner (1986) and more recent field studies by Turner in June-July 1988, except where otherwise noted.

GEOLOGICAL SETTING OF THE JASON DEPOSIT

The Jason deposits are located in the eastern Yukon near Macmillan Pass close to the border with the Northwest Territories. The Jason deposits belong to a group of stratiform zinc-lead and stratiform barite deposits which occur in carbonaceous shales and cherts of the Middle to Upper Devonian Lower Earn Group in the Macmillan Pass Area (Fig. 1). The Jason South/Main zone, Jason End zone, and Tom East/West zone stratiform Zn-Pb deposits, and the Nidd conglomerate-hosted Fe-Zn prospect occur adjacent to synsedimentary faults within a proposed pull-apart basin of Late Devonian age (Fig. 1). Minor mafic volcanic rocks are associated with the Nidd prospect. The pull-apart basin is bounded by northeast-trending normal faults, and by northwest-trending normal and strike-slip faults interpreted to have been active during the Devonian; strike-slip faults were first recognized by Abbott (1982). Devonian age stratiform barite deposits occur peripheral to the pull-apart basin.

The Lower Earn Group was subdivided by Carne (1979) into a lower silty argillite (unit 1), a chert pebble conglomerate (unit 2), a siltstone (unit 3A) and an uppermost carbonaceous chert (unit 3B) (Fig. 2). The Jason and Tom deposits occur near the transition from unit 3A to unit 3B. At the Jason deposit a thick sequence of sedimentary breccias, referred to here as unit 3C, occurs at this transition (Fig. 2).

The Jason South/Main stratiform Zn-Pb deposit (hereafter referred to as the "Jason deposit") occurs on both the southern (South zone) and northern (Main zone) limbs of a faulted, southeast plunging syncline (Fig. 3, 4). Within the syncline, conglomerate and sandstone of unit 2 are overlain successively by siltstone (unit 3A) and by sedimentary breccias interbedded with carbonaceous siliceous shale and siltstone (unit 3C) (Fig. 4). Breccias are composed of clasts of units 1, 2 and 3A. There are two stratiform sulphide horizons: an upper horizon, up to 25 m thick, which is interbedded with siliceous shale and sedimentary breccier (B unit 3C), and a lower horizon up to 55 m thick, which is interbedded with thinbedded siltstone at the top of unit 3A. Both sulphide horizons terminate up-dip against the Jason fault on the south side of the syncline. The Jason fault juxtaposes strata of the Silurian to Lower Devonian Road River Group, and basal Lower Earn Group against younger Lower Earn Group strata (units 2 to 3B). The indurated and mineralized nature of the Jason fault is distinct from other local faults. Isopachs of the sedimentary breccia beds within unit 3C are lobe like in plan, and trend at high angle to the Jason fault. The breccia beds thin away from the Jason fault.

CHARACTER OF THE JASON DEPOSIT

Two distinct ore types occur within the Jason deposit: (1) veined and massive iron carbonate-sulphide adjacent to the Jason fault that grades outwards into (2) widespread finely laminated barite, sulphide, and chert. The distal laminated mineralization is divided into facies based on mineralogy (Fig. 5). Proximal massive ores are divided into facies based on the mineralogy of the massive or "bedded" component of the ores, but this may be overprinted by later discordant mineralization.

The barite-sulphide facies comprise a large bulk of the Jason deposit and is composed of monomineralic, millimetre-scale laminae of barite, chert, sphalerite or galena, or bi-minerallic laminae of sphalerite+chert, sphalerite+galena, and barite+galena. Farther from the Jason fault fine laminae of pyrite and sphalerite are interbedded with carbonaceous chert (quartz-sulphide facies). Toward the Jason fault, laminae of the barite-sulphide facies are interbedded with massive beds of sphalerite+galena, or galena+pyrite (Pb-Zn-Fe sulphide facies). Locally, erosional scour textures occur within the Pb-Zn-Fe facies and the barite-sulphide facies; sedimentary breccias locally include clasts of stratiform mineralization.

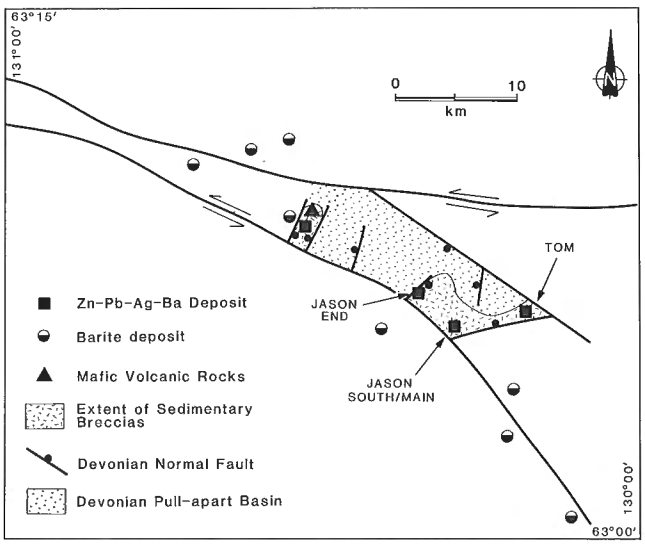

Figure 1. Distribution of Late Devonian age faults, sedimentary breccias, stratiform Zn-Pb-Ba deposits and stratiform barite deposits in the Macmillan Pass area (from Turner, 1988).

Adjacent to the Jason fault, massive pyrite (pyrite facies) is interbedded with beds of sphalerite-galena. The pyrite facies is in abrupt contact with overlying, but unaltered sedimentary breccias (Fig. 5). The massive pyrite locally displays fine grained collimorphic textures, pseudomorphic after barite, and is cut by quartz-sulphide veinlets. Within the lower horizon near the breccia pipe, irregular bands, veins and massive bodies of pyrite overprint bedded pyrite.

Iron carbonate facies rocks comprise much of the upper and lower horizons near the Jason fault (Fig. 5). In the lower horizon, siltstone strata are progressively replaced by (1) quartz and muscovite; (2) siderite; (3) pyrrhotite; and (4) ankerite-galena (Fig. 6).

A breccia pipe cuts the lower horizon and extends from the Jason fault to the sedimentary breccias overlying unit 3A (Fig. 5). This breccia is composed of angular fragments of silicified siltstone in a variable matrix of siderite, ankerite, muscovite, pyrrhotite, quartz, galena, and pyrite. The mineral paragenesis in the breccia is similar to that found in the proximal iron carbonate facies. Where the breccia body cuts bedded pyrite of the pyrite facies, pyrrhotite has replaced pyrite.

Overlying the breccia body are sedimentary breccias which are cut by patchy veinlets of ferroan carbonate and pyrrhotite (Fig. 5). Above this is the iron carbonate facies of the upper horizon, massive, mottled and veined rock composed of a complex assemblage of ankerite, galena, pyrite, pyrrhotite, quartz with minor fragments of silicified siltstone. On the fringe of the iron carbonate facies, barite-sulphide facies are silicified and replaced by banded and massive ankerite.

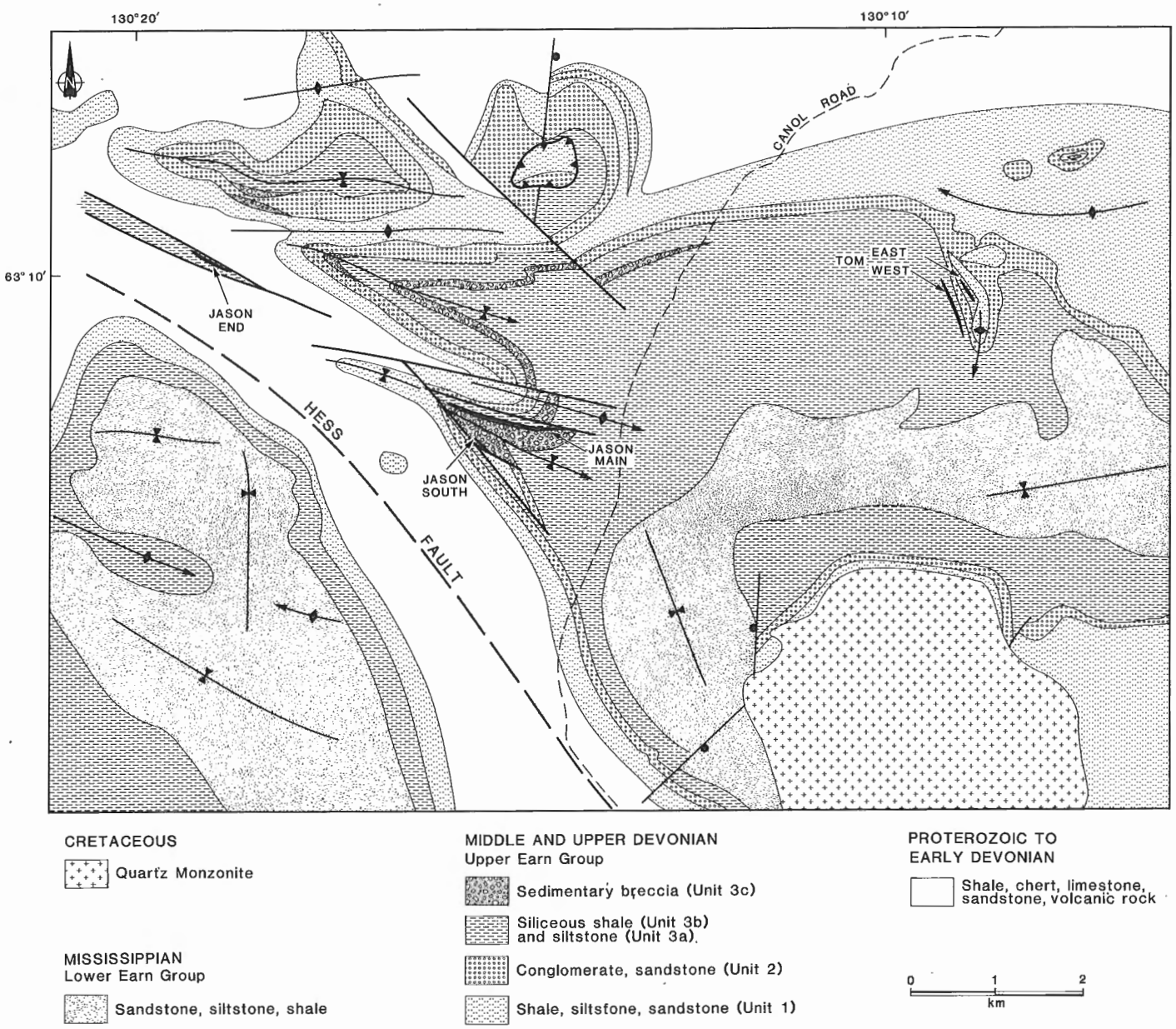

Figure 2. Bedrock geological map of the Jason deposit area (modified after Abbott, 1983; McClay and Bidwell, 1986).

DISCUSSION ON THE CHARACTER OF THE JASON DEPOSIT

The occurrence of sedimentary breccias interbedded within, and overlying, the stratiform deposit indicates movement on the Jason fault coincided with the hydrothermal activity that formed the Jason deposit (Fig. 5). Resedimentation and scour textures, and graded sulphide laminae are evidence of subaqueous sulphide sedimentation. The wedge-shaped, cross-sectional profile of the deposit likely reflects hydrothermal deposition within a bathymetric low adjacent to the Jason fault scarp.

The massive and veined proximal mineralization represents subsurface processes related to replacement of previously mineralized rocks in the upflow zone of the hydrothermal system (Fig. 8). The ferroan carbonate replacement of stratiform mineralization, quartzose siltstone and illitic mudstone reflects CO_2-rich fluids. Brecciation and ferroan carbonate precipitation followed earlier silicification of the sediments, perhaps reflecting rupture of a silicified cap coincident with CO_2 effervescence in the hydrothermal fluids. Extensive replacement of early siderite and pyrite by pyrrhotite may indicate evolution of the hydrothermal fluids to lower $^{f}S_2$ and/or $^{f}O_2$. Whether this sulphur was derived from reaction with earlier-formed stratiform sulphides or sulphates, or introduced with the hydrothermal fluids remains to be determined. It is important to note, however, that the vent complex is almost exclusively developed within the earlier-formed stratiform mineralization.

Early-formed alteration was both pervasive (e.g. silicification) and bedding controlled (e.g. siderite), superposed alteration (e.g. ankerite-galena) replaced early bedding-controlled alteration and developed along fractures during progressive induration of the sediments. Massive pyrite formed by in situ precipitation from rising fluids, and replaced sediments immediately below the seafloor (Fig. 8). Massive galena and sphalerite beds represent sulphide sedimentation or resedimentation adjacent to the vent. Resedimentation of this galena-sphalerite sediment suggests the vent area was a positive bathymetric feature on the seafloor.

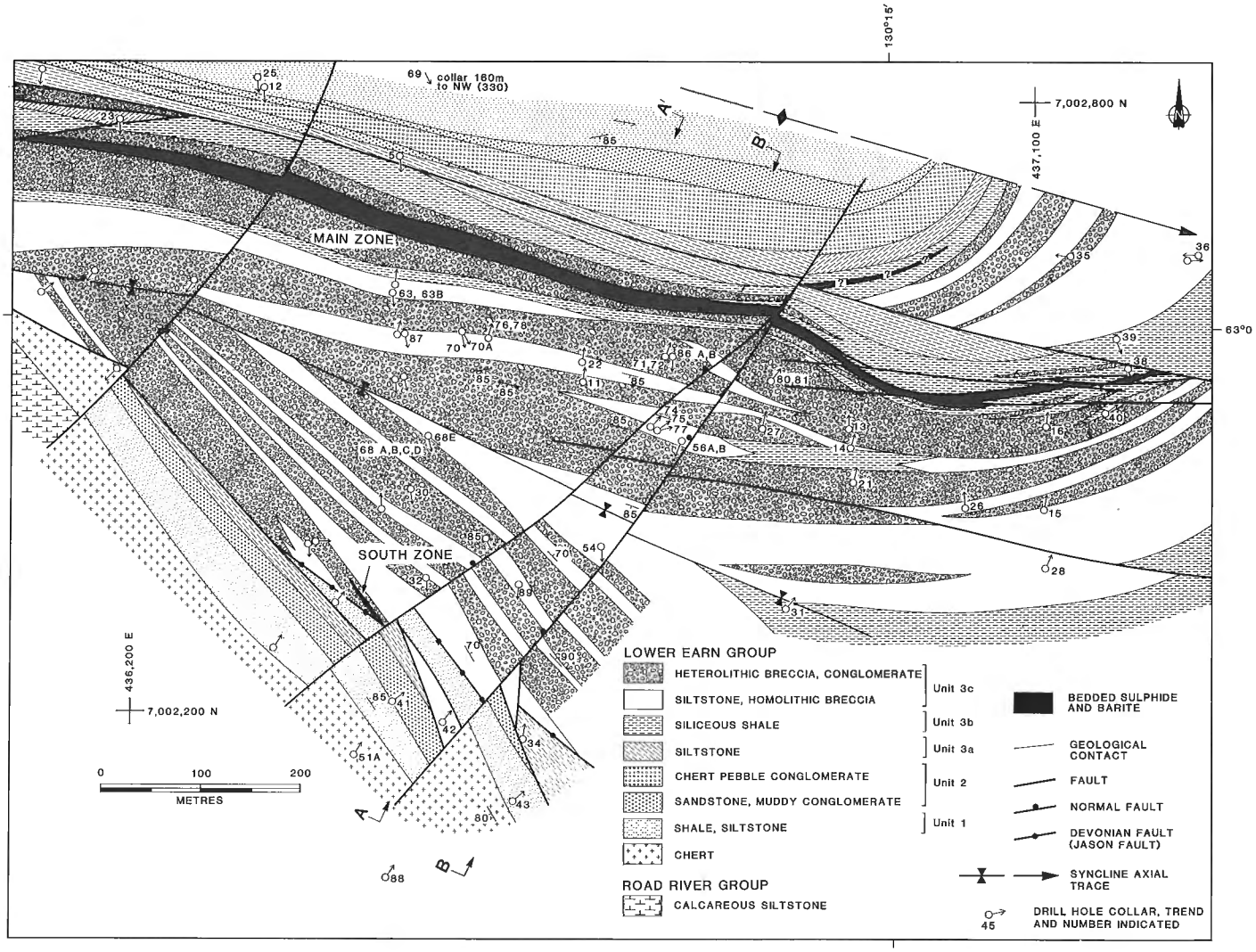

Figure 3. Bedrock geological map of the Jason South/Main deposit area.

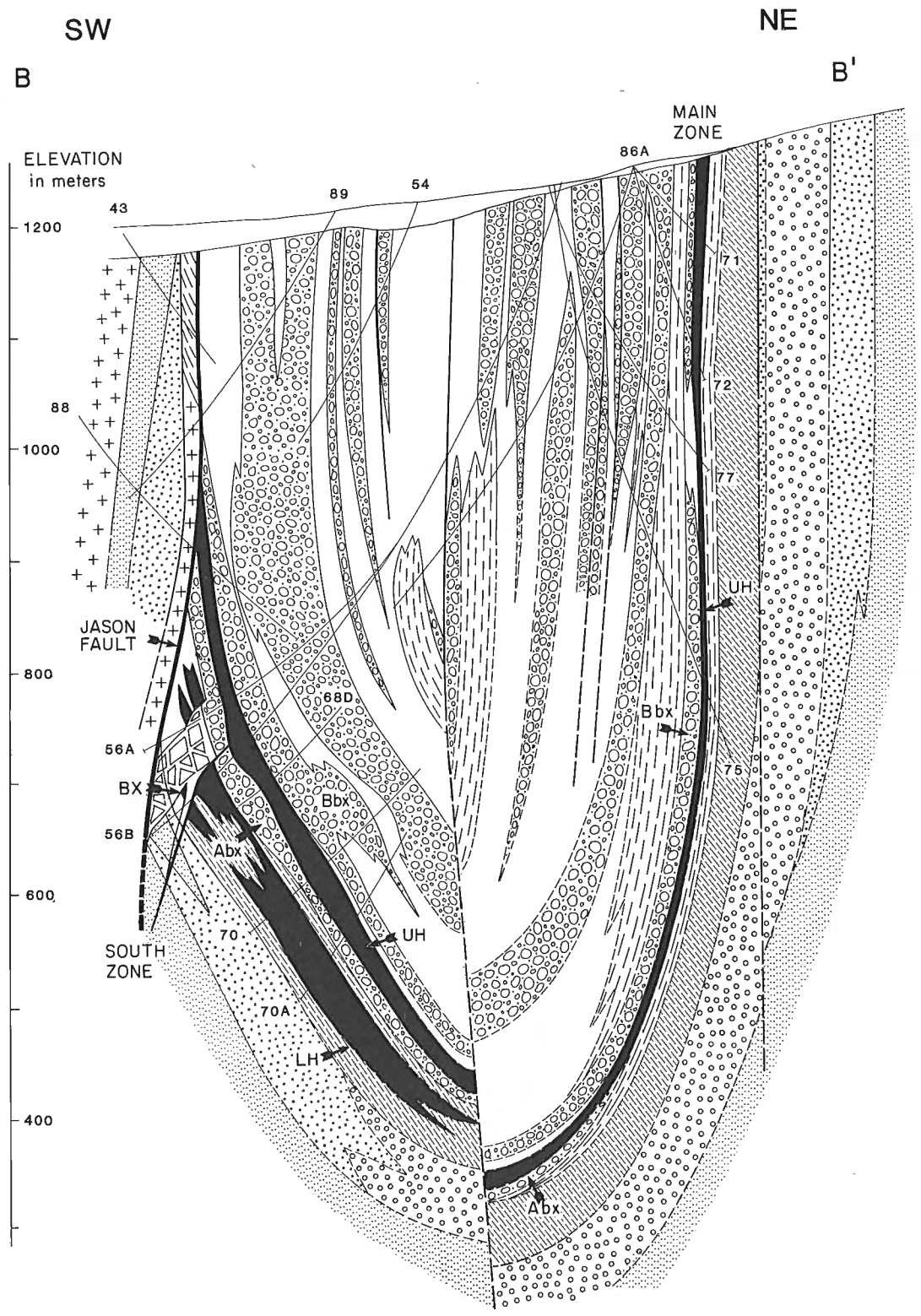

Figure 4. Geological cross-section B-B'' looking west across the South and Main zones. Several features are indicated: upper horizon (UH), lower horizon (LH) and individual sedimentary breccia units (Abx, Bbx) (modified after Turner, 1986). Refer to Figure 3 for legend.

STABLE AND STRONTIUM ISOTOPE STUDIES

A comprehensive sulphur, carbon, oxygen, hydrogen and strontium isotope study of sulphide, barite, carbonate, quartz, and muscovite minerals, and inclusion fluids, from the Jason deposit is currently in progress. Samples were selected that formed in different parts of the deposit and at different times. Analysis of carbonate-sulphide-silicate and sulphate-sulphide-silicate associations will allow for the comparison of carbon, sulphur, oxygen and strontium isotope trends. Several questions critical to understanding the genesis of the Jason deposit in particular, and stratiform sediment-hosted deposits in general, will be addressed: (1) what were the primary sources of carbon and reduced sulphur; (2) what was the origin of water in the hydrothermal fluids; (3) how did the hydrothermal fluids evolve and mix with seawater; and (4) what is the genetic relationship between local and widespread ferroan carbonate alteration and the stratiform base-metal deposits.

Isotopic analyses are reported relative to the following standards: ^{13}C, PDB; ^{34}S, CDT.

Source of sulphur

Ohmoto et al. (in press) proposed that the source of sulphur in stratiform sediment-hosted deposits is a reduced, sulphur- and metal-bearing brine. In constrast, Goodfellow and Jonasson (1984) and Goodfellow (1987) suggested stratiform sulphide deposition in the Selwyn Basin by reaction between a sulphur-poor but metal-bearing brine and H_2S in anoxic bottom waters.

Gardner and Hutcheon (1985) reported a range of $\partial^{34}S$ for 22 sulphide samples from the Jason deposit of 8.5 to 17.7, samples from the vent complex (their "Facies A") comprise a greater range (8.5 to 17.7) than for distal stratiform sulphides (10.2 to 15.6; their "Facies C"). Vent sulphides tend to have higher $\partial^{34}S$ than laminated sulphides.

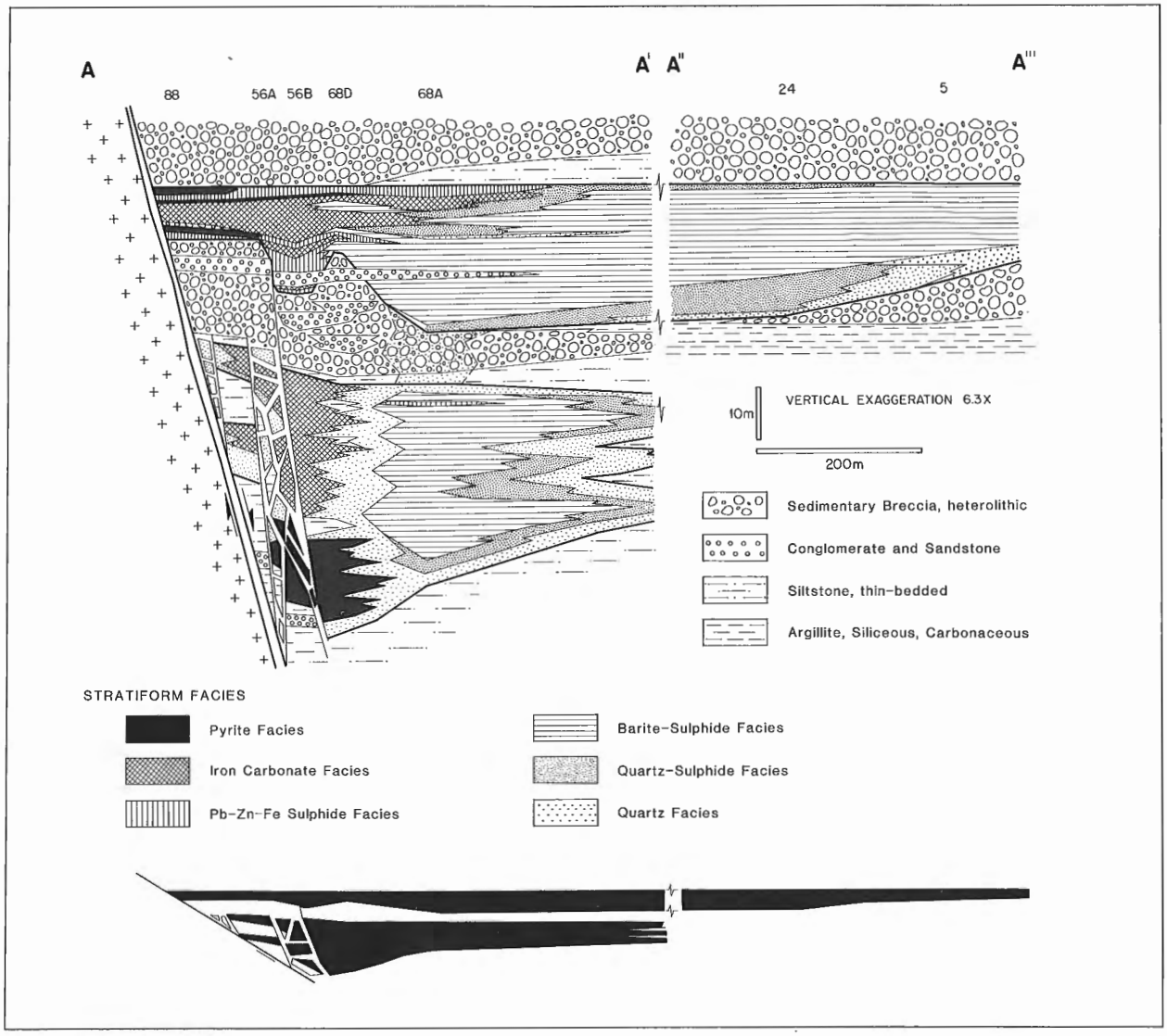

Figure 5. Restored stratigraphic cross-section A-A' across the trend of the Jason fault illustrating distribution of internal facies within the stratiform deposits. Heavy black line encloses hydrothermal facies. Upper section has 6.3X vertical exaggeration; true scale cross-section shown in solid black.

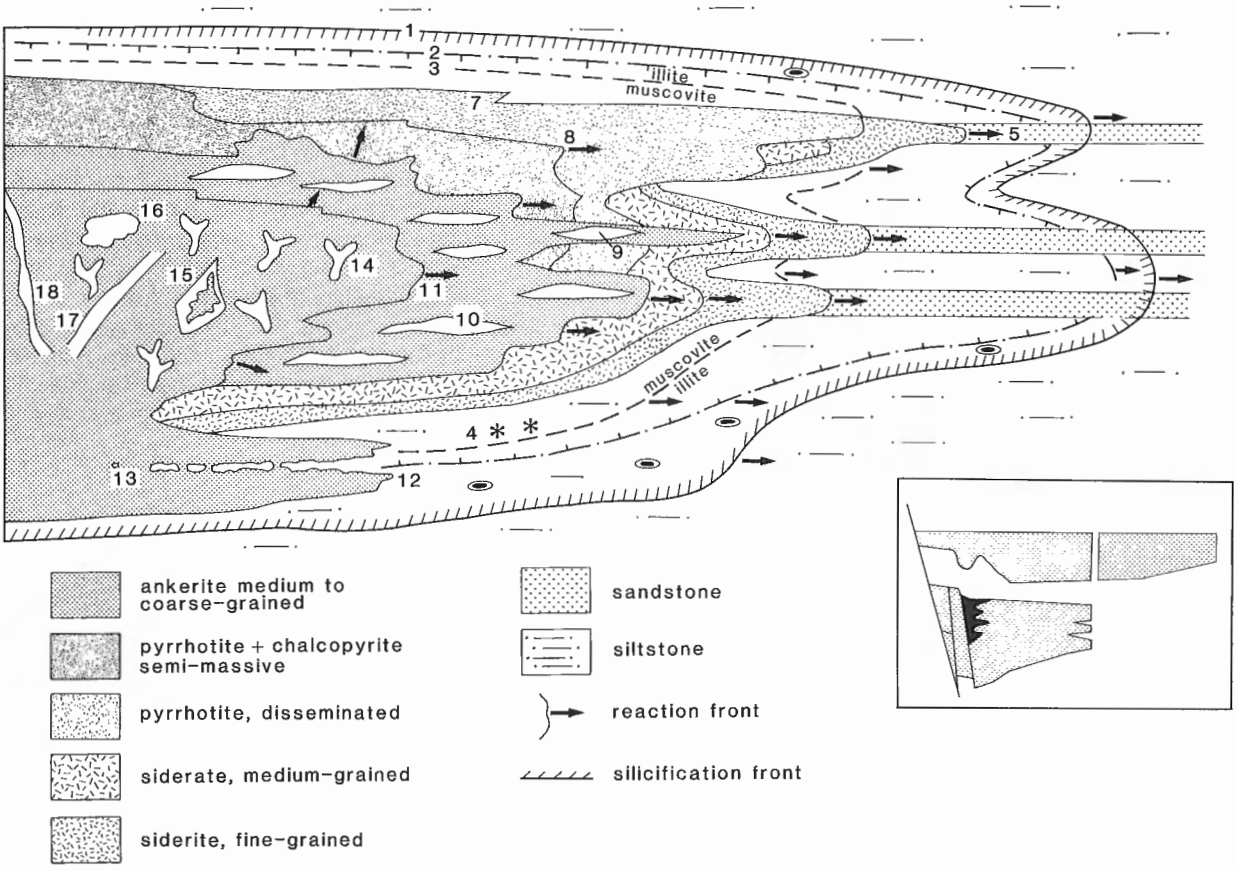

Figure 6. Schematic diagram of mineral relationships within the iron carbonate facies of the lower horizon adjacent to the breccia body as indicated in inset diagram. Numbers on figure refer to specific relationships: (1) extent of silicification; (2) extent of destruction of organic matter; (3) extent of muscovite replacement of illite; (4) coarse grained muscovite rosettes; (5) replacement of sandstone laminae by fine grained siderite; (6) extent of medium grained siderite; (7) replacement of siderite by disseminated pyrrhotite; (8) replacement of siderite by semi-massive pyrrhotite and minor chalcopyrite; (9) bedding parallel ankerite-quartz-galena veins; (10) amalgamation of parallel ankerite-quartz-galena veins; (11) extent of massive ankerite-galena; (12) replacement of siltstone by ankerite; (13) corroded fragments of siltstone in ankerite matrix; (13) galena "lace" interstitial to ankerite; (14) irregular ankerite veins and pods; (15) ankerite-quartz-galena-pyrobitumen pod; (16) quartz nodule; (17) ankerite-galena-quartz-muscovite vein; and (18) pyrrhotite-pyrite-muscovite vein.

For example, $\partial^{34}S$ of pyrrhotite (13.5, 16.0, 17.4, 17.7) and galena (8.5, 9.9, 14.7, 13.8, 14.7, 15.0, 17.0) from the vent complex, and sphalerite (20.0, 22.5) and galena (17.7, 22.5) in proximal, replacement-type ores in the End Zone are greater than sphalerite (10.2, 11.0, 14.5), and galena (11.2, 11.9, 12.0) in the laminated sulphides. Other sulphur isotope analyses of laminated sulphides at Jason also have lower $\partial^{34}S$. Nine sphalerite-galena concentrates have low $\partial^{34}S$ values (4.0 to 14.5; Turner, unpublished data). Although the number of samples is small and therefore may not be representative of the entire deposit, inspection of these data suggest that sulphides in the vent complex have higher $\partial^{34}S$ than sulphides in the laminated ores. The heavier sulphur in the vent complex may reflect introduction of heavy hydrothermal sulphur; it may also represent high temperature inorganic reduction of sulphate in laminated barite during replacement.

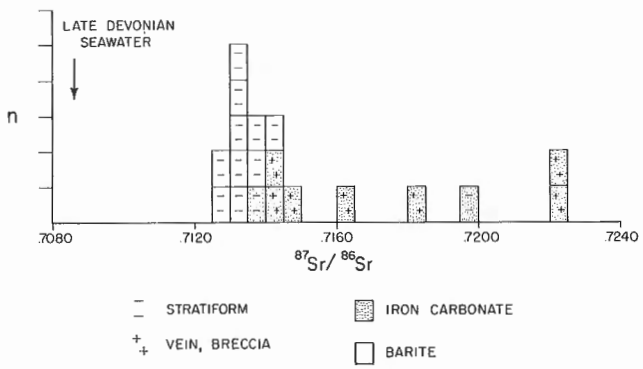

Figure 7. Histogram of $^{87}Sr/^{86}Sr$ ratios for ferroan carbonate and barite samples; strontium isotope composition for Late Devonian age seawater from Burke et al. (1982).

Analyses of delta $\partial^{34}S$ of laminated and disseminated pyrite in carbonaceous siliceous shale of the upper part of unit 3B near the Jason deposit range from 22 to 34‰ (Goodfellow and Jonasson, 1984). Goodfellow and Jonasson (1984) and Goodfellow (1987) determined the sulphur isotopic composition of the ambient water column sulphate based on sedimentary pyrite; diagenetic pyrite was also used to reflect water column sulphate based on evidence in modern starved sedimentary environments where rapid exchange of sulphate occurs between pore fluids and the overlying water column. Determination of the isotopic composition of sulphate in seawater, contemporaneous with formation of the Jason deposit, requires sampling sedimentary and diagenetic pyrite stratigraphically equivalent to the stratiform deposit. It is unclear if any of the pyrite sampled by Goodfellow and Jonasson (1984) are stratigraphically equivalent to the Jason deposit. Their data suggest rapid variation in $\partial^{34}S/^{32}S$ ratio of basin waters during the Late Devonian.

Exhalative environment: brine pool or bouyant plume

Two end-member hydrothermal exhalative environments occur within the modern ocean: (i) mixing with seawater, i.e. hydrothermal precipitation from a buoyant plume discharged into ambient seawater (e.g. East Pacific Rise) and (ii) mixing with a brine pool, i.e. hydrothermal precipitation within a brine pool ponded on the seabottom (e.g. Atlantis II deep, Red Sea). Studies of modern hydrothermal exhalative environments suggests that strontium isotopes are an important tool for deciphering the exhalative environment of fossil deposits. For example, Sr isotopic values for anhydrite in the presently active Atlantis II deep brine pool, Red

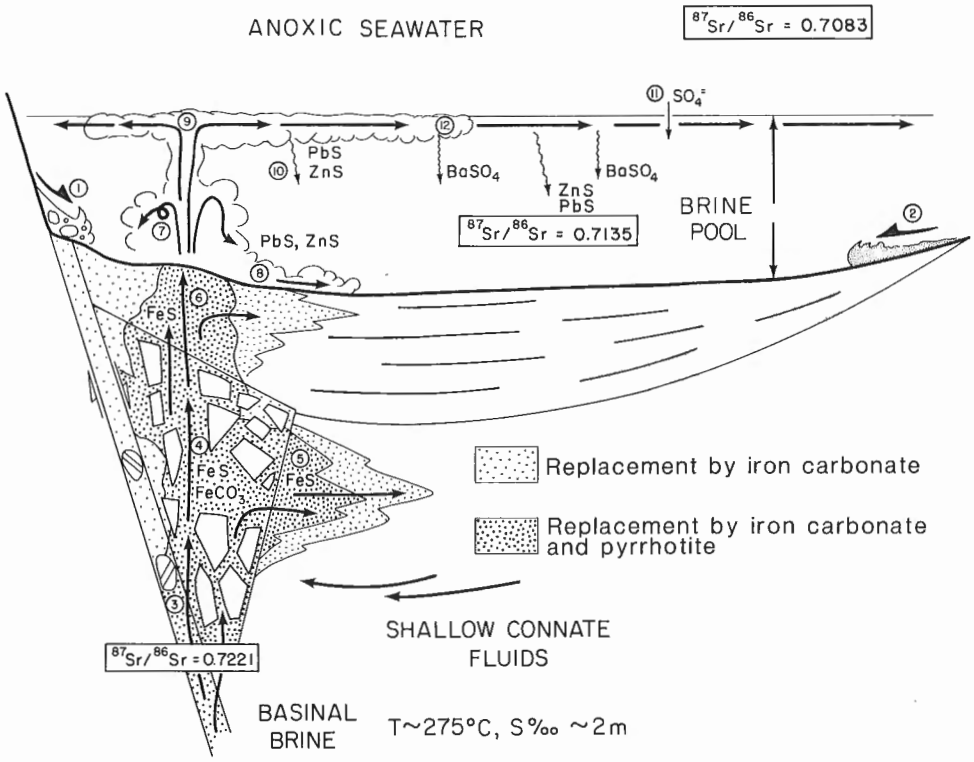

Figure 8. Interpretive cross-section of hydrothermal vent and brine pool environment illustrating processes active during formation of the Jason deposit: (1) debris flow from active fault scarp; (2) chert-silt turbidity flow; (3) upflow of reduced metal-rich hydrothermal fluid (T = 275°C, 2m NaCl equivalent; Gardner and Hutcheon, 1985); (4) brecciation of indurated silicified silts and muds, precipitation of ferroan carbonate and muscovite; (5) lateral infiltration of hydrothermal sediments by hydrothermal fluids causing silicification, alteration of illite to muscovite, and progressive replacement by siderite and pyrrhotite; (6) replacement of early formed laminated hydrothermal sediments of barite, silica and zinc and lead sulphide by banded to massive and veined ferroan carbonate, pyrrhotite, galena and pyrite; (7) venting of hydrothermal fluids; rapid sedimentation of sphalerite and galena creating a vent mound; (8) resedimentation of sulphides from vent mound; (9) entrainment of sulphide particles in bouyant hydrothermal plume to top of brine pool; (10) sedimentation of entrained sulphide during lateral spread of plume along brine interface; segregation of mineral particulate due to differental settling rates; (11) diffusion of seawater sulphate into brine pool; (12) precipitation of barite from mixing of brine pool sulphate and barium in hydrothermal fluid.

Sea (Zierenberg and Shanks, in press), show a distinct shift from ambient seawater values, whereas sulphates forming in bouyant plume vent sites along ocean ridges display values that range from those of basaltic crust to coeval seawater (Albarede et al., 1981).

A reconnaissance suite of 10 carbonate and 9 barite samples from the Jason deposit indicates a range of $^{87}Sr/^{86}Sr$ ratio from 0.7129 to 0.7144 in barite and 0.7137 to 0.7221 in carbonates (Fig. 7). Detectable rubidium occurred in only one barite sample. High Rb/(Rb+Sr) ratios (0.38 and 0.55) were measured for 2 carbonates which had high $^{87}Sr/^{86}Sr$ ratios (i.e. 0.7196 and 0.7221), perhaps suggesting some contamination of those two samples by radiogenic strontium. Barite samples, regardless of stratigraphic position within the stratiform bodies, have a narrow range of strontium isotope ratios, ($^{87}Sr/^{86}Sr$ = 0.7126-0.7144), which is distinctly higher than for Late Devonian seawater ($^{87}Sr/^{86}Sr$ = 0.7083; Burke et al., 1982). Analogous to the Atlantis II deep, these data suggest that barite precipitated from a stable brine, in this case ponded adjacent to the Jason fault. A plot of $^{87}Sr/^{86}Sr$ versus 1/Sr for barite form a linear trend suggesting mixing of a more radiogenic, strontium-rich hydrothermal fluid with less radiogenic, strontium-poor seawater.

Subsurface mixing

Strontium isotopic ratios of the eight carbonate samples with low Rb/(Rb+Sr) ratios in the vent complex range over a large interval (i.e. 0.7221 to 0.7137). Carbonates in the "deep" parts of the fault and breccia body generally have higher $^{87}Sr/^{86}Sr$ than "shallower" carbonates replacing barites. Laminated barites are the least radiogenic. A three-component mixing model for strontium comprising (1) reaction between a radiogenic (hydrothermal) fluid and a more radiogenic shallow sediment, and (2) mixing of the evolved (reacted) fluid with a less radiogenic seawater is under consideration. Early siderite replacing Lower Earn Group siltstone is distinctly more radiogenic than later, vein-controlled ankerite. In our model, siderite would have formed at lower water/rock ratios than ankerite precipitated in younger fractures.

It is anticipated that the vent complex formed under steep physical-chemical gradients (e.g., temperature, $^{f}O_2$, $^{f}S_2$, pH) in which the hydrothermal fluid evolved rapidly, and that these conditions varied markedly over the life of the hydrothermal system. Sampling of minerals representing different paragenetic stages of the vent complex will attempt to constrain time-space evolution of fluid composition.

Evolution of the hydrothermal sedimentary environment

The sedimentary record preserved in the laminated sulphide-sulphate-silica stratigraphy provides a history of the hydrothermal depositional environment. Seventeen analyses of laminated barite, studied by Gardner and Hutcheon (1985), yielded an average $\partial^{34}S$ of 24.4+/-1.2. A systematic increase in $\partial^{34}S$ occurs with increasing stratigraphic position in one hole in the South zone (DDH81-68, 4 samples). This trend is also noted in 5 barite samples from both stratiform horizons in DDH81-68A (Turner, unpublished data) and correlates with a slight but consistent shift to less radiogenic strontium isotope ratios in the same barite samples. In contrast, Gardner and Hutcheon (1985) reported 2 sections in the Main zone that appear to show a general decrease in $\partial^{34}S$ with increasing stratigraphic position (TR-3, 7 samples; DDH77-25, 3 samples).

Ferroan carbonate alteration

Late Devonian stratiform deposits in the Macmillan Pass area are intimately associated with carbonization. The proximal replacement zone of the Jason South/Main deposit is dominated by an ferroan carbonate minineralogy, as are those in the Tom deposit (Carne, 1979) and the Jason End zone (Gardner and Hutcheon, 1985). Extensive ferroan carbonate alteration also occurred within calcareous shales of the upper Road River Group and siltstone and conglomerates of unit 1 and unit 2 of the Lower Earn Group. This alteration is composed of pervasive and porphyroblastic ferroan carbonate cut by quartz, ferroan carbonate and pyrite veins, and is widespread over several kilometres on the Jason property, from the End zone area east to the South zone/Main zone. Ferroan carbonate alteration is also associated with mafic volcanic flows, tuffs and low-grade base metal mineralization at the Nidd property, and basaltic flows/sills and volcaniclastic rocks in the upper Road River Group in the Macmillan Pass area.

The origin of the ferroan carbonate is unclear. Based on delta ^{13}C analyses of 5 ankerites from the Tom deposit (−2.7+/−0.3), and an estimated range of temperature of formation (100 to 250°C), a calculated isotopic composition of the carbon of the ankerite-forming fluid is −2.3 to −7.5‰ (Ansdell, 1985). This range closely matches that of CO_2 degassed from the mantle (e.g. Kilauea; Taylor, 1986; Taylor and Gerlach, 1988) but could conceivably be derived from a restricted mixture of carbon from organic matter and limestone in strata below the Tom. Such a scenario is consistent with the mixing of mantle fluids (e.g. CO_2) with base metal-bearing fluids derived from basinal clastic rocks during formation of the stratiform Zn-Pb deposits.

ACKNOWLEDGMENTS

Preparation and stable isotopic analyses of selected samples are being carried out in laboratories at the GSC and the Ottawa-Carleton Centre for Geoscience Studies/GSC Stable Isotope Laboratory, University of Ottawa. Determination of $^{87}Sr/^{86}Sr$ of carbonates and barite was conducted by Geochron Laboratories Ltd., Cambridge, Mass.; additional analyses are underway at the Geochronology Laboratory, Lithosphere and Canadian Shield Division, GSC Ottawa. We thank Rick Bailes and Abermin Resources for their continued support of this project, and Ian Jonasson for helpful editing of a draft of this manuscript. Thanks also go to Cal Sahnnon of Abermin for his generous hospitality at the Jason camp and to Christine Davis for her able drafting.

REFERENCES

Abbott, J.G.

1982: Structure and stratigraphy of the Macmillan Fold Belt: evidence for Devonian faulting; *in* Yukon Geology and Exploration 1981; Department of Indian Affairs and Northern Development (Canada), Northern Affairs Program, Exploration and Geological Services Division, Whitehorse, Yukon, p. 22-33.

1983: Geology of the Macmillan Fold Belt 105O-SE and parts of 105P-SW (1:50,000); Department of Indian Affairs and Northern Development (Canada), Northern Affairs Program, Exploration and Geological Services Division, Whitehorse, Yukon, Open File Maps.

Albarede, F., Michard, A., Minster, J.F., and Michard, G.

1981: $^{87}Sr/^{86}Sr$ ratios in hydrothermal waters and deposits from the East Pacific Rise at 21N; Earth and Planetary Science Letters, v. 55, p. 229-236.

Ansdell, K.M.

1985: Fluid inclusion and stable isotope study of the Tom Ba-Pb-Zn deposit, Yukon Territory; M.S.C. Thesis, University of Alberta, Edmonton, 123 p.

Burke, W.H., Denison, R.E., Hetherington, E.A., Koepnick, R.B., Nelson, H.F., and Otto, J.B.

1982: Variation of seawater $^{87}Sr/^{86}Sr$ throughout Phanerozoic time; Geology, v. 10, p. 516-519.

Carne, R.C.

1979: Geological setting and stratiform mineralization, Tom claims, Yukon Territory: Department Indian Affairs and Northern Development, Open-File Report. EGS 1979-4, 30 p.

Gardner, H.D. and Hutcheon, I.,

1985: Geochemistry, mineralogy and geology of the Jason Pb-Zn deposits, Macmillan Pass, Yukon, Canada; Economic Geology, v. 80, p. 1257-1276.

Goodfellow, W.D.,

1987: Anoxic stratified oceans as a source of sulphur in sediment-hosted stratiform Zn-Pb Deposits (Selwyn basin, Yukon, Canada); Chemical Geology, v. 65, p. 359-382.

Goodfellow, W.D. and Jonasson, I.R.,

1984: Ocean stagnation and ventilation defined by $\partial^{34}S$ secular trends in pyrite and barite, Selwyn Basin, Yukon; Geology, v. 12, p. 583-586.

McClay, K.R., and Bidwell, G.E.,

1986: Geology of the Tom Deposit, Macmillan Pass, Yukon; *in* Morin, J.A., (editor), Mineral Deposits of the Northern Cordillera, Canadian Institute of Mining and Metallurgy, Special Volume 37, p. 100-114.

Ohmoto, H., Kaiser, C.J., and Geer, K.A.,

— Systematics of sulphur isotopes in recent marine sediments and ancient sediment-hosted basemetal deposits; International Conference on Stable Isotopes and Fluid Processes in Mineralization, Geological Society of Australia, Special Publication. (in press)

Taylor, B.E.,

1986: Magmatic volatiles: isotopic variation of C, H, and S. Chapter 7, in Stable Isotopes in High Temperature Processes. Mineralogical Society of America, Reviews in Mineralogy, edited by H.P. Taylor et al., v. 16, p. 185-225.

Taylor, B.E., and Gerlach, T.M.,

1988: Carbon isotopic composition of volcanic gases from early episodes of the 1983 East Rift Zone, Kilauea Volcano, Hawaii; Geological Society of America, Abstracts with Programs, v. 20, n. 7, p. A112.

Turner, R.J.W.

1986: The genesis of stratiform lead-zinc deposits, Jason property, Macmillan pass, Yukon; [Ph.D thesis], Stanford University, Stanford, 205 p.

1988: Targeting mid-Paleozoic massive sulphide deposits; Mining Review, v. 8, n. 6, p. 43-47.

Zierenberg, R.A., and Shanks, W.C. III,

— Isotopic studies of epigenetic features in Atlantis II Deep metalliferous sediment, Red Sea: smectite geothermometry and advective brine mixing; Geochimica and Cosmochimica Acta. (in press)

Interpretation of stream geochemistry leading to the discovery of a secondary zinc deposit, Pelly River, Nahanni map area, Yukon

Wayne D. Goodfellow
Mineral Resources Division

Goodfellow, W.D., Interpretation of stream geochemistry leading to the discovery of a secondary zinc deposit, Pelly River, Nahanni map area, Yukon; in Current Research, Part E, Geological Survey of Canada, Paper 89-1E, p. 31-50, 1989.

Abstract

Follow-up of a high-Zn but low-Pb stream anomaly has led to the discovery of secondary Zn mineralization overlying Road River Group shale and chert in the NW Nahanni map area. These rocks host stratiform Zn-Pb deposits elsewhere in the map sheet. The secondary Zn zone forms mounds of smithsonite, zincian calcite and hemimorphite which are remarkedly similar to secondary Zn mineralization that blankets the Howards Pass deposit. Zinc and Ni contents range up to 18.5 and 1.0 wt. %, respectively.

Detailed studies of the surficial geochemistry of known Pb-Zn deposits combined with thermodynamic modelling of the aqueous chemistry have shown clearly that Pb is fixed, whereas Zn is very mobile under alkaline conditions. The differential solubility of these elements under alkaline conditions has resulted in the separation of Zn from Pb in the secondary environment, and explains the origin of Zn anomalies. Coincident Pb-Zn anomalies only result when the deposit is exposed to physical erosion.

Résumé

En suivant une anomalie fluviatile à contenu élevé de Zn mais faible de Pb, on a découvert une minéralisation secondaire en Zn sus-jacente aux schistes argileux et cherts du groupe de Road River dans le nord-ouest de la région cartographique de Nahanni. Ces roches renferment des gisements de Zn et Pb à d'autres endroits de cette région cartographique. La zone secondaire minéralisée en Zn forme des monticules de smithsonite, de calcite zincifère et d'hémimorphite qui rappellent étonnamment la minéralisation secondaire en Zn recouvrant le gisement de Howard Pass. Les teneurs en zinc et Ni peuvent atteindre 18,5 % et 1,0 % en poids respectivement.

Des études détaillées de la géochimie de surface de gisements connus de Pb et Zn, combinées à la modélisation thermodynamique de la chimie de l'eau, ont clairement démontré que Pb est fixe tandis que Zn est très mobile dans les conditions d'alcanalité. La solubilité différentielle de ces éléments dans des conditions d'alcalinité a permis de séparer Zn de Pb dans le milieu de minéralisation secondaire, et d'expliquer l'origine des anomalies en Zn. Une coïncidence au niveau des anomalies en Zn et Pb ne se produit que lorsque le gisement est exposé à l'action de la désagrégation mécanique.

INTRODUCTION

Stream sediment geochemistry has been used successfully by exploration companies to discover sediment-hosted stratiform Pb-Zn deposits in the Selwyn Basin, Yukon. Sediment anomalies identified during exploration programs are commonly rated according to 1) the intensity of Pb and Zn anomalies, and 2) whether or not these anomalies are coincident. This approach obviously worked since both the Howards Pass (XY) and Anniv deposits were discovered by coincident Pb and Zn anomalies. One of the factors that resulted in the elimination of potentially good exploration targets on the basis of these criteria applies to streams draining calcareous shales of the Road River Group that are buffered at an alkaline pH by carbonate minerals and are unable to transport Pb in solution. Under these alkaline conditions, Pb anomalies are associated only with deposits which have undergone active physical erosion. Spring-fed streams draining deposits which are poorly exposed or shallowly buried, by contrast, typically display high Zn values but background Pb contents because of the low solubility of the latter in alkaline ground waters. As a result, exploration programs that consider only coincident Pb and Zn anomalies automatically exclude shallowly buried deposits from consideration.

This paper reports on the application of surficial geochemical studies of the Howards Pass and Anniv stratiform Zn-Pb deposits in the interpretation of high-Zn and low-Pb stream sediment anomalies identified in the Nahanni map sheet by reconnaissance geochemical methods (Goodfellow, 1982). During the evaluation of one Zn anomaly, a zone of secondary Zn mineralization (henceforth referred to as the Pelly River deposit) was discovered at the headwaters of the Pelly River. Although primary Pb-Zn sulphides have not yet been discovered in this area, the remarkable similarity of this deposit to secondary mineralization overlying the Howards Pass Pb-Zn deposit (Jonasson et al., in press), the high Zn content of the secondary zone and its location overlying basinal shales of the Road River Group which are correlative with those hosting Zn-Pb deposits elsewhere in the Nahanni map area, all indicate a high potential for stratiform Pb-Zn sulphide mineralization.

TECTONOSTRATIGRAPHIC SETTING OF SELWYN BASIN

The Nahanni map area (NTS 105I) straddles the Yukon-Northwest Territories border and comprises part of the Selwyn Basin and adjacent Mackenzie Carbonate Platform (Fig. 1). The Selwyn Basin is an elongate fault-controlled epicontinental marine basin that formed due to subsidence accompanying rifting of the western passive margin of North America (Goodfellow et al., 1983; Goodfellow and Jonasson, 1986; Tempelman-Kluit, 1981). It is bounded to the east and north by the Mackenzie Carbonate Platform and dissected by Cassiar Platform. The western margin is not preserved. Most of the extensional faulting during the Paleozoic was probably due to the reactivation of structures formed during the initial rifting of the craton at about 780 Ma.

The Selwyn Basin is underlain by a thick syn-rift sequence of Hadrynian-Cambrian feldspathic grits which

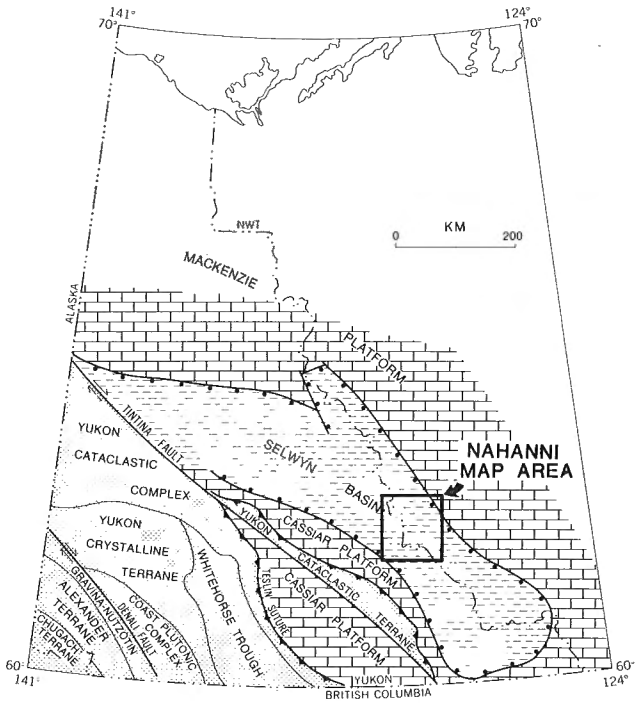

Figure 1. Yukon tectonic elements from Tempelman-Kluit (1981) and the location of the Nahanni map area (NTS 105I).

fine upward into maroon and green shales (Fig. 2). From the Cambrian until the onset of block faulting in the Late Devonian, the Selwyn Basin behaved as an extremely stable basin which was starved of sediment from the adjacent continent. As a result, carbonaceous chert and mudstone of the Road River Group (Fig. 2) are predominant except during the Middle to Late Silurian when the sediments were bioturbated and less carbonaceous due to the destruction of organic matter by organisms. In the Late Devonian, block faulting of the cratonic margin produced grabens into which clastics of the Earn Group (Fig. 2) were shed from areas uplifted elsewhere in the Selwyn Basin. By the latest Devonian (Famennian), the shedding of brown clastics from the west over the Selwyn Basin and adjacent carbonate platforms heralded the end of the Selwyn Basin.

On a regional scale, strata of the Selwyn Basin have been folded about west-northwest-trending axes that plunge consistently northwest (Gordey, 1978). In the Nahanni map area, the major folds are open although units are internally tightly folded, except in the northwest sector where strata have been more tightly folded.

Stratiform sediment-hosted Pb-Zn deposits of Early Silurian (e.g. Howards Pass, Anniv, Hug and Pab; Fig. 2) and Devonian (e.g. Nor) age occur in the Nahanni map sheet. The Early Silurian deposits are hosted by cherty limestone and calcareous carbonaceous shale and chert of the Road River Group (Goodfellow and Jonasson, 1986). The Nor and numerous barren sedimentary barite deposits (e.g. Oro, GHMS, Summit Lake) occur in black clastics and chert of the Lower Earn Group. Carbonaceous chert and shale of the Earn Group can be differentiated from similar rocks of the Road River Group by higher pyrite and lower carbonate contents.

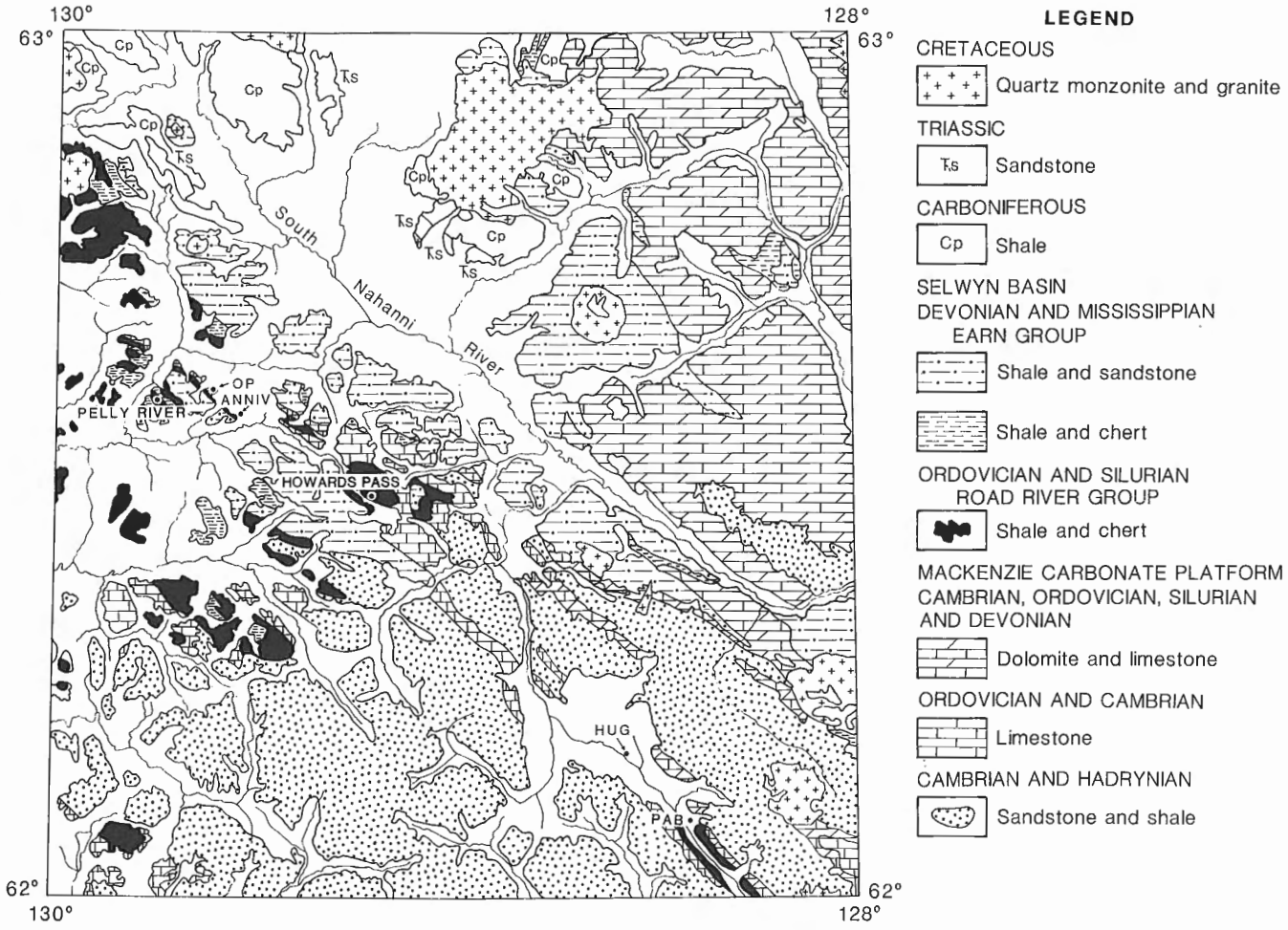

Figure 2. Geological map and Early Silurian stratiform Pb-Zn deposits, Nahanni map sheet. Geology simplified from a 1:125 000 scale geological map of the area by Gordey (1981).

SAMPLING AND ANALYTICAL METHODS

Sediment samples were collected in active streams from fine silt accumulated under or behind boulders, trapped in living moss or deposited near stream banks where flow velocities were lower. All sediment samples were air-dried in the field and shipped to Geological Survey of Canada laboratories where they were sieved to minus-80 mesh (177 microns) and subsequently ground to minus-150 mesh (105 microns) in a ceramic ball-mill. All elements were determined by atomic absorption spectrometry (AAS) after HNO_3/HCl digestion except P_2O_5 which was determined by X-ray fluorescence (XRF).

Water samples were collected from streams and springs in 250 ml polyethylene bottles. All samples were analyzed for Zn, Mn, Ca, Mg and Fe by AAS; for F, SO_4^{-2} and Cl by DIONEX and specific ion electrode methods; and for U by laser-induced fluorescence using a SCINTREX UA-3.

Rocks were collected from surface exposures, crushed and ground to minus-150 mesh, and analyzed as follows. The major element oxides SiO_2, Al_2O_3, TiO_2, Fe_2O_3, MnO, MgO, CaO, Na_2O, K_2O and P_2O_5 were determined by Induction Coupled Plasma-Emission Spectrometry (ICP-ES) after a total acid digestion. H_2O was evolved by heating a flux in a modified "Penfield Tube", then dissolved in an organic solvent and titrated with Karl Fisher reagent. Total carbon was determined by burning a sample in an induction furnace and the resulting CO_2 absorbed in a solution of triethanolamine in acetone and titrated with sodium methylate-methanol. Carbonate CO_2 was evolved with HCl, absorbed and titrated as described above. Organic carbon was calculated as the difference between total carbon and carbonate carbon. Total sulphur was analyzed by burning a sample in an induction furnace to generate SO_2 which was measured iodometrically using an automatic titrator. All trace and minor elements were determined by ICP-ES after a total digestion.

PELLY RIVER SECONDARY ZINC DEPOSIT

Geological setting

The Pelly River secondary Zn deposit occurs in the northeast section of the Nahanni map area (see Fig. 2) along a north-flowing tributary of the Pelly River (see Fig. 5a). The deposit is best exposed in a 2 m high mound (see Fig. 5b) which appears to have dammed the stream and resulted in the formation of a meadow upstream from the secondary zone.

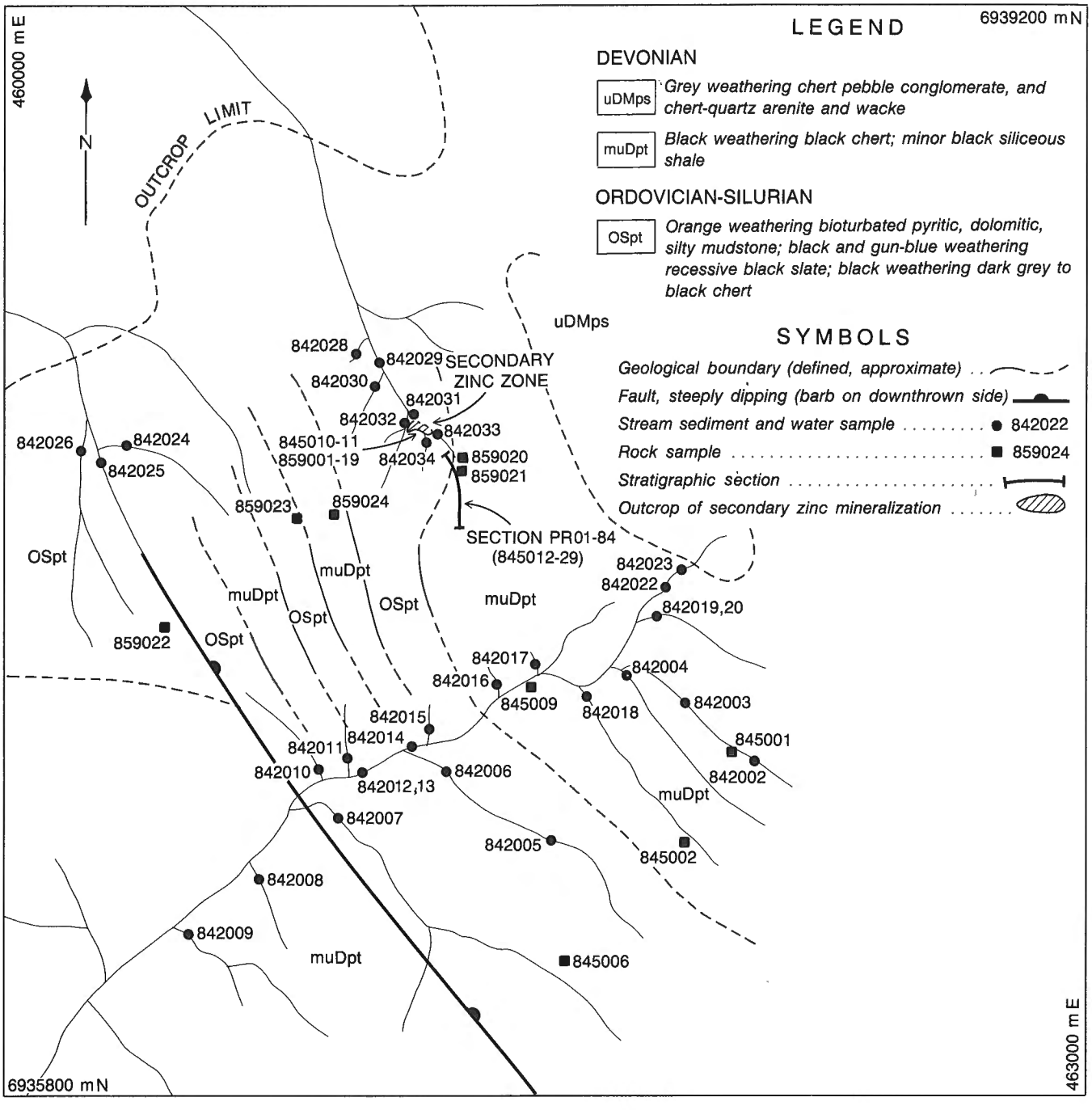

GSC

Figure 3. Geology of the Pelly River area showing the secondary Zn zone, and stream and rock sample locations. Stream sediment and water, and rock chemical data are listed in Tables 1 to 5.

The geology in the Pelly River area consists of tightly folded Ordovician-Silurian shale and chert of the Road River Group and Devonian-Mississippian black chert and clastics of the Earn Group (Fig. 3). The exposure of bioturbated mudstone and phosphatic chert immediately upstream from the secondary Zn occurrence demonstrates that this secondary mineralization blankets strata of the Road River Group and occurs near the horizon which hosts the Howards Pass stratiform sulphide deposit (Goodfellow and Jonasson, 1986). At the Howards Pass deposit, primary Zn-Pb mineralization is hosted in Early Silurian cherty limestone and carbonaceous chert which directly underlie phosphatic chert of the Road River Group. At the Pelly River deposit, the secondary Zn zone now covers rocks that are time equivalent and geochemically similar to sedimentary rocks which host sedimentary Zn-Pb mineralization elsewhere in the Nahanni map sheet.

A partial stratigraphic section of the Road River and Earn groups (Fig. 4) was measured and sampled upstream from the Pelly River deposit (section is located on Fig. 3). Sample 105I 845012, which was taken about 10 m upstream

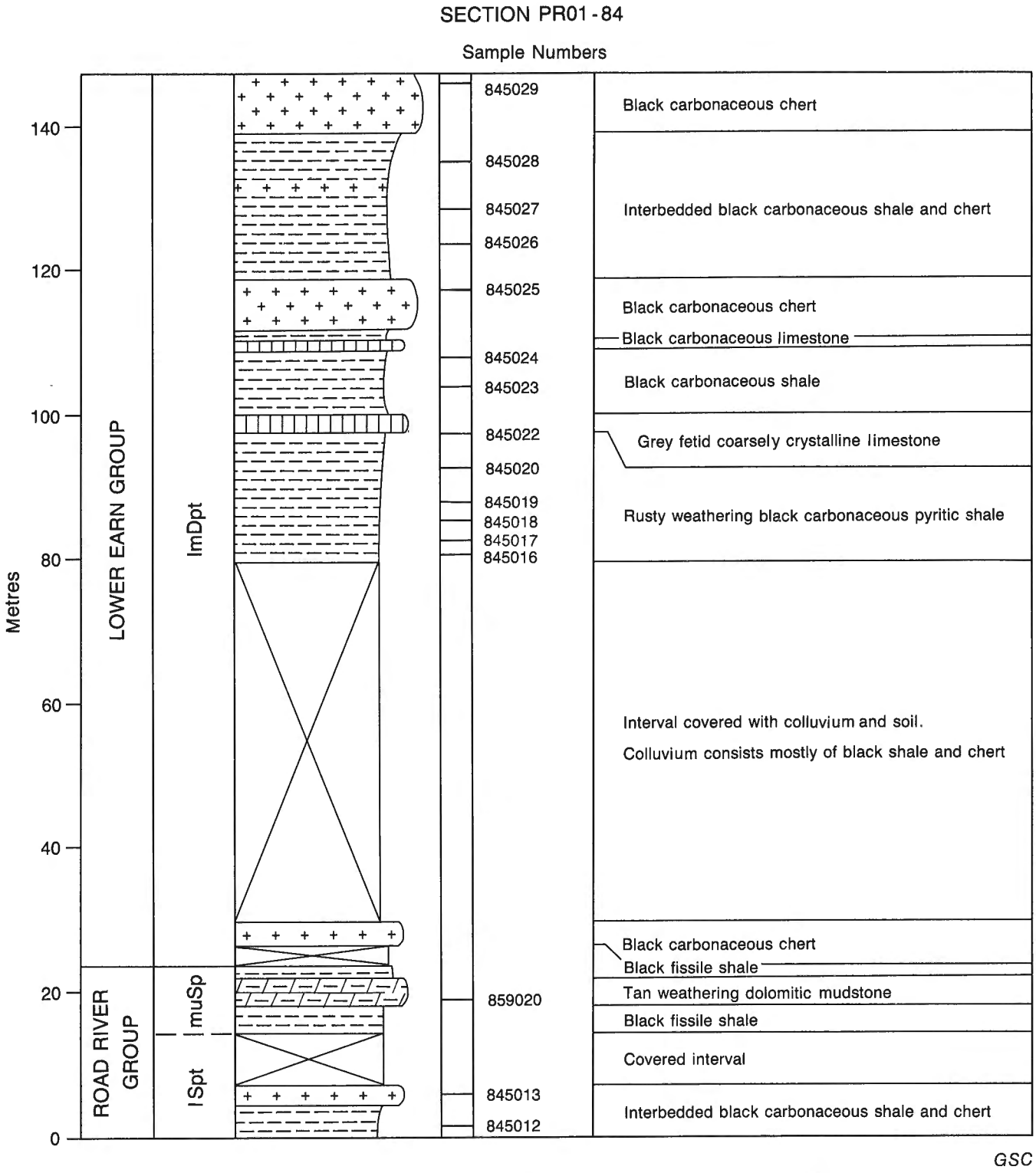

Figure 4. Partial stratigraphic section of the Road River and Lower Earn groups, near the Pelly River secondary Zn deposit. Sample numbers refer to those listed with chemical data in Table 1. Section is located on Figure 3.

Table 1a. Major element analyses of section PR01-84, Pelly River Secondary Zn deposit

Sample Numbers		SiO_2	TiO_2	Al_2O_3	Fe_2O_{3T}	MnO	MgO	CaO	Na_2O	K_2O	H_2O_T	CO_2	C-org	P_2O_5	S
105I	845012	72.3	0.56	10.4	3.8	0.03	1.29	1.67	0.0	2.87	4.2	0.0	3.3	1.34	0.19
	845013	53.4	0.62	12.6	4.2	0.03	2.61	2.80	0.2	3.71	-	4.2	0.1	0.16	3.49
105I	859020	65.0	0.72	15.3	6.0	0.01	1.32	0.10	0.7	3.96	-	0.0	0.0	0.08	1.60
105I	845016	65.1	0.84	15.9	3.0	0.00	1.61	0.14	0.0	4.57	5.0	0.0	0.6	0.08	0.51
	845017	52.7	0.72	11.3	2.1	0.00	0.59	0.13	0.0	3.83	-	0.0	0.3	0.12	3.71
	845018	64.4	0.89	16.7	1.4	0.00	0.95	0.14	0.0	5.18	4.2	0.0	1.0	0.05	0.31
	845019	63.4	0.82	16.0	2.0	0.00	0.79	0.78	0.1	4.91	3.7	0.0	1.5	0.53	0.21
	845020	51.5	0.42	7.2	7.2	0.13	5.35	8.22	0.0	2.36	3.8	10.5	2.0	0.23	0.02
	845022	3.6	0.08	0.7	0.4	0.05	19.8	29.2	0.0	0.18	0.4	40.9	0.4	0.03	0.01
	845023	94.2	0.09	2.9	0.6	0.00	0.30	0.49	0.2	0.67	1.0	0.5	1.0	0.06	0.28
	845024	77.3	0.24	4.7	1.1	0.01	1.68	4.79	0.0	1.31	2.1	3.2	1.4	1.60	0.08
	845025	94.0	0.07	1.2	0.0	0.00	0.10	0.14	0.0	0.21	1.3	0.0	3.3	0.08	0.19
	845026	65.0	0.62	14.5	3.5	0.01	1.73	0.21	0.5	3.91	5.8	0.0	1.4	0.25	0.51
	845027	72.7	0.70	12.3	2.6	0.01	1.45	0.34	0.3	3.44	4.1	0.0	1.5	0.33	0.08
	845028	75.4	0.59	10.6	1.9	0.00	1.00	0.50	0.0	2.87	4.3	0.0	2.1	0.30	0.32
	845029	89.3	0.07	1.4	0.1	0.00	0.01	0.27	0.0	0.28	1.2	0.0	6.7	0.26	0.16

Notes: All elements and element oxides expressed in wt.%

Table 1b. Minor and trace element analyses of section PR01-84

Sample Numbers		Cu	Pb	Zn	Mo	Co	Ni	Cd	Ag	V	Ba
105I	845012	91	11	1474	38	3	115	32	1.9	840	0.87
	845013	28	8	330	2	11	47	6	<0.1	120	6.09
105I	859020	31	19	170	6	10	39	0.8	<0.1	92	0.86
105I	845016	21	8	119	4	<1	21	1.5	0.8	200	0.95
	845017	12	20	61	4	<1	7	0.8	1.5	170	15.11
	845018	12	13	41	6	<1	11	1.4	1.4	250	2.95
	845019	30	10	138	4	<1	31	1.4	0.8	260	4.61
	845020	43	12	3800	250	159	365	61	<0.1	980	1.11
	845022	24	9	525	8	1	39	17	<0.1	165	1.22
	845023	19	4	103	2	2	22	4.2	2.2	40	0.26
	845024	150	8	1032	14	3	133	30	1.8	585	0.61
	845025	44	5	133	44	<1	80	2.8	0.2	1140	0.23
	845026	58	21	302	20	1	40	2.5	1.0	320	0.87
	845027	154	12	535	38	3	54	1.4	2.0	1200	1.21
	845028	30	6	134	6	<1	40	2.5	0.6	335	0.55
	845029	19	8	15	6	<1	70	1.3	0.7	660	0.33

Notes: All elements expressed in ppm, except for Ba which is in weight percent.

Table 2a. Sample descriptions, Pelly River area

Sample No.		Lithological Description	Group
105I	845001	Black carbonaceous fissile pyritic shale	Lower Earn Group
	845002	Black massive carbonaceous chert	Road River Group
	845003	Black massive carbonaceous chert	Road River Group
	845004	Black carbonaceous chert with pale grey stripes	Road River Group
	845005	Black finely laminated carbonaceous chert	Road River Group
	845006	Black carbonaceous graptolitic fissile shale	Road River Group
	845007	Black carbonaceous graptolitic fissile shale	Road River Group
	845008	Black carbonaceous graptolitic fissile shale	Road River Group
	845009	Black carbonaceous shale	Road River Group
	845013	Black carbonaceous chert, near secondary Zn mineralization	Road River Group (?)
	859014	Black carbonaceous chert, near secondary Zn mineralization	Road River Group (?)
	859015	Black carbonaceous chert, near secondary Zn mineralization	Road River Group (?)
	859018	Black carbonaceous chert, underlying secondary Zn mineralization	Road River Group (?)
	859019	Black carbonaceous chert	Road River Group
	859020	Rusty weathering pyritic dolomitic mudstone	Road River Group
	859021	Black carbonaceous chert, with white stripes	Earn Group
	859022	Dark grey siliceous limestone	Earn Group
	859023	Black carbonaceous shale	Road River Group
	859024	Orange weathering pyritic, dolomitic mudstone	Road River Group

Table 2b. Major element analyses of shale, chert and limestone from the Pelly River area

Sample No.		SiO_2	TiO_2	Al_2O_3	Fe_2O_{3T}	MnO	MgO	CaO	Na_2O	K_2O	H_2O_T	CO_2	C-org	P_2O_5	S
105I	845001	78.8	0.56	12.1	0.5	0.0	0.66	0.05	0.3	2.55	3.4	0.0	2.3	0.07	0.13
	845002	90.6	0.16	3.1	0.6	0.0	0.09	0.10	0.0	0.66	1.8	0.0	1.8	0.13	0.10
	845003	97.0	0.07	1.4	0.2	0.0	0.02	0.12	0.0	0.11	0.6	0.0	1.4	0.11	0.11
	845005	88.2	0.18	3.0	0.9	0.01	0.23	0.28	0.0	0.66	2.2	0.0	3.7	0.23	0.14
	845006	81.0	0.29	4.3	0.5	0.0	0.24	0.04	0.0	1.21	2.7	0.0	7.7	0.09	0.12
	845007	72.1	0.90	9.9	1.0	0.01	1.19	0.66	0.0	2.39	4.7	0.0	7.0	0.80	0.32
	845008	80.5	0.40	6.9	1.4	0.00	0.62	0.44	0.1	1.67	3.2	0.0	4.8	0.22	0.07
	845009	74.4	0.57	11.1	4.5	0.03	0.99	0.40	0.5	3.07	3.1	0.0	0.6	0.28	0.02
105I	859013	85.5	0.24	4.67	0.17	0.01	0.33	0.17	0.02	0.88	2.4	0.0	3.3	0.03	0.16
	859014	91.4	0.05	1.46	0.71	0.01	0.09	0.21	0.01	0.33	1.3	0.0	2.1	0.11	0.10
	859015	88.8	0.07	1.62	0.41	0.01	0.10	1.84	0.01	0.34	1.0	0.1	1.2	1.32	0.15
	859018	89.9	0.13	2.91	0.10	0.01	0.19	0.10	0.01	0.53	1.5	0.0	2.4	0.03	0.16
	859019	92.4	0.03	0.87	0.19	0.01	0.06	0.10	0.01	0.25	0.6	0.0	1.0	0.07	0.08
	859020	65.0	0.72	15.3	5.9	0.01	1.32	0.10	0.70	3.96	-	0.0	0.1	0.08	1.60
	859021	86.8	0.11	2.46	0.60	0.01	0.20	1.82	0.01	0.72	1.8	0.0	3.6	1.51	0.09
	859022	3.74	0.03	0.75	0.30	0.06	19.9	29.2	0.01	0.34	0.5	44.1	1.0	0.03	0.13
	859023	77.7	0.53	9.09	1.06	0.01	0.97	0.09	0.02	2.23	4.1	0.1	3.6	0.11	0.13
	859024	28.2	0.26	5.27	3.35	0.14	11.9	17.9	0.33	1.29	1.7	27.7	0.6	0.03	0.09

Notes: All elements and element oxides expressed in wt.%

Table 2c. Minor and trace element analyses of shale, chert and limestone from the Pelly River area

Sample	Number	Cu	Pb	Zn	Mo	Co	Ni	Cd	Ag	V	Ba
105I	845001	14	12	29	18	<1	12	1.5	0.2	600	0.45
	845002	78	7	164	40	<1	35	26	1.6	3200	0.48
	845003	29	8	27	4	<1	22	1.4	1.3	480	0.09
	845005	79	96	150	18	3	86	2.9	2.0	1110	0.43
	845006	17	4	34	10	<1	60	0.4	1.0	680	0.34
	845007	20	11	38	14	<1	49	0.6	2.0	1120	0.46
	845008	38	4	314	6	2	84	2.3	0.6	300	0.41
	845009	30	11	831	10	6	77	1.2	0.6	130	0.94
105I	859013	4	8	320	10	46	46	6.5	0.9	1700	0.29
	859014	14	<2	1000	14	69	69	22.7	0.5	540	0.22
	859015	17	4	620	12	37	37	16.8	0.9	570	0.20
	859018	6	2	200	6	26	26	3.3	0.7	1000	0.21
	859019	9	3	78	4	15	15	0.8	0.6	160	0.18
	859020	33	12	195	6	31	31	0.8	<0.5	92	0.86
	859021	41	15	58	2	35	35	<0.2	0.7	500	0.22
	859022	18	5	600	4	44	44	1.7	<0.5	62	0.18
	859023	6	9	34	18	32	32	0.6	1.2	1300	0.60
	859024	12	9	135	14	17	17	4.2	<0.5	170	0.36

Notes: All elements expressed in ppm except Ba which is in wt. %

from the secondary Zn zone, consists of interbedded black chert and shale and contains 1.34 wt. % P_2O_5 and 1474 ppm Zn (Table 1). This sample is highly anomalous when compared to rocks of similar age and composition collected remote from Zn-Pb mineralization in the Nahanni map sheet (Goodfellow et al., 1983). The unit from which this sample was collected is overlain by baritic and pyritic cherty shale which underlies wispy laminated bioturbated mudstone. The bioturbated mudstone is Ba-rich and contains large pyrite concretions. This is important since studies of the Howards Pass deposit (Goodfellow, 1984) have shown that this unit displays a marked increase in the content of Ba and density of pyrite concretions towards the sulphide zone.

Rocks of the Road River Group are overlain by interbedded carbonaceous limestone, shale and chert of the Lower Earn Group (Fig. 4). Inspection of Table 1 reveals that these rocks contain elevated levels of Ba, Zn, Cd, Mo, Co, Ni, F_2O_3 and P_2O_5. One sample contains 15.11 wt. % Ba and a second sample contains 3800 ppm Zn. Additional chemical analyses of spot samples of carbonaceous shale and chert from the Pelly River area are given in Table 2 (refer to Fig. 3 for sample locations). Values for most elements approach background levels for shale and chert from the Road River and Lower Earn groups (Goodfellow et al., 1983) with the exception of samples collected near the secondary Zn zone which have elevated Zn, Cd and Ni contents.

Mineralogy and geochemistry

The secondary Zn mineralization displays a cauliflower morphology (Fig. 5c) due to the replacement of multiple layers of moss (Fig. 5d) by Zn-rich ground waters. Upstream from the mound where the meadow has been down-cut by stream erosion, talus consisting of shale and chert clasts cemented by secondary Zn minerals is exposed (Fig. 5e,f).

Individual samples of the secondary zone display a cellular morphology (Fig. 6a,b) very similar to moss which has been replaced by Zn at the Howards Pass deposit (Lee et al., 1984; Jonasson et al., in press). Although the species of moss has not been identified at the Pelly River deposit, it is similar in appearance to *Pohlia wahlenbergii* described at the Howards Pass deposit (Jonasson et al., in press). Detailed examination of samples using a scanning electron microscope-energy dispersive spectral method (SEM-EDS) illustrates that cell walls are replaced and rimmed by zincian calcite, smithsonite and hemimorphite (Fig. 6c,d) which were identified by X-ray methods. There is a consistent paragenesis similar to the Howards Pass secondary zone with Zn-calcite appearing early in the history of moss replacement followed by smithsonite and finally hemimorphite. The cells are either empty or infilled by calcite, zincian calcite and smithsonite. As replacement and crystallization processes progressed, the internal moss structure was obscured by botryoidal clusters of secondary minerals (Fig. 6c). In weathered samples, carbonate minerals dissolved leaving an interlocking network of hemimorphite which commonly forms pseudomorphs after the cellular structure (Fig. 6f).

The Zn content of the secondary zone ranges up to 18.5 wt. % (Table 3). Other elements and compounds accumulated as part of this mineralization are Ni, Cd, Ca, SiO_2, CO_2, Fe_2O_3, Mo and Co. It is notable that lead content is

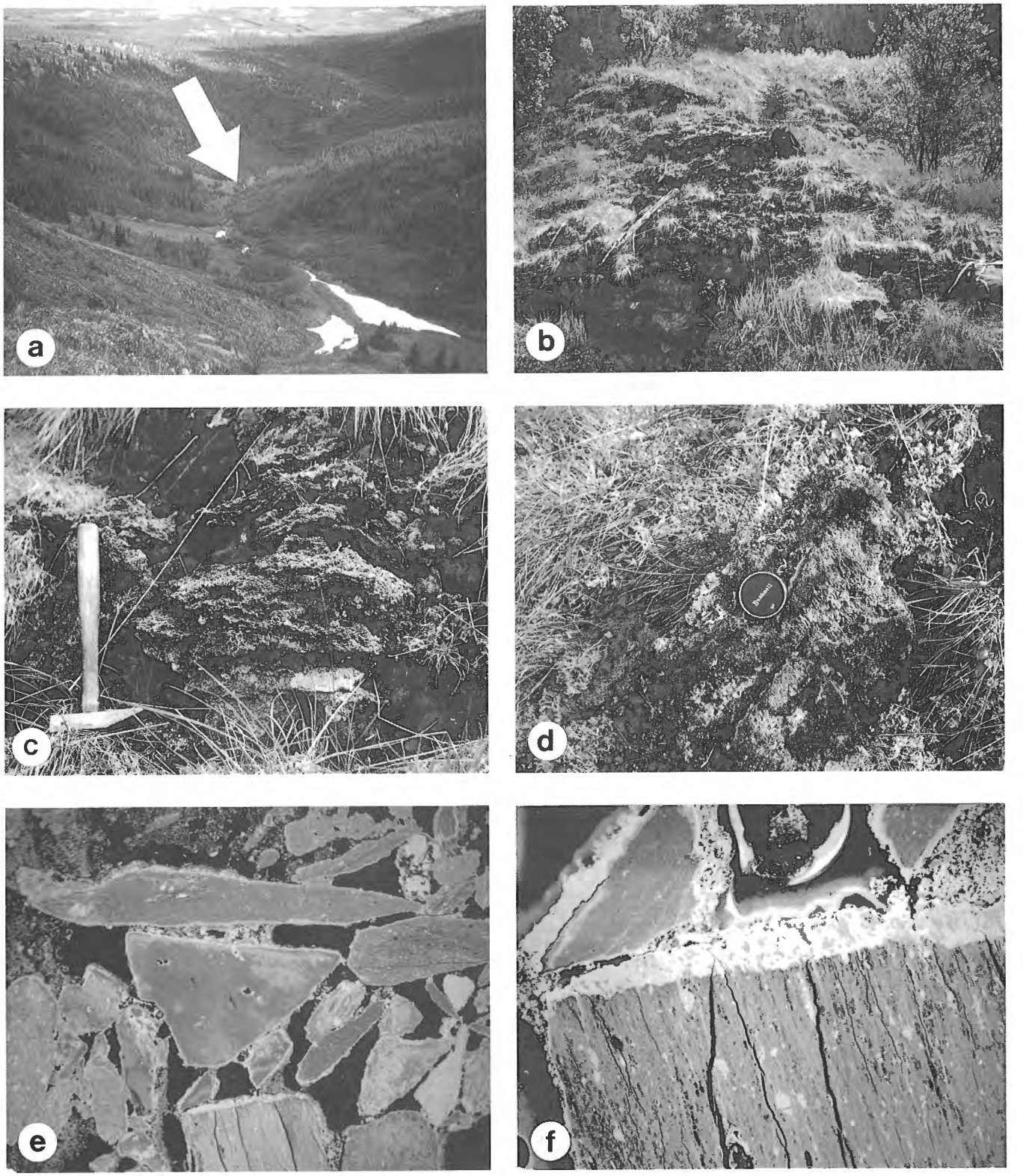

Figure 5. **a)** Stream valley drained by a tributary of the Pelly River and containing the Pelly River secondary Zn deposit (located with a white arrow). Green meadow formed by the damming effect of secondary Zn mineralization; **b)** View looking south of the secondary Zn zone showing its mound-like morphology. Pack sack at right for scale; **c)** Close-up view of mound in Fig. 5b showing cauliflower morphology; **d)** Close-up view of mound in (b) showing moss layers which are now replaced by secondary Zn minerals; **e)** Scanning electron microscope backscattered electron image (SEM-BSE) of talus about 10 m from the secondary Zn deposit which is cemented by hemimorphite and smithsonite; **f)** Blowup of (e) showing hemimorphite and smithsonite rimming talus clasts.

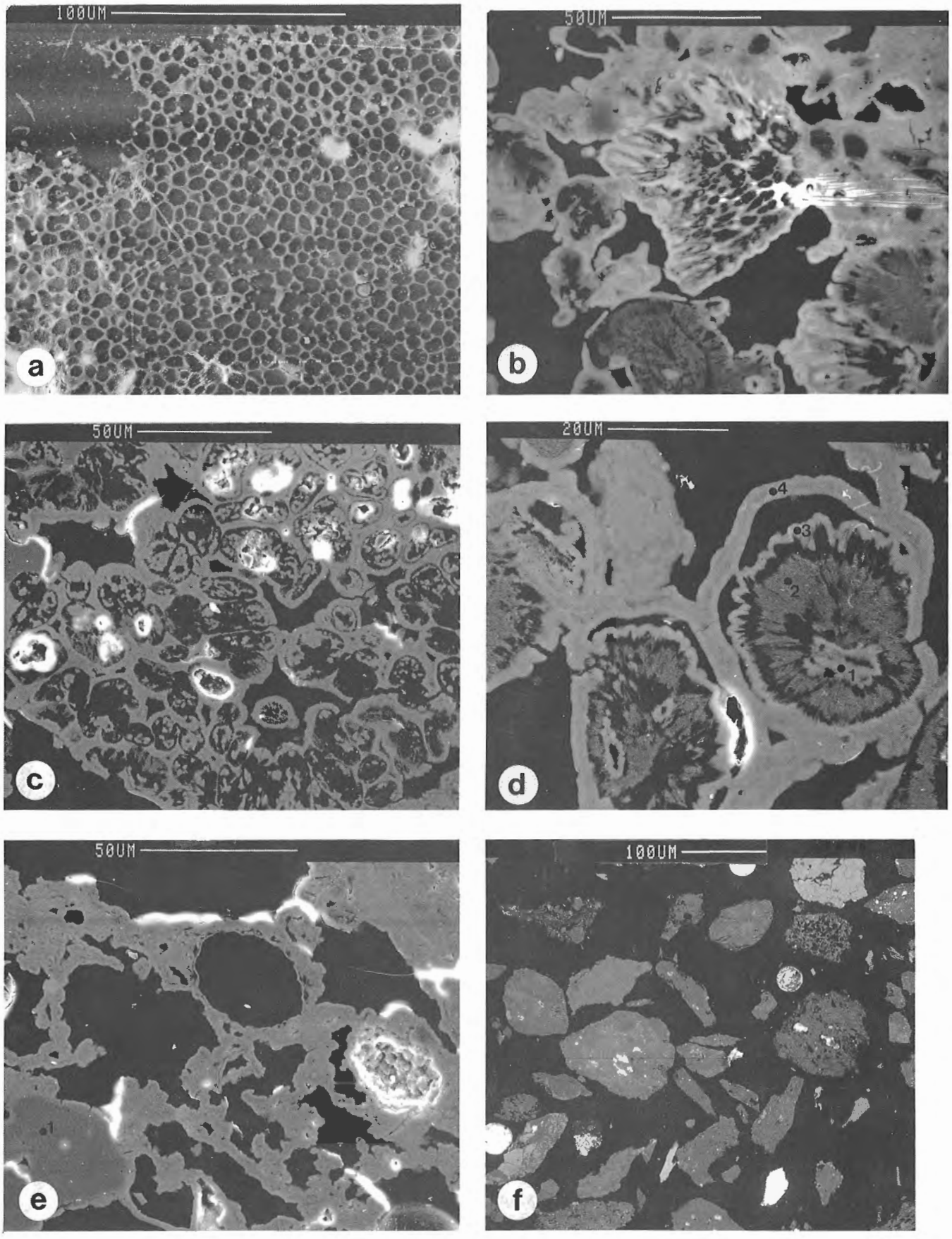
100UM
a
50UM
b
50UM
c
20UM
4
3
2
1
d
50UM
1
e
100UM
f

relatively very low (<150 ppm) and Ni reaches a value close to 1 wt. % in sample 105I 859011. SEM-EDS examinations of the distribution of elements in this sample indicate that Ni, Fe and Cd are associated with Zn in smithsonite and hemimorphite. This element association is similar to that described by Jonasson et al. (in press) for the secondary Zn zone overlying the Howards Pass deposit. Other elements shown in Table 3 are bound in chert and shale talus which comprises a variable component of each sample.

Stream geochemistry

Sediment from streams draining the Pelly River area were shown to contain anomalously high Zn contents (Fig. 7), but background Pb levels (Goodfellow, 1982; Bonham-Carter and Goodfellow, 1986; Ellwood et al., 1986). Furthermore, these high-Zn sediments were collected from streams which were also shown to be alkaline and chemically similar to those draining the calcareous Road River Group and the carbonate-rich portion of the Howards Pass deposit (Goodfellow, 1983). Because of the low measured Pb contents in water from streams draining both the Howards Pass (Goodfellow, 1983) and Anniv Zn-Pb deposits, and considering the thermodynamic limits placed on the hydromorphic transport of Pb under alkaline conditions, high-Zn anomalies in the Pelly River area were investigated in greater detail. The spatial distributions of Zn in sediment and water from streams draining the Pelly River area (Fig. 8 and 9) show the area near the secondary zone to be highly anomalous in Zn. There is also a high correlation of anomalous Zn with Cd and Ni in stream sediment. Lead, however, is less than 35 ppm in all stream sediment samples (Table 4) and below detection (<2 ppb) in stream water samples (Table 5). Water samples from the streams draining the secondary Zn zone are generally alkaline with pH values greater than 8.0.

DISCUSSION

The dispersion of elements in streams draining stratiform sphalerite-galena deposits is controlled by: 1) the exposure of the mineralization to physical erosion by streams or mass weathering; and 2) the chemical mobility of Zn and Pb in groundwaters and streams. Deposits such as Howards Pass and Anniv, which have been down-cut by streams, are reflected in the surficial environment by intense and widespread coincident Zn and Pb anomalies (Goodfellow, 1983). Stream sediment collected from streams draining the Howards Pass deposit, for example, contain corroded galena and sphalerite grains along with secondary Zn minerals eroded from the secondary Zn zone (Fig. 6f). Water samples collected from streams draining both the Howards Pass and Anniv deposits, however, are concentrated in Zn but depleted in Pb (Table 6). Even pore waters taken from a Zn-rich bog with Zn contents up to 35 wt. % at Howards Pass (Jonasson et al., in press) are markedly depleted in Pb relative to Zn.

The separation of Zn from Pb in the secondary environment is controlled mostly by pH. Under highly alkaline conditions, Zn is mobile as a divalent ion while Pb forms an insoluble carbonate (i.e. cerussite) at pH values greater than 5.5. This is readily apparent if the stability fields for aqueous and mineral species of Zn (Fig. 10) are compared with those of Pb (Fig. 11). The conditions for each of these Log a_{O2}-pH predominance diagrams are accurately constrained by chemical measurements of stream, seep and pore waters. The range and average of pH values for water samples from the Howards Pass, Anniv and Pelly River deposits are plotted on each diagram for comparison. The fact that average pH values plot near the Zn^{2+}-$ZnCO_3$ boundary for all three areas (Fig. 10) indicates a pH control on the solubility of Zn in solution. This is in contrast to the predominance diagram of Pb species which shows average pH values for stream, seep and pore fluids plotting in the cerussite field (Fig. 11). Under these highly alkaline conditions, any Pb released to ground waters by the oxidation of galena is immediately reprecipitated as a Pb carbonate. The hydromorphic dispersion of Pb from stratiform Zn-Pb deposits hosted by calcareous rocks is therefore extremely limited.

The pH of streams in the Nahanni map area is controlled mostly by the relative contents of carbonate and Fe-sulphides in the underlying bedrock. In streams draining the Mackenzie Carbonate Platform, for example, the pH ranges between 8.2 and 8.4 pH units (Goodfellow, 1982). In the Selwyn Basin, however, which hosts large stratiform Zn-Pb deposits, the pH of streams displays a large range because of variable carbonate contents. The Road River Group, which is host to several large deposits including the Howards Pass and Anniv deposits, is typically carbonate-rich whereas the Lower Earn Group, which also hosts major base metal deposits, is carbonate-poor and more pyritic. As a result, streams draining rocks of the Road River Group are buffered at an alkaline pH while those draining the pyritic shales of the Earn Group are commonly acidic. In some areas underlain by Earn Group strata, pH values as low as four have been measured due to generation of sulphuric acid by the oxidation of sulphides. Under these acidic conditions, both Pb and Zn are mobile in stream water and can therefore generate coincident hydromorphic anomalies. This thermodynamic prediction of Pb transport under low pH conditions is confirmed by high Pb contents measured in acidic streams draining the Tom and Nor stratiform Pb-Zn deposits (Goodfellow, 1983).

Figure 6. **a)** SEM-BSE showing a cross section of moss cellular structure, Pelly River deposit, sample 105I 859011; **b)** Same as (a) except different area; **c)** Blowup of (a) showing coalescing concentrically zoned cellular structures; **d)** Detail of (a) showing botryoidal structure infilled with smithsonite (1) and radially distributed calcite (2), and replaced by smithsonite (3) which is circled by hemimorphite (4). Black areas represent open space; **e)** SEM backscatter image of a circular interlocking network of hemimorphite. All of the smithsonite and calcite has been leached out except for one patch of calcite (1) in the bottom-left portion of the image; **f)** Minus-80 mesh (<177 microns) fraction of active sediment from a stream draining the Howards Pass deposit. White patch at bottom-center of diagram is a detrital galena grain. Other white grain and pale grey grains consist of sphalerite and secondary Zn minerals which have been eroded from the secondary zone overlying the sulphide deposit.

Table 3a. Field descriptions of samples from secondary zinc mineralization, Pelly River

Sample Numbers	Lithological Description
105I 845010	Creamy coloured calcite and smithsonite replacing layers of moss, giving the sample a cauliflower morphology.
105I 845011	Shale and chert talus cemented with calcite and smithsonite.
105I 859001	Creamy coloured calcite and smithsonite replacing several layers of moss.
105I 859002	As above except one metre up section from previous sample.
105I 859003	As above except two metres up section from sample 859001.
105I 859004	Black chert talus cemented with calcite and smithsonite.
105I 859006	Creamy coloured calcite and smithsonite replacing moss layers; morphology well preserved.
105I 859007	As above, except 0.5 metres up section from sample 859006.
105I 859008	Black shale and chert talus cemented by creamy-tan coloured Zn-carbonates.
105I 859009	Mixture of cemented talus and moss replaced by Zn-rich carbonates.
105I 859010	Creamy coloured Zn-rich carbonates replacing multiple layers of moss.
105I 859011	Alternating bands of cemented talus and replaced moss. Zn bound mostly in hemimorphite.
105I 859012	Black chert talus cemented with creamy coloured carbonate.
105I 859016	Black chert cemented with creamy-tan coloured hemimorphite.
105I 859017	Black chert cemented with creamy-tan coloured hemimorphite.

Table 3b. Major and trace element analyses of the Pelly River secondary Zn deposit.

Sample Number		Weight Percent										
		SiO_2	TiO_2	Al_2O_3	Fe_2O_{3T}	MnO	MgO	CaO	Na_2O	K_2O	H_2O_T	CO_2
105I	845010	26.3	0.11	0.9	1.1	0.7	0.26	36.9	n.d.	0.20	2.2	24.9
	845011	10.81	0.09	1.5	1.0	0.5	0.29	45.3	n.d.	0.34	2.9	32.3
105I	859001	3.62	0.01	0.35	3.71	2.36	0.27	45.2	0.01	0.10	3.6	34.5
	859002	2.05	0.01	0.25	1.35	0.17	0.19	50.2	0.01	0.07	2.2	41.3
	859003	1.56	0.01	0.27	0.27	0.05	0.20	53.7	0.01	0.11	1.2	43.1
	859004	10.3	0.07	1.48	0.66	0.05	0.43	46.7	0.02	0.45	1.8	36.4
	859005	69.8	0.41	7.14	2.08	0.02	1.79	4.16	0.11	2.57	2.0	4.3
	859006	4.78	0.03	0.63	0.55	0.07	0.30	48.2	0.01	0.20	1.9	37.7
	859007	2.95	0.02	0.43	0.43	0.03	0.29	50.4	0.03	0.16	1.6	40.4
	859008	42.0	0.29	5.78	1.99	0.08	1.08	20.5	0.09	1.51	3.6	15.5
	859009	32.5	0.19	3.67	1.56	0.12	0.63	21.3	0.06	0.97	6.3	17.1
	859010	19.4	0.11	2.34	1.93	0.11	0.57	31.9	0.03	0.57	5.6	24.9
	859011	33.4	0.10	2.59	1.64	0.16	0.57	10.0	0.04	0.61	12.3	7.6
	859012	64.6	0.32	5.85	8.69	0.01	0.65	0.97	0.02	1.05	7.1	0.0
	859016	73.0	0.29	5.95	2.22	0.04	0.46	1.29	0.08	1.10	4.2	0.0
	859017	62.9	0.41	7.23	2.90	0.04	0.88	1.38	0.08	1.88	6.2	0.3
		C-org	P_2O_5	S	Zn	Pb	Ni	Cd	Co	Mo	Ag	Cu
105I	845010	1.1	0.20	0.20	23660	11	1300	390	10	10	0.1	24
	845011	1.4	0.22	0.27	34550	3	1830	392	5	10	F0.1	30
105I	859001	0.7	0.30	0.25	26000	<2	1452	778	591	184	1.0	22
	859002	0.5	0.19	0.29	9950	4	325	402	23	4	1.1	14
	859003	0.3	0.12	0.29	5600	3	130	284	4	4	0.6	7
	859004	0.7	0.34	0.39	6000	6	216	233	3	4	0.5	13
	859005	2.5	0.30	0.77	650	133	36	5	4	16	0.5	29
	859006	1.1	0.16	0.31	9500	4	349	219	8	6	0.5	9
	859007	0.0	0.15	0.38	6800	2	191	182	4	2	0.7	6
	859008	1.1	0.98	0.27	17500	4	1116	221	14	6	0.9	55
	859009	1.0	0.44	0.27	60000	12	5810	265	13	8	1.5	48
	859010	0.6	0.30	0.17	50000	9	2490	260	16	6	0.5	30
	859011	1.7	0.40	0.17	185000	6	9160	121	18	14	4.3	110
	859012	3.4	1.59	0.25	1000	18	353	97	1	84	3.1	45
	859016	1.0	0.90	0.49	38000	10	1678	31	1	24	1.4	105
	859017	2.2	0.62	0.16	72000	8	3660	58	9	14	1.9	132

Notes: Zn, Pb, Ni, Cd, Co, Mo, Ag and Cu expressed in ppm;
all other elements or element oxides in wt.%.

Table 4. Chemical analyses of the minus-80 mesh fraction of stream sediments, Pelly River area

Sample Number		Cu	Pb	Zn	Mo	Co	Ni	Mn	Cd	Ag	Fe	V	Ba	P_2O_5
105I	842003	72	31	124	39	3	33	54	3.1	2.8	2.3	1120	2800	0.60
	842004	70	23	184	44	3	43	90	1.9	6.2	2.3	940	2000	0.90
	842005	201	20	1832	14	20	199	480	7.5	2.4	4.0	440	8350	1.04
	842006	186	21	1831	12	17	201	540	10.2	1.8	3.6	470	7200	1.27
	842007	187	22	2680	21	17	285	440	22.7	2.2	3.8	700	13000	1.43
	842008	117	16	778	11	8	95	248	8.8	1.6	2.7	560	6000	0.82
	842011	84	15	3050	16	6	270	248	34.1	1.0	2.3	880	7350	0.82
	842013	82	18	4930	16	7	671	640	24.5	1.6	2.0	600	2800	0.88
	842014	71	17	3200	6	9	253	232	17.6	0.9	2.9	440	4800	0.59
	842015	106	15	915	10	9	150	720	14.2	1.7	2.1	750	6100	0.85
	842017	156	16	2720	38	15	279	840	22.4	2.4	3.0	1000	8000	1.39
	842018	78	13	1369	22	16	211	770	18.5	1.1	3.6	430	7800	0.53
	842019	17	17	73	<1	7	18	580	<0.1	<0.1	2.6	90	1500	0.25
	842020	60	19	177	28	4	50	96	1.9	6.1	2.2	660	2300	0.81
	842022	61	29	125	41	2	20	54	4.0	3.9	2.7	1400	3500	0.72
	842023	62	23	160	38	4	49	100	2.2	6.2	2.2	720	2200	0.79
	842024	101	13	6000	8	10	528	440	37.7	0.8	2.6	290	3000	0.35
	842025	78	10	1809	20	10	190	440	12.8	1.0	2.7	440	8800	0.48
	842026	112	9	2520	10	9	287	180	15.8	1.0	2.6	320	5200	0.43
	842027	84	12	2930	24	7	170	148	31.0	1.4	1.8	1100	9600	0.72
	842028	62	11	873	36	8	85	600	16.4	1.1	2.2	680	14500	1.02
	842029	175	14	4940	40	23	349	760	44.5	1.2	2.8	700	7800	1.02
	842030	217	13	5980	44	27	499	880	57.6	1.5	2.8	700	8000	1.11
	842031	93	11	1905	22	7	200	96	24.6	1.3	2.3	700	7500	0.90
	842032	257	16	25540	22	18	1707	2000	90.3	2.9	1.9	820	5400	2.17
	842033	103	14	4270	46	22	298	760	41.6	1.4	3.1	700	9500	0.76
	842034	65	12	3660	14	12	399	440	38.1	0.8	2.6	400	8000	0.53
	842035	403	23	2370	52	16	252	285	25.8	2.9	3.6	1650	15750	1.10
	842036	112	29	1253	28	18	106	280	16.3	1.2	4.3	500	430	0.51
	842037	20	12	75	2	9	15	1000	<0.1	<0.1	2.6	105	1000	0.23

Notes: - P_2O_5 expressed as wt.%
- all other elements in ppm

Table 5. Chemical analyses of stream water, Pelly River area

Sample Number		Zn	Mn	Fe	U	F	Ca	Mg	CO_3	SO_4	Cl	pH
105I	842002	2	<5	<10	0.30	<20	0.2	0.1	1.0	1.4	0.21	4.3
	842003	10	<5	<10	0.02	<20	0.4	0.3	1.0	2.4	0.25	4.6
	842004	26	<3	<10	0.01	<20	0.8	0.4	1.0	4.4	0.12	4.5
	842005	103	<5	<10	2.40	200	29	18	122	29	0.22	8.1
	842006	94	<5	<10	3.20	320	36	20	135	38	0.20	8.1
	842007	62	<5	<10	1.90	160	22	13	86	25	0.16	8.0
	842008	19	<5	<10	1.70	150	19	12	76	22	0.24	8.0
	842009	22	<5	<10	9.00	230	66	35	217	94	0.90	8.4
	842010	36	<5	<10	0.01	330	45	24	191	29	0.25	8.4
	842011	363	<5	<10	1.68	260	32	18	99	62	0.35	7.8
	842012	209	<5	<10	5.00	330	36	19	123	55	0.18	7.9
	842013	393	<5	<10	4.60	540	56	25	195	56	0.27	8.4
	842014	67	<5	<10	1.70	200	27	15	118	18	0.25	8.2
	842015	72	<5	<10	5.00	400	39	21	149	48	0.27	8.3
	842016	60	<5	<10	7.20	540	80	42	297	79	0.23	8.4
	842017	203	<5	<10	1.90	260	25	14	105	17	0.13	7.8
	842018	2	<5	<10	2.80	240	28	15	114	24	0.11	8.2
	842019	36	11	<10	0.03	53	1.0	0.1	1.0	6	0.10	4.5
	842022	47	27	<10	0.07	72	1.7	0.6	0.1	10	0.24	4.2
	842023	192	38	22	0.09	180	3.5	0.8	1.0	26	0.21	4.1
	842024	1604	<5	<10	3.9	580	45	25	155	80	0.24	7.9
	842025	27	<5	<10	7.0	420	61	32	191	103	0.23	8.2
	842026	235	<5	<10	11.4	420	55	28	175	84	0.29	8.3
	842027	1094	<5	<10	6.4	370	41	19	132	16	0.27	8.1
	842028	146	<5	99	0.34	80	3.1	1	1.0	2.6	0.19	6.3
	802029	770	<5	<10	7.2	580	56	22	137	99	0.22	8.1
	842030	829	18	<10	7.6	600	56	22	140	105	0.20	8.1
	842031	73	<5	<10	3.7	860	39	14	101	69	0.23	8.2
	842032	1407	<5	<10	9.6	640	50	24	131	115	0.21	8.0
	842033	531	<5	<10	2.5	320	32	17	113	39	0.16	7.8
	842034	566	<5	<10	10.2	500	77	32	229	103	0.25	8.2
	842035	195	<5	<10	2.1	115	19	9.5	53	36	0.09	7.8
	842036	20	<5	<10	4.0	92	25	16	102	33	0.15	8.1

Notes: Zn, Mn, Fe, U and F expressed in ppb; all other elements in ppm.

Table 6. Average, minimum and maximum geochemical values for stream, spring and pore waters from the Howards Pass and Anniv Zn-Pb deposits, and from the Pelly River secondary Zn deposit.

AREA	Zn	Pb	Cd	CO_3	SO_4	SiO_2	pH	Ni
HOWARDS PASS (seeps)								
Average	156	2.8	1.6	49	49	1.9	7.9	n.d.
Maximun	1397	15	14	115	287	4.3	8.5	n.d
Minimum	3	2.0	0.3	0.6	2	0.15	4.7	n.d
HOWARDS PASS (streams)								
Average	114	< 3.1	< 1.1	82	25	n.d.	7.6	n.d
Maximum	1815	14	11	221	70	n.d.	8.5	n.d
Minimum	1	< 2.0	< 0.5	0	16	n.d.	4.7	n.d.
HOWARDS PASS (pore waters)								
Average	3583	37	n.d.	152	166	6.5	8.2	81
Maximum	13260	110	n.d.	223	216	9.5	8.5	204
Minimum	131	2	n.d.	98	82	4.2	7.8	23
ANNIV (stream)								
Average	284	n.d.	n.d.	42	19	n.d.	7.7	n.d.
Maximum	1369	n.d.	n.d.	124	121	n.d.	8.2	n.d.
Minimum	2	n.d.	n.d.	0.6	19	n.d.	6.1	n.d.
PELLY RIVER (stream)								
Average	323	n.d.	n.d.	60	45	n.d.	7.3	n.d.
Maximum	1604	n.d.	n.d.	137	115	n.d.	8.4	n.d.
Minimum	2	n.d.	n.d.	0.1	2	n.d.	4.1	n.d.

Notes: - Zn, Pb, Cd and Ni in ppb; all other elements expressed in ppm
n.d. = not determined

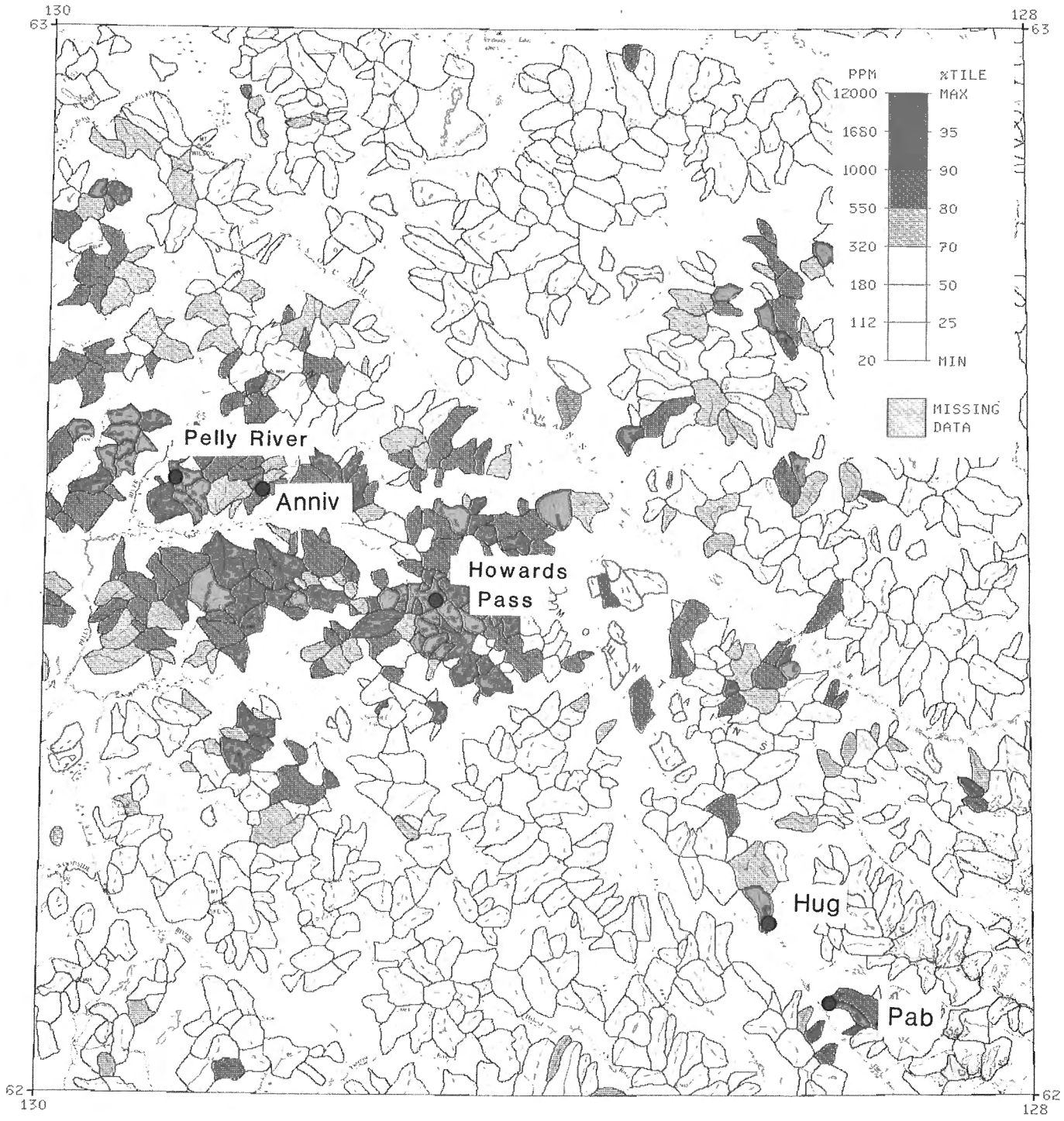

Figure 7. Catchment basin map of the Nahanni map area highlighting basins drained by streams containing sediment which are anomalous in Zn (Ellwood et al., 1986 from data published by Goodfellow, 1982).

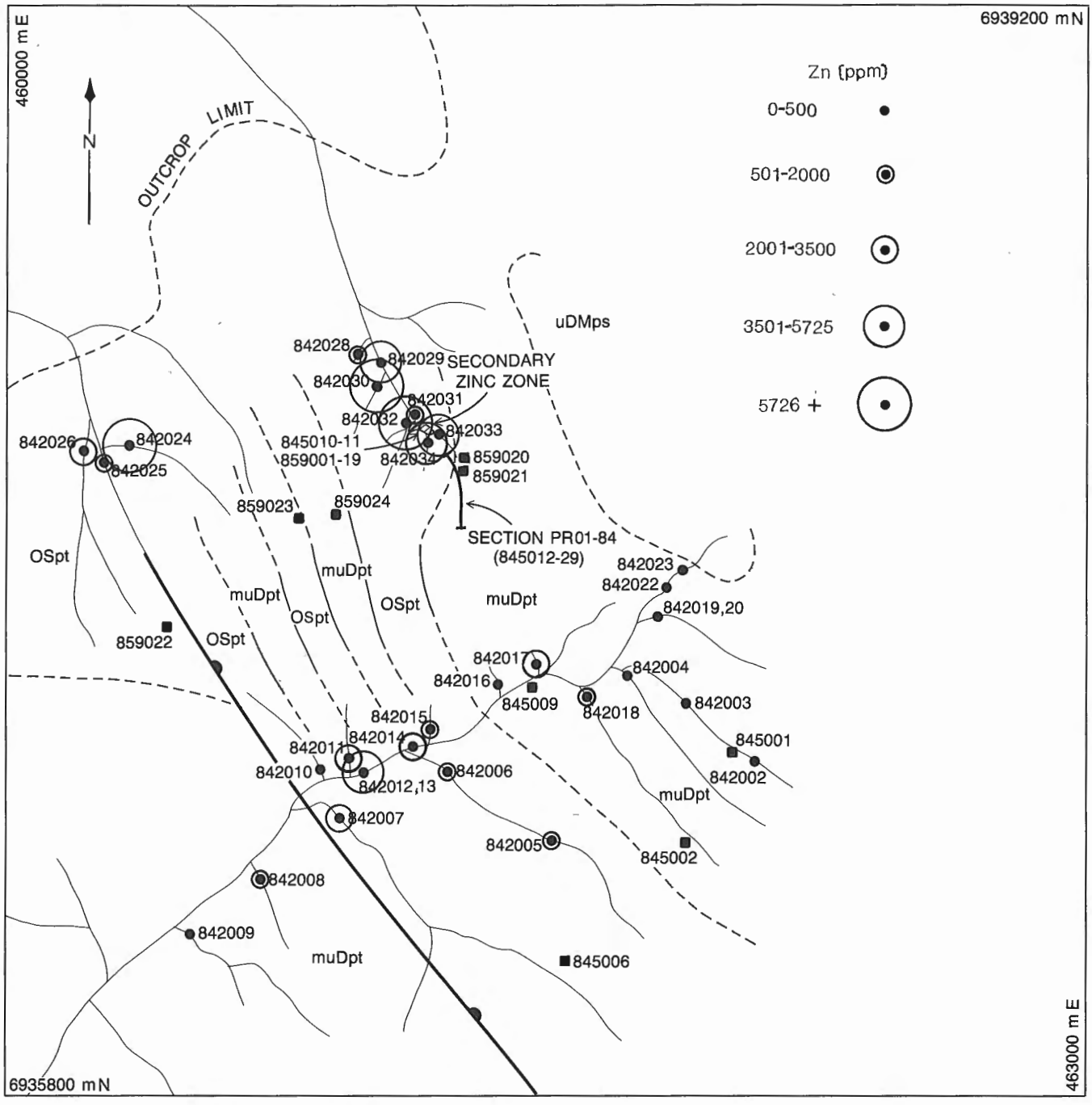

Figure 8. Symbol map of the Pelly River area showing the distribution of Zn in the minus-80 mesh fraction of stream sediment. Raw chemical data for all elements determined are listed in Table 4.

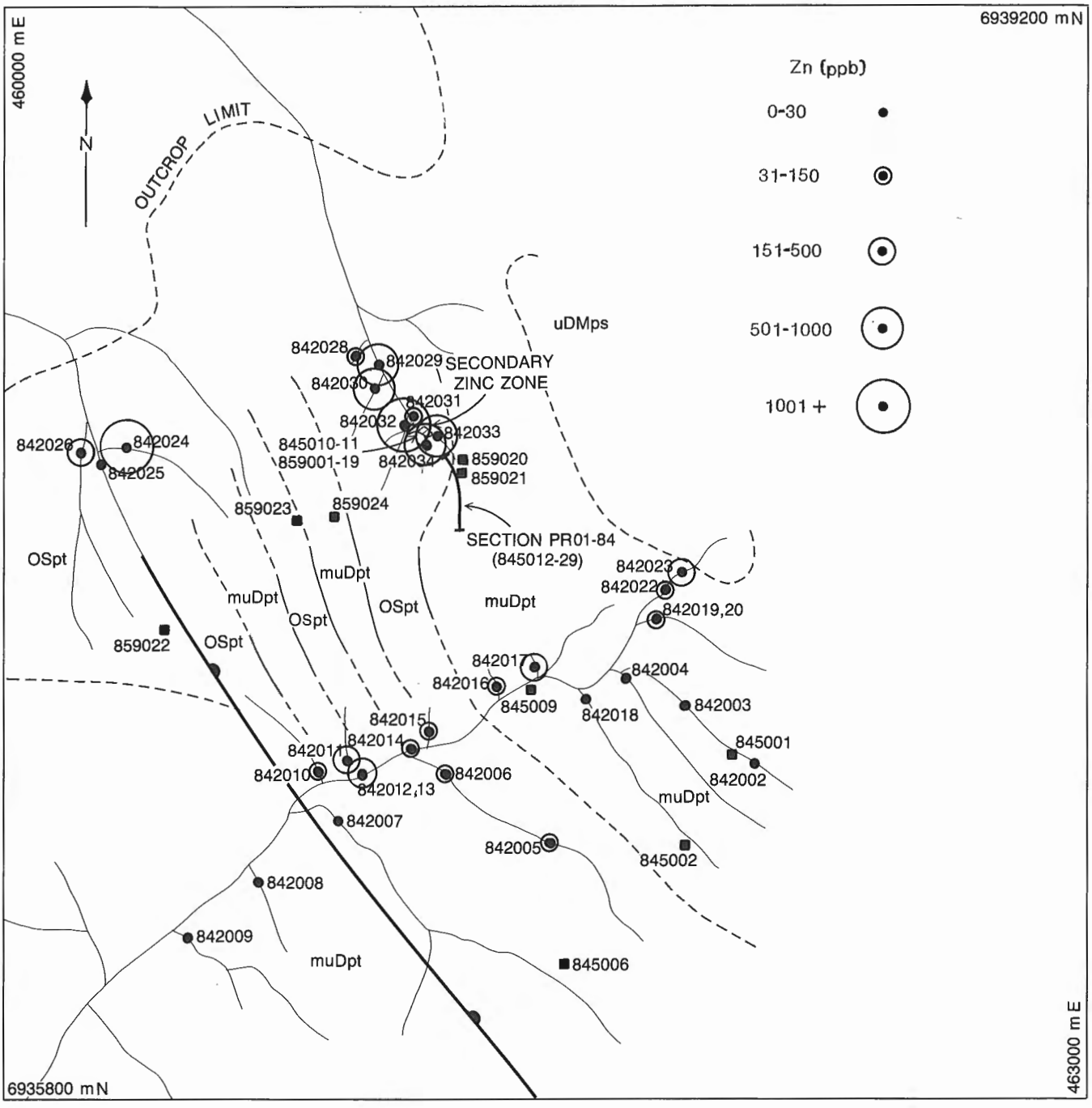

Figure 9. Symbol map of the Pelly River area showing the distribution of Zn in stream water. Raw chemical data for all elements determined are listed in Table 5.

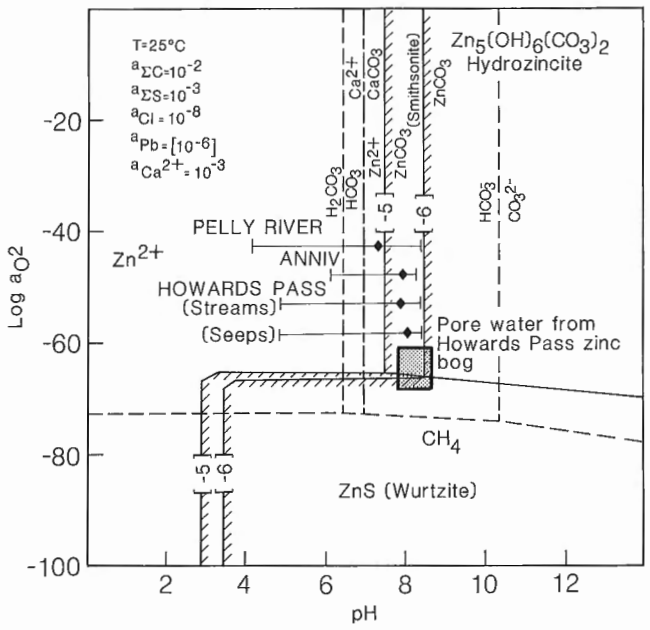

Figure 10. Log $^aO_2$-pH predominance field diagram of aqueous and mineral species in the Zn-Ca-C-S-Cl system. Thermodynamic data from Helgeson (1969), Sangameshwar and Barnes (1983) and Fouillac and Criaud (1984). Stability fields were calculated and plotted using SOLUPLOT which was written by C.M. Bethke (unpublished report, Pennsylvania State University, 1981). Activities of all ligands were calculated from measured data by computer program EQ3NR (Wolery, 1983).

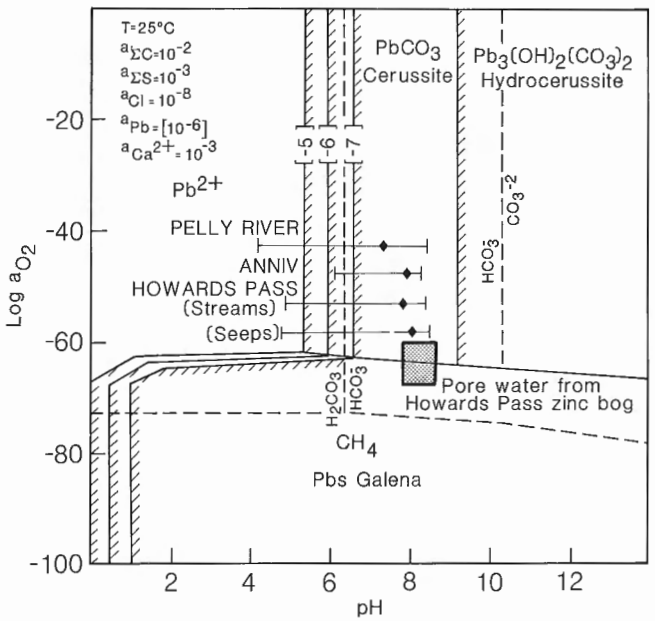

Figure 11. Log $^aO_2$-pH predominance field diagram of aqueous and mineral species in the Pb-Ca-C-S-Cl system. Thermodynamic data from Helgeson (1969), Sangameshwar and Barnes (1983) and Fouillac and Criaud (1984). Stability fields were calculated and plotted using SOLUPLOT which was written by C.M. Bethke (unpublished report, Pennsylvania State University, 1981). Activities of all ligands were calculated from measured data by computer program EQ3NR (Wolery, 1983).

CONCLUSIONS

1. Under alkaline pH conditions, such as those measured in streams draining calcareous rocks of the Road River Group which host Early Silurian stratiform Zn-Pb deposits (e.g. Howards Pass and Anniv deposits), Zn is dispersed in solution whereas Pb is not. The separation of Zn from Pb in the secondary environment is due to their different chemical behaviours at high pH. Stream anomalies generated under these conditions are typically Zn-rich and Pb-poor except where the deposit is exposed and sulphides and/or their oxidation products are dispersed by clastic processes.

2. Because ground waters penetrate fractured rocks well below the surface before discharging at the break in slope, elements transported in solution (e.g. Zn) offer an important advantage over chemically immobile elements (e.g. Pb) in detecting stratiform Zn-Pb deposits concealed at depth. This is particularly true for highly alkaline waters due to the precipitation of Pb as a carbonate under these conditions. As a result, areas drained by streams with high Zn but low Pb contents should not be excluded from follow-up investigation by exploration geologists but instead should be evaluated for shallowly buried stratiform Zn-Pb mineralization using ore-forming and ore-associated elements which are commonly dispersed more widely in host rocks.

3. A secondary Zn deposit was discovered in the Pelly River area by following up a high-Zn and low-Pb stream sediment anomaly outlined by a regional geochemical survey of the Nahanni map area (Goodfellow, 1982). Other areas in the Selwyn Basin drained by streams with similar geochemical characteristics also have a high potential to host stratiform Zn-Pb mineralization.

4. The mineralogical and chemical similarities of the Pelly River secondary zone to secondary Zn mineralization overlying the Howards Pass deposit combined with its occurrence near the horizon which hosts Early Silurian deposits elsewhere in the Nahanni map sheet, indicate that the source of Zn is probably stratiform Zn-Pb mineralization. Further support for this conclusion is provided by high Zn, Cd and P_2O_5 contents of carbonaceous shales just upstream from the secondary Zn zone.

ACKNOWLEDGMENTS

Many of my colleagues at the GSC contributed technically to this paper and I am very grateful for their efforts. G.R. Lachance and G.E.M. Hall supervised chemical analyses of rock, sediment and water samples; D.A. Walker and R.N. Delabio contributed to mineral identifications and analyses; G.F. Bonham-Carter assisted during the field operations; R.D. Lancaster supervised drafting of some of the diagrams; and I.R. Jonasson reviewed the paper and offered many helpful suggestions.

REFERENCES

Bonham-Carter, G.F. and Goodfellow, W.D.
1986: Background corrections to stream geochemical data using digitized drainage and geological maps: application to Selwyn Basin, Yukon and Northwest Territories; Journal of Geochemical Exploration, v. 25, p. 139-155.

Ellwood, D.J., Bonham-Carter, G.F., and Goodfellow, W.D.
1986: An automated procedure for catchment basin analysis of stream geochemical data: Nahanni River map area, Yukon and Northwest Territories; Geological Survey of Canada, Paper 85-26.

Fouillac, C. and Criaud, A.
1984: Carbonate and bicarbonate trace metal complexes: critical re-evaluation of stability constants; Geochemical Journal, v. 18, p. 297-303.

Goodfellow, W.D.
1982: Regional stream sediment and water geochemistry of the Nahanni map-area (NTS 105I), Yukon and Northwest Territories (National Geochemical Map NGR 51-1981); Geological Survey of Canada, Open File 868.
1983: Stream sediment and water geochemistry of the Howards Pass (XY) Zn-Pb deposit and Nor Zn-Pb-Ba occurrence, Selwyn Basin, Yukon and Northwest Territories; Geological Survey of Canada, Open File 845, 27 p.
1984: Geochemistry of rocks hosting the Howards Pass (XY) strata-bound Zn-Pb deposit, Selwyn Basin, Yukon Territory, Canada; *in* Proceedings of the Sixth Quadrennial IAGOD Symposium, E. Schweizerbart'sche Verlagsbuchhandlung (Nagele u. Obermiller), Stuttgart, Germany, p. 91-112.

Goodfellow, W.D. and Jonasson, I.R.
1986: Environment of formation of the Howards Pass (XY) Zn-Pb deposit, Selwyn Basin, Yukon; *in* Mineral Deposits of Northern Cordillera, ed. J.A. Morin CIMM Special Volume 37, p. 19-50.

Goodfellow, W.D., Jonasson, I.R., and Morganti, J.M.
1983: Zonation of chalcophile elements about the Howards Pass (XY) Zn-Pb deposit, Selwyn Basin, Yukon; Journal of Geochemical Exploration, v. 19, p. 503-542.

Gordey, S.P.
1978: Stratigraphy and structure of the Summit Lake area, Yukon and Northwest Territories. *in* Current Research, Geological Survey of Canada, Paper 78-1A, p. 43-48.
1981: Geology of Nahanni map area, Yukon Territory and District of Mackenzie; Geological Survey of Canada, Open File 780.

Helgeson, H.C.
1969: Thermodynamics of hydrothermal systems at elevated temperatures and pressures; American Journal of Science, v. 267, p. 729-804.

Jonasson, I.R., Goodfellow, W.D., Walker, D.A., and Jackson, L.E. Jr.
—: Secondary zinc mineralization in post-glacial sediments and talus at Howards Pass, Yukon, Canada — mineralogy, geochemistry and genesis; *in* Weathering, its Products and Deposits, ed. S.S. Augustithis Theophrastus Publications, Greece, 55 p. in press.

Lee, J., Jonasson, I.R., and Goodfellow, W.D.
1984: Metal accumulation by byrophytes in some zinc-rich blanket bogs, Selwyn Mountains, Yukon Territory; Canadian Journal of Botany, v. 62, p. 722-728.

Sangameshwar, S.R. and Barnes, H.L.
1983: Supergene processes in zinc-lead-silver sulfide ores in carbonates; Economic Geology, v. 78, p. 1379-1397.

Tempelman-Kluit, D.J.
1981: Geology and mineral deposits of southern Yukon; *in* Yukon Geology and Exploration 1979-80, Department of Indian Affairs and Northern Development (Canada), Exploration and Geological Services Division, Whitehorse, Yukon, p. 1-31.

Wolery, T.M.
1983: EQ3NR — a computer program for geochemical aqueous speciation — solubility calculations: user's guide and documentation; Lawrence Livermore Laboratory, University of California, 89 p.

Revised stratigraphy and structure in the Thompson-Shuswap-Okanagan map area, southern British Columbia

Andrew V. Okulitch
Institute of Sedimentary and Petroleum Geology, Calgary

Okulitch, A.V., Revised stratigraphy and structure in the Thompson-Shuswap-Okanagan map area, southern British Columbia; in Current Research, Part E, Geological Survey of Canada, Paper 89-1E, p. 51-60, 1989.

Abstract

Revisions to stratigraphy and structure of the Thompson-Shuswap-Okanagan map area are based on compilation of studies made in the area since 1979 and current fieldwork. Strata west of the complex had been correlated with Hadrynian to Upper Triassic units in the Kootenay Arc, east of the complex. New data indicate that the Tsalkom, Sicamous and Eagle Bay formations are Cambrian to Devonian and that the Silver Creek Formation may be Precambrian.

The South Fosthall Pluton, originally dated as Ordovician, is now known to be Eocene. The Whiterocks Mountain syenite, once correlated with Paleocene intrusions, is a complex of Jurassic suites.

The contact between the Tsalkom and Silver Creek formations is interpreted as a Mesozoic thrust fault. That between the Sicamous and Eagle Bay formations is interpreted to be a deformed stratigraphic contact.

Eocene volcanic rocks southwest of Shuswap Lake have been tilted on north-trending normal faults that may be associated with a major west-dipping detachment fault.

Résumé

Les révisions apportées à la stratigraphie et à la structure de la région cartographique de Thompson, Shuswap et Okanagan, sont basées sur la compilation d'études faites dans le secteur depuis 1979 et sur des travaux de terrain récents. À l'ouest du complexe de Shuswap, on a corrélé des strates avec les unités allant de l'Hadrynien au Trias supérieur dans l'arc de Kootenay à l'est du complexe. De nouvelles données indiquent que les formations de Tsalkom, Sicamous et Eagle Bay sont d'âge cambrien à dévonien et que la formation de Silver Creek peut être précambrienne.

Le pluton de South Fosthall, initialement attribué à l'Ordovicien, est maintenant placé dans l'Éocène. La syénite de Whiterocks Mountain, autrefois corrélée avec les intrusions d'âge paléocène, est un complexe de séries jurassiques.

On a interprété le contact entre les formations de Tsalkom et de Silver Creek comme étant une faille chevauchante d'âge mésozoïque. Le contact entre les formations de Sicamous et d'Eagle Bay est considéré comme un contact stratigraphique déformé.

Les roches volcaniques d'âge éocène situées au sud-ouest du lac Shuswap ont basculé le long des failles de direction nord, qui sont peut-être associées à une faille de décollement importante, inclinée vers l'ouest.

INTRODUCTION

Significant advances in the understanding of regional tectonics and ages of rock units in southern British Columbia as well as active mineral exploration, require revision of Open File 637 (Okulitch, 1979). Selected areas in the Thompson-Shuswap-Okanagan map area (Fig. 1) were re-examined, and data published since 1979 were integrated to make these revisions. Several current projects in the area (M. Bardoux, R.L. Brown, S.D. Carr and B. Johnson of Carleton University, pers. comm., 1988) continue to clarify understanding of the geological evolution, but data and working hypotheses from these, although generously shared and discussed, are specifically excluded from this report. The geology of the Clearwater and Vavenby areas and east and west of southern Adams Lake (Schiarizza and Preto, 1984; Schiarizza, 1983; 1986) has been extensively revised; these revisions are not repeated here in detail.

STRATIGRAPHY

The ages of units within the Shuswap Assemblage (now part of the Shuswap Metamorphic Complex as redefined in Okulitch, 1984) remain unknown, although tentative correlation of the western part of the complex within the map area with Hadrynian clastic strata of the Horsethief Creek Group has been suggested (e.g. Journeay and Brown, 1986).

The Silver Creek, Tsalkom, Sicamous and Eagle Bay formations (Jones, 1959) are largely unfossiliferous and not amenable to isotopic dating; correlations were based on regional lithological comparisons only.

The age of the Silver Creek Formation (PP_{SC}) remains uncertain; it is likely pre-Ordovician, being the probable host unit to the Little Shuswap Gneiss ($_{L}Ogn$) (Okulitch, 1985). Typical lithologies in the Silver Creek Formation (quartzite, mica schist and minor amphibolite and marble) occur within Lower Cambrian and Hadrynian strata in northern parts of the Shuswap Complex and in the Kootenay Arc, and in Proterozoic (Aphebian or Helikian) platformal strata in the Monashee Complex (Journeay and Brown, 1986). Any correlations remain tenuous.

The structurally overlying Tsalkom Formation ($C\text{-}O_T$) of ultramafic to intermediate (mostly basic) metavolcanic rocks was postulated to be of Permian age, correlative with the Kaslo Group in the Kootenay Arc and the Fennell Formation in the northwestern corner of the map area. The lithological correlation was influenced by the proposed correlation of overlying pelites of the Sicamous Formation with Triassic strata. However, additional comparisons among the Tsalkom and Fennell formations and Cambro-Ordovician volcanics in the Kootenay Arc (Jowett Formation), as well as revision of the probable age of the Sicamous Formation (see below), suggest that the Tsalkom Formation is equivalent to the Jowett Formation of the Kootenay Arc.

The calcareous pelites of the Sicamous Formation ($C\text{-}O_S$) also remain undated. The formation was correlated, on the basis of apparent continuity across an area of limited exposure west of the southern end of Adams Lake through a possible facies change from calcareous to non calcareous

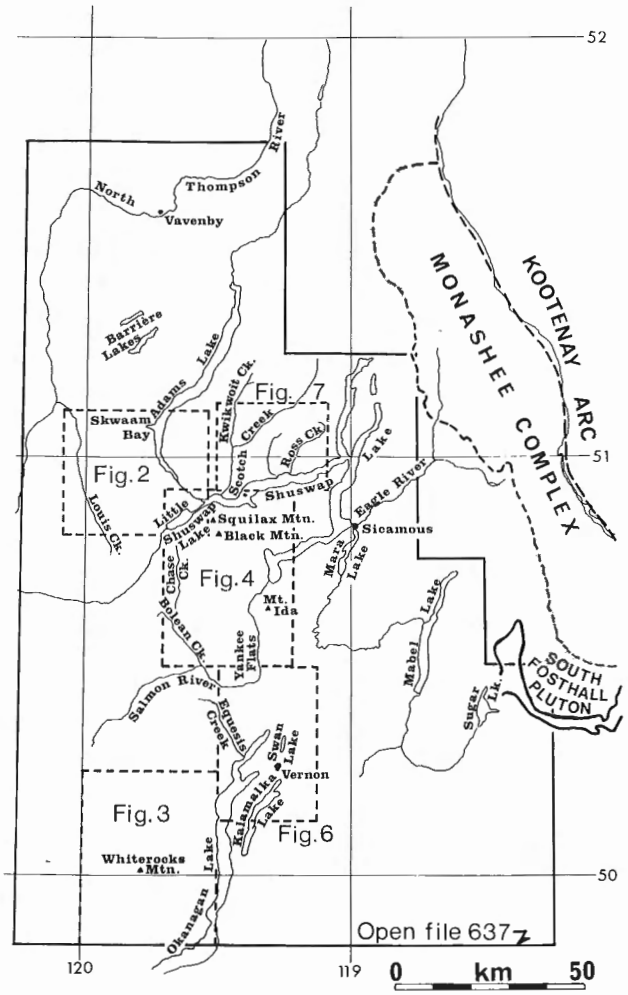

Figure 1. Geographic features of the study area and locations of revised maps (Figures 2, 3, 4, 6 and 7). Distribution of the South Fosthall Pluton from Parrish et al. (1988). Legend for symbols on all figures in Table 1.

pelite, with fossiliferous Upper Triassic strata. Overlying metavolcanic strata in stratigraphic continuity with the Sicamous Formation were suggested to be equivalent to those of the Nicola Group (TrJ_N) and not part of the Eagle Bay Formation as previously mapped (Jones, 1959). However, after additional study, no obvious stratigraphic or structural break is apparent between these metavolcanics and structurally higher units of the Eagle Bay. Comparison of the Sicamous Formation with pelites of the Cambro-Ordovician Index Formation and Upper Triassic Slocan Group in the Kootenay Arc, has suggested greater similarity with the Index rather than the Slocan (P.B. Read, pers. comm., 1982). The metavolcanic unit tentatively assigned to the Nicola Group is returned to the Eagle Bay Formation. The Sicamous Formation is correlated with lower Paleozoic strata of the Kootenay Arc. Schiarizza and Preto (1984) correlated pelitic strata west of southern Adams Lake (Fig. 2) with dated Carboniferous units immediately to the north. It is possible that pelites of both Carboniferous and Cambro-Ordovician age are present in this area. Without paleontological confirmation, correlations and age assignments remain speculative.

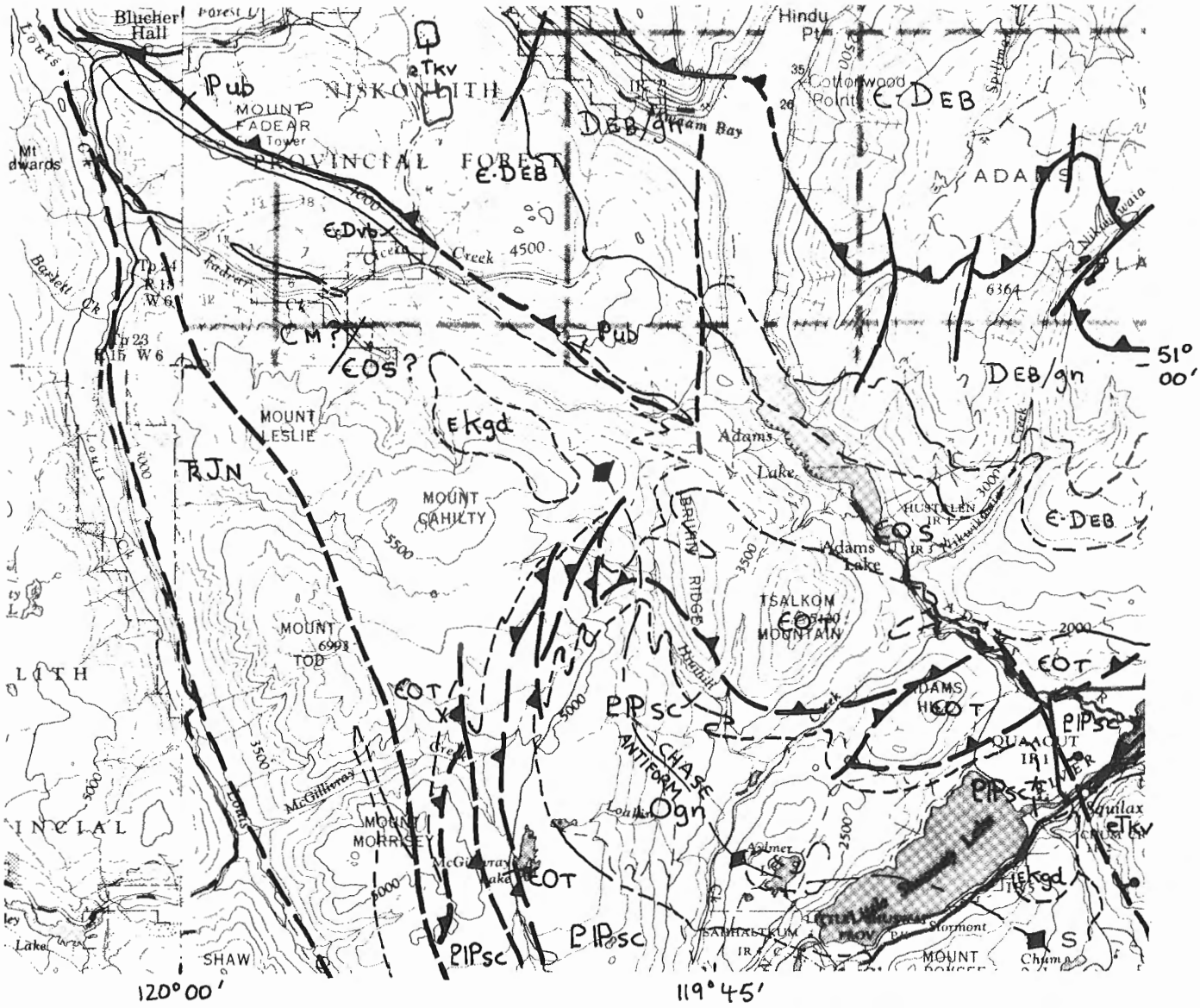

Figure 2. Revisions of geology west of southern Adams Lake and Adams River. Data in the northern half from Schiarizza and Preto (1984). Scale = 1:250 000. See Table 1.

The Eagle Bay Formation ($C\text{-}D_{EB}$) was correlated with formations of the Cambro-Ordovician Lardeau Group, Kootenay Arc, on the basis of its pre-Late Devonian age (Okulitch et al., 1975) and considerable lithological similarities. The Tshinakin Limestone member ($lC\text{-}_T$) was suggested to be a possible equivalent of the Lower Cambrian Badshot Formation. Archaeocyathids and other fauna from the Tshinakin Limestone near Vavenby collected by P. Schiarizza, have confirmed its Early Cambrian age (B.S. Norford unpublished internal report, Geological Survey of Canada, 1985). Felsic tuff (D_{EB}) near Skwaam Bay, Adams Lake is Devonian (387 $\pm$ 4 Ma) (R.L. Armstrong, pers. comm., 1981). Felsic volcanics east of Adams Lake are likely part of this unit and include foliated granitic rocks (D_{EB}/gn) that may be coeval and cogenetic with them and the mid-Devonian Mount Fowler Batholith ($_LDg$). This unit is interpreted to be stratigraphically high in an overturned and over-thrust succession, and no equivalent to this unit occurs in the Kootenay Arc beneath unconformably overlying Carboniferous strata of the Milford Group. The age range and lithological diversity of this formation suggest that it should be raised to group status, and this will be initiated in a later paper.

Carboniferous clastic strata near Clearwater and the Barrière lakes, and west of Adams Lake were assigned to the Milford Group (C_M) of the Kootenay Arc because of lithological and faunal similarities (Okulitch and Cameron, 1976). Although subsequently included in the Eagle Bay Formation (Schiarizza, 1983; Schiarizza and Preto, 1984), the clear age differences, lithological distinctions and possible differing structural histories (cf. Okulitch, 1985, p. 1422 for discussion of this last point) support treatment of these units as separate stratigraphic entities.

With the exception of the enigmatic Silver Creek Formation, this succession is presently considered correlative to lower to mid-Paleozoic strata of the Kootenay Arc, in keeping with suggestions made by Dawson (1898). Correlations to the north remain less certain but the lower to mid-Paleozoic parts of the Snowshoe, Cariboo and Black Stuart

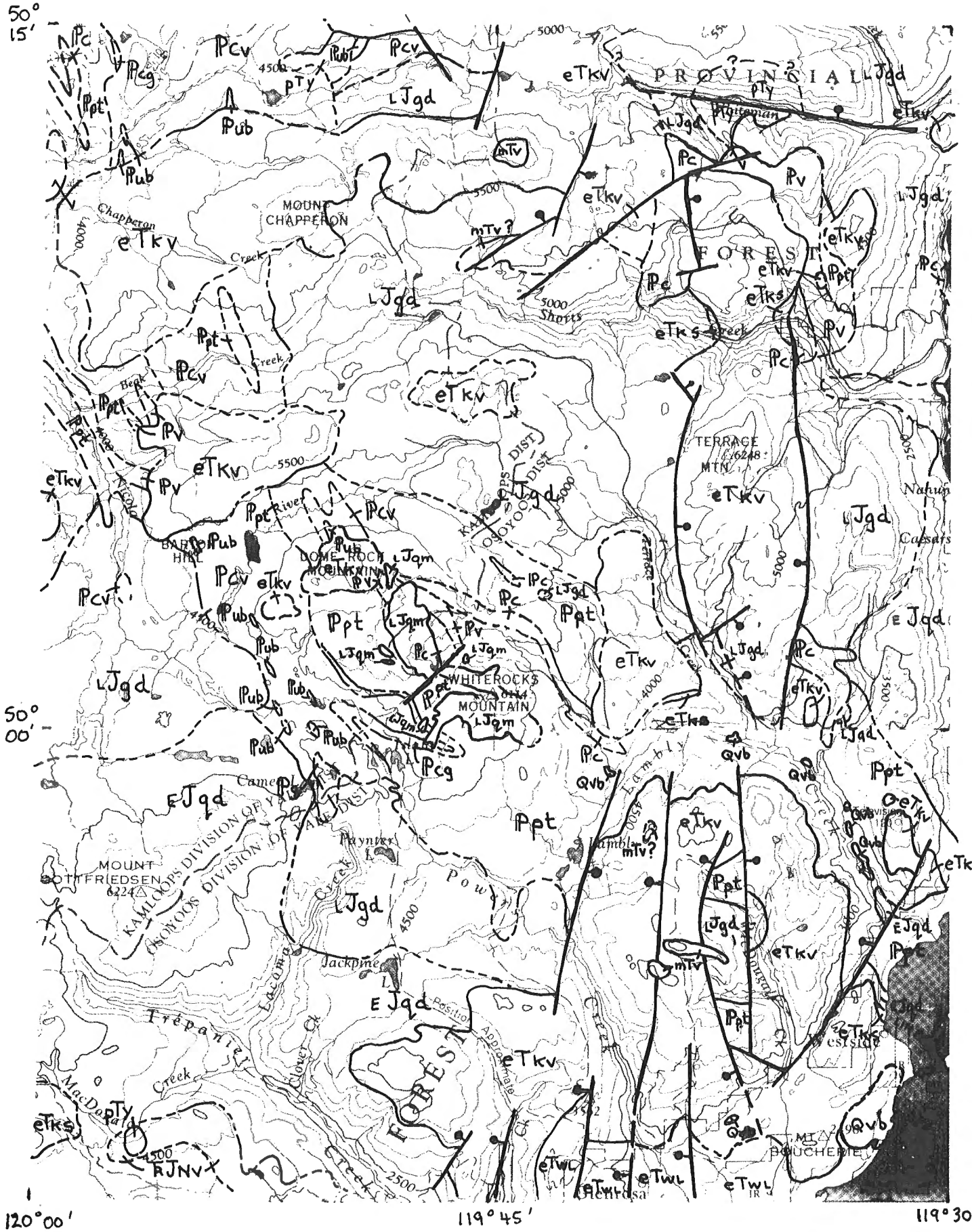

Figure 3. Revisions of geology west of Okanagan Lake. Data from the Whiterocks Mountain area from Mehner (1982). Data for Eocene volcanic rocks from Church (1980a, b). Scale = 1:250 000. See Table 1.

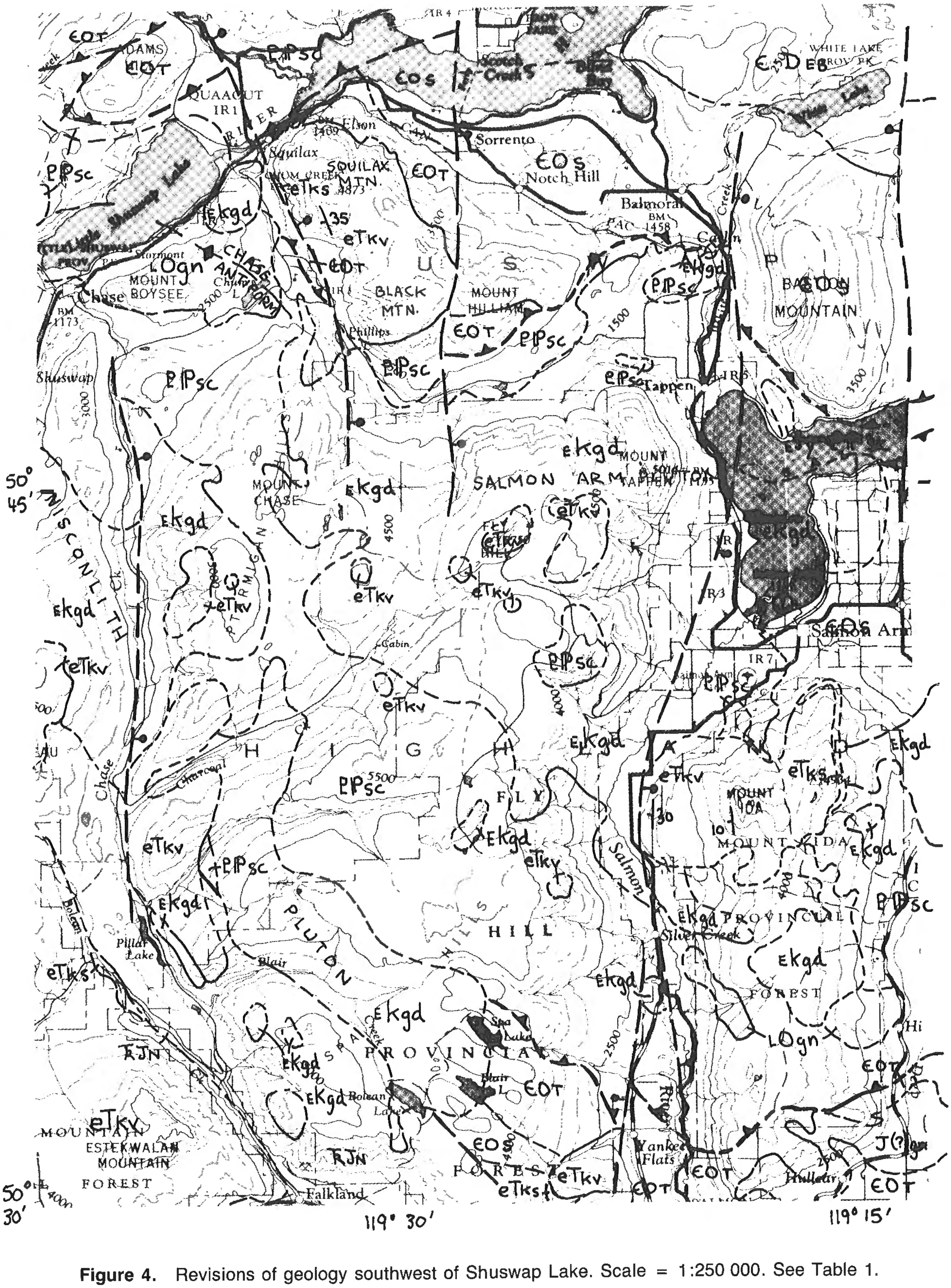

Figure 4. Revisions of geology southwest of Shuswap Lake. Scale = 1:250 000. See Table 1.

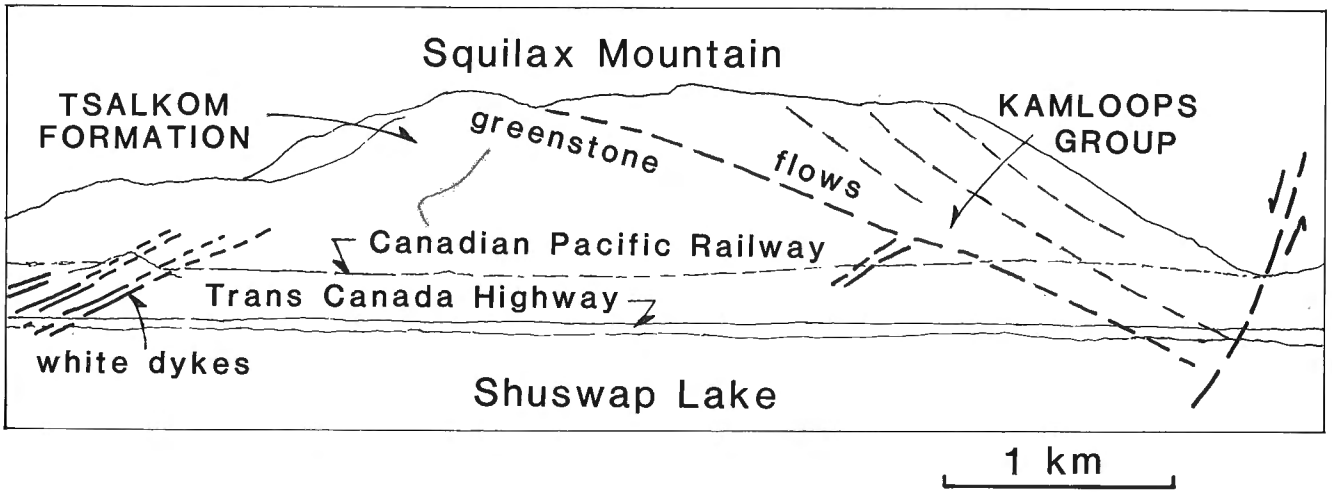

Figure 5. Composite sketch from photographs of Squilax Mountain. View facing south from the delta of the Adams River.

groups in the Quesnel Lake region (Struik, 1988) are probable candidates.

The Fennell Formation is now known to include volcanic flows, chert and minor clastics of pre-mid-Devonian, Carboniferous and Permian ages (Schiarizza and Preto, 1984).

PLUTONISM

The ages of most plutons in the map area remain unchanged by subsequent work. There are two significant exceptions. The South Fosthall Pluton, in the southeastern part of the map area (Fig. 1), was initially assigned a Late Devonian age on the basis of preliminary analyses (subsequently refined to be Ordovician; Okulitch, 1985). All subsequent isotopic ages obtained in the vicinity of the sample site were Eocene and it has been suggested to be a large glacial erratic exposed in a small roadcut (Parrish et al., 1988). Alternately, it may be a large xenolith. The source pluton presumably lies within the Monashee Complex to the north at higher elevations, or at depth, but has not been found. Foliated plutons to the west in the Mabel and Sugar lakes area designated as possibly of Jurassic age are extensions of the Eocene granitic suite (Parrish et al., 1988). Foliated leucocratic intrusions (the Silver Star Intrusions of Jones, 1959) still farther west near Vernon and north to Mara Lake, are likely of Eocene age (eTgn) (e.g. Solberg, 1976).

The "syenite" stock in the southwestern corner of the map area at Whiterocks Mountain (Fig. 3) was suggested to be of Paleocene age on the basis of similarity to the Paleocene to Eocene Coryell intrusives. Detailed studies by Osatenko (1979), Wilkins (1981) and Mehner (1982) have indicated that the stock is a small intrusive complex of alkalic and calc-alkalic suites with units of syenite-monzonite, pyroxenite and quartz monzonite. Isotopic analyses (Rb-Sr whole rock, U-Pb zircon; R.L. Armstrong, pers. comm., 1988) indicated that the alkalic and calc-alkalic suites are about 145-154 Ma in age (Late Jurassic).

STRUCTURE

The nature of several major fault zones in the map area has been revised by changes in regional correlation of units, by the application of new tectonic models and remapping of select localities. If the present assignment of the Sicamous Formation to lower Paleozoic successions is correct, then a fault must separate it from Triassic pelitic and volcanic strata to the west and southwest (Fig. 3). This fault would presumably extend east-northeast of and parallel to the major fault zone along the North Thompson River, Louis, Bolean and Equesis creeks and be part of that zone. Its exact location is uncertain in that poorly exposed area, and it is placed east of augite porphyries of the Nicola Group.

A thrust fault was postulated to separate the Sicamous Formation and overlying metavolcanics possibly of the Nicola Group, from the structurally overlying Eagle Bay Formation. The structure was necessary if the Sicamous was of Triassic age. Inclusion of the Sicamous in the Cambrian to Devonian succession correlative with strata of the Kootenay Arc does away with the need for such a hypothetical structure. Although similar features have been mapped within the Eagle Bay Formation (Schiarizza and Preto, 1984; Schiarizza, 1986), and others may be expected within a tightly folded and sheared structural succession such as the Sicamous and Eagle Bay formations, few can be reliably mapped and one has not been detected at this level.

The contact between the Silver Creek and Tsalkom formations was suggested to be an unconformity; however, this is unlikely because the contact is a gently folded surface (the Chase Antiform and associated folds to the east) whereas formations above and below the contact contain isoclinal to open polyphase structures (Fig. 4). The contact was interpreted to be a folded low angle fault (Okulitch, 1984), possibly an east-directed thrust; however, the sense of relative motion on this shear zone remains uncertain. Interdigitations of the Silver Creek and Tsalkom formations, interpreted as tight folds, are presently suggested to

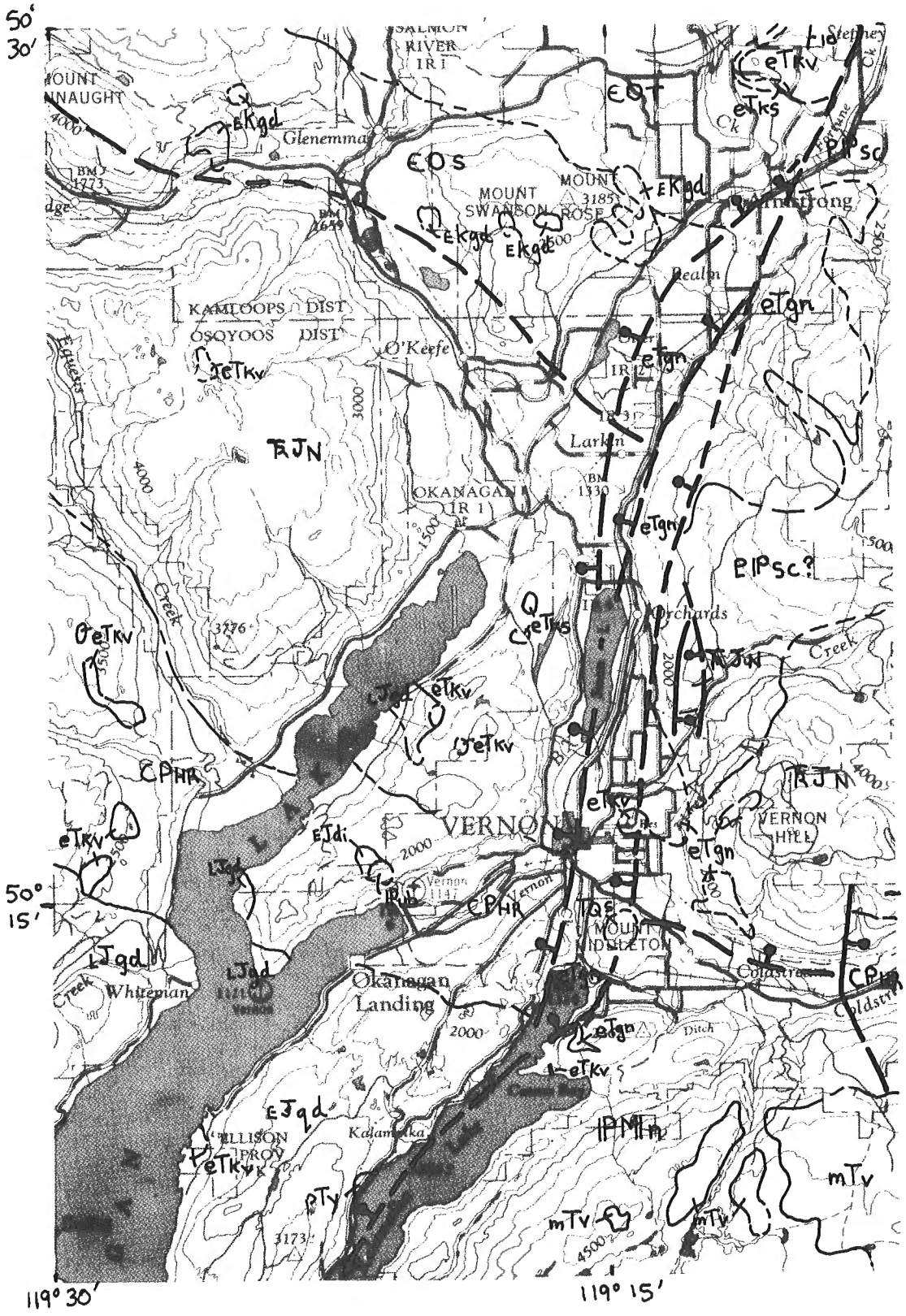

Figure 6. Revisions of geology at the northern end of Okanagan Lake. Data at the northeastern end of Kalamalka Lake from Solberg (1976). Scale = 1:250 000. See Table 1.

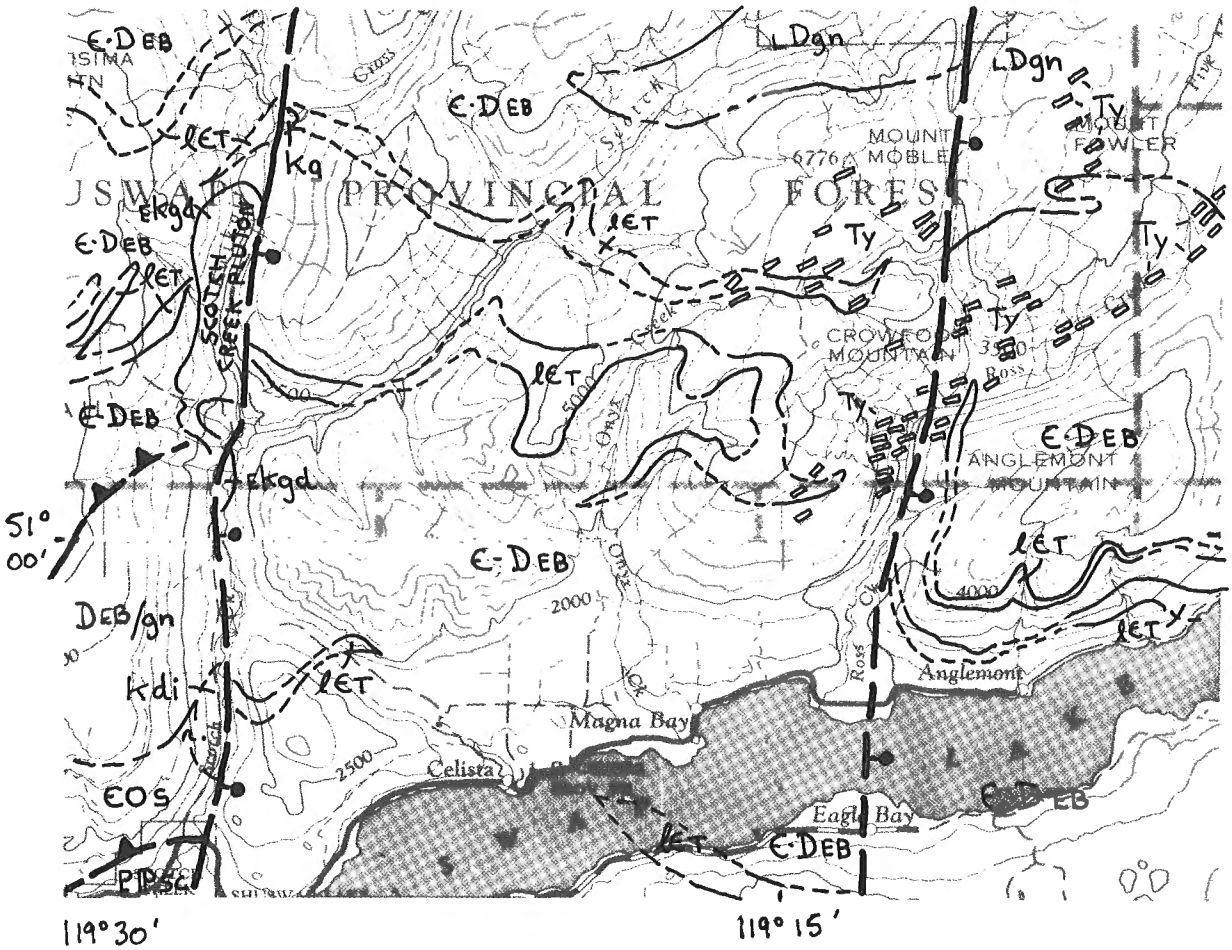

Figure 7. Revisions of geology north of Shuswap Lake near Scotch and Ross creeks. Scale = 1:250 000. See Table 1.

be faulted slivers. This fault must have been active in the late Paleozoic or Mesozoic as it affects a succession that includes units as young as Devonian (Skwaam Bay felsic tuffs) and is warped by folds that are cut by the 108 Ma Salmon Arm Pluton ($_{E}$Kgd).

Documentation of a widespread major episode of extensional tectonism affecting much of the southern Cordillera in the Eocene (cf. Parrish et al., 1988 for a synthesis of current studies) significantly alters interpretations of all late faults and pertubation of isotopic systems in the map area. As this tectonism is the subject of current thesis projects (R.L. Brown, pers. comm., 1988), only observations made independently are reported and regional integration and interpretation of data are not attempted. Journeay and Brown (1986) suggested that the Okanagan Shear Zone (Bardoux, 1985) which extends along the Okanagan Valley to Vernon, passes farther north to Mara Lake and joins the west-dipping fault along the north side of the Eagle River (Jones, 1959; Okulitch, 1979). This structure, interpreted as an east-directed regional thrust (Okulitch, 1984) akin to the Monashee Décollement (Read and Brown, 1981) was shown to be a west-side-down low angle normal fault termed the Eagle River Detachment (Journeay and Brown, 1986). They suggested that this fault may extend northwest to the northern end of Adams Lake, thus much of the central and western part of the map area is allochthonous relative to the high grade rocks of the Shuswap Complex.

Current work focused on the effects of such tectonism on Eocene volcanic strata of the Kamloops Group (eTKv, eTKs) southwest of Shuswap Lake. From map B, Open File 637, it may be inferred that volcanics on Mount Ida and Squilax and Black mountains are tilted down to the west, and the small outlier of volcanics near Yankee Flats south of Mount Ida, is tilted down to the east (Fig. 4). New mapping confirms these relationships. Flows at Mount Squilax dip about 30 degrees west. Moreover, felsic to intermediate feeder dykes below and east of the flows, cutting the Tsalkom Formation, dip east, an expected relationship in a tilted feeder/flow system (Fig. 5). Similar relationships occur on Mount Ida: flows near the summit dip about 15 degrees west and roll over to about 30 degrees in the valley of the Salmon River. Flows on hills west of these localities are at about 1 km greater elevation than those in the intervening valleys, suggesting a minimum of 1 km displacement on northerly-trending east-dipping faults in the valleys. These two faults are antithetic to the Eagle River Detachment. A small west-dipping synthetic fault is presumed to bound the flows at Yankee Flats.

Flows on the Nisconlith Pluton ($_{E}$Kgd) south of Little Shuswap Lake are poorly exposed but can be inferred to dip west from their outcrop distribution. Basal flows and strata to the west and southwest (Ewing, 1981, Fig. 6) are flat-lying and are between 100 and 700 m higher in elevation than the tilted flows, suggesting about 0.5 km displacement on a north-south fault in the valley of Chase Creek.

Table 1. Unit symbols for Figures 2-4, 6 and 7.

Quaternary	Qvb	valley basalt
Tertiary and Quaternary	TQs	breccia and conglomerate
Tertiary		
Miocene	mTv	basalt flows
Eocene	eT_Kv	Kamloops Group volcanic flows and dykes
	eT_KS	Kamloops Group sediment
	seT_{WL}	White Lake Formation
	eTgn	mylonite, granitoid gneiss and leucocratic intrusions
Paleocene	pTy	Coryell Suite syenite
Tertiary(?)	Ty	syenitic dykes
Cretaceous(?)	$_EKgd$	granodiorite
	Kdi	diorite
	Kg	granite
Jurassic	$_LJgd$	granodiorite
	$_EJqd$	quartz diorite
	$_EJdi$	diorite
	$_EJy$	syenite
Triassic and Jurassic	TrJ_N	Nicola Group
Paleozoic and/or Mesozoic	PMn	Okanagan Complex gneiss and schist
Paleozoic	Pc	limestone
	Ppt	argillite, chert
	Pcg	conglomerate
	Pv	volcanic rocks
	Pub	ultramafic rocks, serpentinite
	P_Cv	Chapperon Group
Carboniferous and Permian	CP_{HR}	Harper Ranch Group
Carboniferous	C_M	Milford Group
Devonian	L^{Dg}	Mount Fowler Batholith, foliated granite
	D_{EB}/gn	Eagle Bay Formation felsic volcanic rocks and gneissic intrusions
Ordovician	$_LOgn$	Little Shuswap Gneiss
Cambrian to Devonian	$E\text{-}D_{EB}$	Eagle Bay Formation
Cambrian to Ordovician	EO_S	Sicamous Formation
	EO_T	Tsalkom Formation
Lower Cambrian	lE_T	Tshinakin Limestone
Hadrynian(?) and (?)/or (?) Paleozoic(?)	PP_{SC}	Silver Creek Formation
Geological contacts		
Normal faults		
Thrust faults		

North-south faults in Scotch and Ross creeks north of Shuswap Lake are likely also related to the Eagle River Detachment.

The flat-lying 1 km thick mylonite zone (eTgn) that extends north from Swan Lake, north of Vernon, was re-examined at a new roadcut (Fig. 6). The regional tectonic significance of this feature was not recognized in the course of earlier work (Okulitch, 1979; 1984). The mylonite fabric contains some evidence of top-to-the west transport and is cut by a north-south vertical undeformed mafic dyke. The nearest dated dyke (43 $\pm$ 2 Ma) of similar character (eT_Kv) occurs 15 km to the south near Kalamalka Lake (Solberg, 1976). This may provide an upper limit to the age deformation in the mylonite zone. Deformed leucocratic intrusions (eTgn) (42 $\pm$ 10 Ma) in the same area indicate that some penetrative deformation was restricted to a brief period coeval with regional extensional faulting (52-45 Ma; Parrish et al., 1988). The age of the mylonite zone and its possible relationships to the Okanagan Shear Zone and the Eagle River Detachment are under investigation (R.L. Brown, pers. comm., 1988).

ISOTOPIC AGES AND TECTONISM

Another goal of the present study was to assess intrusive ages and times of metamorphism, and posttectonic cooling in the area north of the main arm of Shuswap Lake, north to the North Thompson River. Eocene extensional faulting

and uplift (e.g. Journeay and Brown, 1986; Parrish et al., 1988), accompanied by granitic intrusions, has perturbed isotopic systems to varying degrees within and adjacent to the Shuswap Metamorphic Complex. This orogenic episode had not been recognized in the southern Canadian Cordillera at the time Open File 637 was released except as "an enigmatic Tertiary thermal event" (Okulitch, 1978).

Original ages of metamorphism (126-154 Ma) and intrusion (80-98 Ma) are preserved by the K-Ar isotopic system in biotite, muscovite and hornblende west of Adams Lake, near the western end of Shuswap Lake and west of Mabel Lake (Mathews, 1981). This is typical of rocks in the hanging wall of major Eocene detachment faults, as summarized by Parrish et al. (1988). Rocks in the footwall were intruded, rapidly uplifted and cooled at 52-45 Ma (Parish et al., 1988). In areas of poor exposure, therefore, the location of such structures can be restricted by isotopic analyses. East and north of Shuswap Lake, and south of the North Thompson River, east of Vavenby, mica K-Ar and zircon fission track ages from the Devonian Mount Fowler Batholith ($_{L}$Dgn) and small intrusions of presumed Mesozoic age, range from 43 to 54 Ma (Okulitch, 1979). At one locality, however, 400 m above the Eagle River Detachment, north of Sicamous, and at another, near the transition from low to high grade rocks east of Vavenby, K-Ar from hornblende yielded dates of 92 to 107 Ma (Okulitch, 1979). Cooling through a considerable range in temperature apparently occurred during one or more episodes over about 50 million years in the hanging wall.

To investigate more fully the thermal effects of Eocene tectonism in this zone, samples were collected from intrusions within low and high grade rocks from Shuswap Lake to the North Thompson River in the northernmost part of the map area. Two hitherto unmapped bodies were found during this work (Fig. 7): a small plug of biotite hornblende(?) granite (Kg) at the junction of Cross and Kwikoit creeks and a stock of hornblende microdiorite (Kdi) on the western side of lowermost Scotch Creek (K.L. Daughtry, pers. comm., 1988). It is anticipated that isotopic analyses will provide insights about the plutonic and thermal history of this area as well as place broad limits on the zone where Eocene detachment faults may lie.

REFERENCES

Bardoux, M.
1985: The Kelowna detachment zone, Okanagan Valley, south-central British Columbia; *in* Current Research, Part A, Geological Survey of Canada, Paper 85-1A, p. 333-339.

Church, B.N.
1980a: Geology of the Kelowna Tertiary outlier (west half); British Columbia Ministry of Energy, Mines and Petroleum Resources, Preliminary Map 39.
1980b: Geology of the Terrace Mountain Tertiary outlier; British Columbia Ministry of Energy, Mines and Petroleum Resources, Revised Preliminary Map 37.

Dawson, G.M.
1898: Map sheet 11 (Shuswap sheet) British Columbia; Geological Survey of Canada, Map 604.

Ewing, T.E.
1981: Regional stratigraphy and structural setting of the Kamloops Group, south-central British Columbia; Canadian Journal of Earth Sciences, v. 18, p. 1464-1477.

Jones, A.G.
1959: Vernon map area, British Columbia; Geological Survey of Canada, Memoir 296.

Journeay J.M. and Brown, R.L.
1986: Major tectonic boundaries of the Omineca belt in southern British Columbia: a progress report; *in* Current Research, Part A, Geological Survey of Canada, Paper 86-1A, p. 81-88.

Mathews, W.H.
1981: Early Cenozoic resetting of potassium-argon dates and geothermal history of the north Okanagan area, British Columbia; Canadian Journal of Earth Sciences, v. 18, p. 1310-1319.

Mehner, D.T.
1982: The geology of the Whiterocks Mountain alkalic complex in south-central British Columbia; M.Sc. thesis, University of British Columbia.

Okulitch, A.V.
1973: Age and correlation of the Kobau Group, Mount Kobau, British Columbia; Canadian Journal of Earth Sciences, v. 10, p. 1508-1518.
1978: Discussion of results of K-Ar radiometric analyses; *in* Age Determinations and Geologic Studies, K-Ar Isotopic Ages, Report 13, ed. R.K. Wanless, R.D. Stevens, G.R. Lachance, and R.N. Delabio, Geological Survey of Canada, Paper 77-2, p. 24-26.
1979: Lithology, stratigraphy, structure and mineral occurrences of the Thompson-Shuswap-Okanagan area, British Columbia; Geological Survey of Canada, Open File 637.
1984: The role of the Shuswap Metamorphic Complex in Cordilleran tectonism: a review; Canadian Journal of Earth Sciences, v. 21, p. 1171-1193.
1985: Paleozoic plutonism in southeastern British Columbia; Canadian Journal of Earth Sciences, v. 22, p. 1409-1424.

Okulitch, A.V. and Cameron, B.E.B.
1976: Stratigraphic revisions of the Nicola, Cache Creek and Mount Ida groups based on conodont collections from the western margin of the Shuswap Metamorphic Complex, south-central British Columbia; Canadian Journal of Earth Sciences, v. 13, p. 44-53.

Okulitch, A.V., Wanless, R.K., and Loveridge, W.D.
1975: Devonian plutonism in south-central British Columbia; Canadian Journal of Earth Sciences, v. 12, p. 1760-1769.

Osatenko, M.J.
1979: Assessment report of geology, soil geochemistry, percussion and diamond drilling on the Dobbin property (Tad 1-3, 5-12, 14, and Esperon 11 claims), Tadpole Lake, Vernon and Nicola Mining Districts, N.T.S. 82L/4W; British Columbia Ministry of Energy, Mines and Petroleum Resources, Assessment Report 7596.

Parrish, R.R., Carr, S.D., and Parkinson, D.L.
1988: Eocene extensional tectonics and geochronology of the southern Omineca Belt, British Columbia and Washington; Tectonics, v. 7, p. 181-212.

Read, P.B. and Brown, R.L.
1981: Columbia River fault zone: southeastern margin of the Shuswap and Monashee complexes, southern British Columbia; Canadian Journal of Earth Sciences, v. 18, p. 1127-1145.

Schiarizza, P.
1983: Geology of the Barrière River-Clearwater area (82M/4,5,12; 92P/1,8,9); British Columbia Ministry of Energy, Mines and Petroleum Resources, Preliminary Map 53.
1986: Geology of the Vavenby area (82M/12 and parts of 5 and 11); British Columbia Ministry of Energy, Mines and Petroleum Resources, Open File Map 1986-5.

Schiarizza, P. and Preto, V.A.
1984: Geology of the Adams Plateau-Clearwater area (82L/13; 82M/3,4,5,6,12; 92P/1,8,9); British Columbia Ministry of Energy, Mines and Petroleum Resources, Preliminary Map 56.

Solberg, P.
1976: Structural relations between the Shuswap and "Cache Creek" complexes near Kalamalka Lake, southern British Columbia; M.Sc. thesis, University of British Columbia.

Struik, L.C.
1988: Structural geology of the Cariboo gold mining district, east-central British Columbia; Geological Survey of Canada, Memoir 421.

Wilkins, A.L.
1981: K-Ar and Rb-Sr dating of the Whiterocks Mountain alkalic complex in the Intermontane Belt west of Okanagan Lake, south-central British Columbia; B.Sc. thesis, University of British Columbia.

Ordovician conodonts identify the oldest sediments in the Intermontane Belt, Olalla, south-central British Columbia

S.M.L. Pohler, M.J. Orchard and D.J. Tempelman-Kluit
Cordilleran and Pacific Geoscience Division, Vancouver

Pohler, S.M.L., Orchard, M.J., and Tempelman-Kluit, D.J., Ordovician conodonts identify the oldest sediments in the Intermontane Belt, Olalla, south-central British Columbia; in Current Research, Part E, Geological Survey of Canada, Paper 89-1E, p. 61-67, 1989.

Abstract

Ordovician and Triassic conodonts are reported from limestones near Olalla in south-central B.C. Middle to Late Ordovician conodonts found in limestone lenses in the Shoemaker Assemblage are the only record of this age in the entire Intermontane Belt and represent a further stratigraphic anomaly within this complex region of the Cordillera. The Ordovician fauna has enigmatic faunal affinity. Two Triassic conodont faunas of Ladinian and Carnian age are reported from the nearby "Olalla Limestone".

Résumé

On signale la présence de conodontes de l'Ordovicien et du Trias dans des calcaires, près d'Olalla, dans la région centre-sud de la C.-B. Des conodontes de l'Ordovicien moyen et supérieur, trouvés dans des lentilles de calcaire de l'assemblage de Shoemaker, sont la seule évidence de cette période dans toute la zone intermontagneuse et représentent une autre anomalie stratigraphique au sein de cette région complexe de la Cordillère. La faune ordovicienne a une affinité faunique énigmatique. On signale la présence de deux faunes de conodontes du Trias (Landinien et Carnien) dans les calcaires d'Olalla avoisinants.

INTRODUCTION

In the Olalla area of south-central B.C. (Fig. 1), structurally intermixed strata referred to as the Shoemaker Assemblage (Wheeler and McFeely, 1987) comprise greenstone, silicified tuff, chert breccia and minor limestone of dominantly Paleozoic age. They are found in proximity to Mesozoic volcanic and sedimentary strata of the Nicola Group, including the "Olalla Limestone". In terms of western Cordilleran geology these rocks are part of the Quesnel Terrane (Okanagan Subterrane) of the Intermontane Superterrane (Wheeler and McFeely, 1987). The regional relationships of these rocks, which have undergone polyphase deformation and low grade metamorphism (Read and Okulitch, 1977), are poorly understood. Of particular interest are limestones within both groups (i.e. Shoemaker Assemblage and Nicola Group) that have yielded conodonts and other fossils.

GEOLOGICAL SETTING

The study area was first mapped by Bostock (1940, 1941), who referred massive and ribbon chert to the Shoemaker Formation and meta-andesites and related intrusive rocks to the Old Tom Formation. Later, Rice (1947) found that these rocks, along with Bostock's Independence and Bradshaw formations, could not be distinguished farther south (in the Princeton map area) and combined them in one group comprising "green and grey chert, grey argillite and cherty argillite, limestone, and green andesite, locally altered to quartz-mica schist and gneiss". Rice (1947) also noted the presence of small lenses of interbedded limestone that are the subject of this study. Milford (1984) referred to the assemblage as the Apex Mountain Group and interpreted the depositional environment to be a deep ocean basin with basalts being generated along a spreading ocean ridge; he postulated an eastward-dipping subduction zone in the east. Shallow water sediments within the assemblage were explained as deposits atop isolated seamounts or a high standing ridge. The time-frame provided by earlier fossil data reported by Read and Okulitch (1977), Monger (1977), and Milford (1984) is from Early Carboniferous to Late Triassic.

Problems have arisen because diverse ages have been reported from a single locality. Of particular note is the record of Siluro-Devonian stromatoporoids, tabulate corals, and bryozoa, Carboniferous foraminiferids, and Triassic conodonts from limestones in Shoemaker Creek (Read and Okulitch, 1977; Milford, 1984). The two older faunas are clearly anomalous because several samples from this site, including matrix from the original fossil samples (in GSC collections in Calgary), have yielded identical Triassic conodonts, namely Carnian paragondolellids (see below). The implied history of redeposited carbonates needs careful study.

Most of the fossils from chert of the Shoemaker Formation provide unambiguous mid-Carboniferous ages. Milford (1984) reported on several radiolarian faunas and more recently, F. Cordey (Université de Paris) recovered a microfauna from chert that includes conodonts reported herein as Late Devonian (Famennian).

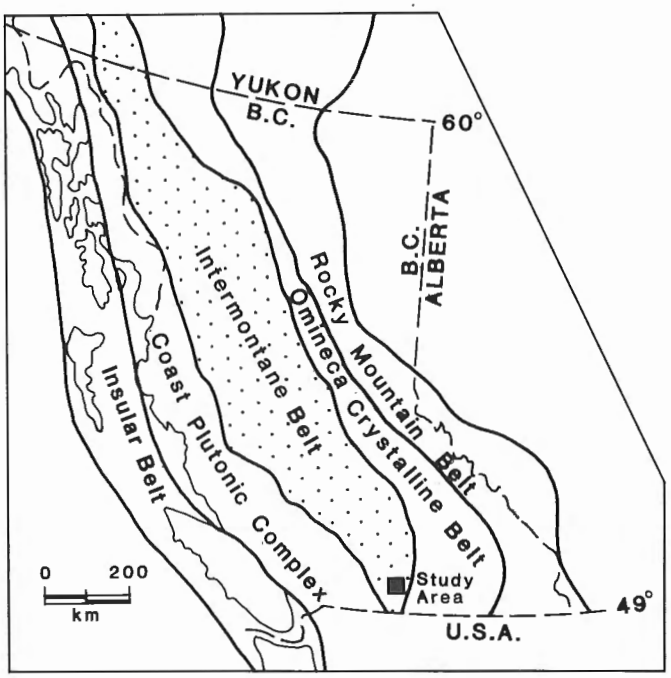

Figure 1. Location of study area.

The most recent collections from rocks of the Shoemaker Assemblage suggest a further dimension to the complex stratigraphy. Ordovician conodonts reported herein represent a significantly older stratigraphic record than has been suspected previously. The full significance of this discovery awaits further analysis of the regional geology.

SAMPLE LOCATIONS

Conodont and petrographic samples were collected from two localities in early 1988 east and west of Highway 3A between Olalla and Keremeos Forks Indian Reserve 12A (Fig. 2). The western locality is situated near Cedar Creek alongside a dirt road branching off Highway 3A about 3 km north of Olalla. Two outcrops of limestone are present. The most extensive outcrop (49°18′20″- 30″, 119°49′20″ - 25″), about 2 km from Highway 3A, is a 150 m long, 10 m thick body from which seven 3-4 kg samples were taken (samples Ced 2-8) at a spacing of between 10 and 50 m. It could not be determined whether this limestone represents a single block or is part of a continuous outcrop. A thin band of green tuff(?) separating two limestone bodies near the west end of the outcrop may either be matrix within which the limestone sits or an interbedded horizon. No other stratigraphic contacts were observed. In a second limestone outcrop, about 1.5 km off the highway, small limestone lenses occur in a sheared matrix of clastic metasediments (Plate 2, fig. 1); four samples were collected (B9-12). On the east side of Keremeos Creek near the confluence with Cedar Creek two limestones outcrop at an elevation of between 3000 and 3500 ft (Fig. 2). Six samples were collected from this, the upper "Olalla Limestone" (Ol 1-6); two samples were collected from the lower limestone (Ol 7-8).

BIOSTRATIGRAPHY

Of the 11 samples collected from Cedar Creek only three (Ced 2, 3 and 6) from the largest limestone body yielded conodonts (Table 1; Plate 1, fig. 1-9); those from the limestone lenses closer to the highway were barren. Two other samples collected earlier by J.C. Milford (GSC Loc. No. C-158537) and by one of the authors (T-K; GSC Loc. No. C-149527) yielded small faunas. Poor preservation precludes specific assignment of most specimens. Conodont CAI is between 5 and 6 and many conodonts are broken or otherwise distorted.

The presence of *Belodina*? sp. indicates that the fauna cannot be older than Whiterockian. The Olalla specimens have been assigned to this genus with question because insufficient material is available to determine whether *Belodina* Ethington or *Pseudobelodina* Sweet is present.

Only one species of *Strachanognathus, S. parvus* Rhodes, is known. It ranges from Arenig to Ashgill in age (Löfgren, 1978; Orchard, 1980, Pohler et al., 1987; Serpagli, 1967). A single oistodiform element has been assigned to *Oistodus venustus*? Stauffer s.f. Nowlan et al. (1988) questionably included this form species in *Paroistodus* Lindström along with the form species *Acodus ? mutatus* (Branson and Mehl). The genus *Paroistodus*? sensu Nowlan et al. is known from Middle to Late Ordovician. Acodiform elements resembling *Acodus ? mutatus* are found in the Cedar Creek material but they have striations along the base which, according to Nowlan et al. (1988), are typical of *Dapsilodus* Cooper rather than *Paroistodus*? Also, the costation of the acodiform elements is similar to that seen in *Belodella*? n. sp. (see below), and one of them carries small denticles on the upper margin. The acodiform like elements are therefore included with the latter genus.

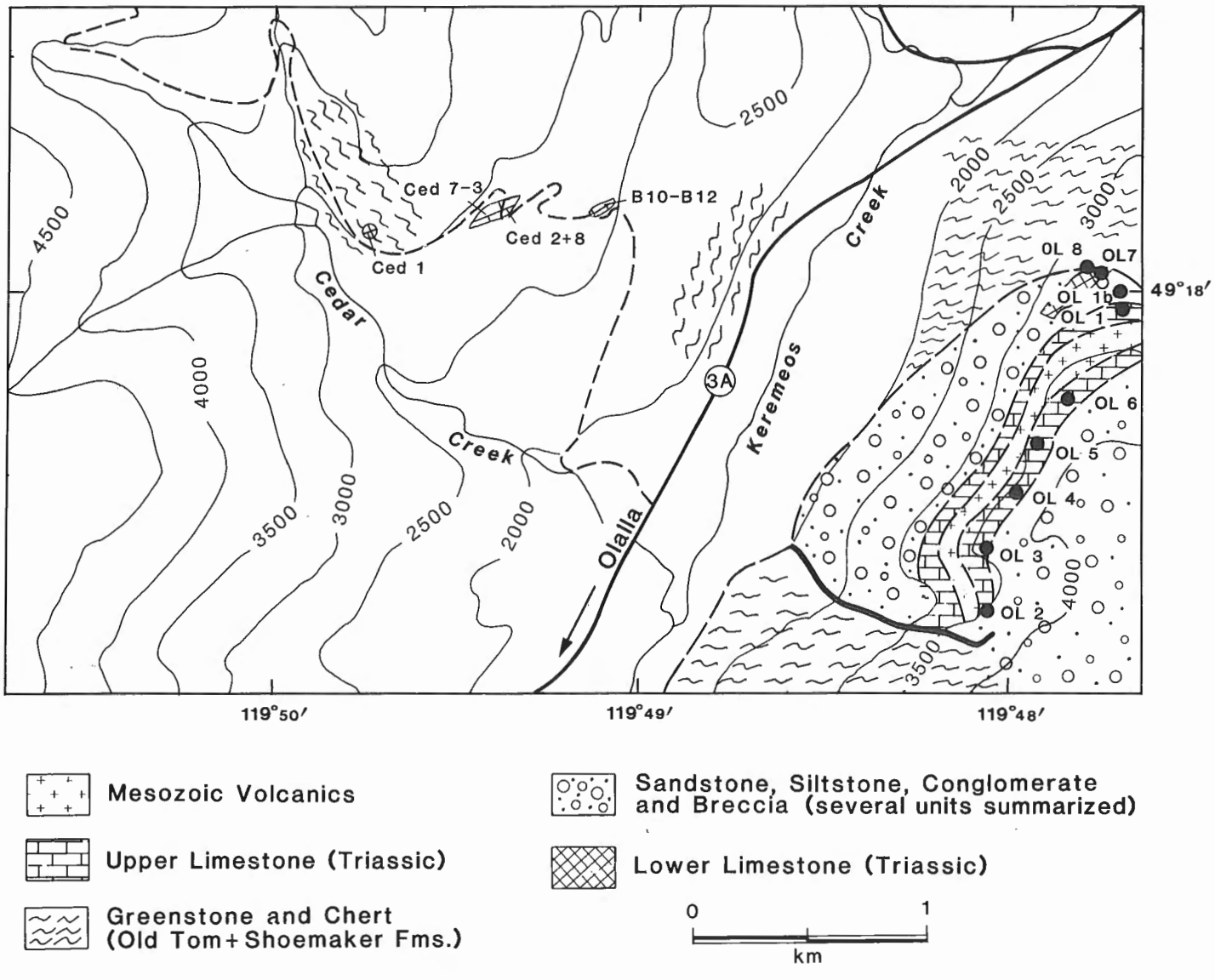

Figure 2. Ordovician and Triassic sample localities in the Olalla area (geology adapted from Read and Okulitch, 1977 and Ross and Barnes, 1972).

Table 1. Numerical data on conodont taxa from Cedar Creek

GSC/Sample number Taxa	C-149527 86-TO-34B	C-158537 Milford	C-158484 Ced 2	C-158485 Ced 3	C-158488 Ced 6
Strachanognathus parvus Rhodes	2	2	—	2	—
Belodina? sp.	3	1	4	—	—
Oistodus venustus Stauffer s.f.	1	—	—	—	—
Protopanderodus sp.	2	—	—	—	—
Drepanoistodus sp.	1	—	—	—	—
Belodella? sp.	9	7	12	8	1
unidentified simple cones	3	—	—	—	—

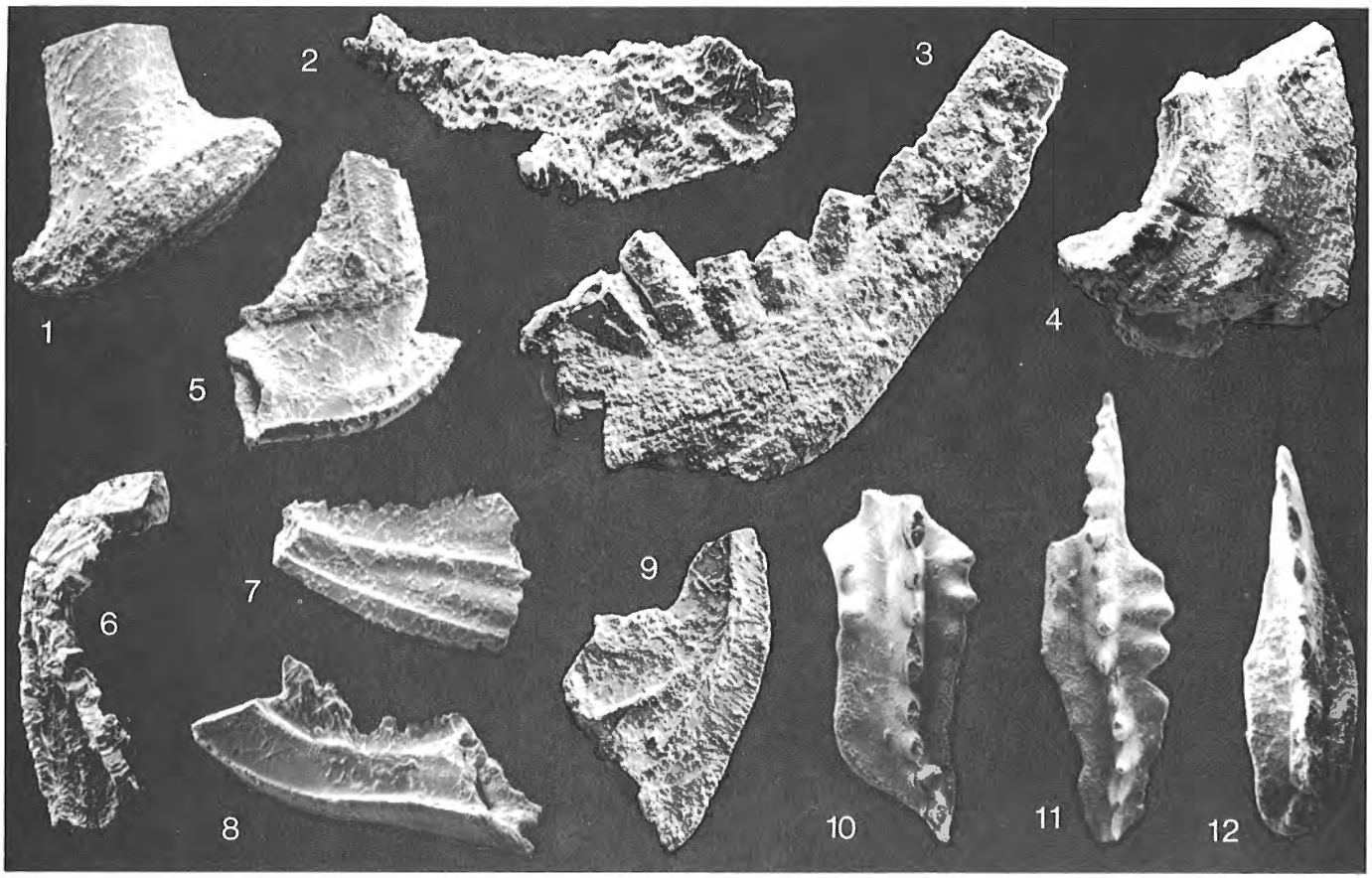

Plate 1. Ordovician (fig. 1-9) and Triassic (fig. 10-12) conodonts from Olalla. All Ordovician specimen are from the Shoemaker Assemblage at Cedar Creek (GSC Loc. No. C-149527); Triassic specimens are from the "Olalla Limestone" (Nicola Group).

Figure 1. Drepanoistodus sp. Inner lateral view, suberectiform element, x100, GSC 81221.
Figure 2. *Oistodus venustus*? Stauffer. Inner lateral view, x90, GSC 81222.
Figure 3. *Belodina* sp. Outer lateral view, x70, GSC 81223.
Figure 4. *Protopanderodus* sp. Outer lateral view, x90, GSC 81224.
Figure 5. *Strachanognathus parvus* Rhodes. Lateral view, x100, GSC 81225.
Figures 6-9. *Belodella*? n. sp. 6, 8. Lateral views of two different triangular elements. Note lateral flexure visible in fig. 6., x100, GSC 81226 and 81228 respectively. 7. Plano-convex element, inner lateral view. Note costation on lateral faces, x100, GSC 81227. 8. Biconvex element? lateral view. Note costae on lateral faces, x100, GSC 81229.
Figures 10, 11. *"Epigondolella" mungoensis* (Diebel). 10. Upper view, x100, GSC 81230; 11. Upper view, x90, GSC 81231. Both from GSC Loc. No. C-158353.
Figure 12. *"Paragondolella"* ex gr. *polygnathiformis* (Budurov and Stefanov). Upper view, x100, GSC 81232. GSC Loc. No. C-158500.

Table 2. Petrography of samples from Cedar Creek and "Olalla Limestone".

Sample number Field #/GSC #	Dunham classification	Folk classification	Description
Ced 1 C-158483	—	—	Breccia with clasts of brown and black radiolarian chert, matrix siliceous.
Ced 2 C-158484	—	Sparite	Fragmented neospar crystals, cemented by another generation of neospar. Stylocumulate in pore spaces
Ced 3 C-158485	—	Sparite	Similar to Ced 2.
Ced 4 C-158486	—	Sparite	Similar to Ced 2; some echinoderm fragments present.
Ced 5 C-158487	—	Sparite	Like Ced 4 with addition of "peloid ghosts".
Ced 6 C-158488	Wackestone-packstone	Biopelmicrite	Peloids + echinoderms in neomorph mud matrix.
Ced 7 C-158489	—	Sparite	Like Ced 5
Ced 8 C-158490	Wackestone-packstone	Biopelmicrite	Like Ced 6
B 9 C-158491	—	Sparite	Similar to Ced 2
B 10 C-158492	—	Sparite	Sparite and microspar, some echinoderm fragments.
B 11 C-158493	—	Sparite	Similar to B 10
B 12 C-158494	Wackestone-packstone	Biopelmicrite	Similar to Ced 8
Ol 1 C-158353	Wackestone	Pelmicrite	Finegrained peloids, cortoids, echinoderm fragments and shell debris; lithoclasts of quartz and shale.
Ol 2 C-158496	Grainstone	Pelsparite	Similar to Ol 1, components in microspar matrix or neomorph cement.
Ol 3 C-158497	Grainstone	Pelsparite	Similar to Ol 2.
Ol 4 C-158498	Rudstone	Lithosparite	Rounded clasts, 4-5 different microfacies: intrapelmicrite, pelmicrite, biomicrite, biopelmicrite. Matrix replaced by neomorph spar.
Ol 5 C-158499	—	Microsparite	Echinoderm fragments and ghosts of peloids.
Ol 6 C-158500	Wackestone	Pelmicrite	Cortoids, peloids, echinoderm fragments.
Ol 7 C-158351	Packstone	Poorly washed Biosparite	Crionoid fragments, shell debris.

Belodella? n. sp. is an enigmatic species which dominates the Cedar Creek fauna. Because of the lack of suitable oistodiform elements it cannot be decided whether *Ansella* Fåhraeus and Hunter or *Belodella* Ethington is present. All recovered elements are characterized by a short cusp, a long base, and small denticles along the upper margin; most are laterally flexed (Plate 1, fig. 6-9). In addition, all specimens have one or two costae on the lateral faces. Single lateral costae are typical of *Ansella*, but the lateral flexure of the cusp is characteristic of *Belodella* (e.g. *Belodella erecta* (Rhodes and Dineley)), as is the lack of oistodiform elements. None of the species of either genus shows a similar morphology to the Cedar Creek form which is therefore regarded as a new species.

The genus *Ansella* is only known from Ordovician strata (Fahraeus and Hunter, 1985), whereas *Belodella* ranges from the Silurian (possibly Ordovician) into the Devonian. The other two species present in the collection, *Drepanoistodus* sp. and *Protopanderodus* sp. are indicative of an Ordovician age. In summary, the conodont fauna cannot be dated at present more precisely than Middle or Late Ordovician.

The co-occurrence of *Ansella* or *Belodella, Belodina* and *Strachanognathus* has not been reported previously. *Ansella* together with *Belodina* has been observed, for example in the Middle Ordovician of the Monitor Range, Nevada (Harris et al., 1979), and possibly in the Sichuan Province of China (Jiang and An, 1985), and on the Siberian Platform (Moskalenko, 1983). *Ansella* with *Strachanognathus* occurs in the Middle Ordovician of New World Island, Newfoundland (Fåhraeus and Hunter, 1985), and *Belodina* co-occurs with *Strachanognathus* in the lower Upper Ordovician of Shaanxi, China (Yu and Wang, 1986). None of the occurrences recorded in the literature comprise all three genera together. This suggests either transport, reworking or a unique biofacies for the limestones at Cedar Creek.

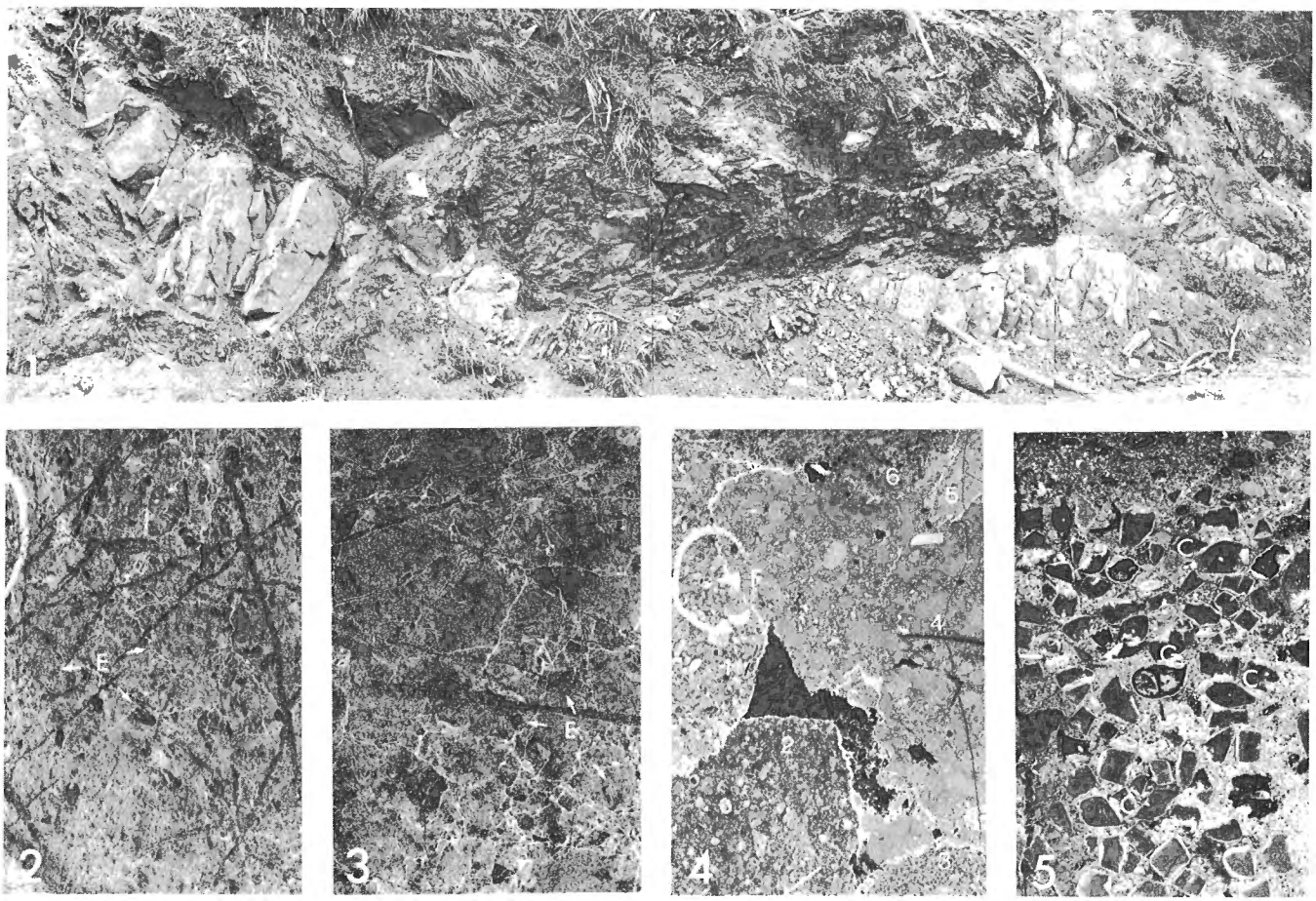

Plate 2.

Figure 1. Locality of samples B 9-11 near Cedar Creek. Melange with "limestone fish" in a shale matrix.
Figure 2. Negative print of thin section of Ordovician limestone at Cedar Creek. Note echinoderm fragments (E) in microspar matrix. x10.
Figure 3. Negative print of thin section from limestones shown in Figure 1. Note similarity of fabric, deformation and composition to Figure 2. x10.
Figure 4. Negative print of thin section from upper "Olalla Limestone" (Triassic). Rudstone with different types of lithoclasts numbered 1-6. F = foraminiferid. x10.
Figure 5. Negative print of thin section from lower "Olalla Limestone" (Triassic). Limestone is composed dominantly of crinoid columns typically with rhomboidal cross sections (C) and few gastropods (G). x10.

Conodonts from the "Olalla Limestone" comprise two faunas. The first, from the lower limestone (Ol-1; GSC Loc. No. C-158353; 49°17′59″, 119°47′53″), consists entirely of *'Epigondolella" mungoensis* (Diebel). This is a cosmopolitan species that characterizes late Ladinian strata throughout North America, Europe and Asia. In southern British Columbia, the same species is known in limestones outcropping about 10 km northwest of Grand Forks on Highway 3 as far north as Phoenix, and also in the most westerly Nicola Group outcrops in Ashcroft map area on Highway 1 near Martel. A late Ladinian limestone is therefore widely, though irregularly, developed in southern British Columbia and seems to represent an initial phase of carbonate deposition early in the history of the Nicola Group. The younger fauna from the higher outcrop of the "Olalla Limestone" (Ol-6;, GSC Loc. No. C-158500; 49°17′55″, 119°47′57″) contains representatives of the *"Paragondolella" polygnathiformis* (Budurov and Stefanov) group and is Carnian in age. This is a far more common age for Nicola Group carbonates and correlates with faunas known throughout Penticton, Hope and Ashcroft map areas. It is also the same age and composition as the conodont fauna from Shoemaker Creek (GSC Loc. No. C-046935). Read and Okulitch (1977) reported a slightly younger (Carnian-Norian boundary) conodont fauna from the Olalla locality, but the collection is apparently lost.

CARBONATE LITHOFACIES

The limestones from which the Ordovician conodonts were collected are highly fractured and recrystallized. No bedding is visible. Thin sections prepared from the rocks (Table 2) are dark grey due to disseminated carbon resulting from heating of organic matter. In some thin sections, peloids and fine grained echinoderm debris in a lime mud (now microspar) matrix (Plate 2, fig. 2) are recognized. A similar microfacies occurs in samples from the nearby unproductive limestones which may therefore be of the same age (Plate 2, fig. 1, 3; Table 2).

Among the samples from the Triassic limestones (Table 2) three different microfacies can be distinguished: (1) poorly washed biomicrite dominantly composed of crinoid columns with a curious rhombic cross-section (Plate 2, fig. 5); (2) a wackestone (pelsparite) composed of peloids, cortoids and rare echinoderm fragments in a neomorphosed lime mud matrix; (3) a polymict carbonate microconglomerate with centimetre-sized lithoclasts (i.e. peloidal grainstone, packstone and wackestone and ?bindstone) of shallow water origin. The matrix is sparse and a coarse silt or fine grained quartz sand (Plate 2, fig. 4).

Microfacies (1) occurs in the lower "Olalla Limestone" which was unproductive. Microfacies (2) occurs in the upper limestone which yielded the Ladinian-Carnian conodonts. Microfacies (3) occurs also in the upper limestone. All of the limestones are most likely shelf or shelf-edge lithologies with the exception of the microconglomerate which could be found in a carbonate slope setting.

REFERENCES

Bostock, H.S.
1940: Map of the Keremeos area; Geological Survey of Canada, Map 341A.
1941: Map of the Olalla area; Geological Survey of Canada, Map 628A.

Fåhraeus, L.E. and Hunter, D.R.
1985: Simple-cone conodont taxa from the Cobbs Arm Limestone (Middle Ordovician), New World Island, Newfoundland; Canadian Journal of Earth Sciences, v. 22, p. 1171-1182.

Harris, A.G., Bergström, S.M., Ethington, R.L., and Ross, J.R., Jr.
1979: Aspects of Middle and Upper Ordovician conodont biostratigraphy of carbonate facies in Nevada and southeast California and comparison with some Appalachian successions; Brigham Young University Geology Studies, v. 26, 7-43.

Jiang Huai-cheng and An Tai-xiang
1985: Conodont biostratigraphy of the Ordovician of SE Sichuan; Acta Micropalaeontologica Sinica, v. 2, p. 14-27.

Löfgren, A.
1978: Arenigian and Llanvirnian conodonts from Jamtland, northern Sweden; Fossils and Strata, v. 13, 161 p.

Milford, J.C.
1984: Geology of the Apex Mountain Group, north and east of the Similkameen River, south-central British Columbia; unpublished M.Sc. thesis, University of British Columbia, 108 p.

Monger, J.W.H.
1977: Upper Paleozoic rocks of the western Canadian Cordillera and their bearing on Cordilleran evolution; Canadian Journal of Earth Sciences, v. 14, 1832-1859.

Moskalenko, T.
1983: Conodonts and biostratigraphy in the Ordovician of the Siberian Platform; Fossils and Strata, v. 15, p. 87-94.

Nowlan, G.S., McCracken, A.D., and Chatterton, B.C.
1988: Conodonts from Ordovician-Silurian boundary strata, Whittaker Formation, Mackenzie Mountains, Northwest Territories; Geological Survey of Canada, Bulletin 373, 99 p.

Orchard, M.J.
1980: Upper Ordovician conodonts from England and Wales; Geologica and Palaeontologica, v.14, p. 9-44.

Pohler, S.M.L., Barnes, C.R., and James, N.P.
1987: Reconstructing a lost faunal realm: conodonts from megaconglomerates of the Ordovician Cow Head Group, western Newfoundland; in Conodonts: Investigative techniques and applications, R.L. Austin (ed.), British Micropalaeontological Society Series, p. 341-362.

Read, P.B. and Okulitch, A.V.
1977: The Triassic unconformity of south-central British Columbia; Canadian Journal of Earth Sciences, v. 14, p. 606-638.

Rice, H.M.A.
1947: Geology and mineral deposits of the Princeton map-area, British Columbia; Geological Survey of Canada, Memoir 243, 136 p.

Ross, J.V. and Barnes, W.C.,
1972: Evidence for "Caribooan Orogeny" in the Southern Okanagan Region of British Columbia; Canadian Journal of Earth Sciences, v. 9, p. 1693-1702.

Serpagli, E.
1967: I conodonti dell" Ordoviciano Superiore (Ashgilliano) delle Alpi Carniche; Bollettino della Societa Paleontologica Italiana, v. 6, p. 30-111.

Wheeler, J.O. and McFeely, P.
1987: Tectonic assemblage map of the Canadian Cordillera and adjacent parts of the United States of America; Geological Survey of Canada, Open File 1565.

Yu Fen-ling and Wang Zhi-hao
1986: Conodonts from Beiguoshan Formation in Long Xian, Shaanxi; Acta Micropalaeontologica Sinica, v. 3, p. 99-108.

Implications of Early Eocene Ladybird granite in the Thor-Odin — Pinnacles area, southern British Columbia

Sharon D. Carr[1]
Cordilleran and Pacific Geoscience Division, Vancouver

Carr, S.D., Implications of Early Eocene Ladybird granite in the Thor-Odin — Pinnacles area, southern British Columbia; in Current Research, Part E, Geological Survey of Canada, Paper 89-1E, p. 69-77, 1989.

Abstract

Ladybird granite suite Early Eocene plutons and pegmatite sheets are extensive in the southern Thor-Odin — Pinnacles area of southern British Columbia. The suite is primarily confined to a specific crustal level (the Ladybird zone) bounded at the base by Mesozoic thrust faults (Monashee décollement and Cariboo thrust) and at the top by Eocene extensional faults (Columbia River fault, Beaven — Cherryville fault system and, farther west, the Okanagan fault). Part of the stratigraphy of the Ladybird zone is correlated with upper Paleozoic to Upper Triassic Milford, Kaslo and Slocan groups.

A major first phase isoclinal nappe deforms the Upper Triassic Slocan Group, indicating a Mesozoic age for the earliest recognized deformation at this crustal level. The Early Eocene Ladybird suite also postdates four phases of folding in the Pinnacles area and cuts thrust faults at the base of the Ladybird zone. Ladybird intrusive rocks are penetratively deformed, indicating significant Eocene regional strain.

Résumé

Les plutons et les couches de pegmatite de l'Éocène inférieur de la série de granite de Ladybird sont fort répandus dans la région sud de Thor-Odin — Pinnacles dans le sud de la Colombie-Britannique. La série est principalement confinée à un niveau crustal particulier (la zone de Ladybird) qui est limité à la base par des failles chevauchantes du Mésozoïque (décollement de Monashee et chevauchement de Cariboo) et au sommet par des failles de distension de l'Éocène (faille du fleuve Columbia, réseau de failles de Beaven — Cherryville et, plus à l'ouest, la faille d'Okanagan). Une partie de la stratigraphie de la zone de Ladybird est corrélée avec les groupes de Kaslo, Slocan et Milford mis en place entre le Paléozoïque supérieur et le Trias supérieur.

Une grande nappe isocline de première phase déforme le groupe de Slocan du Trias supérieur, faisant remonter au Mésozoïque la déformation reconnue la plus ancienne à ce niveau crustal. La série de Ladybird de l'Éocène inférieur est aussi postérieure à quatre phases de plissement dans la région de Pinnacles et recoupe des failles de chevauchement à la base de la zone de Ladybird. Les roches intrusives de Ladybird sont déformées par pénétration, signe qu'une déformation régionale intense s'est produite pendant l'Éocène.

[1] Department of Earth Sciences, Carleton University and Ottawa-Carleton Geoscience Centre, Ottawa, Ontario K1S 5B6

INTRODUCTION

The southern Thor-Odin and Pinnacles region consists of high-grade polydeformed rocks which lie south of the Monashee Complex (Thor-Odin dome) in the Omineca Belt of southern British Columbia (Fig. 1). This area comprises three main tectonostratigraphic packages or sheets that were deformed at different crustal levels at different times and have been juxtaposed by major faults (Fig. 2). The lowest sheet contains Precambrian basement rocks overlain by stratified mantling gneisses and is exposed in Thor-Odin dome. It lies in the footwall of easterly-directed, Mesozoic shear zones (Monashee décollement and Cariboo thrust) that are well exposed on the southwest flank of Thor-Odin on

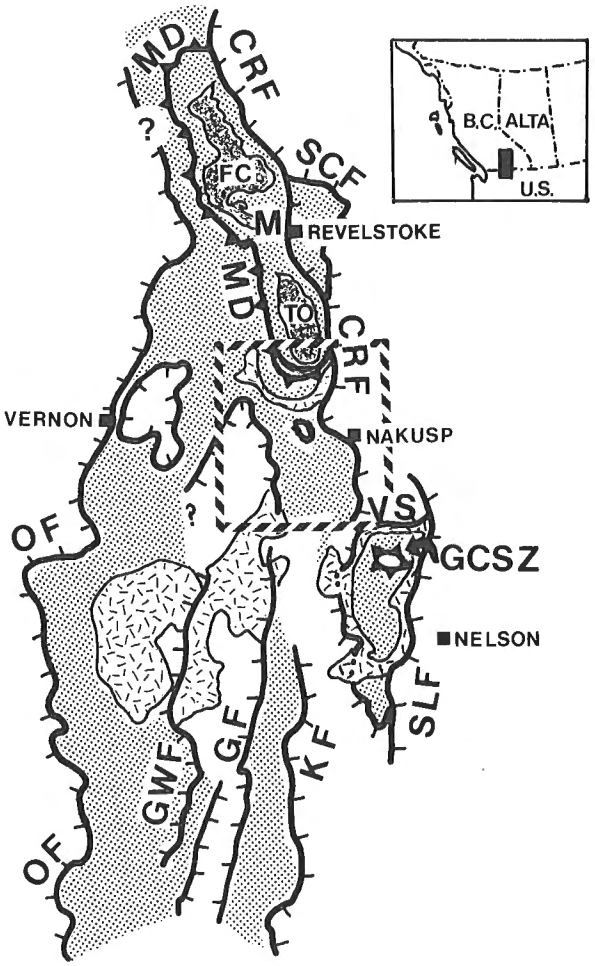

Figure 1. Tectonic map of southern Omineca belt, modified from Parrish et al. (1988). Features shown with patterns are the Early Eocene Ladybird suite (granite pattern), areas of metamorphic rocks characterized by 45-60 Ma K-Ar mica dates (grey stipple) and basement rocks of the Monashee complex (dark grey). Major thrust faults within Monashee (M) and Valhalla (V) complexes are the Monashee décollement (MD) and Gwillim Creek shear zones (GCSZ). Basement rocks of the Monashee complex are exposed in Frenchman Cap (FC) and Thor-Odin (TO). Eocene normal faults are the Columbia River fault (CRF), Granby fault (GF), Greenwood fault system (GWF), Kettle fault (KF), Okanagan fault (OF), Slocan Lake fault (SLF) and Valkyr shear zone (VS).

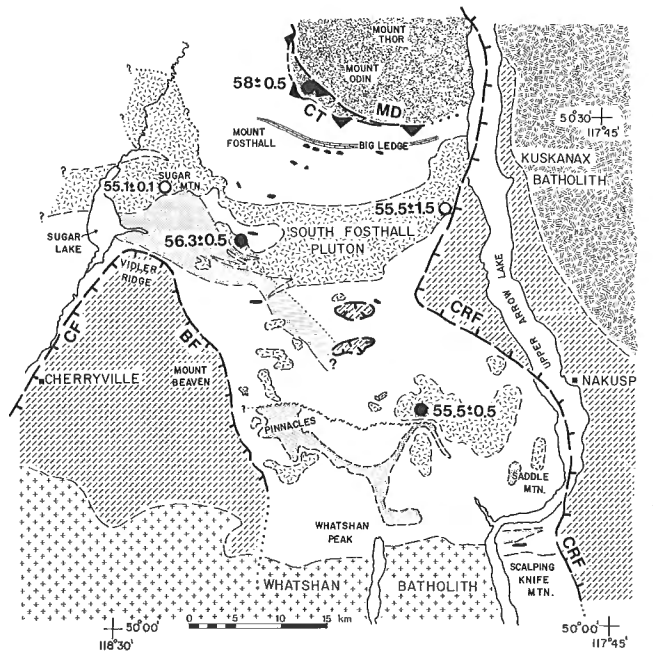

UPPER PLATE ROCKS

- MIDDLE JURASSIC KUSKANAX BATHOLITH
- LATE CRETACEOUS WHATSHAN BATHOLITH
- UPPER PALEOZOIC - MESOZOIC SCHIST, MARBLE, ARGILLITE, GREENSTONE AND VOLCANIC ROCKS

LADYBIRD PLATE

- EARLY EOCENE LADYBIRD GRANITE SUITE
- CALCAREOUS QUARTZITE, CALC-SILICATE, MARBLE, AND META-CONGLOMERATE
- ULTRAMAFIC ROCKS
- EMPRESS MARBLE
- UNDIVIDED METAMORPHIC ROCKS

MONASHEE COMPLEX

- UNDIVIDED BASEMENT AND MANTLING GNEISSES
- NORMAL FAULT: BR = BEAVEN FAULT; CF = CHERRYVILLE FAULT; CRF = COLUMBIA RIVER FAULT
- THRUST FAULT; CT = CARIBOO THRUST; MD = MONASHEE DECOLLEMENT
- PINNACLES FAULT
- U-Pb DATING LOCALE (Parrish et al., 1988); DATES IN Ma.
- U-Pb DATING LOCALE (Carr, unpublished data 1988); DATES IN Ma.

Figure 2. Generalized geology of the Thor-Odin—Pinnacles area. Compiled from Carr (unpub. data, 1986-1988), Read (1979), Read and Wheeler (1976), Reesor and Moore (1971) and Hyndman (1969).

Cariboo Alp (Coleman, 1989). Above the Cariboo thrust is a second panel of rocks (the Ladybird zone) that encompasses the southern flank of Thor-Odin and Pinnacles domes and extends southwards for 45 km to the Whatshan batholith (Fig. 2). It comprises a sequence of late Proterozoic(?) to Mesozoic paragneiss and schist intruded by Early Eocene leucogranite plutons, stocks and pegmatite sheets. This distinctive suite of intrusive rocks was previously termed the Ladybird granite in the Valhalla region (Fig. 1; Parrish et al., 1988a), and the name is herein applied to similar Early Eocene leucogranites and pegmatites in the Thor-Odin — Pinnacles area. The South Fosthall pluton (Fig. 2), originally thought to be of Paleozoic age (Okulitch, 1985), is the only Ladybird intrusive body in the region that is named. In the Thor-Odin — Pinnacles area, the Ladybird intrusives are exclusive to this second panel of rocks, thus it is informally named the Ladybird zone. It is bounded on the east and west sides by outwardly-dipping, regional-scale Eocene normal faults: the Columbia River fault zone on the east and the Beaven — Cherryville fault system on the west (Fig. 2). Rocks in the hanging wall of these faults are referred to in this paper as upper plate rocks and consist of unmetamorphosed to medium grade, upper Paleozoic to Lower Jurassic rocks intruded by Middle Jurassic and Late Cretaceous batholiths (Read and Wheeler, 1976; Read, 1979; Okulitch, 1979; Parrish and Wheeler, 1983).

Identification of high grade rocks, major boundaries, metamorphic breaks, and low grade stratigraphy was carried out by Jones (1959). Detailed mapping of units and the concept of a mantled gneiss dome in Thor-Odin was published by Reesor and Moore (1971); metamorphism and a large fold in Pinnacles were described by Reesor and Froese (1968, 1969). The Columbia River fault, the klippen of low grade rocks and the southern part of the Beaven fault were mapped by Read (1979). Duncan (1984) interpreted the evolution of Thor-Odin dome in terms of fold interference. Parrish et al. (1988a) presented geochronological and structural arguments that are consistent with exhumation of the complex due to Eocene extension.

The purpose of this project is to study the relationship between Mesozoic compression and Eocene extension, plutonism and tectonic denudation. The results will contribute to the interpretation of seismic reflection data collected in the area in 1988 as part of LITHOPROBE. This paper, based on about six months of field mapping in the Thor-Odin — Pinnacles area, focuses on the geology of the Ladybird zone and Eocene normal faults and implications for the tectonic history.

EOCENE NORMAL FAULTS

The Columbia River fault zone

The trace of the east-dipping Columbia River normal fault extends north-south for about 200 km and bounds the eastern margin of the Monashee Complex (Frenchman Cap and Thor-Odin) and Pinnacles dome (Fig. 1; Parrish and Armstrong, 1988; Brown et al., 1986; Lane, 1984). The fault appears to die out to the south in the Cariboo Creek stock on the northwestern flank of Valhalla complex. The displacement in the central part of the fault is estimated to be in the order 20-30 km (Parrish et al., 1988a). Locally the fault is an irregular corrugated surface with grooves and scoop-shaped ramps and flats; however, regionally the fault zone dips 30° east. Mylonites in the footwall indicate that some of the movement on the Columbia River fault occurred at high grade below the brittle-ductile transition. Throughout the eastern half of the Thor-Odin — Pinnacles region, fold hinges and sillimanite bearing lineations are transposed into an east-west orientation and stocks and pegmatites of the Early Eocene Ladybird granite suite are foliated and lineated with unannealed protomylonitic to mylonitic fabrics. Within about a kilometre of the fault trace, ductile mylonitic fabrics are overprinted by brittle structures and sillimanite grade rocks have undergone retrogression to chlorite grade. Deformation in the upper plate is apparently predominantly brittle.

The Eocene age of the fault is constrained by fabric relationships and geochronology of the South Fosthall pluton (Fig. 2). The pluton, which has an igneous fabric on the southwestern flank of Thor-Odin (Sugar Mountain), is transposed into a mylonitic sheet in the footwall of the fault. The Early Eocene U-Pb zircon dates (55 $\pm$ 1.5 and 55 $\pm$ 1 Ma), Rb-Sr dates of synkinematic muscovite (53.9 $\pm$ 0.8, 56.0 $\pm$ 0.9 and 59.7 $\pm$ 1.2 Ma) and Middle Eocene K-Ar mica dates (45.5 $\pm$ 0.9, 47.1 $\pm$ 0.9 and 47.1 $\pm$ 1.3 Ma) constrain the timing of the structure (Parrish et al., 1988a).

The Beaven — Cherryville fault system

The Beaven fault is a northwest trending normal fault that dips about 45° west and bounds the western side of Pinnacles dome (Fig. 2). The southern part was initially mapped by Read (1979). It is exposed on the ridges west of Pinnacles Peak and on Vidler Ridge. Exposure is poor in the intervening area but cataclastic rocks are exposed on the Outlet and Cherry Creek logging roads and logged areas. The Beaven fault has been mapped for some 30 km and is inferred to die out to the south in the Whatshan batholith. The Cherryville fault, first mapped by Jones (1959), extends for about 20 km and the magnitude of the dip is not known.

The Beaven and Cherryville normal faults dip towards each other and join at their northern ends, resulting in a klippe of low grade rocks surrounded on three sides by high grade rocks of the Ladybird zone (Fig. 2). Contrary to inferences by Jones (1959) and Okulitch (1979), the fault system does not continue northwards in Sugar Lake and the Shuswap River valley. On the shores of Sugar Lake, rocks are well exposed at low water, and east-west trending stratigraphic units, contacts and metamorphic isograds match on both sides of the lake.

Footwall rocks (Ladybird zone) consist of sillimanite $\pm$ staurolite $\pm$ muscovite bearing gneiss and schist and Ladybird granite and pegmatite. The hanging wall is primarily composed of cleaved and folded shale, chlorite $\pm$ biotite bearing fine grained schist, minor limestone and sandstone, intermediate to mafic volcanic rocks and augite porphyry. These rocks are correlated with the Upper Triassic Slocan Group (Jones, 1959; Read 1979; Okulitch, 1979)

and possibly the Lower Jurassic Rossland Group. The metamorphic grade is generally low; however, garnet, staurolite and kyanite occur only in fine grained schists in the immediate hanging wall of the Beaven fault west of Pinnacles Peaks.

The Beaven fault is predominantly a brittle fault. In the north, on Vidler Ridge, deformation is brittle and is confined to a narrow (about 60 m) zone. Twenty kilometres south, on a ridge southwest of the Pinnacles, an elongate fault bounded package of rocks in the footwall is mylonitic and is interpreted as a footwall horse. This coincides with the area of garnet, kyanite and staurolite in hanging wall rock indicating that deeper levels of the fault are exhumed in this region.

Westerly-directed discrete shear zones

There are discrete 10 cm to 50 m wide zones of shear in Ladybird rocks in the western part of the region, near Sugar Lake and in the Silver and Park hills between the Shuswap River valley and Mabel Lake. Asymmetry of mylonitic fabrics indicates a westerly-directed shear sense and it may be that these shears are related to the Okanagan fault zone (Fig. 1). There is a regional divergence of Eocene transport directions along a north-south axis in the Thor-Odin/Pinnacles area.

Contrasting thermal and metamorphic histories of upper and lower plates of Eocene normal faults

The upper plate of the Columbia River fault and Beaven — Cherryville fault system is generally at much lower grade (chlorite $\pm$ biotite $\pm$ staurolite) than the predominantly high grade (sillimanite-K-feldspar or sillimanite-muscovite) Ladybird zone, although there are some local exceptions to this. Metamorphism in the upper plate is pre-Middle Jurassic whereas rocks in the Ladybird zone were at high grade in the Eocene. The 161.6 $\pm$ O.5 Ma Galena Bay stock (Parrish and Armstrong, 1988) and the 173 $\pm$ 5 Ma Kuskanax batholith crosscut isograds in the hanging wall of the Columbia River fault placing a minimum age on the metamorphism (Read and Wheeler, 1976; Read and Brown, 1981; Parrish and Wheeler, 1983; Parrish et al., 1988a). The Ladybird zone was hot in the Eocene as 55-58 Ma Ladybird intrusions and pegmatites do not impose contact metamorphism on country rocks and in some areas both Ladybird granite and country rock were deformed together at high grade. This conclusion is supported by mineral dating of the South Fosthall pluton in the footwall of the Columbia River fault which records an Eocene cooling history (Parrish et al., 1988a) and Late Paleocene and Early Eocene U-Pb dates on metamorphic zircons in four amphibolite samples (Carr, unpublished data, 1988).

THE LADYBIRD ZONE

Stratigraphy of metamorphic rocks in the Ladybird zone

For the purpose of this paper, the stratigraphy of the Ladybird zone can be broadly divided into three packages. Immediately overlying the Monashee décollement/Cariboo thrust is a 3 km thick package of semi-pelitic and psammitic gneisses with up to about 30 % garnet-bearing amphibolite intruded by up to 30 % pegmatite. These rocks are probably correlative with Upper Precambrian Windermere stratigraphy. They are overlain by a second package of rocks which is well exposed as an east-west trending belt in the Big Ledge area and on the north flank of Mount Fosthall. It comprises a siliceous sequence overlain by the prominent Empress marble (Fig. 2) and graphitic calcareous schists which contain ultramafic lenses. These rocks are correlated with the Cambrian Hamill, Mohican, Badshot and overlying Lardeau (Höy, 1977) on the basis of lithologic similarity and on 550-500 Ma model lead ages on stratiform galena in calcareous schists of the Mohican Formation equivalent in Big Ledge (Duncan, 1984).

The third package of rocks extends from south of Mount Fosthall to the southern part of Pinnacles dome and Scalping Knife Mountain on the east shore of Arrow Lake (Fig. 2). Four marker units were identified in a well exposed corridor along the western side of the area and are apparently correlative with upper Paleozoic to Triassic rocks described by Klepacki (1983, 1985a, 1985b) in the Goat Range of the Kootenay Arc 40 km to the east. The map units are: 1) a distinctive calcareous quartzite—marble marker unit underlain by semipelitic rocks, 2) a heterogeneous sequence of pelite, semi-pelite, and psammite with amphibolite and ultramafic rocks, 3) an amphibolite with clasts, and 4) a very thick pelite with minor marble and psammitic rocks. This succession is correlated respectively with the Milford Group, Kaslo Group, Marten conglomerate and Slocan Group on the basis of lithologic similarity. This is consistent with designations made for units on Scalping Knife Mountain by Read and Wheeler (1976). Further structural work is required before thicknesses can be assigned to the map units.

The Ladybird zone has undergone polyphase deformation. There is an early metamorphic foliation containing high grade minerals. Since few F_1 structures have been observed and none were observed in pelites, it is uncertain whether this fabric is S_1 or S_2. S_1 or S_2 is folded by syn-metamorphic, asymmetric, north-verging folds (F_2 or F_3; Fig. 3) and refolded by more upright syn-metamorphic folds (F_3 or F_4). A crenulation cleavage, penetrative in pelitic rocks, is post-metamorphic (F_4 or F_5). There is structural and stratigraphic evidence that these folds are imposed on an F_1 nappe which has an inverted limb that extends for at least 15 km. The correlation of some of the stratigraphy in the Ladybird zone with rocks as young as Upper Triassic indicates that the folds, including F_1 folds must be Mesozoic structures.

Vidler calc-silicate

The calc silicate is well exposed east of Sugar Lake (Sugar Mountain, Vidler Ridge and Sitkum Creek), on Scalping Knife Mountain, on Saddle Mountain and in Pinnacles peaks (Fig. 1). It is a white- to buff-weathering quartzite with varying amounts of calcite, and marble interlayers at all scales (Fig. 4). The calcite weathers out giving it a distinctive texture; it was described by Jones (1959) as the "pitted quartzite." The calc silicate unit includes rare amphibolite

and semi-pelitic rocks. This unit may be equivalent to the McHardy assemblage of the Milford Group as described by Klepacki (1985b).

Ultramafic bearing unit

This unit overlies the calc-silicate unit and is well exposed southeast of Vidler Ridge, on Sitkum Plateau, on Twin Peaks and on Scalping Knife Mountain (Fig. 2). This unit is probably correlative with the ultramafic-bearing succession at Nemo Lakes north of the Valhalla complex (Parrish, 1981) and may be part of the Lower Permian Kaslo Group. It is a heterogeneous sequence of interlayered amphibolite, rusty weathering semi-pelites and psammites (± hornblende), sillimanite schist (± staurolite) and pods of magnesian ultramafic rocks which have olivine, anthophyllite and enstatite as major phases (Fig. 5). Where they are well exposed (Scalping Knife Mountain and Sitkum Plateau), the ultramafic pods can be traced for hundreds of metres and appear to stay at the same stratigraphic position relative to enclosing rocks. They probably represent tectonically boudinaged bodies of metamorphosed serpentinite. If this ultramafic unit represents the tectonic base of thrusted Quesnel terrane, any structural evidence for such a boundary has been obliterated by younger deformation.

Mount Mafic amphibolite

This hornblende amphibolite unit is restricted in occurrence to the headwaters of Cherry Creek and Cusson Creek with a strike length of about 6 km. It is mostly homogeneous but some horizons contain pancake shaped clasts and may have a breccia or conglomerate protolith. Clasts within a mafic matrix range from crystal size to 20 by 10 cm. They consist of hornblende clots, felsic clasts (± hornblende), and rare diorite, magnesian ultramafic rock, psammite and semipelite clasts (Fig. 6). This unit may be correlative with the Marten conglomerate in the Goat Range which lies unconformably on the Kaslo Group and is overlain unconformably by the Slocan Group (Klepacki, 1985b).

Figure 3. Three phases of superposed folds in semipelite; F_2 axial surface trace (outlined by pebbles) is folded by upright F_3 and overprinted by late F4 crenulation.

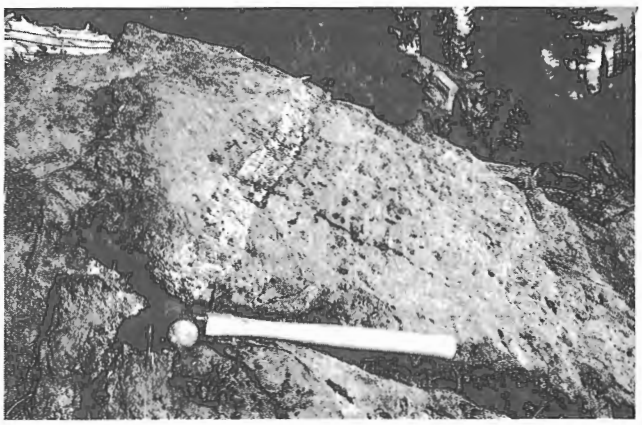

Figure 5. Ultramafic pod from east of Vidler Ridge.

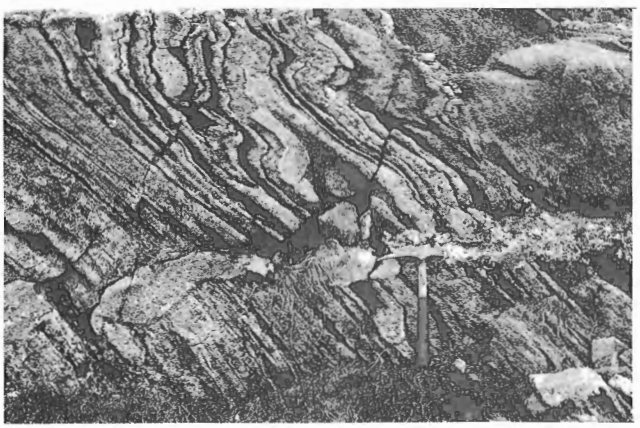

Figure 4. Westward view of calcareous quartzite with thin recessive marble interlayers. North-verging, asymmetric F_2 folds are superimposed on F_1 Z-folds; all fabrics are cut by a slightly deformed sill of Ladybird granite.

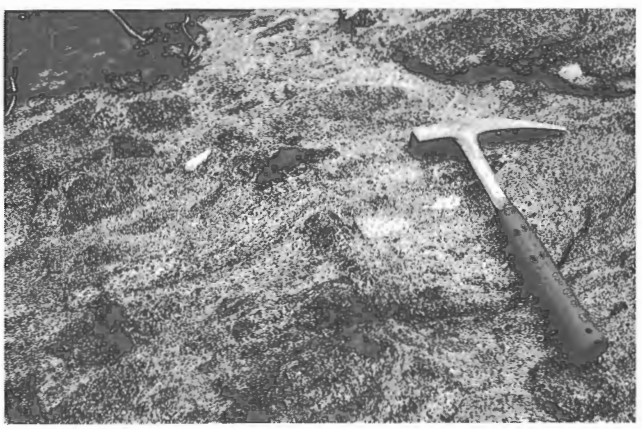

Figure 6. Clasts of diorite, mafic and felsic amphibolite and psammite in the Mount Mafic amphibolite from Cherry Creek.

The Snow Mountain schist

This schist is thought to be the youngest stratigraphic package in the Ladybird zone, correlative with the Upper Triassic Slocan Group, and occurs southeast of Vidler Ridge and west of Pinnacles peaks. It is predominantly a coarse, black weathering, sillimanite-muscovite-biotite schist that has minor quartzite interlayers from 1 mm to 20 cm thick (Fig. 7). On the west side of the area, in the footwall of the Beaven fault and on the shores of Sugar Lake, the schist is orange weathering and contains staurolite crystals up to 15 cm long. Kyanite is present in some locations. The schist contains clean marble, quartzite, semi-pelitic layers and minor felsic (tuffaceous?) layers.

The Ladybird granite

The Ladybird granite, first mapped as the "Valhalla series" by Little (1957, 1960, 1961), comprises homogeneous, biotite ($\pm$ muscovite, $\pm$ garnet) bearing leucocratic quartz monzonite to granite batholiths, stocks and pegmatites. It was first dated (Carr et al., 1987; Parrish et al., 1988a) in Valhalla complex where U-Pb zircon dates on plutons, stocks and pegmatites range from 59 $\pm$ 1 (syn-kinematic) to 56 $\pm$ 1.5 Ma (post-kinematic). The results of subsequent regional mapping and geochronology indicate that exposure of Early Eocene Ladybird granite is extensive throughout the metamorphic terrane (Fig. 1; Parrish et al., 1988a).

In the southern Thor-Odin—Pinnacles area, Ladybird intrusions and pegmatite are ubiquitous. The largest volume of Ladybird occurs on the south flank of Thor-Odin between the Cariboo thrust and the South Fosthall pluton. This region is in the bottom portion of the Ladybird sheet. A broad belt north of the South Fosthall pluton was mapped by Reesor and Moore (1971) in terms of greater or less than 50 % pegmatite. Stratigraphy seems to be more or less intact amongst the granitic rocks; marker units and stratigraphic packages can be mapped across the pegmatite sheets. Stockwork and thick pegmatite sheets are predominant in the central and eastern part of Pinnacles dome. The lowest volume of Ladybird occurs between the South Fosthall pluton and Pinnacle peaks, in the southwestern part of the region in the footwall of the Beaven fault, and south of Pinnacles near Whatshan peak. In these areas, Ladybird rocks occur as isolated stocks rather than sheets.

The South Fosthall pluton has been dated at two locales yielding 55 $\pm$ 1.5 Ma and 55 $\pm$ 0.1 Ma ages (U-Pb zircon and monazite; Parrish et al., 1988a). Recent U-Pb work on pegmatites is summarized on Figure 2; a pegmatite which crosscuts sheared rocks of the Monashee décollement—Cariboo thrust zone is 58 $\pm$ 0.5 Ma, a very weakly deformed pegmatite 10 km east of Sugar Lake on Sitkum Creek is 56.3 $\pm$ 0.5 Ma and a lineated and foliated pegmatite northeast of Whatshan Peak is 55.5 $\pm$0.5 Ma (Carr, unpub. data, 1988).

Contact relationships of the Ladybird granite suite

Pinnacles

In the area between the South Fosthall pluton and the Whatshan batholith, the Ladybird suite consists of granite stocks and sheets, pegmatite sheets (Fig. 8) and pegmatite stockwork (Fig. 9). These clearly postdate at least four phases of folding. Ladybird rocks are generally weakly deformed to undeformed in the central and western part of the area

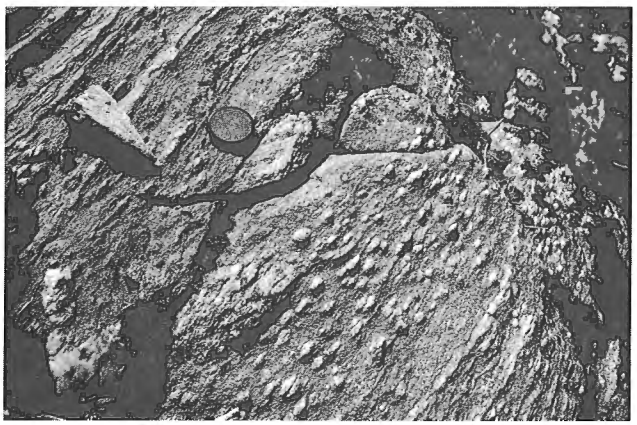

Figure 7. Prominent sillimanite porphyroblasts in Snow Mountain schist unit from north of Pinnacles peaks.

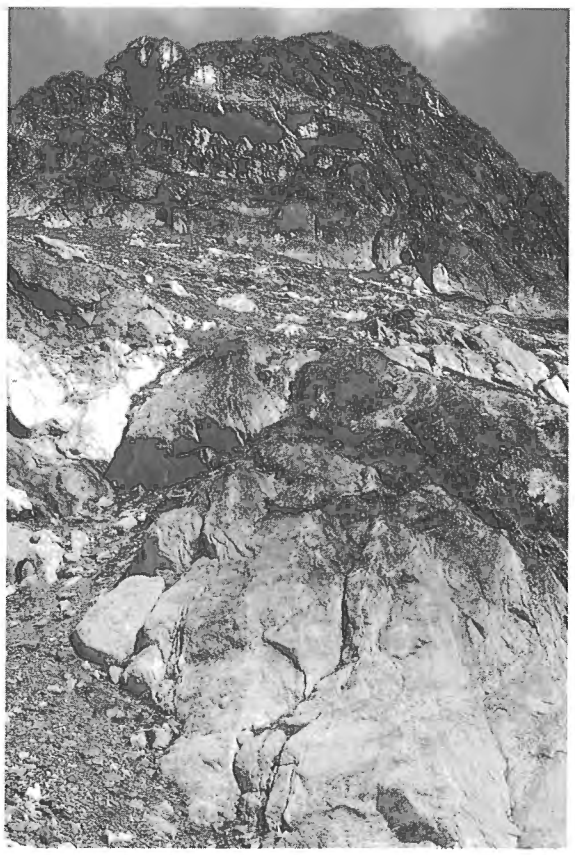

Figure 8. Cliff (about 150 m high) in Pinnacles peaks area composed of 10-50 m thick, undeformed, coarse, muscovite-garnet bearing pegmatite sheets with rusty weathering paragneiss screens.

and are protomylonitic to mylonitic in the footwall of the Columbia River fault. For example, pegmatite dykes on Saddle Mountain on the west shore of Arrow Lake are mylonitic.

Southern flank of Thor-Odin

The southern flank of Thor-Odin between the Cariboo thrust and the South Fosthall pluton represents the lowermost part of the Ladybird sheet. It has suffered more penetrative Eocene strain than higher levels in the sheet which are exposed farther south. Ladybird rocks are predominantly concordant or sub-concordant with the metamorphic foliation. In the Pinnacles area Ladybird rocks post-date folding, however, on the southern flank of Thor-Odin, late open upright folds deform the Ladybird granite.

Strain in the Ladybird varies systematically throughout the region. On the west side in the Sugar Lake area, the texture is predominantly a primary igneous fabric. There are westerly-directed discrete shear zones as previously discussed. On the eastern flank of Thor-Odin, fabrics are protomylonitic and mylonitic in the footwall of the Columbia River fault (Vanstone and Pingston creeks).

In the central part of the area, the Ladybird rocks are foliated and well lineated with an east-west oriented lineation. There appears to be a strain gradient within this central area. Pegmatites about 1 km above the Cariboo thrust fault are highly strained, mylonitic (Fig. 10) and boudined. Asymmetric fabrics indicate an easterly-directed shear sense. Additional U-Pb dating is underway to confirm that these highly strained pegmatites are in fact part of the Early Eocene Ladybird granite suite. Paragneiss is highly strained and attenuated, fold hinges are rotated into the stretching lineation and sheath folds are present. This high strain decreases southward. On Mount Fosthall (Fig. 2) the pegmatites are deformed; however, Mesozoic superposed fold geometry is still preserved. This strain gradient and the mylonitic fabrics indicate that there was significant Eocene strain at or near the base of the Ladybird zone. This strain is younger than that associated with the Cariboo thrust (Coleman, 1989). It may be an extensional structure which predates or is contemporaneous with the Columbia River fault. The geometry of the structure is analogous to the Valkyr shear zone in the Valhalla complex; however, the structural level and thermal history above and below the strained zone differ from Valhalla complex.

CONCLUSIONS

On the basis of field and geochronological studies, the following conclusions can be drawn.

The Thor-Odin — Pinnacles area comprises three main tectonostratigraphic packages or sheets that were deformed at different crustal levels at different times and have been juxtaposed by major faults. Basement and mantling gneisses form the lower sheet (Monashee Complex) and are bounded on the top by thrust faults (Monashee décollement and Cariboo thrust; Coleman, 1989). This is overlain by the Ladybird zone, a sequence of Proterozoic to Mesozoic paragneisses and schists intruded by Early Eocene Ladybird leucogranite plutons, stocks and pegmatite sheets. The Ladybird intrusives are exclusive to this panel of rocks (this has interesting implications for the origin and the emplacement history of the Ladybird suite). The Ladybird zone underwent Eocene penetrative strain and cooled in Paleogene time. The Ladybird zone, within the area of study, is bounded on the east and west sides by Eocene normal faults; the Columbia River fault zone, the Beaven — Cherryville fault system and farther to the west, the Okanagan fault. The upper plate comprises upper Paleozoic to Triassic rocks that were deformed and metamorphosed prior to the intrusion of both Middle Jurassic (Kuskanax) and Late Cretaceous (Whatshan) batholiths.

The volume of Early Eocene (58-55 Ma) leucogranite plutons, stocks and pegmatite is significant, making up more than 50 % of the rocks near the base of the plate and more than 30 % in Pinnacles area. The distribution of Ladybird granite in a fault bounded sheet is the same configuration as Valhalla complex where Ladybird granite is underlain by

Figure 9. Post-tectonic Ladybird pegmatite crosscuts fabric in country rock in Pinnacles peaks area.

Figure 10. Well developed mylonitic fabric in Ladybird pegmatite from north of Margie Lake near the base of the Ladybird sheet about 600 m above the Cariboo thrust.

the Gwillim Creek shear zones and bounded on the top by the Valkyr—Slocan Lake normal fault system (Carr et al., 1987; Parrish et al., 1988b).

Fabric studies in conjunction with geochronology allow the timing of the Columbia River fault to be determined. Movement is bracketed by the Early Eocene U-Pb zircon dates on the deformed South Fosthall pluton, Rb-Sr dates of synkinematic muscovite and Middle Eocene K-Ar mica dates.

The metamorphism in the Ladybird zone is younger than the pre-Middle Jurassic metamorphism (Parrish and Wheeler, 1983) typical of the upper plate of Eocene normal faults. This is supported by 1) Eocene mineral cooling ages (see above), 2) contact relationships of Early Eocene Ladybird suite (no contact aureoles), 3) sillimanite- and hornblende-bearing country rocks were deformed with intrusive Ladybird granite (transposed folds and lineations), and 4) four amphibolite samples yielded metamorphic zircons which are Late Paleocene and Early Eocene (Carr, unpub. U-Pb data, 1988).

From north to south, a transect through the Ladybird zone is exposed. The deepest levels are exposed on the southern flank of Thor-Odin and higher levels occur in Pinnacles. This is a function of the structural orientation of the rocks and exhumation of deeper levels of the Ladybird sheet along the central part of the Columbia River fault. There is a zone of high strain at or near the base of the Ladybird zone which decreases upwards. This may represent an easterly-directed zone of strain which preceded or was contemporaneous with motion on the Columbia River fault. The geometry is analogous to the Valkyr shear zone — Slocan Lake fault zone in the Valhalla complex (Carr et al., 1987); however, the structural level of the strain zone and the thermal history of under- and overlying rocks differs.

In the central and eastern part of the area, penetrative mylonitic fabrics in the Ladybird granite are easterly-directed; however, there are discrete westerly-directed shear zones on the western side of the area which may be related to the Okanagan fault system. A north-south trending axis of diverging Eocene transport directions occurs in the Thor-Odin — Pinnacles area.

The metamorphic rocks in the Ladybird sheet have been polydeformed in the Mesozoic. An early foliation, which may be S_1 or S_2, contains high grade minerals. It is folded by syn-metamorphic, asymmetric, north-verging folds (F_2 or F_3) and refolded by more upright syn-metamorphic folds (F_3 or F_4). A crenulation cleavage, penetrative in pelitic rocks, is post-metamorphic (F_4 or F_5). There is structural and stratigraphic evidence that these folds are imposed on an F_1 nappe which has an inverted limb that extends for at least 15 km. Crosscutting relationships of the Ladybird granite in the Pinnacles area demonstrate that folding predates the intrusion of the Ladybird suite.

Metamorphic stratigraphy on the western side of the area has been correlated with Upper Mississippian to Pennsylvanian Milford Group, Lower Permian Kaslo Group, Permian Marten conglomerate and Upper Triassic Slocan Group. Folding of rocks as young as Late Triassic indicates that polyphase folding, including F_1 isoclinal nappes is Mesozoic.

At the inferred base of Quesnel terrane where magnesian ultramafic rocks are present, structures associated with obduction have been obliterated by younger deformation.

ACKNOWLEDGMENTS

This project was funded by LITHOPROBE University Supporting Geoscience Grant number 85, NSERC Operating Grant A2693 to R.L. Brown, EMR Research Agreement 227/04/88, the Geological Survey of Canada, and a Geological Society of America research grant. I would like to acknowledge an NSERC postgraduate scholarship. I am grateful to Dick Brown and Randy Parrish for advice and discussion, and particularly to Randy for his patience in teaching U-Pb geochronology and for access to geochronological facilities. I thank Peter Read for providing unpublished maps of the Columbia River fault and the Beaven fault and Vicki Coleman and Brad Johnson for field assistance.

REFERENCES

Brown, R.L., Journeay, J.M., Lane, L.S., Murphy, D.C., and Rees, C.J.
1986: Obduction, backfolding and piggyback thrusting in the metamorphic hinterland of the southeastern Canadian Cordillera; Journal of Structural Geology, v. 8, p. 255-268.

Carr, S.D., Parrish, R.R., and Brown, R.L.
1987: Eocene structural development of the Valhalla complex, southeastern British Columbia; Tectonics, v. 6, p.175-196.

Coleman, V.J.
1989: The Cariboo Duplex at the southern boundary of the Monashee Complex, Southern British Columbia; *in* Current Research, Part E, Geological Survey of Canada, Paper 89-1E.

Duncan, I.J.
1984: Structural evolution of the Thor-Odin gneiss dome; Tectonophysics, v. 101, p. 87-130.

Höy, T.
1977: Big Ledge; *in* Geology in British Columbia 1975, British Columbia Department of Mines and Petroleum Resources, p. G12-G18.

Hyndman, D.W.
1969: Petrology and Structure of Nakusp Map-area, British Columbia; Geological Survey of Canada, Bulletin 161, 95 p.

Jones, A.G.
1959: Vernon map area, British Columbia, Geological Survey of Canada Memoir 296, 186 p.

Klepacki, D.W.
1983: Stratigraphic and structural relations of the Milford, Kaslo and Slocan groups, Roseberry Quadrangle, Lardeau map area, British Columbia; *in* Current Research, Part A, Geological Survey of Canada, Paper 83-1A, p. 229-233.
1985a: Stratigraphic and structural relations of the Milford, Kaslo and Slocan groups, Lardeau and Nelson map areas, British Columbia; *in* Current Research, Part A, Geological Survey of Canada, Paper 85-1A, p. 277-286.
1985b: Stratigraphy and structural geology of the Goat Range area, southeastern British Columbia; unpublished Ph.D. thesis, Massachusetts Institute of Technology, 252 p.

Lane, L.S.
1984: Brittle deformation in the Columbia River fault zone near Revelstoke, southeastern British Columbia; Canadian Journal of Earth Sciences, v. 21, p. 584-598.

Little, H.W.
1957: Kettle River, east half, British Columbia; Geological Survey of Canada, Map 6-1957.
1960: Nelson map-area, west half, British Columbia, Geologic Survey of Canada, Memoir 308, 205 p.
1961: Kettle River, west half, British Columbia, Geologic Survey of Canada, Map 15-1961.

Okulitch, A.V.
1979: Thompson-Shuswap-Okanagan; Geologic Survey of Canada, Open File 637.
1985: Paleozoic plutonism in southeastern British Columbia; Canadian Journal of Earth Sciences, v. 22, p. 1409-1424.

Parrish, R.R.
1981: Geology of the Nemo Lakes Belt, northern Valhalla Range, southeast British Columbia; Canadian Journal of Earth Sciences, v. 18, p. 944-958.

Parrish, R.R., and Wheeler, J.O.
1983: U-Pb zircon age of the Kuskanax batholith, southeastern British Columbia; Canadian Journal of Earth Sciences, v. 20, p. 1751-1756.

Parrish, R.R., Carr, S.D., and Parkinson, D.L.
1988a: Eocene extensional tectonics and geochronology of the southern Omineca belt, British Columbia and Washington; Tectonics, v. 7, p. 181-212.

Parrish, R.R., Price, R.A., and Carr, S.D.
1988b: Late Cretaceous-Paleogene metamorphism in the core zone of the Cordilleran orogen: Valhalla complex of southeastern British Columbia; Geological Society of America, Abstracts with Programs, v. 19, p. 800.

Parrish, R.R., and Armstrong, R.L.
1988: The ca. 162 Ma Galena Bay stock and its relationship to the Columbia River fault zone, southeast British Columbia; *in* Radiogenic Age and Isotopic Studies: Report 1, Geological Survey of Canada, Paper 87-2, p. 25-32.

Read, P.B.
1979: Geology and mineral deposits, eastern part of Vernon east-half map-area; Geological Survey of Canada, Open File 658.

Read, P.B., and Wheeler, J.O.
1976: Geology of Lardeau west-half map area; Geological Survey of Canada, Open File 288.

Read, P.B., and Brown, R.L.
1981: Columbia River fault zone: southeastern margin of the Shuswap and Monashee complexes, southern British Columbia; Canadian Journal of Earth Sciences, v. 18, p. 1127-1145.

Reesor, J.E., and Froese, E.
1968: Petrology and structure, Pinnacle peaks map-area, British Columbia; *in* Report of Activities, Part A, Geological Survey of Canada, Paper 68-1A, p. 111-112.
1969: Structural and petrological study of Pinnacle Peaks gneiss dome, British Columbia; *in* Report of Activities, Part A, Geological Survey of Canada, Paper 69-1A, p. 139-140.

Reesor, J.E., and Moore, J.M.
1971: Petrology and structure of Thor-Odin gneiss dome, Shuswap metamorphic complex, British Columbia; Geological Survey of Canada, Bulletin 195, 149 p.

Eocene stratigraphy, age of the Coryell batholith, and extensional faults in the Granby Valley, southern British Columbia

Sharon D. Carr[1] and David L. Parkinson[2]
Lithosphere and Canadian Shield Division

Carr, S.D. and Parkinson, D.L., Eocene stratigraphy, age of the Coryell batholith, and extensional faults in the Granby Valley, southern British Columbia; in Current Research, Part E, Geological Survey of Canada, Paper 89-1E, p. 79-87, 1989.

Abstract

Middle Eocene volcanic and clastic strata, west of the Grand Forks metamorphic core complex, are correlative with the Marron (lower Kitley Lake and Yellow Lake members) and Kettle River formations. They are exposed as klippen in the hanging wall of the Jones fault, a shallow dipping normal fault that predates, and is exposed in the upper plate of, the west-dipping Granby normal fault which bounds the western margin of the Grand Forks complex. Both the Jones and Granby faults are high crustal level, brittle extensional structures.

U-Pb zircon geochronology of the Coryell syenite yields a 51.1 ± 0.5 Ma age of crystallization. The Jones and Granby faults are younger than 51 Ma as they both truncate Coryell intrusions. These westerly-directed faults are therefore slightly younger than the easterly-directed Kettle and Valkyr-Slocan Lake normal fault systems farther to the east, which are intruded by 51 Ma Coryell syenite.

Résumé

Les strates volcaniques et clastiques de l'Éocène, à l'ouest du complexe central métamorphique de Grand Forks, ont été corrélées avec les formations de Marron (membres inférieurs de Kitley Lake et de Yellow Lake) et de Kettle River. Elles affleurent sous forme de klippes au toit de la faille de Jones, faille normale de faible inclinaison, antérieure à la faille normale de Granby de plongement ouest et limitant la marge ouest de Grand Forks, et qui affleure dans le bloc supérieur de cette seconde faille. Les failles de Jones et Granby sont toutes deux des structures fragiles de distension, situées à un niveau élevé de la croûte.

La géochronologie déterminée par datation à l'aide de la méthode U-Pb appliquée au zircon, de la syénite de Coryell, a permis d'évaluer à 51,1 ± 0,5 Ma l'âge de la cristallisation. Les failles de Jones et Granby sont plus récentes que 51 Ma, étant donné qu'elles tronquent toutes deux des intrusions de Coryell. Ces failles de direction ouest sont par conséquent légèrement plus récentes que les réseaux de failles normales de Kettle et Valkyr-Slocan Lake; ces failles de direction est se trouvent plus à l'est et sont traversées par la syénite de Coryell âgée de 51 Ma.

[1] Department of Earth Sciences, Carleton University and Ottawa-Carleton Geoscience Centre, Ottawa, Ontario, K1S 5B6
[2] Department of Geological Sciences, University of California, Santa Barbara, CA 93106

INTRODUCTION

Exhumation of high grade metamorphic terranes on regionally extensive normal faults during Eocene extension is an important part of the protracted tectonic history of the Omineca Belt (Parrish et al., 1988). The Grand Forks-Kettle complex lies in the central part of the extended terrane and is bounded by outward dipping, regionally extensive normal faults: the Kettle fault on the east and the Granby fault on the west (Fig. 1). These and other ductile and/or brittle normal fault systems have inferred displacements on the order of 20-40 km and are thought to have accommodated up to 80-120% extension across the belt (Parrish et al., 1988).

This study describes the structure of high crustal level, brittle extensional Jones and Granby faults and Eocene stratigraphy on the western flank of the Grand Forks-Kettle complex and is based on one week of field mapping and one U-Pb zircon date. The map area (Fig. 2) is adjacent to that of Preto (1970). A 51.1 $\pm$ 0.5 Ma U-Pb zircon date on Coryell syenite in the footwall of the Jones fault and upper plate of Granby fault places a maximum age on these extensional structures.

GEOLOGY

Rocks from three different structural levels are exposed on the western flank of the Grand Forks complex (Fig. 2). The structurally lowest zone consists of high-grade gneiss and intrusive rocks exposed in the Grand Forks complex and is bounded on the top by the west-dipping Granby normal fault. The middle zone, which is made up of predominantly Middle Eocene Coryell syenite that intrudes low-grade upper Paleozoic to Mesozoic rocks and Middle Jurassic Nelson intrusives, is bounded on the bottom by the Granby fault and on the top by the Jones fault. The highest zone comprises klippen of Middle Eocene volcanic and clastic strata in the hanging wall of the Jones fault. Late steeply-dipping brittle faults, with displacements of less than 1 km, truncate all rock units as well as the Jones and Granby faults.

The Granby fault

The west-dipping Granby fault bounds the western margin of the Grand Forks complex (Fig. 1). Footwall rocks of the complex comprise polydeformed sillimanite-grade paragneiss of uncertain age and variably deformed Middle Jurassic and Late Cretaceous-Paleocene plutonic rocks (Little 1957; Preto, 1970; this study). The timing of deformation and metamorphism in the complex is uncertain.

The trace of the Granby fault, a well-defined topographic lineament, extends north-south along strike for 50-60 km (Fig. 1). It dies out to the south in Washington; the northern termination is uncertain due to poor exposure and lack of detailed mapping. In some places the fault is a single cataclastic zone separating upper and lower plate rocks and in others it is a complex, 0.5-1.5 km thick zone of anastomosing faults (Fig. 2; see also Preto, 1970). Isolated ductile shear zones were observed in granitoid rocks in the footwall of the Granby fault; however, the predominant fabric is brittle. Regionally the fault appears to dip 25-35 degrees to the west (determined from structure contours) but locally there are 2-3 km long steeply-dipping segments interpreted as reactivated zones.

The Granby fault juxtaposes unmetamorphosed and greenschist facies hanging wall rocks against sillimanite-grade paragneiss in the footwall. The magnitude of displacement is uncertain; however, 1) the metamorphic juxtaposition (sillimanite-chlorite) is significant, and 2) there are no hanging wall/footwall cutoffs, indicating that the displacement is large, perhaps on the order of tens of kilometres as suggested by Parrish et al. (1988). The Granby fault truncates the 51.5 $\pm$ 0.5 Ma (U-Pb zircon) Coryell syenite and Middle Eocene Marron Formation (Fig. 2) and therefore movement is Middle Eocene or younger.

The Jones fault

Isolated exposures of Eocene volcanic rocks are bounded at their base by a brittle fault, herein named the Jones fault (it is well exposed near Jones Creek; Fig. 2). The fault surface is presently flat lying or very gently dipping either east or westward (Fig. 3). It has been reoriented by the Granby fault and late steep faults (Fig. 2) and it may also be folded.

Klippen were mapped on the ridge between the Granby River and Lynch Creek where hanging wall volcanic rocks are juxtaposed against footwall Coryell syenite (Fig. 4). At the northern end of the ridge, the fault is a cryptic surface with a thin (<1 m) ultracataclasite zone in a 3-4 m thick fractured zone, whereas at the southern end of the ridge (south of Jones Creek), the fault is a 20-30 m thick breccia zone with gouge zones and quartz veins. Coryell syenite fault rocks are composed of chalky fine grained cataclasite with closely spaced fractures and gouge zones (Fig. 5). Greenschist facies retrograde alteration minerals include chlorite, epidote and sericite. Primary biotite and hornblende, ubiquitous in the protolith, are not present in fault rocks. Hanging wall volcanic fault rocks, which are generally more coherent than the syenite, fracture into hard splinters which are often coated with chlorite, epidote and pyrite.

The sense of displacement of the Jones fault is uncertain. On the ridge between the Granby River and Lynch Creek (Fig. 2), volcanic flows and bedding in a conglomerate dip to the east. This orientation would be geometrically consistent with west-directed movement on the Jones fault if these rocks are upright, as their stratigraphic correlation indicates. However, westward dips are reported in the region by Little (1957) and the structure in the upper plate is unknown.

The original geometry and orientation of the fault is uncertain; it may have been listric or planar and this makes it difficult to estimate displacement. In the case of a planar fault, the angular relationship between flow banding and conglomerate bedding in the hanging wall and the present orientation of the fault can be used to place some constraints on the dip of the active fault. Restoration of bedding to the horizontal requires that the Jones Creek fault had an original strike of 000° to 028° and a dip of 60° to 80° degrees west. The extrusive volcanic rocks and mesozonal Coryell syenite are both Middle Eocene. Assuming a vertical separation of

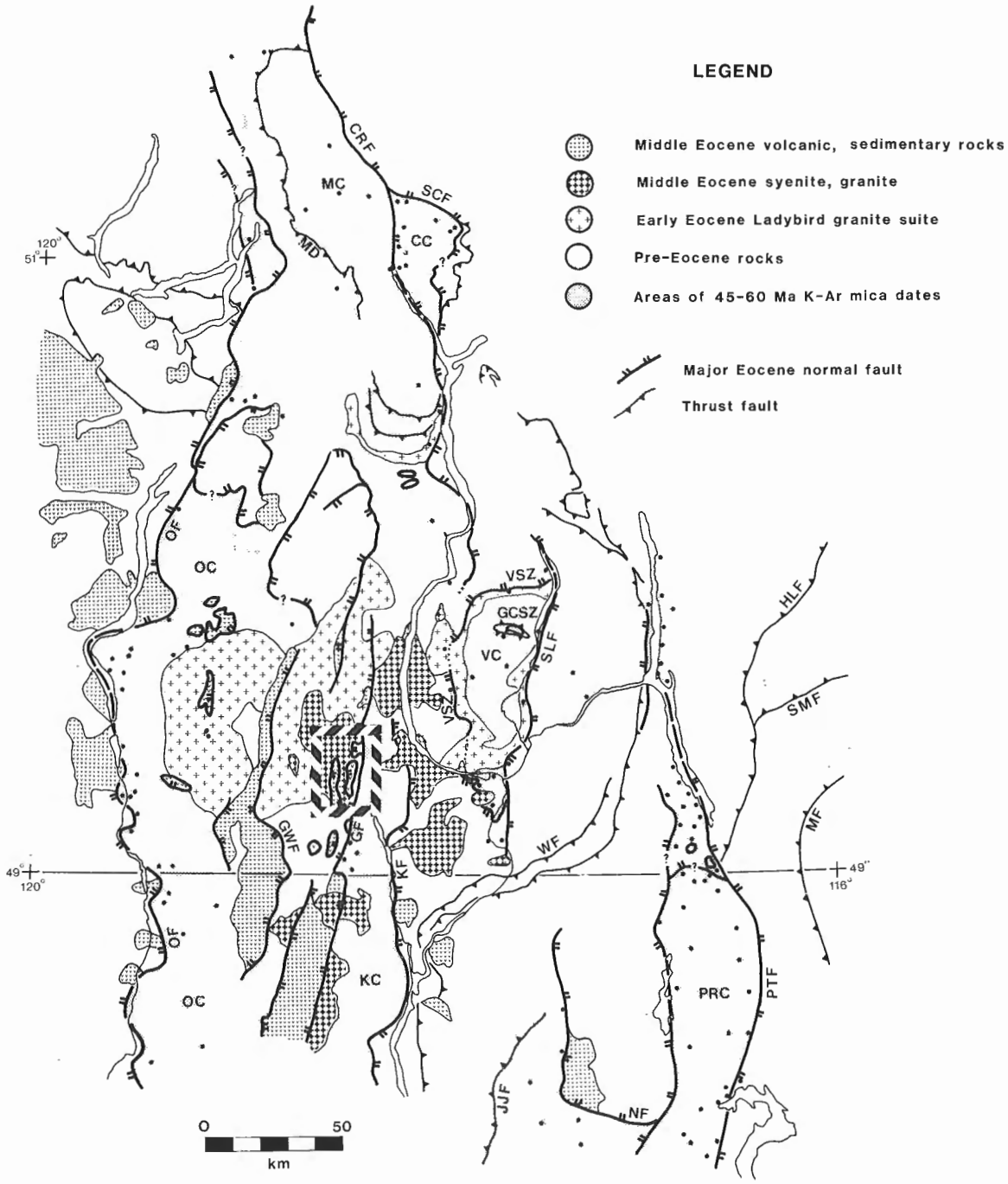

Figure 1. Tectonic map of southern British Columbia and northern Washington modified from Parrish et al. (1988). Metamorphic complexes and faults are designated as follows: CC, Clachnacudainn complex; CRF, Columbia River fault; GCSZ, Gwillim Creek shear zones; GF, Granby fault; GWF, Greenwood fault system (see below); HLF, Hall Lake fault; JJF, Jumpoff Joe fault; KC, Grand Forks-Kettle complex; KF, Kettle River fault; MC, Monashee complex; MD, Monashee decollement; MF, Moyie Fault; NF, Newport fault; OC, Okanagan complex; OF, Okanagan Valley fault; PRC, Priest River complex; PTF, Purcell Trench fault; SCF, Standfast Creek fault; SLF, Slocan Lake fault; SMF, St. Mary fault; VC, Valhalla complex; VSZ, Valkyr shear zone; WF, Waneta fault. GWF (Greenwood fault system) is a composite system of west-dipping normal faults including Deadwood Ridge, parts of Greyhound and Windfall Creek, and McCarren Creek faults of Little (1983), with offset measured in kilometres. For the sake of clarity, a fault trace, termed GWF, is shown which predominantly bounds the Eocene strata on the east. Dots show locations of 45-60 Ma K-Ar dates.

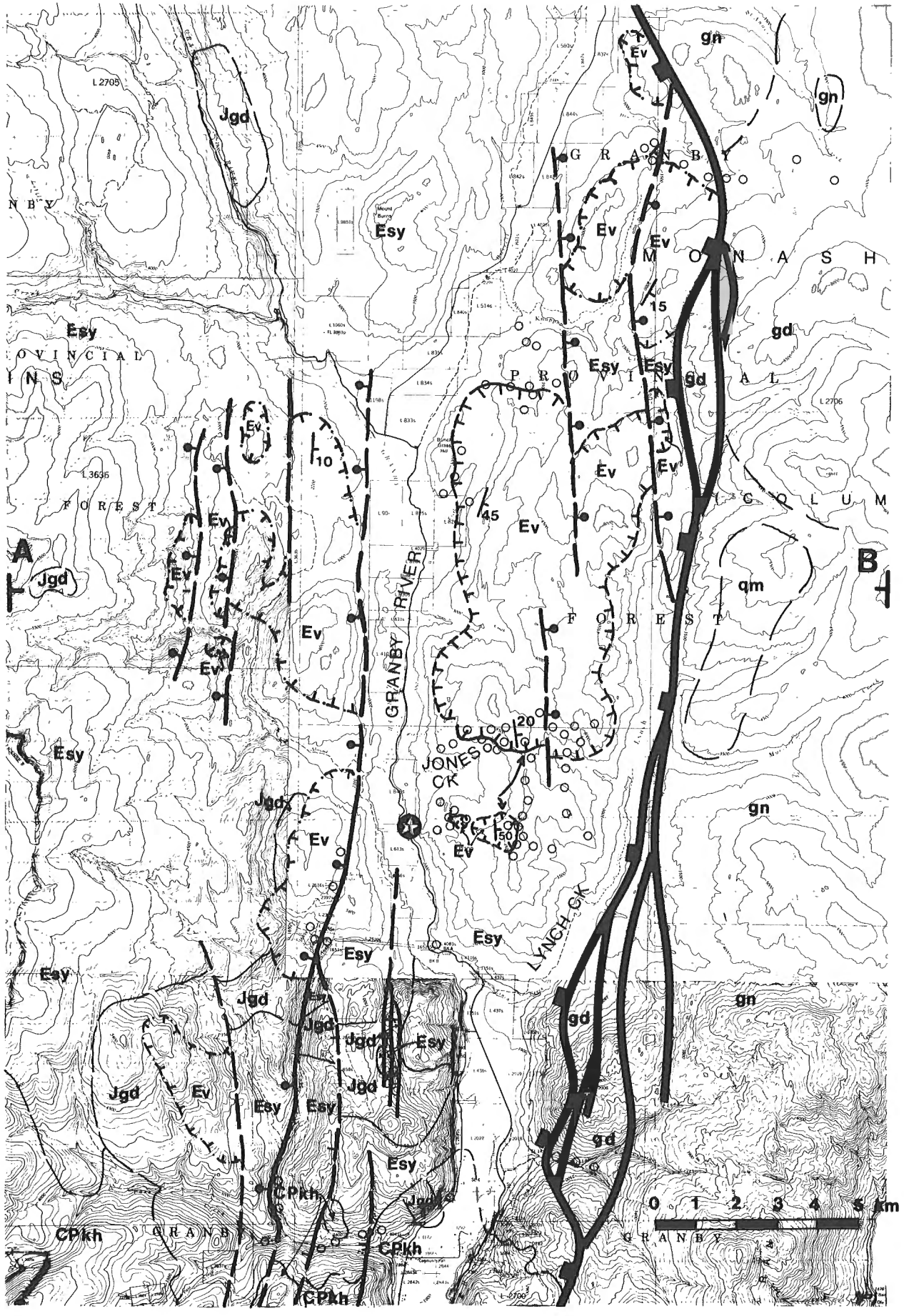
A
B
Jgd
Esy
Ev
gn
gd
qm
CPkh
GRANBY RIVER
JONES CK
LYNCH CK
GRANBY
MONASH
FOREST
PROVINCIAL
COLUM
10
15
20
45
50
0 1 2 3 4 5 km

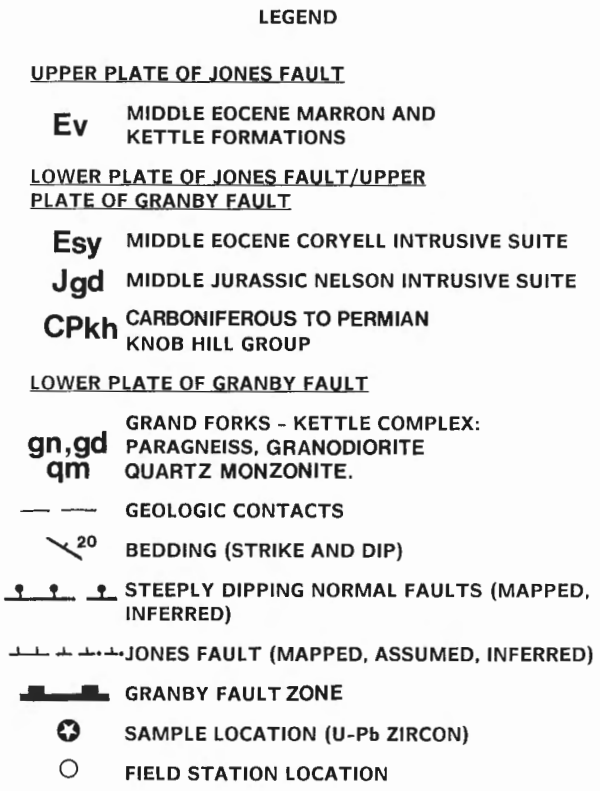

Figure 2. Geological map of the Granby River area compiled from Carr and Parkinson (this study), Little (1957) and Preto (1970). See box on Figure 1 for location. Cross section AB is shown in Figure 3.

5-13 km, a displacement of 5.5-15 km is required if the active Jones fault was a steeply-dipping planar structure with westerly displacement.

The dissected flat-lying configuration of the Jones fault, with Tertiary strata dipping into the fault plane, is typical of many extensional faults in the Great Basin extended terrane (Coney, 1980; Davis et al., 1980; Wernicke, 1985), and this style has not previously been described in the extended terrane of southern British Columbia.

Steep normal faults

Steeply-dipping brittle faults which crosscut all rock units are younger than both the Jones and Granby faults. These faults were mapped in the southern part of Fig. 2 and were found to correspond to prominent north-south lineaments on aerial photographs. One of these faults is well exposed for 7 km along Rock Candy Creek. Coryell syenite occurs in both the hanging wall and footwall so that the amount of offset is unknown. The fault is a 0.5-1 km thick zone of incoherent, fractured rock with discrete gouge zones and pervasive chlorite alteration. Gouge zones and a fault breccia-hosted fluorine deposit at Kennedy mine dip 70 degrees to the west.

Steep normal faults in the central part of the map area were inferred on the basis of interpretation of aerial photographs and geological relationships (Little, 1957). They range from 4-14 km in strike length, and cross-section interpretation of displaced contacts indicates that displacements are on the order of tens to hundreds of metres. They may be listric; this would account for present orientations of the Jones fault in the western part of the area (Fig. 3).

Upper plate of Granby fault/lower plate of Jones fault

There are three rock units in the structural zone which lie in the footwall of the Jones fault and the hanging wall of the Granby fault (Fig. 2): 1) upper Paleozoic-early Mesozoic Knob Hill Group; 2) Middle Jurassic intrusive rocks; and 3) Eocene Coryell intrusive rocks.

Knob Hill Group

The Knob Hill Group, thought to be part of an allochthonous terrane accreted in the late Triassic (Monger et al., 1982), consists of poorly bedded chert, andesitic to basaltic greenstone and minor argillite and limestone (Little, 1983). The thickness is unknown and there may be several unconformities within the group. Ages of pre-Carboniferous, Permian and Triassic to (?) Early Jurassic have been determined from fossils (Little, 1983). Isolated exposures of Knob Hill greenstone and siltstone occur in the southern part of the Granby map area (Fig. 2).

Middle Jurassic Nelson intrusives

Middle Jurassic plutons and batholiths, originally mapped as "Nelson series" by Little (1957, 1961), comprise heterogeneous plutons which consist of biotite granodiorite, hornblende-biotite granodiorite and minor granite phases. Leucocratic, mafic and pegmatite dykes and schist and paragneiss screens are common. The fabric and crystal size is variable ranging from an undeformed igneous texture with porphyritic or equigranular texture to foliated orthogneiss with boudinaged and folded dykes. Knob Hill Group rocks occur as pendants in the Nelson intrusives. Both the Knob Hill Group and Nelson intrusives are intruded by Coryell along sharp contacts, or by dykes of Coryell with chilled margins.

Coryell intrusives

The extensive Middle Eocene Coryell intrusive suite is exposed from the Okanagan fault in the west to the Valhalla complex in the east (Fig. 1). The main lithology is a pink- to buff-weathering syenite (Fig. 6) but there are minor phases of mafic biotite-rich monzonites, grey-weathering granite to quartz syenite (Little, 1957) and ultramafic to mafic intrusives which are exposed in the Franklin Camp 20 km to the north (Drysdale, 1914; Keep and Russell, 1988). In contrast to the heterogeneous Nelson intrusives, most phases of the Coryell suite are homogeneous in composition and fabric. The syenite is typically coarse grained and porphyritic with euhedral crystals (Fig. 6). White or pink aplitic to coarse grained feldspathic dykes are common. Ductile penetrative fabrics were not observed in Coryell intrusions in the Granby valley area. Coryell intrudes all other rock units in the region with the exception of Eocene and Miocene volcanics (Little, 1957; this study).

U-Pb zircon geochronology of Coryell syenite

A Coryell sample, collected from a coarse syenite phase 4.75 km north of the junction of Lynch Creek and the Granby River (Fig. 2), is 51.1 ± 0.5 (U-Pb zircon). Standard mineral separation techniques were used to separate zircons. Dissolution and U and Pb separation were done using techniques modified from Krogh (1973). U and Pb isotopic analyses were run on a MAT 261 multicollector. All geochronological work was done at the University of California at Santa Barbara. Table 1 contains the data for 2 zircon fractions which are both concordant at 51.1 ± 0.5 Ma. This is the same as a 51.5 ± 0.5 Ma U-Pb zircon age of a posttectonic syenite in Valhalla complex (Carr et al., 1987; Parrish et al. 1988).

The Coryell syenite places constraints on the age of Eocene extensional faulting in the Granby area. The Jones and Granby faults are both younger than 51 Ma as they truncate Coryell intrusions. This is similar to timing established

Table 1. U-Pb Analytical data for zircon, Coryell syenite, Granby River area, British Columbia.

Analysis #, size[a]	wt[b] (mg)	U, ppm	Pb,[c] ppm	$^{206}Pb/^{204}Pb$[d]	^{208}Pb[e] %	$^{206}Pb/^{238}U$, ± 2 SEM%[f]	$^{207}Pb/^{235}U$ ± 2 SEM%[f]	$^{207}Pb/^{206}Pb$ ± 2 SEM%[f]	$^{207}Pb/^{206}Pb$[g], age, error Ma
50-150 mag	7.4	178	1.2	609	20.7	0.00795 (1.0) 51.1 ± 0.5 Ma	0.05171 (1.0) 51.2 ± 0.5 Ma	0.04718 (.3)	58 ± 8
+105 nonmag	3.4	396	2.8	500	21.6	0.00795 (1.0) 51.1 ± 0.5 Ma	0.05155 (1.0) 51.3 ± 0.5 Ma	0.04724 (.4)	61 ± 10

[a]sizes (i.e. 50, +105) refer to average size of zircons in microns.
[b]weighing error 0.1 mg.
[c]radiogenic ^{206}Pb.
[d]measured ratio, corrected for ^{205}Pb-^{235}U spike and fractionation.
[e]radiogenic Pb
[f]corrected for blank Pb and U, common Pb, errors quoted are 2 standard errors of the mean in percent, age errors in Ma.
[g]corrected for blank and common Pb, errors quoted are 2 standard errors of the mean in Ma.

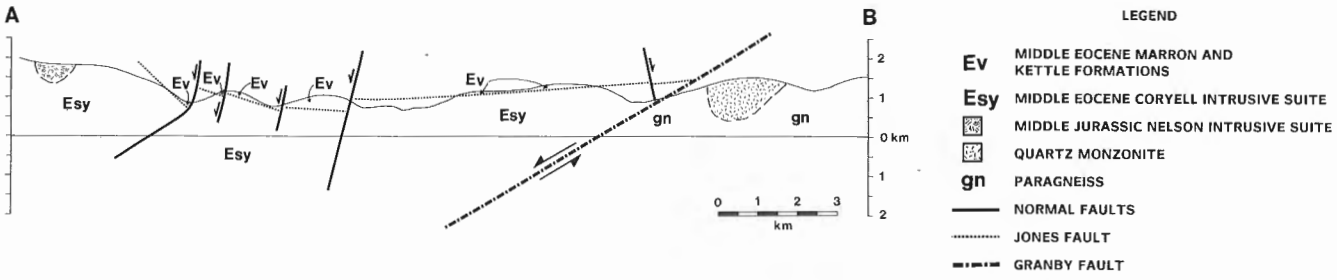

Figure 3. East-west cross section (see Fig. 2 for location). Jones fault with upper plate Marron and Kettle River formations and lower plate Coryell syenite is cut by the Granby fault.

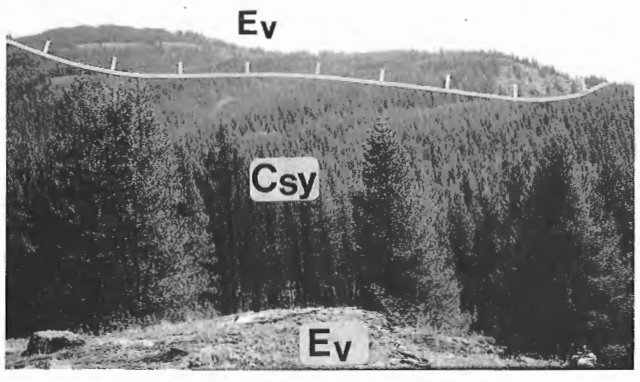

Figure 4. Eastward view of klippen of Marron volcanics (Ev), on ridge-top and in foreground, in upper plate of Jones fault (southeast of Jones Creek; Fig. 2). Footwall Coryell syenite (Csy) underlies the treed slopes in the middle distance.

Figure 5. Fractured cataclasite in Jones Creek fault zone. Protolith is coarse Coryell syenite (compare with protolith in Fig. 6).

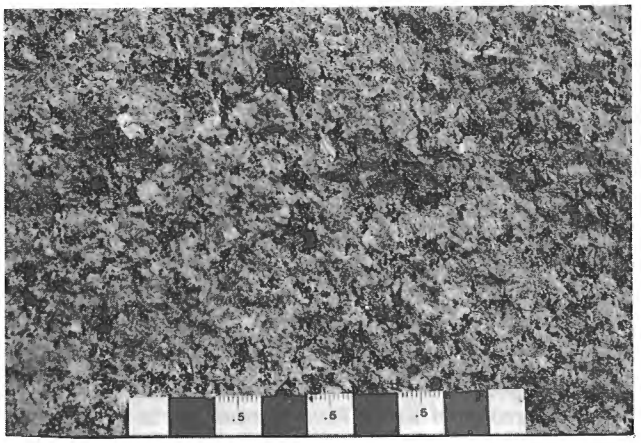

Figure 6. Pink-weathering hornblende bearing Coryell syenite from Granby valley dating locale (shown on Fig. 2) is representative of the main phase of the Coryell intrusive suite in southern British Columbia.

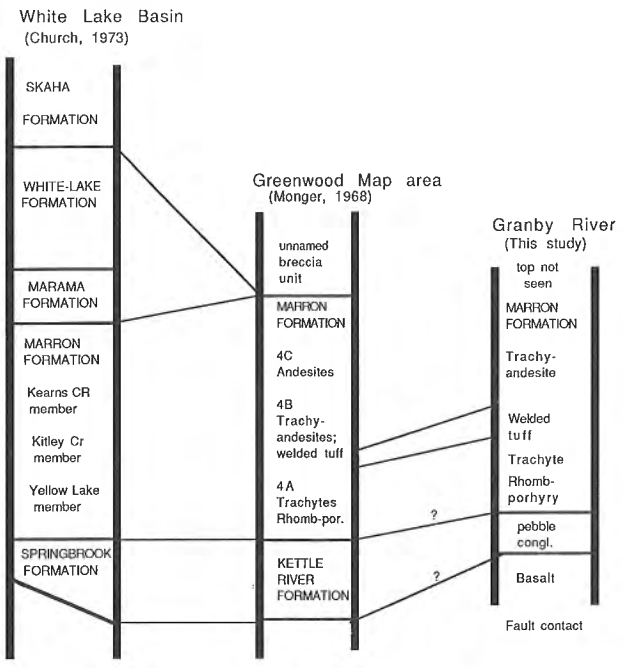

Figure 7. Summary of correlation of Eocene stratigraphy in southern British Columbia.

for the westerly-directed Okanagan fault (Parkinson, 1985; Carr et al., 1987; Parrish et al., 1988) and is in contrast to easterly-directed fault systems (Kettle and Valkyr-Slocan Lake faults) which are intruded by 51 Ma Coryell syenite (Parrish et al., 1988).

Upper plate of Jones fault

Eocene stratigraphy — Granby area

Volcanic and sedimentary rocks west of the Grand Forks complex were mapped by Little (1957) as Phoenix Volcanic

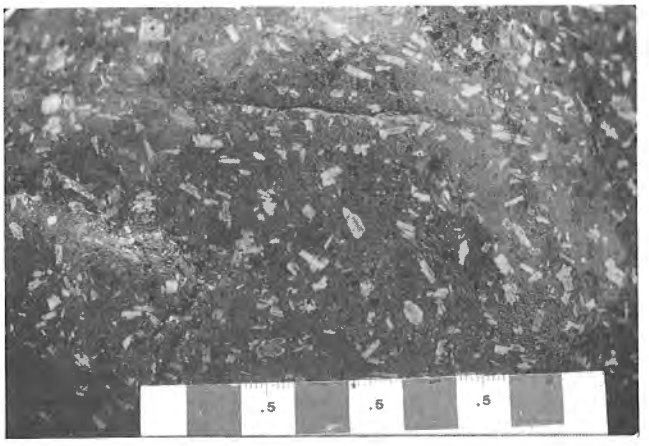

Figure 8. Trachyandesite with feldspar, pyroxene and biotite phenocrysts from the Marron Formation northeast of Jones Creek.

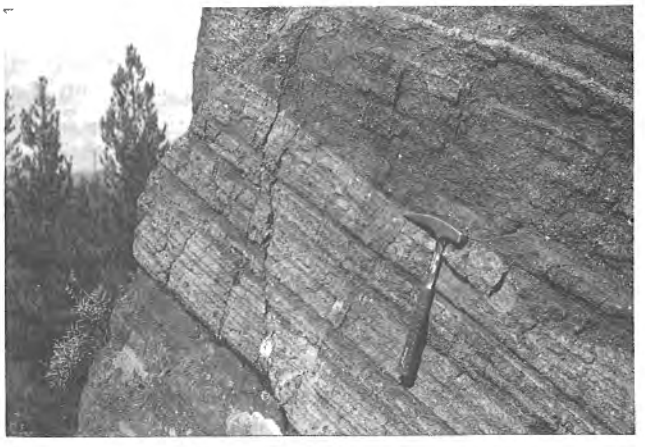

Figure 9. Well-bedded immature conglomerate with subangular basalt clasts of the Kettle River Formation on Bunch Grass Hill. The conglomerate is overlain and underlain by alkali basalt of the Marron Formation.

group and were subsequently correlated with and renamed the Marron Formation (Monger, 1968; Church, 1973). The most extensive exposures, located on the ridge between the Granby River and Lynch Creek (Fig. 2) were examined in this study (Fig. 7). The exposed section is <200 m thick. The lowest exposed horizons are alkaline basalt or basaltic andesite with phenocrysts of biotite, pyroxene and feldspar (plagioclase and rhombohedral anorthoclase). Trachyte and trachyandesite overlie the basaltic rocks and constitute the predominant lithology. They are brown or tan-brown with coarse grained creamy white to pink feldspar phenocrysts (Fig. 8). Biotite and altered pyroxenes are common in the more mafic sections. Along the ridge crest, the upper part of the exposed section consists of a grey to brown flow-banded trachytic tuff unit. The flow banding strikes 350-010° and dips $\sim$50 degrees to the east. The tuff contains clear to white feldspar phenocrysts and flattened pumice fragments. The flattened pumice fragments and flow banding illustrate the welded nature of this unit.

East of Bunch Grass Hill (Fig. 2), a red-weathering well-bedded pebble conglomerate unit at least 40 m thick occurs within the alkaline basalt unit (Fig. 9). Coarse grained greywacke and conglomerate contain angular fragments of red and green basaltic clasts in a calcareous matrix. Bedding is well defined by thin 1-20 cm beds and dips 35 to 55 degrees to the southeast.

Regional stratigraphy of Middle Eocene Kettle River and Marron formations

Eocene volcanic and sedimentary rocks are exposed west of Greenwood, in the Kettle valley, in northern Washington and west of the Okanagan valley (Bostock, 1941; Little, 1961, 1983; Monger, 1968; Church, 1973; Pearson and Obradovich, 1977; Church et al., 1983; see Fig. 1 and Fig. 7). In the Greenwood area, the ~600-1200 m thick clastic Kettle River Formation sits unconformably on upper Paleozoic stratigraphy and Mesozoic intrusions (Little, 1983). It is composed of stratified feldspathic and lithic volcanic sandstone with conglomeratic horizons up to 100 m thick and rare porphyritic dacite. Conglomerate occurs at all stratigraphic horizons and the clasts consist of chert, greenstone, quartz-feldspar porphyry and dacitic tuff (Little, 1983). The Kettle River Formation is of Middle Eocene age based on spores and microflora (Rouse and Mathews, 1961; Little, 1983) and correlates with the Kettle River Formation in the Kelowna area in the Okanagan valley (Church et al., 1983; Fig. 7) and the O'Brien Creek Formation in northern Washington (Pearson and Obradovich, 1977). Pearson and Obradovich (1977) reported a K-Ar biotite date of 53.1 ± 1.5 Ma from a tuff unit within the O'Brien Creek Formation.

The ~600-1800 m thick Marron Formation overlies and interdigitates with the Kettle River Formation (Monger, 1968; Little, 1983). In the Greenwood area, the Marron was divided by Monger (1968) into three units (from oldest to youngest): 4A) sodic trachytes, or alkaline basalts; 4B) trachyandesite to andesite; and pyroxene andesite; and 4C) biotite-pyroxene andesite, or hornblende andesite (Fig. 7). These units are correlated with the Yellow Lake, Kitley Lake and Kearns Creek members of the Marron Formation in the White Lake basin (Church, 1973; Little, 1983). The Greenwood area tuff was dated by Mathews (1964) as 49 ± 2 Ma (K-Ar on biotite); equivalent units in the White Lake basin section studied by Church (1973) farther west, give K-Ar biotite dates of 52.9 ± 1 Ma.

Correlation of Eocene volcanic and clastic strata in the Granby area

The volcanic section in the Granby area is mafic at the base and becomes increasingly felsic upsection. There is a conglomerate unit near the base and a flow-banded tuff near the top of the exposed section (Fig. 7). The volcanic rocks correlate well with the lower Yellow Lake and Kitley Lake members of the Marron Formation in both the Greenwood and White Lake areas as described by Monger (1968), Church (1982) and Little (1983). The conglomerate is probably correlative with conglomerates in the Kettle River Formation (Monger, 1968) implying that the Kettle River and Marron Formations are intercalated.

CONCLUSIONS

Detailed mapping of rocks west of the Grand Forks-Kettle Complex in the Granby valley and U-Pb geochronology support the following conclusions.

1) Isolated exposures of intercalated volcanic and clastic rocks, which occur exclusively in the upper plate of the Granby fault, are correlative with the Middle Eocene Marron Formation (lower Yellow Lake and Kitley Lake members) and Kettle River formation of the Greenwood area and White Lake basin.

2) There are three generations of Eocene normal faults in the map area. The oldest is the Jones fault which has klippen of Marron and Kettle River formations in the hanging wall. The fault is presently shallow dipping. It is truncated by the regionally extensive, moderately west-dipping Granby fault which bounds the western margin of the high grade Grand Forks complex. The youngest structures are steep normal faults, of apparently minor displacement (< 1 km), which may have in part reactivated the Granby fault. The Jones fault has been reoriented by movement on the Granby fault and late brittle faults so the orientation and geometry of the active fault is unknown.

This study raises questions about the kinematics, displacement and active geometry of the high crustal level, Eocene extensional faults in southern British Columbia. Further work must be done, perhaps in better exposed areas, to better constrain the fault systems.

3) Coryell syenite is a regionally extensive plutonic suite that is exposed from the Valhalla complex in the east to the Okanagan valley in the west. A sample from the Granby River valley yields a 51.1 ± 0.5 Ma U-Pb zircon date. This is the same as a 51.5 ± 0.5 Ma U-Pb zircon date from a posttectonic stock in the Valhalla complex (Carr et al., 1987; Parrish et al., 1988).

4) The Coryell syenite places constraints on the age of Eocene extensional faulting in the Granby area. The Jones and Granby faults are both younger than 51 Ma as they truncate Coryell intrusions. This is similar to timing established for the Okanagan fault (Parkinson, 1985; Parrish et al., 1988) and is in contrast to easterly-directed fault systems (Kettle and Valkyr-Slocan Lake faults) which are plugged by 51 Ma Coryell syenite (Carr et al., 1987; Parrish et al., 1988).

5) In contrast to the Okanagan, Columbia River and Valkyr-Slocan Lake faults which have a mid-crustal level mylonitic history, the Jones and Granby faults are higher level brittle structures. They occur near the central part of the extended terrane where Eocene transport directions diverge. The dissected flat-lying configuration of the Jones fault, with Tertiary strata dipping into the fault plane, is typical of the extensional faults in the Great Basin extended terrane (Coney, 1980; Davis et al., 1980; Wernicke, 1985).

To the east of the Grand Forks complex, the normal faults are east dipping and easterly directed, and in the Granby region and farther west, the faults are west dipping and westerly directed. The Granby area preserves high level structures which may not be as far travelled as upper plate rocks on the perimeter of the extended terrane.

ACKNOWLEDGMENTS

We would like to thank Randy Parrish for introducing us to the geology of the area, for stimulating discussions and for comments on the manuscript.

REFERENCES

Bostock, H.S.
1941: Okanagan Falls map-area; Geological Survey of Canada, Map 627A.

Carr, S.D., Parrish R., and Brown, R.L.
1987: Eocene Structural Development of the Valhalla complex, Southeastern British Columbia; Tectonics, v. 6, p. 175-196.

Church, B.N.
1973: Geology of the White Lake Basin; British Columbia Department of Mines and Petroleum Resources, Bulletin 61, 120 p.
1982: Notes on the Penticton Group: a progress report on a new stratigraphic subdivision of the Tertiary, south-Central British Columbia; B.C. Ministry of Energy, Mines and Petroleum Resources, Geological Fieldwork, 1981, Paper 1982-1, p. 12-16.

Church, B.N., Ewing, T.E., and Hora, Z.D.
1983: Volcanology, structure, coal and mineral resources of early Tertiary outliers in south-Central British Columbia; Geological Association of Canada, Field Trip Guidebook No. 1, 91 p.

Coney, P. J.
1980: Cordilleran metamorphic core complexes: an overview; Geological Society of America, Memoir 153, p. 7-31.

Davis, G.A., Anderson, J.L., and Frost, E.G.
1980: Mylonitization and detachment faulting in the Whipple-Buckskin-Rawhide Mountains terrane, southeastern California and western Arizona; Geological Society of America, Memoir 153, p. 79-129.

Drysdale, C.W.
1914: Franklin Mining Camp, west Kootenay, British Columbia; Geological Survey of Canada, Map 97A.

Keep, M. and Russell, J.K.
1988: Geology of the Averill Plutonic Complex, Franklin Mining Camp; British Columbia Ministry of Energy, Mines and Petroleum Resources, Paper 1988-1, p. 49-53.

Krogh, T.E.
1973: A low contamination method for hydrothermal decomposition of zircon and extraction of U and Pb for isotopic age determinations, Geochimica et Cosmochimica Acta, v. 37, p. 485-494.

Little, H.W.
1957: Kettle River, east half, British Columbia; Geological Survey of Canada, Map 6-1957.
1961: Kettle River, west half, British Columbia; Geological Survey of Canada, Map 15-1961.
1983: Geology of the Greenwood map-area, British Columbia; Geological Survey of Canada, Paper 79-29.

Mathews, W.H.
1964: Potassium-Argon Date Determination of Cenozoic Volcanic Rocks from British Columbia; Geological Society of America Bulletin, v. 75, p. 465-468.

Monger, J.W.H.
1968: Early Tertiary stratified rocks, Greenwood map-area, B.C.; Geological Survey of Canada, Paper 67-42, 39 p.

Monger, J.W.H., Price, R.A., and Tempelman-Kluit, D.J.
1982: Tectonic accretions and the origin of the duo major metamorphic and plutonic wells in the Canadian Cordillera; Geology, v. 10, p. 70-75.

Parkinson, D.
1985: U-Pb geochronology and regional geology of the southern Okanagan Valley, British Columbia: the western boundary of a metamorphic core complex; M.Sc. thesis, University of British Columbia, 149 p.

Parrish, R.R., Carr, S.D., and Parkinson, D.L.
1988: Eocene extensional tectonics and geochronology of the Southern Omineca Belt, British Columbia and Washington; Tectonics, v. 7, p. 181-212.

Pearson, R.C. and Obradovich, J.D.
1977: Eocene rocks in northeast Washington–radiometric ages and correlation; U.S. Geological Survey, Bulletin 1433, 41 p.

Preto, V.A.
1970: Structure and petrology of the Grand Forks Group, British Columbia; Geological Survey of Canada, Paper 69-22, 80 p.

Rouse, G.E. and Mathews, W.H.
1961: Radioactive dating of plant bearing deposits; Science, v. 133, p. 1079-1080.

Wernicke, B.
1985: Uniform-sense normal simple shear of the continental lithosphere; Canadian Journal of Earth Sciences, v. 22, p. 108-125.

The Cariboo duplex at the southern boundary of the Monashee Complex, southern British Columbia

Vicki J. Coleman[1]
Cordilleran and Pacific Geoscience Division, Vancouver

Coleman, V.J., The Cariboo duplex at the southern boundary of the Monashee Complex, southern British Columbia; in Current Research, Part E, Geological Survey of Canada, Paper 89-1E, p. 89-93, 1989.

Abstract

The Monashee décollement, a westerly-rooted, east-verging ductile shear zone displaced rocks of the Selkirk Allochthon eastward across the Monashee Complex. The décollement is located in Cariboo Alp on the southwest flank of Thor-Odin, where it underlies the Cariboo duplex.

The duplex is bounded by the Monashee décollement (sole thrust) and the Cariboo thrust (roof thrust), and contains fault-bounded imbricate slices. Kinematic studies indicate a consistent upper plate to-the-northeast sense of shear throughout the duplex. Displacement along the duplex was concurrent with and outlasted F2 folding; fault-bounded horses are sheared-off limbs of large F2 folds. The Cariboo thrust juxtaposes packages of rocks with different metamorphic assemblages. Dating of an undeformed, discordant pegmatite reveals that the structures observed in Cariboo Alp are older than 58 ± 0.5 Ma.

As the thrust slices swing around the western side of Thor-Odin, they become greatly attenuated and stretching lineations become E-W trending, recording an easterly-directed sense of shear.

Résumé

Le décollement de Monashee, zone de cisaillement ductile enracinée à l'ouest et orientée vers l'est, a déplacé des roches de l'allochtone de Selkirk vers l'est à travers le complexe de Monashee. Le décollement est situé dans Cariboo Alp sur le flanc sud-ouest de Thor-Odin où il repose sous le duplexe de Cariboo.

Le duplexe est délimité par le décollement de Monashee (chevauchement subhorizontal) et par le chevauchement de Cariboo (chevauchement supérieur), et renferme des lambeaux imbriqués limités par des failles. Des études de cinématique révèlent la présence d'une plaque supérieure ininterrompue dans le sens nord-est du cisaillement dans l'ensemble du duplexe. Le déplacement le long du duplexe s'est produit pendant et après le plissement F_2; les intercalations stériles limitées par des failles sont des flancs de grands plis F_2 détachés par cisaillement. Le chevauchement de Cariboo jouxte des ensembles de roches présentant différentes associations métamorphiques. La datation d'une pegmatite discordante non déformée révèle que les structures observées dans Cariboo Alp sont antérieures à 58 ± 0,5 Ma.

À mesure que les lambeaux de charriage contournent le flanc ouest de Thor-Odin, ils s'atténuent considérablement et les linéations s'allongent dans une direction E-O, leur imprimant ainsi un sens de cisaillement orienté vers l'est.

[1] Department of Earth Sciences, Carleton University and Ottawa-Carleton Geoscience Centre, Ottawa, Ontario, K1S 5B6

INTRODUCTION

The Monashee décollement is a westerly-rooted, east-verging ductile shear zone which carried cover rocks of the Selkirk Allochthon eastward across core and mantling gneisses of the Monashee Complex of the Shuswap metamorphic terrane of southeastern British Columbia (Brown and Read, 1983; Journeay, 1986; Brown and Journeay, 1987). Displacement on the Monashee décollement is thought to have occurred originally in the Middle Jurassic with major reactivation in the Late Cretaceous (Brown and Journeay, 1987; Journeay, 1986).

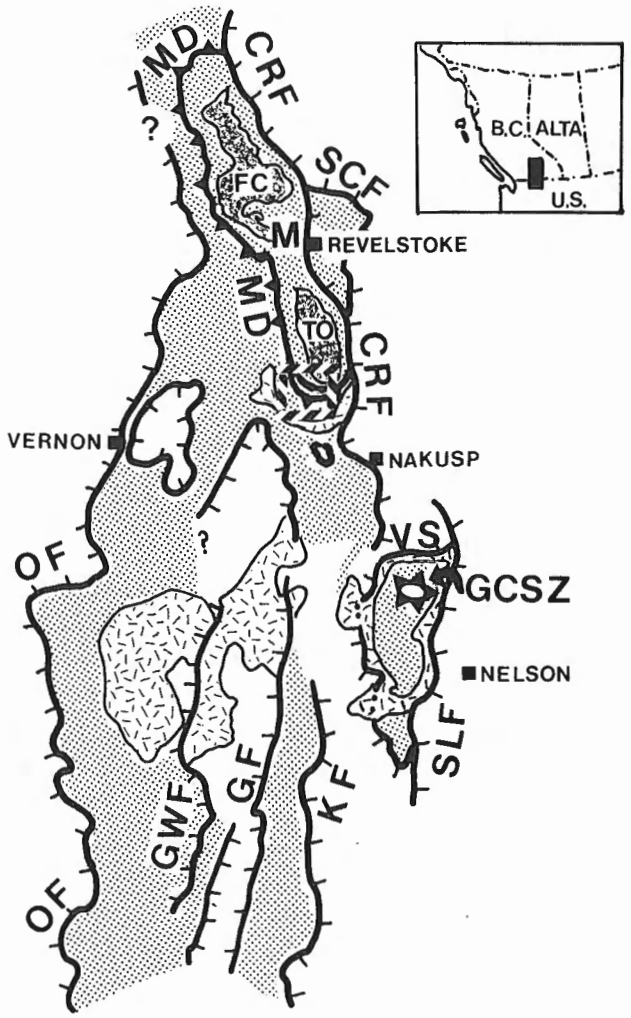

Figure 1. Tectonic sketch map of southern Omineca belt, modified after Carr (1989). Features shown with patterns are the Early Eocene Ladybird suite (granite pattern), areas of metamorphic rocks characterized by 45-60 Ma K-Ar mica dates (grey stipple) and basement rocks of the Monashee Complex (dark grey). Major thrust faults within Monashee (M) and Valhalla (V) complexes are the Monashee décollement (MD) and Gwillim Creek shear zones (GCSZ). Basement rocks of the Monashee complex are exposed in Frenchman Cap (FC) and Thor-Odin (TO). Eocene normal faults are the Columbia River fault (CRF), Granby fault (GF), Greenwood fault system (GWF), Kettle fault (KF), Okanagan fault (OF), Slocan Lake fault (SLF), and Valkyr shear zone (VS). Box marks location of Cariboo Alp (Fig. 2).

A Master's project has been started at Carleton University to study the décollement on the southwest flank of Thor-Odin, a structural culmination in the Monashee Complex (Fig. 1 and 2). This study confirms the location of the décollement proposed by Journeay and Brown (1986) in Cariboo Alp.

Reesor and Moore (1971) originally mapped slices of both basement and cover rocks in Cariboo Alp. Duncan (1984) recognized these as thrust slices but interpreted them to have northerly-directed movement, oriented at right angles to local fold hinges. Results of the present study indicate that the fault-bounded slices in Cariboo Alp are part of a duplex structure, herein named the Cariboo duplex (Fig. 3 and 4), which was formed by an apparent upper plate to-the-northeast shearing event. These results are preliminary; mapping will be continued next summer.

THE CARIBOO DUPLEX

The Cariboo duplex is bounded by northwest-southeast trending sole and roof faults, the Monashee décollement and the Cariboo thrust respectively, which dip to the southwest. In between the sole and roof thrusts are fault-bounded imbricate slices or horses (Fig. 2 and 3). There is a consistent, strong northeast-southwest stretching lineation and a southwestward dipping mylonitic foliation. The duplex is characterized by recrystallized and annealed mylonitic fabrics,

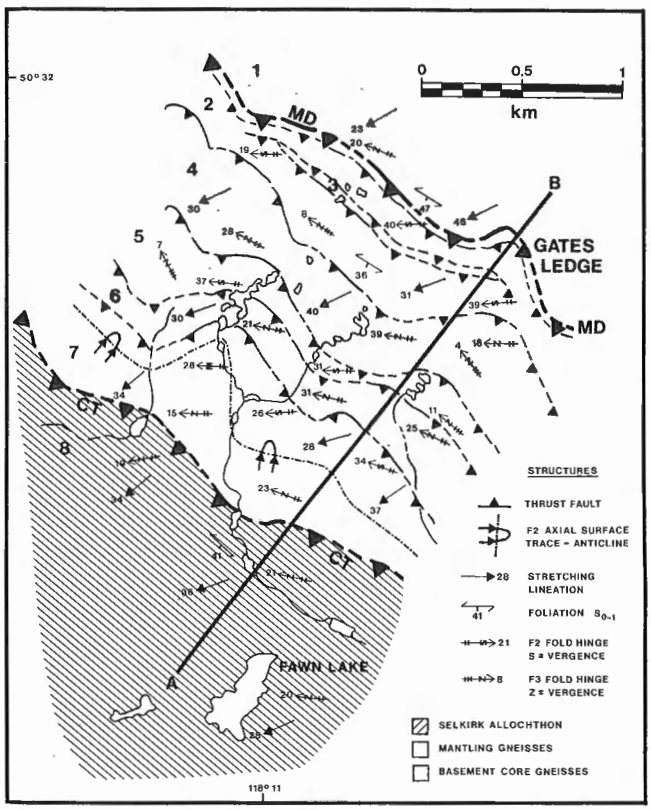

Figure 2. Simplified map of Cariboo Alp. See Figure 1 for regional location. MD = Monashee décollement. CT = Cariboo thrust. Numbered units are referred to and described in the text.

sheath folds, and strong transposition of stratigraphy. Figure 4 is a representation of the possible geometry of the Cariboo duplex.

Below the sole thrust (Monashee décollement), are basement core gneisses (labelled 1 in Fig. 2 and 3). They consist predominantly of folded migmatitic biotite-quartz-feldspar ± garnet ± sillimanite ± kyanite gneisses, with varying proportions of these three main constituents. Boudins of amphibolite are also present.

The horses (units 2-7 in Fig. 2 and 3) are thrust slices of both mantling and basement core gneisses. The mantling gneiss slices (labelled 2, 5, 7 in Fig. 2 and 3) are composed of interlayered rusty-weathering semipelite and quartz-feldspar paragneiss, psammite, pelite, and quartzite. Some of the quartzite units are quite clean and up to 25 m in thickness. A minor amount of marble and calc-silicate is also present. Boudins and discontinuous layers of amphibolite are common.

Basement thrust slices 3 and 4 (Fig. 2 and 3) consist mainly of layered impure psammites with interlayers of pelite and migmatitic biotite-quartz-feldspar gneiss. The middle basement slice (4 in Fig. 2 and 3) contains units up to 20 m in thickness with diopside - hornblende - quartz clots in a psammitic matrix. The southern basement slice (labelled 6 in Fig. 2 and 3) is much like the basement core gneisses north of the duplex (1 in Fig. 2 and 3). It is predominantly folded migmatitic biotite-quartz-feldspar gneiss with pelitic interlayers.

The vergence of phase-two folds changes abruptly at each thrust contact of the horses. The thrust slices are sheared-off limbs of large phase two folds. An overturned phase two antiform was mapped in the most southern mantling gneiss slice (7 in Fig. 2 and 3; the "fold zone" of Reesor and Moore (1971)).

Above the roof thrust (Cariboo thrust), there is a thick package of metasediments consisting of mainly rusty metasandstone and semipelite, some of which contain up to 30% migmatite pods. Very minor quartzite and marble are present. Amphibolite boudins and layers are very common.

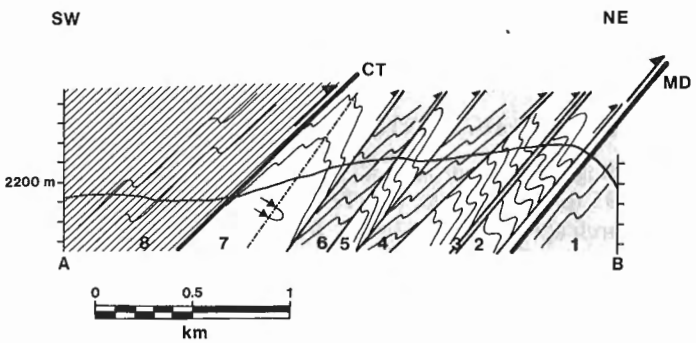

Figure 3. Southwest-northeast cross-section through Cariboo Alp. See Figure 2 for the location of the section A-B and symbols used. Fold patterns in cross-section represent F2 minor folds. Horizontal scale = vertical scale.

These metasediments are best correlated with rocks of the late Proterozoic Lower Horsethief Creek Group based on lithological similarities (Brown et al., 1978; Pell and Simony, 1987). Above the Cariboo thrust there is a significant increase in the amount of discordant pegmatite. To the south, upward in the section, concordant, sheared pegmatite appears.

Below the Cariboo thrust, the pelitic metamorphic assemblage is sillimanite - kyanite - garnet - biotite - quartz - K-feldspar. The sillimanite occurs as mats of fibrolite in the stretching lineation. The kyanite blades have been progressively replaced and overgrown by sillimanite. These blades of kyanite are not as well oriented as the fibrolite, yet look as if they have been rotated towards the stretching direction.

Above the Cariboo thrust, the rocks of the Selkirk Allochthon have a pelitic metamorphic assemblage of sillimanite - garnet - biotite - quartz - K-feldspar. No relict kyanite has been found in the hanging wall of the roof thrust.

Around the western side of Thor-Odin (Fig. 1) these thrust slices assume a more northerly trend and become greatly attenuated. Stretching lineations swing around from a northeast-southwest trend to an east-west trend and record an easterly-directed sense of shear.

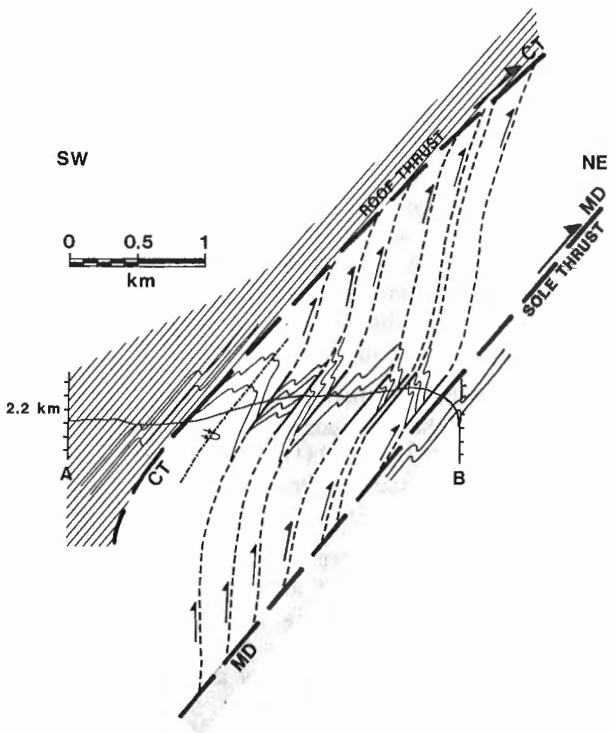

Figure 4. A possible geometry of the Cariboo duplex. See Figures 2 and 3 for the location of the southwest-northeast section A-B and for the symbols used. Horizontal scale = vertical scale.

DISCUSSION

The sole thrust of the Cariboo duplex is the Monashee décollement. In the northern half of the Monashee Complex the décollement has been documented as a shear zone which carried late Proterozoic (Windermere) and Lower Paleozoic rocks of the Selkirk Allochthon eastward across Proterozoic core and mantling gneisses (Brown and Read, 1983; Journeay and Brown, 1986; Journeay, 1986; Scammell, 1987; Bosdachin and Harrap, 1988). In Cariboo Alp, however, the décollement has cut farther down-section and is here located directly above the basement core gneisses.

The Cariboo thrust is interpreted to be a major boundary based on the following data: (1) it truncates major F2 structures, (2) the fault separates packages of rocks with different metamorphic assemblages, (3) it separates different stratigraphic packages, and (4) the fault juxtaposes packages of rocks with different structural styles (e.g. the frequency of minor folds decreases markedly above the Cariboo thrust). The Cariboo thrust may be correlated with Journeay's (1986) MD2 mapped on the west flank of Frenchman Cap dome.

There are insufficient data to determine the amount of displacement across the duplex but it is probably quite large as one of the basement thrust slices is not readily correlated with the adjacent basement core gneisses and the allochthonous mantling gneiss thrust sheets are not easily correlated with autochthonous mantling gneisses to the north (which are mapped as infolds within basement core gneisses).

Kinematics

Kinematic indicators are well preserved throughout the duplex. Mylonitic rocks contain a strong consistent southwest-trending stretching lineation (defined by pulled-apart mats of sillimanite and biotite, quartz rodding, and various pressure shadows) and a predominantly southwestward-dipping mylonitic foliation.

Kinematic indicators that were used in the field to determine the sense of shear included C-S fabrics (Berthe et al., 1979), shear bands (Platt, 1984), rotated asymmetric porphyroclasts and rotated boudins (Hanmer, 1984, 1986; Passchier and Simpson, 1986).

Kinematic indicators were considered reliable, because independent and consistent structures were observed throughout Cariboo Alp (*see* Fig. 2 for spatial distribution of data). These mylonitic fabrics consistently record an upper plate to-the-northeast sense of shear.

Relative timing

Displacement along the Cariboo duplex postdates, or at least outlasted, two deformational events. Early first phase folds are northerly-verging with very shallowly plunging hinges. F1 folds were mapped on the basis of stratigraphic symmetry within the Cariboo duplex, and to the north as infolds of mantling gneisses within the basement core gneisses. F1 folds are also found as refolded folds or as rootless isoclines with hinges parallel to the stretching lineation.

Synmetamorphic, northerly-verging phase-two folds plunge gently to moderately to the west and are the dominant fold type observed in outcrop. F2 folds have been variably rotated towards parallelism with the stretching lineation, and sheared-off limbs of these folds are common. Sheath folds are also present.

Shearing and formation of the duplex was partially coeval with F2 folding but continued after the folding was completed. Fault-bounded horses within the duplex are sheared-off limbs of large F2 folds.

After formation of the duplex, reactivation of the Cariboo thrust resulted in the juxtaposition of different metamorphic assemblages. Kyanite has not been found in the hanging wall, but occurs in the footwall where it is partially replaced by sillimanite.

Postmetamorphic open, upright third phase folds postdate the upper plate to-the-northeast mylonitic fabric. F3 folds are observed as broad warps and crenulations.

A discordant, undeformed pegmatite which cuts across all the thrust slices and structures in Cariboo Alp has been dated at 58 $\pm$ 0.5 Ma (S.D. Carr, pers. comm., 1988). The structures preserved in Cariboo Alp are pre-Eocene structures.

CONCLUSIONS

1) The Cariboo duplex is bounded by a sole thrust, the Monashee décollement, and a roof thrust, the Cariboo thrust, and contains fault-bounded imbricate slices in between.

2) The shear zone exhibits consistent upper plate to-the-northeast sense of shear.

3) The Cariboo thrust truncates large phase-two structures and juxtaposes packages of rocks with different metamorphic assemblages.

4) The structures observed in Cariboo Alp are older than 58 $\pm$ 0.5 Ma.

5) As the thrust slices swing around the western side of Thor-Odin, they become greatly attenuated and linear structures become East-West trending, recording an upper plate to-the-east sense of shear.

ACKNOWLEDGMENTS

Funding for this project is provided by operating grant A2693 to R.L. Brown, a LITHOPROBE grant, and EMR research agreement 227-04-88. Receipt of an NSERC postgraduate scholarship is gratefully acknowledged. The enthusiastic supervision of Richard L. Brown is appreciated. Thanks go to Sharon Carr and Brad Johnson for very helpful discussions and suggestions. Lise Bender provided cheerful assistance in the field. LITHOPROBE Contribution number 86.

REFERENCES

Berthe, D., Chouckroune, P. and Jegouzo, P.
1979: Orthogneiss, mylonite and non-coaxial deformation of granites: the example of the South Amorican Shear Zone; Journal of Structural Geology, v. 1, p. 31-42.

Bosdachin, R. and Harrap, R.M.
1988: Stratigraphy and structure of the Monashee complex and overlying rocks adjacent to the Trans - Canada Highway, west of Revelstoke, B.C.; *in* Current Research, Part E, Geological Survey of Canada, Paper 88-1E, p. 19-23.

Brown, R.L. and Journeay, J.M.
1987: Tectonic denudation of the Shuswap metamorphic terrane of southeastern British Columbia; Geology, v. 15, p. 142-146.

Brown, R.L. and Read, P.B.
1983: Shuswap terrane of British Columbia: a Mesozoic "core complex"; Geology, v. 11, p. 164-168.

Brown, R.L., Tippett, C., and Lane, L.S.
1978: Stratigraphy, facies changes and correlations in the northern Selkirk Mountains, southern Canadian Cordillera; Canadian Journal of Earth Sciences, v. 15, p. 1129-1140.

Carr, S.D.
1989: Implications of Early Eocene Ladybird granite in the Thor-Odin—Pinnacles area, southern British Columbia; *in* Current Research, Part E, Geological Survey of Canada, Paper 89-1E.

Duncan, I.J.
1984: Structural evolution of the Thor-Odin gneiss dome; Tectonophysics, v. 101, p. 87-130.

Hanmer, S.K.
1984: The potential use of planar and elliptical structures as indicators of strain regime and kinematics of tectonic flow; *in* Current Research, Part B, Geological Survey of Canada, Paper 84-1B, p. 133-142.
1986: Asymmetric pull-aparts and foliation fish as kinematic indicators; Journal of Structural Geology, v. 8, p. 111-122.

Journeay, J.M.
1986: Stratigraphy, internal strain and thermotectonic evolution of northern Frenchman Cap Dome: exhumed duplex structure, Omineca Hinterland, S.E. Canadian Cordillera; unpublished Ph.D. thesis, Queen's University, 350 p.

Journeay, J.M. and Brown, R.L.
1986: Major tectonic boundaries of the Omineca Belt in southern British Columbia: a progress report; *in* Current Research, Part A, Geological Survey of Canada, Paper 86-1A, p. 81-88.

Passchier, C.W. and Simpson, C.
1986: Porphyroclast systems as kinematic indicators; Journal of Structural Geology, v.8, p. 831-843.

Pell, J. and Simony, P.
1987: New correlations of Hadrynian strata, south-central British Columbia; Canadian Journal of Earth Sciences, v. 24, p. 302-313.

Platt, J.P.
1984: Secondary cleavages in ductile shear zones; Journal of Structural Geology, v. 6, p. 439-442.

Reesor, J.E. and Moore, J.M.
1971: Petrology and structure of Thor-Odin gneiss dome, Shuswap Metamorphic Complex, British Columbia; Geological Survey of Canada, Bulletin 195, 149 p.

Scammell, R.J.
1986: Stratigraphy, structure and metamorphism of the north flank of the Monashee Complex, southeastern British Columbia: a record of Proterozoic extension and Phanerozoic crustal thickening; unpublished M.Sc. thesis, Carleton University, 205 p.

Metamorphism and structure of the Mount Cheadle area, Monashee Mountains, British Columbia

Scott G. Digel[1], E.D. Ghent[1], and P.S. Simony[1]
Cordilleran and Pacific Geocience Division, Vancouver

Digel, S.G., Ghent, E.D., and Simony, P.S., Metamorphism and structure of the Mount Cheadle area, Monashee Mountains, British Columbia; in Current Research, Part E, Geological Survey of Canada, Paper 89-1E, p. 95-100, 1989.

Abstract

In the Mount Cheadle area, fibrolite occurs sporadically in kyanite metapelites over an area of at least 200 km² and through a vertical section of 2000 m. This large zone of co-existence is in marked contrast to the sharp, well-defined isograd to the southeast. Garnet-plagioclase-quartz-kyanite geobarometry and garnet-biotite Fe-Mg exchange thermometry yield estimates of 595 ± 12 °C and 5.5 ± 0.6 kbar respectively across the area. It is suggested that the widespread but sporadic occurrence of fibrolite in these kyanite metapelites is at least partly controlled by heat and fluids released during the crystallization of granitic rock at depth.

Résumé

Dans la région du mont Cheadle, on trouve par endroits de la fibrolite dans des métapélites à kyanite sur une surface d'au moins 200 km² et jusqu'à une profondeur de 2000 m. Cette zone étendue de coexistence présente un contraste frappant avec l'isograde abrupte et bien définie au sud-est. La géobarométrie de l'ensemble grenat, plagioclase, quartz et kyanite et la thermométrie des échanges de Fe et Mg dans la biotite à grenat donnent des estimations de 595 ± 12 °C et de 5,5 ± 0,6 kbar respectivement en travers de la région. La présence répandue mais dispersée de la fibrolite dans ces métapites à kyanite peut, semble-t-il, être au moins partiellement contrôlée par la chaleur et les fluides libérés pendant la cristallisation de la roche granitique en profondeur.

[1] Department of Geology and Geophysics, University of Calgary, Calgary, Alberta, T2N 1N4

INTRODUCTION

During the summer of 1987 and part of 1988, extensive sampling and detailed mapping at a scale of 1:24 000 was undertaken in an area of southeastern British Columbia centred on Mount Cheadle (Fig. 1). The main purpose of the study is to map the area over which kyanite and sillimanite coexist, north of the area mapped by Doucet et al. (1985) and south of Bone Creek (Fig. 1). In the Mica Dam area to the southeast, Ghent et al. (1980) described the kyanite-sillimanite isograd as a thin zone corresponding to a steeply-dipping surface which contrasts with the large zone of coexistence of kyanite and sillimanite mapped in the Mount Cheadle area (MCA).

The project area is situated on the northeastern margin of the Shuswap Metamorphic Complex (SMC) which has been studied by Campbell (1968), and workers from the University of Calgary and elsewhere over the last 15 years. The regional stratigraphy, structure, and metamorphism have been described by Ghent et al. (1977), Simony et al. (1980), and Raeside and Simony (1983).

GEOLOGY OF THE MOUNT CHEADLE AREA

Lithologies

A variety of lithologies outcrop in the MCA (Fig. 2). Metasediments and interlayered metabasites of the Upper Precambrian Horsethief Creek Group (HTCG) are dominant and all are intruded by locally abundant pegmatite pods and layers. Mineral assemblages for the different lithologies are given in Table 2; mineral abbreviations are given in Table 1. The semipelite-amphibolite unit outcrops over most of the field area with a thin calc-silicate zone (lower marble?) and the lower pelite being infolded into the semipelite-amphibolite unit. Two previously unreported foliated metacarbonatites were found near Gum and Serpentine creeks.

Metapelites are the only rocks in which kyanite is abundant. Kyanite is commonly surrounded by rims of muscovite in fibrolite-bearing samples. Prismatic sillimanite has not been found. Fibrolite typically occurs in two habits: as small knots intergrown with biotite and, more commonly,

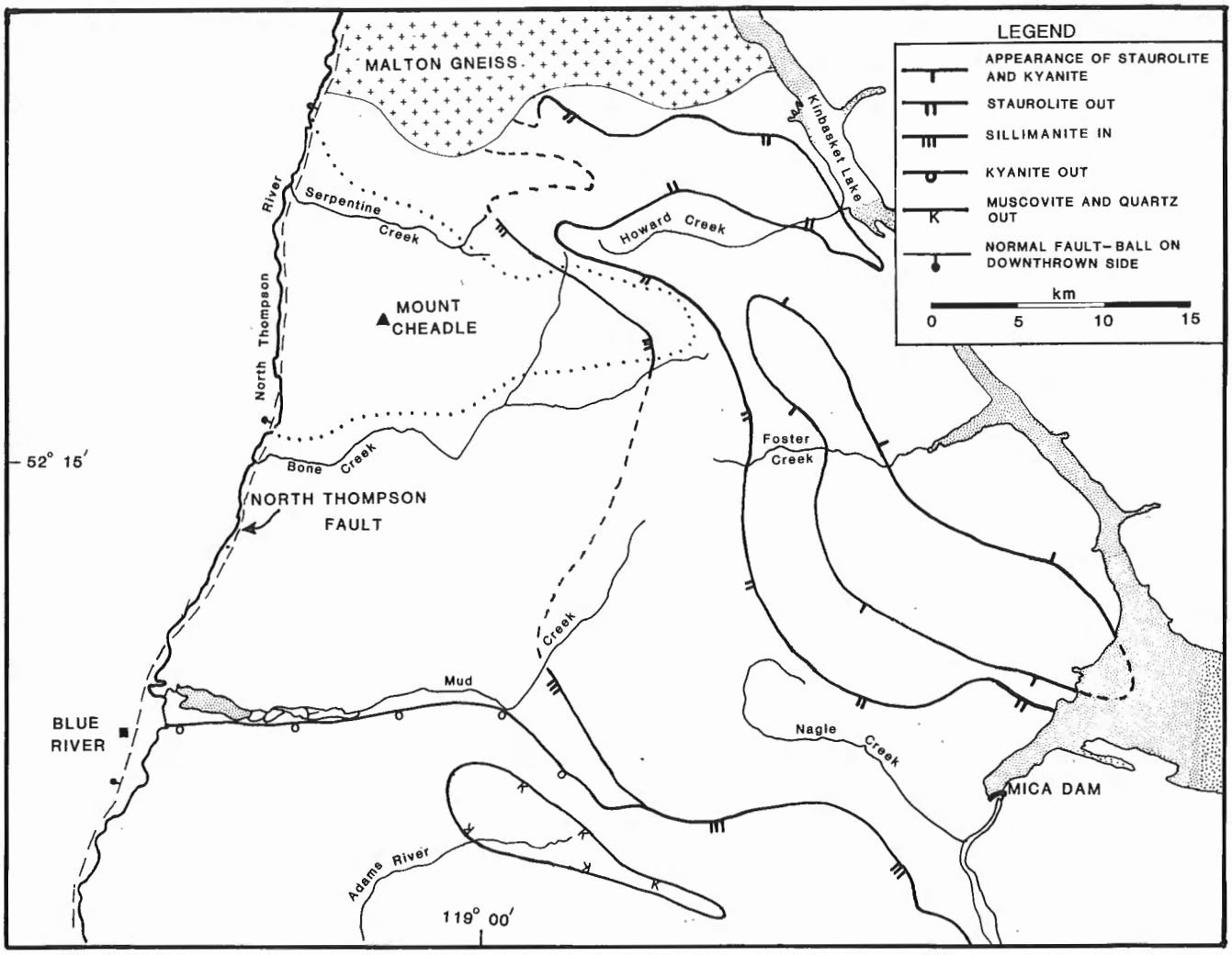

Figure 1. Map of isograds in metapelitic rocks near the northeastern margin of the Shuswap Metamorphic Complex. The study area is outlined by dots. Kyanite and fibrolite coexist between the sillimanite in and kyanite out isograds. Modified from Sevigny and Ghent (1986) and unpublished mapping by S.G. Digel.

as oriented masses intimately intergrown with quartz as nodules and layers. Thickly layered metapelites (> 2 m thick) are common only in the lower pelite.

A metre-thick zone of calc-silicate and semipelite interlayered on a scale of about 30 cm define the contact between the lower pelite and the semipelite-amphibolite unit in the MCA. This calc-silicate zone may represent the lower marble which may be thin due to nondeposition of tectonic thinning in the MCA.

Metabasites are common in the semipelite-amphibolite unit. They are typically less than 4 m thick but are extremely regular in thickness. Layers as thin as 3 cm may be traceable for tens of metres along strike. Some metabasites containing clinopyroxene and scapolite appear to be the product of reaction of more "typical" metabasite (Hbl + Pl + Qtz) with thin carbonate layers. Clinopyroxene and scapolite are present only in these "carbonated" metabasites.

Pegmatite pods and dykes up to 15 m thick are found throughout the study area and intrude all lithologies. Field relations vary widely in that some pegmatites are clearly folded by F_3 whereas others are not. On the outcrop scale, pegmatites are roughly parallel to S_{1+2}; however, on close inspection most can be seen to truncate the host layering and in some cases have forcibly "pushed aside" the country rock. Pegmatites may be extremely coarse grained with individual muscovite and biotite crystals locally exceeding 15 cm.

The Gum Creek carbonatite outcrops at 6700 feet (2040 m) on the edge of a ridge just south of Gum Creek as a layer about 10 m thick. The body is parallel to the main layering in the area and the foliation in the carbonatite is also parallel to the local S_{1+2} indicating that the carbonatite is pre-metamorphic. The Serpentine Creek carbonatite is a small (< 100 m^2) body poorly exposed at 4500 feet (1370 m) along a logging road.

Table 1. List of mineral abbreviations. After Kretz (1983).

Ap	Apatite	Arf	Arfvedsonite
Brl	Beryl	Bt	Biotite
Cal	Calcite	Cpx	Clinopyroxene
Dol	Dolomite	Grt	Garnet
Gr	Graphite	Hbl	Hornblende
Ilm	Ilmenite	Kfs	K-feldspar
Ky	Kyanite	Mag	Magnetite
Ms	Muscovite	Ol	Olivine
Py	Pyrite	Qtz	Quartz
Rt	Rutile	Sil	Sillimanite
Spn	Sphene	Tur	Tourmaline
Zo	Zoisite		

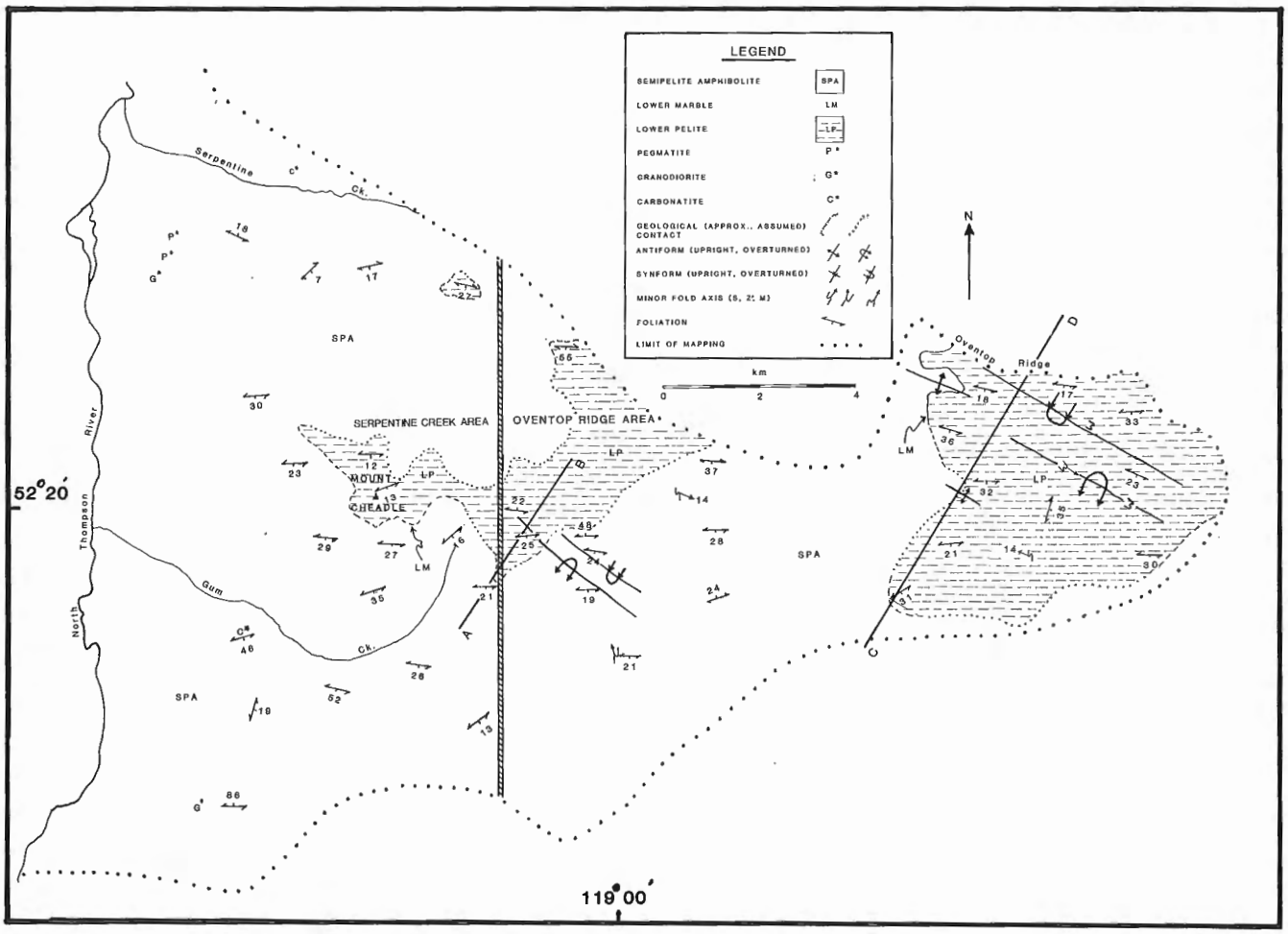

Figure 2. Geological sketch map of the Mount Cheadle area. The hatched bar is the boundary between the Serpentine Creek and Oventop Ridge area.

Structure

The region has been affected by three phases of deformation. During phases 1 and 2, large tight folds were formed. Transposition of the earlier structure and recrystallization during phase 2 led to the development of a pervasive, intense foliation mapped as S_{1+2} (Simony et al., 1980). Phase three structures are sporadically developed. The phase 1 structures are associated with formation of the Scrip Nappe (Raeside and Simony, 1983) with the bulk of the area occupied by the inverted lower limb and with the lower pelite occupying the core of the nappe (Figs. 2 and 3).

In general, the S_{1+2} foliation dips gently to moderately southwest and the amount of phase 3 folding increases from east to west across the study area (Fig. 3). The Mount Chea-

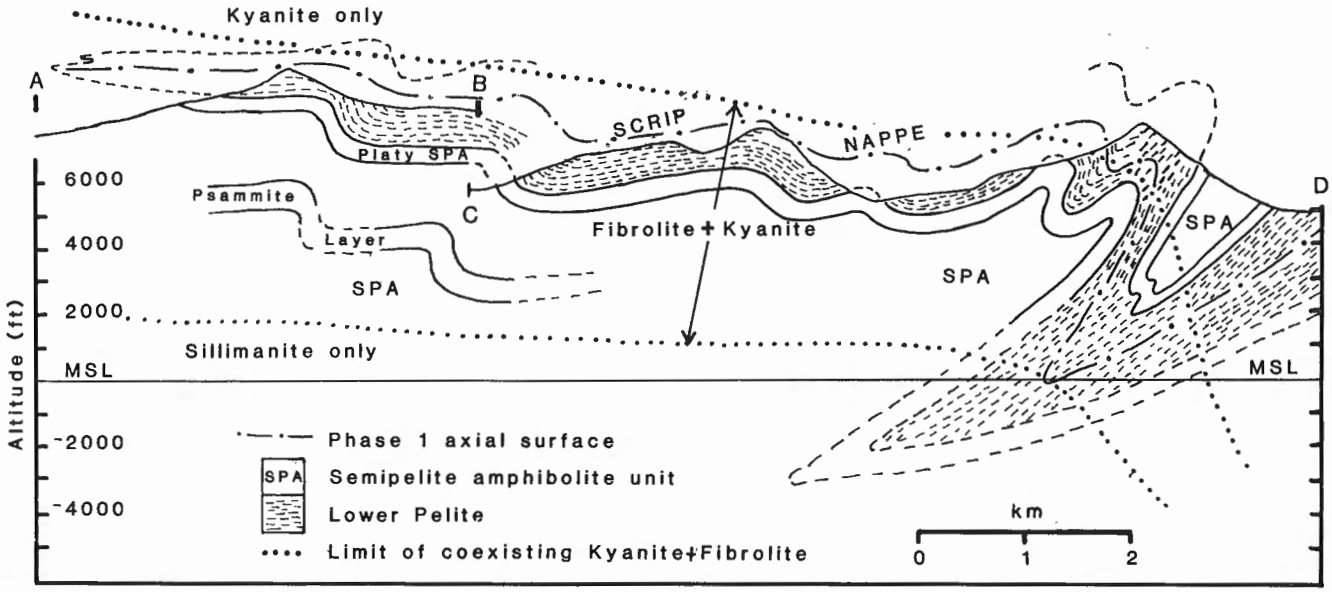

Figure 3. Combined cross-sections through the Mount Cheadle area.

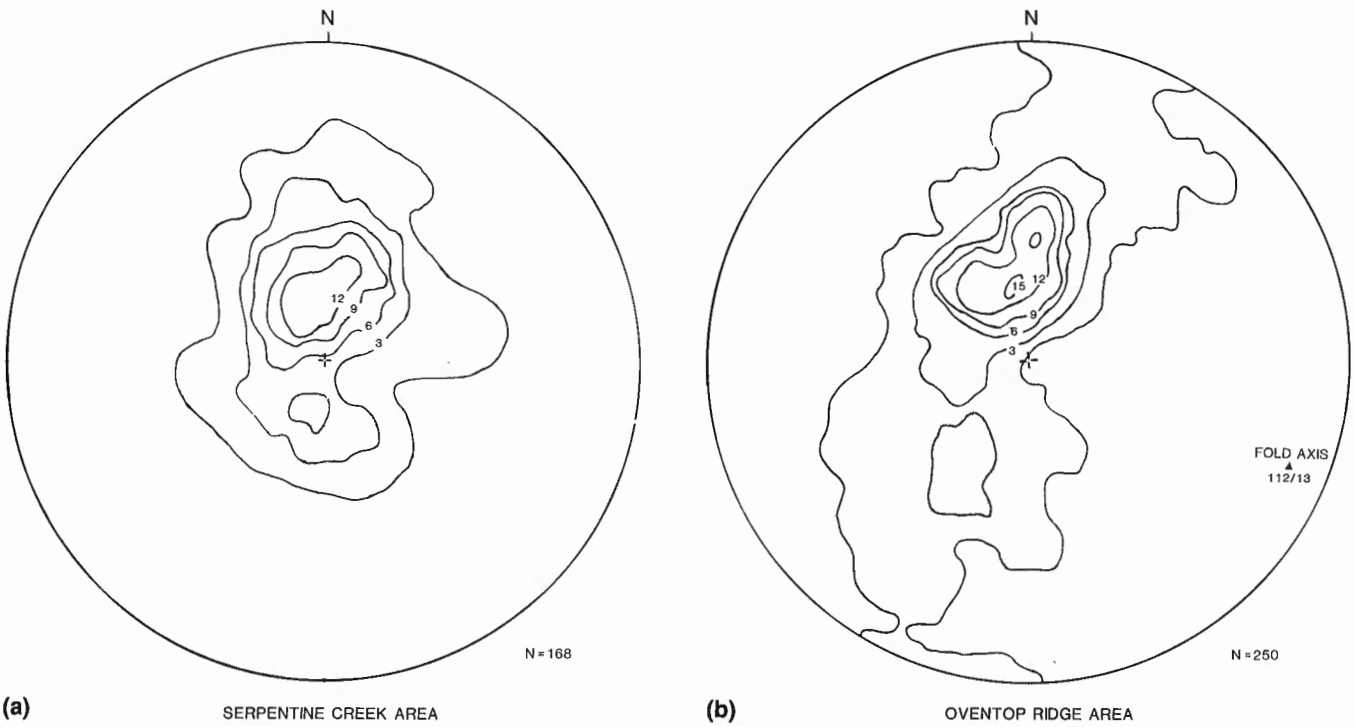

Figure 4. Equal area stereographic projections of poles to S_{1+2} in the Serpentine Creek (a) and Oventop Ridge areas (b).

Table 2. Typical mineral assemblages.

Metapelite: Qtz + Ms + Bt + Pl + Grt + Ky ± Sil, Ap, Gr, Tur, Py
Calc-silicate: Qtz + Cal + Cpx + Kfs ± Zo, Hbl, Bt, Grt, Pl, Sca, Spn, Zo, Gr
Metabasite: Pl + Qtz + Ap ± Grt, Bt, Spn, Rt, Ilm
Pegmatite: Qtz + Pl + Ms + Bt ± Grt, Tur
Granodiorite: Pl + Kfs + Qtz + Grt + Bt + Hbl + Ap + Mag + Tur
Carbonatite: Cal + Bt + Ap ± Arf, Cpx, Pl, Dol, Ol, Kfs, Opaques

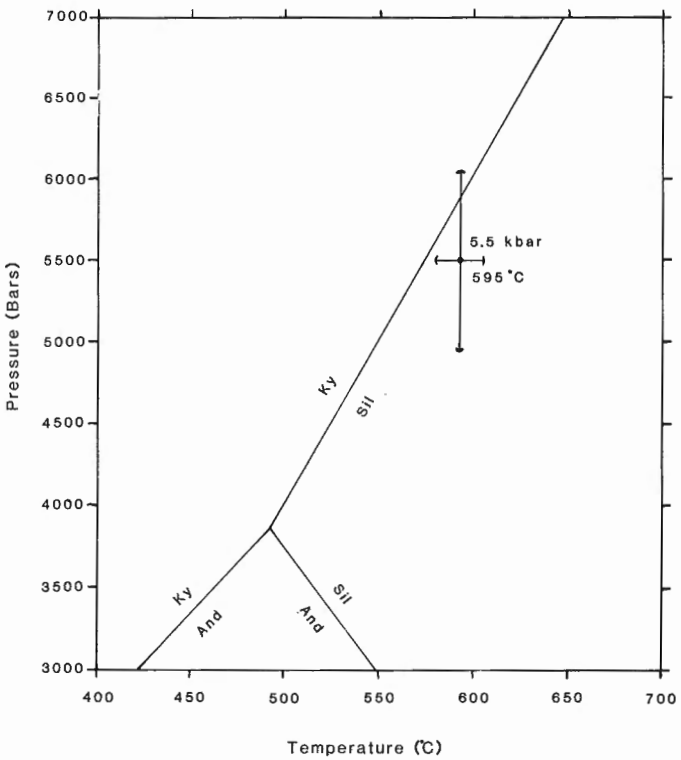

Figure 5. Average pressure-temperature conditions as determined from 11 metapelites in the Mount Cheadle area. Vertical and horizontal bars represent one standard deviation (0.6 kbar and 12°C respectively).

dle area has been divided into two sections of differing structural complexity-the Serpentine Creek area in the west and the Oventop Ridge area in the east (Fig. 2). The change from a relatively simple structure in the west to a more extensively folded area in the east is evident when poles to the S_{1+2} are plotted on equal area stereonets (Figs. 4a and b). Two generations (F_2 and F_3) of folds are superimposed on the gently-dipping limb of the Scrip Nappe in the MCA. The great circle defined by poles to S_{1+2} in Figure 4b is due to the presence of abundant, relatively small-scale (tens of metres wavelength), upright F_3 folds in the east half of the field area.

Kyanite-sillimanite relations

The most common aluminosilicate mineral in the metapelites is kyanite, which is present in rocks of suitable composition throughout the entire study area. By contrast, coarsely crystalline sillimanite (cross-section > 10 μm as defined by Kerrick, 1987) has not been identified. Fibrolite occurs sporadically over much of the study area including the valley bottoms and the highest peaks traversed, a vertical distance in excess of 2000 m over an area of about 200 km^2. The large area and thick section of coexistence of kyanite and fibrolite is in marked contrast with the relatively sharp and steeply-dipping isograd mapped to the southeast in the Mica Dam area (Ghent et al., 1980). Metapelites containing fibrolite without kyanite were not found, suggesting that the distribution of these minerals does not define a simple isogradic surface. Fibrolite is restricted to foliation-parallel layers and pods containing abundant quartz. References to similar quartz-fibrolite associations are common in the literature (e.g. Losert, 1968; Kerrick, 1987).

Conditions of metamorphism and the kyanite-sillimanite isograd

Preliminary estimates of pressure and temperature associated with metamorphism have been made using the assemblages Grt-Pl-Ky-Qtz (database of Berman et al., 1985) and Grt-Bt (calibration of Ferry and Spear, 1978) in metapelites. Across the field area pressure and temperature are essentially constant at 595 ± 12°C and 5.5 ± 0.6 kbar (mean and one standard deviation) respectively (Fig. 5). Calculations using other equilibria in metabasites give similar results. These data and the map pattern indicate that kyanite and fibrolite coexist in a sheet-like zone at least 2000 m thick (Fig. 3). Within this zone, the pressure-temperature conditions must have been near the kyanite-sillimanite curve in P-T space (Fig. 5). Regionally, this sheet dips southeastward under the metamorphic low between Foster Creek and Mica Dam (Fig. 1 and 3). The thick sheet wedges out southeastward (Fig. 3) into the sharp and steeply-dipping isogradic surface southwest of Mica Dam. We suggest that the nucleation and growth of fibrolite within the kyanite metapelites occurred only at sites where factors influencing reaction kinetics (i.e. localized deformation and presence of fluid) were favourable. This resulted in the sporadic occurrence of fibrolite in metapelites on both map and outcrop scales. A probable source of heat, mechanical energy, and fluid which could initiate fibrolite growth is the intrusion and crystallization of granitic rocks similar to those described by Sevigny and Ghent (1986) in the Adams River area where deeper structural levels of HTCG stratigraphy are exposed. Heat produced from the crystallizing granites could raise the temperature of the overlying rock package to conditions favourable for fibrolite growth. Movement of fluid from the granites and deformation (kinetic controls) along structural weaknesses in HTCG rocks such as the S_{1+2} foliation would restrict development of fibrolite to the localized, thin layers observed in the field.

Doucet et al. (1985) favoured structural rotation (by F_3) of the kyanite-sillimanite isograd to subhorizontal over the thermal effects of granitic intrusion to explain the large area of coexistence of kyanite and fibrolite. The lack of significant F_3 structures and the absence of metapelites containing sillimanite without kyanite suggest that folding of a simple isograd such as that described by Ghent et al. (1980) is not responsible for the distribution of kyanite and fibrolite in the Mount Cheadle area.

CONCLUSIONS

Detailed mapping and sampling show that the thick vertical section over which kyanite and sillimanite coexist mapped by Doucet et al. (1985) continues considerably farther north into the Mount Cheadle area (MCA). Metamorphic conditions throughout the MCA approximate those of the kyanite-sillimanite isograd (595°C and 5.5 kbar). The intrusion and crystallization of synkinematic and synmetamorphic granitic rocks at depth is believed to have brought the temperature of overlying kyanite-bearing HTCG rocks to P-T conditions near the kyanite-sillimanite curve. The sporadic occurrence of fibrolite within this rock package corresponds to the outcrop-scale localization of deformation and fluids (i.e. along S_{1+2}) and the kinetic influence of this localization on the fibrolite-forming reaction.

ACKNOWLEDGMENTS

This study forms part of the senior author's M.Sc. thesis research at the University of Calgary. It is funded by EMR research agreements 224-04-87 and 50-88 held by Simony and Ghent and NSERC operating grant A4379 to Ghent. Thanks are due to Ron Arksey and Carlo Aiello for their field assistance, Gary Foreman and Todd McCready of Yellowhead Helicopters for their timely flying, and to Brian Hannis for his expediting services from Valemount. Len Gal reviewed an earlier draft of the manuscript.

REFERENCES

Berman, R.G., Brown, T.H., and Greenwood, H.J.
1985: An internally consistent thermodynamic data base for minerals in the system Na_2O - K_2O - CaO - MgO - FeO - Fe_2O_3 - Al_2O_3 - SiO_2 - TiO_2 - H_2O - CO_2. Atomic Energy of Canada Ltd. Technical Report 377, 62 p.

Campbell, R.B.
1968: Canoe River, British Columbia; Geological Survey of Canada, Map 15-1967.

Doucet, P.D., Ghent, E.D., and Simony, P.S.
1985: Metamorphism in the Monashee Mountains east of Blue River, British Columbia; in Current Research, Part A, Geological Survey of Canada, Paper 85-1A, p. 69-71.

Ferry, J.M., and Spear, F.S.
1978: Experimental calibration of the partitioning of Fe and Mg between garnet and biotite; Contributions to Mineralogy and Petrology, v. 66, p. 113-117.

Ghent, E.D., Simony, P.S., Mitchell, W., Perry, J., Robbins,D., and Wagner, J.
1977: Structure and metamorphism in the southeast Canoe River area, British Columbia; in Report of Activities, Part C, Geological Survey of Canada, Paper 77-1C, p. 13-17.

Ghent, E.D., Simony, P.S., and Knitter, C.C.
1980: Geometry and pressure-temperature significance of the kyanite-sillimanite isograd in the Mica Dam area, British Columbia; Contributions to Mineralogy and Petrology, v. 74, p. 67-73.

Kerrick, D.M.
1987: Fibrolite in contact aureoles of Donegal, Ireland; American Mineralogist, v. 72, p. 240-254.

Kretz, R.
1983: Symbols for rock-forming minerals; American Mineralogist, v. 68, p. 277-279.

Losert, J.
1968: On the genesis of nodular sillimanitic rocks; 23rd International Geological Congress, v. 4, p. 109-122.

Raeside, R.P. and Simony, P.S.
1983: Stratigraphy and deformational history of the Scrip Nappe, Monashee Mountains, British Columbia; Canadian Journal of Earth Sciences, v. 20, p. 639-650.

Sevigny, J.H. and Ghent, E.D.
1986: Metamorphism in the northern Adams River area, northeastern Shuswap Complex, Monashee Mountains, British Columbia; in Current Research, Part B, Geological Survey of Canada, Paper 86-1B, p. 693-698.

Simony, P.S., Ghent, E.D., Craw, D., Mitchell, W., and Robbins, D.B.
1980: Structural and metamorphic evolution of the northeast flank of the Shuswap Complex, southern Canoe River area, British Columbia; Geological Society of America, Memoir 153, p. 445-461.

Stratigraphy, structure and metamorphism of the Mt. Lulu area, Cariboo Mountains, British Columbia

R.T. Walker[1] and P.S. Simony[1]
Cordilleran and Pacific Geoscience Division, Vancouver

Walker, R.T. and Simony, P.S., Stratigraphy, structure and metamorphism of the Mt. Lulu area, Cariboo Mountains, British Columbia; in Current Research, Part E, Geological Survey of Canada, Paper 89-1E, p. 101-107, 1989.

Abstract

Fieldwork has revealed an overturned north-facing metasedimentary package of Horsethief Creek Group strata previously mapped as lower Kaza. A large scale antiformal anticline is interpreted placing this overturned package in contact with a thinned and attenuated Horsethief Creek Group sequence overlying an orthogneiss equivalent to basement gneisses of the Malton Range. Lying within the core of the antiform is a small intrusive ultramafic body. At least three phases of deformation have affected the strata of the area. Phase one resulted in the overturned panel while phases two and three produced folds with coaxial, generally northwest-plunging fold axes, superimposed on the limbs of the phase one structure.

Metamorphic grade is dominantly within the kyanite stability field with development of quartz to quartz-plagioclase (trondhjemitic) leucosome and biotite-garnet melanosome. Abundance of migmatite increases from east to west. Initial estimates suggest temperatures and pressures of metamorphism range from 565-682 °C and 620-780 MPa.

Résumé

Des travaux sur le terrain ont mis au jour un ensemble de strates métasédimentaires renversées du groupe de Horsethief Creek, dirigé vers le nord et cartographié comme appartenant auparavant au groupe inférieur de Kaza. Un important anticlinal antiforme mettrait cet ensemble renversé en contact avec une séquence amincie et atténuée du groupe de Horsethief Creek qui repose sur un orthogneiss équivalent aux gneiss de socle des chaînons Malton. Un petit corps ultramafique intrusif est logé dans le coeur de l'anticlinal. Au moins trois phases de déformation ont modifié les couches de la région. La première phase a produit le renversement du panneau, tandis que les deuxième et troisième phases ont produit des plis dont les axes coaxiaux plongent en général vers le nord-ouest et sont surimposés sur les flancs de la structure produite par la première phase.

Le degré de métamorphisme se situe principalement dans le champ de stabilité de la kyanite avec formation de leucosome quartzique à quartzo-plagioclastique (trondhjémitique) et de mélanosome à biotite et grenat. L'abondance de migmatite augmente d'est en ouest. Les premières estimations des plages de température et de pression de métamorphisme se situent entre 565 et 682 °C et entre 620 et 780 MPa respectivement.

[1] University of Calgary, Department of Geology and Geophysics, Calgary, Alberta T2N 1N4

INTRODUCTION

Mapping at 1:20 000 scale was carried out during the 1987 and 1988 field seasons in the Cariboo Mountains of southeast central British Columbia (Fig. 1). The field area is located southwest of Valemount, on the eastern edge of the Omineca Crystalline Belt (Fig. 1). Based on reconnaissance mapping (1:250 000), Campbell (1968, 1973) assigned metasediments of the area to the Upper Proterozoic (Hadrynian) Kaza Group. The present study suggests modification of this interpretation.

Over the past fifteen years correlations have been made within Hadrynian Windermere Supergroup strata from Purcell and Selkirk Mountains (Brown et al., 1978; Poulton and Simony, 1980) into the Monashee Mountains (Morrison, 1982; Raeside, 1982). Recently, these correlations have been extended into the Cariboo Mountains (Pell and Simony, 1987). Subsequent work (Currie and Simony, 1987) extended these correlations northwards into the Allan Creek area.

The objectives of this study are: 1) to extend work in the southern Cariboo Mountains (Currie and Simony, 1987; Dechesne, 1986; Pell, 1984; Pell and Simony, 1987) northward, 2) determine the processes of migmatization, 3) examine a thin slice of orthogneiss and determine its origin and 4) attempt to determine the setting of the field area in the large-scale nappe structure of the region.

STRATIGRAPHY

Horsethief Creek Group

Previous work in the Cariboo Mountains (Currie and Simony, 1987) established the presence of an overturned, north-facing metasedimentary succession of Hadrynian Horsethief Creek Group (Fig. 2) which consists, in stratigraphic order, of the lower grit division, lower pelite division, and the lower marble and semipelite — amphibolite division (Ghent et al., 1977; Pell and Simony, 1987; Raeside, 1982; Simony et al., 1980).

In the Mt. Lulu area, the lower grit division is composed of psammite and granule conglomerate (''grit'') with pelite, semipelite and minor leuco-amphibolite. Granule conglomerate bands up to 3 m thick are composed of feldspar and quartzite clasts 1 cm or less in diameter, generally with poor grading. The lower grit division forms a resistant unit more than 400 m thick; no stratigraphic base has been observed.

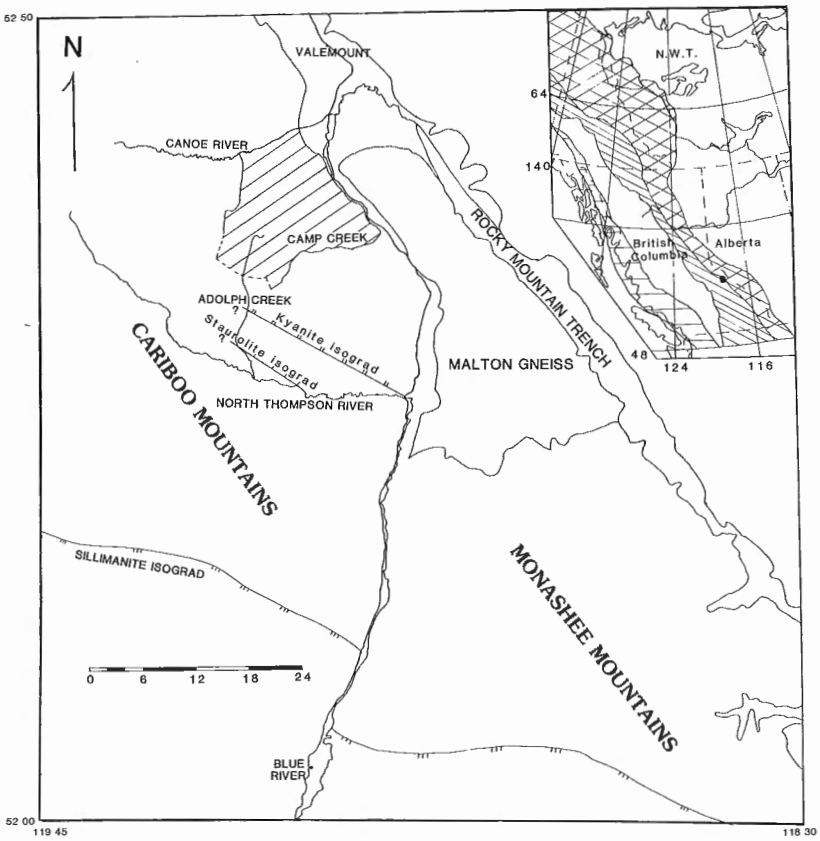

Figure 1. Local geographic map showing position of field area (hatched) in the Cariboo Mountains southwest of Valemount. Note the position of the Malton gneiss directly east of the field area, across the Albreda valley. The inset shows the field area (black square) in relation to the five geological belts of the Cordillera. The field area is located on the eastern margin of the Omineca Crystalline Belt (slanted line pattern) (modified after Tipper et al., 1981).

The lower pelite division is a recessive unit up to 150 m thick consisting of orange-brown weathering muscovite-biotite schist with abundant garnet, kyanite and migmatite at the appropriate metamorphic grade.

The lower pelite division is overlain by what is possibly an equivalent of the lower marble or lower carbonate division of Raeside (1982). The unit consists of calcareous psammite and calc- silicate bands together with pelitic and semipelitic layers about 50 m thick.

The lower carbonate division is, in turn, overlain by the semipelite-amphibolite division (SPA), which is divisible into four subdivisions. The basal 150 m of the SPA consists of pelite and semipelite with minor amphibolite. The pelites include only minor kyanite-bearing horizons. Amphibolite bodies are 2-10 m thick and consist of hornblende, plagioclase and biotite. Some of the larger bodies are boudinaged. The basal pelites grade up into about 150-200 m of platy semipelite alternating with 1-4 cm thick garnet and/or biotite amphibolite layers. Semipelite beds are 1 to 2 cm thick and are separated by biotitic partings.

The third subdivision of the SPA consists of coarse psammite, quartzite and pebble to boulder conglomerate with only minor amphibolites. This unit undergoes a facies change from east to west, from a sequence of pebble and boulder conglomerate, quartzite, psammite and biotite amphibolite to a sequence consisting of grits, psammite and quartzite with pelitic partings and only minor amphibolite. The eastern pebble to boulder conglomerate has clasts from 0.5-10 cm across. These are rounded to well-rounded. Lithologies include quartzite, marble, calc-silicate, granite and granitoid gneiss. Similar conglomeratic facies have been reported from the SPA elsewhere in the Cariboo Mountains (Dechesne, 1986; L.D. Currie, pers. comm., 1987) and the Monashee Mountains (S.G. Digel, pers. comm., 1987; R.B. Campbell, pers. comm.). Several layers show well defined graded bedding and channel forms several metres thick. Most of the amphibolites in the SPA are relatively thin layers, are continuous for hundreds of metres, and have sharp contacts. These are probably equivalent to Sevigny's (1987) Group 2 amphibolites, representing flows and tuffs. Some thicker, boudinaged amphibolites

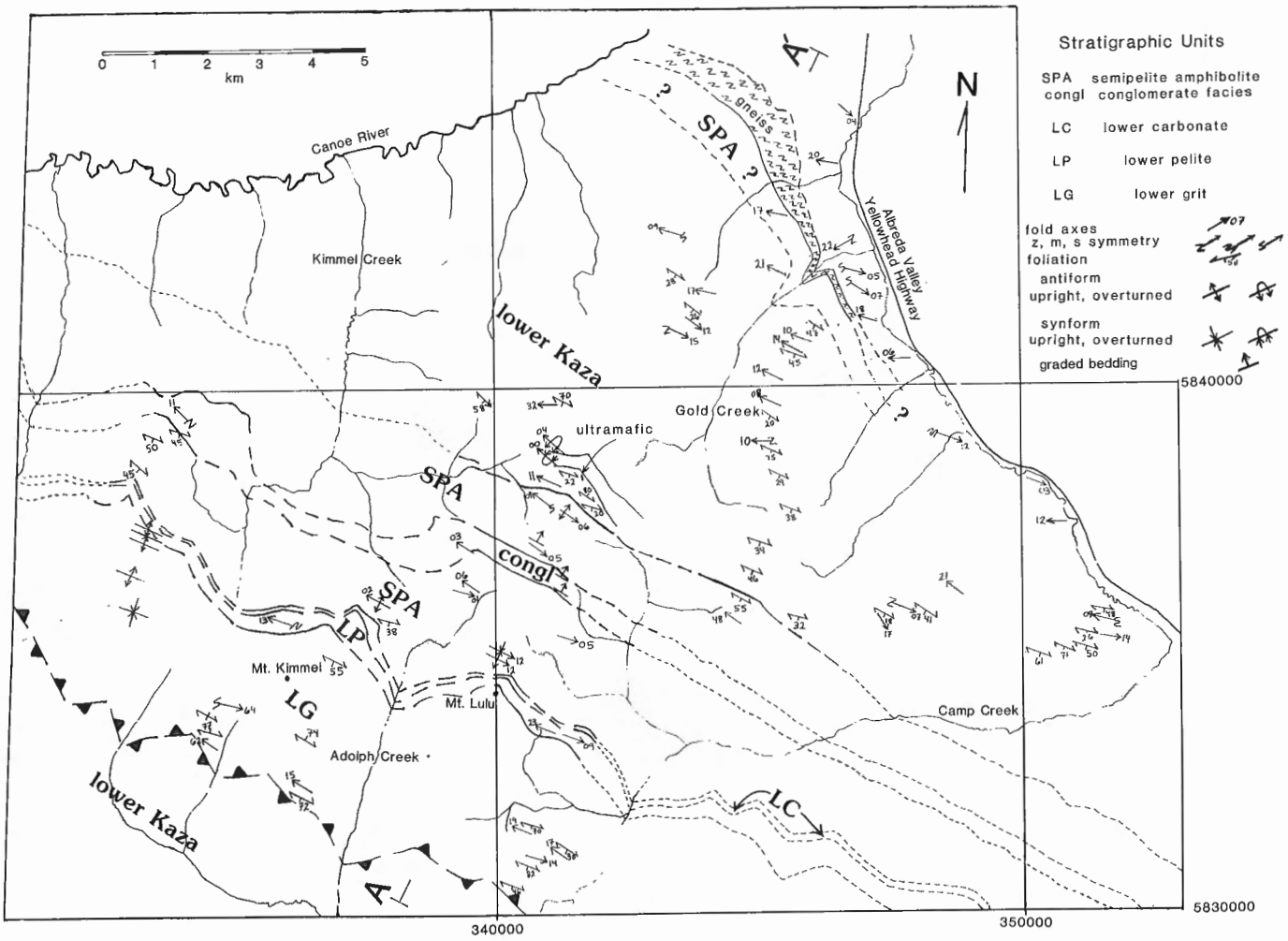

Figure 2. Geological map showing the stratigraphic relations and interpreted structure. The lower two subdivisions of the SPA discussed in the text are grouped into the lower SPA. Stratigraphic contacts are denoted as follows: solid lines designate contacts observed, dashed lines represent extrapolated contacts of probable validity and short dashed lines indicate hypothetical projection with little control. The doubly toothed fault in the southwest corner indicates the lack of control on sense of vergence. The grid is a 10 000 metre UTM grid.

may correspond to Sevigny's (1987) Group 1 amphibolites, interpreted as sills and transposed dykes with some evidence of forceful intrusion (Brown et al., 1978). The fourth subdivision of the SPA consists of pelite and semipelite (70 %) interlaminated with 3 cm to 1 m thick amphibolite layers (30 %). The SPA is at least 1000 m thick. The strata typical of the SPA are in sharp contact with a sequence that closely resembles and could be the lower Kaza Group. The pure white to grey weathering marbles of the Middle Marble (Dechesne, 1986; Pell and Simony, 1987; Raeside, 1982) do not appear to be present. There are three possible interpretations for the absence of the Middle Marble: (1) The lower Kaza is in stratigraphic contact on the SPA with thin layers of calc-silicate and calcareous psammite representing a local facies of the Middle Marble (Figs. 2 and 3); (2) The Middle Marble may have been locally removed by sub-Kaza erosion; or, (3) The contact is a low angle fault possibly connected to the lower Kaza-lower grit contact to the south.

Lower Kaza Group

Biotite-muscovite-rich pelites overlie the calcareous lithologies described above. These pelites dominate a broad band running through the field area and are interpreted as lower Kaza Group (Fig. 2). All lithologies described above are present within the lower Kaza although their proportions are variable. Coarse clastics (grits) and psammites are less abundant and thinner than in the lower grit division. Amphibolites and platy semipelite are more abundant in the SPA. Although the lower pelite, lower SPA and upper SPA all have pelitic intervals, the pelites of the lower Kaza have more abundant biotite, imparting a darker weathering colour than the orange weathering pelites of the Horsethief Creek Group. In addition, the pelites of the lower Kaza are generally richer in kyanite and migmatite. Leucoamphibolites are also more abundant in the lower Kaza than elsewhere in the stratigraphy. Due to the highly folded nature of the unit, an estimate of a stratigraphic thickness is impossible.

Ultramafic rocks

An ultramafic body is present in the lower Kaza Group, in the core of a second-phase synform (Figs. 2 and 3). It underlies about 2000 m^2 and consists of coarse grained green clinopyroxene and black amphibole, magnetite, pyrite, pyrrhotite and black biotite. From an ultramafic core, exposed above snow and talus, the body becomes progressively brecciated and hydrated structurally upwards.

The brecciated zone, 10-15 m thick, is characterized by ultramafic clasts, up to 60 cm long having an oval to elongate shape with a black biotite-hornblende hydrated rind, in a banded plagioclase-quartz-biotite-carbonate matrix in which clast proportion decreases upwards. The banded matrix may have resulted from a hot, dominantly crystalline slurry interacting with a cooler metasedimentary host, liberating fluids composed of H_2O with variable Ca, Na, Si, and CO_2. Black biotite is closely associated and intergrown with black amphibole throughout the exposed ultramafic.

Several metasedimentary bands in the breccia are oblique to the breccia-metasedimentary contact. These bands are inclusions of overlying pelite-semipelite and are irregular in thickness (about 0.5 m) and up to 20 m long. The brecciated zone is overlain by pelitic and semipelitic metasediments.

The presence of metasedimentary screens of overlying metasediments, together with the coarse crystalline nature and brecciation of the ultramafic suggests an intrusive origin. Most shearing within the pod and in the matrix of the breccia is probably tectonic but the possibility of emplacement- related shearing and banding cannot be ruled out.

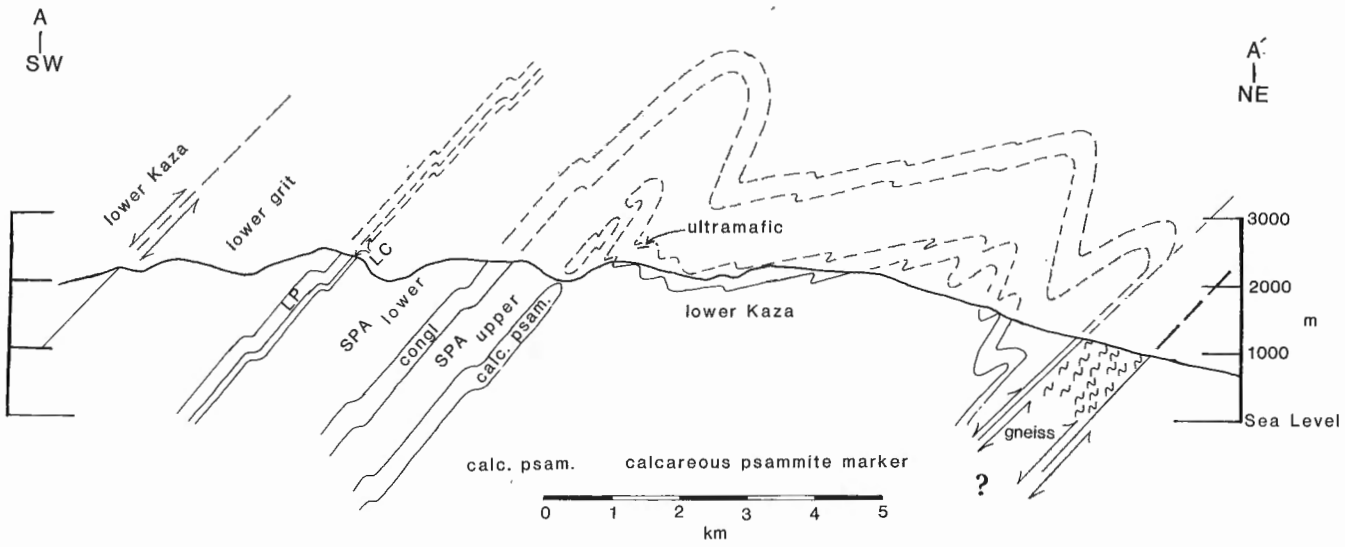

Figure 3. Hypothetical cross-section along A-A' (Fig. 2). This interpretation indicates an overturned Horsethief Creek Group panel rising to the northeast into an antiform with lower Kaza in the core, having a width of about 6 km from limb to limb. A key feature of this interpretation is the postulated connection of conglomerate within the SPA with that lying immediately above the orthogneiss. The gneiss is shown in sheared contact with upper SPA pelitic lithologies on its structural top and in fault contact with underlying lower Kaza lithologies.

Felsic and mafic gneisses

In the northeast part of the field area, alternating felsic and mafic gneisses outcrop in a belt some 300 m thick and 3000 m long (Fig. 2). Felsic gneiss layers consist predominantly of plagioclase, alkali feldspar and biotite with subordinate quartz. Feldspar augen reach 1 cm in length. Felsic layers are up to 2 m thick with 1-5 cm thick biotitic partings and have sharp contacts with mafic bands. The mafic layers are 1-2 m thick and are composed of either biotite, amphibole and plagioclase or garnet amphibolite.

The high proportion of alternating felsic and mafic layers together with the granitic appearance suggests two possible origins for the gneisses: 1) a sheared granitoid intrusive body, or 2) an infold or fault slice of basement related to the Malton Gneiss, exposed to the east across the Albreda valley (Fig. 2).

Of the two hypotheses, the latter is preferred for several reasons: (1) the gneisses show similar lithologies to those described in the Malton Range (Morrison, 1982) and in the Bulldog Creek area (McDonough, 1984; McDonough and Simony, 1984), (2) the presence of highly sheared, stretched cobble to boulder conglomerate and other metasediments immediately overlying the gneisses, (3) lack of apophyses into "host" metasediments, and (4) lack of metasedimentary xenoliths.

Pegmatites

Pegmatite bodies, ranging in thickness from 3 cm to 3 m are present throughout the field area and consist of coarse grained plagioclase, quartz and muscovite with minor garnet. Some bodies are transposed and deformed with host lithologies whereas others crosscut foliation and folds of host lithologies, therefore representing different generations.

It seems probable from crosscutting relations that pegmatite bodies were intruded prior to, and after, phase three deformation. Pegmatites that cut across foliations and preexisting folds have small apophyses into host lithologies. Neither these apophyses nor megacrysts of post-tectonic pegmatite show evidence of strain.

STRUCTURE

At least three deformational events have affected the area. Phase one, D_1, resulted in the overturning of a succession of Horsethief Creek Group strata south of Camp Creek (Currie and Simony, 1987) and in the southern part of the field area (Figs. 2 and 3). This south-dipping, north-facing panel of Horsethief Creek Group strata is interpreted to be in thrust contact with lower Kaza strata in the Mt. Lulu area. Locally, schistosity associated with early D_1 structures is refolded in the cores of the phase-two folds that are typically well preserved in competent lithologies such as the lower grit division and the conglomeratic facies of the SPA.

A regional foliation is approximately parallel to the axial planes of phase two folds. It is subparallel to bedding everywhere except in the tight phase two hinge zones. Fold styles for second phase deformation range from parallel to similar, tight to isoclinal northeast-verging folds which typically have an axial planar cleavage. The style of these mesoscopic folds is highly dependent upon lithology. Fold axes generally plunge northwest but vary in orientation through horizontal to shallowly southeast plunging.

Third-phase deformation resulted in variably developed crenulation cleavages and a wide range of fold styles. The main structures affecting the map pattern are third phase folds, which range from open to tight, inclined folds and are coaxial with phase two.

Even later, minor deformation is present throughout the field area as fracture planes, shear planes and spaced crenulations. The strike of the fracture and shear planes are similar to the trend of the crenulations and range between N40°E and N80°E.

The thin orthogneiss sheet on the northeast side of the map area is bounded on the east by pelite, probably lower Kaza Group, and on the southwest by a thick panel of lower Kaza strata. Faults of uncertain age bound the gneiss.

METAMORPHISM

At the southeastern edge of the field area, two occurrences of apparently stable staurolite were found. Slightly to the west, staurolite was observed with kyanite. North and west of this, only kyanite (with migmatite) are present. These relations suggest the existence of a staurolite-out isograd spatially related to both kyanite-in and migmatite-in isograds. Compositional variation in staurolite together with variations in aH_2O *may* result in narrow divariant fields rather than univariant curves for disappearance of staurolite and generation of migmatite. The remainder of the field area is at kyanite grade, with kyanite present in both metasediments and leucosome. Leucosome, 5-40% by volume, is trondhjemitic in composition. It is best developed in pelitic rocks as layers parallel to foliation, in crenulation hinges, and as lenses. Leucosome is present to a lesser extent in semipelite and psammite, imparting a gneiss-like appearance to these lithologies. Melanosome, not always developed, consists of biotite ± garnet. Phases in equilibrium throughout the area are: gar+bi+musc+qtz+ky+plag.

Conditions of metamorphism

Metamorphic temperatures and pressures reached 565-682°C and 620-780 MPa. Staurolite is present in topographically and structurally low positions in the eastern part of the area. In addition, phase-two fold axes plunge generally northwest and metamorphic grade increases westward, toward structurally higher levels. Therefore, mineral assemblages apparently indicate an inverted metamorphic sequence.

Garnet and biotite are ubiquitous in the area and therefore give a consistent mineral pair by which temperatures obtained from different portions of the field area can be compared. Temperatures obtained from garnet-biotite geothermometry are consistent with the presence of kyanite and absence of staurolite. The calibrations used (Thompson, 1976; Ferry and Spear, 1978; Newton and Haselton, 1981;

Ganguly and Saxena, 1984) give temperatures ranging from 565 to 682°C. Each calibration gives a similar temperature range, indicating an increase in grade consistent with the appearance of kyanite and migmatite (Raeside, 1982), from east to west. Calcite-dolomite and two feldspar determinations gave significantly lower temperatures. These results may represent equilibration under retrograde P-T conditions.

Pressures obtained using garnet-plagioclase-kyanite-biotite-quartz geobarometry (Ghent, 1976) range from 620 to 780 MPa. Plagioclase compositions are relatively constant, varying from 0.24 to 0.26 anorthite, but the Ca content in garnet is more variable.

Migmatites

Migmatites in the area consist of trondhjemitic leucosome, consisting of plagioclase and quartz, and melanosome (biotite ± garnet). Trondhjemite, 5-40 %, by volume, is present throughout most of the area. Typically plagioclase constitutes from 0-60 % of the leucosome and the anorthite component in plagioclase is between 0.24 and 0.26.

The temperatures obtained by geothermometry just overlap experimentally determined melting temperatures, particularly if high P_{H_2O} and the presence of incompatible elements (Pichavant 1987, 1981) further depress the melting curves. Therefore, partial melting along the Ab(An)-qtz cotectic could have been involved in formation of migmatite.

It is a almost certain that metamorphic segregation operated in these rocks, because they are known to have undergone at least three phases of deformation. Silica is highly mobile, in contrast to Al (Ashworth, 1985; Harris, 1974) and therefore is able to diffuse under a pressure gradient. In some outcrops along the eastern boundary of the field area, quartz is the *only* phase present in crenulation hinges. Farther north and west, some leucosomes have quartz cores with plagioclase or plagioclase-quartz rims. Possibly an initial leucosome related to metamorphic segregation was followed by a plagioclase contribution due to advanced stages of metamorphic segregation and/or anatexis. The amount of anatexis is not known.

CONCLUSIONS

Correlations tentatively indicate that lower units of the Horsethief Creek Group, which underlie the Middle Marble, are present in the Cariboo Mountains. An overturned sequence identified south of Camp Creek (Currie and Simony, 1987) continues northwards and is folded by a series of megascopic third phase antiforms and synforms resulting in steeply folded semipelite-amphibolite (SPA) north of Mt. Lulu. Lower Kaza lithologies are present structurally above an inverted Horsethief Creek Group panel, having been carried on a first phase fault, and are folded as well by second and third phase folds. Carried within the Lower Kaza are both an ultramafic intrusive pod and a fault-slice or infold of gneiss. Structural relations indicate that the ultramafic body represents an intrusion, grading from a recognizable ultramafic core upward to a highly brecciated zone. The gneiss has no discernable apophyses or other features indicating injection, is overlain by a sheared pebble to boulder conglomerate and is highly foliated. It is thus thought to be basement, equivalent to parts of the Malton Gneiss exposed immediately across the Albreda valley.

Most of the area is at kyanite grade. Abundant leucosome has developed by metamorphic segregation and perhaps anatexis, primarily in pelites. Leucosome (with or without melanosome) is developed in host lithologies parallel to foliation or as irregularly shaped lenses. Metastable staurolite with kyanite and no leucosome was seen in thin sections from two localities and without kyanite in two outcrops on the eastern edge of the field area. Therefore, it is probable that metamorphic grade increases northward and westward from staurolite to kyanite grade on the eastern slopes of the Cariboo Mountains.

ACKNOWLEDGMENTS

Able assistance in the field was provided by Chris Slind, Keith Mountjoy, Raj Damodaran and "Lad". Bryan Hannis was most helpful with expediting services throughout the summer, and Yellowhead Helicopters provided safe airborne transportation during the fly camp portion of field-work. We would like to acknowledge stimulating discussions with L. Currie, T. Gordon, E.D. Ghent, D. Murphy, etc. Field-work was financed through EMR Research agreements to P.S. Simony and E.D. Ghent.

REFERENCES

Ashworth, J.R.
1985: Introduction; in Migmatites, J.R. Ashworth (editor), Blackie and Son, Glasgow, 302 p.

Brown, R.L., Tippet, C.R., and Lane, L.S.
1978: Stratigraphy, facies changes and correlations in the northern Selkirk Mountains, southern Canadian Cordillera; Canadian Journal of Earth Sciences, v. 15, p. 1129-1140.

Campbell, R.B.
1968: Canoe River, British Columbia; Geological Survey of Canada, Map 15-1967.
1973: Structural cross-section and tectonic model of the southeastern Canadian Cordillera; Canadian Journal of Earth Sciences, v. 10, p. 1607-1620.

Currie, L.D. and Simony, P.S.
1987: Geology of the Allan Creek area, southeastern Cariboo Mountains, British Columbia; in Current Research, Part A, Geological Survey of Canada, Paper 87-1A, p. 713-718.

Dechesne, R.G.
1986: The geology of the southern Cariboo Mountains near Blue River, British Columbia; unpublished M.Sc. thesis, University of Calgary, Alberta, 262 p.

Ferry, J.M. and Spear, F.S.
1978: Experimental calibration of the partitioning of Fe and Mg between biotite and garnet; Contributions to Mineralogy and Petrology, v. 66, p. 113-117.

Ganguly, J. and Saxena, S.K.
1984: Mixing properties of alumino-silicate garnets: constraints from natural and experimental data, and applications to geothermobarometry; American Mineralogist, v. 69, p. 88-97.

Ghent, E.D.
1976: Plagioclase-garnet-Al_2SiO_5-quartz: a potential geobarometer-geothermometer; American Mineralogist, v. 61, p. 1654-1660.

Ghent, E.D., Simony, P.S., Mitchell, W., Perry, J., Robbins, D., and Wagner, J.
1977: Structure and metamorphism in southeast Canoe River area, British Columbia; in Report of Activities, Part C, Geological Survey of Canada, Paper 77-1C, p. 13-17.

Harris, N.B.W.
1974: Some migmatite types and their origins, from the Barousse Massif, Central Pyrenees; Geological Magazine, v. 111, p. 319-328.

McDonough, M.R.
1984: Structural evolution and metamorphism of basement gneisses and Hadrynian cover, Bulldog Creek area, British Columbia; unpublished M.Sc. thesis, University of Calgary, Alberta, 163 p.

McDonough, M.R. and Simony, P.S.
1984: Basement gneisses and Hadrynian metasediments near Bulldog Creek, Selwyn Range, British Columbia; in Current Research, Part A, Geological Survey of Canada, Paper 84-1A, p. 99-102.

Morrison, M.L.
1982: Structure and petrology of the Malton Gneiss Complex, British Columbia; unpublished Ph.D. thesis, University of Calgary, Alberta, 164 p.

Newton, R.C. and Haselton, H.T.
1981: Thermodynamics of the garnet-plagioclase-Al_2SiO_5-quartz barometer; in Thermodynamics of Minerals and Melts, R.C. Newton, A. Navrotsky and B.J. Wood (editors), Springer-Verlag, p. 131-147.

Pell, J.
1984: Stratigraphy, structure and metamorphism of Hadrynian strata in the southeastern Cariboo Mountains, B.C.; unpublished Ph.D. thesis, University of Calgary, Alberta, 185 p.

Pell, J. and Simony, P.S.
1987: New correlations of Hadrynian strata, south-central British Columbia; Canadian Journal of Earth Science, v. 24, p. 302-313.

Pichavant, M.
1981: An experimental study of the effect of boron on a water saturated haplogranite at 1 kbar vapour pressure; Contributions to Mineralogy and Petrology, v. 76, p. 430-439.
1987: Effects of B and H_2O on liquidus phase relations in the haplogranite system at 1 kbar; American Mineralogist, v. 72, p. 1056-1070.

Poulton, T.P. and Simony, P.S.
1980: Stratigraphy, sedimentology and regional correlation of the Horsethief Creek Group (Hadrynian, late Precambrian) in the northern Purcell and Selkirk Mountains, British Columbia; Canadian Journal of Earth Sciences, v. 17, p. 1708-1724.

Raeside, R.P.
1982: Structure, metamorphism and migmatization of the Scrip Range, Mica Creek, British Columbia; unpublished Ph.D. thesis, University of Calgary, Alberta, 204 p.

Sevigny, J.H.
1987: Field and stratigraphic relations of amphibolites in the late Proterozoic Horsethief Creek Group, northern Adams River area, British Columbia; in Current Research, Part A, Geological Survey of Canada, Paper 87-1A, p. 751-756.

Simony, P.S., Ghent, E.D., Craw, D., Mitchell, W., and Robbins, D.B.
1980: Structural and metamorphic evolution of northeast flank of Shuswap Complex, southern Canoe River area, British Columbia; in Geological Society of America, Memoir 153, M.P. Crittenden, Jr., P.J. Coney, and G.H. Davis (editors), p. 445-461.

Thompson, A.B.
1976: Mineral reactions in pelitic rocks: II. Calculation of some P-T-X (Fe-Mg) phase relations; American Journal of Science, v. 276, p. 425-454.

Tipper, H.W., Woodsworth, G.J., and Gabrielse, H.
1981: Tectonic Assemblage Map of the Canadian Cordillera and adjacent parts of the United States of America; Geological Survey of Canada, Map 1505A.

Regional geology of the McLeod Lake map area, British Columbia

L.C. Struik
Cordilleran and Pacific Geoscience Division, Vancouver

Struik, L.C., Regional geology of the McLeod Lake map area, British Columbia; in Current Research, Part E, Geological Survey of Canada, Paper 89-1E, p. 109-114, 1989.

Abstract

Upper Cretaceous(?) to Miocene dextral strike-slip and related crustal extension (and erosion) are interpreted to have generated the present topography of the bedrock in the McLeod Lake map area. Much of that bedrock topography was filled by Pleistocene glacial deposits. Tertiary basalt, sedimentary rocks, and plutons were probably generated by the transform plate motions recorded by the strike-slip and extension structures. Crustal shortening, accommodated by thrust overlap and folds, in part preceded the Late Cretaceous and younger tectonics. Pre-Tertiary bedrock consists of the Triassic and Jurassic Takla Group; upper Paleozoic Slide Mountain Group basalt and sediments; the Pennsylvanian Cache Creek Group limestone and basalt; the pre-Mesozoic sedimentary protolith to the Wolverine Metamorphic Complex; Lower Paleozoic carbonates sediments and minor basalts; and upper Precambrian clastic rocks.

Résumé

Un rejet horizontal dextre et une extension (et l'érosion) crustale associée qui dateraient du Crétacé supérieur (?) au Miocène, seraient à l'origine du relief actuel du socle de la région de la carte de McLeod Lake. Une grande partie du socle a été recouverte de dépôts glaciaires du Pléistocène. Des basaltes, des roches sédimentaires et des plutons du Tertiaire sont probablement le résultat des mouvements de plaques indiqués par les structures à rejet horizontal et la structure d'extension. Le racourcissement de la croûte, sous forme de chevauchement et de plis, a précédé en partie la dynamique tectonique du Crétacé supérieur et plus récente. Le socle pré-tertiaire est constitué du groupe de Takla du Trias et du Jurassique; des basaltes et des sédiments du groupe de Slide Mountain du Paléozoïque supérieur; des calcaires et des basaltes du groupe de Cache Creek du Pennsylvanien; de la roche originelle sédimentaire pré-mésozoïque du complexe métamorphique de Wolverine; des sédiments carbonatés et des basaltes secondaires du Paléozoïque inférieur; et des roches clastiques du Précambrien supérieur.

INTRODUCTION

The McLeod Lake map area (Fig. 1, 2) is transected by Highway 97, is permeated by logging roads, and has one town, Bear Lake.

TERTIARY BASALT

The youngest indurated rock of the area remains as volcanic necks supporting the Teapot and Coffeepot mountains and as nearly flat flows mainly in the western part of the McLeod Lake map area. The basalt contains ultramafic nodules that were probably derived from the mantle (Brearley, 1986). The flat lying flows were erupted in the Late Oligocene or Miocene (the age of the Teapot basalt from a K-Ar whole rock date, Ross, 1983). The same basalt occurs as dykes in the Wolverine Complex on Mount MacKinnon and those dykes are subparallel to the extension cracks formed by earlier, probably Eocene and Oligocene, tectonics (E. Deville, pers. comm., 1988).

Tertiary conglomerate, sand, and siltstone

Poorly consolidated sediments are exposed along several of the larger river channels, under the Miocene basalt and within the Parsnip River valley. To preserve those sediments there must have been topographic depressions (basins) where the sediment could be deposited from still or slow moving water. The plant remains found in the deposits suggest continental swamp or lake conditions. From the sediments we can infer that river channels, swamps and lakes existed during the early and middle(?) Tertiary. The conglomerate must have been derived from fast flowing rivers and because it contains locally derived clasts implies steep topography.

EAGLET PLUTON

The Eaglet Pluton at Eaglet Lake was mylonitized along a splay of the McLeod Lake Fault (Struik and Fuller, 1988). The deformation was ductile and therefore took place while the pluton was in the middle or lower crust. The pluton was dated as 36 Ma (Wanless et al., 1970). It, and presumably some of the adjacent country rock, must have still been rising after 36 Ma.

Biotite granodioritic plutons like the Eaglet Pluton are intruded by miarolitic granite and feldspar porphyry rhyolite. If those granodiorites are the same age as the Eagle Pluton (36 Ma) then the granites and rhyolites should be younger. A rhyolite dyke complex intrudes the gneisses, schists, granitic pegmatites and biotite-granodiorite plutons on Mount MacKinnon. The dyke complex probably formed by crustal stretching and so that stretching should be younger than 36 Ma - if the granodiorites have the same age as the Eaglet Pluton. Rhyolite flows are found west and east of Mount MacKinnon and probably are surface lavas fed by the rhyolite dyke systems such as on Mount MacKinnon. The uplift of the Wolverine Complex and its rhyolite dyke system must therefore still postdate the stretching and emplacement of the dykes.

The rhyolite dykes, miarolitic granite, biotite-granodiorite and garnet-biotite and muscovite granite are confined to the Wolverine Complex, however, rhyolite flows northeast of Carp Lake may be erupted onto rocks of the Takla Group. The miarolitic granite has associated concentrations of galena and molybdenite between Eaglet Lake and the Fraser River.

The high grade metamorphic rocks of the Wolverine Complex must have been uplifted because the gneisses and schists and plutons that intrude them formed at middle or lower crustal levels. Yet adjacent to those metamorphic rocks and separated from them by shallowly-dipping mylonitic and brittle shear zones are chlorite grade rocks that were always at relatively shallow depths. The high grade metamorphic rocks must have risen at least 6-10 km compared with 2-4 km for the low-grade rocks. This difference in uplift implies that the chlorite grade rocks moved down

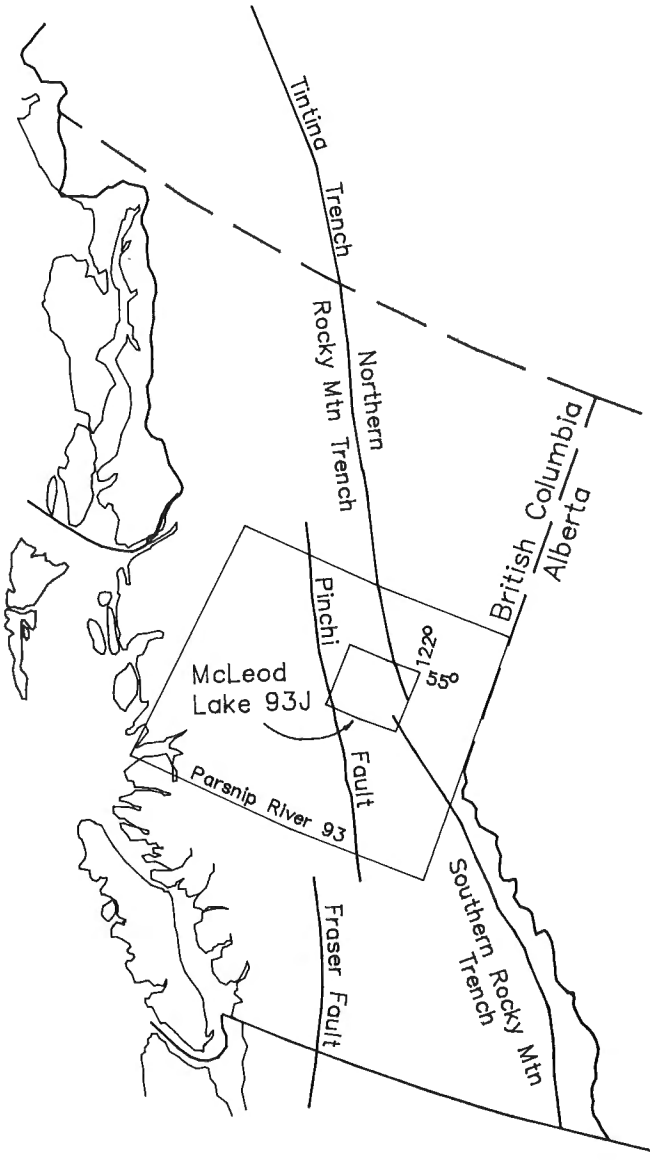

Figure 1. Location of the McLeod Lake map area within British Columbia.

relative to the high grade rocks. That sense of motion, top down, was seen at several of the exposed mylonitic zones between the high and low grade rocks. Metamorphic rocks of the Wolverine Complex probably were uplifted during the middle Tertiary because plutons like the Eaglet Pluton intrude the Wolverine Complex. This uplift is younger than the Eocene thrust faults in the Rocky Mountains (Price, 1965).

Monger (1985) described middle Tertiary movement along the Fraser Fault system in southwest British Columbia. The Fraser Fault system and the McLeod Lake extension complex are probably linked by an en echelon system of dextral strike-slip faults and pull-aparts, and the similar ages are therefore not fortuitous. Price and Carmichael (1985) suggested the same link but preferred an Eocene or older age for tectonism. The Pinchi Fault, that separates the Takla and Slide Mountain groups from the western, age-equivalent Cache Creek Group, may be part of that en echelon system (Struik, 1988c).

STRIKE-SLIP FAULTS

Two sets of fault trends are present in the region. The younger follows the trend of the McLeod Lake Fault; this is a more northerly trend (160°) than the older Northern Rocky Mountain Trench Fault system (140°). The offset of structures related to the Northern Rocky Mountain Trench Fault by those related to the McLeod Lake Fault is best expressed in the Rocky Mountains east of the Parsnip River, although that may be a matter of exposure. The same style of intersecting faults is seen in the regional pattern between the Crooked and Parsnip Rivers and perhaps within the area of the Wolverine Complex (Fig. 3). Each of these fault sets is ascribed to dextral strike-slip systems (E. Deville, pers.

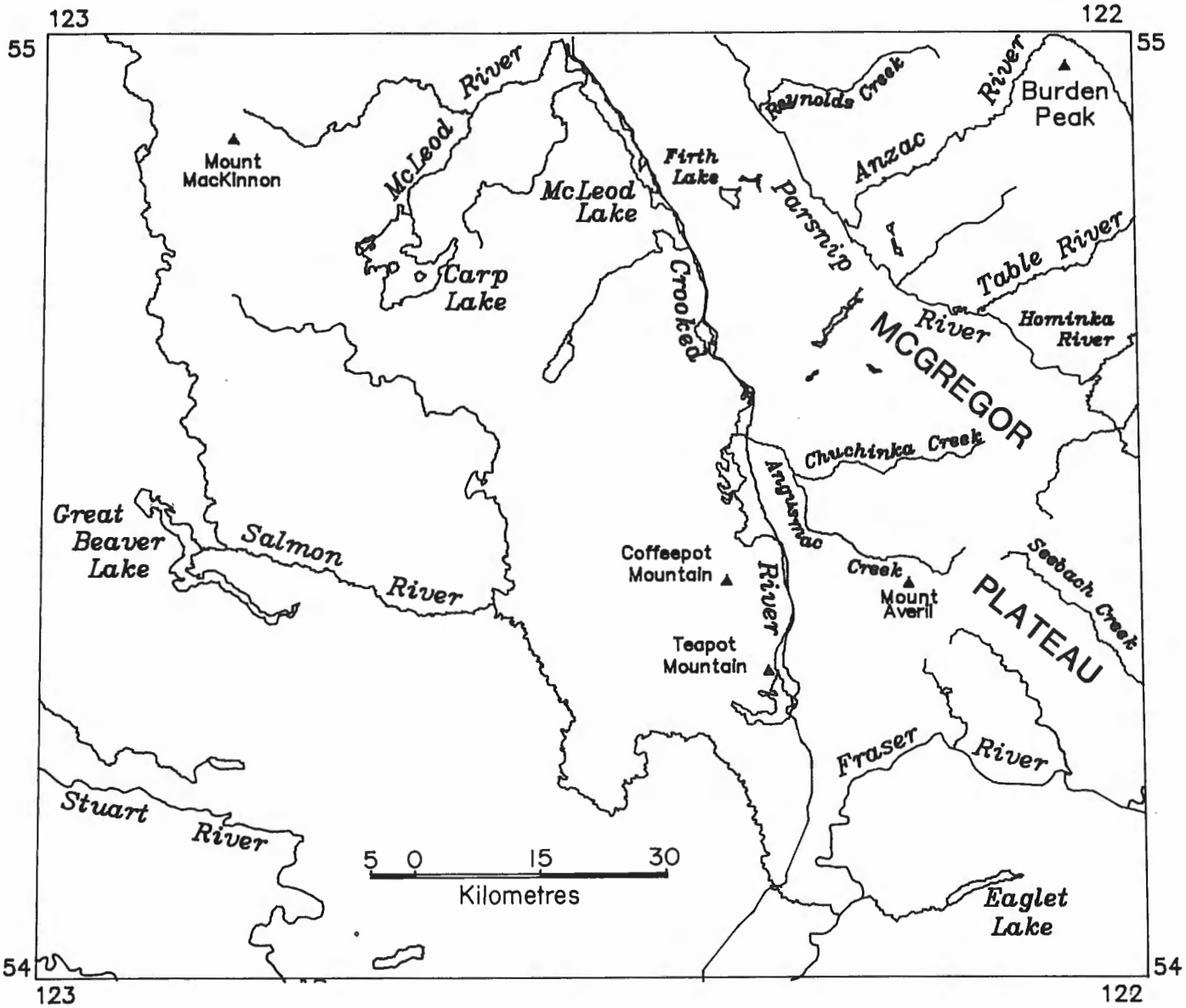

Figure 2. Geographic features of the McLeod Lake map area that are referred to in the text.

comm., 1988; Taite, 1989). We have suggested that the McLeod Lake system is middle Tertiary; perhaps the Parsnip River system is early to late early Tertiary. The Upper Cretaceous or Paleocene clastic rocks along Reynolds Creek (Muller and Tipper, 1969) may have filled a depression generated by movement along the Parsnip system, suggesting a late Cretaceous or Paleocene age to some of the movement along the Parsnip system.

CRETACEOUS AND JURASSIC

Within the Rocky Mountains and perhaps the McGregor Plateau, east- and west-directed thrust faults are probably cut by the strike-slip faults of the Parsnip and McLeod systems and are therefore older, perhaps Cretaceous. The more shallowly-dipping east-directed thrusts appear to be older than the westerly directed ones. Inferred thrust faults within the McGregor Plateau are offset by the Parsnip set of strike-slip faults.

Folds in rocks east of the McLeod Lake Fault might be the same age as the easterly and westerly thrusts, although certainly some of the folds along the Parsnip valley were generated during strike-slip motion on the Northern Rocky Mountain Trench Fault (Taite, 1989). The interplay between the strike-slip and thrust faulting is not known: some of the thrust faults may have formed while strike-slip motion was taking place. Close to the Parsnip strike-slip faults, easterly-directed folds are refolded; the best example is between the Table and Hominka rivers. Kink bands common in the slates of the Rocky Mountains have the correct sense of shear and orientation to have been made by dextral strike-slip motion along the Parsnip faults. Those kink bands deformed the slaty cleavage that is axial planar to regional folds; therefore the Parsnip fault system may have had some motion on it after the folding.

Folds west of the McLeod Lake Fault can be grouped for discussion into those of the Wolverine Complex and those of the "cover" rocks to the Wolverine Complex. Within the Wolverine Complex syn-metamorphic isoclinal and tight folds of gneiss, schist and granitic pegmatite are intruded by biotite granodiorite and rhyolite dykes and are broken by brittle extension faults. Folds in the Takla and Slide Mountain groups might all be small ones related to fault motions of various types. For example, folds of Takla Group rocks along the McLeod River appear to have formed during thrust and strike-slip faulting.

By extrapolation of thrust relationships in the Prince George map area to the south the Slide Mountain and Takla groups were thrust onto the rocks now incorporated in the Wolverine Metamorphic Complex. They were thrust before the mid-Cretaceous (100 Ma) because the Naver Pluton of that age intrudes the thrust fault at the base of the Slide Mountain Group in the Prince George map area (Struik, 1985). Presumably that thrusting was part of a compressional event that thickened the crust and induced metamorphism, but is that the metamorphism seen in the Wolverine Complex? The rocks of the Wolverine Complex, like those of the Shuswap Metamorphic Complex (Parrish et al., 1988) may have been held at depth long after the initial collisional thickening and the metamorphism and tectonics we now see were frozen into the rocks during the later Tertiary uplift.

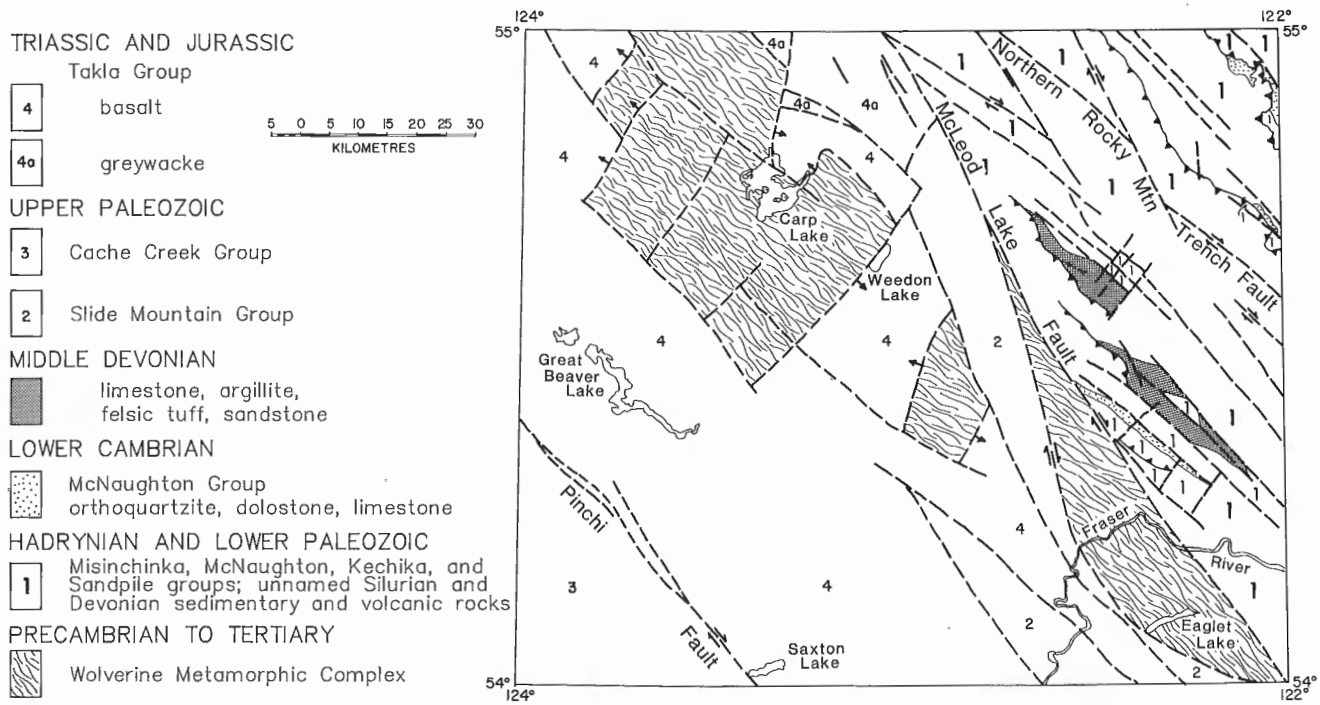

Figure 3. Some pertinent geology of the McLeod Lake map area. Significant changes from previous maps include 1) the thrust faults, 2) the Devonian units, 3) the distribution of Takla Group greywacke and 4) the distribution of some of the northwest trending strike-slip faults.

TRIASSIC AND UPPER PALEOZOIC

Within the McLeod Lake map area, the tectonic and stratigraphic history of the Slide Mountain and Takla groups is mostly hidden. But presumably it is similar to that of those rocks to the north and south (*see* Struik, 1985; 1988a; Ferri and Melville, 1988; Struik, 1988a, b). The rocks of the Takla Group encompass the Middle Triassic to Lower Jurassic (Struik, 1988d) and the Slide Mountain Group the upper Paleozoic (Nelson, 1988; Struik, 1988a). Greywacke and lithic tuff of the Takla Group similar to that on Tabor Mountain east of Prince George (Struik, 1985) underlies a large area between McLeod and Carp lakes and extends northward into the Pine Pass map area (Fig. 3). They were mapped as Slide Mountain Group by Muller and Tipper, 1969). The Cache Creek Group, which is mainly represented by limestone and minor basalt in the southwest corner of the McLeod Lake map area, appears to be mainly upper Carboniferous (Pohler et al., 1989).

EARLY PALEOZOIC AND PRECAMBRIAN

Early Paleozoic and Precambrian rocks are confined to the area east of the McLeod Lake Fault. Presently we recognize eight sequences of rock ranging in age from Middle Devonian to late Precambrian: 1) Middle Devonian sandstone, tuff, argillite, and limestone; 2) Lower Devonian(?) (''tapioca sandstone'') dolostone, sandy dolostone, quartzite and basalt; 3) Lower Silurian limestone, dolostone, and shale; 4) Ordovician dolostone, limestone and quartzite; 5) Upper Cambrian and Lower Ordovician limestone, dolostone, slate and phyllite; 6) Lower Cambrian dolostone and quartzite; 7) Lower Cambrian(?) quartzite, siltstone and slate; and 8) upper Precambrian phyllite, siltite, and grit.

Middle Devonian

Givetian limestone, as dated by macrofossils (Muller and Tipper, 1969) and microfossils (M.J. Orchard, pers. comm., 1988) forms the base of the Middle Devonian sequence (Fig. 3), most of which was mapped by Muller (Muller and Tipper, 1969) as Silurian Sandpile Group (*see* Struik, 1989 for details). Rhyolitic and dacitic tuff and flows are characteristic of the unit.

Lower Devonian(?)

Under the Givetian limestone of the Middle Devonian sequence is a unit of thinly laminated dolostone and silty dolostone, quartzite, and sandy limestone and dolostone that is very much like the ''tapioca sandstone'' of the McDame map area (Gabrielse, 1963). Locally calcareous basalt agglomerate, pillows, and flows are intercalated with the sandy units. Basalt with unknown contact relationships and previously mapped as Silurian by Tipper et al. (1979) may be part of this ''tapioca'' sequence.

Lower Silurian

Lower Silurian slate, limestone and dolostone probably underlies the tapioca sandstone unit (*see* Struik, 1989 for details). The Silurian rocks are dated by graptolites and conodonts.

Ordovician

The Sandpile Group, a fossil-rich sequence of reefal dolostone and limestone with various units of white quartzite appears to span much of the Ordovician (Sandpile Group). Its relationship with the Lower Silurian rocks is unknown.

Upper Cambrian and Ordovician(?)

Blue-grey slate and phyllite probably underlie the Ordovician rocks and in turn overlie algal limestone, and thinly bedded limestone and sandy limestone probably of Late Cambrian and Early Ordovician age (Kechika Group of Muller and Tipper, 1969). The algal limestone contains various sizes and shapes of algal pellets and blobs. It overlies a sequence of thinly bedded limestone and orange-weathering sandy limestone. North of Seebach Creek on the Chuchinka Forest Road these rocks are intruded by a basalt dyke; the basalt that is similar to that in the Lower Devonian(?) sequence to the northwest.

Lower Cambrian

The relationship between the Upper and Lower Cambrian rocks is uncertain. East of the Parsnip River, Lower Cambrian dolostone and quartzite caps the exposed sequence (*see* Struik, 1989 for further details). Near Mount Averil in the south-central part of the map area, *Archeocyathid*-bearing limestone and associated white quartzite typical of the Lower Cambrian are not interlayered as they are east of the Parsnip River. For instance at Mount Averil, white coarse grained quartzite directly overlies olive slate and siltstone with minor white quartzite (comparable to the upper part of the Misinchinka Group of the Rocky Mountains) and had only minor calcareous-matrixed quartzite in a nearly 100% quartzite unit. However, east of the Parsnip River at Burden Peak, the possibly equivalent quartzite unit has dolomitic quartzite and dolostone units near its base and throughout the sequence. Also many of the dolostone beds at Burden Peak have *Archeocyathids* indicating the sequence is almost entirely from the late Early Cambrian. Although 100 m of quartzite and slate mapped as part of the upper Misinchinka Group underlies the Lower Cambrian(?) quartzite at Mount Averil, most of the Misinchinka Group rocks of the map area are exposed east of the Parsnip River (*see* Struik, 1989 for details). The upper Misinchinka Group may be mainly Lower Cambrian because it is gradational with the overlying *Archeocyathid*-bearing quartzite-dolostone sequence.

Upper Precambrian

The Cambrian-Precambrian contact may lie between the olive and olive-grey slate and siltstone and white quartzite of the upper Misinchinka Group and the grey and dark grey siltstone and slate immediately overlying the grit unit of the Misinichinka Group (Struik, 1989). The bottom of the grit unit is covered.

REFERENCES

Brearley, M.
1986: Ultramafic xenoliths from British Columbia, Canada: petrological and dissolution studies; unpublished Ph.D. thesis, University of Alberta, Edmonton, Alberta.

Ferri, F. and Melville, D.M.
1988: Manson Creek mapping project (93N/09); in Geological Fieldwork 1987, British Columbia Ministry of Energy, Mines and Petroleum Resources, Paper 1988-1, p. 169-180.

Gabrielse, H.
1963: McDame map-area, Cassiar District, British Columbia; Geological Survey of Canada, Memoir 319.

Harms, T.A., Nelson, J., and Bradford, J.
1988: Geological transect across the Sylvester Allochthon north of the Blue River, northern British Columbia (104P/12); in Geological Fieldwork 1987; British Columbia Ministry of Energy, Mines and Petroleum Resources, Paper 1988-1, p. 245-248.

Mansy, J.-L. and Gabrielse, H.
1978: Stratigraphy terminology and correlation of upper Proterozoic rocks in Omineca and Cassiar mountains, north-central British Columbia; Geological Survey of Canada, Paper 77-19.

Monger, J.W.H.
1985: Structural evolution of the southwestern Intermontane belt, Ashcroft and Hope map areas, British Columbia; in Current Research, Part A, Geological Survey of Canada, Paper 85-1A, p. 349-358.

Muller, J.E. and Tipper, H.W.
1969: Geology, McLeod Lake, British Columbia; Geological Survey of Canada, Map 1205A.

Parrish, R.R., Carr, S.D., and Parkinson, D.L.
1988: Eocene extensional tectonics and geochronology of the southern Omineca Belt, British Columbia and Washington; Tectonics, v. 7, p. 181-212.

Pohler, S., Orchard, M.J., and Struik, L.C.
1989: Preliminary biostratigraphy of conodonts from McLeod Lake map area, British Columbia; in Current Research, Part E, Geological Survey of Canada, Paper 89-1E.

Price, R.A.
1965: Flathead map-area, British Columbia and Alberta; Geological Survey of Canada, Memoir 336.

Price, R.A. and Carmichael, D.M.
1985: Geometric test for Late Cretaceous-Paleogene intracontinental transform faulting in the Canadian Cordillera; Geology, v. 14, p. 468-471.

Ross, J.V.
1983: The nature and rheology of the Cordilleran upper mantle of British Columbia: inferences from peridotite xenoliths; in Continental Tectonics: Structure, Kinematics and Dynamics, M. Friedman and M.N. Toksoz (eds.), Tectonophysics, v. 100, p. 321-358.

Struik, L.C.
1985: Pre-Cretaceous terranes and their thrust and strike-slip contacts, Prince George (east half) and McBride (west half), British Columbia; in Current Research, Part A, Geological Survey of Canada, Paper 85-1A, p. 267-272.
1988a: Structural geology of the Cariboo gold mining district, east-central British Columbia; Geological Survey of Canada, Memoir 421.
1988b: Crustal evolution of the eastern Canadian Cordillera; Tectonics, v. 7, p. 727-747.
1988c: Exploring the Parsnip; Mining Review, v. 8, no. 4, p. 66-68.
1988d: Regional imbrication within Quesnel terrane, central British Columbia: as suggested by conodont ages; Canadian Journal of Earth Sciences, in press.
1989: Devonian, Silurian, Cambrian and Precambrian stratigraphy, McLeod Lake area, British Columbia; in Current Research, Part E, Geological Survey of Canada, Paper 89-1E.

Struik, L.C. and Fuller, E.A.
1988: Preliminary report on the geology of McLeod Lake area, British Columbia; in Current Research, Part E, Geological Survey of Canada, Paper 88-1E, p. 39-42.

Taite, S.P.
1989: Deformation in the Parsnip River valley, McLeod Lake map area, British Columbia; in Current Research, Part E, Geological Survey of Canada, Paper 89-1E.

Tipper, H.W., Campbell, R.B., Taylor, G.C., and Stott, D.F.
1979: Parsnip River, British Columbia; Geological Survey of Canada, Map 1424A.

Wanless, R.K., Stevens, R.D., Lachance, G.R., and Delabio, R.N.
1970: Age determinations and geological studies K-Ar isotopic ages, report 9; Geological Survey of Canada, Paper 69-2A, 78 p.

Deformation in the Parsnip River valley, McLeod Lake map area, British Columbia

S.P. Taite[1]
Cordilleran and Pacific Geoscience Division, Vancouver

Taite, S.P., Deformation in the Parsnip River valley, McLeod Lake map area, British Columbia; in Current Research, Part E, Geological Survey of Canada, Paper 89-1E, p. 115-118, 1989.

Abstract

At the confluence of the Parsnip and Hominka rivers, intense flattening and associated dextral shear may have occurred because of motion along the Northern Rocky Mountain Trench Fault. Considerable northeast-trending shortening has been accommodated by both D_1 folding and pressure solution. Subsequent crenulation cleavage (D_2) could have formed in the same stress regime as the folds, whereas the younger kink bands (D_3) may have been produced by a stress regime related to the younger McLeod Lake Fault.

Résumé

À la confluence des rivières Parsnip et Hominka, s'est peut-être produit un aplatissement intense accompagné d'un cisaillement dextre, causés par un mouvement survenu le long de la partie nord de la faille du sillon des Rocheuses. Un raccourcissement considérable de direction nord-est a été rendu possible à la fois par un plissement (D_1) et la dissolution par compression. Il est possible que la crénulation ultérieure (D_2) soit apparue dans les mêmes conditions de contraintes que les plis, tandis que les flexures répétées plus récentes (D_3) résultent peut-être d'un régime de contraintes apparenté à la faille plus récente de McLeod Lake.

[1] Department of Geological Sciences, University of British Columbia, 6339 Stores Road, Vancouver, B.C. V6T 2B4

INTRODUCTION

Regional mapping of the McLeod Lake map sheet was first published by Muller and Tipper in 1969. Further mapping of the area was conducted during the 1987 and 1988 field seasons to improve on the understanding of both the distribution of lithologies and the local tectonic history (Struik and Fuller, 1988).

The McLeod Lake map area occupies a key tectonic position, in that a major fault system, the Northern Rocky Mountain Trench, may terminate within its bounds. It and the through-going McLeod Lake Fault are believed to accommodate large dextral offsets (Gabrielse, 1985), but the nature and the amount of offset are poorly constrained.

During the 1988 field season a zone of intense deformation was found along the trend of the Northern Rocky Mountain Trench, on the eastern flank of the Parsnip River Valley (Fig. 1). Steeply dipping fabrics within this zone trend parallel to the Northern Rocky Mountain Trench. The style and geometry of small-scale structures indicates that considerable shortening has been accommodated, and is likely related to movement along the southern extension of the Northern Rocky Mountain Trench.

The oldest lithologies exposed east of the Parsnip River Valley are fine-to coarse-grained clastic sedimentary rocks of the Precambrian middle Misinchinka Group. These are conformably overlain by black slates, phyllites, quartzites and brown schistose greywackes of the upper Precambrian to lower Cambrian upper Misinchinka Group, which are overlain by unnamed Lower Cambrian quartzites, sandstones, black shales and dolomites (Muller and Tipper, 1969).

Figure 2. Isoclinal folds indicative of D_1 deformation.

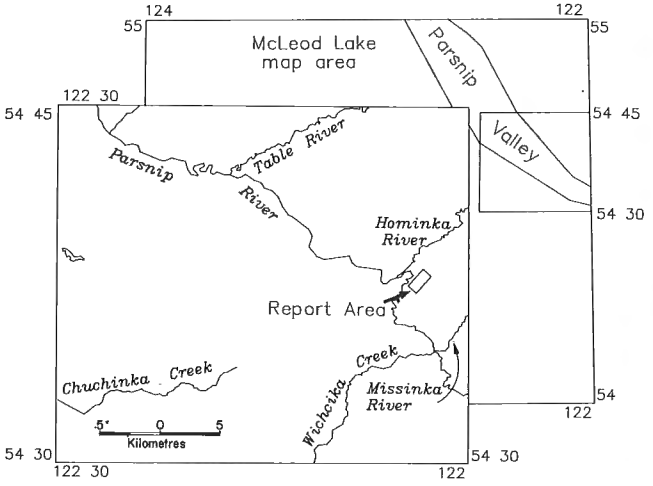

Figure 1. The location of the zone of deformation on the eastern flank of the Parsnip River valley, McLeod Lake map sheet. The southern extension of the Northern Rocky Mountain Trench is thought to be located in the Parsnip River valley.

Figure 3. Pressure solution cleavage surfaces axial planar to D_1 folds.

Figure 4. Asymmetric pull-apart structures within quartzites and phyllites indicating dextral shear. Note the D_2 crenulation cleavage in phyllitic layer under the Canadian dollar.

DEFORMATION

The zone of intense deformation occurs within greywackes, quartzites, and phyllites of the upper Misinchinka Group. Within this zone, tight folds with well defined axial planar fabrics become progressively tighter towards a central core region where compositional layering is completely transposed about rootless isoclines. Boundaries for the belt trend parallel to the Parsnip River Valley, and have been arbitrarily defined as the first appearance of abundant outcrop scale folds with well developed axial planar fabrics. The total width of the zone is uncertain; approximately 300 — 500 m of strongly deformed rocks are exposed discontinuously in logging roadcuts in locations just south of the Hominka River and just north of the Missinka River.

Structural fabrics found within the fold belt have been attributed to three distinct deformation events. The first phase, D_1, is characterized by open to tight folds with upright axial surfaces striking approximately 135-145° (Fig. 2). Within the core of the fold belt, compositional layering has been completely transposed about rootless isoclines, and axial surfaces are marked by both a strong foliation and a well developed pressure solution cleavage (Fig. 3). Both foliation and pressure solution cleavage surfaces are at a small angle to compositional layering within the core of the fold belt. Layering has been disrupted inhomogeneously, and kinematic indicators (asymmetric folds and pinch and swell structures) found within the fold belt are indicative of both dextral and sinistral shear deformation; dextral shear kinematic indicators are the most abundant (Fig. 4). Minor folds at the boundaries of the fold belt are symmetric, towards the core they become increasingly asymmetric, with a dextral sense of rotation.

The second recognizable deformation event, D_2, is a crenulation cleavage refolding the transposed foliation of D_1 and striking approximately 95-105°. The pervasive cleavage is well developed within phyllites in the core of the fold belt but is not observed towards the boundaries (Fig. 4).

D_3, the third observed phase of deformation, is characterized by both a non-pervasive, well developed kinking of D_1 and D_2 structures, and a very broad, shallow warping of the D_1 axial planer foliation on a 5 — 10 m scale. Northerly trending axial planes are vertical and D_3 fold axis plunge at 85-90° (Fig. 5).

DISCUSSION

The most notable characteristic of this area is the intense deformation seen concentrated in a relatively narrow zone. Considerable shortening across the zone has been accommodated by both the D_1 folding and the pressure solution cleavage. Abundant asymmetric fabrics indicate there was also a component of dextral offset during deformation, and because the transposition surfaces parallel the Northern Rocky Mountain Trench, the formation of this zone could be related to movement along the Trench. The formation of

Figure 5. D_3 kink bands that strike approximately north-south.

D_1 and D_2 structures may have been related to the same stress regime, with the compressional axis perpendicular to the D_1 foliation plane. The D_3 kink bands may have formed in response to a younger and differently oriented stress regime related to movement along the McLeod Lake Fault.

REFERENCES

Gabrielse, H.
1985: Major dextral transcurrent displacements along the Northern Rocky Mountain Trench and related lineaments in north-central British Columbia ; Geological Society of America, Bulletin, v. 96, p. 1-14.

Muller, J.E. and Tipper, H.W.
1969: Geology of the Mcleod Lake map area, British Columbia ; Geological Survey of Canada, Map 1204A.

Struik, L.C. and Fuller, E.A.
1988: Preliminary report on the geology of the McLeod Lake area, British Columbia; in Current Research, Part E, Geological Survey of Canada, Paper 88-1E, p. 39-42.

Devonian, Silurian, Cambrian and Precambrian stratigraphy, McLeod Lake map area, British Columbia

L.C. Struik
Cordilleran and Pacific Geoscience Division, Vancouver

Struik, L.C., Devonian, Silurian, Cambrian and Precambrian stratigraphy, McLeod Lake map area, British Columbia; in Current Research, Part E, Geological Survey of Canada, Paper 89-1E, p. 119-124, 1989.

Abstract

The Devonian sequence, in descending order, consists mainly of sandstone, cherty felsic tuff, slate-argillite, and limestone, and was previously included mainly in older units. The described and measured Silurian section consists of slate, dolostone and limestone and its age is constrained at its base by graptolites and conodonts. The sequence includes several bedding-parallel detachments. The Cambrian-Precambrian sequence, in de-ascending order, consists of 6 mappable units: dolostone; quartzite; quartzite-siltstone; siltstone-quartzite; siltstone; and grit. The Cambrian-Precambrian boundary may be above the siltstone unit.

Résumé

La séquence dévonienne, de haut en bas, se compose principalement de grès, de tuf felsique cherteux, d'argilite, d'ardoise et de calcaire, et a autrefois été principalement placée dans des unités plus anciennes. La coupe silurienne, décrite et mesurée se compose d'ardoise, de calcaire dolomitique et de calcaire; on a défini l'âge de cette coupe d'après les graptolites et conodontes trouvés à sa base. Cette séquence comprend plusieurs décollements parallèles au litage. La séquence cambrienne et précambrienne, de haut en bas, se compose de six unités cartographiables de calcaire dolomitique; de quartzite; de quartzite et microgrès; de microgrès et quartzite; de microgrès; et, de grès grossiers. La limite entre le Cambrien et le Précambrien pourrait se situer au-dessus de l'unité composée de microgrès.

INTRODUCTION

Remapping in the McLeod Lake map area is part of a larger program that will re-evaluate the regional geology of central British Columbia. Mapping started in summer of 1987 (Struik and Fuller, 1988) and should continue in 1989.

The Rocky Mountain Trench has a kink in it (Fig. 1). That kink in central British Columbia forms a series of ridges called the McGregor Plateau; bound to the east by the Northern Rocky Mountain Trench and to the west by the Crooked River valley and the Southern Rocky Mountain Trench (Fig. 1 and 2). The plateau contains lower Paleozoic stratigraphy which appears to be akin to that found in the Rocky, Omineca, and Cassiar mountains. Part of this sequence previously mapped as Triassic, Devonian and Silurian by Muller and Tipper (1969) and as Devonian and Silurian by Tipper et al. (1979) is here interpreted mainly as Devonian. Another part of that sequence is a Silurian section that contains graptolites and conodonts at its base. That 122 m section is described. East of the Rocky Mountain Trench, upper Precambrian and Lower Cambrian rocks are here subdivided into six units.

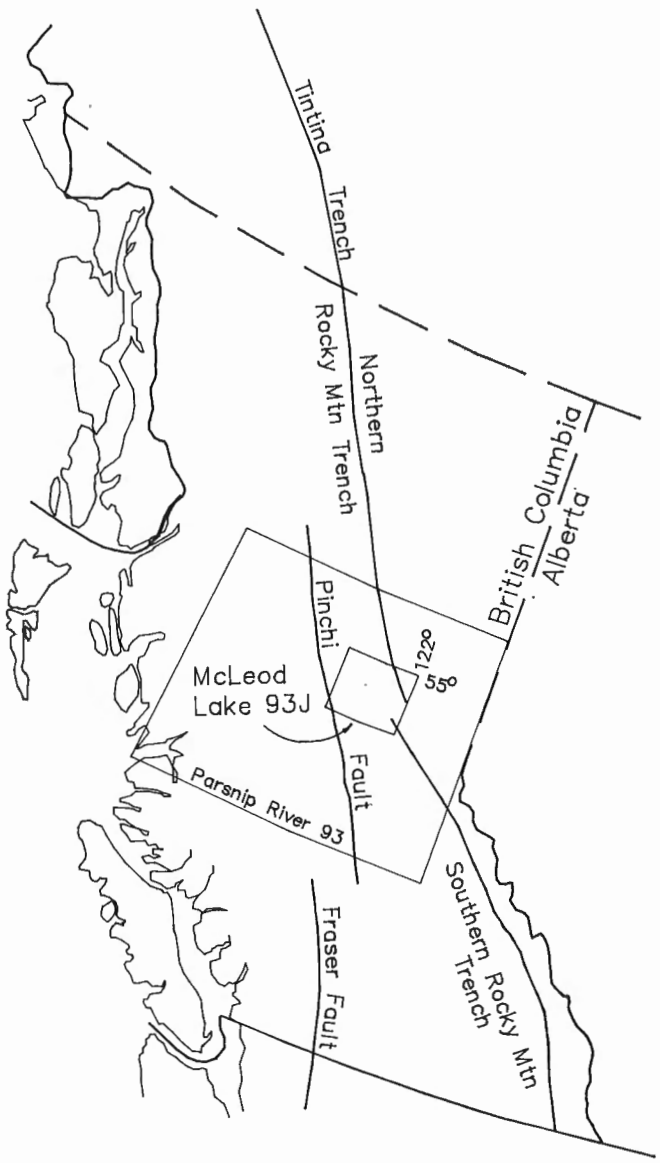

Figure 1. Location of the Mcleod Lake map area in British Columbia.

DEVONIAN ROCKS

Muller and Tipper (1969) described a sequence of limestone and dolostone that they interpreted to be Devonian. This sequence consists of four units assigned to the Middle Devonian. In descending order these are: 1) limestone; 2) felsic and intermediate cherty tuff and welded flow banded rhyolite; 3) slate, black argillite and chert; and 4) limestone (Fig. 3). The succession is most completely (but poorly) exposed in the area east of Mount Averil at the headwaters of Angusmac Creek.

The *sandstone unit* is recessive, dusty and ash grey, fine grained, and overlies the tuff unit abruptly in several places (the contact was not seen). In places, the sandstone weathers brown and has irregular elongate patches that look like horizontal worm burrows. North of Angusmac Creek, dark grey slate is interbedded with the sandstone. Beds of the sandstone are thin (3-10 cm) and ill-defined. The thickness of the unit is greater than 50 m and no younger rocks were recognized in this sequence.

The *tuff unit* gradationally overlies the slate-argillite unit, is mostly cherty, olive and olive-grey, and in 3-8 cm beds. The beds have wispy internal laminations and locally load casts. In places feldspar crystals (0.5 mm) float in the cherty matrix. South and west of Tacheeda Lakes, flow-banded rhyolite or dacite overlies the slate-argillite unit and is assumed to be laterally equivalent to the cherty tuff sequence. The tuff unit may be as thick as 300 m, but generally is between 50-100 m thick.

The *slate-argillite unit* has a lower part of slate and an upper part of argillite and chert; however, the slate may be partly laterally equivalent to the argillite. The slate is dark grey, locally siliceous, and is thinly interbedded (3-10 mm) with lesser amounts of a white weathering siltstone(?) that may be altered felsic tuff. The argillite is dark grey and mostly black, and is generally siliceous. Near the top of the sequence it is cherty and grades into black chert, which in turn grades into grey and olive cherty tuff. From a structural interpretation the slate-argillite unit may be about 250 m thick, but folds and thrust faults, seen in places, have likely thickened the sequence. Rocks of the slate-argillite unit are probably the same as those of the Tacheeda Lakes Canyon section along the Tacheeda Forest Service Road southwest of Tacheeda Lakes. There, as in several other places, the unit contains limestone beds (dark grey, 0-10 cm thick).

The *limestone unit* at the base of the succession has well defined even bedding (5-60 cm thick) and is generally grey and dark grey, finely crystalline with local stubby worm-like forms that appear to be *Amphipora*. The unit varies from 5 m to possibly greater than 100 m thick (from a structural interpretation). The thickness variation may be because the unit was deposited onto an unconformity. Beneath the limestone at the headwaters of Angusmac Creek is cream dolostone, similar to rocks assigned to the Silurian

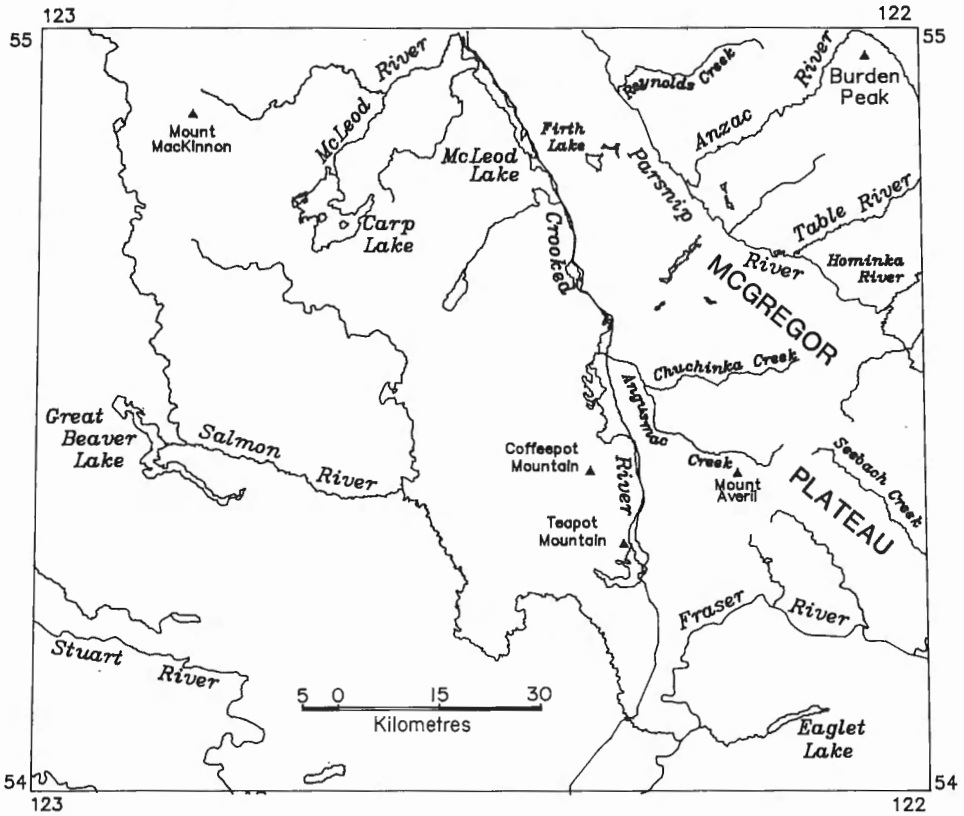

Figure 2. Geographic features of the McLeod Lake area that are referred to in the text.

and Ordovician Sandpile Group. The limestone was dated as partly Givetian by Muller and Tipper (1969). Givetian conodonts have been extracted from similar limestone to the north near Tacheeda Lakes (S. Pohler, pers. comm., 1988).

Regional relationships

Generally the Middle Devonian Angusmac succession rests on cream finely sugary dolostone, typical of rocks associated with the "tapioca" sandstone sequence described by Gabrielse (1963) for the McDame map area. The "tapioca" sandstone may be Early Devonian (H. Gabrielse, pers. comm., 1988). East of Redrocky Creek the Angusmac succession may rest on the Ordovician and Cambrian Kechika Group. South of Tacheeda Lakes, rhyolite of the tuff unit appears to overlie agglomeratic basalt formerly mapped as part of the Silurian (Tipper et al., 1979). Perhaps the contact is an unconformity or the basalt is part of a bimodal volcanic suite with the rhyolite. The bimodal hypothesis requires basalts of both Devonian and Silurian age, because basalts have also been mapped within the "tapioca" sandstone equivalent sequence.

SILURIAN SECTION

Along the Chuchinka Forest Service road, a cut exposes a section of slate, limestone and dolostone 122 m thick. The base of the section has been dated by graptolites and conodonts as Early Silurian. The sequence has been recognized in other places and is distinct from others in the area

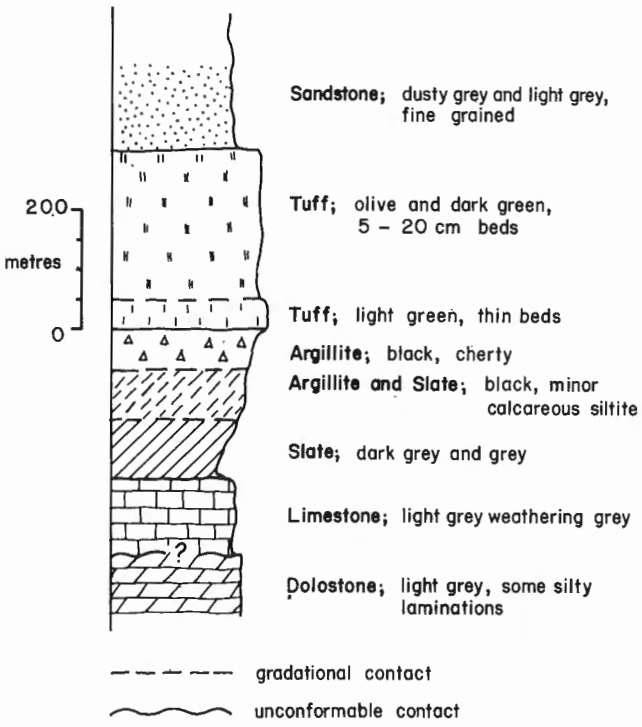

Figure 3. Stratigraphy of the Middle Devonian sequence from above the possible unconformity on the dolostone. Except for the basal limestone these rocks were previously mapped as Triassic, Silurian or Ordovician (Muller and Tipper, 1969; Tipper et al., 1979).

that are lumped into an undifferentiated Ordovician and Silurian unit that Muller and Tipper (1969) assigned to the Sandpile Group. At least three distinct units can be recognized in the rocks formerly assigned to the Sandpile Group and the section description in Appendix A is a step in the differentiation of those rocks. Brian Norford identified the graptolites and Susan Pohler and Mike Orchard identified the conodonts (see also Pohler et al., 1989).

These Silurian rocks probably overlie a sequence of richly fossiliferous Ordovician limestone and dolostone with lesser amounts of thin orthoquartzite beds. They may be overlain by Silurian or Devonian dolostone, quartzose dolostone, quartzite and basalt, part of which is similar to the "tapioca" sandstone of the McDame map area in northern British Columbia (Gabrielse, 1963).

CAMBRIAN AND PRECAMBRIAN ROCKS

East of the Rocky Mountain Trench, dolostone containing *Archeocyathids* overlies quartzite, slate and grit that are therefore interpreted to be Cambrian and possibly Precambrian. The exposed sequence can be subdivided into six mappable units; from top to bottom they are: 1) dolostone, 2) quartzite, 3) quartzite-siltstone, 4) siltstone-quartzite, 5) siltstone, and 6) grit.

The *dolostone unit* consists of reefal dolostone, siltstone and minor limestone and grades upward into interbedded quartzite and dolostone. In the area of Burden Peak this Lower Cambrian unit is overthrust by the siltstone-quartzite unit. Rocks of the dolostone unit are well exposed south of Burden Peak, and are described in Appendix A.

The *quartzite unit* consists of coarse- and medium-grained orthoquartzite, dolostone and minor slate. It underlies the dolostone unit in gradational continuity and, like the dolostone, is Early Cambrian from the presence of *Archeocyathids*. Measured sections of the quartzite unit are described in Appendix A.

The base of the quartzite unit lies some 60 m below the measured sections, and the intervening interval has quartzite, dolostone, calcareous quartzite, siltstone and slate. Downward in the interval, thick beds of white quartzite and orange weathering dolostone are separated by thicker and thicker intervals of interbedded slate, medium- and fine-grained quartzite, calcareous quartzite and siltstone (5 - 20 cm thick beds). The slate is olive and olive-grey and the siltstone and quartzite are mainly white. The contact with the underlying quartzite-siltstone unit is gradational and is drawn, going down section, at the last appearance of dolostone and bundles of coarse grained white quartzite beds.

The *quartzite-siltstone unit* is some 700 m thick south of Burden Peak; but that estimate may be too thick because it does not compensate for some of the tight folds within the central part of the sequence. The top of the sequence consists of 100 m of mostly white quartzite (7-25 cm beds) with thinner interbeds of olive siltstone and olive-grey slate. The base of the sequence (200 m thick) resembles the top of the sequence and is separated from it by about 400 m of thinly interbedded olive fine grained quartzite, siltstone and slate.

The *siltstone-quartzite unit* resembles the central part of the overlying unit and is approximately 750 m thick. The contact with the overlying unit is gradational.

The *siltstone unit* is approximately 200-400 m thick and its siltstone, fine grained quartzite and slate are mainly grey, dark grey and black. The contact with the overlying unit is suspected to be sharp although it is nowhere well exposed. Perhaps that contact is the boundary between Cambrian and Precambrian rocks. The lower part of the sequence consists mainly of grey slate or phyllite. Near the contact with the underlying grit unit the slate may contain one or two 30-70 cm beds of grit, but appears to be underlain directly by 5-10 m bundles of grit beds, that have been assigned to the grit unit.

The *grit unit* consists of grit and phyllite or slate. The grit beds are from 25-100 cm thick and form bundles some 8-25 m thick. Between the bundles are grey and olive-grey phyllites. The grit is generally very coarse sand to granule in grain size, but in places is a pebble conglomerate. The poorly sorted clasts consist of quartz and 6-12 % feldspar and the matrix is of muscovite and chlorite. About 200-300 m of the grit unit are exposed, with the base unseen. The grit unit is similar to the middle Miette and Kaza groups of the McBride map area to the south and the Swannell Formation and middle Misinchinka Group to the northwest and north, and therefore is assigned to the Precambrian (*see* Mansy and Gabrielse, 1979 for the distribution of the grit unit).

REFERENCES

Gabrielse, H.
1963: McDame map-area, Cassiar District, British Columbia; Geological Survey of Canada, Memoir 319.

Mansy, J.-L. and Gabrielse, H.
1978: Stratigraphy terminology and correlation of upper Proterozoic rocks in Omineca and Cassiar mountains, north-central British Columbia; Geological Survey of Canada, Paper 77-19.

Muller, J.E. and Tipper, H.W.
1969: Geology, McLeod Lake, British Columbia; Geological Survey of Canada, Map 1205A.

Pohler, S., Orchard, M.J., and Struik, L.C.
1989: Preliminary biostratigraphy of conodonts from McLeod Lake map area, British Columbia; in Current Research, Part E, Geological Survey of Canada, Paper 89-1E.

Struik, L.C. and Fuller, E.A.
1988: Preliminary report on the geology of McLeod Lake area, British Columbia; in Current Research, Part E, Geological Survey of Canada, Paper 88-1E, p. 39-42.

Tipper, H.W., Campbell, R.B., Taylor, G.C., and Stott, D.F.
1979: Parsnip River, British Columbia; Geological Survey of Canada, Map 1424A.

APPENDIX A

Description of measured sections from parts of the McLeod lake map area

SILURIAN

Chuchinka Forest Road

(Starts at UTM N6039855 E535450, ends at UTM N6040050 E535750)
Measured by L.C. Struik

Unit		Thickness in metres Unit	Above base
	Top of section, covered with glacial drift		
31	Limestone, white, finely to moderately crystalline	10	121.2
30	Limestone, light grey weathering grey, brecciated	2	111.2
29	Limestone, khaki	1.5	109.2
28	Limestone, dark grey, thick bedded thinly laminated, invaded by many thin calcite veins	4	107.2
	Covered	10	103.7
27	Limestone, dark grey	3	93.7
26	Limestone, grey, thin bedded	2	90.7
25	Limestone, grey, thick bedded	2	88.7
24	Limestone, light grey, thin bedded	1	86.7
23	Limestone, grey, 30 cm beds, permeated with calcite veins	1	85.7
22	Limestone, light grey, some khaki weathering breccia in thin layers, thin bedded	4	84.7
	Breccia and gouge of limestone and dolomitic limestone, overlying units are oriented differently than those below this fault	3	80.7
21	Limestone, dolomitic, grey, some 1-4 mm crinoid and shell fragments, brecciated near the gouge zone	15	77.7
20	Limestone, dolomitic, dark grey, 4-8 cm spaced ripples some of which are linear and others with nodes, approximately 2% 1-4 mm crinoid and shell fragments, 40-60 cm beds	9	62.7
19	Limestone, dolomitic, dark grey, buff, weathering, even 2-7 cm beds, thinner bedded near the base. Detachment, bedding parallel	6.3	53.7
18	Limestone, dark grey, 2-5 cm beds. Fault, bedding-plane detachment	2	47.4
17	Dolostone and dolomitic limestone, dark grey, 10-20 cm beds	1.6	45.4
16	Dolostone, grey, 2-4 cm beds	1.5	43.8
15	Dolostone and dolomitic limestone, dark grey, 20-50 cm beds	10.9	42.3
14	Limestone, black, thin bedded, some interbeds of black argillite. Fault, bedding-plane detachment	1.8	31.4
13	Limestone, dolomitic, dark grey, 10-25 cm beds, ripples in interference pattern nodes (some of which have concentrations of crinoid and shell debris), beds thin downsection, thin black slate at base	4.9	29.6
12	Limestone, black, 2-6 cm beds, minor black slate beds, includes a bedding-plane detachment	2.3	24.7
11	Limestone, black, platy, minor 8-15 cm beds that weather brown	2.1	22.4
10	Slate and lesser amounts of argillite, black, 0.3-3 cm beds, a lens of dark grey limestone	.7	20.3
9	Limestone, dark grey, 3-15 cm beds possible desiccation cracks	.8	19.6
8	Slate and argillite, black, 3-7 mm layers	.2	18.8
7	Limestone and slate, dark grey and black, limestone is thinly platy	.4	18.6
6	Dolostone, dark buff weathering dark grey, mostly breccia and stockwork of calcite veins	6	18.2
5	Dolostone, dark grey, 1-15 cm beds, lots of calcite veins some of which have vugs	3	12.2
4	Limestone and slate, black, thin platy beds, graptolitic	3	9.2
3	Limestone and slate, black thinly bedded	1.5	6.2
2	Limestone, dark buff weathering dark grey, 1-15 cm beds, conodonts	.7	4.7
1	Slate and limestone, black, thinly bedded, platy, brachiopods (some rhynchonellids), graptolites: *Monograptus* spp., *M.* ex gr. *M. priodon* (Bronn), *M.* ex gr. *M. spiralis* (Geinitz), *Stomatograptus grandis* (Suess) (collection is Early Silurian, Late Llandovery as identified by B.S. Norford). Base of section, covered with glacial drift	4	4

CAMBRIAN-PRECAMBRIAN

Dolostone unit

Description, in descending order, of the dolostone unit south of Burden Peak

–Quartzite, white, coarse and medium grained and lesser amounts of dolostone, orange weathering; about 50 m thick under a thrust fault

–Dolostone, orange weathering, with poorly preserved *Archeocyatha*; about 15 m thick

–Siltstone and fine grained sandstone, khaki and olive-grey, thinly bedded, some jellyfish-like imprints; about 8 m thick
–Limestone, grey, locally pelletal, minor bioclastic debris that may be bits of trilobite; about 2 m thick
–Dolostone, orange weathering, poorly preserved *Archeocyatha*; about 50 m thick.

Quartzite unit

The following description of the quartzite unit comes from 2 sections south of Burden Peak.

Section 2

(Starts at UTM N6039855 E535450, ends at UTM N6040050 E535750)
Measured by L.C. Struik

Unit		Thickness in metres Unit	Above base
Top of exposure. This section underlies the dolostone as described above for the area south of Burden Peak.			
29	Quartzite, white, very coarse, coarse and medium grained, 0.5-1.5 m thick beds	6.1	64.5
28	Dolostone, cream, weathers tan, coarse quartz sand grains	.2	58.4
27	Quartzite, white, coarse and medium grained, 0.3-1.5 m thick beds.	4.9	58.2
	Covered	2.3	53.3
26	Quartzite, white, medium grained,	3.2	51
	Covered	.8	47.8
25	Quartzite, white, coarse grained, planar crossbedded.	4.4	47
	Covered	2.1	42.6
24	Quartzite, white, fine grained	3	40.5
23	Dolostone, cream, weathers tan	1.5	37.5
	Covered, probably quartzite	1.5	35
22	Dolostone, cream, weathers tan. finely crystalline, *Archeocyatha*	1.6	34.5
21	Quartzite, pale yellow, fine grained	1.5	32.9
20	Dolostone, cream, weathers tan.	1.3	31.4
	Covered	1.4	30.1
19	Quartzite, white, thinly bedded fine and medium grained.	.7	28.7
	Covered	2.5	28.0
18	Dolostone, cream, weathers tan, some reticulated layers.	1	25.5
	Covered	3.5	24.5
17	Dolostone, tan, 15-20 cm beds, *Archeocyatha*	1	21
16	Quartzite, white, medium and fine grained.	1.3	20
	Covered	1.7	18.7
15	Dolostone, laminated tan and brown, some 10 cm thick phyllitic layers, discontinuous exposure	2.35	17
14	Quartzite, laminated tan and white, weathers grey, medium grained	.7	14.65
13	Dolostone, grey, weathers tan, finely crystalline	.95	13.95
12	Quartzite, white, medium grained	2.5	13
11	Dolostone, light grey, finely crystalline, 15-20 cm beds	4.5	10.5
10	Quartzite, white and cream, medium and very coarse grained, some pebble conglomerate, 0.3-1.6 m beds	6	6
Base of section approximately laterally equivalent to the top of the following section.			

Section 1

(starts at UTM N6086855 E558450, ends at UTM N6087205 E558225)
Measured by Ted Fuller and Robert Mahood

Unit		Thickness in metres Unit	Above base
9	Quartzite, white, medium grained	4.5	46.5
8	Dolostone, pink, pitted reticulate weathering, possible *Archeocyatha*	7.5	42
7	Quartzite, white, medium grained	6.6	34.5
6	Quartzite, white, medium-coarse grained, massive, disseminated pyrite cubes (<1 mm).	5.9	27.9
	Covered	1	22
5	Dolostone, cream, very pale, green and pink, weathers brown, *Archeocyatha*	12	21
4	Dolostone, cream, weathers brown, pelletoidal, abundant *Archeocyatha*	2.5	9
3	Dolostone, cream, weathers brown finely crystalline, bioturbated	3	7.5
2	Dolostone, cream, weathers brown, floating coarse quartz grains, laminated	1.8	4.5
1	Quartzite, white, coarse grained, some calcite cement, planar cross-bedded, paleoflow to the north	2.7	2.7
Base of exposure. Along strike to the south the sequence is underlain by quartzite and lesser dolostone that downsection is interbedded with increasing amounts of slate and siltstone.			

Preliminary biostratigraphy of conodonts from McLeod Lake map area, British Columbia

S.M.L. Pohler, M.J. Orchard, and L.C. Struik
Cordilleran and Pacific Geoscience Division, Vancouver

Pohler, S.M.L., Orchard, M.J., and Struik, L.C., Preliminary biostratigraphy of conodonts from McLeod Lake map area, British Columbia; in Current Research, Part E, Geological Survey of Canada, Paper 89-1E, p. 125-126, 1989.

Abstract

Of 60 conodont samples processed from the west half of McLeod Lake map area 18 were productive yielding conodont faunas ranging from Early Ordovician to Middle Devonian in age. Early Ordovician faunas, recovered from near Parsnip River and Seebach Creek are of Late Tremadoc age (Fauna C of North America). Middle Ordovician faunas also occur near Seebach Creek, Middle to Late Ordovician faunas near Chuchinka and Seebach Creeks. Early Silurian conodonts were found at Chuchinka Creek and Middle Devonian conodonts near Tacheeda Lake and in the northwest of the map area.

Résumé

Parmi les 60 échantillons de conodontes traités, provenant de la moitié ouest de la carte de McLeod Lake, 18 ont été productifs, renfermant des faunes de conodontes dont l'âge varie de l'Ordovicien inférieur au Dévonien moyen. Les faunes de l'Ordovicien inférieur, récupérées près de la rivière Parsnip et du ruisseau Seebach, appartiennent au Trémadocien supérieur (faune C de l'Amérique du Nord). Les faunes de l'Ordovicien moyen se retrouvent aussi près du ruisseau Seebach, les faunes de l'Ordovicien moyen à supérieur se trouvent près des ruisseaux Chuchinka et Seebach. Des conodontes du Silurien inférieur ont été trouvés au ruisseau Chuchinka, et d'autres du Dévonien moyen, près du lac Tacheeda et dans le nord-ouest de la carte.

About 60 of the 200+ conodont samples collected by one of us (LCS) from the west half of the McLeod Lake map area have been processed and picked for conodonts. Of these, 18 were productive and most produced Ordovician conodonts. Silurian and Devonian conodonts were recovered from five samples (Fig. 1). The Ordovician samples produced Early, Middle and Middle to Late Ordovician faunas.

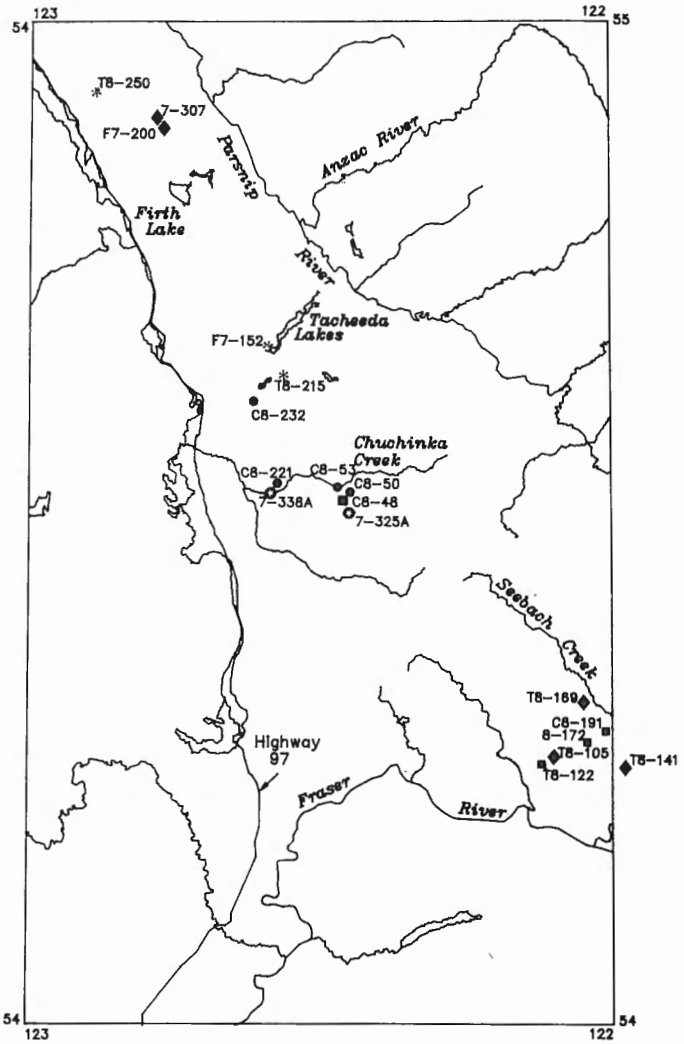

Figure 1. West half of McLeod Lake map area illustrating localities of productive conodont samples. Symbols indicate different age: Diamonds = Early Ordovician, squares = Middle Ordovician, circles = Middle to Late Ordovician, stars = Early Silurian, asterisks = Devonian.

Early Ordovician conodonts retrieved from near Parsnip River comprise a sparse fauna with *Variabiloconus bassleri* (Furnish) as the only determinable index fossil. Samples collected near Seebach Creek had higher yields, giving *V. bassleri, Rossodus manitouensis* Repetski and Ethington, and *Acontiodus propinquus* Furnish. All species are typical of North American Midcontinent Fauna C and indicate an early Canadian (late Tremadoc) age (Ethington and Clark, 1971).

Middle Ordovician conodonts have been found near Chuchinka Creek in a sample containing *Panderodus* sp., *Belodina* sp., *Leptochirognathus* sp., and *Drepanoistodus suberectus* (Branson and Mehl). One fauna from near Seebach Creek yielded *Appalachignathus* sp.

Middle to Late Ordovician localities cluster around Chuchinka Creek. Conodont faunas recovered are dominated by species of *Panderodus* and *Belodina* along with *Drepanoistodus suberectus* (Branson and Mehl). *Plectodina* sp. and *Phragmodus* sp. are rare components of the fauna. The latter occurred in two samples from Seebach Creek together with *Protopanderodus* sp., *Dapsilodus* sp., *Belodina* sp., and *Panderodus* sp.

Determination of more precise stratigraphic levels should be possible following further taxonomic study of the conodont faunas recovered, supplemented by the processing of additional samples currently underway.

The two early Silurian faunules collected near Chuchinka Creek are both dominated by *Panderodus* spp. but differ in their accessory species. One sample contains species of *Pterospathodus pennatus* (Walliser), *Oulodus fluegeli* (Walliser), *Walliserodus, Carniodus,* and a new platform genus; a second, probably older faunule produced similar oulodids and panderodids together with *Pterospathodus celloni* (Walliser) and *Distomodus*.

Three Devonian collections have been recovered. The largest, from Tacheeda Lakes, contains *Polygnathus parawebbi* Chatterton, *Icriodus* sp., and *Belodella* sp.; on the basis of the first species, a mid-Eifelian through mid-Givetian age is indicated (Klapper and Johnson, 1980). A small faunule from the northwest part of the map area contains *Polygnathus* ex gr. *linguiformis* Hinde and *?Neopanderodus*, of Middle Devonian age. A third collection from south of Tacheeda Lakes contains poorly preserved, but less thermally altered, icriodids and lanceolate polygnathids of probable Givetian to Frasnian age.

REFERENCE

Ethington R.L. and Clark, D.L.,
1971: Lower Ordovician conodonts in North America; Geological Society of America, Memoir, 127, p. 63-82.

Klapper, G. and Johnson, J.G.
1980: Endemism and dispersal of Devonian conodonts; Journal of Paleontology, v. 54, p. 400-455.

Permian-Triassic boundary beds in the Cache Creek Group, Marble Range, near Jesmond, British Columbia

J.M. Beyers[1] and M.J. Orchard
Cordilleran and Pacific Geoscience Division, Vancouver

Beyers, J.M. and Orchard, M.J., Permian-Triassic boundary beds in the Cache Creek Group, Marble Range, near Jesmond, British Columbia; in Current Research, Part E, Geological Survey of Canada, Paper 89-1E, p. 127-132, 1989.

Abstract

The Marble Canyon Formation (Cache Creek Group) near Jesmond consists of lower and upper parts from which three conodont faunas are known. In the lower limestone, a Late Permian ***Iranognathus - Hindeodus - Neogondolella*** *association occurs. In the upper limestone, a fauna dominated by* ***Ellisonia****-like elements, probably Early Triassic, gives way to one characterized by representatives of Early Triassic* ***Neospathodus****. The iranognathids are similar to a species from high in the Upper Permian of south China and are here placed in the* ***I. nudus*** *group. Similarly, an element which resembles Chinese and transcaucasian latest Permian neogondolellids is referred to the* ***Neogondolella subcarinata*** *group. A fourth fauna containing "****Hindeodus parvus****", a guide species for the basal Triassic (Griesbachian), is reported from the Porcupine Creek area of the Marble Range, and represents the oldest Triassic known from the Canadian Cordillera. These occurrences show that the Marble Canyon Formation includes strata close to the Permian-Triassic boundary, and perhaps one of the most extensive records for the interval in North America.*

Résumé

La formation de Marble Canyon (groupe de Cache Creek) proche de Jesmond se compose de niveaux inférieurs et supérieurs dans lesquels on a identifié trois faunes de conodontes. Dans le calcaire inférieur, existe l'association d'âge permien supérieur: ***Iranognathus - Hindeodus - Neogondolella****. Dans le calcaire supérieur, une faune dominée par des éléments comparables à* ***Ellisonia****, probablement d'âge triasique inférieur, fait place à une faune caractérisée par des représentants de l'espèce* ***Neospathodus*** *d'âge triasique inférieur. Les Iranognathidés rappellent une espèce située à un niveau élevé du permien supérieur de la Chine méridionale et sont placés ici dans le groupe* ***I. nudus****. Également, un élément qui ressemble au Néogondolellidés chinois et transcaucasiens du sommet du Permien est attribué au groupe* ***Neogondolella subcarinata****. On a signalé une quatrième faune contenant "****Hindeodus parvus****", espèce repère du Trias basal (Griensbachien), dans la région de Porcupine Creek du chaînon Marble; elle correspond au niveau le plus ancien du Trias que l'on ait rencontré dans la Cordillère canadienne. La présence de ces fossiles montre que la formation de Marble Canyon contient des strates proches de la limite entre le Permien et le Trias, et constitue peut-être l'une des colonnes chronostratigraphiques les plus complètes de cet invervalle en Amérique du Nord.*

[1] Department of Geological Sciences, University of British Columbia, 6339 Stores Rd., Vancouver B.C. V6T 2B4

INTRODUCTION

This report is a further contribution to a study of conodont biostratigraphy of Cache Creek Terrane. Limestones of the Cache Creek Group in south-central British Columbia are mostly confined to the Central Belt, one of three lithostratigraphic units into which the group has been divided (Monger and McMillan, 1984). The limestones form the Marble Canyon Formation of Duffell and McTaggart (1952), which underlies the Marble Range and extends from Cornwall Hills in the south to Jesmond in the north (Fig. 1). As part of this study, more than 300 conodont samples were collected from widely separated outcrop areas in Cornwall Hills, Marble Canyon, Pavilion Mountain, Clinton, Porcupine Creek and Jesmond (Fig. 1).

One result of our investigation is the discovery of very young Permian and very old Triassic carbonates in the northern part of the Marble Range, near Jesmond in Bonaparte Lake map area (92P). Figure 2 gives a stratigraphic column based on a section near Jesmond, where the outcrop consists of lower and upper parts separated by a covered interval. Outcrop in the lower beds is typically disrupted and poorly bedded limestone, commonly but unevenly dolomitized; crinoid columnals are the only obvious fauna. Thin sections show a recrystallized calcareous matrix, with echinoderm plates and poorly preserved fusulinids. In the upper part of the section, outcrop is usually well bedded and much more complete (Fig. 3), but the limestones are similarly recrystallized. Laterally discontinuous algal laminations occur at several horizons (Fig. 2). In thin section the fabric shows distinctive pelleting, wavy laminations and bird's eye structures.

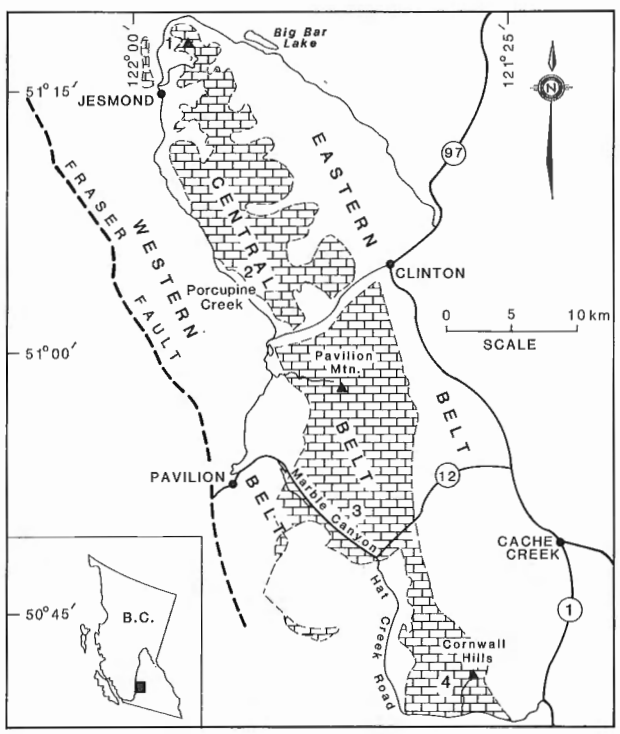

Figure 1. Map of study area showing numbered localities discussed in text.

CONODONTS FROM NORTHERN MARBLE RANGE

We recognize three conodont faunas in the section near Jesmond (Fig. 2; Orchard and Beyers, 1988). The oldest fauna is identified as Permian on the basis of conservative elements of *Hindeodus*, iranognathids here referred to the *I. nudus* group, possible diplognathodids akin to *D. movschovitschi*, and neogondolellids of the *N. subcarinata* group. This association is unknown elsewhere in North America and is of particular interest in terms of both its apparent very young Permian age, and its Tethyan faunal affinity.

The second fauna, of probable Triassic age, consists exclusively of ramiform elements which are here grouped provisionally in the genus *Ellisonia* (Plate 1, fig. 3). These ellisonids are a problematic group and need further study. The Jesmond occurrences in the lower metres of the upper section (Fig. 2) occupy a stratigraphic position that implies an Early Triassic age. Some ellisonids are long ranging but many morphotypes of the Jesmond fauna appear to be of Early Triassic aspect (Sweet, 1970b).

The third, and youngest fauna is dominated by species of *Neospathodus*, including *N. triangularis* and *N. homeri*

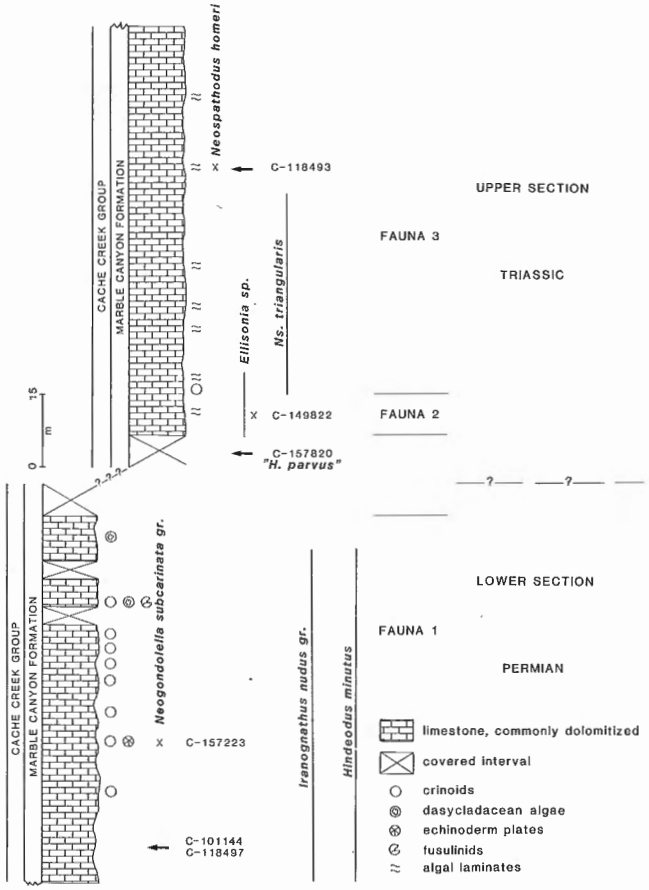

Figure 2. Jesmond. Stratigraphic column based on measured sections separated by covered interval, showing ranges of fauna and sample location. Arrows indicate approximate position of specimens located outside of section.

(Plate 1, fig. 5). These two species have been reported from Spathian strata in Pakistan, Nevada, Greece and Italy; *N. triangularis* is present also in Bulgaria (Ziegler, 1977; Perri and Andraghetti, 1987).

A fourth fauna from the Porcupine Creek area some 20 km south of Jesmond contains "*Hindeodus parvus*" (Plate 1, fig. 8-9), a species that is reported elsewhere from Permian-Triassic boundary beds.

DISCUSSION

Iranognathus

Members of the Late Permian genus *Iranognathus* are known from Iran and China; Wardlaw (1988) also reported "species of *Iranognathus*" from the Salt Range. Two species, *I. unicostatus* and *I. tarazi*, were originally described from Iran by Kozur et al. (1975). Later (Kozur et al., 1978) the stratigraphic position of *I. tarazi* was shown to fall within the *Haydenella - Pseudowellerella* bearing strata near Julfa, and within the lower part of stratum 7 in the Abadeh section. Subsequently, the same species has been reported from the upper Wuchiaping and lower Shangsi formations in south China (Wang et al., 1987).

The absence of all but one ridge on the upper surface of the basal cup of *I. unicostatus*, a feature which sets it apart from *I. tarazi*, may be the expression of a morphological simplification in the genus. This trend may have continued to produce a third recently described Upper Permian species, *Iranognathus nudus*, which is characterized by the absence of ornamentation on the cup. This species occurs in cherty limestones of the Shangsi Formation in the Qiaoting section near the town of Nanjiang, Sichuan Province, south China (Wang et al., 1987), where it is found throughout all but the uppermost few metres of the Shangsi Formation. This unit, which has been referred to the Changxingian, is overlain paraconformably by the Triassic (Wang et al., 1987).

Figure 3. Bedded limestones of the Lower Triassic upper section, Jesmond. Maximum bed thickness 20 cm.

All *Iranognathus* species have pustulose micro-ornamentation on the carina (Wang et al., 1987). Many specimens from Jesmond (e.g. Plate 1, fig. 6-7) show pustules in addition to fused carinal denticles. Other specimens do not clearly show this micro-ornamentation and therefore resemble, at least superficially, supposed diplognathodids such as "*D.*" *movschovitschi* from the lower Dzhulfian of Akhura (Kozur, 1975; Orchard, 1984). The distinction between simple iranognathids and diplognathodids of the Upper Permian needs to be examined closely.

A further problem arises from the uncertainty about carina profile in these Upper Permian scaphate elements. In the Jesmond specimens, the carina rises posteriorly and then descends abruptly (this forms a lateral profile that is similar to that of *Hindeodus julfensis* (Teichert et al., 1973) from the Dzhulfian in Iran). The lateral profile of the holotype of *Iranognathus nudus* was not illustrated by Wang et al. (1987), and therefore we cannot be certain that the Jesmond material is the same. We express this uncertainty by referring the B.C. material to the *I. nudus* group. In addition, we are still unclear about intraspecific variation in denticulation and profile of the carina, and the size and shape of the basal cavity. Pending clarification of this, the Jesmond specimens are regarded as Late Permian rather than as specifically Changxingian.

Neogondolella

Neogondolella subcarinata belongs to a complex of Upper Permian neogondolellids which have in common a broad, lachrimiform platform. Variations in length and height of the carina, absence or presence of a posterior brim, the outline of the keel, and relative platform dimensions, have resulted in the recognition of several subspecies (Clark and Wang, 1988). *Neogondolella s. subcarinata* was originally reported from the Ali Bashi Formation at Kuh-e-Ali Bashi near Julfa (Teichert et al., 1973), from the ravine close to the Dorasham II railway station and the village of Akhura in Soviet transcaucasia, and from the upper part of stratum 7 in the section at Kuh-e-Khambast near Abadeh (Kozur et al., 1978). At all four of these localities the appearance of *N. subcarinata* coincides with that of the ammonoid *Phisonites* (Kozur et al., 1978), recording the beginning of the Dorashamian stage as established by Rostovtsev and Azaryan (1973). In south China *Neogondolella subcarinata* and affiliated taxa are well represented, ranging to the top of the Permian as illustrated by Clark and Wang (1988). At a second Chinese locality, the Selong section in Nyalam County, Xizang (Tibet) Province, the base of the *Ophiceras sakuntala* Zone in the Lower Formation of the Tulong Group coincides with the top of the ranges of a *Neogondolella subcarinata* subspecies and a further related species, *N. deflecta* (Yao and Li, 1987).

N. ex gr. *subcarinata* is an element newly recorded from Jesmond. This species (Plate 1, fig. 1), from 32 m above the base of the lower limestone (Fig. 2), features a high blade with semi-fused denticles, which decrease in height posteriorly, becoming the low, fused carinal nodes of the platform. The cusp is pronounced and inclined posteriorly

and is surrounded by a very narrow brim; the platform, thick and widest at mid-length, possesses distinct adcarinal grooves. At the geniculation point located about one third from the anterior end, the outer margin veers sharply inward, then tapers gradually towards the anterior. In these respects it resembles most closely *Neogondolella s. subcarinata* Sweet and is consequently tentatively referred to the *N. subcarinata* group. It differs from *Neogondolella leveni* (from the lower Dzhulfian of Akhura in Soviet transcaucasia; Kozur, 1975) in the lack of a node at the geniculation point, and from *N. orientalis* (from 1 m below the base of the Ali Bashi Formation at Kuh-e-Ali Bashi in Iran and from the mid-portion of the *Vedioceras* beds at Dorasham II in the USSR; Teichert et al., 1973) by a carina extended to the posterior platform end. The range encompassed by the *leveni-orientalis-subcarinata* lineage is Dzhulfian to Changxingian (Kozur, 1975; Clark and Wang, 1988). In China, a *N. s. subcarinata* assemblage zone is assigned to the lower Changxingian (Zhao et al., 1981). As with *Iranognathus*, we prefer to assign a broad Late Permian age to the Jesmond material pending further study.

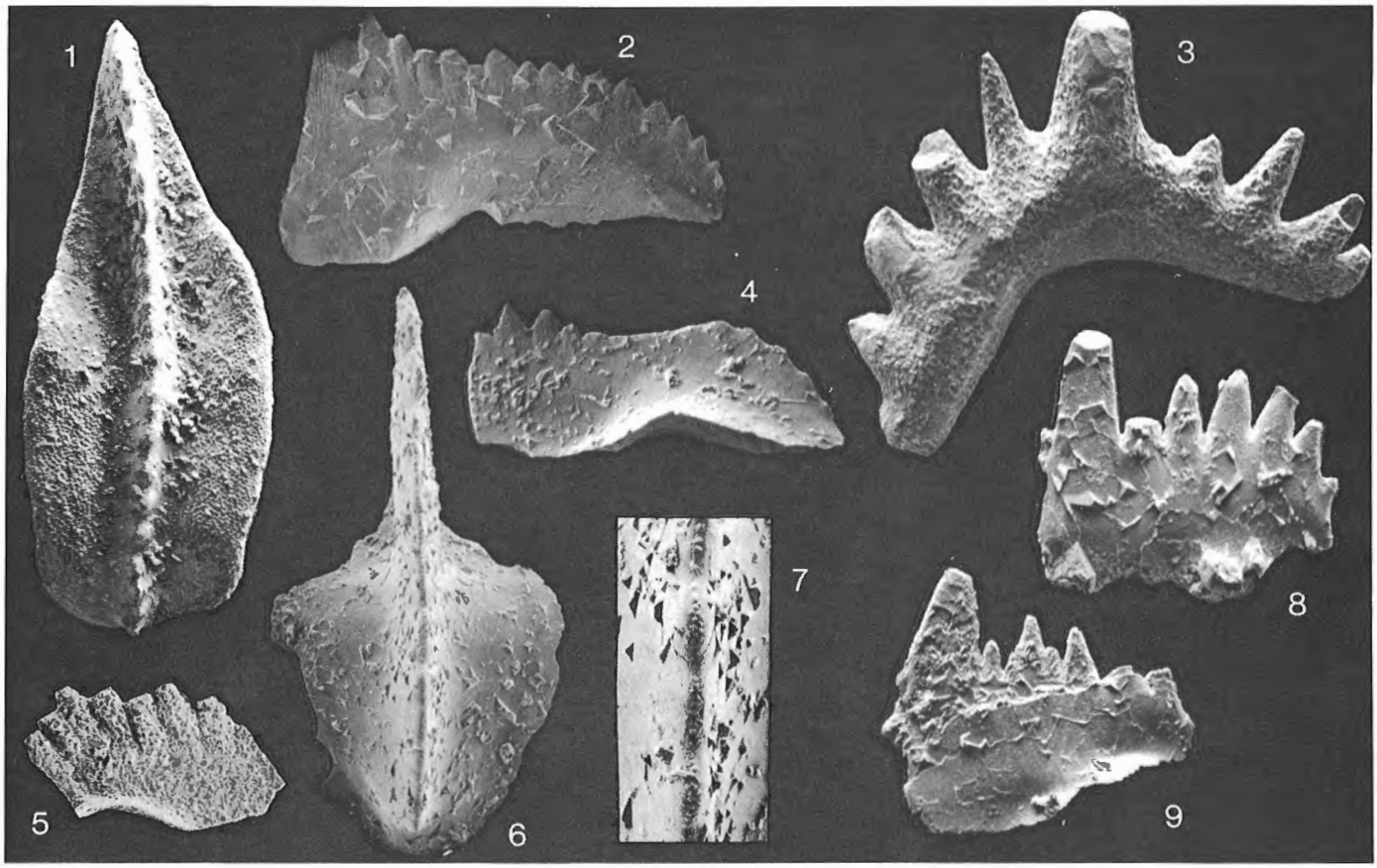

Plate 1.
(Localities are described in Table 1)
Figure 1. *Neogondolella* ex gr. *subcarinata* Sweet. Upper view, GSC 81233 x60, from C-157223.
Figure 2. *Hindeodus minutus* (Ellison). Lateral view, GSC 81234 x100, from C-118497.
Figure 3. *Ellisonia* sp. Inner view, GSC 81235 x50, from C-149822.
Figures 4, 6-7. *Iranognathus* ex gr. *nudus* Wang, Ritter & Clark. 4. Lateral view, GSC 81236 x90. 6. Upper view, GSC 81237 x100. 7. Close up of carina in upper view, GSC 81237 x250. All from C-118497.
Figure 5. *Neospathodus homeri* (Bender). Lateral view, GSC 81238 x100, from C-118493.
Figures 8-9. "*Hindeodus parvus*" Kozur & Pjatakova. 8. Lateral view, GSC 81239 x100. 9. Lateral view, GSC 81240 x100. All from C-157820.

Table 1. Locality registry
GSC Loc. No. C-118493. Sample no. 84MJO-JLO-2, NTS 92P/5W, 51°18′29″, 121°54′30″, Jesmond fire lookout access road, below lookout.
GSC Loc. No. C-118497. Sample no. 84MJO-JLO-7, NTS 92P/5W, 51°17′51.5″, 121°54′35.8″, Jesmond fire lookout access road, 50 m downhill from second switchback, elevation 5550 ft.
GSC Loc. No. C-157223. Sample no. 87OF-B-J-A6-B, NTS 92P/5W, 51°17′53.1″, 121°54′34.5″, Jesmond access road, from bare hill above second switchback.
GSC Loc. No. C-149822. Sample no. 86OF-B-SW3-JAR-70, NTS 92P/5W, 51°17′58.8″, 121°54′31.8″, Jesmond access road, above third switchback.
GSC Loc. No. C-157820. Sample no. 87OF-B-PORCCK-1, NTS 92P/4, 51°04′17.6″, 121°49′19.7″, 2.9 km from beginning of dirt road which leaves Jesmond road 5.5 km N of its junction with Kelly Lake road.

Hindeodus

Conservative species of the conodont *Hindeodus (H. minutus* or *H. typicalis* of different authors) are found throughout the Ali Bashi and lower Elikah formations in northern Iran (Sweet, 1979); they are shown to range from the top of stratum 4 through strata 5, 6 and 7 (Kozur et al., 1978) and into the base of the Triassic stratum 8 (Sweet, 1973) near Abadeh. *Hindeodus typicalis* also spans the Permian-Triassic boundary interval in the southern Alps of Italy, occurring in both the Permian Bellerophon and the Triassic Werfen formations (Assereto et al., 1973; Perri and Andraghetti, 1987); at Guryul Ravine in Kashmir where it ranges from the upper Zewan Formation into the Khunamuh Formation (Sweet, 1970a); and, in its type section in the Salt Range of Pakistan, in the Permian Chhidru and Triassic Mianwali formations (Sweet, 1970b). Sweet (in Teichert and Kummel, 1976) noted that this species dominated what he termed the "younger" of two faunas at Kap Stosch in east Greenland, present in the Permian *Martinia* shale facies and Triassic beds of the Wordie Creek Formation. However, at the Qiaoting section of south China, *H. minutus* is present only in the Permian Shangsi Formation, and has not been reported from overlying Triassic strata (Wang et al., 1987). In the Great Basin of the United States, in southwestern Montana, the species occurs well above the base of the Triassic Dinwoody (Schock et al., 1981).

The younger *Hindeodus parvus*, thought by many to be the adenticulate morphotype of *Isarcicella isarcica* (Ziegler, 1977; Paull, 1982; Perri and Andraghetti, 1987), appears with *Claraia* in the Karabaglyar Formation of Soviet transcaucasia and in stratum 8 at the section near Abadeh according to Kozur et al. (1978) who also reported the presence of forms transitional between *H. minutus* and "*H. parvus*" in *Paratirolites* beds of the Dorasham II section, interpreting this as evidence for the presence of the entire Upper Permian. "*Hindeodus parvus*" appears about 10 m above the base of the black shales of the Khunamuh Formation at Guryul Ravine (see Sweet, 1970a, and 1979, p. 241, for revisions to the earlier data). *Isarcicella isarcica* occurs over a short interval a few metres above the base of the Werfen Formation in Italy (Perri and Andraghetti, 1987), and is present in the lowermost Dinwoody of northwestern Utah (Paull, 1982), serving once more as an Early Triassic indicator. However, at the Selong section in Tibet, Yao and Li (1987) show the range of "*Hindeodus parvus*" as overlapping with the upper parts of those of *Neogondolella subcarinata* and *N. deflecta*, becoming numerous only in the *Ophiceras sakuntala* Zone, after their disappearance.

The fauna from a thin-bedded limestone along Porcupine Creek in the Marble Range (Plate 1, fig. 8-9) lacks elements with accessory lateral denticles. If the adenticulate morphotype does not represent a variety of *Isarcicella isarcica*, it may well be slightly older although Paull (1982) assigns a lowermost, but not basal, Triassic position to all morphotypes of the species.

SUMMARY

Conodonts demonstrate that the Marble Canyon Formation of the Cache Creek Group is Early Triassic as well as Late Permian in age. Triassic strata are now known to occur in many parts of its outcrop area, although some of these could be separated from the Marble Canyon Formation *per se*. The discovery of "*Hindeodus parvus*" documents the first Griesbachian west of the Canadian Rocky Mountains. This compliments Dienerian, Smithian and Spathian strata recorded here, and earlier (Orchard, 1981, 1984; Orchard and Beyers, 1988). On the basis of elements belonging to the *Neogondolella subcarinata* and *Iranognathus nudus* groups, we know that the Jesmond limestones may well represent the youngest Permian in North America. The Permo-Triassic systemic boundary occurs in the Marble Canyon Formation and more complete sections may be sought in the Marble Range.

ACKNOWLEDGMENTS

Some of the costs of Beyers' fieldwork and research were borne by a NSERC Operating Grant No. 581450. We thank R. Manley for assistance in the field. Christine Davis drafted Figures 1 and 2. P. Krauss photographed the specimens on Plate 1.

REFERENCES

Assereto, R., Bosellini, A., Fantini Sestini, N. and W.C. Sweet
1973: The Permian-Triasscic boundary in the southern Alps (Italy); in The Permian and Triassic systems and their mutual boundary, Logan, A. and Hills, L.V. (eds.), Canadian Society of Petroleum Geologists, Memoir 2, p. 176-199.

Clark, D.L. and Wang, C.-y.
1988: Permian neogondolellids from south China: significance for evolution of the *serrata* and *carinata* groups in North America; Journal of Paleontology, v. 62, p. 132-138.

Duffell, S. and McTaggart, K.C.
1952: Ashcroft map-area, British Columbia; Geological Survey of Canada, Memoir 262.

Kozur, H.
1975: Beiträge zur Conodontenfauna des Perm; Geologisch-Paläontologische Mitteilungen Innsbruck, v. 5, no. 4, p. 1-44.

Kozur, H., Mostler, H. and Rahimi-Yazd, A.
1975: Beiträge zur Mikrofauna permotriadischer Schichtfolgen- Teil II: Neue Conodonten aus dem Oberperm und der basalen Trias von Nord- und Zentraliran; Geologisch- Paläontologische Mitteilungen Innsbruck, 5, no. 3, p. 1-23.

Kozur, H., Leven, E. Ya., Lozovskii, V.R. and Pyatakova, M.V.
1978: Conodontal sequence of Permian and Triassic boundary strata of Transcaucasia; Byulleten' Moskovskogo Obshchestva Ispytatelei Prirody (Bulletin of the Moscow Society of Naturalists), Geology Section, v. 53, p. 15-23.

Monger, J.W.H. and McMillan, W.J.
1984: Bedrock geology of Ashcroft (92I) map area; Geological Survey of Canada, Open File 980.

Orchard, M.J.
1981: Triassic conodonts from the Cache Creek Group, Marble Canyon, southern British Columbia; in Current Research, Part A, Geological Survey of Canada, Paper 81-1A, p. 357-359.
1984: Pennsylvanian, Permian and Triassic conodonts from the Cache Creek Group, Cache Creek, Southern British Columbia; in Current Research, Part B, Geological Survey of Canada, Paper 84-1B, p. 197-206.

Orchard, M.J. and Beyers, J.M.
1988: Conodont biostratigraphy of the Cache Creek Group in the Marble Range of south-central British Columbia; in Current Research, Part E, Geological Survey of Canada, Paper 88-1E, p. 159-162.
Paull, R.K.
1982: Conodont biostratigraphy of Lower Triassic rocks, Terrace Mountains, northwestern Utah; Utah Geological Association, Publication 10, p. 235-250.
Perri, M.C. and Andraghetti, M.
1987: Permian-Triassic boundary and Early Triassic conodonts from the southern Alps, Italy; Rivista Italiana di paleontologica e stratigrafia, v. 93, p. 291-328.
Rostovtsev, K.O. and Azaryan, N.R.
1973: The Permian-Triassic boundary in Transcaucasia; in The Permian and Triassic systems and their mutual boundary, Logan, A. and Hills, L.V. (eds.), Canadian Society of Petroleum Geologists, Memoir 2, p. 89-99.
Schock, W.W., Maughan, E.K. and Wardlaw, B.R.
1981: Permian-Triassic boundary in southwestern Montana and western Wyoming; Field Conference and Symposium Guidebook to southwest Montana, Montana Geological Society, p. 59-69.
Sweet, W.C.
1970a: Permian and Triassic conodonts from a section at Guryul Ravine, Vihi District, Kashmir; University of Kansas Paleontological Contributions, Paper 49, p. 1-10, Lawrence/Kansas.
1970b: Uppermost Permian and Lower Triassic conodonts of the Salt Range and Trans-Indus Ranges, West Pakistan; in Stratigraphic boundary problems: Permian and Triassic of West Pakistan, Kummel, B. and Teichart, C. (eds.), University of Kansas Paleontological Contributions, Special Publication 4, p. 207-275, Lawrence/Kansas.
1973: Late Permian and Early Triassic conodont faunas; in The Permian and Triassic systems and their mutual boundary, Logan, A. and Hills, L.V. (eds.), Canadian Society of Petroleum Geologists, Memoir 2, p. 630-646.
1979: Graphic correlation of Permo-Triassic rocks in Kashmir, Pakistan and Iran; Geologica et Palaeontologica, v. 13, p. 239-248.
Teichert, C. and Kummel, B.
1976: Permian-Triassic boundary in the Kap Stosch area, East Greenland, with an appendix by W.C. Sweet; Meddelelser om Groenland, v. 197, 54 pp.
Teichert, C., Kummel, B. and Sweet, W.
1973: Permian-Triassic strata, Kuh-E-Ali Bashi, northwestern Iran; Bulletin of the Museum of Comparative Zoology, v. 145, p. 359-472.
Wang, C.-Y., Ritter, S. M. and Clark, D. L.
1987: The *Sweetognathus* complex in the Permian of China: Implications for evolution and homeomorphy; Journal of Paleontology, v. 61, p. 1047-1057.
Wardlaw, B.R.
1988: Permian conodonts from the Salt Range, Pakistan; Annual Meeting of the Geological Society of America, Abstracts with Programs, v. 20, p. 393-394.
Yao, J. and Li, Z.
1987: Permian-Triassic conodont faunas and the Permian-Triassic boundary at the Selong section in Nyalam County, Xizang, China; Kexue Tongbao, v. 32, p. 1555-1560.
Zhao, J.-K., Sheng, J.-Z., Yao, Z.-Q., Liang, X.-L., Chen C.-Z., Rui, L. and Liao, Z.-T.
1981: The Changhsingian and Permian-Triassic boundary of south China; Bulletin of the Nanjing Institute of Geology and Palaeontology, Academia Sinica, v. 2, no. 2, p. 1-85.
Ziegler, W.
1977: Catalogue of conodonts, v. 3; E. Schweizerbart'sche Verlagsbuchhandlung, Stuttgart, 574 p.

Stratigraphy and structure in east Spatsizi map area, north-central British Columbia

C.A. Evenchick
Cordilleran and Pacific Geoscience Division, Vancouver

Evenchick, C.A., Stratigraphy and structure in east Spatsizi map area, north-central British Columbia; in Current Research, Part E, Geological Survey of Canada, Paper 89-1E, p. 133-138, 1989.

Abstract

In northeastern-most Spatsizi map area the unconformity between the Cretaceous nonmarine Sustut Group and its upper Paleozoic to lower Mesozoic basement of volcanic and granitoid rocks is offset by normal faults. As a result, both Sustut Group and its basement outcrop in the topographically lowest area (the Stikine River valley) although the unconformity is flat-lying or gently warped.

The Bowser Lake Group in southeast Spatsizi map area is divided loosely into four lithological units that vary from monotonous, marine, very fine grained sandstone and siltstone (Ashman Formation) to a unit of coarsening-up cycles of siltstone, sandstone and conglomerate with rare coal. Tight to open folds vary from upright to overturned to the northeast, and accommodated up to 50% shortening, with an unknown amount of shortening along thrust faults. A newly recognized thrust fault has the eastern-most known Spatsizi Group in its hanging wall.

Résumé

Dans la partie la plus au nord-est de la région cartographique de Spatsizi, la discordance entre le groupe non marin de Sustut du Crétacé et son soubassement de roches volcaniques et granitoïdes du Paléozoïque supérieur au Mésozoïque inférieur est décalée par des failles normales. Ainsi, le groupe de Sustut et son soubassement affleurent dans la zone topographiquement la plus basse (la vallée de la rivière Stikine) même si la discordance est plane ou légèrement ondulée.

Le groupe de Bowser Lake dans le sud-est de la région cartographique de Spatsizi est divisé en gros en quatre unités lithologiques qui varient d'un grès et d'une aleurolite à grain très fin, monotones et marins (formation d'Ashman) à une unité cyclique d'aleurolites, de grès et de conglomérats à grain croissant, avec un peu de charbon. Les plis, serrés à ouverts, varient de dressés à déversés vers le nord-est, et donnent lieu à un raccourcissement de 50%, avec un degré de raccourcissement inconnu le long des chevauchements. Un chevauchement repéré récemment loge dans sa lèvre supérieure le groupe de Spatsizi relevé le plus à l'est.

INTRODUCTION

Field mapping in Spatsizi (104 H) was extended outward from the central part of the map area covered in previous summers (Evenchick 1986, 1987, 1988) to include: the northwest Eaglenest Range; south of Tuaton Lake and Stikine River; southwest of the Nass River; and the shoreline of the Stikine River (Fig. 1). The first three areas are underlain by diverse sedimentary facies of the Middle Jurassic to Lower(?) Cretaceous Bowser Lake Group, an intensly deformed unit of marine and nonmarine clastic rocks. The Stikine River is underlain by fluvial sediments of the mid- to Upper Cretaceous Sustut Group and its pre-Middle Jurassic basement of sedimentary, volcanic, and plutonic rocks.

ACKNOWLEDGMENTS

Field work was expedited by the able assistance of Tim Plommer (Capilano College) and Kelly Sexsmith (University of British Columbia); we were accompanied for several weeks by Peter Mustard (Carleton University) and Charlie Roots (GSC). The continued co-operation of the staff of Gulf Canada at the Klappan camp, and of Northern Mountain Helicopters is greatly appreciated. Christine Davis drafted the diagrams.

STIKINE RIVER GEOLOGY

Contacts between the Sustut Group and its basement

The primary purpose in mapping the shoreline geology of the Stikine River was to refine the contact between the Sustut Group and its basement. Reconnaissance mapping by Eisbacher (1974), and Gabrielse and Tipper (1984) showed the river valley in northeast Spatsizi map area to be underlain by the Tango Creek Formation, the lower of two formations in the Sustut Group. The position of the contact is critical to estimates of thickness of the Sustut Group at the undeformed northeast margin of the Sustut Basin. However, exposures of bedrock on the northeast side of the Spatsizi Plateau are rare; there is little to no exposure for the 300 m of elevation between the lowest flat-lying resistant conglomerates of the Sustut Group and the river valley, which is mostly filled by Quaternary sediment. Outcrops along the river vary from one or two metres high, and extending several metres along the shore, to cliffs 10 to 15 m high and tens of metres along the shore. The following discussion focuses on the geology in the northeast part of the map area because it is the only place where the map is significantly changed at 1:250 000 scale from that of Gabrielse and Tipper (1984). The geology of the Stikine River in west Spatsizi map area was compiled by Gabrielse and Tipper (1984) from unpublished 1:50 000 scale maps of P.B. Read (Geotex Consultants).

The distribution of map units is shown in Figure 2. The flat-lying unconformity between the basal Tango Creek Formation and its basement is exposed only at an elevation of 1200 m (4000 ft) in a tributary of Diamond Creek. Southwest-dipping Tango Creek Formation is exposed on the banks of the Stikine River, 7 km east-southeast of the unconformity and 250 m lower in elevation. However, flat-lying Sustut Group on the Spatsizi Plateau precludes simple folding to bring the unconformity down to the river. The contact between Sustut Group and its basement in the Stikine River is interpreted to be a dip-slip fault for two reasons. First, steeply dipping normal faults are consistent with the structural style (Evenchick, 1987, 1988). Second, the fault is roughly along trend of the Griffith Fault, a major northeast-trending dip-slip fault with the same sense of displacement that is required to offset the unconformity northeast of the Stikine River (southeast-side-down).

In Diamond Creek the contact between the Sustut Group and its basement is covered. It seems unlikely that this contact is an unconformity; the 30 m gap in exposure between Tango Creek Formation and volcanic rocks is at a prominent eastern-northeast-trending lineament, interpreted here to be a northwest-side-down fault.

Northwest of Diamond Creek the position of the unconformity is constrained only by flat-lying Sustut Group on the Spatsizi Plateau, and exposures of basement rocks in the Stikine River as far northwest as 7 km southeast of the confluence of the Stikine and Pitman rivers. Tango Creek Formation outcrops in the Stikine River 4 km northwest of the northwestern-most outcrops of basement. The unexposed contact in the river is shown tentatively as a dip-slip fault because the gap in exposure is roughly on trend with the Black Fox Fault, another important northeast-trending dip-slip fault (Evenchick, 1987). Northwest of the fault(?) the unconformity is inferred to be several kilometres northeast of the Stikine River. Tango Creek Formation in the Stikine River above and below the junction with the Pitman River

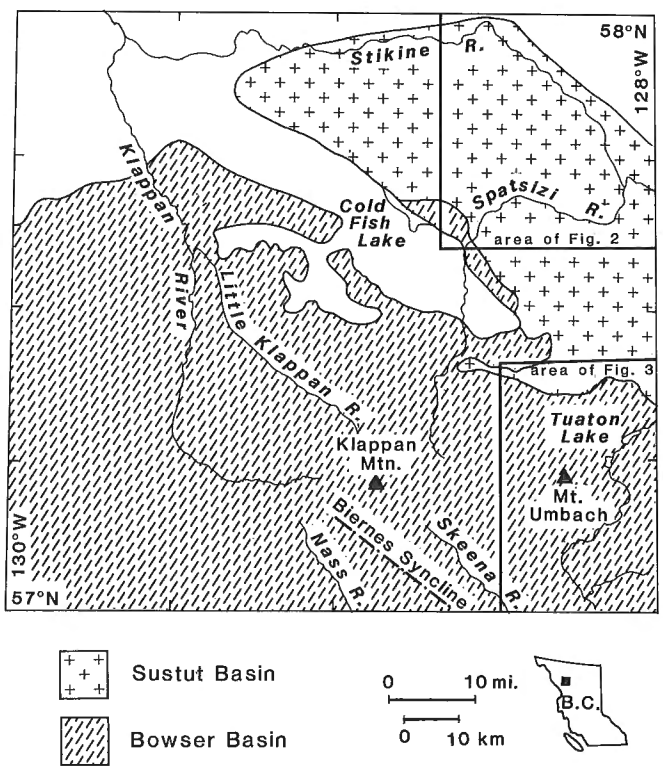

Figure 1. Regional geological and geographic features in Spatsizi map area, with the location of Figures 2 and 3.

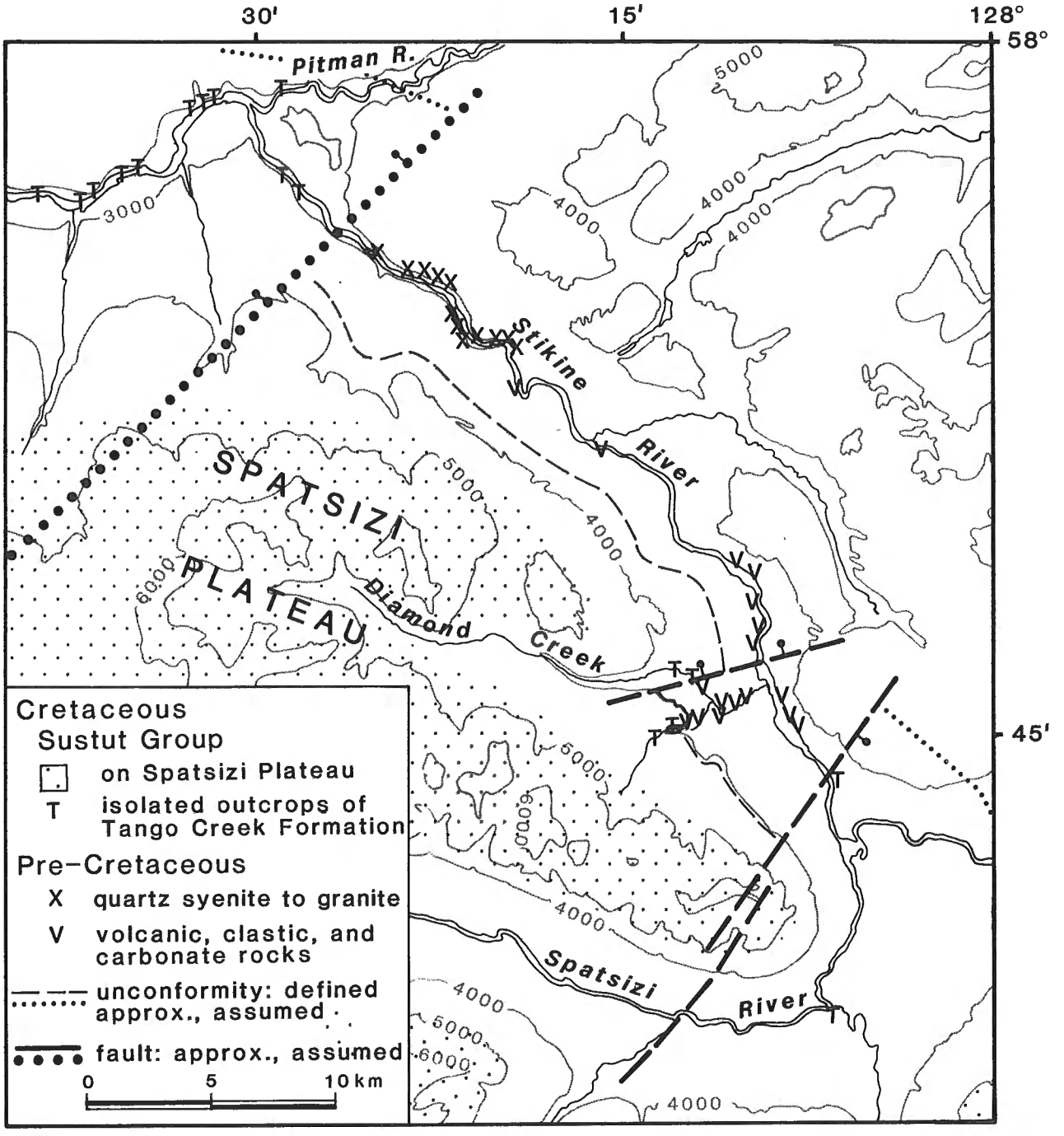

Figure 2. Regional geology of northeast Spatsizi map area showing the contact between the Sustut Group and its basement. Elevations are in feet above sea level.

dips gently to moderately south and south-southeast, and the Tango Creek Formation outcrops as far east as 3 km up the Pitman River (Geological Survey of Canada, 1957).

Basement lithologies

On the northeast side of the Sustut Basin the most common basement rock is feldspar porphyry similar to that in the Middle to Upper Triassic Stuhini Group. In contrast, on the southwest side of the basin, the Sustut Group overlies a structurally complex basement of Cold Fish volcanics, Spatsizi Group, and Bowser Lake Group (Evenchick, 1988). Also present on the northeast side are upper Paleozoic or lower Mesozoic thin-bedded carbonates, clastic rocks and volcanic rocks and an undeformed quartz syenite to granite pluton of unknown age. Similar granitoid lithologies in the Stikine and Hotailuh batholiths are Late Triassic or mid(?)-Jurassic (Anderson, 1984).

The absence of Bowser Lake Group northeast of the Sustut Basin reflects either overlap of the northeast depositional edge of the Bowser Lake Group by the Sustut Group or pre-Sustut deformation and erosion of the Bowser Lake Group, as demonstrated on the southwest side of the Sustut Basin (Evenchick, 1988).

BOWSER LAKE GROUP SOUTH OF TUATON LAKE AND STIKINE RIVER

Sedimentary rocks in the intensely deformed area south, southwest, and west of Tuaton Lake and the Stikine River (Fig. 3) can be grouped loosely into four lithological units based on grain size. Studies of sedimentary environments and regional correlation are underway.

Fine sandstone and siltstone

Medium grey to black-weathering fine sandstone and siltstone underlie areas northwest, west and southeast of Tuaton Lake (Fig. 3). The recessive, commonly very dark-weathering unit varies from laminated to thin-bedded to massive. Where bedding is apparent, black finer grained beds alternate with brown or grey coarser beds of fine clastics. The unit includes less than 10 % medium grained, massive or faintly parallel-laminated sandstone in beds 0.5 to 2 m thick, and massive pebble conglomerate 2 to 10 m thick. Trace fossils are common locally; most are either curved unbranched black traces 1 mm across and less than 10 mm long, or are branching curved burrows up to 6 mm across and several centimetres long.

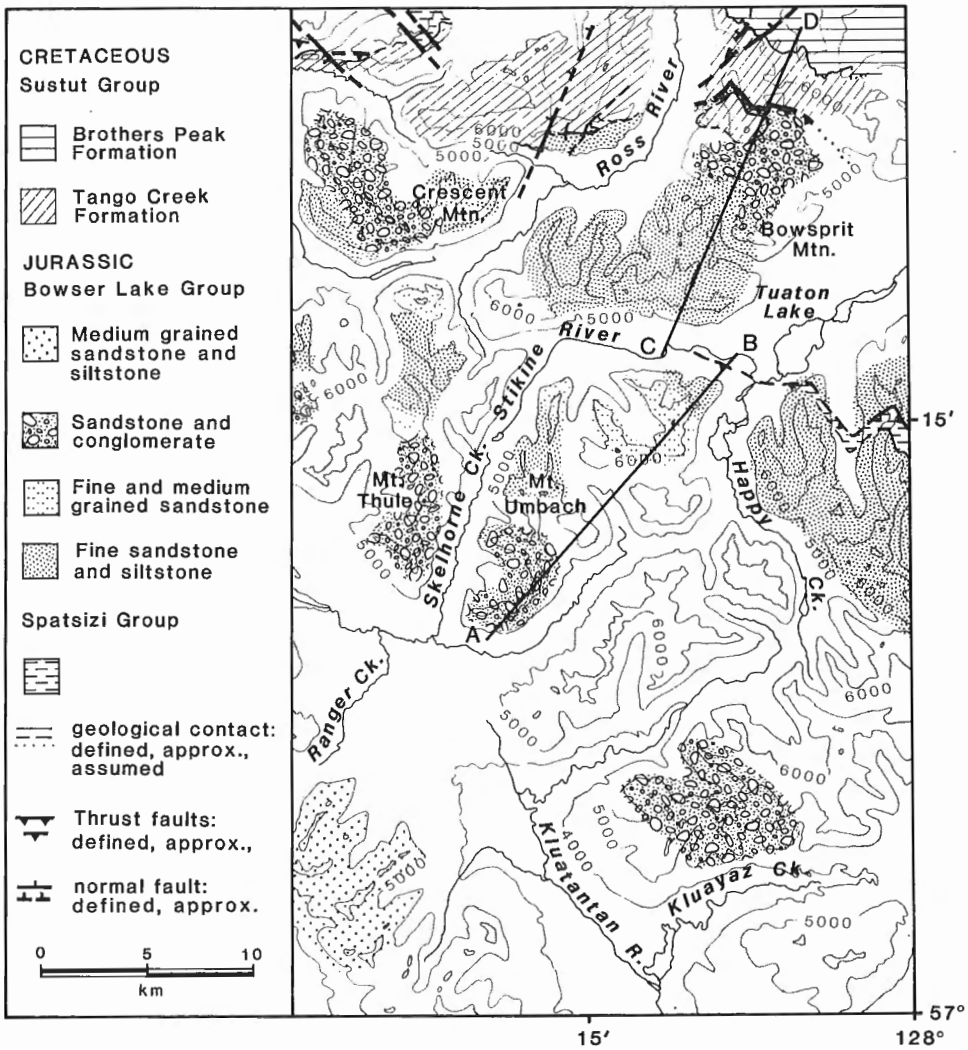

Figure 3. Regional geology of southeast Spatsizi map area, showing the general distribution of lithological units of the Bowser Lake Group, and the location of sections AB and CD in Figure 5. Elevations are in feet above sea level.

The thickness of the unit is poorly known because of the difficulty in recognizing repetition of stratigraphy in the monotonous sequence. Southeast of Tuaton Lake it is thickened structurally by a thrust fault that has Spatsizi Group in its hanging wall. The unit is at least 300 m thick in the footwall of the thrust fault, and similar rocks stratigraphically overlying the Spatsizi Group in the hanging wall are at least 300 m thick. The unit is similar to the Ashman Formation in its fine grain size, weathering characteristics, and stratigraphic position relative to the Spatsizi Group, although here it lacks the abundant chert pebble conglomerate lenses so common near the base of the Ashman Formation in the Eaglenest Range to the northwest.

At Bowsprit Mountain the fine clastic unit grades up into a coarser clastic unit that gradually includes increasing amounts of medium grained sandstone and pebble conglomerate. Southwest of Tuaton Lake it appears to be overlain by a unit of dominantly fine-to medium-grained sandstone. A northwest-trending belt of the same general lithologies on the northern ridges of Mt. Umbach and Thule are of unknown stratigraphic position relative to the fine clastics to the north.

Fine-and medium-grained sandstone

A resistant unit of dominantly fine-and medium-grained sandstone, with minor very fine sandstone or siltstone, coarse sandstone, and pebble conglomerate, outcrops in two northwest trending belts (Fig. 3). Bedding varies from thin-bedded to medium-and thick-bedded, has vague parallel lamination, or is massive. Pelecypods, belemnites and trace fossils similar to those in the fine clastic unit are common locally. The northern of the two belts overlies the finer clastic unit southwest of Tuaton Lake but has structurally com-

Figure 4. View northwest to folded conglomerate (most resistant members) and sandstone south of Mt. Umbach.

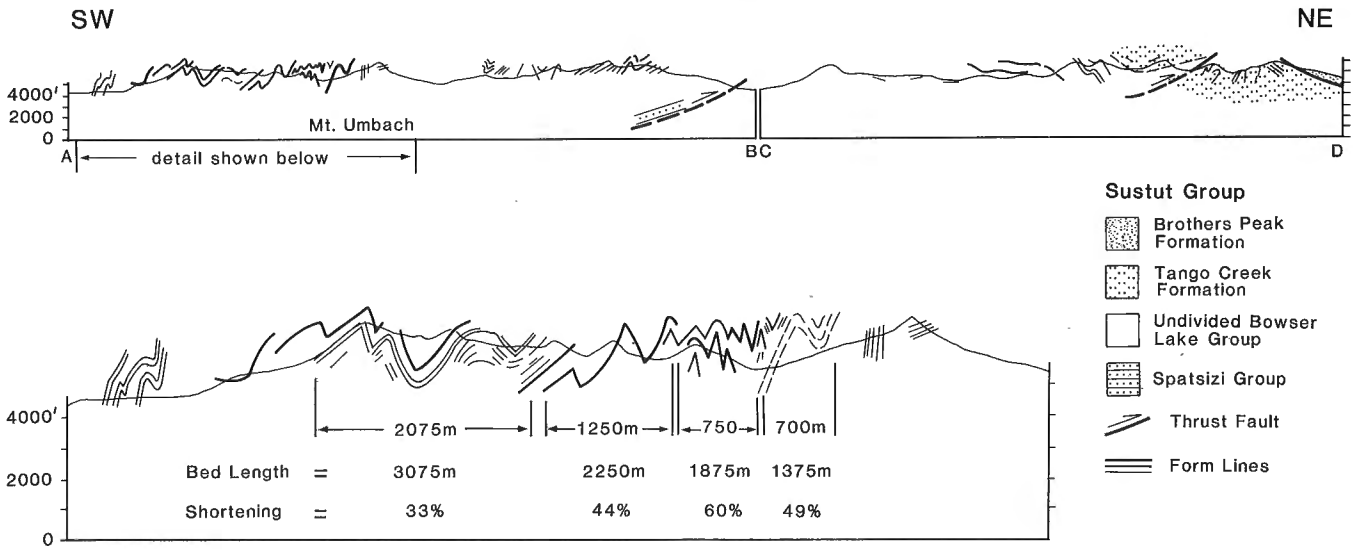

Figure 5. Cross-sections of southeast Spatsizi map area; see Figure 3 for location of sections AB and CD.

plex relationships with the belt of fine clastics to the southwest. The southern sandstone belt appears to overlie the unit of fine, recessive dark clastics and underlie a coarser clastic unit.

Sandstone and conglomerate

A resistant-weathering unit of pebble conglomerate, sandstone, siltstone, and minor coal underlies the rugged, well exposed area between Mt. Thule and Kluayaz Creek (Fig. 3 and 4). Siltstone, sandstone and conglomerate occur in coarsening-up cycles. Conglomerate members are 5-30 m thick, are commonly clast-supported, with clasts less than 6 cm across. Pelecypods and belemnites occur in or near medium grained sandstones and trace fossils are present in finer sandstone. Plant debris is more abundant than in units described above, which have only rare fragments of plants. Segments of silicified logs are rare, but imprints of large wood fragments on the bases of coarse sandstone and conglomerate beds are common.

Medium grained sandstone and siltstone

In the southwest corner of the region (Fig. 3) is a unit of medium grained sandstone and black and brown siltstone and mudstone. Sandstone occurs as laterally discontinuous members 1-3 m thick, alternating with fine dark siltstone or mudstone in members 1-10 m thick. Tabular crossbeds are common. Delicate fossil plants are abundant; fossilized trees are common locally; and marine fossils are absent. The unit, at least 500 m thick, is assumed to overlie the marine sediments to the northeast, and is interpreted as fluvial.

STRUCTURAL STYLE

Figure 5 depicts the structural style across the area. The general relationships between Bowser Lake and Sustut groups are shown in section CD. The internal details of the structure are poorly known in the fine clastic unit, although many thrust faults, overturned folds, and open upright folds are apparent. Details of the structure farther south are well displayed in units with local markers of resistant conglomerate or sandstone that are continuously exposed for several kilometres across anticlines and synclines (section AB). Although there are several areas where the stratigraphic relationships of beds on either side of a fault or area of poor exposure are unknown, the amount of shortening represented by folds can be estimated by measuring the bed length of individual markers around folds and comparing the bed length with the present horizontal distance between the ends of the beds (Fig. 5). From the comparison of bed lengths, individual members are shortened 33 %, 44 %, 60 %, and 49 %. The average shortening of 44 % is clearly a minimum because there is an unknown amount of shortening accommodated on thrust faults.

SUMMARY

Northeast Spatsizi map area is underlain by the Cretaceous Sustut Group and its basement of upper Paleozoic and lower Mesozoic rocks. The unconformable contact between the Sustut Group and its basement is offset by steeply dipping normal faults that may be the extensions of large-scale, long-lived, dip-slip faults to the southwest. Southeast Spatsizi map area is underlain by intensely shortened marine and nonmarine clastic rocks that can be loosely grouped into four lithological units that vary from monotonous, marine, very fine grained sandstone and siltstone to a unit of coarsening-up cycles of siltstone, sandstone and conglomerate with rare coal. The monotonous fine grained clastic unit correlates with the Ashman Formation, and stratigraphically overlies Spatsizi Group in the hanging wall of a newly recognized thrust fault. Open to tight northeast-verging folds in southeast Spatsizi map area accommodated an average of 44 % shortening. The large amount of shortening compares with shortening in regions to the north and northwest where folds and thrust faults accommodated at least 50 % shortening (Evenchick, 1987,1988).

REFERENCES

Anderson, R.G.
1984: Late Triassic and Jurassic magmatism along the Stikine Arch and the geology of the Stikine batholith, north-central British Columbia; in Current Research, Part A, Geological Survey of Canada, Paper 84-1A, p. 67-73.

Eisbacher, G.H.
1974: Sedimentary and tectonic evolution of the Sustut and Sifton basins, north-central British Columbia; Geological Survey of Canada, Paper 73-31, 57 p.

Evenchick, C.A.
1986: Structural style of the northeast margin of the Bowser Basin, Spatsizi map area, north-central British Columbia; in Current Research, Part B, Geological Survey of Canada, Paper 87-1B, p. 733-739.
1987: Stratigraphy and structure of the northeast margin of the Bowser Basin, Spatsizi map area, north-central British Columbia; in Current Research, Part A, Geological Survey of Canada, Paper 87-1A, p. 719-726.
1988: Structural style and stratigraphy in northeast Bowser and Sustut basins, north-central British Columbia; in Current Research, Part E, Geological Survey of Canada, Paper 88-1E, p. 91-95.

Gabrielse, H. and Tipper, H.W.
1984: Bedrock geology of Spatsizi map area (104H); Geological Survey of Canada, Open File 1005.

Geological Survey of Canada
1957: Stikine River area, British Columbia; Geological Survey of Canada, Map 9-1957.

The Nisling Schist in eastern Dezadeash map area, Yukon

Philippe Erdmer[1]
Cordilleran and Pacific Geoscience Division, Vancouver

Erdmer, P., The Nisling Schist in eastern Dezadeash map area, Yukon; in Current Research, Part E, Geological Survey of Canada, Paper 89-1E, p. 139-144, 1989.

Abstract

From reconnaissance study of a 150 km² area, the Nisling assemblage includes quartz-biotite schist with minor amphibolite, marble, quartzite, and skarn. High-temperature regional metamorphism that developed assemblages up to sillimanite-K-feldspar (no muscovite) in pelite predated the intrusion of Eocene granite and of Triassic(?) granodiorite. All penetrative fabrics in the schist terrane are older than the Eocene intrusion. Further study will help establish whether the terrane is an exotic block of continental crust or a slice of North American basement which may be highly allochthonous.

Résumé

Selon une étude de reconnaissance d'une superficie de 150 km², l'assemblage de Nisling renferme du schiste à quartz-biotite avec un peu d'amphibolite, de marbre, de quartzite et de skarn. Le métamorphisme régional à haute température qui a produit des assemblages allant jusqu'à du sillimanite-K-feldspath (pas de muscovite) dans la pélite a précédé l'intrusion de granite de l'Éocène et de granodiorite du Trias (?). Toutes les structures pénétrantes dans le terrain schisteux sont antérieures à l'intrusion de l'Éocène. Une étude plus poussée permettrait d'établir si le terrain est un bloc exotique de la croûte continentale ou un lambeau du socle nord-américain qui serait fortement allochtone.

[1] Department of Geology, University of Alberta, Edmonton, Alberta, T6G 2E3

INTRODUCTION

The Nisling assemblage of the northwestern Cordillera (Wheeler and McFeely, 1987) is a poorly-known metamorphosed passive continental margin succession. It is exposed as a discontinuous schist terrane along several hundred kilometres of the eastern margin of the Coast Plutonic Complex, west of the dominantly oceanic rocks of the Intermontane Belt.

In northwestern British Columbia, field relations suggest that the Nisling assemblage may represent the western basement of Stikinia (Monger and Berg, 1984). In southwestern Yukon, the rocks were originally included in the undivided metamorphic complex of the Yukon Group (e.g. Kindle, 1952; Wheeler, 1961). Although the premetamorphic stratigraphy remains obscure, reconnaissance work (Tempelman-Kluit, 1974; Christie, 1957; Werner, 1977, 1978) has provided evidence of protoliths of possible Paleozoic and Proterozoic age that underwent pre-Early Triassic regional metamorphism and deformation. This orogenic imprint is not recorded in neighbouring terranes and is older than the proposed time of accretion of this part of the Cordillera to North America.

The Nisling terrane has been interpreted as a rifted ribbon of North American crust that was returned during early Mesozoic collision (Tempelman-Kluit, 1979). Alternatively, it may be either uplifted cratonic (autochthonous North American) basement, or part of an exotic continent of unknown paleogeographic position. An understanding of the internal structure, age, and tectonic significance of the terrane is required to delineate the western extent of the craton beneath the northern Cordillera, and will contribute to a more conclusive interpretation of surrounding parts of the orogen as being either thick- or thin-skinned.

Study of the Nisling terrane has begun in northern British Columbia (Mihalynuk and Rouse, 1988; L. Currie, pers. comm., 1988). To evaluate the potential and scope of detailed studies in the Yukon, the Nisling terrane near Kusawa Lake in Dezadeash map area (Fig. 1) was examined in July 1988. Specific objectives were to search for possible orthogneiss slices in the cores of structural culminations within the schist, to investigate the conditions of pre-Mesozoic deformation and metamorphism, and to establish the extent of fabric overprinting by intrusions of the Coast Plutonic Complex.

ROCK TYPES

Psammitic to pelitic medium grained quartz-rich biotite schist (Fig. 2) underlies about 80 % of the area mapped. It is light grey with a salt-and-pepper texture, and weathers rusty brown. Fine grained muscovite is common; garnet and/or sillimanite in small amounts occur in many outcrops of the most pelitic layers. Local fine grained quartz-rich layers have an appearance similar to low-grade, grey, nearly translucent siltstone. Sulphide-rich layers a few millimetres thick are common near the quartz-rich layers. Coarse grained muscovite schist forms thin (10 — 50 cm) layers within the biotite schist. The biotite schist commonly includes a migmatite phase in layers a few centimetres thick, subparallel to compositional layering.

White, medium- to coarse-grained, saccharoidal-weathering marble forming resistant ribs on ridge tops occurs in layers commonly several tens of metres thick, and up to 100 m thick. The rock is more than 95 % calcite, with minor phlogopite, diopside, and clinozoisite. It is similar to distinctive marble reported elsewhere in the terrane (e.g. Tempelman-Kluit, 1974). Wispy 5 to 150 cm thick layers of actinolite-diopside marble and garnet-diopside-vesuvianite calc-silicate occur within the biotite schist. These appear compositionally distinct from the thick, pure marble units, and may result in part from young contact metamorphism, as inferred by Kindle (1952). However, the distribution of sizeable granitic bodies does not appear related to the occurrence of marble and calc-silicate.

Well-foliated plagioclase-hornblende-biotite amphibolite underlies about 10 % of the terrane. It grades locally into pale green actinolite-biotite schist and into well-banded garnet-hornblende-diopside-biotite paragneiss.

Nearly translucent quartzite forms layers up to several tens of metres thick within the biotite schist. It is commonly coloured grey by minute hematite or graphite inclusions, and weathers light orange to brown.

Contacts between rock types are parallel to the main foliation. Hybrid or gradational rocks with compositions between end-members are common and locally form layers several tens of metres thick. All units are cut by at least two generations of granitic pegmatite and/or aplite veins in most outcrops.

Medium- to coarse-grained, foliated hornblende-biotite granodiorite to tonalite forms sills and layers up to several hundred metres thick within the schists. The granodiorite cuts across compositional layering at low angles, and is cut by massive biotite granodiorite to granite dykes, sills and plutons. Previous regional mapping (Kindle, 1952) interpreted foliated granodiorite to be a marginal phase of the Coast Intrusions. However, although the massive granitic rocks are typical of younger units of the Coast Plutonic suite, the foliated granodiorite is distinctly different. It cannot be traced into a massive phase or into K-feldspar-rich rock (granite). There is local structural concordance of foliation in the granodiorite with that in the schist, and not with contacts of massive intrusions. Massive granitic rocks cut the schist in many places; no deflection of existing foliation is observed and no contact fabric is developed. For these reasons, it is probable that at least some foliated hornblende granodiorite of the Coast Plutonic Complex in Dezadeash and Whitehorse map areas is a separate unit, lithologically and structurally identical to the Aishihik batholith to the north (*see* Tempelman-Kluit, 1974) which has yielded U-Pb zircon ages near 220 Ma (S. Johnston, pers. comm., 1988). Triassic or older intrusives are also present to the south in Atlin map area: Werner (1978) and Bultman (1979) reported foliated Triassic granodiorites cutting the schist terrane.

Massive, medium grained, homogeneous, equigranular, grey, biotite and/or hornblende granodiorite to quartz monzonite or granite that cuts all the above rocks constitutes part of the Coast Plutonic Complex. Minor clinopyroxene is characteristic. Biotite and hornblende form aggregates of

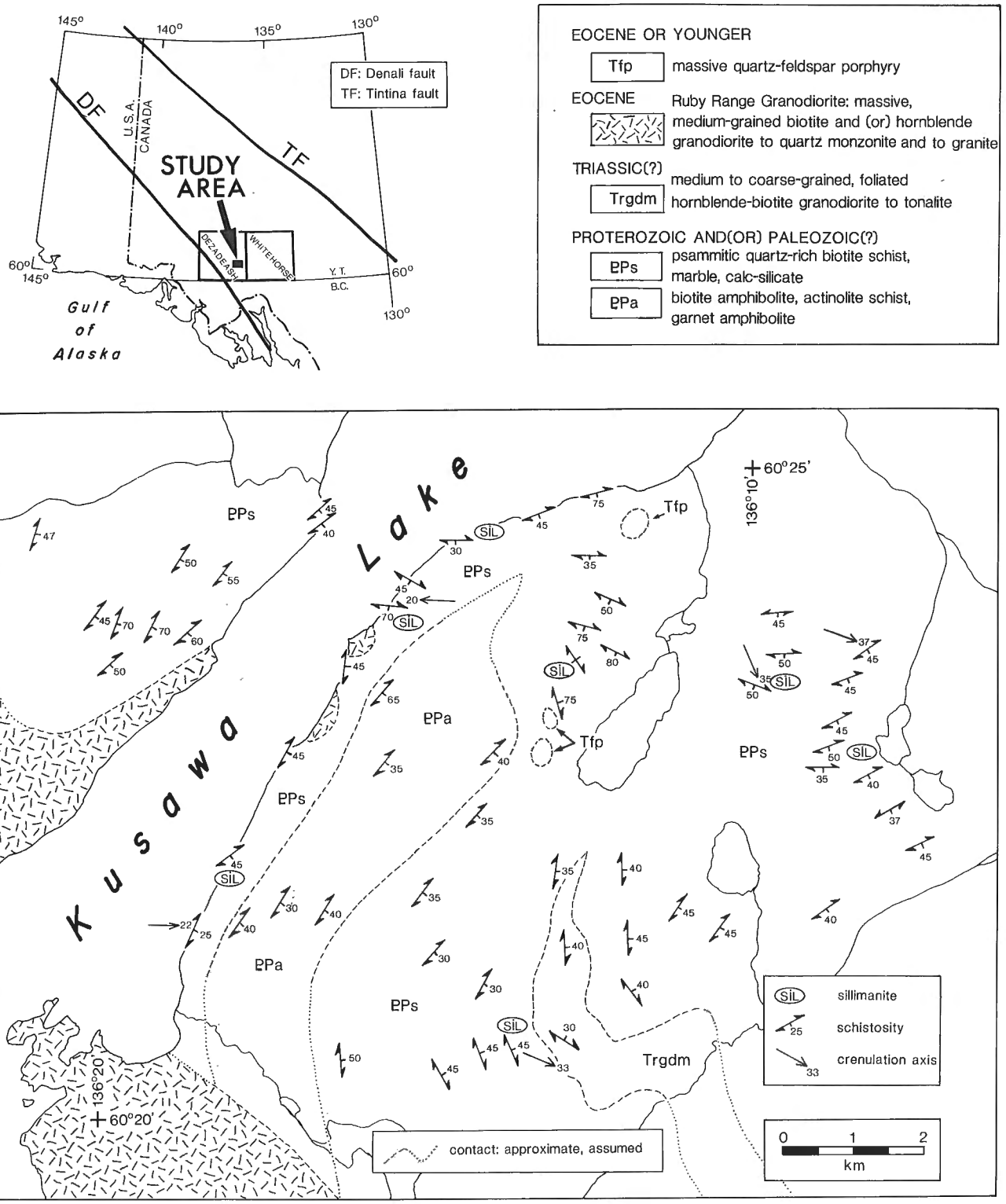

Figure 1. Geology of part of the Nisling terrane east of Kusawa Lake.

small, nearly equant crystals. The felsic minerals commonly form an interlocking fine grained mosaic, suggesting a relatively rapid cooling. Dykes and sills cutting the older rocks are common, as are sharp-edged inclusions of schist and foliated granodiorite in outcrops of granite breccia. No penetrative fabric attributable to intrusion was noted in either host or intrusive. A sample of the granodiorite from the study area gave a K-Ar biotite date of 56.4 $\pm$ 1.8 Ma, and on this basis the unit has been included in the Ruby Range Granodiorite (Farrar et al., 1988). Alternatively, part of the unit may be older, i.e. Cretaceous, and could include or be reset by the Ruby Range Granodiorite or the Nisling Range Alaskite (about 52 to 57 Ma old, Tempelman-Kluit and Wanless, 1975; Farrar et al., 1988).

Fresh, massive, fine grained quartz-feldspar porphyry occurs in several discrete plugs up to 200 m across. The light grey to buff rock is resistant and forms distinctive blocky outcrops on ridges. It fractures readily into flinty, angular fragments and has only a thin (2 to 3 mm) weathered rind. It is correlated with similar subvolcanic rocks of Tertiary age in surrounding areas (e.g. unit Tfp of Tempelman-Kluit, 1974).

STRUCTURE

Fabric elements in the schistose rocks other than the foliated granodiorite are (1) compositional layering and colour banding in hand specimen or outcrop, assumed to be transposed bedding, (2) a strong schistosity, defined by micas in schist; hornblende in amphibolite; and calcite and/or amphibole in marble and calc-silicate, (3) a weaker crenulation schistosity that overprints the main schistosity locally in mica-rich layers, (4) a strong quartz rodding and/or streaking in quartz-rich layers, parallel to hinges of flattened (isoclinal) folds of the main schistosity, and (5) a coarse crenulation lineation resulting from small open folds of the main schistosity and parallel to the trace of the weaker crenulation schistosity (which is axial-planar to the crenulations).

Compositional layering and the main schistosity are everywhere parallel and dip generally southeast except where reoriented by southeast-plunging folds. Mesoscopic folds are relatively common where lithological layering is strong but difficult to discern elsewhere. Folds are generally round, isoclinal structures (Fig. 3). Axes are parallel to regional fold axes and are mainly southeast-plunging.

A comparison of lineation attitudes near Kusawa Lake with structures along strike to the northwest and southeast shows that structural patterns are uniform over large areas. Together with the fact that massive plutons clearly cut fabrics in the schist, this suggests that no regional penetrative fabric was imposed by the youngest Coast intrusions. The main fabrics are thus pre-Eocene; if the foliated granodiorite unit is Triassic, at least one post-Triassic, pre-Eocene penetrative fabric is developed. However, as the foliated granodiorite cuts schistosity and crenulations in its host, the bulk of fabric in the schist is probably older than Late Triassic.

METAMORPHISM

Much of the schist terrane was metamorphosed to amphibolite facies, as shown by the wide distribution of sillimanite in muscovite-bearing rocks southeast of Kusawa Lake (Fig. 1) and the local occurrence of sillimanite and K-feldspar (muscovite absent or reacting out). Diagnostic maximum-phase assemblages are: garnet-muscovite-sillimanite-biotite-plagioclase-quartz and sillimanite-biotite-K-feldspar-plagioclase-quartz in pelite, diopside-actinolite-phlogopite-grossular-calcite-quartz in calc-silicate or marble, and garnet-hornblende-plagioclase-quartz-biotite in amphibolite.

Mineral assemblages are either pre- or syn-kinematic; synkinematic sillimanite fibres define the coarse (late) crenulation locally. A weak retrogression in the form of sericitization of feldspars and moderate recrystallization of the margins of some porphyroblasts has affected all the foliated rocks including the foliated granodiorite. This retrogression is thought to reflect a thermal overprint by the youngest phases of the Coast Plutonic Complex.

Figure 2. Quartz-biotite semi-pelitic schist from the east shore of Kusawa Lake.

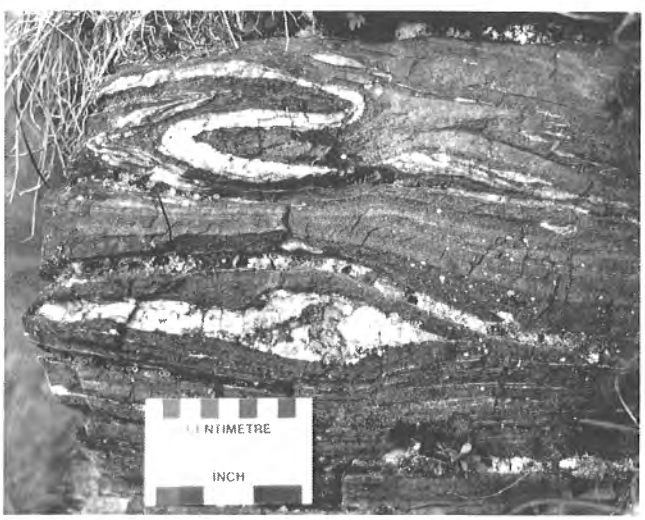

Figure 3. Folded quartz and aplite veins in mica-amphibolite.

PROTOLITH AND AGE OF REGIONAL ASSEMBLAGES

A significant number of isotopic age determinations are now available from parts of the Coast Belt of southwesternmost Yukon and northwesternmost British Columbia. Most are from granitoid rocks but a few are from metamorphic rocks. Although most are K-Ar determinations, there is enough spread in the numbers to suggest a protracted emplacement history for the Coast Plutonic Complex and its satellitic intrusions.

Plutons giving Triassic, Jurassic(?), mid-Cretaceous, Late Cretaceous, and Eocene dates occur. Several bodies of Triassic age are mentioned above; other plutons, including those of the Klotassin suite, are possible candidates (Tempelman-Kluit and Wanless, 1975; Morrison et al., 1979). Plutons of possible Jurassic age are suggested by some isotopic results (Tempelman-Kluit and Wanless, 1975; Bultman, 1979). Granitoid intrusions of mid-Cretaceous age include the Nisling Range granodiorite suite and the Coffee Creek quartz monzonite (Tempelman-Kluit and Wanless, 1975), and others (Morrison et al., 1979; Bultman, 1979; Farrar et al., 1988). Bodies of Late Cretaceous age are referred to by Morrison et al. (1979), Bultman (1979), and Barker et al. (1986). Isotopic results that may record Late Cretaceous plutonism are reported from the Ruby Range batholith by Christopher et al. (1972), Tempelman-Kluit and Wanless (1975), Farrar et al. (1988), and Dodds and Campbell (1988). Bodies of Eocene age are widespread in both Yukon and British Columbia (Wheeler and McFeely, 1987). The Coast Plutonic Complex is thus the locus of repeated intrusive activity, a significant part of which is older than the collision of Terrane II with North America proposed by Monger et al. (1982).

The protolith of the Nisling assemblage near Kusawa Lake is interpreted to be largely pre-Triassic and to include rocks of Paleozoic and Proterozoic ages. However, Eisbacher (1976) suggested that the Kluane Schist, exposed immediately north of the map area, may be the metamorphic equivalent of the Late Jurassic to Early Cretaceous Dezadeash Group. From K-Ar results, its metamorphism may be early Tertiary in age (Stevens et al., 1982; Farrar et al., 1988). The relation of the Kluane Schist to the Nisling Schist is unknown. Correlation of parts of these assemblages is possible but both assemblages are poorly studied. Another assemblage of young metamorphic rocks is Late Cretaceous or older orthogneiss identified southwest of the study area, near Skagway (Barker et al., 1986).

SUMMARY AND CONCLUSIONS

1. Rock types, structures, and relations within the Nisling assemblage near Kusawa Lake are similar to those along strike to the northwest and southeast. This suggests that the schist terrane may be distinct from both the Coast and Intermontane belts along several hundred kilometres.
2. Parts of the area are underlain by foliated hornblende granodiorite of possible Triassic age that intruded the schist terrane and is cut by massive Eocene plutons.
3. The peak of prograde metamorphism occurred during a high-temperature (sillimanite-K-feldspar-migmatite) regional, synkinematic event.
4. The peak of metamorphism predated the intrusion of the foliated granodiorite and of massive granitic rocks. Both the schist and the foliated granodiorite were retrograded during a static thermal event inferred to be Eocene or older.
5. No basement to the schist assemblage has been identified in the study area. Gneissic basement may be preserved as screens in younger plutons. Augen gneiss reported in granite to the north has not yet been investigated.
6. Some plutons of the Coast Plutonic Complex were emplaced at relatively shallow levels. They cut high-grade penetrative fabrics, and do not appear to have disturbed regional (older) structural trends.
7. As exposure is excellent, abundant data can be collected through detailed mapping. Studies of the Nisling assemblage in southern Yukon would help resolve the question of this terrane's possible correlation with North American shelf and cratonic rocks to the east. These studies are suitable for thesis research and would complement work in progress in northern British Columbia.

ACKNOWLEDGMENTS

Support from EMR and DIAND in the form of funding and logistical assistance made the fieldwork possible. Careful and useful reviews of this report by C.J. Dodds and G.J. Woodsworth are gratefully acknowledged.

REFERENCES

Barker, F., Arth, J.G., and Stern, T.W.
1986: Evolution of the Coast batholith along the Skagway traverse, Alaska and British Columbia; American Mineralogist, v. 71, p. 632-643.

Bultman, T.R.
1979: Geology and tectonic history of the Whitehorse Trough west of Atlin, British Columbia; unpublished Ph.D. thesis, Yale University, New Haven, CT., 284 p.

Christie, R.L.
1957: Geology of Bennett map-area, British Columbia; Geological Survey of Canada, Map 19-1957.

Christopher, P.A., White, W.H., and Harakal, J.E.
1972: K-Ar dating of the "Cork" (Burwash Creek) Cu-Mo Prospect, Burwash Landing area, Yukon Territory; Canadian Journal of Earth Sciences, v. 9, p. 918-921.

Dodds, C.J. and Campbell, R.B.
1988: Potassium-Argon ages of mainly intrusive rocks in the Saint Elias Mountains, Yukon and British Columbia; Geological Survey of Canada, Paper 87-16, 43 p.

Eisbacher, G.H.
1976: Sedimentology of the Dezadeash flysch and its implications for strike-slip faulting along the Denali Fault, Yukon Territory and Alaska; Canadian Journal of Earth Sciences, v. 13, p. 1495-1513.

Farrar, E., Clark, A.H., Archibald, D.A., and Way, D.C.
1988: Potassium-argon age of granitoid plutonic rocks, southwest Yukon Territory, Canada; Isochron/West, no. 51, p. 19-23.

Kindle, E.D.
1952: Dezadeash map-area, Yukon Territory; Geological Survey of Canada, Memoir 268.

Mihalynuk, M. and Rouse, J.
1988: Geology of the Tutshi Lake area, NTS 104M/15; British Columbia Geological Survey Branch, Open File Map 1988-5.

Monger, J.W.H., Price R.A., and Tempelman-Kluit, D.J.
1982: Tectonic accretion and the origin of the two major metamorphic and plutonic welts in the Canadian Cordillera; Geology, v. 10, p. 70-75.

Monger, J.W.H. and Berg, H.C.
1984: Lithotectonic terrane map of western Canada and southeastern Alaska; Part B *in* Lithotectonic Terrane Maps of the North American Cordillera, edited by N.J. Silberling and D.L. Jones, United States Geological Survey Open File Report 84-523.

Morrison, G.W., Godwin, C.I., and Armstrong, R.L.
1979: Interpretation of isotopic ages and $^{87}Sr/^{86}Sr$ initial ratios for plutonic rocks in the Whitehorse map area, Yukon; Canadian Journal of Earth Sciences, v. 16, p. 1988-1997.

Stevens, R.D., Delabio, R.N., and Lachance, G.R.
1982: Age determinations and geological studies, K-Ar isotopic ages, Report 16; Geological Survey of Canada, Paper 82-2.

Tempelman-Kluit, D.J.
1974: Reconnaissance geology of Aishihik Lake, Snag, and part of Stewart River map-areas, west-central Yukon; Geological Survey of Canada, Paper 73-41.
1979: Transported cataclasite, ophiolite, and granodiorite in Yukon: evidence of arc-continent collision; Geological Survey of Canada, Paper 79-14.

Tempelman-Kluit, D.J. and Wanless, R.K.
1975: Potassium-argon age determinations of metamorphic and plutonic rocks in the Yukon Crystalline Terrane; Canadian Journal of Earth Sciences, v. 12, p. 1895-1909.

Werner, L.J.
1977: Metamorphic terrane, northern Coast Mountains west of Atlin Lake, British Columbia; in Report of Activities, Part A, Geological Survey of Canada, Paper 77-1A, p. 267-269.
1978: Metamorphic terrane, northern Coast Mountains west of Atlin Lake, British Columbia; in Current Research, Part A, Geological Survey of Canada, Paper 78-1A, p. 69-70.

Wheeler, J.O.
1961: Whitehorse map-area, Yukon Territory; Geological Survey of Canada, Memoir 312.

Wheeler, J.O. and McFeely, P.A.
1987: Tectonic assemblage map of the Canadian Cordillera and adjacent parts of the United States of America; Geological Survey of Canada, Open File 1565.

A stratigraphic, plutonic, and structural framework for the Iskut River map area, northwestern British Columbia

R.G. Anderson
Cordilleran and Pacific Geoscience Division, Vancouver

Anderson, R.G., A stratigraphic, plutonic, and structural framework for the Iskut River map area, northwestern British Columbia; in Current Research, Part E, Geological Survey of Canada, Paper 89-1E, p. 145-154, 1989.

Abstract

Iskut map area includes four, unconformity-bounded, tectonostratigraphic assemblages: 1) Paleozoic Stikine assemblage; 2) Triassic-Jurassic volcano-plutonic complexes of Stikinia; 3) Middle and Upper Jurassic Bowser overlap assemblage; and 4) Tertiary Coast Plutonic Complex.

Early Devonian to Early Permian limestones and volcanics make up the Stikine assemblage and include intensely deformed rocks.

Distinctive porphyritic dykes link Upper Triassic and metallogenically-important Lower Jurassic volcanics with their plutonic equivalents. Basinal sedimentary and distal tuffaceous Lower and Middle Jurassic rocks mark the end of Triassic-Jurassic volcanism.

Siliciclastics of the Middle and Upper Jurassic Bowser Lake Group are part of an overlap assemblage deformed into orthogonal crossfolds.

Tertiary, post-tectonic, felsic plutons characterize the Coast Plutonic Complex. Eastward younging of strata from west to east and local zones of high strain attest to intrusion and uplift of the Coast Plutonic Complex.

Résumé

Le secteur de carte d'Iskut comprend quatre assemblages tectonostratigraphiques limités par des discordances stratigraphiques: 1) l'assemblage paléozoïque de Stikine; 2) les complexes volcano-plutoniques triasiques-jurassiques de Stikinia; 3) les assemblages de Bowser, du Jurassique moyen et supérieur, recouvrant partiellement les autres; 4) le complexe plutonique côtier du Tertiaire.

Des calcaires du Dévonien inférieur au Permien inférieur constituent l'assemblage de Stikine et comprennent des roches intensément déformées.

Des dykes prophyritiques distinctifs relient le Trias supérieur (groupe de Stuhini) et les roches volcaniques du Jurassique inférieur, importantes du point de vue de la métallogénèse (groupe de Hazelton) à leur équivalent plutonique. Les roches de bassins sédimentaires et les roches tufacées distales du groupe de Spatsizi du Jurassique inférieur et moyen marquent la fin du volcanisme triasique et jurassique.

Les roches clastiques siliceuses du groupe de Bowser Lake du Jurassique supérieur font partie d'un assemblage de recouvrement déformé en plis transverses orthogonaux.

Les plutons felsiques tertiaires post-tectoniques caractérisent le complexe plutonique côtier. Les strates dirigées vers l'est et les zones locales de déformation élevée témoignent de l'intrusion et du soulèvement du complexe plutonique côtier.

INTRODUCTION

Iskut River map area (56-57°N, 130-132°W; NTS 104 B) encompasses an important geological transect through the west-central Cordillera. Stratigraphic, plutonic, structural, and metamorphic transitions among Paleozoic Stikine assemblage, Mesozoic Stikinian, Middle and Upper Jurassic Bowser Basin, and Mesozoic(?)-Tertiary Coast Belt rocks occur in the map area. Precious metal lode deposits in the Silbak-Premier-Big Missouri, Suphurets and Stonehouse-Snip-Bronson Creek camps in the map area attract increasingly intense exploration interest.

The Cassiar-Stewart and old Granduc roads provide access to the eastern part of the region (Fig. 1a). Helicopter and fixed wing aircraft service to the new Bronson Creek airstrip remain the principal transportation links with Stewart, Terrace and Smithers.

Easy access via the Stikine and Iskut rivers fostered early mineral exploration in the western and central parts of the map area beginning in the 1880s. Discovery and development of the Stewart mining camp in the early 1900s led to regional geological surveys of increasingly expanded scope (e.g., McConnell, 1910, 1911; O'Neill, 1919; Schofield and Hanson, 1922; Hanson, 1929, 1935; Kerr, 1948; Geological Survey of Canada, 1957). Grove (1971, 1986) established the modern stratigraphic, plutonic and metallogenic framework for the Stewart mining district. Galley (1981), Alldrick (1983, 1984, 1985, 1987), Alldrick et al. (1986, 1987), Alldrick and Britton (1988), Britton and Alldrick (1988), and Brown (1987) have refined and extended the Jurassic stratigraphy around the Silbak Premier and Big Missouri mines north to the Sulphurets camp.

Fieldwork in 1985 and 1986 focused on stratigraphy at locations where fossil collections had been made by earlier workers; on the regional distribution of plutonic rocks; and on transects where metamorphic and/or structural transitions between Intermontane and Coast belts might have been anticipated. In 1987 and 1988 the macro- and micro-fossil identifications on 1985 and 1986 collections were completed.

This overview highlights Paleozoic and Mesozoic stratigraphy and plutonic episodes in the Iskut River map area. The focus is on well-dated strata; implicit is the importance of macro- and microfaunal biostratigraphy in precise correlation of the predominantly volcanogenic stratigraphy, which is characterized by abrupt facies changes. The stratigraphy and plutonic framework are most simply described in terms of four tectonostratigraphic elements: Paleozoic Stikine assemblage, Triassic and Jurassic Stikinian strata and plutons, Middle and Upper Jurassic Bowser Lake Group overlap assemblage; and Tertiary Coast Plutonic Complex.

Of particular interest to mineral explorationists are the Lower Jurassic volcanics and associated alkaline granitic rocks and related dykes of the Stikinian assemblage: many of the precious metal vein deposits seem to be associated with them (e.g. Silbak-Premier, Big Missouri, Silver Butte, Sulphurets).

PALEOZOIC STIKINE ASSEMBLAGE

Paleozoic Stikine assemblage rocks (Fig. 1a; Monger, 1977) are most extensively exposed in discontinuous outcrops in and around the Iskut ice field in the northern part of the map area. The assemblage is distinguished by biostratigraphically important coralline reef limestone members (e.g. Pitcher, 1960) and intercalated mafic to felsic volcanics.

Sr and Nd isotopic studies on samples of Devonian to Upper Jurassic rocks from the map area (Samson et al., 1987, in prep.) suggested that a young, geochemically and isotopically primitive crust underlies this part of Stikinia and its oldest strata.

The Lower to Middle Devonian (Early Devonian-post-Pragian) unit (Fig. 2) near Forrest Kerr Creek comprises at least four distinct coralline limestone members interlayered with mafic volcaniclastics, felsic crystal tuff, pebble conglomerate and siliceous shale. The unit contains the most penetratively deformed rocks in the area; these exhibit at least two phases of deformation. Locally, steeply west-northwest-dipping schistosity is overprinted by a gently south-southwest plunging crenulation whose axial plane dips steeply southeast. Elsewhere, kink bands are superimposed on layer-parallel schistosity in a felsic crystal tuff. The east-southeast, subvertical orientation of the kink bands is coplanar with late structures described by Holbek (1988) in Stikine assemblage rocks in the Mess Creek area north of the map area.

Mississippian (Viséan-Namurian) rocks (Fig. 2) north of Newmont Lake near the headwaters of Forrest Kerr Creek include thick-bedded coralline reef limestone interbedded with distinctive chert and pillowed basalt, hyaloclastite and epiclastic rocks. The thick-bedded nature of the Mississippian limestone, local coarse bioclastic texture (large crinoid columnals) and association with pillowed basalt flows distinguishes it from Permian equivalents.

Lower Permian (Asselian-Sakmarian or Leonardian) strata (Fig. 2) include important, thin-bedded coralline limestone and volcanic arc-like mafic to felsic volcanic flows, tuffs and volcaniclastics. Around Newmont Lake, the plagioclase-phyric intermediate to felsic volcanics resemble Jurassic Hazelton Group-equivalent rocks in the region; their intercalation with the limestone members is an important distinction. South of the Iskut River, Permian volcanic rocks are commonly green and of low greenschist grade; contact metamorphism by nearby Jurassic to Tertiary plutons is likely an important factor in the metamorphic overprint. Near Zippa Mountain, Lower Permian limestone is complexly deformed and overlain apparently unconformably by mafic volcanics (of Late Triassic age?). A striking structure in the fold complex is an isoclinal fold overturned to the south-southeast with a north-northeast fold axis.

Upper Triassic and upper Lower Jurassic (Toarcian) limestone members occur as nunataks or on the flanks of the Iskut ice field where their geological relations with the Stikine assemblage are poorly known. If these members are part of the Stikine assemblage, the assemblage partly overlaps in age (e.g. late Paleozoic to Early Jurassic) with other

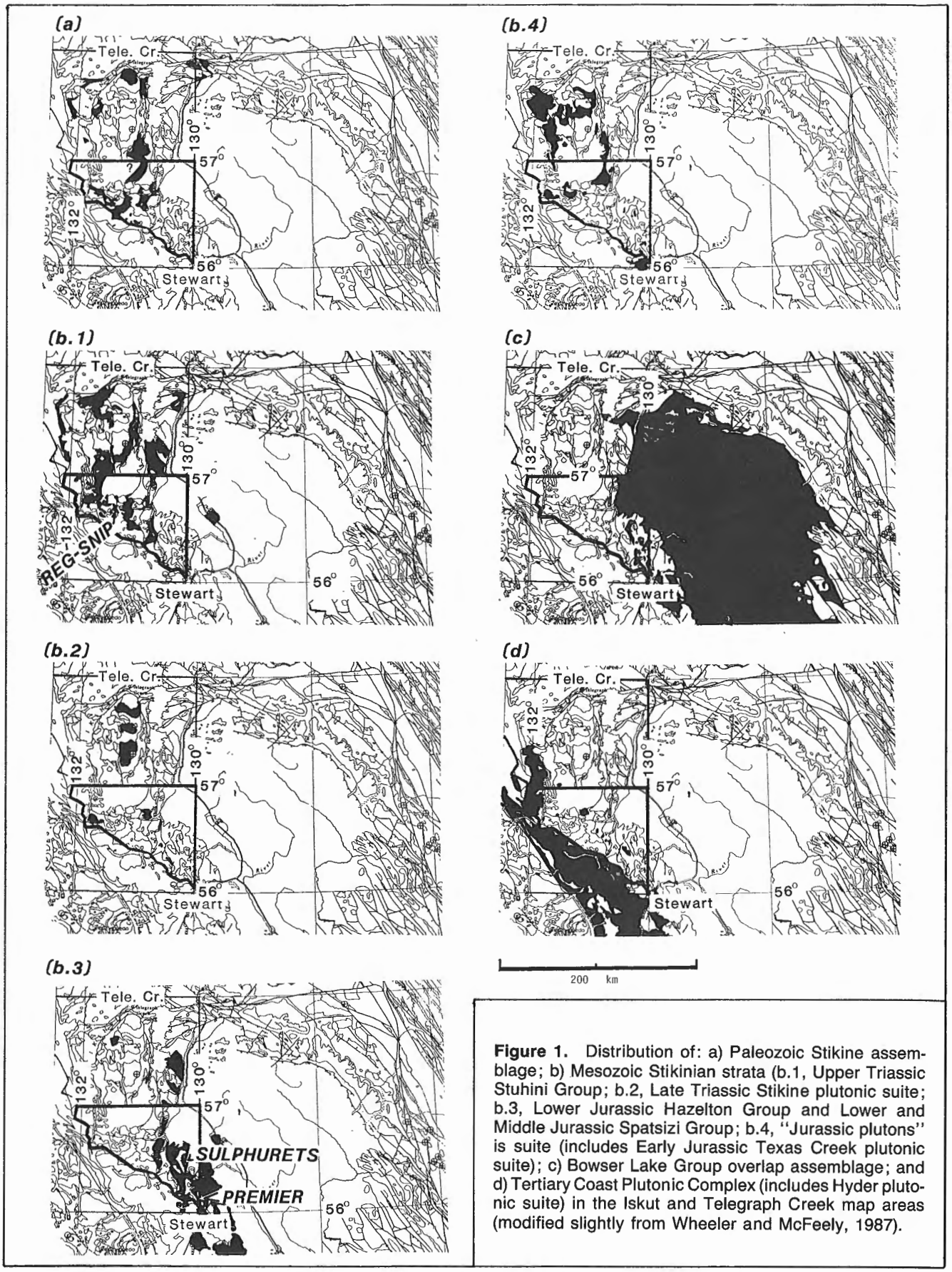

Figure 1. Distribution of: a) Paleozoic Stikine assemblage; b) Mesozoic Stikinian strata (b.1, Upper Triassic Stuhini Group; b.2, Late Triassic Stikine plutonic suite; b.3, Lower Jurassic Hazelton Group and Lower and Middle Jurassic Spatsizi Group; b.4, "Jurassic plutons" is suite (includes Early Jurassic Texas Creek plutonic suite); c) Bowser Lake Group overlap assemblage; and d) Tertiary Coast Plutonic Complex (includes Hyder plutonic suite) in the Iskut and Telegraph Creek map areas (modified slightly from Wheeler and McFeely, 1987).

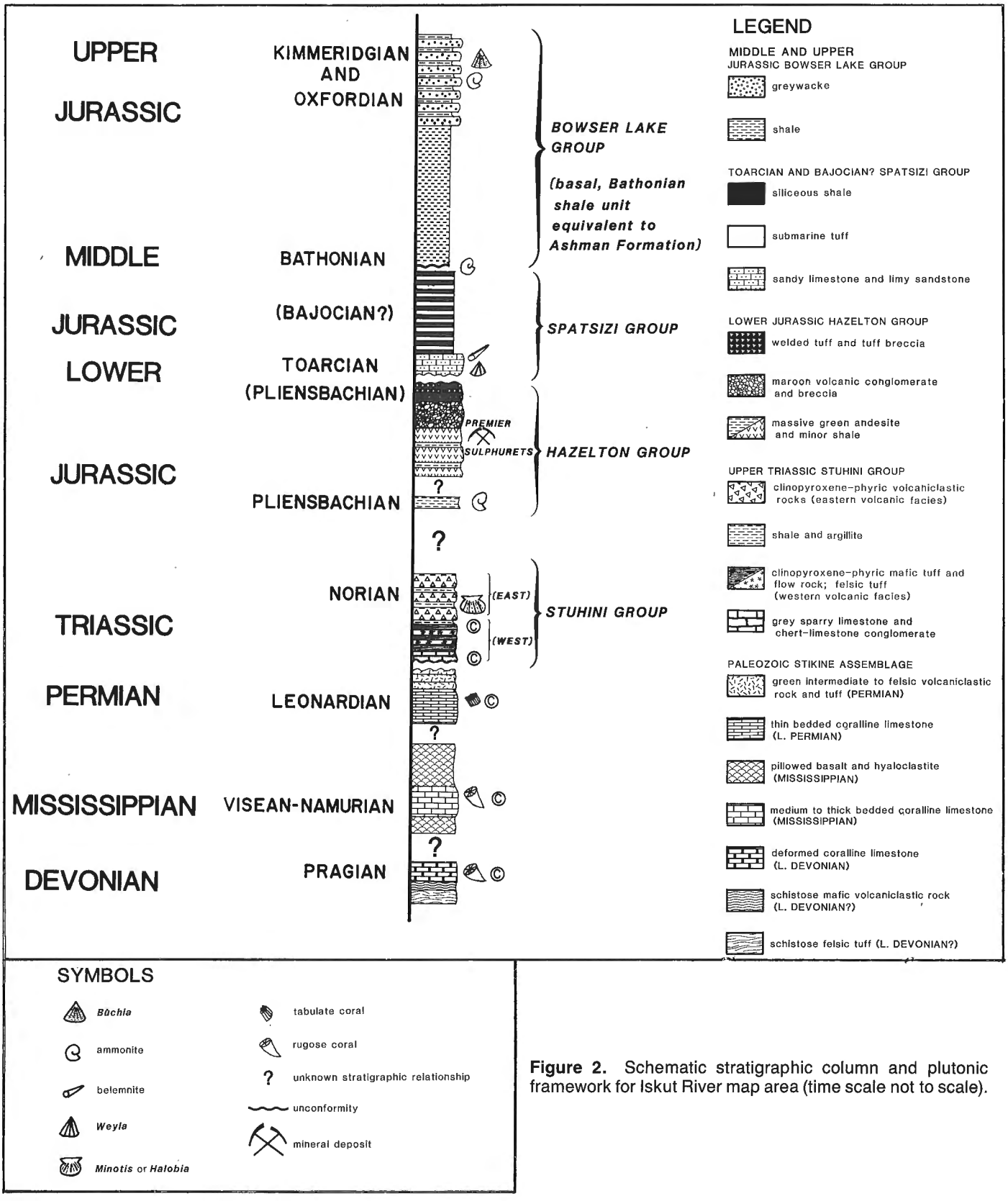

Figure 2. Schematic stratigraphic column and plutonic framework for Iskut River map area (time scale not to scale).

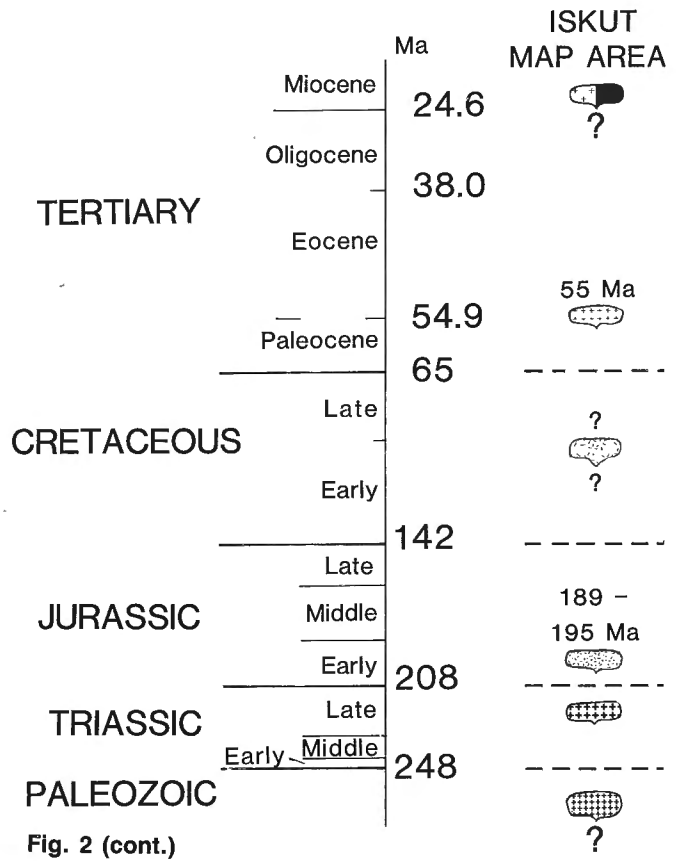

Fig. 2 (cont.)

Cordilleran Paleozoic-Mesozoic assemblages of oceanic affinity (e.g. Cache Creek Group in southern B.C.; Cordey et al., 1987) but differs from them in stratigraphic detail, overall age range, fusulinid taxonomy and tectonic association. Moreover, conodont colour alteration index values are generally greater than 5 for Permian and older strata and less than 5 for Triassic strata and suggest a widespread Permo-Triassic thermal event. Similar relations had been recognized along the eastern Stikine Arch between Permian and Middle Triassic rocks (Read, 1983) and may corroborate an earlier proposed Permo-Triassic "Tahltanian orogeny" (Souther and Armstrong, 1966; Souther, 1971). Stratigraphic relations on the flanks of the Stikine assemblage culmination suggest important sub-Triassic and sub-Toarcian unconformities, as well.

MESOZOIC STIKINIA STRATIGRAPHY

Paleozoic to Middle Jurassic strata formally define the Stikinia terrane (Monger and Berg, 1984). However, the Stikine assemblage occurs as scattered outcrops throughout the northern part of Stikinia and its stratigraphy and age range differs in detail from place to place (Monger, 1977). Coextensive, lithologically similar and coeval Upper Triassic and Lower Jurassic strata and associated plutonic suites give Stikinia its most regionally recognizable "fingerprint" and are metallogenically the most favourable for precious metal deposits.

Toarcian and Bajocian rocks provide recognizable, well-dated, upper bounding strata with respect to the economically important Lower Jurassic volcanics. Facies changes in the Lower to Middle Jurassic units (included with the Spatsizi Group to the northeast; Thomson et al., 1986) suggest the inception of a "proto-Bowser Basin" in the Toarcian and Bajocian.

Stuhini Group and Stikine plutonic suite

Stratigraphy

Upper Triassic, Stuhini Group volcanic and sedimentary rocks show marked facies changes from northwest to southeast (Fig. 1b.1 and 2). To the northwest, distinctly bimodal, basalt and rhyolite flows and tuff overlie an important, well-dated, Upper Triassic limestone member. The limestone extends from Mount Choquette at least as far south as Iskut Mountain and possibly as far east as Mount Verrett. The marker unit locally includes coarse limestone and chert breccia and conglomerate whose facies are interpreted as marking the Late Triassic slope break of the Stikine assemblage. Decimetre-scale growth faults are common in the volcanics and suggest that synvolcanic earthquake activity gave rise to the chert-limestone coarse clastic deposits. East-southeasterly-trending bimodal basalt-rhyolite feeder dykes in Paleozoic Stikine assemblage limestone signal the cessation of long-lived carbonate sedimentation and breakup and drowning of the carbonate reef complex in the Late Triassic. Coarse grained clinopyroxene±hornblende phenocrysts are characteristic of the mafic flows. Thin, interlayered micrite layers, on Mount Choquette contain Late Triassic conodonts.

These facies are dissimilar to the type Stuhini Group (Souther, 1971; Monger, 1980) or with Stuhini Group rocks along the eastern Stikine Arch (e.g. Anderson, 1983). They may be the key to any correlations with Mesozoic Alexander Terrane strata to the north and west of the map area (Gehrels and Saleeby, 1987; Gehrels et al., 1987; MacIntyre, 1984).

To the southeast, on McQuillan Ridge and east of Storie Creek, Upper Triassic rocks include predominant, mafic flows and volcaniclastics and minor, intercalated *Monotis*- or *Halobia*-bearing shale (Grove, 1986; Gunning, 1985). Clinopyroxene- (±hornblende)- phyric basalt and andesitic basalt also characterize the Stuhini Group's eastern facies but felsic volcanics appear to be absent.

Plutonism

Clinopyroxene gabbro and diorite, biotite-hornblende quartz monzodiorite and biotite alkali-feldspar megacrystic quartz monzonite represent the compositional range of the Late Triassic Stikine plutonic suite (Fig. 1b.2 and 2; Woodsworth et al., in press) in the region. The plutons are massive, inclusion-bearing and cospatial with the thickest accumulations of Stuhini Group volcanics. Ultramafite (hornblendite, hornblende clinopyroxenite) inclusions are rare but important because they indicate the coeval and cospatial relationship between felsic granitoids (Stikine plutonic suite) Late Triassic Alaskan-type ultramafite suite (Polaris suite) characteristic of northern Stikinia and Quesnellia (Woodsworth et al., in press). East-southeast-trending, porphyritic dykes are prominent in all plutons. Bimodal, rhyolite and clinopyroxene- and/or "bladed"

plagioclase-phyric basalt dykes are common in the Warm Spring Mountain pluton associated with the bimodal volcanics in the west. Clinopyroxene-porphyry basalt and hornblende-porphyry andesitic basalt dykes crosscut plutons on McQuillan Ridge and near the confluence of McLymont Creek and Iskut River in the east. Except for the western rhyolite dykes, the orientation, phenocryst mineralogy and composition of the dykes are typical of, and consistent within, the Stikine plutonic suite along the northern and western margin of the Bowser Basin.

Hazelton Group and Texas Creek plutonic suite

Stratigraphy

Lower Jurassic (Pliensbachian?) volcanics and minor sedimentary rocks dominate in the southeastern and central part of the Iskut River map area (Fig. 1b.3 and 2). The rocks appear to be the most prospective for precious metal lode deposits.

Lower Jurassic volcanics are characterized by significant and abrupt facies changes and, although generally unfossiliferous, are commonly correlated with the Telkwa Formation of the Hazelton Group (Tipper and Richards, 1976). From a regional mapping perspective, the recognizable Upper Triassic Stuhini Group and upper Lower Jurassic (Toarcian) member of the Spatsizi Group serve as useful bounding marker strata for the heterogeneous unit (*see* also Alldrick, 1983, 1984, 1985, 1987; Alldrick et al., 1986, 1987; Brown, 1987; Alldrick and Britton, 1988; Britton and Alldrick, 1988).

A regionally extensive Pliensbachian(?) volcanic stratigraphy includes: lowermost mafic and intermediate volcanic flows and volcaniclastics interlayered with two shale or argillite horizons (Unuk River Formation of Grove, 1986); medial maroon and green epiclastic volcaniclastics and tuff (Grove's (1986) Betty Creek Formation); and an uppermost, aerially extensive and distinctive, felsic welded tuff and tuff breccia (locally known as the Monitor Lake rhyolite; Grove's (1986) Salmon River Formation, in part, and Alldrick's (1987) Mount Dilworth "formation", in part). Overlying the uppermost andesite unit locally is a alkali-feldspar porphyritic volcanic flow which is considered an extrusive equivalent of the "Premier porphyry" dykes (Alldrick, 1985; Brown, 1987). Some precious metal veins appear to be localized along the contact between the two units in parts of the Stewart camp (e.g. Silver Butte; R. Britten, pers. comm., 1988).

Fragments of the alkali-feldspar-phyric andesite occur in the medial maroon epiclastic unit (Brown, 1987) and no "Premier porphyry" dykes intrude the epiclastic member. The epiclastics apparently rest unconformably on the basal andesite unit (Grove, 1971) and represent a volcanic hiatus.

Near the Kay property, the felsic volcanics underlie Bajocian rocks and are known to be Pliensbachian (Donnelly, 1976). Regionally, the felsic volcanics represent the terminal eruptive event in Early Jurassic volcanism. If correlative with the Dilworth "formation" (Alldrick, 1987) to the east, isotopic and faunal ages for basal and uppermost members of the Lower Jurassic Hazelton Group suggest that Early Jurassic volcanism was restricted to the Pliensbachian.

Plutonism

Early Jurassic plutons (189-195 Ma; Texas Creek plutonic suite; Alldrick et al., 1986, 1987; Brown, 1987; Woodsworth et al., in press) are widespread, distinctive and metallogenically important (Fig. 1b.4 and 2). Two plutonic styles are widespread. One comprises calc-alkaline (biotite-) hornblende granodiorite and quartz monzodiorite plutons crosscut by alkali-feldspar-phyric andesite dykes (e.g. Texas Creek pluton and "Premier porphyry" dykes near Silbak Premier mine). The other consists of biotite syenite plutons (e.g. dated Early Jurassic Galore Creek syenite and undated syenitic plutons near Mitchell Glacier (Kirkham, 1963) and the confluence of the Craig and Iskut rivers near the Snip deposit (Kerr, 1948)). The typical green- weathering appearance of the calc-alkaline suite indicates the suite's widespread alteration to chlorite and epidote. Discrete, east-trending mylonite zones in the Texas Creek pluton are locally distinctive (Smith, 1977). The importance of Early Jurassic alkaline plutonism (e.g. as alkali-feldspar porphyry dykes or syenite plutons) in the localization of precious metal lodes has been recognized for some time.

Alldrick and others (1986, 1987) and Brown (1987) have clearly documented the close spatial, temporal and genetic link between Texas Creek and Summit Lake plutons (the Texas Creek plutonic suite) and Pliensbachian volcanics via the "Premier porphyry" dykes. The quartz monzodiorite and granodiorite plutons are characterized by prismatic hornblende and common, widespread alteration of mafic minerals and plagioclase to chlorite and epidote. Plutons of similar composition, mafic mineralogy and alteration state occur west of Middle Mountain and near Iskut and Katete mountains in the western part of the map area. The western members of the Texas Creek plutonic suite appear to lack "Premier porphyry" dykes.

Deformation

Moderately west-dipping foliation and gently to moderately west-southwest-plunging mineral, pencil and stretching lineation characterize deformation of the Pliensbachian rocks in the Stewart camp (Grove, 1971; Brown 1987). West-dipping foliation conspicuous structure in chloritic andesite or porphyritic rocks along the Granduc road near Cascade Creek and along parts of the Silbak Premier-Big Missouri roads, is the youngest structural element in the area (Brown, 1987). At one locality, asymmetry of deformed fragments suggests west over east movement of the upper plate. East of Storie Creek, Gunning (1987) documented a steeply west-dipping, post-Toarcian reverse fault.

Well-developed, but unusual, discrete, subvertical, east-trending mylonite zones are conspicuous in parts of the Texas Creek pluton (Smith, 1977). Biotite lineation developed in the foliation plane is collinear with other linear fabrics and yields an anomalous (and likely reset) Eocene K-Ar date (Brown, 1987).

Gently to moderately west-southwest-plunging, collinear, lineations developed in Pliensbachian (commonly) to Bathonian (rarely) rocks are the most extensive fabric in the region. Lineation varieties include: biotite mineral lineation (in mylonitized Texas Creek pluton); fragment stretching lineation (in volcanic conglomerates on the Granduc road and maroon epiclastic rocks on Bear River Ridge); and pencil lineation outlined by two intersecting cleavages.

The ductile nature of some of these fabrics is in contrast to disharmonic, brittle regime fold patterns developed in Bajocian(?) and Middle and Upper Jurassic rocks. Regionally, the zones of high strain mark the eastern margin of the Coast Plutonic Complex in the southeastern part of the map area. Geological constraints on the age of the ductile structures are apparently contradictory. The fabrics are most extensively developed in all members of the Pliensbachian volcanic strata. In the Silbak Premier camp, west-dipping foliation in drillcore is annealed near quartz breccia ore (A. Randall, pers. comm., 1988) which is considered coeval with the cospatial Pliensbachian "Premier" porphyry dykes. If the linear and planar fabrics are cogenetic, and if collinearity of ductile mineral lineations, stretching lineations and pencil lineations indicate contemporaneity, the structures are post-Bathonian (Brown, 1987).

Spatsizi Group

Upper Lower and lower Middle Jurassic strata (Toarcian and Bajocian) are perhaps the most useful biostratigraphic and lithostratigraphic units of the Jurassic strata. Similar Toarcian rocks can be recognized as far north as the Stikine Arch north of the Stikine River (Anderson, 1983). The Toarcian and Bajocian rocks are coeval with and in part lithological correlatives with formations within the formally defined Spatsizi Group (Thomson et al., 1986).

Buff, sandy limestone contains *Weyla* bivalves and belemnites whose temporal overlap is restricted to the Toarcian (H.W. Tipper, pers. comm., 1985). The sub-Toarcian unconformity is recognized regionally but is best demonstrated east of Storie Creek where Toarcian strata unconformably overly *Monotis*-bearing Upper Triassic Stuhini Group (Gunning, 1986). From Mount Dilworth north to Storie Creek, there is an increase in shale at the expense of limestone in Toarcian rocks (Fig. 3).

Bajocian(?) rocks conformably overlie Toarcian limestone and comprise a sedimentologically unique alternation of white tuff and black, radiolarian-bearing siliceous shale (Brown, 1987). An identical, well-dated (Bajocian) unit, formally defined as the Quock Formation of the Spatsizi Group (Thomson et al., 1986) in the Spatsizi map area to the northeast was informally described as the "pajama beds" to depict the distinctive dark and light strata. In the Iskut map area, bed thickness and tuff:shale ratio decrease in Bajocian(?) rocks from Monitor Lake north to the Mitchell Glacier near the present southern limit of Middle and Upper Jurassic Bowser Lake Group (Fig. 3). Detailed stratigraphy of the Bajocian unit has the potential to predict the location of submarine hydrothermal exhalative vents.

Facies changes in the Toarcian and Bajocian rocks suggest a shale-out to the north in both units. The changes may anticipate the Bowser Basin's inception by 10-15 Ma.

MIDDLE AND UPPER JURASSIC BOWSER OVERLAP ASSEMBLAGE

Middle and Upper Jurassic (Bathonian to Oxfordian-Kimmeridgian) Bowser Lake Group rocks occur mainly in the northeastern part of Iskut River map area (Fig. 1c) and consist of monotonous, medium bedded green to brown, plagioclase-rich greywacke which predominates over *Buchia*-bearing, thin-bedded shale (Fig. 2). Paucity of marker beds in the Bowser Lake Group frustrate detailed mapping and regional correlation of distinctive northerly- and easterly-trending cross fold axes. Along the northern part of the basin, basal chert-rich conglomerates derived from a proximal, Cache Creek terrane highland to the north identifies the Bowser Lake Group as an overlap assemblage (Monger and Berg, 1984).

The Bathonian member (Ashman Formation-equivalent) comprises uniform shale or argillite containing local buff carbonate lenses or concretions. Evidence for a sub-Bathonian unconformity is best developed near Tom MacKay Lake where *Iniskinites*-bearing shale (Gunning, 1986) overlies lower members of the Pliensbachian volcanics (Donnelly, 1976; Grove, 1986). Oxfordian to Kimmeridgian greywacke and shale unit predominate over much of the northeastern part of the map area.

Deformation

Regional-scale synclines (e.g. Dilworth (Grove, 1971) and Tom MacKay Lake synclines (Gunning, 1987; Grove, 1986)) involve Pliensbachian to Bathonian rocks. Although the distribution of Bowser Lake Group and of older rocks are concordant on a map- scale, there is evidence for two, orthogonal fold events which distinguish the Bathonian rocks (Gunning, 1986). There is evidence of disharmonic folding in Bathonian rocks above a structural detachment in the Silbak Premier area (Brown, 1987). In the northeastern part of the Iskut River map area, orthogonal folds developed about north- and west-trending fold axes distinguish the structural style of the Oxfordian-Kimmeridgian rocks as well. Typically, tight, north-trending folds were overprinted by gentle folding about west-trending axes. In a few localities, the chronology of orthogonal folding is reversed.

PLUTONISM AND EASTERN LIMIT OF THE COAST BELT

Plutonic rocks occur throughout the Iskut map area but dominate in the southwest (Fig. 1d). In the past, geologists have included all granite plutons as part of the Coast Plutonic Complex (CPC).

More mapping and, especially, isotopic dating remain to be done to define the plutonic episodes and their plutonic styles within the map area. At least four episodes are recognized (Fig. 2; Woodsworth et al., in press): Late Triassic (Stikine plutonic suite), Early Jurassic (Texas Creek plutonic suite), Eocene (Hyder plutonic suite), and Oligocene-Miocene. Paleozoic and mid-Cretaceous plutonism seem likely but are unknown from intrusive relations or isotopic age data.

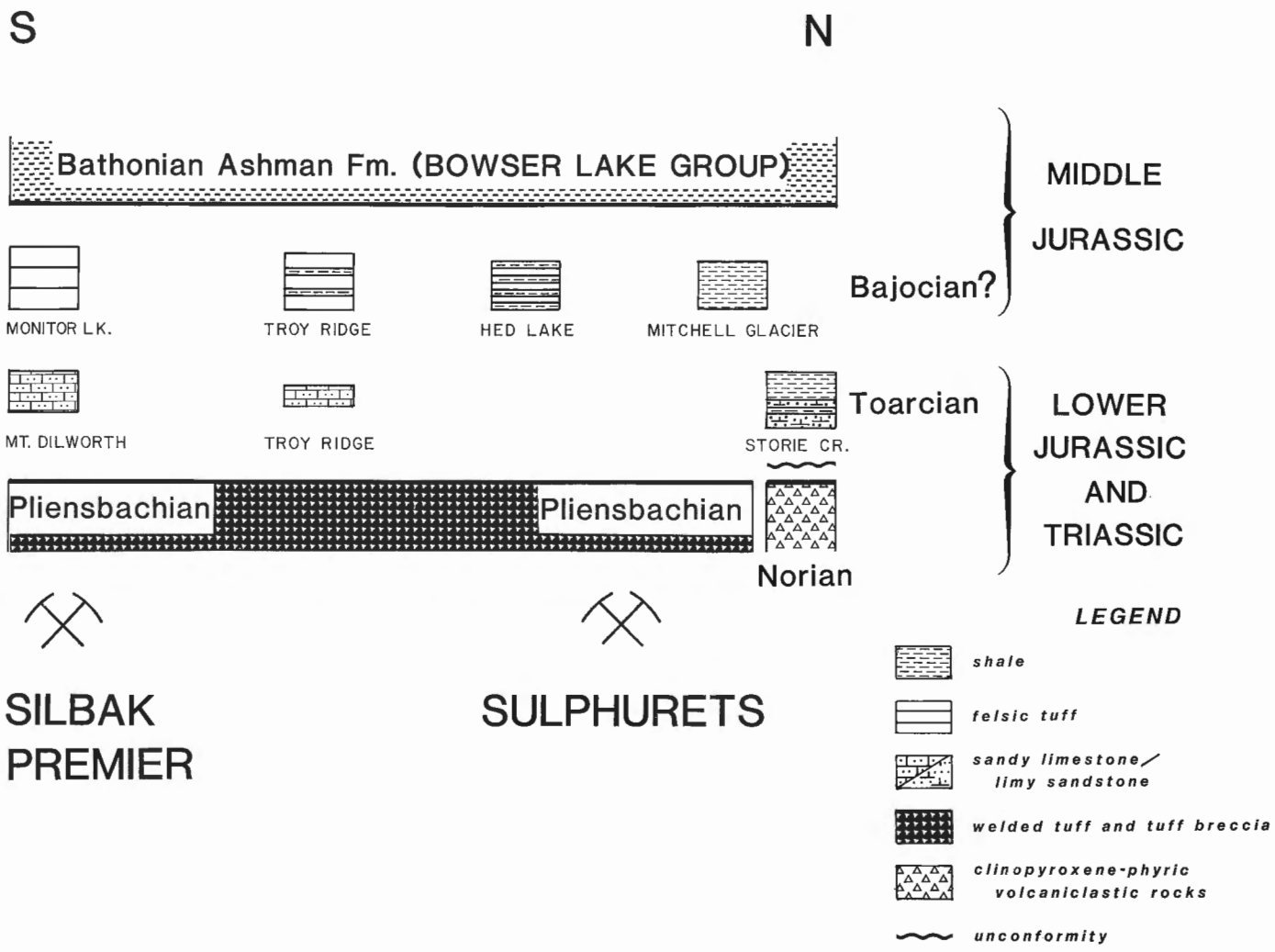

Figure 3. Schematic facies changes in Toarcian and Bajocian(?) rocks along of a north-south transect the eastern margin of the Iskut map area. Bounding Pliensbachian felsic welded tuff and tuff breccia (Alldrick's (1987) Dilworth "formation", in part) and Bathonian shale (Ashman Formation-equivalent) strata shown for reference.

Late Triassic and Early Jurassic plutons are coeval and cospatial with Stuhini Group and Hazelton Group-equivalent volcanic rocks. Their plutonic styles reveal a direct link to the volcanics via distinctive porphyritic dykes. Eocene plutons apparently lack dykes and volcanic equivalents. The Coast Plutonic Complex' eastern boundary, from Stewart northwest to Elbow Mountain and the Stikine River, is defined largely by the eastern limit of Eocene plutonism and is coincident with the international boundary. From Elbow Mountain north to the map area's boundary, the Stikine River marks the boundary between mid-greenschist grade metamorphic rocks and Tertiary plutons to the west and low greenschist grade rocks and Late Triassic-Early Jurassic plutonic suites and volcanic equivalents to the east.

Tertiary plutons (50-55 Ma; Hyder plutonic suite (Buddington, 1929; Smith, 1977; Woodsworth et al., in press; Anderson, unpub. U-Pb data) are more siliceous, biotite-rich, and less altered than Mesozoic plutons. Monzogranite, quartz monzonite and granodiorite predominate but minor monzodiorite and microdiorite (e.g. Portland dyke swarm) occur. The plutons lack dykes and preserved volcanic equivalents. Tertiary plutons crosscut all regional structural fabric, are considered post-tectonic but locally, where they comprise bimodal diorite-granite (e.g. Portland dyke swarm), indicate extension (perhaps as much as 30%; Brown, 1987).

There is good evidence for Oligocene-Miocene (18-25 Ma) ultra-potassic magmatism (Brown, 1987); it is mainly represented by scattered biotite minette lamprophyre dykes. A fresh, gabbro-syenite complex (Kerr, 1948), south of the Quaternary Hoodoo Mountain peralkaline volcanic complex, may be part of the Oligocene-Miocene alkaline suite.

SUMMARY

Early Devonian to Early Permian coralline limestone reef and mafic to felsic volcanic rocks make up the Stikine assemblage and include some of the most intensely deformed rocks in the region. Distinctive porphyritic dykes link Upper Triassic and Lower Jurassic volcanics with their plutonic equivalents. Lower and Middle Jurassic basinal limestone, radiolarian-bearing siliceous shale and tuff mark the end of the Triassic-Jurassic volcanic arc-building event. Middle and Upper Jurassic fine- and medium- grained siliciclastics are part of an overlap assemblage which, to the north, demonstrably links Stikinia and Cache Creek terranes. Post-tectonic, fresh, felsic plutons of mainly Tertiary age characterize the Coast Plutonic Complex along the southwest margin of the map area. Younging of strata from west to east attests to intrusion and uplift of the Coast Plutonic Complex. The eastern margin of the complex is defined by: the extent of the Tertiary plutons and local zones of high strain in the southeast; intrusive contacts in the central part of the map area; and an abrupt increase in metamorphic grade and change in plutonic style across the Stikine River in the west.

Unconformities seem to bound the major stratigraphic assemblages. Stratigraphic relationships among members of the Stikine assemblage are poorly known. The regionally extensive Permo-Triassic event is marked by local polymict conglomerate, a regional decrease in conodont colour alteration index with age and, possibly, an angular unconformity between recumbent isoclinally folded Lower Permian limestone and overlying Upper Triassic(?) mafic volcanics(?). A regionally important sub-Toarcian unconformity and a local but metallogenetically important Pliensbachian unconformity characterize the Lower Jurassic strata in the area.

The Lower Jurassic Hazelton Group and alkaline members of the cogenetic Early Jurassic Texas Creek plutonic suite have proved the most productive and prospective for precious metal lodes. Fossiliferous Upper Triassic Stuhini Group and Lower to Middle Jurassic Spatsizi Group strata provide recognizable, biostratigraphically restricted, bounding markers which define the economically important but mainly unfossiliferous and heterogeneous Lower Jurassic volcanic strata of the Hazelton Group metallotect.

ACKNOWLEDGMENTS

The contribution of macro- and microfossil identifications by W. Bamber, E. Carter, T. Poulton, H.W. Tipper, T. Tozer, and M.J. Orchard is implicit in this preliminary stratigraphic framework. M. Andrews, J. Beekmann, M. Gunning, D. Mathison, and D. Mustard, all members of the "A-team" over the years, have made special and important contributions to the geological mapping of the Iskut River map area. Careful compilation and preparation of draft diagrams by Art Calderwood is appreciated.

REFERENCES

Alldrick, D.J.
1983: Salmon River Project, Stewart, British Columbia; in Geological Fieldwork, 1982, British Columbia Ministry of Energy, Mines and Petroleum Resources, Paper 1983-1, p. 183-195.
1984: Geologic setting of the precious metal deposits in the Stewart area; in Geological Fieldwork, 1983, British Columbia Ministry of Energy, Mines and Petroleum Resources, Paper 1984-1, p. 149-164.
1985: Stratigraphy and petrology of the Stewart mining camp (104B/1); in Geological Fieldwork, 1984, British Columbia Ministry of Energy, Mines and Petroleum Resources, Paper 1985-1, p. 316-341.
1987: Geology and mineral deposits of the Salmon River valley, Stewart area, NTS 104 A and 104 B; British Columbia Ministry of Energy, Mines and Petroleum Resources, Geological Survey Branch, Open File Map 1987-22.

Alldrick, D.J. and Britton, J.M.
1988: Geology and mineral deposits of the Sulphurets area (NTS 104 A/5, 104 A/12, 104 B/8 and 104 B/9); British Columbia Ministry of Energy, Mines and Petroleum Resources, Geological Survey Branch, Open File Map 1988-4.

Alldrick, D.J., Mortensen, J.K., and Armstrong, R.L.
1986: Uranium-lead age determinations in the Stewart area; in Geological Fieldwork, 1985, British Columbia Ministry of Energy, Mines and Petroleum Resources, Paper 1986-1, p. 217-218.

Alldrick, D.J., Brown, D.A., Harakal, J.E., Mortensen, J.K., and Armstrong, R.L.
1987: Geochronology of the Stewart mining camp (104 B/1); in Geological Fieldwork, 1986, British Columbia Ministry of Energy, Mines and Petroleum Resources, Paper 1987-1, p. 81-92.

Anderson, R.G.
1983: The geology of the Hotailuh Batholith and surrounding volcanic and sedimentary rocks, north-central British Columbia; unpublished Ph.D. thesis, Carleton University.

Britton, J.M. and Alldrick, D.J.
1988: Sulphurets map area (104A/05W, 12W; 104B/08E, 09E); in Geological Fieldwork, 1987, British Columbia Ministry of Energy, Mines and Petroleum Resources, Paper 1988-1, p. 199-210.

Brown, D.A.
1987: Geological setting of the volcanic-hosted Silbak Premier Mine, northwestern British Columbia (104 A/4, B1); unpublished M.Sc. thesis, University of British Columbia, 216 p.

Buddington, A.F.
1929: Geology of Hyder and vicinity, southeastern Alaska; United States Geological Survey, Bulletin 807, 124 p.

Cordey, F., Mortimer, N., DeWever, P., and Monger, J.W.H.
1987: Significance of Jurassic radiolarians from the Cache Creek terrane, British Columbia; Geology, v. 15, p. 1151-1154.

Donnelly, D.A.
1976: Study of the volcanic stratigraphy and volcanogenic mineralization on the Kay claim group, northwestern British Columbia; unpublished B.Sc. thesis, University of British Columbia, 61 p.

Galley, A.
1981: Volcanic stratigraphy and gold-silver occurrences on the Big Missouri claim group, Stewart, British Columbia; unpublished M.Sc. thesis, University of Western Ontario, 181 p.

Gehrels, G.E. and Saleeby, J.B.
1987: Geologic framework, tectonic evolution, and displacement history of the Alexander terrane; Tectonics, v. 6, p. 151-174.

Gehrels, G.E., Saleeby, J.B., and Berg, H.C.
1987: Geology of Annette, Gravina, and Duke Islands, southeastern Alaska; Canadian Journal of Earth Sciences, v. 24, p. 866-881.

Geological Survey of Canada
1957: Stikine River area, Cassiar District, British Columbia; Geological Survey of Canada, Map 9-1957.

Grove, E.W.
1971: Geology and mineral deposits of the Stewart area, British Columbia; British Columbia Department of Mines and Petroleum Resources, Bulletin 58, 219 p.
1986: Geology and mineral deposits of the Unuk River-Salmon River-Anyox area; British Columbia Ministry of Energy, Mines and Petroleum Resources, Bulletin 63, 434 p.

Gunning, M.H.
1986: Late Triassic to Middle Jurassic (Norian to Oxfordian) volcanic and sedimentary stratigraphy and structure in the southeastern part of the Iskut map sheet, north-central British Columbia; unpublished B.Sc. thesis, University of British Columbia, 85 p.

Hanson, G.
1929: Bear River and Stewart map-areas, Cassiar District, B.C.; Geological Survey of Canada, Memoir 159, 84 p.
1935: Portland Canal area, British Columbia; Geological Survey of Canada, Memoir 175, 175 p.

Holbek, P.M.
1988: Geology and mineralization of the Stikine Assemblage, Mess Creek area, northwestern B.C.; (abstract), Smithers Exploration Group-G.A.C., Cordilleran Section, Program and Abstracts, p. A50-51.

Kerr, F.A.
1948: Lower Stikine and western Iskut river areas, British Columbia; Geological Survey of Canada, Memoir 246, 94 p.

Kirkham, R.
1963: The geology and mineral deposits in the vicinity of the Mitchell and Sulphurets glaciers, northwest British Columbia; unpublished M.Sc. thesis, University of British Columbia, 122 p.

MacIntyre, D.G.
1984: Geology of the Alsek-Tatshenshini rivers area (114 P); in Geological Fieldwork 1983, British Columbia Ministry of Energy, Mines and Petroleum Resources, Paper 1984-1, p. 173-184.

McConnell, R.G.
1910: Portland Canal District; Geological Survey of Canada, Summary Report 1910, p. 59-90.
1911: Salmon River district, B.C.; Geological Survey of Canada, Summary Report 1911, p. 50-56.

Monger, J.W.H.
1977: Upper Paleozoic rocks of the western Canadian Cordillera and their bearing on Cordilleran evolution; Canadian Journal of Earth Sciences, v. 14, p. 1832-1859.
1980: Upper Triassic stratigraphy, Dease Lake and Tulsequah map-areas, northwestern British Columbia; in Current Research, Part B, Geological Survey of Canada, Paper 80-1B, p. 1-9.

Monger, J.W.H. and Berg, H.C.
1984: Part B--Lithotectonic terrane map of western Canada and southeastern Alaska; in Lithotectonic Terranes Maps of the North American Cordillera, N.J. Silberling and D.L. Jones (eds.), United States Geological Survey, Open-File Report 84-523.

O'Neill, J.J.
1919: Salmon River district, Portland Canal mining division, B.C.; Geological Survey of Canada, Summary Report 1919, p. 7-11.

Pitcher, M.G.
1960: Fusulinids of the Cache Creek Group Stikine River area, Cassiar District, British Columbia, Canada; unpublished M.Sc. thesis, Brigham Young University, 64 p.

Read, P.B,
1983: Geology, Classy Creek (104J/2E) and Stikine Canyon (104J/1W), British Columbia; Geological Survey of Canada, Open File 940.

Samson, S., Patchett, J., Gehrels, G., McClelland, W.M., and Anderson, R.G.
1987: Nd isotopes and the origin of the accreted Alexander and Stikine terranes in the Canadian Cordillera; (abstract), E.O.S. v. 69, p. 1548.

Schofield, S.J. and Hanson, G.
1922: Geology and ore deposits of Salmon River district, British Columbia; Geological Survey of Canada, Memoir 132, 81 p.

Smith, J.G.
1977: Geology of the Ketchikan D-1 and Bradfield Canal A-1 quadrangles, southeastern Alaska; United States Geological Survey, Bulletin 1425, 49 p.

Souther, J.G.
1971: Geology and mineral deposits of the Tulsequah map-area, British Columbia; Geological Survey of Canada, Memoir 362, 84 p.
1972: Telegraph Creek map-area, British Columbia; Geological Survey of Canada, Paper 71-44, 38 p.

Souther, J.G. and Armstrong, J.E.
1966: North central belt of the Cordillera of British Columbia; in Tectonic History and Mineral Deposits of the Western Cordillera; Canadian Institute of Mining and Metallurgy, Special Volume 8, p. 171-184.

Thomson, R.C., Smith, P.L., and Tipper, H.W.
1986: Lower to Middle Jurassic (Pliensbachian to Bajocian) stratigraphy of the northern Spatsizi area, north-central British Columbia; Canadian Journal of Earth Sciences, v. 23, p. 1963-1973.

Tipper, H.W. and Richards, T.A.
1976: Jurassic stratigraphy and history of north-central British Columbia; Geological Survey of Canada, Bulletin 270, 73 p.

Wheeler, J.O. and McFeely, P.
1987: Revised tectonic assemblage map of the Canadian cordillera and adjacent parts of the United States of America; Geological Survey of Canada, Open File 1565.

Woodsworth, G.J., Anderson, R.G., and Armstrong, R.L.
— Plutonic Regimes, Chapter 15 in Cordilleran Orogen: Canada; H. Gabrielse and C.J. Yorath (eds.), Geological Survey of Canada, Geology of Canada, no. 4, (also Geological Society of America, the Geology of North America, v. G-2). (in press).

Metamorphism, deformation and geochronology of the Ecstall-Quaal rivers area, Coast Plutonic Complex, British Columbia

S.A. Gareau[1]
Cordilleran and Pacific Geoscience Division, Vancouver

Gareau, S.A., Metamorphism, deformation and geochronology of the Ecstall-Quaal rivers area, Coast Plutonic Complex, British Columbia; in Current Research, Part E, Geological Survey of Canada, Paper 89-1E, p. 155-162, 1989.

Abstract

New U-Pb zircon dates and recent fieldwork show that a first deformational event produced both a strong planar fabric and isoclinal folds. This event postdates the intrusion of the 378 Ma Big Falls orthogneiss and may predate that of the 192 Ma Johnson Lake body. The deformed rocks were refolded by more open structures and subjected to late large-scale folding. This deformation was followed by intrusion of the undeformed mid-Cretaceous Ecstall quartz diorite. The Paleogene intrusion of the Quottoon tonalite and related pegmatites induced a sillimanite-grade aureole on metamorphic rocks closest to the pluton.

The strong fabric in the Quottoon pluton indicates intrusion into a tectonically active zone which may be the southern analogue of the Work Channel lineament. Except for a 2 km wide zone adjacent to the Quottoon pluton, fabrics in the metamorphic belt are not related to a Paleogene shear zone, but may in part represent a post-Devonian shear zone that was an important tectonic boundary.

Résumé

De nouvelles datations par la méthode U-Pb sur le zircon et de récents travaux de terrain, montrent qu'un premier épisode de déformation a produit à la fois une fabrique plane bien définie et des plis isoclinaux. Cet épisode est ultérieur à l'intrusion de l'orthogneiss de Big Falls de 378 Ma, et précède peut-être celui du corps intrusif de Lake Johnson de 192 Ma. Les roches déformées ont été à nouveau plissées par des structures plus ouvertes, et soumises à un plissement tardif de grande échelle. Cette déformation a été suivie de l'intrusion de la diorite quartzique d'Ecstall, non déformée, d'âge crétacé moyen. L'intrusion paléogène de la tonalite de Quottoon et des pegmatites apparentées ont créé une auréole du degré de la sillimanite dans les roches métamorphiques les plus proches du pluton.

La fabrique très bien définie du pluton de Quottoon indique que l'intrusion s'est produite dans une zone tectoniquement active qui est peut-être l'analogue méridional du linéament de Work Channel. À l'exception d'une zone de 2 km de large proche du pluton de Quottoon, les fabriques caractérisant la zone métamorphique ne sont pas reliées à une présence d'une zone de cisaillement paléogène, mais représentent peut-être en partie une zone de cisaillement post-dévonienne qui représente une importante limite tectonique.

[1] Ottawa-Carleton Geoscience Centre, Department of Earth Sciences, Carleton University, Ottawa, Ontario K1S 5B6

INTRODUCTION

Mapping in the area between the Ecstall River and Douglas Channel, begun in 1987, continued in 1988. The objectives are to document the rock types, metamorphism, deformational styles and ages of metamorphic rocks in a 10-15 km wide northerly-trending belt bounded in the west by the mid-Cretaceous Ecstall pluton and on the east by the Paleogene Quottoon tonalite. This belt is located along the southern extension of the Work Channel lineament which has been interpreted by Crawford et al. (1987) as a large and steep ductile shear zone with upward Paleogene movement of the eastern block. Thus, a second objective consists of characterizing this major tectonic boundary south of the Skeena River.

The Work Channel lineament in the Prince Rupert area is a zone of steep structural fabric separating the western and central belts of the Coast Plutonic Complex (Fig. 1). Farther to the south, in the Ecstall-Quaal rivers area, steep fabrics are present near the Ecstall River (Fig. 2). There the foliation strikes northwest to north and dips steeply east, the lineation plunges steeply to the north, and isoclinal folds are steeply inclined (Gareau, 1988). Rocks of igneous origin abound to the west, whereas metasedimentary rock dominates the eastern side of the region (Fig. 2). However, steep structures cannot be followed north of Big Falls Creek and along Douglas Channel. In addition, away from the Ecstall river, units described in Table 1 (*see* also Gareau, 1988) are no longer restricted to a particular side of the metamorphic belt (Fig. 2).

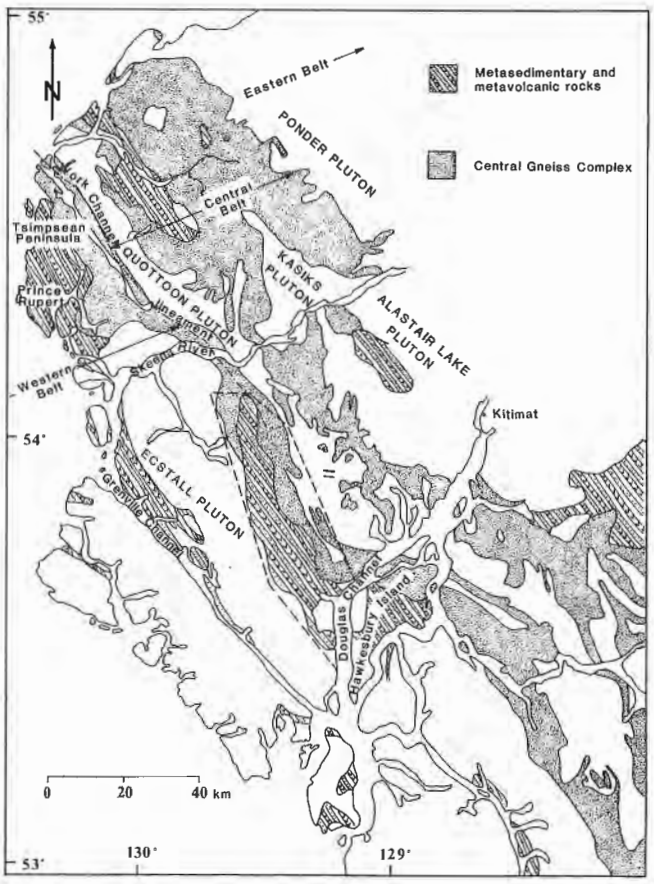

Figure 1. Generalized geological map of part of the Coast Plutonic Complex between latitudes 53 and 55° N. After Hutchison (1982) and Roddick (1970).

LITHOLOGIC NOTES

Along the northern shore of Douglas Channel (Fig. 2), well-layered metasedimentary rocks are confined to the westernmost part of the metamorphic belt. The Big Falls orthogneiss is not present along Douglas Channel. Areas where it might be expected are instead underlain by the homogeneous and undeformed, coarse grained epidote-biotite-hornblende quartz dioritic Kitkiata pluton. Where present,

Table 1. Description of major lithologies in Ecstall River-Douglas Channel area.

PLUTONIC ROCK	Aplite and pegmatite dykes	Leucocratic, variable amounts of biotite, muscovite and garnet.
	Quottoon pluton (57.1 Ma)	Strongly foliated and lineated biotite-hornblende tonalite. Fabric concordant with that of metamorphic host with which it is in gradational contact.
	Ecstall body	Homogeneous and undeformed medium grained epidote-hornblende-biotite quartz diorite in sharp contact with folded metamorphic rock.
	Kitkiata pluton	Homogeneous and undeformed coarse grained epidote-biotite-hornblende quartz diorite in very sharp contact with country rock.
	Hornblende diorite	Coarse grained and non to weakly lineated. Associated rusty-weathering coarse hornblendite.
ORTHOGNEISS	Johnson Lake body (192 Ma)	Medium grained epidote-biotite-hornblende tonalite. Weakly foliated and cross-cutting regional fabric at northern end; strongly foliated and concordant at southern end.
	Big Falls body (378 Ma)	Quartz-feldspar-muscovite-biotite ± garnet ± hornblende augen gneiss with minor fine grained amphibolitic inclusions and hornblende-bearing tonalitic layers.
	Foch Lake body	Medium grained, feldspar blastoporphyritic, titanite-epidote-biotite gneiss. Sharp contact with metamorphic rock is folded.
METAVOLCANICS	Mafic	Fine grained chlorite-hornblende-zoisite ± biotite ± calcite schist with less than 30% Carich plagioclase + quartz.
	Intermediate to felsic	Biotite-quartz semi-schist of varying grain size. Felsic component less than 20% of rock. Possibly cogenetic with Big Falls orthogneiss.
METASEDIMENTS		White to grey, locally pyritiferous, quartzite interlayered with biotite-hornblende gneiss, fissile mica schist, black phyllite to metaargillite or Al_2SiO_5-bearing metapelite.
BIOTITE-HORNBLENDE GNEISS	Well layered	Medium grained garnetiferous amphibolite and biotite quartz dioritic to granodioritic gneiss. Rare epidote + garnet-rich pods.
	Homogeneous	Lineated, fine to medium-grained, locally garnetiferous, epidote ± biotite ± hornblende gneiss. Epidote and granitoid clasts locally present.

the Big Falls orthogneiss is everywhere spatially associated with mafic hornblende-chlorite, locally clastic, volcanic rock and biotite semi-schist. Although finer grained, the biotite semi-schist similar to the orthogneiss; this suggests that the volcanic rocks may be cogenetic with the Big Falls body.

Hornblende-chlorite schist occurs along Douglas Channel on the northeast side of Kitkiata Inlet. The schist is in gradational contact with a homogeneous, strongly lineated, locally clastic epidote ± biotite ± hornblende ± garnet gneiss (Fig. 3). This is in contrast with the very sharp contact between the same two units in the Ecstall River area.

Along Douglas Channel, a second gradational contact separates the homogeneous gneiss from well-layered medium grained garnetiferous amphibolite and more felsic biotite gneiss (Fig. 4). West of Foch Lake, the well-layered and homogeneous gneisses are cut by a medium grained, feldspar blastoporphyritic titanite-epidote-biotite gneiss.

STRUCTURE

Three types of folds occur throughout the Ecstall-Quaal rivers area. Isoclinal folds and very strong planar fabrics (Fig. 5) are attributed to a first deformational event (D1). No widespread macroscopic asymmetric fabric typical of shear zones was seen with this intense deformation. Such fabrics may have been present but, if so, were largely destroyed during more recent metamorphism and deformation of the region. These D-1 features are refolded by more open structures of 1-5 m amplitude. Fabric elements related to this second fold generation are locally rotated around moderately to steeply inclined large-scale (hundreds of metre) folds generally striking northwest and dipping steeply either northeast or southwest. Folding is most apparent in well-layered metasedimentary rocks, although small-scale folds in other units attest to the deformation of all rocks.

METAMORPHISM AND PLUTONISM

The deformed rocks contain typical amphibolite facies peak metamorphic assemblages such as andesine-biotite-epidote-hornblende-almandine in mafic volcanic rocks and andesine-muscovite-biotite-almandine in pelitic rocks. Abundant chlorite in the basic rocks is partly retrograde. In metasedimentary rocks, kyanite and staurolite are locally present and sillimanite occurs close to the eastern edge of the metamorphic belt. One episode of metamorphism postdates at least one deformational event, because randomly oriented hornblende crosscuts the fabric of a chlorite schist and a foliated amphibolite contains garnet overgrowing a foliation itself folded by late large-scale folds.

On the west the deformed metamorphic rocks are intruded by the Ecstall pluton. The contact is sharp and the medium grained epidote-hornblende-biotite quartz diorite has a weakly foliated margin less than 1 km and generally less than 100 m wide. Within 2 km of the gradational contact with the Quottoon pluton, the metamorphic rocks are coarser grained and locally contain sillimanite. These observations are consistent with the thermal metamorphism resulting from the intrusion of the Paleogene biotite-hornblende tonalite. Partial melting of the metamorphic rocks may have occurred rarely where migmatites are present within 50 m of the contact.

Leucocratic pegmatite dykes increase in density and degree of deformation over 2.5 km towards the contact with the Quottoon pluton. The fabric in these rocks (Fig. 6) parallels that of the adjacent metamorphic rock, itself concordant with the strong foliation and lineation at the western margin of the Quottoon pluton (Fig. 7). These observations indicate that the Quottoon tonalite was intruded into a tectonically active zone. As attested by the various states of deformation of the relatively young pegmatites, only the easternmost part of the metamorphic belt was affected by this Paleogene deformation which is otherwise essentially undetectable in the previously intensely deformed metamorphic rocks.

U-Pb GEOCHRONOLOGY

Dating of zircons from five samples collected during the 1987 field season gave the following preliminary results.

A moderately foliated and weakly lineated, coarse grained, (biotite)-hornblende tonalite (sample 246-1, Fig. 2) from the Quottoon pluton gave an essentially concordant date of 57.1 Ma. This date is in agreement with results of Armstrong and Runkle (1979) and is interpreted as the emplacement age of the Quottoon pluton in the Ecstall River area.

A 59.0 +0.8/−1.3 Ma date was obtained from a sample of foliated, coarse grained, leucocratic epidote-biotite quartz dioritic dyke collected in the metamorphic belt about 1 km west of the Quottoon pluton contact (sample 140-2, Fig. 2). The pegmatitic zircons show minor Pb inheritance. The dated sample belongs to a series of leucocratic dykes increasing in density and degree of deformation towards the Quottoon pluton. Their intrusion appears related to and essentially coeval with intrusion of the Quottoon pluton.

Two samples from the Johnson Lake orthogneiss were dated at 192 +8/−4 Ma. Sample 139-5 is located very close to the Paleogene dyke (Fig. 2), in the zone of high Paleogene strain. The strong foliation and lineation in the titanite-epidote-biotite-hornblende metagranodiorite is concordant with that of the surrounding rocks. Collected close to the small body's northern contact which crosscuts the regional fabric (Fig. 2), sample 218-2 is similar in composition, but differs in the intensity of the foliation which is very weak to non-existent. Since sample 139-5 was collected from that part of the metamorphic belt that has been affected by Paleogene deformation, whereas sample 218-2, being farther from the Quottoon pluton, was located outside the Paleogene deformation aureole, it is possible that the strong foliation of sample 139-5 was produced solely during late Paleogene deformation. If this was the case, the anomalous absence of strong foliation in the Johnson Lake orthogneiss may shed some light on the timing of deformation in the metamorphic rocks. Since all metamorphic rocks of the region, including compositionally very similar orthogneiss, possess the very strong fabric attributed to D-1, it is possible that the virtually unfoliated Johnson Lake orthogneiss has been intruded after this deformation period.

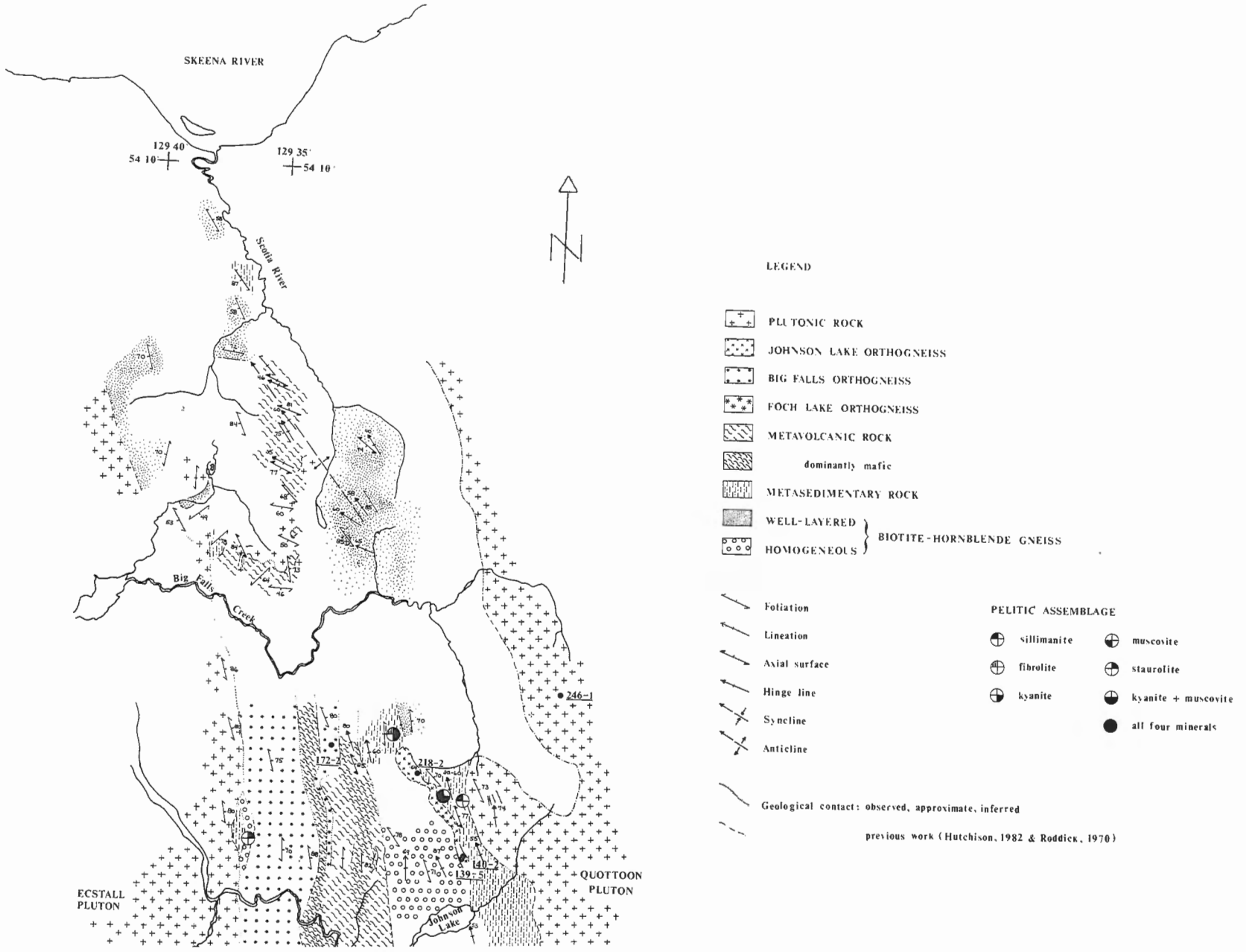
SKEENA RIVER
129 40
54 10
129 35
54 10
Scotia River
Big Falls Creek
246-1
172-2
218-2
140-2
139-5
ECSTALL PLUTON
QUOTTOON PLUTON
Johnson Lake
LEGEND
PLUTONIC ROCK
JOHNSON LAKE ORTHOGNEISS
BIG FALLS ORTHOGNEISS
FOCH LAKE ORTHOGNEISS
METAVOLCANIC ROCK
dominantly mafic
METASEDIMENTARY ROCK
WELL-LAYERED
HOMOGENEOUS
BIOTITE-HORNBLENDE GNEISS
Foliation
Lineation
Axial surface
Hinge line
Syncline
Anticline
PELITIC ASSEMBLAGE
sillimanite
fibrolite
kyanite
muscovite
staurolite
kyanite + muscovite
all four minerals
Geological contact: observed, approximate, inferred
previous work (Hutchison, 1982 & Roddick, 1970)

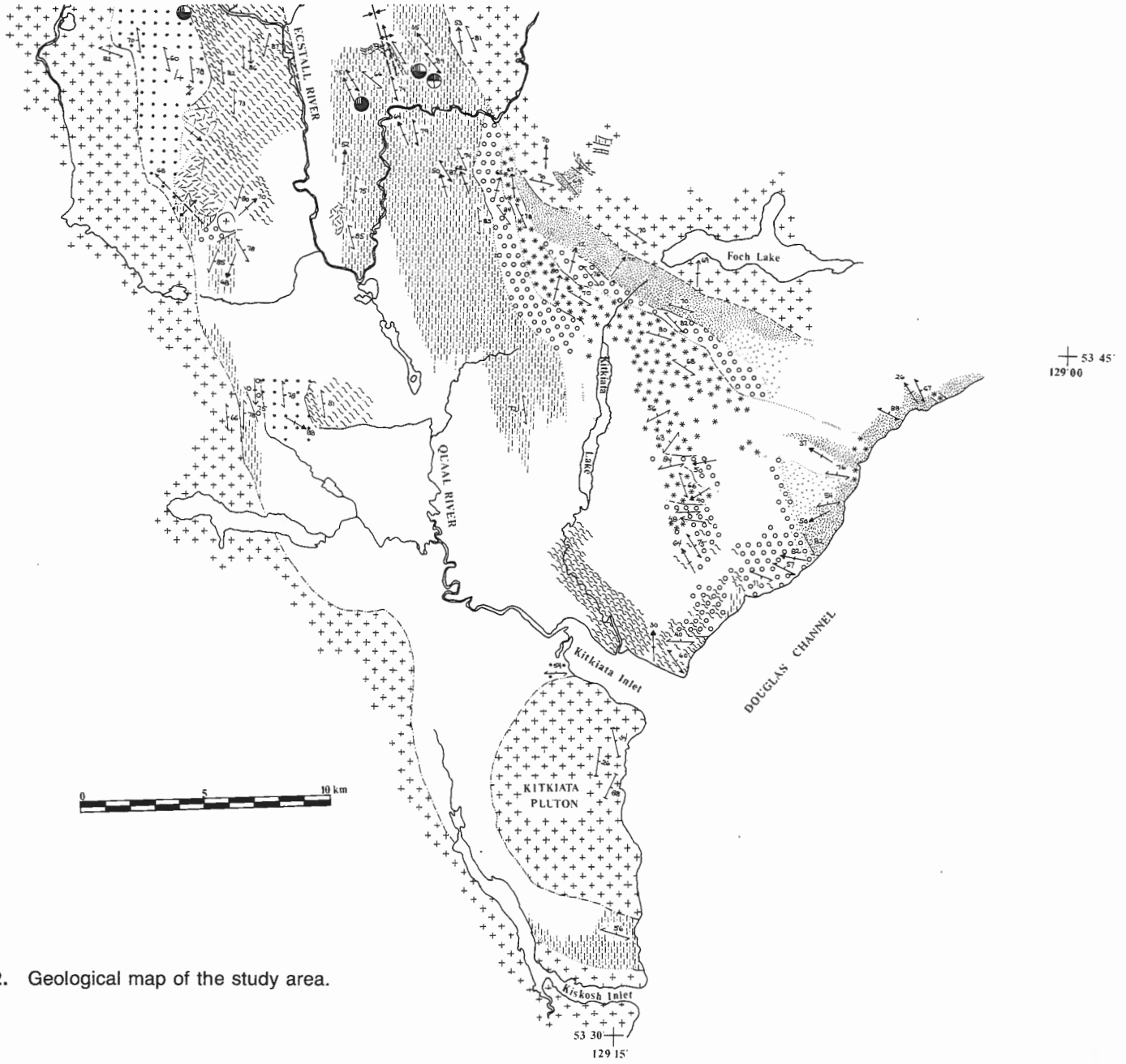

Figure 2. Geological map of the study area.

Figure 3. Homogeneous biotite-hornblende gneiss containing stretched epidote-rich and granitoid clasts. Ridge north of Johnson Lake.

Figure 4. Well-layered biotite-hornblende gneiss. The dark layers consist of medium-grained garnetiferous amphibolite and lighter grey layers of biotite-feldspar gneiss. White pegmatitic material is folded with the gneiss. Minor folds are related to late large-scale deformation of the metamorphic rock. Northwest of Kitkiata Lake.

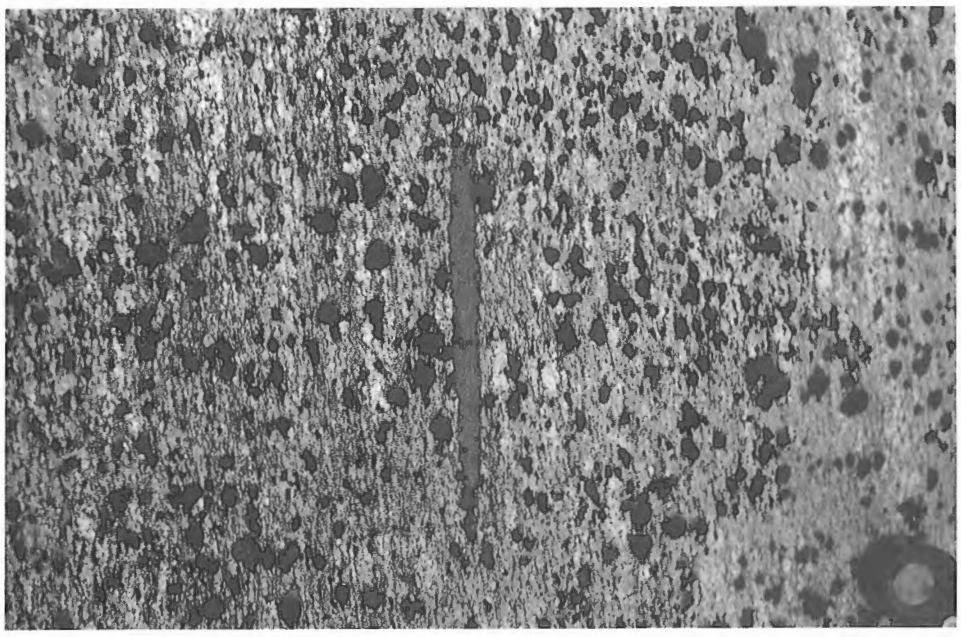

Figure 5. Strongly foliated biotite-muscovite Big Falls orthogneiss. The strong planar fabric is typical in the rocks of the Estall-Quaal rivers metamorphic belt and is attributed to D-1. Ridge south of Big Falls Creek.

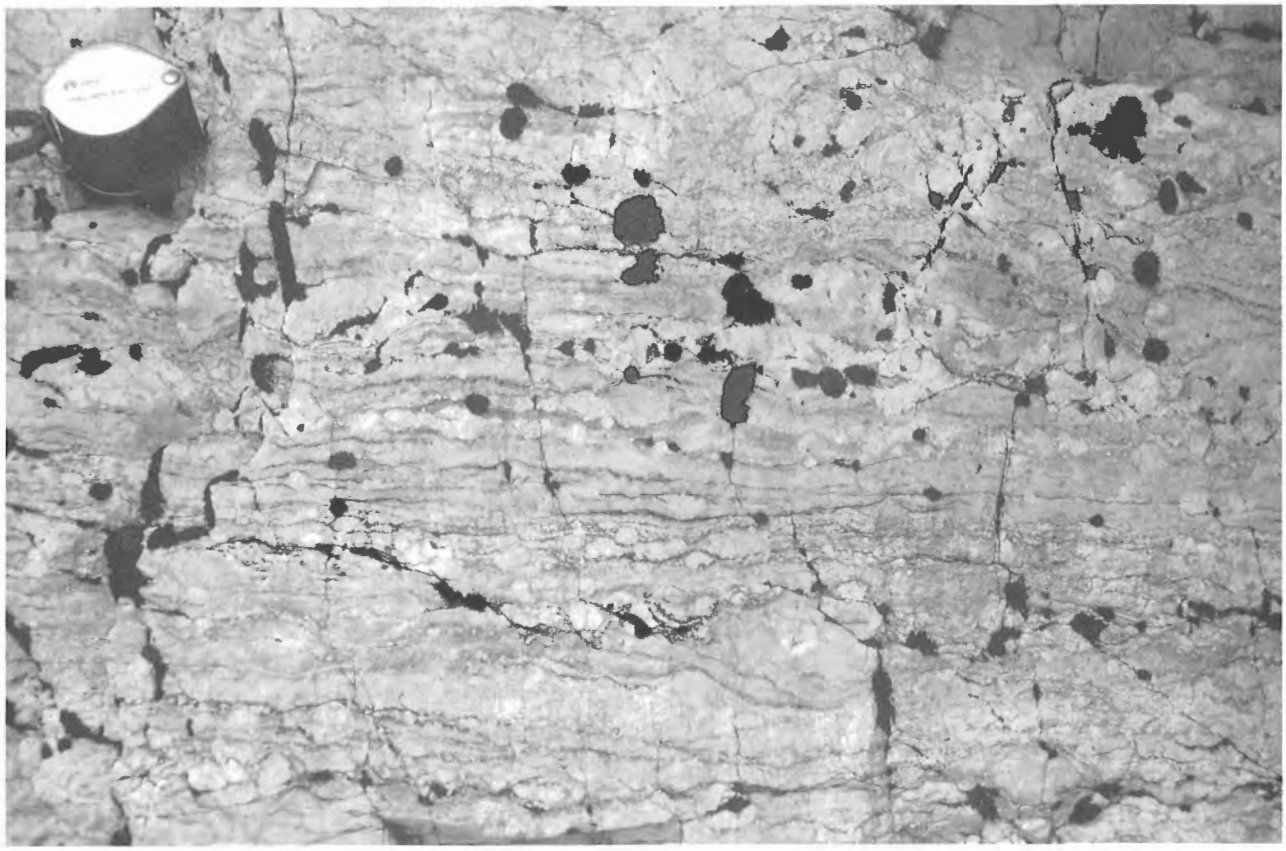

Figure 6. Strongly deformed leucocratic pegmatite dyke located close to the Quottoon pluton contact. This dyke belongs to a suite of pegmatites that intrude the metamorphic rocks mostly in a 2.5 km wide band adjacent to the Quottoon pluton. Their concentration and degree of deformation increase towards the Quottoon contact. Ridge north of Johnson Lake.

The strongly foliated biotite-muscovite augen gneiss collected from within the Big Falls body (sample 172-2, Fig. 2) was dated at 378 +14/−9 Ma. This is interpreted as an emplacement age predating all deformation documented in the metamorphic belt.

CONCLUSION

The Paleogene Quottoon tonalite was intruded into a tectonically active zone which may be the southern analogue of the Work Channel lineament. Paleogene deformation is reflected only in the easternmost 2 km of the Ecstall-Quaal rivers metamorphic belt.

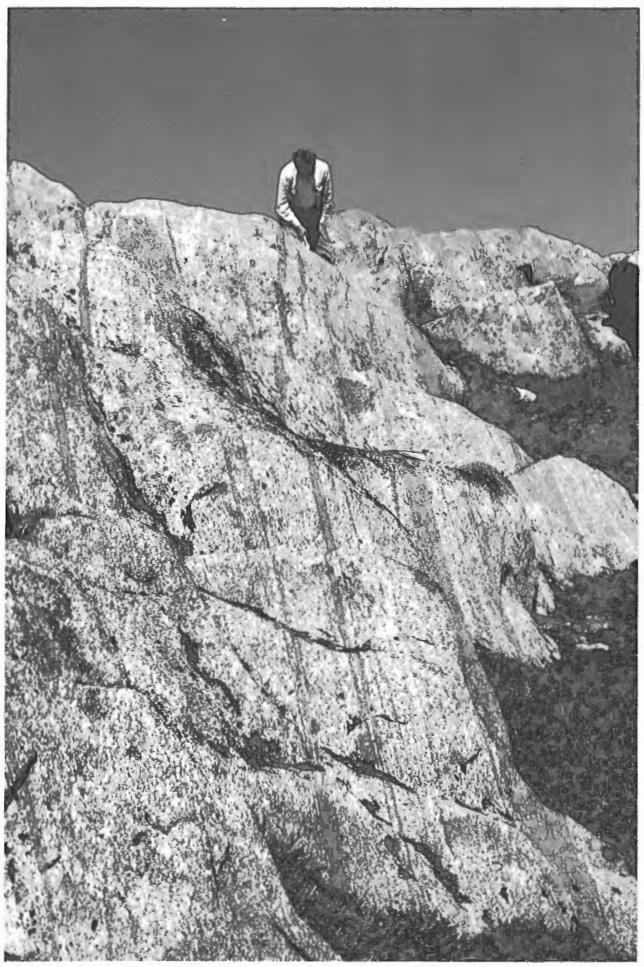

Figure 7. Deformed Quottoon pluton. In this rock, mafic inclusions emphasize the strong fabric present in the Paleogene Quottoon tonalite. Ridge immediately north of Foch Lake.

In the metamorphic belt, deformation and amphibolite facies metamorphism in siliceous and semi-pelitic to pelitic sedimentary rocks, mafic to felsic volcanic rocks and intrusive bodies postdated emplacement of the Devonian Big Falls orthogneiss and predated intrusion of the mid-Cretaceous Ecstall pluton. A very strong fabric and isoclinal folding were initially produced, perhaps in a major ductile shear zone acting as an important tectonic boundary. The intrusion of the Johnson Lake orthogneiss may have postdated this first deformational event. Later deformation produced more open structures that in turn were deformed by late large-scale folds.

ACKNOWLEDGMENTS

George Skippen and Glenn Woodsworth's generous support is gratefully acknowledged. I wish to thank Randy Parrish who introduced me to the art of U-Pb dating and provided advice and insightful discussions while visiting me in the field. The U-Pb data were obtained in the facilities of the Geochronology Section, Lithosphere and Canadian Shield Division of the Geological Survey of Canada. Help in the field by Tania Hale, Frances Noone, Kathleen Dixon and Jorg Beekman is also greatly appreciated. Many thanks to Dave Newman and Garry Thomsen (Okanagan Helicopters Ltd.) for providing professional flying and resourceful help. The manuscript was reviewed by R.R. Parrish and G.J. Woodsworth.

REFERENCES

Armstrong, R.L. and Runkle D.
1979: Rb-Sr geochronometry of the Ecstall, Kitkiata and Quottoon plutons and their country rocks, Prince Rupert region, Coast Plutonic Complex, British Columbia; Canadian Journal of Earth Sciences, v. 16, p. 387-399.

Crawford, M.L., Hollister, L.S., and Woodsworth, G.J.
1987: Crustal deformation and regional metamorphism across a terrane boundary, Coast Plutonic Complex, British Columbia; Tectonics, v. 6, p. 343-361.

Gareau, S.A.
1988: Preliminary study of the Work Channel lineament in the Ecstall River area, Coast Plutonic Complex, British Columbia; in Current Research, Part E, Geological Survey of Canada, Paper 88-1E, p. 49-55.

Hutchison, W.W.
1982: Geology of the Prince Rupert-Skeena map area, British Columbia: Geological Survey of Canada, Memoir 394, 116 p.

Roddick, J.A.
1970: Douglas Channel — Hecate Strait map-area, British Columbia: Geological Survey of Canada, Paper 70-41, 56 p.

A note on the Coast-Intermontane belt transition, Mount Waddington map area, British Columbia

Margaret E. Rusmore[1] and G.J. Woodsworth
Cordilleran and Pacific Geoscience Division, Vancouver

Rusmore, M.E. and Woodsworth, G.J., A note on the Coast-Intermontane belt transition, Mount Waddington map area, British Columbia; in Current Research, Part E, Geological Survey of Canada, Paper 89-1E, p. 163-167, 1989.

Abstract

Recent fieldwork shows that the extensive Late Cretaceous thrust belt developed in low grade rocks of the western Intermontane Belt extends west into the Coast Plutonic Complex. Amphibolite-facies metamorphic and granitoid rocks comprise the southwesternmost thrust sheet seen to date. Field observations suggest that metamorphic grade increases upwards within individual thrust sheets. Metamorphic grade also increases from northeast to southwest along a given structural horizon. The protolith for the metamorphic rocks between Nude and Mosley creeks was probably Lower Cretaceous clastic rocks that are exposed in thrust sheets east of Nude Creek.

Résumé

Des travaux de terrain récents montrent que la vaste zone de charriage du Crétacé supérieur, formée dans des roches peu métamorphisées de la zone intramontagnarde occidentale, se prolonge à l'ouest jusque dans le complexe plutonique côtier. Les roches métamorphiques du faciès des amphibolites et les roches granitoïdes comprennent la nappe de charriage la plus distante observée au sud-ouest. Les observations faites sur le terrain suggèrent que le degré de métamorphisme augmente vers le haut, dans les nappes de charriage individuelles. Le degré de métamorphisme augmente aussi du nord-est au sud-ouest le long d'un horizon structural précis. Les roches originelles qui ont donné naissance aux roches métamorphiques situées entre les ruisseaux Nude et Mosley étaient probablement des roches clastiques du Crétacé inférieur qui affleurent dans des nappes de charriage à l'est du ruisseau Nude.

[1] Department of Geology, Occidental College, Los Angeles, CA 90041

INTRODUCTION

The eastern margin of the Coast Belt is well exposed in the northeastern part of the Mount Waddington map area. Previous work in the region showed that a northwest-striking Late Cretaceous thrust belt lies just east of the Coast Belt (Tipper, 1969; Rusmore and Woodsworth, 1988). Regionally the thrust belt dips southwest toward plutonic and metamorphic rocks of the Coast Plutonic Complex that comprise the Coast Belt, although dips reverse locally. Results from two previous field seasons demonstrated that the thrust belt involves Triassic rocks correlative with Stikinia, Lower Cretaceous clastic rocks, and Lower Cretaceous(?) volcanic strata. Thrust sheets apparently moved toward the northeast, parallel to a consistent elongation lineation. We have continued our work in the area to discover whether the Coast Plutonic Complex (CPC) is involved in the thrusting, document the structural and metamorphic history of the CPC in this area, and investigate stratigraphic relations between Triassic and Cretaceous units.

Work in the past summer focused on mapping across the strike of the belt west of Nude Creek and along the southeastern part of the thrust system, near Tredcroft Glacier. About five weeks of fieldwork were planned, but bad weather cut the number of working days nearly in half. Mapping was done on a scale of 1:20 000, and is currently being compiled onto a 1:50 000 base. This report summarizes our field observations and preliminary conclusions; further laboratory and fieldwork is planned to verify and expand the tentative conclusions given here.

MARGIN OF THE COAST PLUTONIC COMPLEX

The main result of our fieldwork is the recognition that the thrust belt extends into the Coast Plutonic Complex. Metamorphic and plutonic rocks mapped as the Coast Plutonic Complex by Roddick and Tipper (1985) make up the southwesternmost and structurally highest thrust sheets observed to date. Schists in these thrust sheets were derived from volcanic and clastic protoliths. Protoliths for most of the metaclastic rocks were probably part of the sequence of Lower Cretaceous sedimentary rocks (informally called the Cloud Drifter formation; Rusmore and Woodsworth, 1988) exposed in thrust sheets to the east (Fig. 1). Sandstone, siltstone, and conglomerate compose the Cloud Drifter formation, and these rocks are common protoliths for the schists. Clasts in metaconglomerates are similar to those in the Cloud Drifter formation; felsic volcanic and granitoid clasts are the most common types in both units. The Cloud Drifter formation contains distinctive planar-laminated and trough-bedded sandstones, and metamorphosed equivalents of these are locally recognizable in the schists.

Amphibolite occurs both as layers in the pelitic and psammitic schists and as separate thrust slices. Amphibolite layers in the schists may have been derived from basaltic sandstones typical of the Cloud Drifter formation. The amphibolite thrust slices offer no distinctive features by which to correlate them with volcanic units exposed in thrust sheets to the east.

Metamorphic grade increases structurally upward across the thrust belt, from sub-greenschist facies rocks exposed on the eastern edge of the belt to sillimanite/andalusite-staurolite-garnet-biotite schists in the southwest, near Success Mountain. Field observations suggest that metamorphic grade increases upward within individual thrust sheets. For example, pelites at the base of one sheet near Success Mountain are barely phyllitic and probably contain chlorite, white mica, and perhaps biotite. Near the top of the same sheet, about 400 m structurally higher, andalusite (replaced locally by sillimanite), garnet, staurolite, and biotite are common in pelitic schists. Grade also increases along structural levels; a particular thrust sheet appears more metamorphosed in its southwestern exposures.

Textures visible in hand samples suggest that metamorphism was mainly syn-kinematic, with some mineral growth continuing after deformation ceased. Metamorphic minerals define both a foliation and a lineation. The foliation generally dips gently southwest or northeast and is roughly parallel to the thrusts. Elongate metamorphic minerals define a prominent lineation that trends northeast or southwest and plunges from about 0-25°. This orientation matches elongation lineations present in the lower grade eastern part of the thrust belt (Rusmore and Woodsworth, 1988). Fold styles and orientation are consistent between the lower and higher grade parts of the thrust belt. Mountain-scale recumbent folds occur in low grade sandstones and shales east of Nude Creek (Rusmore and Woodsworth, 1988) and in schists west of it. In the low grade rocks, hinge lines range from perpendicular to the lineation to parallel to it, suggesting that folds have rotated varying amounts towards the lineation direction. An average hinge line calculated from relict bedding attitudes in several folds in the schists parallels the mineral and elongation lineations.

Two tonalitic orthogneiss bodies are involved in the part of the thrust belt mapped this summer. The largest is exposed west of Nude Creek where it lies structurally below a thick imbricate zone (Fig. 1). In outcrop, the rocks show a penetrative schistosity marked by alternating layers of plagioclase+quartz and biotite+hornblende. Schistosity in the orthogneiss is generally parallel to schistosity and cleavage in surrounding schists. A mineral lineation is visible in many samples and parallels the regional orientation of elongation lineations; it trends northeast or southwest and plunges gently. Where viewed perpendicular to the schistosity and parallel to the lineation, plagioclase crystals generally display "tails" of fine grained plagioclase. Most tails appear symmetric in outcrop, suggesting that pure shear dominated at least the last increment of strain. Asymmetric porphyroclasts occur in a few outcrops, but no consistent sense of shear was recognized. Two samples suggested motion toward the northeast, but the opposite sense of shear was recorded in another sample. Study of oriented thin sections and systematic mapping of the orthogneiss is planned to determine the significance of the fabrics.

The contact between the orthogneiss and the surrounding pelitic schists is broadly gradational in the two areas we observed it. Within several metres of the orthogneiss body, bands of orthogneiss 1-2 cm thick appear in the schists and are parallel to the schistosity in the pelites. The bands

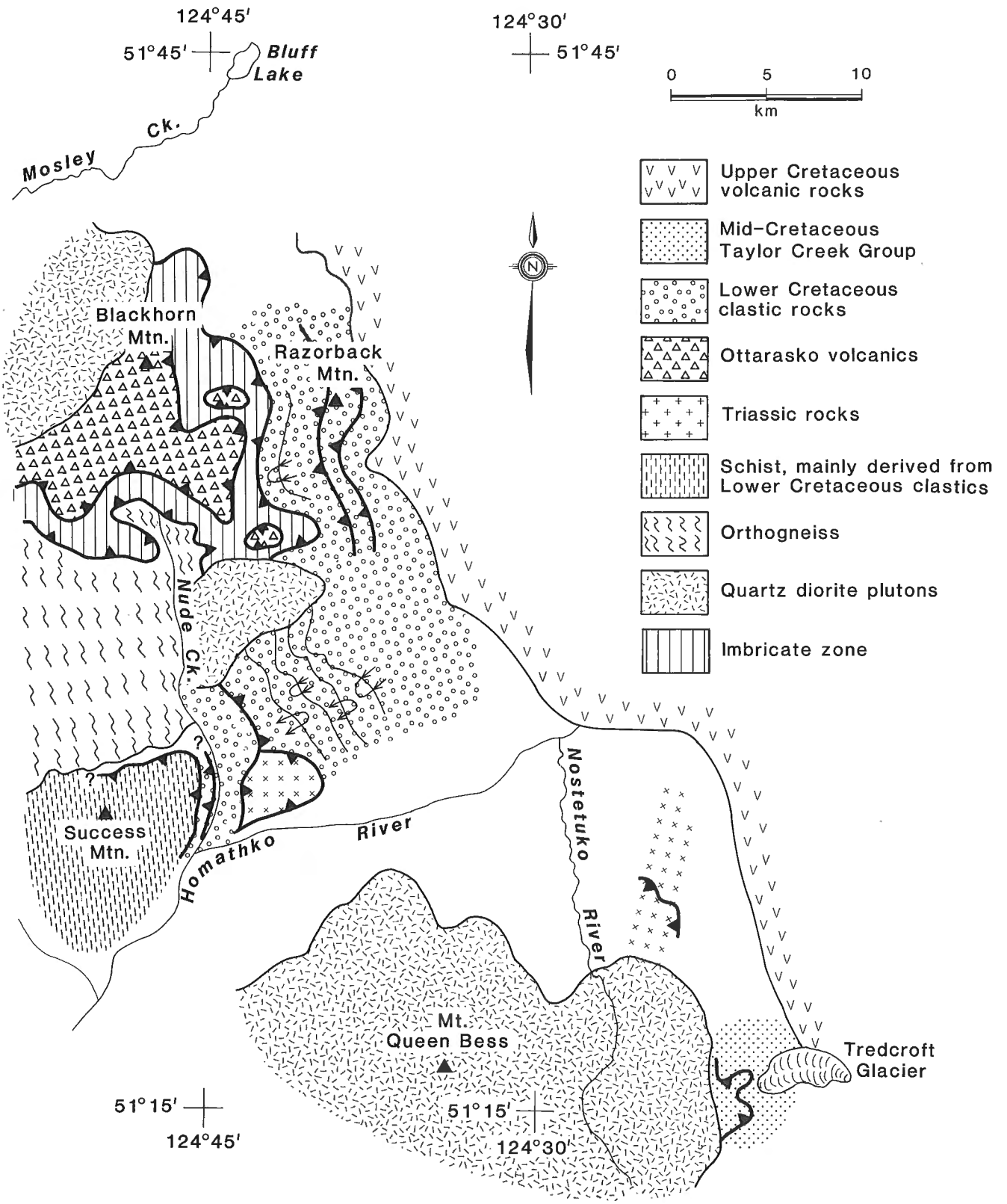

Figure 1. Geological sketch map of part of the Mount Waddington map area.

become thicker and more common closer to the orthogneiss, until schist completely gives way to orthogneiss. Foliations and lineations in both rocks types are parallel, and there is no visible structural break in the contact zone. Although the contact is gradational, the contact zone is more highly strained than the main body of orthogneiss. Mafic inclusions in the orthogneiss are strongly elongated parallel to the mineral lineation near the contact; they become less elongate toward the centre of the body. Within the contact zone, some orthogneiss bands are finer grained and darker than the main body and appear mylonitic. Despite the higher strain, the gradational nature of the contact itself suggests it is not a discrete thrust. Instead, the increased strain probably reflects the presence of the overlying imbricate zone.

Orthogneiss also occurs as a thrust-bound slice about 200 m thick on the east ridge of Success Mountain. The rock is a biotite < hornblende tonalite containing sphene and, locally, garnet. Structurally, the orthogneiss overlies well foliated amphibolite. The contact is sharp and planar; tonalite and amphibolite are mylonitic within a metre or so of the contact. The orthogneiss locally contains about 15-50 % tectonic slices (length:width of about 20:1) of amphibolite with lesser calc-silicate rock and fine grained psammic schist; the rock is what has been called a "banded gneiss" by some other workers in the Coast Plutonic Complex (e.g. Hutchison, 1982). The orthogneiss is structurally overlain by amphibolite and psammitic schist, but the contact is covered.

AGE AND VERGENCE OF THRUSTING

Thrusting and associated folding are probably early Late Cretaceous in age. An upper age limit is provided by a 68 Ma tonalitic pluton that cuts a thrust a few kilometres northeast of Success Mountain (R. Parrish, pers. comm., 1987, in Rusmore and Woodsworth, 1988). Our mapping near Tredcroft Glacier confirms previous workers' conclusions that the mid-Cretaceous Taylor Creek Group is involved in the thrusting (Tipper, 1969; McLaren, 1987). Several thrusts repeat the section on both sides of the glacier, and northeast-verging map-scale folds are common. McLaren (1987) reported a late Early Albian age for the Taylor Creek Group in this area. Thrusting thus occurred between mid-Albian time and 68 Ma.

One goal of mapping in the Tredcroft area was to determine whether rocks younger than the Taylor Creek Group were affected by thrusting. East of Razorback Mountain in the northern part of our study area, Cenomanian(?) rocks of the Kingsvale Group (Tipper, 1969) appear to be overthrust by Hauterivian strata; however, outcrops are poor and the relationship has not been verified elsewhere. In the Tredcroft Glacier area, the contact lies in a rubble-filled valley where contact relationships cannot be determined. Albian strata thus remain the youngest rocks clearly involved in the thrusting. U-Pb dating (in progress) of a deformed dyke from within one of the thrusts may help limit the age of thrusting.

Structures in the Taylor Creek Group support our previous conclusion that thrust sheets moved to the northeast (Rusmore and Woodsworth, 1988). Mesoscopic inclined-plunging folds verge to the northeast and have gently plunging, northwest-trending axes (see McLaren, 1987 for a spectacular view of this type of fold). In several places, a thrust breaks through the overturned northeast limb of an anticline, and carries the fold over a lower plate syncline. Within one thrust, a sandstone bed has been imbricated to form a small duplex structure that indicates northeast-directed thrusting. The presence of these structures leaves little doubt that thrusts sheets moved towards the northeast in this area. Additional support for this conclusion is provided by the fact that the highest grade thrust sheets are found at high structural levels in the southwest part of the thrust belt. Small-scale kinematic indicators are rare throughout the thrust belt; most outcrops record a late-stage flattening event. As mentioned above, the few asymmetric fabrics visible in outcrop suggest both northeast and southwest directed shear. Although the major thrust motion was probably to the northeast throughout the belt, the disparate fabrics hint at a more complex kinematic history.

STRATIGRAPHIC NOTES

The stratigraphy of most low grade units was described in Rusmore and Woodsworth (1988); our new observations about the Taylor Creek Group and relations between Triassic and Cretaceous strata are summarized here.

In the Tredcroft area, the Taylor Creek Group consists of rhyolite breccia and crystal lithic tuff that are conformably overlain by interbedded sandstone and siltstone. The breccia is fine grained with clasts a few millimetres to a centimetre long, and commonly has abundant tuffaceous matrix. Typically it is maroon or green and contains water-clear euhedral to broken quartz crystals, plagioclase crystals and felsic volcanic rock fragments. Locally, glassy black rock fragments are common. One outcrop included woody plant fragments. A few samples looked faintly welded, but no good examples were found. Although most breccias are rhyolitic, green dacitic breccia outcrops in one location. Tuff beds are interspersed throughout the volcanic section, and generally contain scattered to closely packed accretionary lapilli. The high proportion of lapilli in some beds suggests they were concentrated and redeposited by currents; beds containing scattered lapilli are probably air fall tuffs.

The contact between the rhyolite unit and the overlying clastic rocks is gradational over several metres. The clastic rocks resemble those described and mapped as Taylor Creek Group by Tipper (1969). Where exposed on a ridge north of the head of Tredcroft Glacier, conglomerate, sandstone, and tuffaceous siltstone are interbedded with breccia and tuff beds at the top of the volcanic unit. The section grades up to an entirely sedimentary sequence. Conglomerates near the contact are graded, clast-supported and contain mostly siliceous volcanic clasts. Clasts are cemented with a distinctive blue opaline cement.

Because the sedimentary section is highly disrupted by thrusts and folds, we did not attempt to establish a stratigraphy within the sedimentary unit during our brief time in the area. In general, sandstone and siltstone are the dominant;

conglomerate is rare away from the contact with the rhyolite. Sandstones are dark grey to brown, and contain abundant rhyolite and chert grains. Some layers include 2-5 % detrital white mica and scattered biotite. Beds are typically about 0.5-1 m thick and are laterally continuous. Thicker beds contain discontinuous thin (5-10 cm thick) layers of pebbles. Steep, tabular crossbeds are common and trough crossbeds occur in a few places. Given the structural complexity of the area, we hesitate to interpret paleocurrent directions until we have better defined the structure.

A small panel of the Lower Cretaceous Cloud Drifter formation also outcrops in the Tredcroft Glacier area. The outcrops strongly resemble those east of Nude Creek, and consist of sandstone, siltstone and minor conglomerate. Conglomerates contain abundant siliceous volcanic and granitoid clasts and only a few mafic volcanic clasts. A pebble count showed the main clast types to be siliceous volcanic clasts (59 %), granitoid rocks (33 %), and andesite (8 %). Fragments of *Inoceramus*, belemnites, and pelecypods are locally abundant in sandstones, but none were well enough preserved to be useful for age determination.

The stratigraphically lowest part of the Cloud Drifter formation in this area consists of black pebbly mudstone. Pebbles in the mudstone include abundant siliceous volcanics, with lesser amounts of plagioclase crystals, andesite, and plant fragments. Although not found elsewhere in the formation, the similarity in clast types suggests that the pebbly mudstones are part of the Cloud Drifter formation.

Orange-weathering andesite breccia and aquagene tuff outcrop 30 m structurally below the lowest beds in the Cloud Drifter formation north of Tredcroft Glacier. Fresh samples are green and contain small plagioclase phenocrysts and scattered clumps of chlorite that appear to have replaced hornblende phenocrysts. Breccia textures are visible in some outcrops, and a few display small andesite fragments embedded in tuff. Prismatic calcite fragments and weathering pits in one outcrop are probably *Inoceramus* fragments. McLaren (1987) also reported *Inoceramus* in this or nearby outcrops.

The contact between the andesite and the Cloud Drifter formation is covered by scree, but two lines of evidence suggest that the contact is depositional. First, the presence of *Inoceramus* in both the andesite and the Cloud Drifter formation suggests an Early Cretaceous age for the andesite. *Inoceramus*, although not restricted to the Hauterivian, is characteristic of Hauterivian strata of the western Intermontane Belt in the Waddington and Taseko Lakes map areas (Jeletzky and Tipper, 1968; Tipper, 1969). Second, the andesite is a possible source for the andesitic pebbles and common plagioclase crystals in the adjacent pebbly mudstone, and andesitic detritus present throughout the Cloud Drifter formation.

The relation between Triassic rocks (Rusmore and Woodsworth, 1988) and the Cloud Drifter formation remains unclear. Tipper (1969) reported a sheared depositional contact between Triassic basalts (his unit 1) and the Cloud Drifter formation (his unit 12) in the Tredcroft Glacier area. In this area, outcrops assigned by Tipper (1969) to his unit 1 appear to be the andesitic breccias described above. The breccias do not resemble Triassic basalts found east of Nostetuko River, nor is it likely they are Triassic, because they contain fragments of *Inoceramus*. Triassic sandy limestone (Tipper, 1969, and pers. comm., 1988), outcrops structurally below outcrops of the Cloud Drifter formation, but this contact is covered with scree. An outcrop of Cloud Drifter formation also occurs on the other side of the Triassic limestone, indicating that at least one of the contacts is a fault.

ACKNOWLEDGMENTS

Kirsten Menking and John Rusmore were excellent field assistants; we thank them for their help and companionship. Mike King of White Saddle Air Services again provided expert helicopter support, and the generous hospitality of Audrey and Jen King made us feel at home while at Bluff Lake. The project was funded by National Science Foundation Grant EAR-8804806 to Rusmore, the Ford Foundation (Menking and Rusmore), and the Geological Survey of Canada (Woodsworth).

REFERENCES

Hutchison, W.W.
1982: Geology of the Prince Rupert-Skeena map area, British Columbia; Geological Survey of Canada, Memoir 394, 116 p.

Roddick, J.A. and Tipper, H.W.
1985: Geology, Mount Waddington (92N) map area; Geological Survey of Canada, Open File 1163.

Rusmore, M.E. and Woodsworth, G.J.
1988: Eastern margin of the Coast Plutonic Complex, Mount Waddington map area, B.C.; in Current Research, Part E, Geological Survey of Canada, Paper 88-1E, p. 185-190.

Tipper, H.W.
1969: Mesozoic and Cenozoic geology of the northeast part of Mount Waddington map-area (92N), Coast District, British Columbia; Geological Survey of Canada, Paper 68-33, 103 p.

Geology of Mission Ridge, near Lillooet, British Columbia

Meg Coleman[1]
Lithosphere and Canadian Shield Division

Coleman, M., Geology of Mission Ridge, near Lillooet, British Columbia; in Current Research, Part E, Geological Survey of Canada, Paper 89-1E, p. 169-175, 1989.

Abstract

The Bridge River terrane of southwest British Columbia has been deformed in the early Tertiary by several major faults and associated internal strain which overprint and obscure Mesozoic accretionary structures. The Mission Ridge fault, a major low-angle east-dipping normal fault, juxtaposes Bridge River schist and phyllite and probable Eocene foliated intrusions in the footwall against folded Paleogene sediments in the hangingwall. Some of the ductile footwall fabric is Paleogene. The Mission Ridge fault has been offset 3.5 km by normal movement on the Marshall Creek fault, a steep west dipping fault. The Marshall Creek fault may correlate with the Relay Creek fault to the northwest; there was probably normal and strike slip movement on this fault system. The northeastern boundary of the Bridge River terrane is the Yalakom Fault, a major northwest trending, complex, transpressional, strike slip fault, which dips 40 ± 10° northeastward, placing Jurassic-Cretaceous Tyaughton basin sediments above Triassic Bridge River Group.

Résumé

Le terrane de Bridge River dans le sud-est de la Colombie-Britannique a été déformé au début du Tertiaire par plusieurs grandes failles et une déformation interne associée qui se superposent à des structures d'accroissement du Mésozoïque et les masquent. La faille de Mission Ridge, grande faille normale légèrement oblique qui plonge vers l'est, jouxte le schiste et la phyllite de Bridge River et des intrusions feuilletées qui datent probablement de l'Éocène, dans la lèvre inférieure, contre des sédiments plissés du Paléogène dans la lèvre supérieure. La structure ductile de la lèvre inférieure date en partie du Paléogène. La faille de Mission Ridge a été décalée sur 3,5 km par un mouvement normal sur la faille de Marshall Creek qui plonge abruptement vers l'est. Cette dernière pourrait être corrélée avec la faille de Relay Creek vers le nord-ouest; il y a probablement eu un mouvement normal et un rejet horizontal qui se sont exercés sur ce réseau de failles. La limite nord-est du terrane de Bridge River est la faille Yalakom, important décrochement de transpression complexe de direction nord-ouest qui plonge à 40 ± 10° vers le nord-est, situant les sédiments du bassin du Tyaughton du Jurassique-Crétacé au-dessus du groupe triassique de Bridge River.

[1] Department of Earth Sciences, Carleton University, and Ottawa-Carleton Geoscience Centre, Ottawa, Ontario

INTRODUCTION AND REGIONAL SETTING

The purpose of this study is to determine the geometry and timing of internal and bounding structures of the Bridge River terrane in the vicinity of one segment of the 1988 Lithoprobe southern Cordilleran transect, near Lillooet, British Columbia (Fig. 1). Specifically, the orientation of the major faults (Yalakom, Marshall Creek, and others) is addressed in order to assist in interpreting the seismic reflection data collected in 1988. The tectonic history of eugeosynclinal rock units at the boundary of the Coast Plutonic Complex and the Intermontane Belt between 50 and 51° N is highly enigmatic. An already complex history of Mesozoic accretion and probable Eocene extension is obscured by Tertiary strike-slip faulting, involving northward movement of more outboard allochthonous terranes during and/or after accretion.

The Bridge River terrane, composed mainly of Middle Triassic to Middle Jurassic (Roddick and Hutchison, 1973; Monger, 1977; Potter, 1986) chert, argillite, basalt, minor limestone, alpine type ultramafic rocks and their metamorphosed equivalents, lies immediately west of the Yalakom Fault, a major strike slip fault (Fig. 1). This terrane has no clear connection to either Terrane I or II of Monger et al. (1982). In a recent study, Potter (1986) suggested that the Bridge River terrane formed during the mid-Mesozoic on the western margin of Terrane I, after accretion of Terrane I but prior to accretion of Terrane II.

Near Lillooet, the northwest-trending Yalakom Fault separates Jurassic-Cretaceous Tyaughton basin sediments

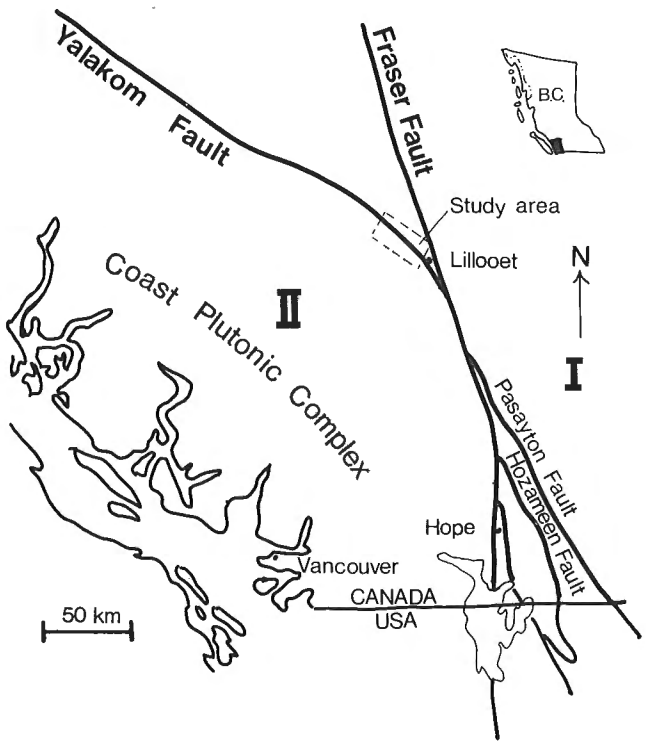

Figure 1. Map of southwestern British Columbia showing the study area and major structural features. I and II refer to Terrane I and Terrane II of Monger et al. (1982).

on the east from the Bridge River Group on the west. The Bridge River Group is deformed by both high- and low-angle northwest-trending faults, which are superimposed on an already complex internal structure.

Recent studies in the area include Potter (1983, 1986), which involved detailed mapping of the southern Shulaps Range including the Shulaps ultramafic complex; a detailed structural analysis of fractures within the Lillooet Group adjacent to the Fraser Fault by Miller (1988); and fission track dating of the Mission Ridge Pluton by Parrish (1983) which revealed significant rapid Oligocene-Miocene uplift.

LITHOLOGIES AND BOUNDING FAULTS

The following map units are described in sequence from the eastern boundary of the map area to the west (Fig. 2).

Lillooet Group

The Lillooet Group consists of marine siltstone, argillite, and conglomerate of volcanic provenance, separated from oceanic crust rocks of the Bridge River Group to the west by the Yalakom Fault (Fig. 2). The Lillooet group has a minimum thickness of 850 m (Duffell and McTaggart, 1952) with ages based on paleontological data which range from Late Jurassic to Early Cretaceous (Duffell and McTaggart, 1952; Trettin, 1961; Jeletzky, 1971).

In the southeast part of the map area the Lillooet Group consists predominantly of interbedded (1-10 cm) argillite and fine grained sandstone layers with cross bedding, graded beds, and load structures. Beds of coarse grained greywacke with occasional argillaceous rip-up clasts occur throughout this part of the unit.

Northwest of Applespring Creek, adjacent the Yalakom Fault, the Lillooet Group consists predominantly of coarse grained greywacke with beds of conglomerate. The distinctive conglomerate beds are lenticular and average 10 m in thickness and 50 m in length, and are composed of a limestone matrix, and about 75% clasts. The clasts include macro-fossil bearing limestone, granitic rocks, and green dacite with feldspar phenocrysts. The clasts are rounded and range from pebble size to cobbles 30 cm in diameter. Similar lenses of conglomerate in the Late Triassic Cadwallader Group were interpreted by Rusmore (1987) as filled channels. Samples of the limestone cobbles were collected for fossil dating. This occurrence of conglomerate is on strike with similar lithologies to the north along the Bridge River described by Leech (1953), but taken together, are in a different geographic area than that of the Cadwallader Group, although they could by correlative.

Yalakom Fault

The north-northwest trending Yalakom Fault separates the Lillooet Group in the eastern hanging wall from the older Bridge River Group to the west in the footwall. Careful field mapping along its trace allows its dip to be estimated as 40 ± 10° eastwards. This fault merges with the north-trending Fraser Fault near Lillooet and extends at least 250 km to the northwest (Fig. 1) with estimated Late Cretaceous-early

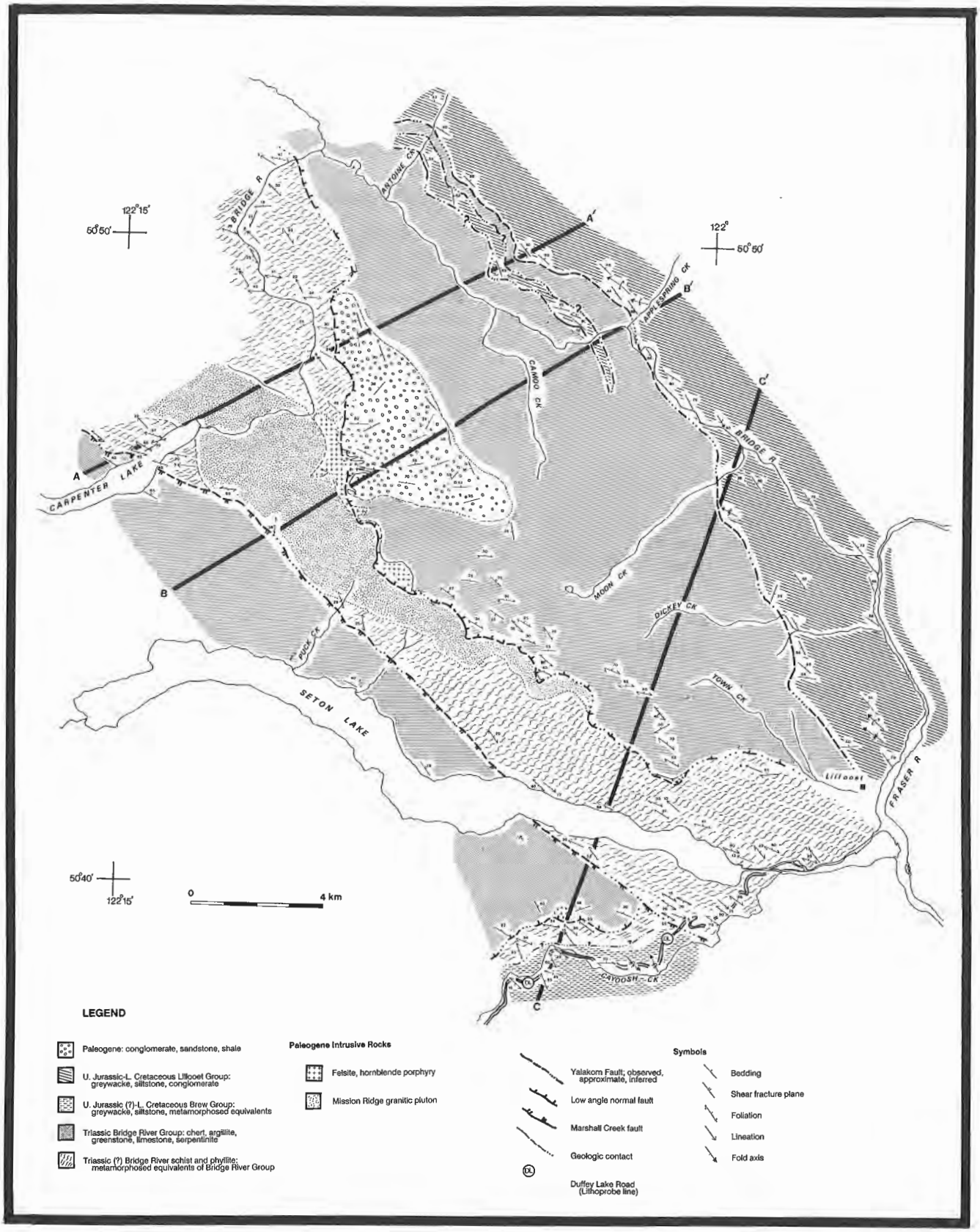

Figure 2. Geological map of the Mission Ridge area. Local relief is more than 2200 m and accounts for the arcuate trace of some of the major faults.

Tertiary right lateral strike slip displacement of 70 to 190 km (Monger, 1985; Tipper, 1969). Rocks of the Lillooet and Bridge River groups show brittle deformation at the fault boundary. Within the southeast end of the map area the fault is characterized by narrow zones of rusty-weathering, fuchsite-bearing, hematized fault breccia. The exact displacement sense on the fault is uncertain.

Bridge River Group

The Bridge River Group between the Yalakom and the low-angle Mission Ridge fault to the west is a chaotic mélange of ribbon chert, greenstone, pillow basalts minor greywacke, limestone olistoliths, and narrow serpentinite zones. It has a structural thickness of 2.5-4.5 km in this structural panel (Fig. 3).

Layers of grey radiolarian chert 1-5 cm thick, are separated by argillite layers 1 mm to 1 cm thick. Fault-bounded blocks of chert have multiple randomly oriented slickenside surfaces. These blocks are generally in fault contact with similarly deformed blocks of the previously mentioned lithologies. In the southern Shulaps Range, Potter (1986) found chert in depositional contact with limestone, greenstone, and sandstone. Ages from radiolaria found along the Bridge River and Carpenter Lake range from Middle Triassic to Middle Jurassic (Potter, 1986; J. Monger, pers. comm., 1988).

Greenstones range from well preserved pillow basalts to highly sheared and chloritized slickenside-bounded blocks. Serpentinized ultramafic rocks occur in discontinuous northwest-trending strands along the Bridge River. Limestone is present as lens-shaped olistoliths as large as 20 m across, and as 50 m thick layers laterally continuous for up to 2 km.

Paleogene sediments

Overlying the Bridge River group in probable sedimentary contact is a 1500 m thick section of well bedded conglomerate, black shale, and coarse grained sandstone. The conglomerate consists of about 70 % rounded clasts up to 15 cm across in a coarse grained sandy matrix. The clasts are mostly lithologies of the Bridge River Group with locally abundant clasts of cream-coloured felsite. None of the clasts were derived from the Bridge River schists, phyllites or associated granitoid intrusives (described below) presently exposed immediately to the west (Fig. 2). Black shales up to 10 m thick occasionally contain *Metasequoia* stems fossils and were collected for palynological dating. These strata are folded into a northwest-trending, northwest-plunging syncline which in turn is truncated by the Mission Ridge fault, described below.

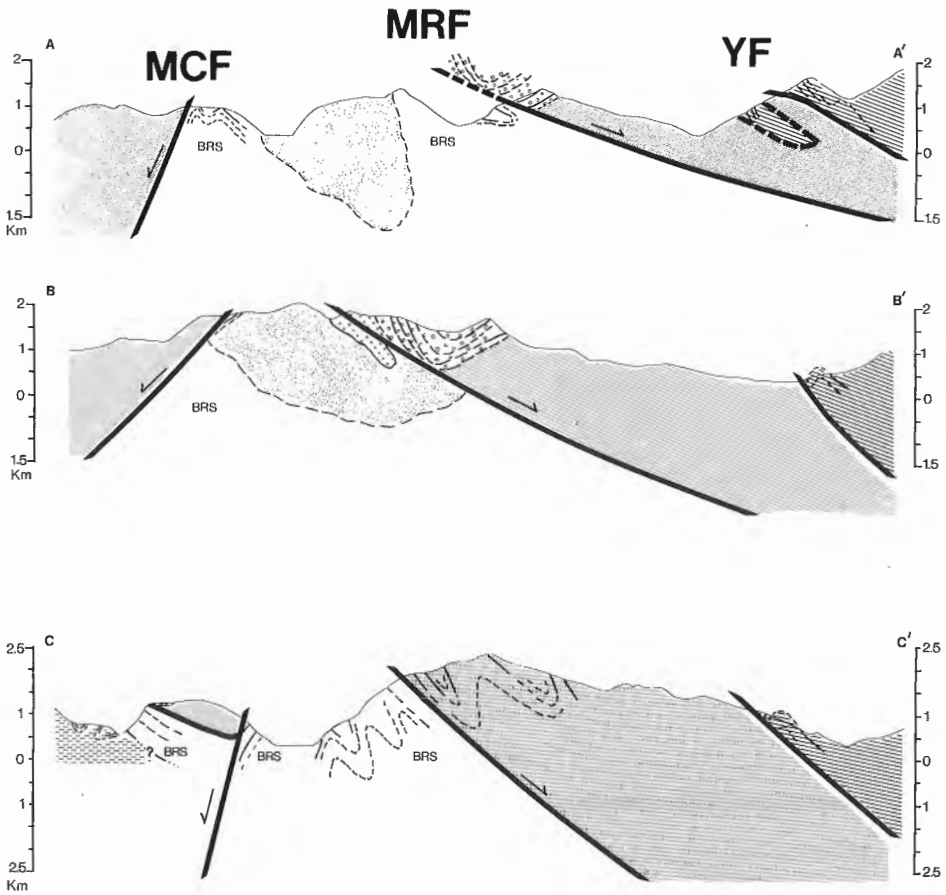

Figure 3. Cross sections A-A', B-B', and C-C'' from corresponding lines on Figure 2. Patterns refer to legend of Figure 2. BRS is Bridge River schist and phyllite; MCF, Marshall Creek fault; MRF, Mission Ridge fault; YF, Yalakom Fault. No vertical exaggeration.

Mission Ridge fault

The Bridge River Group and Paleogene sediments are separated from the underlying Bridge River schist and phyllite and Mission Ridge Pluton by a northeast-dipping low angle normal fault which steepens to the south (Fig. 2), termed here the Mission Ridge fault. The northwest part of this fault within the map area dips 20 ± 5° and truncates both bedding and broad folds within Paleogene sediments in the hanging wall, as well as foliated footwall rocks (cross-section A-A'' and B-B', Fig. 3). To the southeast the fault steepens to a 42 ± 5° dip (line C-C', Fig. 3), where a lower level of the fault zone is exposed; Bridge River Group rocks display a penetrative foliation parallel to the fault plane, particularly in the south.

Bridge River schist and phyllite

Metamorphosed equivalents of the Bridge River Group include well foliated and lineated metachert, phyllite, and chlorite schist; cut by abundant syn- and post-deformational pegmatitic and granitic intrusives (Fig. 4, 5). Metamorphic grade is lower greenschist to lower amphibolite facies.

The metacherts are mylonitic, characterized by layers of quartz 2 mm to 1 cm thick, separated by micaceous pelitic laminations, 1-5 mm thick. Phyllite contains muscovite, biotite, and minor garnet. Chloritized foliated greenstone and greenschist occur in layers 2-15 m thick, and as boudins 2-3 m wide surrounded by metachert and phyllite. Attenuated 1 cm to 2 m thick layers of light grey calcite marble occur locally.

Figure 4. Bridge River schist and phyllite cut by several syn- and post-deformational dykes near northwest end of Seton Lake.

Internal structure of Bridge River schist and phyllite

Pervasive foliation and isoclinal folds deformed by asymmetric folds record at least two stages of penetrative deformation, in part accompanied by significant shear strain. Foliation has a consistent northwest strike with shallow northeast dips. Lineation trends northwest with a shallow plunge. Asymmetric shear bands within appropriate lithologies indicate a consistent northwest over southeast sense of shear (Fig. 6).

Marshall Creek fault

The Bridge River schists are truncated on the west by the high angle Marshall Creek fault, which dips 50-75° or more to the southwest, juxtaposing the Bridge River schists with the lower grade Bridge River Group (Fig. 2).

Figure 5. Foliated late syn-tectonic granitic dyke in Bridge River schist and phyllite, Bridge River canyon.

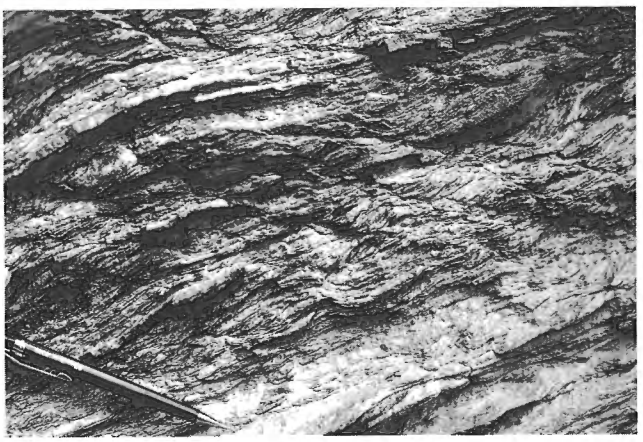

Figure 6. Shear bands in greenschist of Bridge River schist and phyllite with southeast directed sense of shear. In Bridge River canyon, looking northeast.

At the southern end of the map area the fault truncates a low-angle fault to its west. This low angle fault separates Bridge River schists and phyllites from overlying Bridge River Group as does the Mission Ridge fault to the east of the Marshall Creek fault. This low-angle fault is interpreted to be offset by the younger Marshall Creek fault. If it is assumed to be part of the Mission Ridge fault, restoration from cross-section C-C'' (Fig. 3) gives an estimated 3.5 km normal component of displacement on the Marshall Creek fault. This component probably increases to the north in the field area. Farther southeast the Marshall Creek fault juxtaposes the Bridge River schist and phyllite with the Brew Group (Fig. 2), described next.

Brew Group

The Early Cretaceous Brew Group, estimated by Duffell and McTaggart (1952) to be at least 2500 m thick, includes argillite, quartzite, conglomerate and their metamorphic derivatives. Within the map area along the Duffey Lake road, metagreywacke with rip up argillaceous clasts are recumbently folded. The metagreywacke is of greenschist metamorphic grade and muscovite defines the foliation. The nature of the contact between the Brew Group and overlying Bridge River schist and phyllite is unknown.

PALEOGENE INTRUSIVE ROCKS

Mission Ridge Pluton

An elongate foliated coarse grained pluton, termed the Mission Ridge Pluton, ranges in composition from granite to diorite, and intrudes the Bridge River schist and phyllite (Fig. 2). In the northwest part of the map area, the pluton crosscuts the foliation of the country rock and has a weak foliation with the same orientation (Fig. 7). The emplacement of the pluton is interpreted to be late syn-kinematic. Two dykes similar in composition to the Mission Ridge Pluton and with the same structural relationship to the Bridge River schist and phyllite gave Eocene preliminary U-Pb zircon ages (P. van der Heyden, pers. comm., 1988).

Figure 7. Mission Ridge Pluton (foreground) in sharp contact with Bridge River schist and phyllite (background). View to east of Carpenter Lake, above Bridge River canyon.

Felsite

A leucocratic felsite, in part hornblende-phyric, intrudes both hanging wall and footwall rocks of the Mission Ridge fault on the east flank of the Mission Ridge Pluton. The felsite is fractured by the fault and is therefore interpreted to have been emplaced during the last stages of faulting. This felsite is similar in appearance to the felsite clasts in the Paleogene sediments, although it is not necessarily the source of the clasts

DISCUSSION AND CONCLUSIONS

The sequence of tectonic events in this area is incompletely understood, but some relationships have been observed which place important constraints on the geometry, timing, and kinematics of the major fault boundaries. U-Pb dating of intrusions (in progress) will place tighter limits on ages of faulting, plutonism and ductile strain.

The Mission Ridge fault east of the Mission Ridge Pluton truncates southeast-verging mylonitic rocks, probable Eocene intrusions, and Paleogene sediments. Assuming a normal geothermal gradient, at least 12 km of Paleogene displacement is necessary to juxtapose upper greenschist facies rocks of the Bridge River schist and phyllite with subgreenschist rocks of the Bridge River Group and Paleogene sediments.

West-verging folds within the Lillooet Group have axial traces parallel to the Yalakom Fault and may be related to thrusting (in part oblique?); however, this folding event has not definitely been linked to faulting. Fifty kilometres northwest of Lillooet, where the Yalakom Fault is close to vertical, structures including synthetic and antithetic faults fit a model for dextral movement and transpression (Glover et al., 1988).

The Marshall Creek fault, which displaces the Mission Ridge fault, may extend as far northwest as 150 km from where it is truncated by the Fraser fault near Lillooet, if the correlation of the Marshall Creek fault with the Relay Creek fault (Glover et al., 1988), is valid. Glover et al. (1988) have estimated 8 km of right lateral displacement on the Relay Creek fault by restoring truncated units of late Jurassic Relay Mountain group. Post-Eocene displacement on the Marshall Creek fault could involve both a component of strike slip and normal movement.

It is evident from relationships within the Bridge River terrane that several episodes of deformation have taken place since the beginning of the Eocene. All are relevant to placing better timing constraints on the age of major dextral transcurrent faulting of the Fraser-Straight Creek fault system. Although each episode may not have involved either large amounts of displacement or large spans of time, they certainly reveal a complex Tertiary tectonic history. We must first be able to ''undo'' this more recent deformation in order to clarify older accretionary aspects of the Bridge River terrane.

ACKNOWLEDGMENTS

This project was funded by project 850001 of the Geological Survey of Canada (R. Parrish), a NSERC LITHOPROBE Supporting Geoscience Grant number 86 awarded to R. Parrish, and by a research grant from the British Columbia Geological Survey Branch. I am especially grateful to Randy Parrish for suggesting the project, providing advice and discussion, and for reviewing this paper. A thorough introduction to the field area and southwest British Columbia geology by Jim Monger is greatly appreciated. Carole Nuttall and Tiny Adamitz are thanked for their enthusiastic field assistance. LITHOPROBE contribution number 89.

REFERENCES

Duffell, S., and McTaggart, K.C.
1952: Ashcroft map area, British Columbia; Geological Survey of Canada, Memoir 262, 122 p.

Glover, J.K., Schiarizza, P., and Garver, J.I.
1988: Geology of the Noaxe Creek map area (92O/02); in Geological Fieldwork 1986, British Columbia Ministry of Energy Mines and Petroleum Resources, Paper 1988-1, p. 105-123.

Jeletzky, J.A.
1971: Cretaceous and Jurassic stratigraphy of some areas of southwestern British Columbia; in Report of Activities, Part A, Geological Survey of Canada, Paper 71-1A, p. 221-227.

Leech, G.B.
1953: Geology and mineral deposits of the Shulaps Range, southwestern British Columbia; British Columbia Department of Mines, Bulletin 32, 65 p.

Miller, M.G.
1988: Possible pre-Cenozoic left-lateral slip on the Yalakom fault, southwestern British Columbia; Geology, v. 16, p. 584-587.

Monger, J.W.H.
1977: Upper Paleozoic rocks of the western Canadian Cordilleran evolution; Canadian Journal of Earth Sciences, v. 14, p. 1832-1859.

Monger, J.W.H.
1985: Structural evolution of the southwestern Intermontane Belt, Ashcroft and Hope map areas, British Columbia; in Current Research, Part A, Geological Survey of Canada, Paper 85-1A, p. 349-348.

Monger, J.W.H., Price, R.A., and Tempelman-Kluit, D.J.
1982: Tectonic accretion and the origin of the two major metamorphic and plutonic welts in the Canadian Cordillera; Geology, v. 10, p. 70-75.

Parrish, R.R.
1983: Cenozoic thermal evolution and tectonics of the Coast Mountains of British Columbia 1. Fission track dating, apparent uplift rates, and patterns of uplift; Tectonics, v. 2, p. 601-631.

Potter, C.J.
1983: Geology of the Bridge River Complex, southern Shulaps Range, British Columbia: a record of Mesozoic convergent tectonics; unpublished Ph.D. thesis, University of Washington, 192 p.
1986: Origin, accretion, and postaccretionary evolution of the Bridge River terrane, southwest British Columbia; Tectonics, v. 5, p. 1027-1041.

Roddick, J.A., and Hutchison, W.W.
1973: Pemberton (east half) map-area, British Columbia 92 J; Geological Survey of Canada, Paper 73-17, 21 p.

Rusmore, M.E.
1987: Geology of the Cadwallader Group and the Intermontane-Insular superterrane boundary, southwestern British Columbia; Canadian Journal of Earth Sciences, v. 24, p. 2279-2291.

Tipper, H.W.
1969: Mesozoic and Cenozoic geology of the northeast part of Mount Waddington map area (92N), Coast District, British Columbia; Geological Survey of Canada, Paper 68-33.

Trettin, H.P.
1961: Geology of the Fraser River valley between Lillooet and Big Bar Creek; British Columbia Department of Mines and Petroleum Resources, Bulletin 44, 109 p.

Preliminary report on the structural setting along the southeast flank of the Coast Belt, British Columbia

J.M. Journeay and L. Csontos[1]
Cordilleran and Pacific Geoscience Division, Vancouver

Journeay, J.M. and Csontos, L., Preliminary report on the structural setting along the southeast flank of the Coast Belt, British Columbia; in Current Research, Part E, Geological Survey of Canada, Paper 89-1E, p. 177-187, 1989.

Abstract

This area records a complex history of deformation, metamorphism and igneous activity that can be partly linked to progressive shortening and transcurrent displacements along the continental margin of North American since Early Cretaceous. This study outlines the geometry, kinematics and relative timing of major fault systems along the southeast flank of the Coast Belt, between latitudes 49°15′ and 50°30′N.

Three distinct fault systems are recognized 1) an early set of low- and high-angle imbricate thrust faults inferred to have been responsible for the emplacement and southwestward telescoping of the northwest Cascade System and overlying Cascade Metamorphic Core; 2) the Harrison Lake Shear Zone, a right-lateral strike-slip fault that dies out along strike to the north; and 3) a relatively young system of northeast-trending, right-lateral strike-slip faults and associated high-angle reverse faults which may record crustal shortening along the continental margin since middle(?) Tertiary time.

Résumé

L'évolution de cette région est caractérisée par un ensemble complexe d'épisodes de déformation, de métamorphisme et d'activité volcanique, que l'on peut en partie attribuer au raccourcissement progressif de la croûte et à des décrochements survenus le long de la marge continentale de l'Amérique du Nord depuis le Crétacé inférieur. Dans cette étude, on esquisse la géométrie, la cinématique et la chronologie relative des principaux réseaux de failles de long du flanc sud-est de la zone Côtière entre 49°15′ et 50°30′N de latitude.

On a identifié trois réseaux de failles distinctes: 1) un ensemble initial de failles chevauchantes imbriquées, avec fortes et faibles inclinaisons, qui seraient responsables de la mise en place et du télescopage vers le sud-ouest de la partie nord-ouest du système de Cascade et du noyau métamorphique de Cascade sus-jacent; 2) la zone de cisaillement de Harrison Lake, décrochement dextre qui disparaît progressivement au nord le long de sa direction; 3) un système relativement récent de décrochements dextres de direction nord-est, et de failles inverses associées et fortement inclinées, qui témoignent peut-être d'un raccourcissement de la croûte terrestre le long de la marge continentale depuis le Tertiaire moyen (?).

[1] Departement de Geologie, Universite de Budapest, H-1088 Budapest, Muzeum korut 4/A, Hungary

INTRODUCTION

The southern Coast Belt (CB) of the Canadian Cordillera encompasses a wide variety of litho-structural and tectonic units (Fig. 1). These include: 1) Middle Jurassic to late Tertiary igneous rocks of the Coast Plutonic Complex (CPC), 2) Late Triassic to Early Cretaceous volcanic complexes and related sedimentary rocks of the Nooksack and Cadwallader terranes, 3) poly-deformed metamorphic and related plutonic rocks west of the Shuksan Fault, here correlated with the Northwest Cascade System (NWCS) of Brown (1987), and 4) high grade metamorphic and related plutonic rocks east of the Shuksan Fault, considered to be an extension of the Cascade Metamorphic Core (CMC; Monger, 1986).

The western margin of NWCS coincides with the Harrison Lake-Lillooet River Valley, and is defined by a northwest-striking system of ductile and brittle shear zones (Fig. 1). Although locally obscured by the emplacement of late- and post-kinematic plutonic rocks, these shear zones can be traced as far north as Lillooet Lake (50°15′N).

Northwest-striking shear zones east of Harrison Lake (Church Mtn. and Shuksan faults) have previously been interpreted as the products of east-northeast/west-southwest shortening and crustal imbrication (Misch, 1966; Lowes, 1972) associated with the collision of Wrangellia and accreted terranes of the northern Cascades in Early and mid-Cretaceous time (Davis et al., 1978; Monger et al., 1982; Monger, 1986). Recent studies in adjacent parts of northern Washington suggest that many of these fault structures may instead be part of a regional tectonic mélange formed during large-scale dextral transcurrent motion along the continental margin in Late Cretaceous-Early Tertiary time (Brown, 1987). The Harrison Lake Shear Zone (HLSZ; Crickmay, 1930) is recognized as an important strike-slip fault within the region (Monger, 1986), and is interpreted to be part of this tectonic mélange (Brown, 1987).

This paper outlines the geometry, kinematics and timing of fault structures along the western edge of the NWCS and CMC, north of Fraser River. Primary objectives of the study are: 1) to re-examine the history of deformation and metamorphism within these rocks in order to evaluate the proposed mechanisms of tectonic burial, uplift and unroofing within this region, 2) to establish the relative timing relationships and potential for kinematic linkages between deformation within the NWCS and CMC, along the HLSZ and within adjacent parts of the Coast Belt, 3) to determine the potential for structural control on base and precious metal deposits within the Harrison Lake-Pemberton district, and 4) to evaluate the extent to which crustal shortening (by underthrusting) and/or large-scale transcurrent displacements (transpression) may have controlled the structural and thermal evolution of the continental margin (CMC, NWCS and CPC) since Early Cretaceous time. Details of the mapping and results of the field research are shown in Figure 1. This map incorporates the regional mapping and syntheses of Crickmay (1930), Roddick (1965), Roddick and Hutchison (1973), Woodsworth (1977) and Monger (1986) and the detailed work of Reamsbottom (1971, 1974), Lowes (1972), Ray et al. (1984), Ray and Coombes (1985), Gabites (1985) and Arthur (1987).

LITHO-STRUCTURAL UNITS

Correlation of lithological assemblages throughout this part of the Coast Belt is hampered by the lack of fossil control throughout much of the section, by the abundance of plutonic rock and by abrupt variations in both metamorphic grade and structural style across tectonic boundaries. As a result, these lithological assemblages have been grouped together into seven distinct litho-structural units.

Harrison Lake Formation

The Harrison Lake Formation (Crickmay, 1930), which extends along the west side of Harrison Lake, is one of the most complete stratigraphic sections preserved in the southern Coast Belt. It is bounded on the east by brittle and ductile faults of the HLSZ, and on the west by undeformed hornblende granodiorites of the CPC (Fig. 1). The section ranges in age from Early to Middle Jurassic (Early Toarcian-Bajocian fossils; Crickmay, 1930; Arthur, 1987), and is dominated by intermediate to acidic flows and pyroclastic rocks which make up one of two major volcanic complexes within this part of the Nooksack Terrane. The section rests unconformably on Middle Triassic rocks of the Camp Cove Formation to the south, and is overlain by Upper Jurassic to Lower Cretaceous conglomerates of the Fire Lake section (Kent and Penninsula formations).

Metamorphism throughout the Harrison Lake Formation is of sub-greenschist facies, and includes extensive hydrothermal alteration in the lower part of the section. Deformation is limited to the development of large-amplitude regional folds and high-angle brittle faults. Penetrative fabrics are developed only within a narrow zone adjacent to the HLSZ.

Fire Lake section

The base of the Fire Lake section, along the west side of Harrison Lake, ranges in age from Early Cretaceous to Middle Albian, and is dominated by crystal and lithic tuff and associated volcaniclastic conglomerate, sandstone and shale of the Mysterious Creek, Billhook Creek, Kent and Penninsula formations. This assemblage underlies a second major volcanic complex of interlayered mafic flows and crystal tuff (Brokenback Hill Formation). North of Sloquet Creek, the section includes three distinct lithological units: a lower sequence of mafic and felsic metavolcanic flows, flow breccia and crystal tuff, a middle unit of lithic tuff, volcaniclastic wacke, conglomerate and siltstone, and an upper sequence of dark grey phyllite, chlorite schist, volcanic wacke, associated siltstone, and minor limestone. This northern section is lithologically similar to the lower Fire Lake sequence to the south (Penninsula and Brokenback Hill formations), and may well be part of the same stratigraphic sequence. Fossils occur only within limestone slivers of the uppermost lithological unit, and are reported to be of Early Cretaceous age (Roddick, 1965).

The northern section is bounded on the east by thrust faults of the NWCS, and on the west by plutonic and related migmatitic rocks of the CPC (Fig. 1). Rocks of relatively low competence (lithic tuff, volcaniclastic wacke and associated phyllite) are penetratively deformed throughout

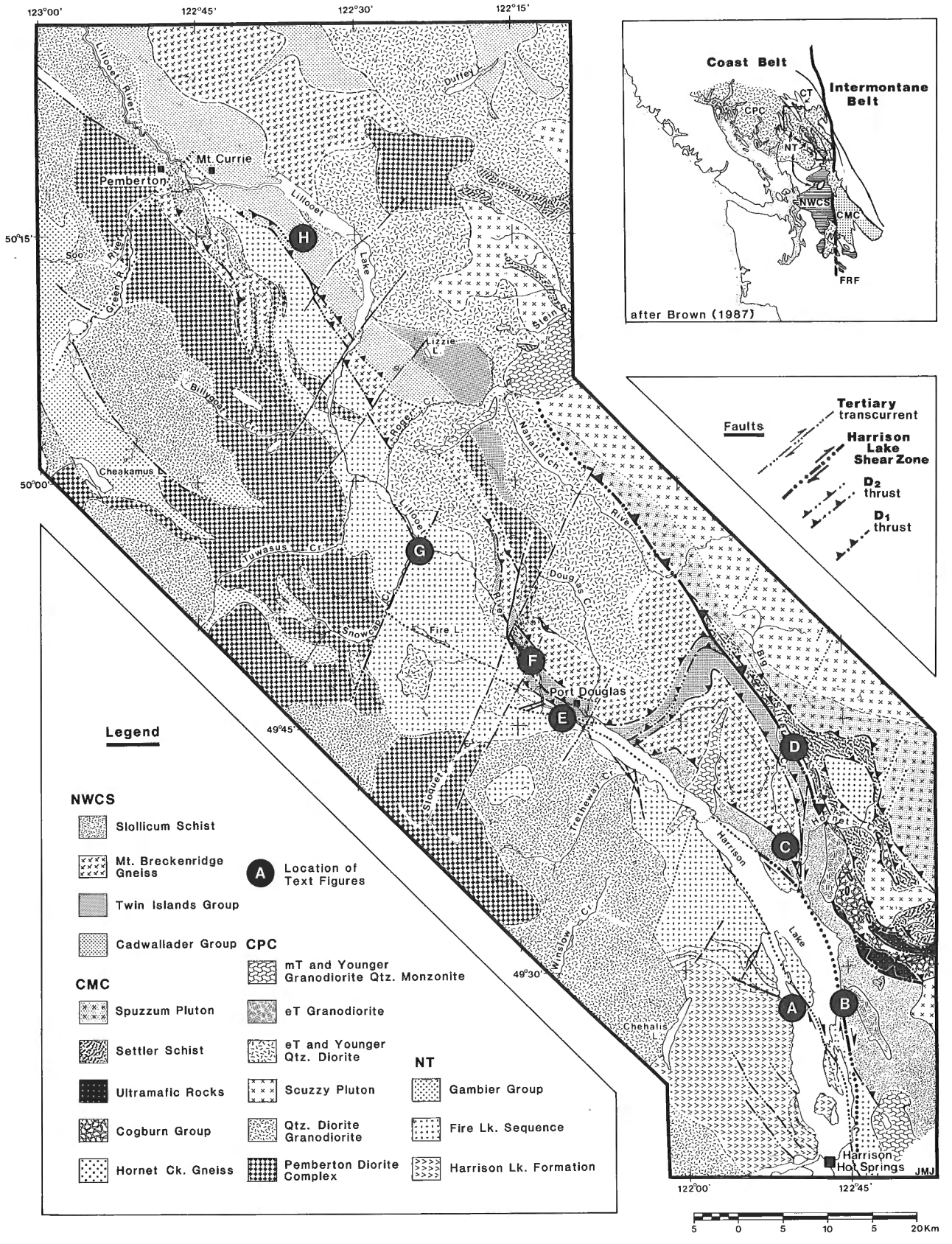

Figure 1. Compilation of geology in the southern Coast Belt, between 49°15′ and 50°30′N. Tectonic elements in this part of the Coast Belt include the Nooksack Terrane, Cadwallader Terrane, Northwest Cascade System (NWCS), Cascade Metamorphic Core (CMC), and varied intrusive igneous suites of the Coast Plutonic Complex (CPC); see inset (after Brown, 1987).

the section. Folded schistosity locally records evidence for two stages of deformation and associated fabric development. Metamorphism varies in grade from lower to upper greenschist facies, and is coeval with the development of early (S_1) flattening foliations.

Cadwallader Group

Characteristic lithologies of the Cadwallader Group, adjacent to and north of Lillooet Lake, include thin-bedded argillite, metavolcanic flows (greenstone), dark grey shale and phyllite, lithic tuff, volcanic wacke, minor conglomerate and limestone. The section is weakly strained, but contains minor structures which record at least two episodes of deformation. It is bounded on the northeast by quartz diorite and granodiorite and on the west by high-angle reverse faults and mixed plutonic rocks of the Pemberton Diorite Complex (Fig. 1).

Twin Islands Group

Metamorphic rocks of the Twin Islands Group (Roddick, 1965) occur in fault-bounded slivers northeast of Harrison Lake and adjacent to Lillooet River (Fig. 1). Dominant lithologies include volcanic conglomerate, hornblende gneiss, intermediate and acidic metavolcanic flows, crystal-lithic tuff, and lesser semi-pelitic, pelitic and talc-sericite schists. Deformation is penetrative and characterized by well-developed flattening foliations and associated down-dip elongation lineations. Metamorphic grade is lower and middle amphibolite facies and was syn-kinematic with respect to D_1 strain. Characteristic minerals include hornblende, garnet, biotite, staurolite, kyanite, and locally sillimanite.

Slollicum schist

The Slollicum schist as defined by Monger (1986) occurs in fault-bounded slivers east of Harrison Lake (Fig. 1). The unit is complexly deformed and consists primarily of interlayered metavolcanic flows and flow breccia, crystal tuff, volcanic wackes and dark grey phyllite, locally with lenses of volcaniclastic conglomerate. Lithological similarities suggest that these rocks may be the higher grade counterpart to the lower Fire Lake sequence. Minor structures indicate at least two episodes of regional folding and associated fabric development, followed by a younger episode of brittle/ductile strain associated with movement along the HLSZ. Metamorphic assemblages range from lower to upper greenschist facies and are syn- to late-kinematic with respect to early D_1 strain.

Cogburn Group

The Cogburn Group is a tectonic mélange of strongly disrupted and imbricated fragments of bedded chert, argillite, metavolcanic flows and minor limestone. Similar lithologies occur to the south in the hanging wall of the Shuksan Thrust (Elbow Lake Formation; Misch, 1966), and to the north in disrupted tectonic slivers of the Bridge River Group. Near the base of the mélange are discontinuous slivers of ultramafic rock and lenses of meta-diorite and gabbro, believed to be part of the Yellow Aster Complex (Lowes, 1972; Gabites, 1985; Monger, 1986).

Settler schist

The Settler schist structurally overlies the Cogburn Group mélange and is structurally interleaved with Late Cretaceous, high pressure granodiorites of the Scuzzy and Spuzzum plutons. It is complexly deformed, and consists predominantly of pelitic and semi-pelitic schist, quartzo feldspathic gneiss, amphibolitic gneiss, minor quartzite and lenses of ultramafic rock. As pointed out by Lowes (1972), these lithologies resemble those of the Chiwakum schist in western Washington, and may in part be correlative with high grade gneisses of the Skagit Metamorphic Suite (Monger, 1986).

Mineral assemblages record at least two distinct episodes of metamorphism; an early Barrovian event characterized by syn- and late-kinematic porphyroblasts of kyanite, staurolite, hornblende, and garnet, and a younger Buchan overprint defined by overgrowths of post-kinematic sillimanite, hornblende and associated lower grade phases.

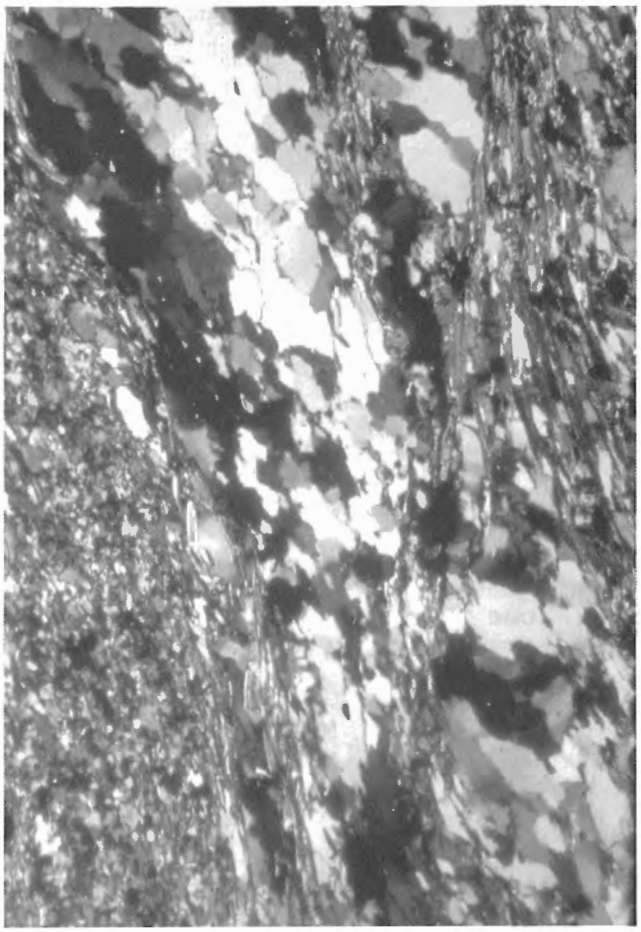

Figure 2. Location E photomicrograph of secondary asymmetric quartz fabrics within sheared quartz-rich horizons in gneissic granodiorite along the contact between slivers of Twin Islands Group. Shear sense indicators record top-to-the-southwest displacement. The view is to the southeast, perpendicular to L_2.

Plutonic rocks

Plutonic suites which either predate or coincide with assembly of the NWCS and CMC in Early to Late Cretaceous time include: 1) foliated Triassic gneisses (225 Ma, U-Pb; Gabites, 1985) of the Hornet Creek complex (Reamsbottom, 1974; Monger, 1986), 2) Middle and Late Jurassic granitoid rocks of the CPC (P. van der Heyden, pers. comm., 1988), 3) Late Cretaceous hornblende granodiorites (96 Ma, U-Pb; Gabites, 1985) and associated leuco-granites of the Mt. Breckenridge Complex (Reamsbottom, 1974; Monger, 1986), and 4) Late Cretaceous high-pressure granodiorites of the Spuzzum and Scuzzy plutons (104 Ma, U-Pb; R.L. Armstrong, pers. comm., 1988; and 86 Ma, U-Pb; R.R. Parrish, pers. comm., 1988), respectively (Richards and McTaggart, 1976; Monger, 1986).

Plutonic rocks of the CPC which postdate the assembly of the NWCS and CMC form much of the southern Coast Belt. They are predominantly granodiorite and quartz diorite in composition, but locally include lesser amounts of granite and gabbro. At least three distinct plutonic suites are recognized: an older suite (age uncertain) of diorite, hornblende granodiorite and lesser amounts of gabbro, quartz diorite and/or biotite granite (Pemberton Diorite Complex); an intermediate suite of hornblende granodiorite and quartz diorite, characterized by K-Ar cooling dates of 19-25 Ma; and a younger suite of quartz monzonite, minor granite, dacite porphyry and miarolitic granodiorite.

STRUCTURAL SETTING

Three distinct fault systems are recognized in the southern Coast Belt (Fig. 1). These include: imbricate thrust faults of the Northwest Cascades System (NWCS) and adjacent Cascade Metamorphic Core (CMC); northwest-striking transcurrent faults of the Harrison Lake Shear Zone (HLSZ); and a crosscutting network of en echelon northeast-striking transcurrent faults and associated high-angle reverse faults.

Northwest Cascade System-Cascade Metamorphic Core

Northwest-striking imbricate fault structures of the NWCS and CMC include both an early set of northeast-dipping syn- to late-metamorphic thrust faults, and a younger set of late- and post-metamorphic high-angle reverse faults. Both sets of fault structures extend northward into the Coast Mountains, where they are intruded and locally obscured by late- and post-kinematic plutons of the CPC.

Geometry and kinematics

Early faults of the NWCS imbricate low grade metamorphic rocks of the Slollicum schist and adjacent Harrison Lake Group, higher grade metamorphic rocks of the Twin Islands Group and related meta-plutonic gneisses of the Mt. Breckenridge Complex (Fig. 1). These faults predate the development of a regional northeast-trending structural culmination centred around Mt. Breckenridge, and have been traced northward along the east side of Lillooet River to Rogers Creek. Individual faults in the system are characterized by discontinuous hanging wall slivers of foliated granite and/or granodiorite, and are recognized in the field by localized zones of high strain (10-20 m wide) in which mylonitic foliations and associated down-dip stretching lineations are well-developed. Kinematic indicators in most of these ductile shear zones yield a consistent upper-plate-to-the southwest sense of displacement (Fig. 2), and support a thrust-imbrication model (Crickmay, 1930; Misch, 1966; Lowes, 1972) for early assembly of the NWCS. The magnitude of tectonic overlap between the NWCS and adjacent parts of the Coast Belt is unknown, but is likely to be tens of kilometres.

Late generation faults of the CMC postdate development of the Mt. Breckenridge antiform, and are responsible for emplacement of the Cogburn Group mélange, high-pressure metamorphic rocks of the Settler schist and foliated granodiorite of the Spuzzum Pluton. Shear zones separating these tectonic slivers dip steeply to the northeast, and locally cut across pre-existing faults of the NWCS. They are characterized by zones of complex folding in which flattening foliations and associated down-dip stretching lineations are both well-developed. Reliable kinematic indicators, seen only along the base of the mélange, consistently yield a northeast-side-up sense of shear (Fig. 3). The basal fault of this system extends northward along Nahatlatch ridge to the headwaters of the Stein River, and southward to the Fraser River, where it is interpreted to be part of the Shuksan Thrust Zone (Lowes, 1972; Monger, 1986).

Figure 3. Location D well foliated gneisses and schists along sheared contact between Cogburn Group and overlying Settler schist. View is to the southeast.

Minor structures

Minor structures associated with both early and late imbrication of the NWCS and CMC are represented by several distinct sets of southwest-verging asymmetric folds and associated axial planar foliations (Fig. 4). Early generation (F_1) folds occur at all structural levels of the thrust belt and display regional variations in both shape and orientation. Folds developed along the leading edge of the thrust belt (NWCS) are typically upright to slightly overturned, with steeply-dipping axial surfaces and shallow north-northwest-plunging hingelines (Fig. 5). At higher structural levels, these folds become increasingly more flattened and overturned with hingelines that are moderately to steeply inclined to the northeast. In regions of highest strain, these folds are tight to nearly isoclinal, and display variable amounts of hinge zone rotation. Axial planar to these early F_1 folds is a well-developed schistosity defined by flattened sedimentary and volcanic clasts and by the preferred orientation of platy metamorphic minerals. In zones of high strain, this foliation contains a down-dip lineation defined by elongate relic phenocrysts, stretched pebbles and clasts, pressure shadows, and the preferred orientation of metamorphic minerals such as actinolite and hornblende.

Overprinting these early structures are a younger set of F_2 minor folds and associated axial planar S_2 crenulations (Fig. 6). As with earlier F_1 structures, these late-stage asymmetric folds are open and upright within basal thrust sheets of the NWCS, and become increasingly more attenuated and inclined at higher structural levels. In zones of high strain, these folds are tight to isoclinal with steeply inclined hingelines that are locally parallel with down-dip stretching lineations.

Variations in the geometry and distribution of both F_1 and F_2 folds reflect regional strain gradients within the NWCS and CMC, and are attributed to flattening and rotational strains associated with thrust imbrication. However, given the uncertainty in the absolute timing of deformation within thrust sheets of the NWCS and CMC, no attempt is made to correlate D_1 and D_2 structures across the Shuksan Thrust.

Relationships between deformation and metamorphism

The earliest episode of metamorphism (M_1 garnet, kyanite and amphibole growth) outlasts F_1 folding and associated fabric development in basal thrust sheets along the leading edge of the NWCS (i.e. Slollicum schist-Twin Islands Group), and is attributed to tectonic burial accompanying early imbrication. Isograds associated with this early episode of metamorphism are in turn cut by younger D_2 shear zones along the base of the Cogburn Group mélange (Lowes, 1972). Sillimanite and hornblende, which occur as late overgrowths adjacent to these crosscutting shear zones (Lowes, 1972), are interpreted to be products of re-heating during renewed overthrusting and westward telescoping of higher grade metamorphic rocks within the core of the metamorphic hinterland.

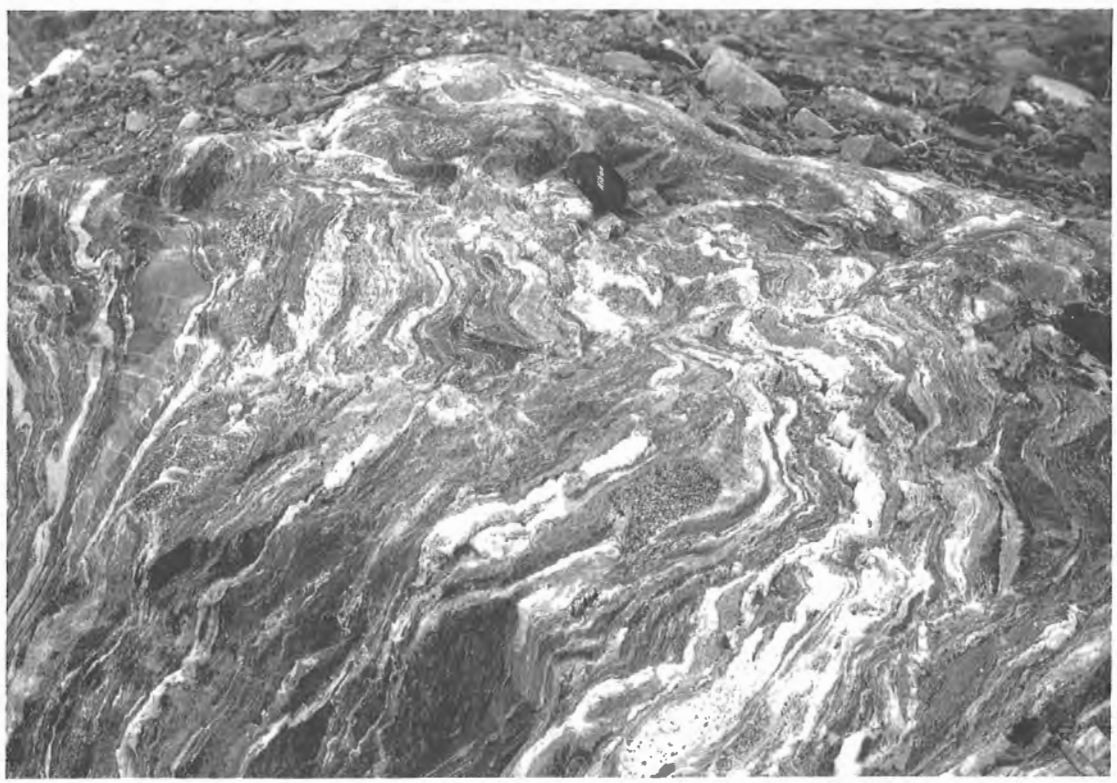

Figure 4. Location F poly deformed meta volcanics of Twin Islands Group within upper thrust sheets of the NWCS north of Harrison Lake. Overprinting relationships record at least two episodes of penetrative deformation in this region.

Figure 5. Location H open, asymmetric F_1 folds developed in multilayered sequence of volcanic wacke and siltstone of the Cadwallader Group, west of Lillooet Lake. Hinge zones plunge southwest and contain a well developed axial planar (S1) cleavage.

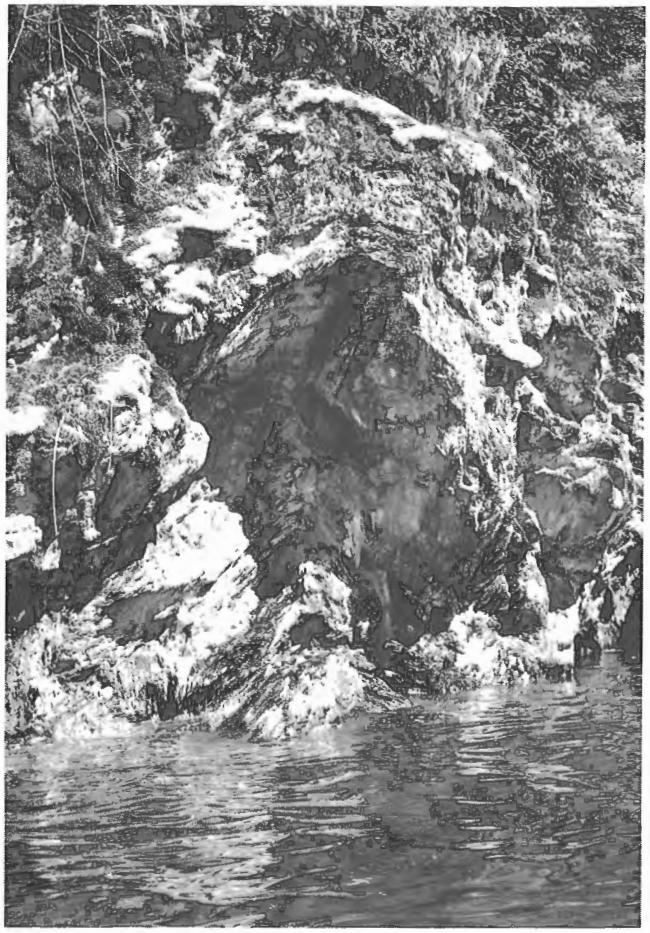

Relative timing

The relative timing of thrust imbrication and associated metamorphism within the NWCS and overlying CMC is bracketed by the involvement of 96 Ma metaplutonic gneiss of the Mt. Breckenridge Complex during early-stage thrusting, and by the emplacement of post-kinematic 86 Ma intrusions of the Scuzzy Pluton (U-Pb dates on zircon; R.R. Parrish, pers. comm., 1988). K-Ar hornblende and Rb-Sr biotite dates range from 66-88 Ma (Gabites, 1985) and give an estimate for the age of post-metamorphic cooling.

Harrison Lake Shear Zone

The Harrison Lake Fault (Fig. 1), initially recognized by Crickmay (1930), is a northwest-striking fault zone which separates foliated metavolcanic and related metasedimentary rocks of the NWCS from weakly deformed and apparently un-metamorphosed rocks of the adjacent Harrison Lake Group (Roddick, 1965; Monger, 1970, 1986; Arthur, 1987). As defined in this study, the Harrison Lake Shear Zone (HLSZ) comprises a network of ductile and brittle strike-slip faults in the Harrison Lake-Lillooet River valleys.

Figure 6. Location C upright F_2 fold hinge in phyllites of Slollicum schist. S_2 slaty cleavage is the form surface. Refolded F_1 fold hinges occur locally.

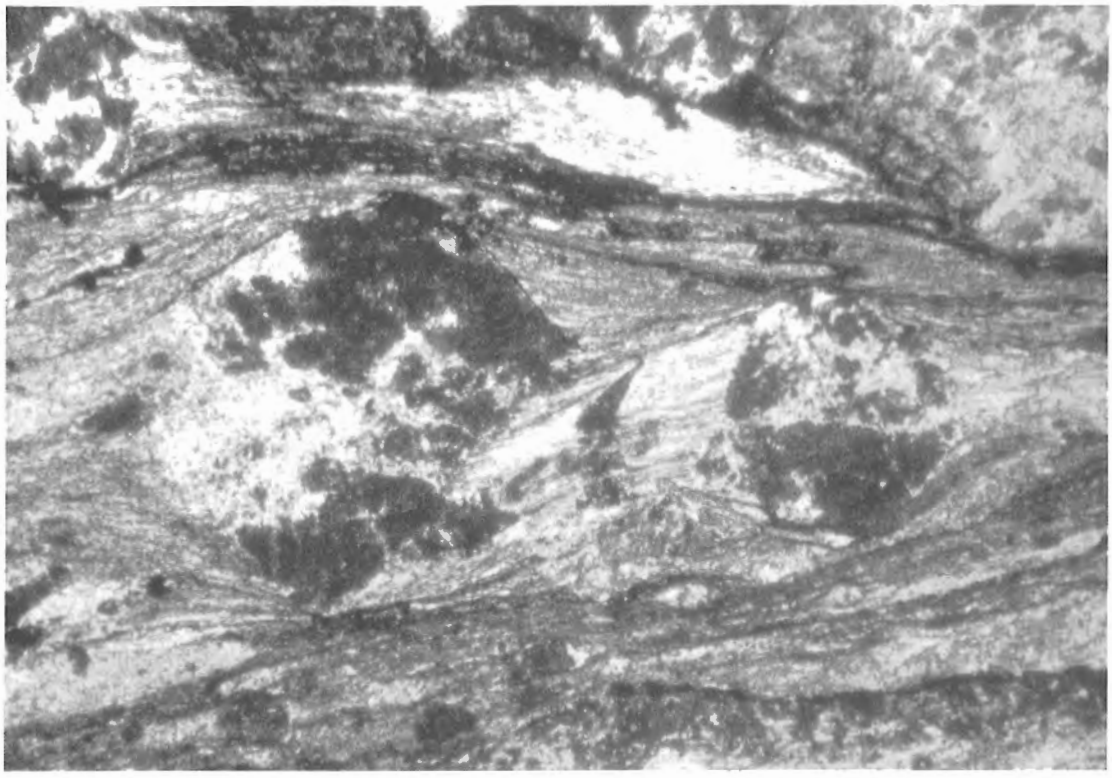

Figure 7. Location B photomicrograph of L-S fabrics in ductile shear zones along the east side of HLSZ. Shear sense indicators record a dextral transcurrent displacement. View is to the northeast, perpendicular to stretching direction.

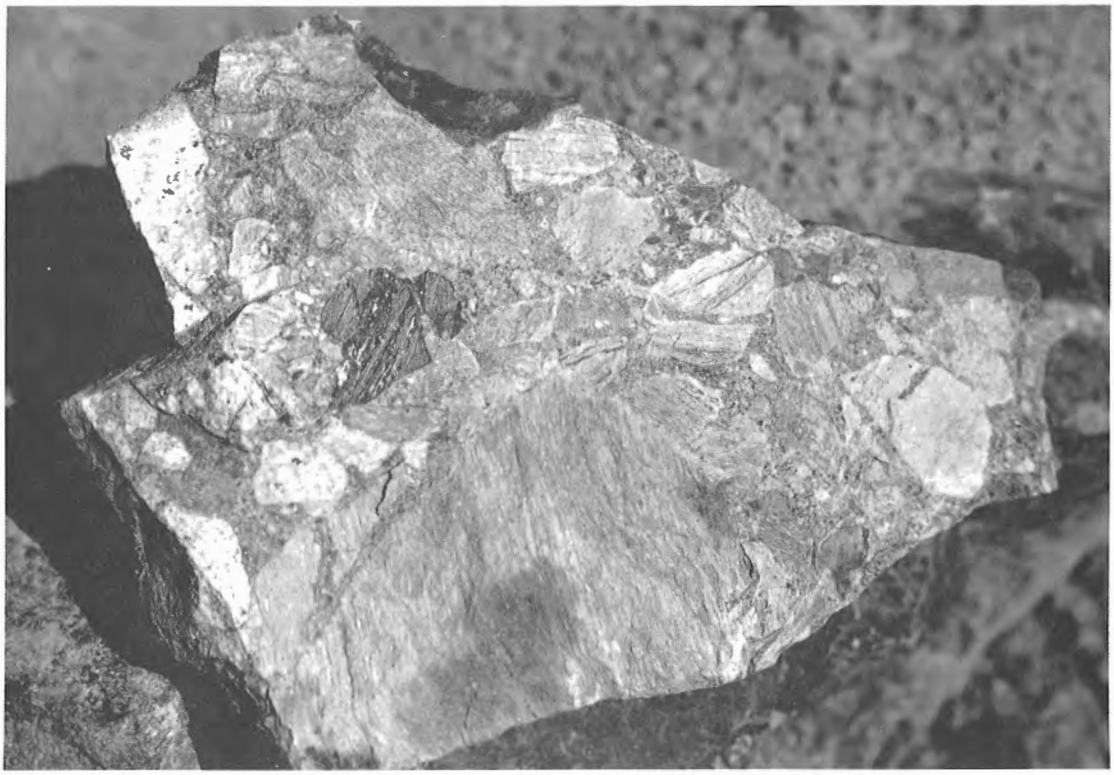

Figure 8. Location G tectonic breccia along the northernmost tip of HLSZ, near confluence of Snowcap Creek and Lillooet River. Breccia fragments are well foliated and include fragments of foliated felsic metavolcanic flows, tuffs and related meta sedimentary rocks of the Fire Lake sequence.

Geometry and kinematics

The western boundary of the shear zone is a northwest-striking brittle fault which separates a well-foliated hanging wall sequence of volcanic rocks and associated phyllites from underlying nonfoliated strata of the Brokenback Hill Formation. The fault is well exposed on Cascade Penninsula and adjacent parts of Long Island, and extends north along the shore of Harrison Lake (Arthur, 1987; Monger, 1986) where it is cut by post-kinematic granodiorite of the Doctors Point Pluton (Fig. 1). Conjugate shear fractures in three separate localities indicate an oblique, right-lateral sense of displacement, but likely record only a small component of net slip across this part of the fault zone.

The eastern boundary of HLSZ, in the vicinity of Cascade Penninsula, is defined by a north-northwest-striking network of closely spaced ductile shear zones (5-10 m wide) in which mylonitic fabrics and associated strike-parallel stretching lineations are locally well developed. This network of shear zones cuts across basal thrusts of the NWCS, and envelops domains of foliated rock in which pre-existing folds and thrust-related fabrics are locally preserved (Fig. 1). Kinematic indicators within fault zones defining this segment of the HLSZ, along with associated minor folds adjacent to these fault strands, yield a consistent sense of oblique, right-lateral displacement (Fig. 7). The amount of displacement across HLSZ increases along strike to the south, but is presently unknown.

The overall geometry of the HLSZ is interpreted to be a leading imbricate fan with strike-slip displacement being partitioned across a network of fault zones in the north, and feeding into a concentrated zone of ductile shear to the south. High-angle brittle faults north of Harrison Lake (Fig. 8), and along Big Silver Creek are considered to be part of this imbricate fan, and collectively define the leading tip of the fault system. Ductile strike-slip shear zones, recognized farther south in the vicinity of the Shuksan thrust (Brown, 1987), may represent the extension of the HLSZ south of the Fraser River (Monger, 1986).

Minor structures

Minor structures associated with strike-slip displacement across the HLSZ include both asymmetric minor folds and well-developed stretching fabrics within zones of ductile strain, and a complex system of both shear and extensional fractures within zones of brittle deformation (Figs. 8,9).

Stretching lineations plunge gently to the northwest and are defined by elongate phenocrysts, pressure shadows and by stretched volcanic, granite and sedimentary clasts and strained fossils. Aspect ratios of deformed clasts in pebble conglomerates along Cascade Penninsula are about 6:1 and record a large component of longitudinal strain. Minor folds and associated crenulations are developed chiefly within foliated rocks along the eastern margin of the shear zone. They occur primarily as asymmetric buckle folds with steeply dipping axial surfaces and inclined hingelines. They are typically overturned to the southeast and are locally reclined in geometry. Differences in the orientation of these folds are attributed in part to variations in the dip of layering prior to buckling.

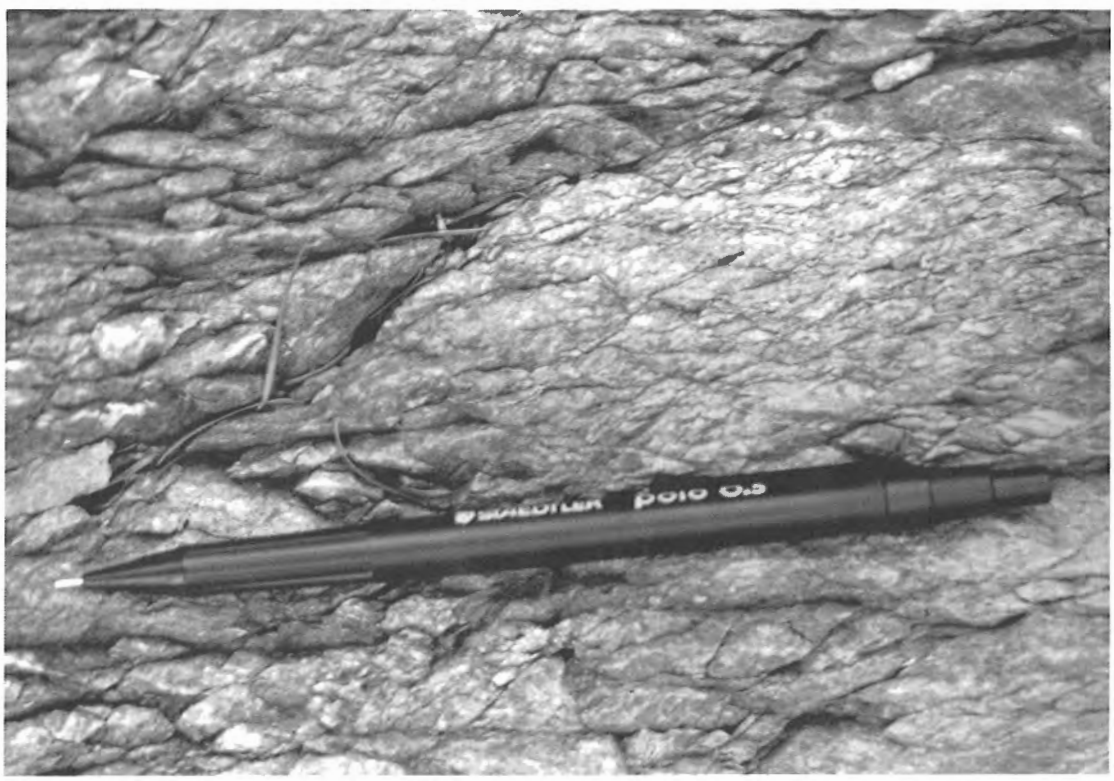

Figure 9. Location A domainal fracture cleavage in low grade volcanics of the Harrison Lake Formation adjacent to brittle fault strands along the west side of HLSZ on Cascade Penninsula.

Relative timing

Displacement across the HLSZ postdates regional metamorphism within the NWCS, and is interpreted to be Late Cretaceous and/or Early Tertiary in age (Monger, 1986). Crosscutting, sheet-like intrusions of undeformed granodiorite (e.g. Doctors Point Pluton) yield K-Ar cooling ages of 22-24 Ma (Ray and Coombes, 1985), and place an upper limit on the timing of strike-slip displacement across this segment of the shear zone.

Tertiary fault system(s)

Tertiary fault structures are represented by a set of northeast-striking dextral transcurrent faults, a conjugate set of northwest-striking high-angle reverse faults and isolated, but locally important east-northeast-striking normal faults. These structures postdate displacement across the HLSZ, and may be kinematically linked as part of part of a regional fault system within the southern Coast Belt.

Transcurrent faults

Northeast-striking transcurrent faults, previously reported by Roddick (1965) and Monger (1986), represent the dominant structural features in the northeast corner of the Vancouver map area (92G) and, together with related high-angle reverse faults, are the major structural features within the southeast corner of the Pemberton map area (92J). Eight new transcurrent fault structures have been mapped (Fig. 1). These faults offset northwest-striking thrust faults of the NWCS and high-angle northwest-striking transcurrent faults of the HLSZ. The transcurrent faults appear to be in part coeval with the emplacement of a relatively young suite of plutonic rocks (about 20-25 Ma) which extends along the southeast margin of the Coast Belt. Brittle structures within these northeast-striking faults yield a consistent right-lateral sense of displacement. Magnitudes of apparent strike-slip displacement range from several hundred metres to as much as 10 km (Snowcap Creek Fault).

High-angle reverse faults

High-angle reverse faults which postdate HLSZ were previously reported along the west side of Harrison Lake by Ray and Coombes (1985), but were of unknown regional significance prior to this study. Several important reverse faults and related fold structures have been mapped within and along the eastern margin of the Pemberton Diorite Complex. In addition, conjugate high-angle reverse faults and related folds mark the boundary between the Fire Lake and Cadwallader groups west of Lillooet Lake (Fig. 1). Kinematic indicators within these shear zones yield both northeast-side-up and southwest-side-up senses of displacement, suggesting that they may be related as a conjugate set. However, the timing relationships between these two sets of faults are unknown. These structures are kinematically compatible with, and may be coeval with the system of northeast-striking transcurrent faults described above.

Kinematic model

The kinematics and relative timing relationships between northeast-striking transcurrent faults and northwest-striking reverse faults suggests that these structures are most likely part of a regional Tertiary fault system (post-26 Ma) that has formed along the continental margin in response to orthogonal (northeast-southwest directed) shortening of the crust. This interpretation suggests the possibility that Eocene and younger deformation (and uplift?) within the southern Coast Mountains may be coupled with subduction along the continental margin.

EXPLORATION POTENTIAL

The leading tip of the Harrison Lake Shear Zone is known to be an important structure in localizing economic gold deposits within southwestern B.C. (Ray et al., 1984; Ray and Coombes, 1985). The gold belt is associated primarily with brittle fault systems along the western margin of the shear zone, and is most likely offset to the north by younger northeast-striking transcurrent faults.

Work this past summer suggests that these younger transcurrent faults may also be important structures in controlling the emplacement of epizonal late Tertiary plutons and in tapping associated hydrothermal systems. It follows that these transcurrent faults may be providing the necessary structural control for localizing economic concentrations of both base and precious metals within the region. This hypothesis is supported by observed spatial relationships between northeast-striking transcurrent faults, post-Miocene plutons and present day hydrothermal systems.

SUMMARY AND REGIONAL TECTONIC SIGNIFICANCE

The southeast flank of the Coast Belt is the locus for a complex history of deformation, metamorphism and igneous activity that can be linked in part to progressive shortening and transcurrent displacement along the continental margin of North America since Early Cretaceous time. Observations outlined above support the following conclusions and preliminary interpretations.

The NWCS was assembled by thrust imbrication of the Twin Islands Group, Slollicum schist and Mt. Breckenridge Gneiss, and is inferred to have been emplaced onto less deformed and unmetamorphosed rocks of the Nooksack terrane (Harrison Lake-Fire Lake groups) in Late Cretaceous time. Shear sense indicators in syn- to late-metamorphic fault zones which separate these tectonic slivers yield consistent upper plate to-the-southwest displacement, and support a thrust imbrication model.

Continued shortening of the crust, following emplacement of the NWCS, is believed to have been accommodated, in part, by southwestward overthrusting and telescoping of the Cascade Metamorphic Core (CMC) along high-angle reverse faults. At this latitude, CMC is defined by high-pressure metamorphic rocks of the Settler schist and related meta-plutonic rocks of the Spuzzum batholith. The basal

thrust of this fault system occurs beneath tectonic slivers of the Cogburn Group mélange, and is inferred to be the northward extension of the Shuksan Thrust.

The presence of CMC schists and gneisses in the hanging wall of the Shuksan Thrust at this latitude suggests that high-pressure schists of the Shuksan Suite, characteristic of the hanging wall south of the Fraser River, may have been tectonically removed during southwest overthrusting and telescoping of the CMC in Late Cretaceous time.

The Harrison Lake Shear Zone (HLSZ) is a right lateral transcurrent fault which splays northward into an imbricate fan of high-angle brittle faults. Displacement increases along strike to the southeast across a network of mylonitic shear zones that apparently feed into major dextral transcurrent faults of the northwest Cascades (Brown, 1987). HLSZ north of the Fraser River is interpreted to be the leading tip of a regional strike-slip fault system that was active some time in the Late Cretaceous and/or early Tertiary. Initiation of HLSZ may reflect either a change in relative plate motions along the continental margin in Late Cretaceous time, or perhaps the crustal response to oblique convergence (transpression) following major contractional events in the southeastern Coast Belt.

The geometry, kinematics and timing relationships between Tertiary faults in the southern Coast Belt suggests that these structures may be part of a regional fault system that has formed along the continental margin in response to a relatively young episode of northeast-southwest shortening. If correctly interpreted, these structures may provide a means of evaluating the crustal response to subduction of the Juan de Fuca Plate beneath North America since middle Tertiary time, and may help to explain patterns of recent uplift within the southern Coast Belt.

ACKNOWLEDGMENTS

This study was begun by J.M. Journeay as a PDF project under the joint supervision of J.W.H. Monger and G.J. Woodsworth; their support and introduction to the geological complexities of the region are greatly appreciated. Reconnaissance work in the Harrison Lake area (JMJ) was carried out in collaboration with Susie Gareau of Carleton University. Mapping responsibilities for the balance of the project were shared with László Csontos, an exchange student from Université de Lille, France. Field research was greatly facilitated and improved by the hard work and good humour of our assistant, Steve Hedberg. Assistance with drafting by Carol N. Journeay is gratefully acknowledged.

REFERENCES

Arthur, A.
1987: Mesozoic stratigraphy and paleontology of the west side of Harrison Lake, southwestern British Columbia; unpublished M.Sc. thesis, University of British Columbia, Vancouver.

Brown, E.H.
1987: Structural geology and accretionary history of the Northwest Cascade System, Washington and British Columbia; Geological Society of America, Bulletin, v. 99, p. 201-214.

Crickmay, C.H.
1930: The structural connection between the Coast Range of British Columbia and the Cascade Range of Washington; Geological Magazine, v. 67, p. 482-491.

Davis, G.A., Monger, J.W.H., and Burchfiel, B.C.
1978: Mesozoic construction of the Cordilleran "collage", central British Columbia to northern California; in Mesozoic Paleogeography of the Western United States, D.G. Howell and K.A. Douglass (eds.), Pacific Section, Society of Economic Paleontologists and Mineralogists, p. 1-32.

Gabites, J.E.
1985: Geology and geochronometry of the Cogburn Creek Settler Creek area, northeast of Harrison Lake, B.C.; unpublished M.Sc. thesis, University of British Columbia, Vancouver, 153 p.

Lowes, B.E.
1972: Metamorphic petrology and structural geology of the area east of Harrison Lake, British Columbia; unpublished Ph.D. thesis, University of Washington, 162 p.

Misch, P.
1966: Tectonic evolution of the northern Cascades of Washington State; Canadian Institute of Mining and Metallurgy, Special Volume 8, p. 101-148.

Monger, J.W.H.
1970: Hope map-area, west half (92H W1/2), British Columbia; Geological Survey of Canada, Paper 69-47, 75 p.
1986: Geology between Harrison Lake and Fraser River, Hope map area, southwestern British Columbia; in Current Research, Part B, Geological Survey of Canada, Paper 86-1B, p. 699-706.

Monger, J.W.H., Price, R.A., and Tempelman-Kluit, D.J.
1982: Tectonic accretion and the origin of two major metamorphic and plutonic welts in the Canadian Cordillera; Geology, v. 10, p. 70-75.

Ray, G.E. and Coombes, S.
1985: Harrison Lake Project (92H/5,12); 92G/9,16); in Geological Fieldwork 1984, British Columbia Ministry of Energy, Mines and Petroleum Resources, Paper 1985-1, p. 120-131.

Ray, G.E., Coombes, S., and White, G.
1984: Harrison Lake Project (92H/5,12; 92G/9); in Geological Fieldwork 1983, British Columbia Ministry of Energy, Mines and Petroleum Resources, Paper 1984-1, p. 42-53.

Reamsbottom, S.B.
1971: The geology of the Mt. Breckenridge area, Harrison Lake, B.C.; unpublished M.Sc. thesis, University of British Columbia, 143 p.
1974: Geology and metamorphism of the Mt. Breckenridge area, Harrison Lake, B.C.; unpublished Ph.D. thesis, University of British Columbia, Vancouver, 155 p.

Richards, T.A. and McTaggart, K.C.
1976: Granitic rocks of the southern Coast Plutonic Complex and northern Cascades of British Columbia; Geological Society of America, Bulletin, v. 87, p. 935-953.

Roddick, J.A.
1965: Vancouver North, Coquitlam and Pitt Lake map-areas, British Columbia; Geological Survey of Canada, Memoir 335, 276 p.

Roddick, J.A. and Hutchison, W.W.
1973: Pemberton (east half) map-area, British Columbia; Geological Survey of Canada, Paper 73-17, 21 p.

Woodsworth, G.J.
1977: Pemberton (92J) map area, British Columbia; Geological Survey of Canada, Open File 482.

Petrography and chemistry of the Meager Mountain volcanic complex, southwestern British Columbia

M.V. Stasiuk[1] and J.K. Russell[1]
Cordilleran and Pacific Geoscience Division, Vancouver

Stasiuk, M.V. and Russell, J.K., Petrography and chemistry of the Meager Mountain volcanic complex, southwestern British Columbia; in Current Research, Part E, Geological Survey of Canada, Paper 89-1E, p. 189-196, 1989.

Abstract

The Meager Mountain volcanic complex is located at the northern end of the Garibaldi volcanic belt and is representative of Canadian Cascade volcanism. It is a dominantly calc-alkaline Quaternary volcano with lavas and pyroclastic rocks ranging in composition from andesite to dacite and Pliocene to Recent in age. Subordinate volumes of peripheral but contemporaneous Pleistocene mafic to intermediate alkaline rocks occur as lava flows and breccias.

Résumé

Le complexe volcanique de Meager Mountain est situé à l'extrémité nord de la zone volcanique de Garibaldi et est représentatif du volcanisme des Cascades au Canada. Il s'agit d'un volcan du Quaternaire essentiellement calco-alcalin dont les laves et les roches pyroclastiques varient en composition de l'andésite à la dacite, et en âge du Pliocène au Quaternaire récent. Des volumes subordonnés des roches alcalines mafiques à intermédiaires du Pléistocène, périphériques mais contemporaines, se présentent sous forme de coulées de laves et de brèches.

[1] Department of Geological Sciences, University of British Columbia, Vancouver, B.C. V6T 2B4

INTRODUCTION

The Meager Mountain volcanic complex is situated about 150 km north of Vancouver in the Coast Mountains, between the Lillooet River and Meager Creek (Fig. 1). The edifice is at the north end of the Garibaldi volcanic belt, the northern extension of the Cascades volcanic belt. The ultimate cause of the Quaternary volcanism is thought to be the subduction of the Juan de Fuca plate beneath the North American plate, and the belt is terminated at the Nootka Fault trend (Green et al., 1988). Reliable K-Ar dates from volcanic rocks within the Meager Mountain complex and within the rest of the Canadian belt range from 2.2 Ma to 2350 years BP. Volcanic rocks vary from basalt through andesite to dacite and the style of volcanism is equally variable, ranging from airfall pyroclastic deposits through pyroclastic flows to lava domes and flows.

Although situated only a short distance from Vancouver, the Meager Mountain volcanic rocks are not as well studied as other Quaternary volcanic centres in British Columbia (e.g. Green, 1981). The Bridge River ash, which represents the youngest volcanic activity in southwestern B.C., was mapped and studied petrographically by Nasmith et al. (1967). Read (1977) produced a 1:20 000 scale geological map of the volcanic complex, under the auspices of B.C. Hydro's exploration program for geothermal energy. Radiometric dates of the rocks have been done by Anderson (1975), Read (1977) and Green et al. (1988). Ages of lavas have been estimated from C^{14} measurements on charred wood by Read (1977) and Green et al. (1988).

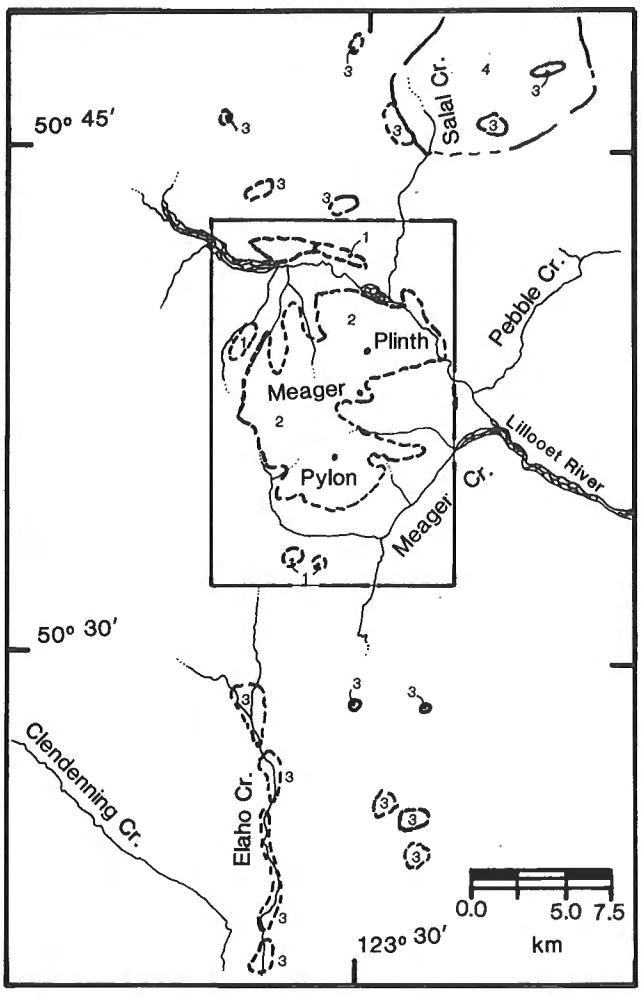

Figure 1. Generalized geology of Meager Mountain volcanic complex (boxed) and surrounding area showing distribution of Quaternary volcanic rocks. 1: Alkaline volcanic rocks (basalt to trachybasalt flows and pyroclastics); 2: Meager Mountain volcanic complex calc-alkaline volcanic rocks; 3: Other areas of Garibaldi Group volcanic rocks (basaltic to rhyodacitic); 4: Salal Creek Pluton (Miocene). Adapted from Woodsworth (1977).

The broad objective of our current project is to add to the existing knowledge of the Meager Mountain complex. Specifically the objectives are twofold: to characterize the chemistry, mineralogy and mineral chemistry of the volcanic complex and to provide a detailed stratigraphic analysis of the volcanic rocks to ascertain the nature of volcanism in the past. During the 1988 field season we sampled younger and fresher volcanic units defined by Read (1977), and sampled and mapped in detail the stratigraphy of the youngest lithological units, named informally the Bridge River assemblage (Read, 1977). In this report we give results of our preliminary field, petrographic and chemical analyses of these rocks (Tables 1, 2, and 3).

GENERAL GEOLOGY

The Garibaldi volcanic belt lies within the Coast Belt and obliquely cuts the regional northwesterly-trending structures (Read, 1977; Green et al., 1988). The basement is a mosaic of plutonic and metamorphic rocks cut by discrete plutons as young as Miocene. The Meager Mountain volcanic rocks mantle the plutonic and metamorphic rocks, and also intrude and disrupt them.

The Meager Mountain volcanic complex is Tertiary to Quaternary and is dominated by the products of calc- alkaline volcanism. Its volcanism both predates and postdates the major recognized glacial periods in southern B.C.; Salmon Springs Glaciation, 50 000 BP, and Fraser Glaciation, 10 000-26 000 BP (Green et al., 1988). The volcanic complex comprises a number of closely spaced intermediate to felsic centres which provide good stratigraphic control on relative ages, and peripheral exposures of basalt flows and basalt pyroclastic rocks. The basaltic rocks are coeval with the intermediate to felsic volcanism. Previous workers have distinguished four episodes of volcanism, including one Tertiary (Pliocene) stage and three Quaternary (Pleistocene and Holocene) stages (Read, 1977; Green et al., 1988).

SUMMARY OF OBSERVATIONS

The petrography of the Meager Mountain volcanic rocks is summarized in Table 2. The petrography of the volcanic suite is discussed with respect to the volcanic assemblages recognized by Read (1977) in order of decreasing age.

Pliocene assemblage

The Pliocene assemblage of volcanics, which forms the base of the volcanic complex, is dominated by slightly altered andesitic breccias and minor aphanitic flows, and is exposed

only in the south and southwest parts of the complex. Read (1977) mapped an extensive, relatively unaltered porphyritic dacite at the top of the assemblage which is characterized in hand sample by abundant, large (4 mm), quartz phenocrysts. In thin section the quartz exhibits undulose extinction and yields biaxial interference figures suggesting significant strain. On this basis, the quartz may not be cognate. The cognate phenocryst and microphenocryst assemblage in decreasing modal abundance is plagioclase >> amphibole > clinopyroxene > biotite.

Pylon assemblage

The Pylon assemblage is the most voluminous and widespread group of volcanic rocks in the complex. The assemblage consists of mainly andesite lavas and was sampled in six localities. In thin section all the andesites are plagioclase + pyroxene porphyritic, contain accessory cubic Fe-Ti oxides and apatite as inclusions within the phenocrysts, and hydrous, mafic minerals which exhibit textural evidence of magmatic resorption. There are, however, two distinct groups which are distinguished on the basis of the (micro-) phenocryst assemblage and the nature of the plagioclase phenocrysts. The first variety of andesite is plagioclase + orthopyroxene porphyritic with additional microphenocrysts of biotite > amphibole > clinopyroxene. Plagioclase also occurs as spongy-textured xenocrysts. The other andesites contain plagioclase + orthopyroxene phenocrysts with microphenocrysts of clinopyroxene > amphibole. Xenocrystic plagioclase in these lavas is characterized by conspicuous vermicular-textured rims which are themselves rimmed by stable, clear jackets of plagioclase. This complex texture represents the effects of initial dissolution of the plagioclase followed by reprecipitation of magmatic plagioclase.

The two andesite groups also appear to have different crystallization sequences (Fig. 2) and slight differences in bulk composition (Table 1). The biotiteabsent andesites, which were collected from the proposed vent area of Read (1977), have relatively less silica than the biotite-phyric andesite lavas. The two andesite subtypes may reflect different stages of magmatic evolution or different magmas. Their existence may imply that The Devastator was not the only centre responsible for the Pylon assemblage andesites.

Capricorn and Plinth assemblages

The Capricorn and Plinth assemblages are composed of felsic volcanic breccias, lava flows and domes, and form the highest peaks in the complex. They were originally mapped by Read (1977) as two packages of rhyodacite flows, domes and pyroclastic rocks, separated stratigraphically by glacial till. One sample of a Capricorn assemblage lava flow and six samples of Plinth assemblage volcanics (both flows and hypabyssal intrusions) were taken for petrographic and chemical study (Tables 1 and 2).

In general, the volcanics of these assemblages share the same mineralogy (Table 2), xenocryst morphology and inferred order of crystallization (Fig. 3). Based on petrography, all samples are plagioclase, quartz and biotite porphyritic with microphenocrysts of amphibole. In several

Table 1. Whole-rock analyses for the Meager Mountain volcanic complex.

Oxide / Name	MM-2A	MM-2B	MM-7	MM-16	MM-20	MM-21	MM-24	MM-25	MM-26	MM-27	MM-28	MM-29
Assemblage	BRA	BRA	BRA	BRA	PYA	PYA	PCA	PYA	PLA	DGA	PYA	PLA
UTM	684121	684121	682124	664124	628038	628038	604034	642038	649085	655079	666082	644089
SiO2	64.12	67.59	68.18	69.71	68.66	66.21	61.45	61.13	65.33	60.62	60.30	68.66
TiO2	0.61	0.51	0.48	0.48	0.47	0.56	0.70	0.76	0.58	0.91	0.86	0.49
Al2O3	15.84	15.28	15.59	15.82	15.48	15.55	16.35	16.45	14.95	16.95	16.85	15.04
Fe2O3	3.92	3.23	3.04	3.14	3.03	3.47	4.72	4.76	3.36	5.92	5.66	3.05
MgO	1.68	1.10	1.14	1.07	1.03	1.46	3.07	2.74	1.54	2.70	2.80	1.12
CaO	3.86	2.98	3.13	2.99	2.96	3.45	4.96	4.68	3.12	5.05	5.03	2.62
Na2O	4.56	4.53	4.65	4.87	4.76	4.33	4.16	4.48	4.68	4.64	4.47	4.68
K2O	2.11	2.45	2.45	2.54	2.50	2.46	1.72	2.11	2.82	1.81	1.63	3.05
P2O5	0.19	0.16	0.15	0.15	0.15	0.18	0.27	0.24	0.23	0.36	0.28	0.17
Total	96.88	97.84	98.80	100.78	99.05	97.66	97.40	97.35	96.60	98.96	97.88	98.88

Oxide / Name	MM-30	MM-32	MM-33	MM-34	MM-35	MM-36	MM-38	MM-39	MM-40
Assemblage	PLA	BRA	DGA	CPA	PYA	PCA	CPA	PLA	PLA
UTM	634109	642119	621080	610080	608106	592101	572095	638097	639103
SiO2	64.55	68.94	68.33	66.16	62.11	65.33	57.99	66.65	66.08
TiO2	0.56	0.47	0.59	0.58	0.70	0.69	0.79	0.51	0.55
Al2O3	15.66	15.69	15.63	15.62	15.90	16.54	17.47	15.36	15.92
Fe2O3	4.09	2.90	2.65	3.70	4.56	4.26	6.39	3.38	3.71
MgO	2.06	1.05	0.98	1.79	2.27	2.04	3.20	1.48	1.64
CaO	3.67	2.97	1.91	3.41	4.23	4.08	5.78	3.14	4.04
Na2O	4.41	4.82	2.48	4.51	4.46	4.76	4.40	4.51	4.39
K2O	2.47	2.49	5.57	2.53	1.90	2.48	1.09	2.59	2.48
P2O5	0.17	0.15	0.21	0.18	0.20	0.27	0.27	0.15	0.17
Total	97.64	99.47	98.36	98.49	96.33	100.47	97.39	97.77	98.98

Labels describe assemblage: BRA, Bridge River; PYA, Pylon; PCA, Pliocene; CPA, Capricorn; DGA, Devastation Glacier; PLA, Plinth. Locations are given by UTM grid references for Zone 10. Analyses are by X-ray fluorescence analysis on pressed glass pellets performed at the University of British Columbia.

samples the biotite and amphibole have reaction coronas indicating disequilibrium with the melt. The groundmass commonly comprises plagioclase, biotite, amphibole, Fe-Ti oxides, apatite and devitrified glass. Xenocrysts of plagioclase are common and have thick vermicular-textured margins which are jacketed by clear plagioclase overgrowths. In this regard the xenocrystic plagioclase is petrographically inseparable from the xenocrysts described in rocks of the Pylon assemblage. These rocks are not strictly rhyodacites, because the only feldspar recognized in thin section is plagioclase. In lieu of glass chemistry the rocks are classified as dacites.

Although Capricorn and Plinth assemblages share many petrographic similarities there are significant variations within the suites. In particular the distribution of xenoliths is not uniform. On the southeast shoulder of Meager Mountain the dacite lavas are choked with monolithic xenoliths up to 0.5 m in diameter. The xenoliths are riddled with miarolitic cavities surrounded by a latticework of slender, zoned, twinned plagioclase and amphibole. Many of the amphiboles are cored by plagioclase, and also contain euhedral crystals of clinopyroxene. The loose, porous texture and euhedral nature of the constituent minerals suggests a juvenile magmatic rather than an accidental assimilation origin for the xenoliths.

Mosaic assemblage

Basalt lava flows and breccias outcrop on the northern, western and southern periphery of the Meager Mountain volcanic complex. Read (1977) grouped and informally named these basaltic volcanic rocks the Mosaic assemblage. The northern basaltic rocks stratigraphically overlie the Plinth assemblage and K-Ar dates establish that the flows on the western edge of the complex are as young as 0.9 Ma (Green et al., 1988). In addition to the exposures of basalt delineated by Read, we have included two southern outcrops which were previously mapped as andesite feeder dykes. These basalts near the southern edge of the complex are significant because they represent a previously unrecognized dissected basaltic vent area. One of the two olivine basalt exposures found preserves subvertical flow laminations as platy joints, is slightly coarser in texture than its nearby extrusive equivalent, and has nearly the same composition (Table 3a). The proximity of these two exposures to basaltic breccia (located only a few hundred metres to the west of the basalt exposures) suggests that the area is a dissected vent and the probable source area for the basalts in the Elaho River valley to the south (Green et al., 1988).

Table 2. Observed mineralogy of the Meager Mountain volcanic rocks.

ASSEMBLAGE and SAMPLE NOS.	MINERALS
Bridge River MM-2a,-2b,-3a,-3b,-3c -7,-16,-32	PL OP AU AM BI
Mosaic Assemblage MM-17,-18,-19,-37	PL OL AU OX
Plinth Assemblage MM-26,-29,-30,-31 -39,-40	PL Q BI AM OX AP
Capricorn Assemblage MM-34	PL Q BI AM OX AP
Pylon Assemblage MM-21,-22,-23 MM-25,-28,-35	PL OP AM BI AU OX AP PL OP AM AU OX AP
Pliocene volcanics MM-24 MM-36	PL AM AU BI PL AM OP AU OX

PL: plagioclase; OL: olivine; OP: orthopyroxene; AU: augite; OX: Fe-Ti oxides; BI: biotite; AM: amphibole; Q: quartz; AP: apatite.

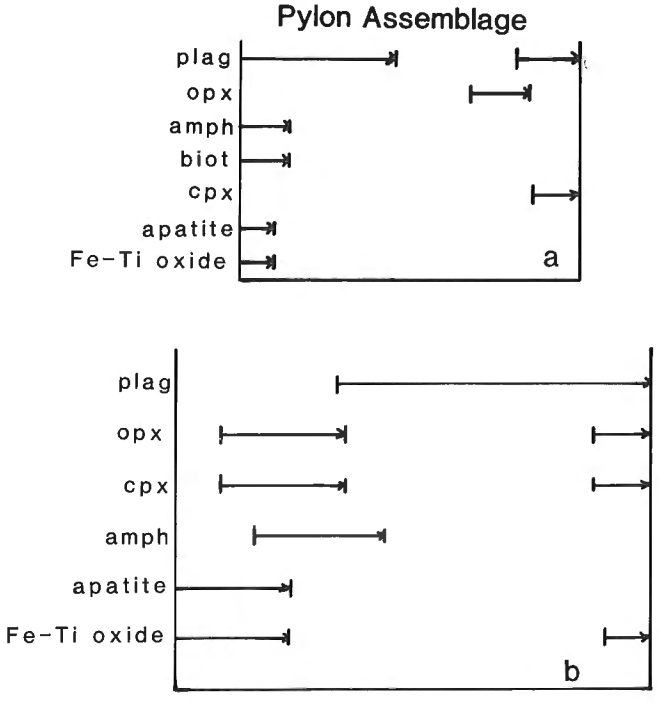

Figure 2. a: Inferred relative crystallization history of biotite-absent andesites (MM-25, 28, 35) of the Pylon assemblage. b: Inferred relative crystallization history of biotite-bearing andesites (MM-21, 22, 23) of the Pylon assemblage.

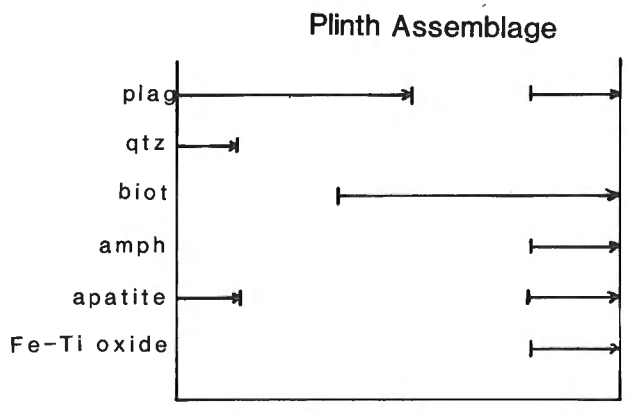

Figure 3. Inferred relative crystallization history of Capricorn and Plinth assemblage dacites (MM-26, 29, 30, 31, 39, 40).

All the basaltic rocks are porphyritic with 10 and 20 % by volume olivine and plagioclase phenocrysts (Tables 2 and 3b). At least one of the basalts contains augite phenocrysts and aluminous spinels occur as inclusions in olivine phenocrysts in every sample. In every case the groundmass contains at least augite, plagioclase, olivine, and oxides. Ca-poor pyroxene was not seen in any of the samples, despite the fact that all of the basalts are holocrystalline (less than 5 % by volume glass). One of the samples contains titanaugite in the groundmass. The petrographic relationships between phenocryst and groundmass phases are summarized in Figure 4. Petrographically these basalts have an alkali olivine basalt affinity; consequently they are not easily related to the calc-alkaline volcanic rocks. The existence of a contemporaneous suite of alkaline basalt within a calc-alkaline suite has not previously been reported for the Garibaldi volcanic belt; however, similar occurrences have been recognized in several Quaternary Mexican calc-alkaline volcanoes (Nelson and Carmichael, 1984; Allan et al., in press; Luhr et al., in press).

These lavas have a large range in chemical composition (Table 3a). The rocks are slightly hypersthene or nepheline normative which corroborates the alkaline affinity defined by the mineralogy (Table 3b). Mineralogically and chemically they are similar to alkaline rocks described from the Mexican volcanic belt (Nelson and Carmichael, 1984; Allan et al., in press; Luhr et al., in press). Another chemical parameter useful to classifying volcanic rocks is the activity of silica in the melt calculated for the whole rock composition (Carmichael et al., 1970; Russell and Nicholls, 1985). Figure 5 shows the values of $aSiO_2$ calculated for the Meager Mountain lavas at their liquidus temperature (Table 3c). These values can be compared to the computed $aSiO_2$ buffering equilibria and the computed liquid lines of descent for a variety of mafic rock types. In terms of this parameter these lavas also exhibit an alkaline affinity as they plot below the stability field of Ca-poor pyroxene.

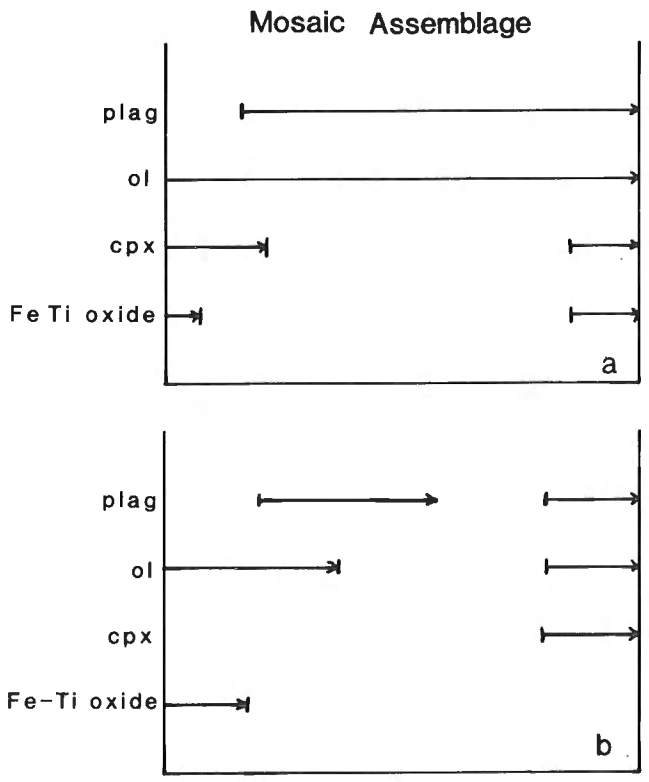

Figure 4. a: Inferred relative crystallization history of Mosaic assemblage alkali-olivine basalts from the south edge of the volcanic complex (MM-18, 19); and b: From the west edge of the volcanic complex (MM-37).

Table 3a. Whole-rock analyses of alkaline rocks of the Meager Mountain volcanic complex (Mosaic assemblage).

Oxide / Name UTM	MM-17 642161	MM-18 604991	MM-19 603994	MM-37 582109
SiO2	50.27	48.23	48.68	49.14
TiO2	1.45	1.54	1.64	1.62
Al2O3	17.07	14.35	14.58	15.71
Fe2O3	1.26	1.48	1.53	1.31
FeO	7.87	9.14	9.44	7.70
MgO	6.30	8.19	9.00	6.52
CaO	8.52	8.48	8.47	9.07
Na2O	3.92	3.38	3.48	3.74
K2O	0.82	0.85	0.84	1.36
P2O5	0.38	0.28	0.30	0.54
Total	98.48	96.43	98.73	97.20

Compositions are measured by X-ray fluorescence analysis on pressed glass powder pellets at the University of British Columbia. Total iron has been recalculated as FeO and Fe2O3 based on a QFM oxygen buffering assemblage (Kilinc et al., 1983) Locations are given by UTM grid references for Zone 10.

Table 3b. Chemical and petrographic characteristics of the alkaline lavas from Meager Mountain volcanic complex.

Name	MM-17	MM-18**	MM-19	MM-37
Normative Constituent				
Or	4.91	5.20	5.02	8.25
Ab	35.68	31.44	31.62	32.43
An	26.93	22.25	21.94	22.65
Ne	0.00	0.00	0.00	1.22
Di	10.73	15.56	14.88	15.94
Hy	5.15	3.43	0.58	0.00
Ol	12.41	17.69	21.40	14.63
Mt	1.34	1.60	1.62	1.41
Il	2.05	2.22	2.31	2.32
Ap	0.81	0.61	0.63	1.16
Petrography:				
Phenocrysts	PL>OL < 10 %	OL,PL < 20 %	OL>PL < 25 %	PL>OL>AU < 25 %
Groundmass:	AU* PL OL OX	AU PL OL OX	AU PL OL OX	AU PL OL OX

* Titanaugite ; ** 2% by volume vesicles with chlorophaeite rims and carbonate amygdules.

Table 3c. Calculated liquidus characteristics of the alkaline lavas.

Name	MM-17	MM-18	MM-19	MM-37
T(°C)	1187	1235	1254	1193
Phase	PL	OL	OL	OL
X(An or Fo)	71	83	84	81
aSiO2	.365	.372	.365	.356

T(°C) is liquidus temperature; X(An or Fo) is mole percent anorthite or forsterite; aSiO2 is the activity of silica in the melt. All calculations are for atmospheric pressure.

Bridge River assemblage

The Bridge River assemblage is a package of felsic volcanics erupted from the northeast side of the volcanic complex 2350 BP (Green et al., 1988). The entire assemblage was erupted over a relatively short period of time, before soil horizons could develop between the individual units. The assemblage is best exposed in the canyon walls of the Lillooet River, a short distance downstream from the junction of Salal Creek with the Lillooet River. Numerous samples were taken of both loose material and rock for granulometric, petrographic and chemical analysis.

Stratigraphy

The oldest lithology of the Bridge River assemblage (Fig. 6) is a pumice lapilli and ash deposit produced by an explosive eruption emanating near the head of Fall Creek on the north slope of Plinth Peak. This initial eruption generated a northeasterly-trending plume of pumice lapilli and ash which crosses into Alberta (Nasmith et al., 1967). The proximal pumice consists mainly of 5-100 mm diameter fibrous pumice, porphyritic (plagioclase, amphibole) vitrophyre, white quartz monzonite and quartz diorite. The glass refractive indices indicate a silica content of approximately 70 % (Williams et al., 1982). The pumice accumulated in the Lillooet River valley and on opposing hill slopes to a depth of 1-2 m, and killed the dense forest which existed in the valley bottom. Preserved, charred stumps, root systems and paleoforest soil are well exposed in the present day Lillooet valley canyon walls.

Before a new soil horizon could develop on the pumice deposit, another eruption (or a continuation of the first eruption) produced a small pyroclastic flow deposit. The deposit preserved today, a grey, non-indurated block and ash deposit, consists almost exclusively of rounded, vesicular pumice blocks in an ashy matrix. The pumice blocks show varying degrees and types of sorting, from unsorted through to normal and reverse sorting. The inconsistent sorting may be the result of the pyroclastic flow being emplaced against the paleotopography of the ancient Lillooet valley wall. The block and ash deposit occurs only at the bottom of the Lillooet valley, and was hot enough to further scorch the trunks of the trees already partly submerged in the initial airfall pumice. It is interesting and enigmatic that the pyroclastic flow did not knock down all the trees in its path even though some were only 30-40 cm in diameter.

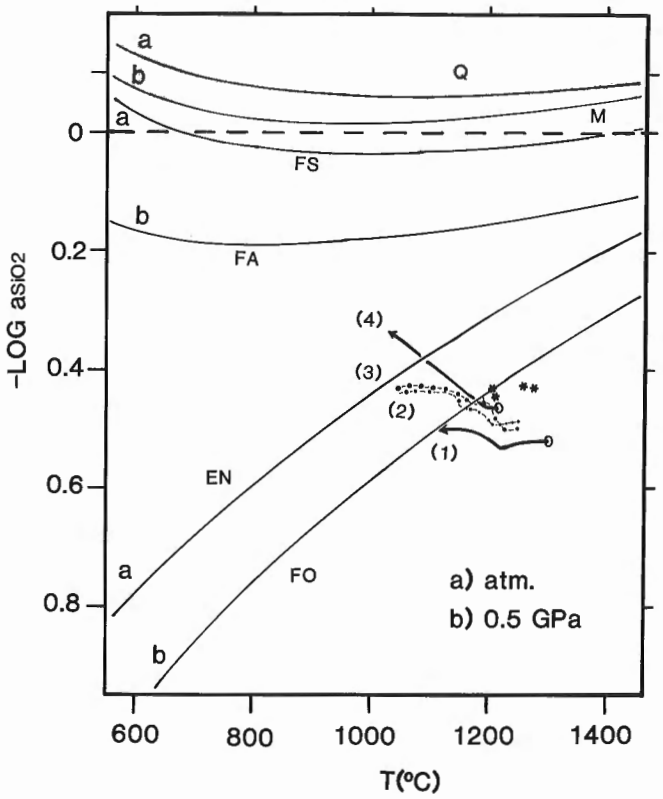

Figure 5. Activity silica versus temperature diagram for alkaline lavas. Solid lines represent the three aSiO2 buffer assemblages Q, Fa-Fs, and Fo-En, calculated at atmospheric pressure (a) and 0.5 GPa. Meager Mountain lavas are plotted as stars. Four curves model the variation in silica activity expected in the differentiation of a Hawaiian alkali olivine basalt (1), alkali olivine basalts from Diamond Craters and Cow Lakes, Oregon (2, 3) and a tholeiite basalt from Thingmuli volcano, Iceland (4). Calculations are after Russell and Nicholls (1985).

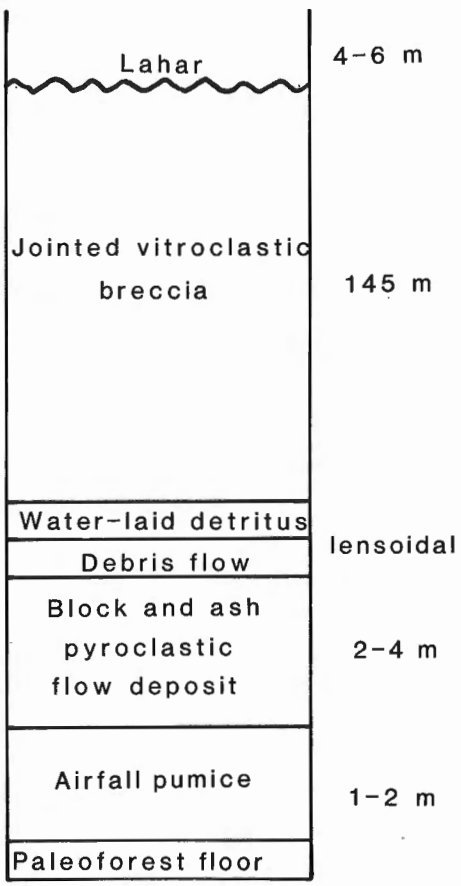

Figure 6. Schematic stratigraphy of the Bridge River assemblage.

A pause in activity followed the pyroclastic flow. Stratified to unstratified high energy debris flow deposits followed by stream-type deposits overly the block and ash deposit. This unit is not volcanic in character and occurs as discontinuous lenses within the present Lillooet valley walls. The detritus is dominated by felsic volcanic rocks and ash, as one would expect in such a recently active area.

The next unit of the assemblage is a cliff-forming well-indurated vitroclastic volcanic breccia up to 145 m thick (Read, 1977). The breccia ranges from matrix-supported to, locally, clast-supported. Ten to twenty per cent of the clasts are dense pumice, and about 5 % are angular quartz monzonite of the Fall Creek pluton, a Miocene intrusion (Read, 1977). The rest of the clasts are composed of felsic vitrophyre identical in thin section to the felsic lava flow which Read (1977) mapped as issuing from the vent area near the head of Fall Creek. The breccia matrix is locally laminated, and the clasts are often arranged in bands and appear flattened. However, there is no evidence to indicate that there was shearing between the laminations. In addition, tree trunks protruding above the previous deposits evidently were not tilted by the emplacement of the breccia because numerous vertical tree moulds can be found in the unit. Thus the breccia did not flow as a lava body or block and ash flow to its position of emplacement. Rather it formed as a glowing avalanche-type deposit caused by the calving of the felsic flow at higher elevations, and filled the valley ahead of its parental flow. Once emplaced, the unit behaved as a cooling unit. The clasts annealed, the unit indurated, and crude vertical cooling joints formed.

Overlying the vitroclastic breccia and its parent lava flow is a debris flow composed of 10-60 % matrix material of angular lithic pebbles to sand. The matrix is unsorted. The larger clasts, up to 5 m in diameter, constitute 40 to 90 % of the unit. Of the large clasts, 40-50 % are vitroclastic breccia and 50-60 % are dacite of the Plinth assemblage. Many of the breccia clasts are radially jointed. The larger clasts are poorly sorted, but an upward decrease in their abundance and some poorly-defined bedding planes indicate that the unit moved as a gravity flow in which the large clasts sorted. The large proportion of older dacite indicates that the unit originated above the head of Fall Creek, perhaps caused by destabilization of the slope due to the recent eruption. The emplacement of the unit must have occurred very shortly after the emplacement of the vitroclastic breccia because it contains jointed breccia clasts torn from the valley-bottom cooling unit while still hot.

Petrography

Petrographic relationships in rocks of the Bridge River assemblage are complex but uniform between pumice blocks, welded breccia, and lava flow. Textures vary from pumiceous, highly vesicular glass to vitroclastic to flow-banded, but in all samples investigated the phenocryst assemblage comprises plagioclase > clinopyroxene > amphibole > biotite. Plagioclase occurs as two populations; i) large xenocrystic phenocrysts up to 5 mm long with spongy textures due to remelting and vestiges of twinning and complex zoning, and ii) clear, twinned microphenocrysts with little zoning. Biotite, as well, has two occurrences: i) rare stable euhedral to subhedral flakes and ii) ragged cores of xenocrystic crystal clots with inclusions of Fe-Ti oxide and coronas of orthopyroxene, Fe-Ti oxide, and clear plagioclase. Xenocrysts(?) of quartz occur rarely. The phenocryst and microphenocryst assemblage of the Bridge River assemblage is, in fact, conspicuously lacking in quartz, but the glassy nature of the rocks and the apparently high silica content of the rocks and glass indicates they are at least dacites and possibly rhyolites.

The pumice blocks found in the Bridge River deposits are commonly banded. In hand sample the banding is defined by 1-3 cm, contorted or shredded bands or wisps of dark pumice hosted by white pumice. The dark pumice is less vesicular and aphanitic compared to host pumice. In thin section the darker material contains abundant plagioclase microphenocrysts with smaller amounts of microphenocrystic Fe-Ti oxides, clinopyroxene, orthopyroxene and amphibole. This darker material also occurs within the vitroclastic breccia as annealed clasts. The presence of these more mafic inclusions suggests that a magma-mixing event preceded the eruption of the Bridge River assemblage.

CONCLUSIONS

The Meager Mountain volcanic complex is a Quaternary volcano of dominantly calc-alkaline flows, domes and breccias and subordinate alkaline olivine basalt lavas and breccia. Rocks of the calc-alkaline suite range in composition from andesite to dacite and are Pliocene to Recent in age. Closely associated in time with the youngest calc-alkaline volcanic rocks are three peripheral occurrences of basaltic and intermediate alkaline flows and breccia. The recognition of this contemporaneous alkaline and calc-alkaline volcanism is significant in that such associations have not been previously documented for the Garibaldi volcanic belt. The discovery of these alkaline rocks may warrant re-investigation of other calc-alkaline volcanoes in the Canadian Cascade belt to ascertain whether this association is more common than presently postulated.

ACKNOWLEDGMENTS

Funding for this research was provided by the Geological Survey of Canada through a Research Agreement Grant to JKR and NSERC Operating Grant A0820 to JKR. We acknowledge helpful discussions with Peter Read and Jamie Allan. Additionally, the senior author was aided in his fieldwork by Chris Vogl (field assistant) and John Goats (Pemberton Helicopters).

REFERENCES

Allan, J.F., Nelson, S.A., Luhr, J.F., Carmichael, I.S.E., and Wopat, M.

—: Pliocene-Recent rifting in SW Mexico and associated alkaline volcanism; in The Gulf and Peninsular Province of the Californias, J.P. Dauphin (ed.), American Association of Petroleum Geologists Memoir Series (in press).

Anderson, R.G.

1975: The geology of the volcanics of the Meager Creek map area, southwestern, British Columbia; unpublished B.Sc. thesis, University of British Columbia, 130 p.

Carmichael, I.S.E., Nicholls, J., and Smith, A.L.

1970: Silica activity in igneous rocks; American Mineralogist, v. 55, p. 246-263.

Green, N.L.

1981: Geology and petrology of Quaternary volcanic rocks: Garibaldi Lake area, southwestern British Columbia; Geological Society of America, Bulletin, v. 92, pt. I, p. 697-702 and pt. II, p. 1359-1470.

Green, N.L., Armstrong, R.L., Harakal, J.E., Souther, J.G., and Read, P.B.

1988: Eruptive history and K-Ar geochronology of the late Cenozoic Garibaldi volcanic belt, southwestern British Columbia; Geological Society America, Bulletin, v. 100, p. 563-579.

Kilinc, A., Carmichael, I.S.E., Rivers, M.L., and Sack, R.O.

1983: The ferric-ferrous ratio of natural silicate liquids equilibrated in air; Contributions to Mineralogy and Petrology, v. 83, p. 136-140.

Luhr, J., Allan, J.F., Carmichael, I.S.E., Nelson, S.A., and Hasenaka, T.

—: Primitive calc-alkaline and alkaline rock types from the Western Mexican volcanic belt; Journal of Geophysical Research (in press).

Nasmith, H., Mathews, W.H., and Rouse, G.E.

1967: Bridge River ash and some other Recent ash beds in British Columbia; Canadian Journal Earth Sciences, v. 4, p. 163-170.

Nelson, S.A. and Carmichael, I.S.E.

1984: Pleistocene to Recent alkalic volcanism in the region of Sanganguey volcano, Nayarit, Mexico; Contributions to Mineralogy and Petrology, v. 85, p. 321-325.

Read, P.B.

1977: Geology of Meager Creek geothermal area, British Columbia; Geological Survey Canada, Open File 603.

Russell, J.K. and Nicholls, J.

1985: Application of Duhem's Theorem to the estimation of extensive and intensive properties of basaltic magmas; Canadian Mineralogist, v. 23, p. 479-488.

Williams, H., Turner, F.J., and Gilbert, C.M.

1982: Petrography: an Introduction to the Study of Rocks in Thin Sections (second edition); W.H. Freeman, San Francisco and Oxford, 626 p.

Woodsworth, G.J.

1977: Geology of the Pemberton (92J) map area; Geological Survey of Canada, Open File 482.

Lithostratigraphy of the Nanaimo Group, Georgia Basin, southwestern British Columbia

T.D.J. England[1]
Cordilleran and Pacific Geoscience Division, Sidney

England, T.D.J., Lithostratigraphy of the Nanaimo Group, Georgia Basin, southwestern British Columbia; in Current Research, Part E, Geological Survey of Canada, Paper 89-1E, p. 197-206, 1989.

Abstract

The lithostratigraphic nomenclature of the Upper Cretaceous Nanaimo Group is reviewed in the light of current confusion regarding rock stratigraphic and time stratigraphic units of the succession. Much of the original lithostratigraphic nomenclature is resurrected, and several new informal names are proposed to replace improper ones. In the Comox Basin, new names are (with the previous name in brackets), the Cottam Point member (Benson Member) for the basal conglomerate beds, and Parksville member (Extension-Protection Formation), and Tsable member (Extension-Protection Formation) for coarse grained units within the Trent River Formation shales. In the Nanaimo Basin, new informal names are the Galiano formation (Geoffrey Formation) and the Mayne formation (Spray Formation). In addition, the basal unit of the Nanaimo Basin, the Benson Formation, is informally subdivided into the Tzuhalem member, a conglomerate facies, and the Saanich member, a sandstone facies.

Résumé

La nomenclature lithostratigraphique du groupe de Nanaïmo du crétacé supérieur est revue à cause de la confusion actuelle qui règne au sujet des strates rocheuses et les unités stratigraphiques de la succession. La nomenclature originale est en grande partie reprise, et plusieurs nouveaux noms officieux sont proposés pour remplacer des appellations impropres. Dans le bassin de Comox, de nouveaux noms remplacent les anciens (entre parenthèses): membre de Cottam Point (membre de Benson) pour les couches basales de conglomérat, et membre de Parksville (formation d'Extension-Protection) et membre de Tsable (formation d'Extension-Protection) pour les unités à gros grain dans les schistes argileux de la formation de Trent River. Dans le bassin de Nanaïmo, de nouveaux noms officieux ont été introduits: formation de Galiano (formation de Geoffrey) et formation de Mayne (formation de Spray). En outre, l'unité basale du bassin de Nanaïmo, la formation de Benson, est divisée officieusement comme suit: membre de Tzuhalem, un faciès de conglomérat, et membre de Saanich, un faciès de grès.

[1] Department of Earth Sciences, Memorial University of Newfoundland, St. John's, Newfoundland A1B 3X5

INTRODUCTION

During the past 130 years, several stratigraphic studies have been made of the Upper Cretaceous Nanaimo Group, the oldest sedimentary sequence of the Georgia Basin in southwestern British Columbia. The early work, summarized by Muller and Jeletzky (1970), was driven by the need to understand the geology of the coal measures, the product of which was then fuelling the economy of British Columbia, and to assess the significant coal resource remaining in the Nanaimo Group on eastern Vancouver Island. The coal resource mostly was exhausted by the late nineteen sixties after some 72 000 000 tons had been mined (Muller and Atchison, 1971). Since the publication by Muller and Jeletzky (1970), much detailed work has continued on the Nanaimo Group, largely in the format of thesis research (which includes 15 or more Master's and 3 Ph.D. theses).

The current work is being undertaken for a dissertation at Memorial University of Newfoundland. The objective is to analyze the evolution of the Georgia Basin, one of the best exposed Upper Cretaceous fore-arc basins in the world. The scope of the research includes both structural and stratigraphic studies, and investigation of the burial history employing standard subsidence and thermal history modelling methods. Vitrinite reflectance data has been obtained for over 600 sites throughout the region. As a result of 1:50 000 scale geological mapping during 1987 and 1988 field seasons, a 1:250 000 scale map of the basin will be produced, incorporating new geological data.

This report focuses on much needed revisions to the lithostratigraphy of the Nanaimo Group, with emphasis on description; stratigraphical and sedimentological interpretations will be left to future discussions. Superscripted numbers on place names refer to numbered locations on Figure 1.

BASIN SETTING

The Georgia Basin is an extensive siliciclastic sediment-filled trough in southwestern British Columbia and northwestern Washington (Fig. 1). It is part of a series of fore-arc basins which developed on the Cretaceous continental margin of western North America (Dickinson, 1976). The Georgia Basin developed on the continental crust of Wrangellia in three distinct depositional episodes: 1) Santonian to Maastrichtian time; 2) during the Paleogene; and 3) during the Neogene (?) and Quaternary. The result of the first episode of sedimentation is the Nanaimo Group, which is preserved in three sub-basins, the Comox, Nanaimo, and Suquash basins (Fig. 1). The Nanaimo Basin and the western part of the Comox Basin, the Alberni outlier, can be considered structural basins, for the distribution of Nanaimo Group in these areas is largely controlled by post-depositional deformation. A true fold and thrust belt, involving all of the Nanaimo Group, developed in the southwestern Georgia Basin sometime during the Tertiary (England, 1988). Alluvial, fluvial, paralic, deltaic, neritic, shelf, and continental slope facies are present in a sedimentary succession that exceeds 3600 m in the Nanaimo Basin, 2000 m in the Comox Basin, and only 300 m (Muller and Jeletzky, 1970) in the Suquash Basin.

LITHOSTRATIGRAPHY

As pointed out by McGugan (1979), revisions to the lithostratigraphy of the Nanaimo and Comox basins proposed by Muller and Jeletzky (1970), contravene the rules of stratigraphic nomenclature (American Commission on Stratigraphic Nomenclature, 1970). Muller and Jeletzky (1970) proposed that several of the formation names of one basin be changed to formation names of the other on the basis of biostratigraphic correlation. Comox Basin formation names replaced by Nanaimo Basin formation names were: lower Trent River Formation to Haslam Formation, upper Trent River Formation to Cedar District Formation, Denman Formation to De Courcy Formation, Lambert Formation to Northumberland Formation (as revised by Muller and Jeletzky, 1970), and Hornby Formation to Gabriola Formation (Fig. 2). Furthermore, several Comox Basin names were to be adopted in the revised Nanaimo Basin stratigraphy: the Benson Formation to Comox Formation (the basal conglomerate being named the Benson Member), the middle unit of the Northumberland Formation to Geoffrey Formation, and the upper unit of the Northumberland Formation to Spray Formation (Fig. 3).

Simplification of lithostratigraphic nomenclature on the basis of biostratigraphy is not in accordance with correct stratigraphic procedure. It ignores the possibility of diachronous formations, which is highly likely given the extent and large paleobathymetric range of the basin. The formational names established by Clapp (1912, 1914), Clapp and Cooke (1917), Mackenzie (1922), and Usher (1952), should be retained to describe the lithostratigraphy of the Nanaimo Group. These names refer to fundamental mappable units in each basin and, because of the alternating coarse and fine grained nature of the formations they are commonly distinguished with ease.

It is thus herein proposed that original names be reinstated so as to accurately describe the lithostratigraphy of the Nanaimo Group. Some additions are informally proposed as a consequence of more detailed work completed since publication of the early schemes. A summary table is given in Table 1.

In the Comox Basin, the uppermost formation is the Hornby Formation, which, in turn, is successively underlain by the Spray, Geoffrey, Lambert, and Denman formations, as described by Usher (1952). Underlying these units are the Trent River and Comox formations, as defined by Mackenzie (1922) and Williams (1924). Subdivision of the Comox Formation by Bickford et al. (1988) into the Dunsmuir and Cumberland members should be retained; however, their designation of Benson Member for the basal unit should be discontinued as the name Benson is used in the Nanaimo Basin as a formational name. Cottam Point member is the informally proposed name for the basal conglomerate of the Nanaimo Group in the Comox Basin, after Cottam Point[1] near Parksville[2] where the conglomerate is well exposed. Usher's (1952) Qualicum Formation has been shown to overlie Comox Formation in boreholes drilled in the southern Comox Basin and can be traced to the northwest to correlate with the Trent River Formation. Therefore, Qualicum Formation need not be retained in this

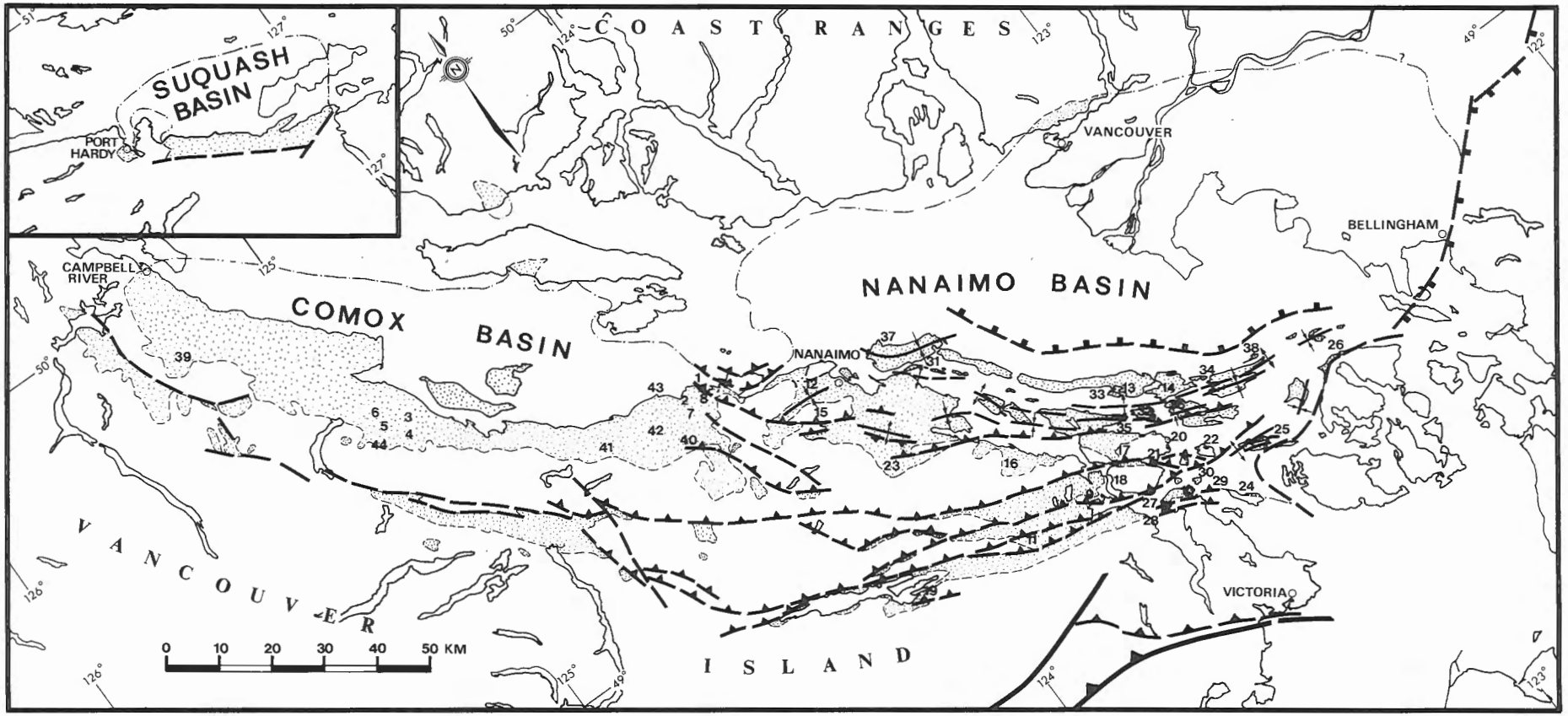

Figure 1. Distribution of the Nanaimo Group in the Georgia Basin. Faults are indicated by thick lines (dashed where inferred), thrust faults with teeth on hanging wall. Approximate basin outline under Georgia Strait indicated by long dash-dot. Bold numbers refer to locations shown by superscripts in the text.

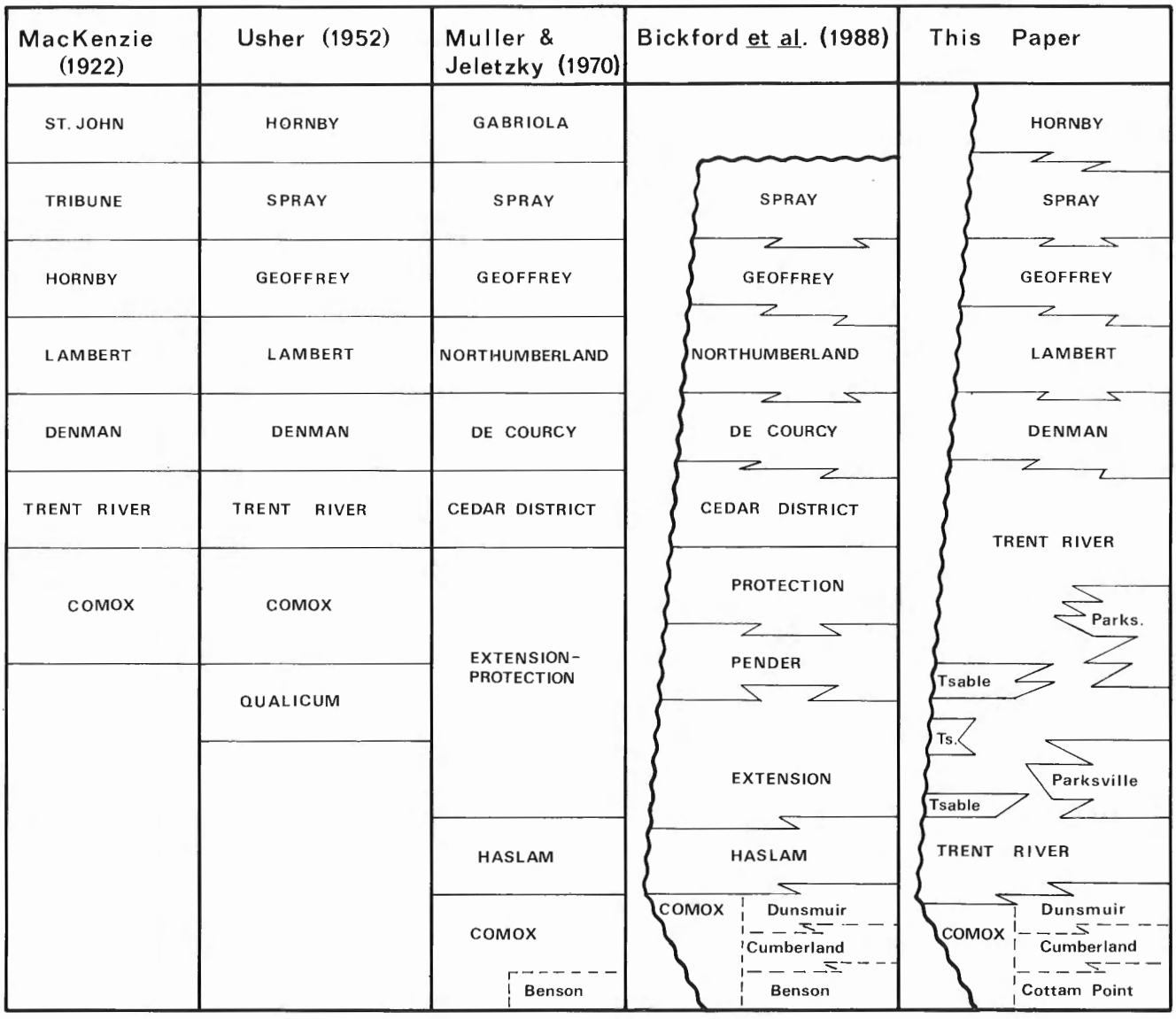

Figure 2. Lithostratigraphic nomenclature of the Comox Basin. Formation names are in upper case, member names are in lower case.

proposed lithostratigraphic scheme. The Trent River Formation locally contains an intermediate conglomerate and sandstone unit which outcrops in the area near Langley Lake[3], north of Tsable River[4]; on lower Bloedel Creek[5]; north of Trent River[6]; and has been intersected in a number of boreholes in the west-central part of the basin (Muller and Jeletzky, 1970). It is suggested that this coarse grained unit be named the Tsable member. Muller and Jeletzky (1970) include this unit in the combined "Extension-Protection Formation"; however, the names "Extension" and "Protection" are used in the Nanaimo Basin. Where the Tsable member is present, the Trent River Formation can be divided into upper and lower members. In the Parksville[2] area, a prominent polymictic conglomerate underlies Little Mountain[7], and conglomerate and sandstone outcrop in the Englishman River valley[8], and along the coast. This coarse grained facies apparently occupies an intermediate position within shales of the Trent River Formation and may be laterally equivalent to parts of the Tsable River member; it cannot be traced to the northwest in the subsurface or in outcrop, and should be given separate status as the Parksville member.

In the Nanaimo Basin, the proposed lithostratigraphic nomenclature is as follows, in upward stratigraphic order. Forming the base of the Nanaimo Group is the Benson Formation, as defined by Clapp (1914), which can be subdivided into two informal units: a basal conglomerate facies, the Tzuhalem member, and a sandstone facies, the Saanich member. The former is named after the prominent exposures on and near Mt. Tzuhalem[9], the latter is named after the extensive sandstone exposures on northern Saanich Peninsula[10]. Overlying the Benson Formation is the Haslam Formation (Clapp, 1914), which Ward (1978) divided into the Haslam Creek member, a massive shale facies exposed on Haslam Creek[23], and the Cowichan Member, a turbidite facies well exposed on the Cowichan River[11]. Overlying the Haslam Formation is the Extension Formation (Clapp, 1914) which Bickford et al. (1988) divided into a lower Northfield member, a siltstone and fine grained sandstone unit overlying the Wellington coal seam and

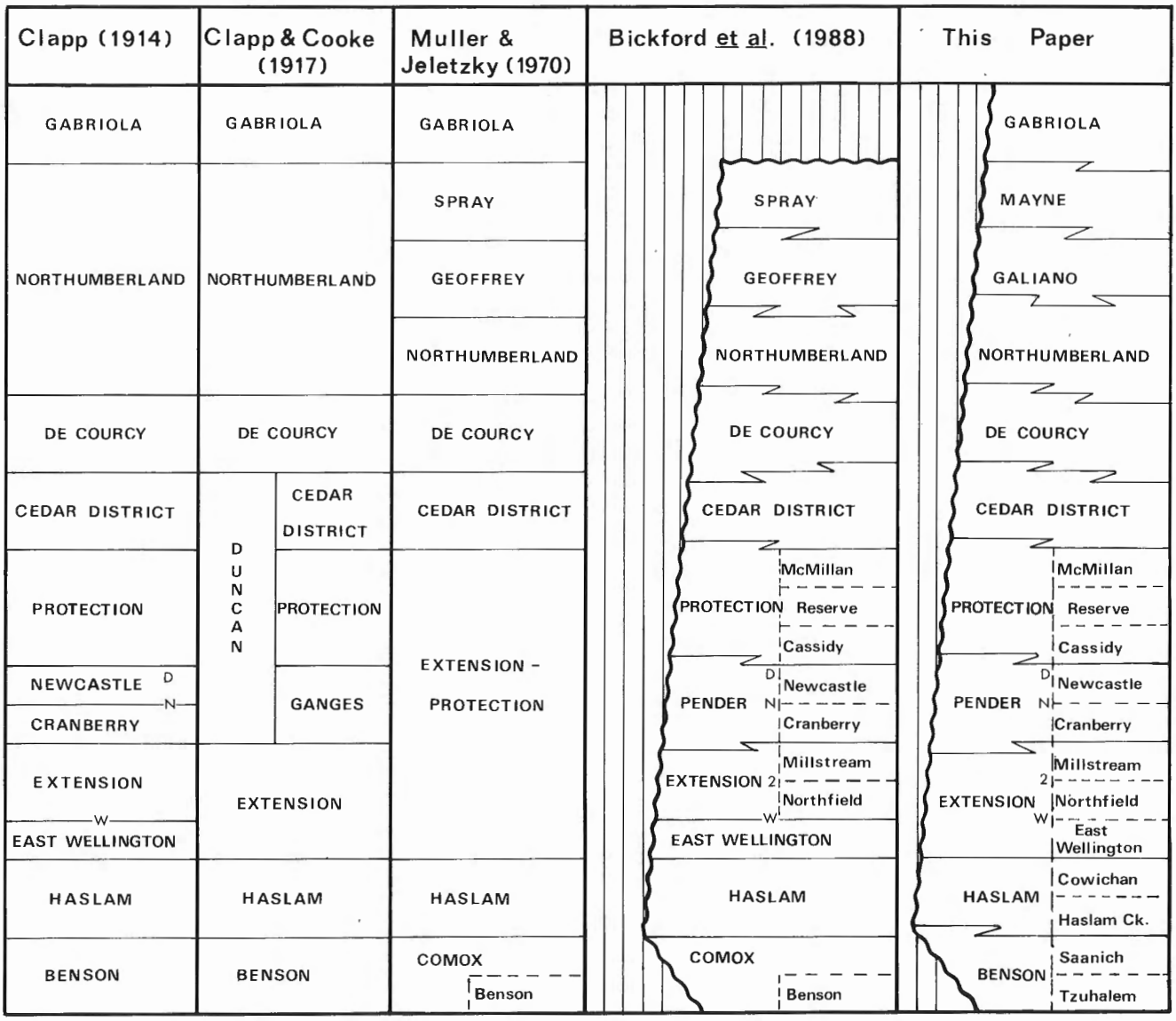

Figure 3. Lithostratigraphic nomenclature of the Nanaimo Basin. Formation names are in upper case, member names are in lower case. W = Wellington Seam, 2 = No. 2 seam, N = Newcastle Seam, D = Douglas Seam. The scheme used in this paper includes Ward's (1978) subdivision of the Haslam Formation.

bounded above by the No. 2 coal seam, and an upper Millstream member, a massive lithic conglomerate exposed along the Millstream River[12]. It is proposed to downgrade Clapp's (1914) East Wellington Formation to member status and include it within the Extension Formation as did Muller and Jeletzky (1970). The East Wellington Formation is a thin-bedded sandstone, less than 15 m thick which overlies the Haslam Formation and underlies the Wellington coal seam. It is only locally developed in the Nanaimo area and is part of the Nanaimo coalfield sequence. Overlying the Extension Formation is the Pender Formation (Ward, 1978) which in the Nanaimo area is divisible into the upper Newcastle member coal measures, and the lower Cranberry member shales (Bickford et al., 1988), separated by the Newcastle coal seam. Previously, these two members had been described as formations (Clapp, 1914). Clapp (1914) placed the base of the Cranberry Formation at the top of the first 25 ft (7.6 m) conglomerate bed of the Extension Formation. The Newcastle Formation includes the Douglas coal seam, which occurs 15 to 75 m below the overlying Protection Formation (Clapp, 1914). In the Nanaimo area, the Protection Formation (Clapp, 1914) is divisible into a lower Cassidy member sandstone and pebble conglomerate, a middle Reserve member comprising coal measures, and an upper McMillan member sandstone (Bickford et al., 1988). The Cedar District and the De Courcy formations (Clapp, 1914) overlie the Protection Formation and consist of dominantly shale and sandstone, respectively; these formations are distributed widely throughout the basin. Overlying the De Courcy Formation is the Northumberland Formation which, as described by Clapp (1914), consists of lower shales and upper shales which are commonly laterally replaced by medial conglomerate and sandstone. Muller and Jeletzky divided Clapp's Northumberland Formation into a lower shale unit, for which they retained the name Northumberland, a middle coarse grained unit which they named the

Table 1. Lithostratigraphy and lithology of the Nanaimo Group in the Comox and Nanaimo basins

COMOX BASIN		
Unit	Lithology	Reference
Hornby Formation	Sst. and cgl.	Usher (1952)
Spray Formation	Sh. and minor sst.	Usher (1952)
Geoffrey Formation	Cgl. and sst.	Usher (1952)
Lambert Formation	Sh. and minor sst.	Usher (1952)
Denman Formation	Sst., cgl., and minor sh.	Usher (1952)
Trent River Formation	Sh., minor cgl., sst. and sh.	Mackenzie (1922)
Tsable member	Cgl., sst. and minor sh.	This paper
Parksville member	Cgl. and sst.	This paper
Comox Formation	Sst., sh. and cgl.	Mackenzie (1922)
Dunsmuir member	Sst. and coal	Bickford et al. (1988)
Cumberland member	Sltst., sst., sh., coal	Bickford et al. (1988)
Cottam Point member	Cgl. and sst.	This paper
NANAIMO BASIN		
Unit	Lithology	Reference
Gabriola Formation	Sst., cgl., minor sh.	Clapp (1914)
Mayne formation	Sh. and minor sst.	This paper
Galiano formation	Cgl., sst., and minor sh.	This paper
Northumberland Formation	Sh. and minor sst.	Muller and Jeletzky (1970)
De Courcy Formation	Sst., cgl. and minor sh.	Clapp (1914)
Cedar District Formation	Sh. and minor sst.	Clapp (1914)
Protection Formation	Sst., sltst., cgl. and coal	Clapp (1914)
MacMillan member	Sst. and sltst.	Bickford et al. (1988)
Reserve member	Sltst., sst. and coal	Bickford et al. (1988)
Cassidy member	Sst. and cgl.	Bickford et al. (1988)
Pender Formation	Sh., sltst., sst., cgl. and coal	Ward (1978)
Newcastle member	Sh., cgl. and coal	Clapp (1914)
Cranberry member	Sst. and sltst.	Clapp (1914)
Extension Formation	Cgl., sst., sltst. and coal	Clapp (1914)
Millstream member	Cgl. and coal	Bickford et al. (1988)
Northfield member	Sltst., sst. and coal	Bickford et al. (1988)
East Wellington mbr.	Sst. and sandy sh.	Clapp (1914)
Haslam Formation	Sh., sltst. and minor sst.	Clapp (1914)
Cowichan member	Sh. and minor sst.	Ward (1978)
Haslam Creek member	Sh. and sltst.	Ward (1978)
Benson Formation	Cgl., sst. and sh.	Clapp (1914)
Saanich member	Sst. and sh.	This paper
Tzuhalem member	Cgl. and sst.	This paper

Geoffrey Formation, and an upper shale succession which they named the "Spray Formation", the latter two formation names coming from Comox Basin nomenclature. Geoffrey and Spray, however, are obviously names preempted in the Comox Basin lithostratigraphic scheme of Usher (1952) and, therefore, cannot be used in the Nanaimo Basin. It is herein proposed that: a) the name Northumberland be retained for the lower shale which overlies the De Courcy Formation; b) the overlying coarse grained unit be named the Galiano Formation after the exposures on Mount Galiano[13]; and c) the succeeding shale unit be named the Mayne formation after the exposures in Miners Bay and Bennett Bay on Mayne Island[14]. At the top of the Nanaimo Group in the Nanaimo Basin is the Gabriola Formation as originally defined by Clapp (1914). The Mayne and Gabriola formations locally interfinger; however, at most localities the contact is transitional over a short section.

In the proposed lithostratigraphic scheme (Table 1), references are given to descriptions of the various units, none of which have been formally defined according to the Code of Stratigraphic Nomenclature (American Commission on Stratigraphic Nomenclature, 1970). In the following section, the new and re-established units discussed above are briefly described and reference sections are indicated. At a later date, all lithostratigraphic units of the Nanaimo Group will be formally defined and supported by type section descriptions.

NANAIMO BASIN

Benson Formation

The Benson Formation was defined by Clapp (1914) as the basal conglomerate of the "Nanaimo series" in the Nanaimo area, named after exposures on the north side of Mt. Benson[15], near Nanaimo. Clapp noted, however, that in some areas the conglomerate grades upward into sandstone that underlies shale of the Haslam Formation. Thick sandstones, intercalated with siltstones and shales, and underlying the Haslam Formation, are well exposed in the southwestern part of the Nanaimo Basin. The conglomerate and sandstone facies can be distinguished readily in the field, and are herein informally named the Tzuhalem and Saanich members, respectively.

Benson Formation, Tzuhalem member

The informally named Tzuhalem member is equivalent to Clapp's (1914) ''Benson conglomerates'', which are reported to be well exposed in the canyon of Haslam Creek[23]. Clapp (1914) described the exposures north and west of Nanaimo, and Clapp and Cooke (1917) described the basal conglomerate in the Cowichan[11] and Chemainus[16] river valleys, and at Mt. Maxwell[17] on Saltspring Island. In the Nanaimo area, Clapp (1914) characterized the conglomerate, where it overlies Upper Triassic volcanic rocks of the Karmutsen Formation, as commonly poorly sorted, coarse grained (pebble to boulder size), composed of subangular to well rounded clasts of green meta-andesites in a matrix of greenish volcanic detritus. In other areas, it is a finer grained, polymictic conglomerate consisting of clasts of Karmutsen volcanics and metasediments and gabbro derived from the Paleozoic Sicker Group. Arkosic sandstone interbeds are common. Clapp and Cooke (1917) described similar lithological character for the conglomerates in the Duncan area[9]. They noted that, where the conglomerate is thick, the lower part is poorly sorted containing angular boulder size clasts, whereas the upper part shows fair sorting and is composed of more varied rounded pebbles of chert, vein-quartz, meta-andesite, granodiorite, and other metamorphic and granitic clasts.

The thickest sections of the Tzuhalem member occur on and near Mt. Tzuhalem[9] and on Mt. Maxwell[17]. The cliffs above Genoa Bay[9] expose 120 m or more of very thick bedded pebble to boulder conglomerate interbedded with medium- to coarse-grained lithic sandstone. The conglomerate is well indurated, poorly sorted, generally matrix supported, the matrix commonly being a greenish-grey to yellowish-grey grit. Boulder conglomerates are well exposed south of Octopus Point, along the west shore of Sansum Narrows[18]. Basal conglomerate forms Baynes Peak on Mt. Maxwell[17] and was described by Hanson (1976) as typically very thick bedded, broadly lenticular, and containing thin sandstone and pebbly sandstone lenses. Hanson estimated the conglomerate unit to be over 180 m thick at Baynes Peak and to be quite thin or absent at other localities on Saltspring Island where it is overstepped by the Haslam Formation. At the top of the cliff at Baynes Peak, the conglomerate is poorly sorted, has pebble to cobble size clasts, is well stratified, and has graded coarse-grained sandstone interbeds.

Over much of the southern Nanaimo Basin, the conglomerate member is much reduced in thickness, forming only 2 to 20 m of poorly sorted conglomerate resting on pre-Cretaceous rocks and underlying the Saanich member. At Mesachie Lake[19], in the Cowichan Lake area, approximately 10 m of poorly organized and poorly sorted greenish-grey conglomerate and sandstone overlie green Karmutsen volcanics. Clasts are pebble to boulder size and are mostly composed of the basement lithology. Numerous bivalve shells are present in the greenish sandstone matrix, some with very thick shells, others disposed as thin coquinas within the sandstone interbeds. Hanson (1976) noted a similar type of facies on the southwest side of Maxwell Creek[17]. At Beaver Point[20] on southeastern Saltspring Island, on Russell Island[21], and on Moresby Island[22], from 2-7 m of poorly sorted cobble to boulder conglomerate is present, composed of assorted subangular metamorphic and igneous rock clasts. Thick bedded, coarse grained sandstone containing pelecypod shells overlies the conglomerates at these localities. On the Saanich Peninsula[10], and on Sidney Island[24], the Tzuhalem member consists of up to 20 m of medium to thick bedded pebbly sandstone and cobble conglomerate. Abundant thick shelled pelecypods and gastropods are present in these beds at Hamley Point on southern Sidney Island[24].

In the San Juan Islands, the Tzuhalem member thickens significantly. On Johns Island[25] and Ripple Island[25] it is represented by over 472 m of conglomerate, sandstone and shale (McLellan, 1927), which clearly underlie the Haslam Formation exposed to the northwest. On Orcas Island[26], Ward (1978) reported 30 m of coarse grained lithic sandstone interbedded with conglomerate, which can be assigned to the Tzuhalem member.

Benson Formation, Saanich member

The Saanich member is an informal name for the thick bedded sandstones of the Benson Formation which are especially well developed in the southern Nanaimo Basin. The most widespread exposure occurs on the northern Saanich Peninsula, where tectonic thickening has resulted in a 1.5 km wide belt extending from Tsehum Harbour[10] to Deep Cove[27]. A minimum thickness of 350 m is estimated for the member in this area. At Hatch Point[28], on the west side of Saanich Inlet, an estimated thickness of over 500 m of Saanich member sandstone is present. In the Mt. Tzuhalem area[9], the member is at least 400 m thick and at Mt. Maxwell[17], Hanson (1976) estimated the unit to be a maximum of over 167 m (includes his middle mudstone and upper sandstone units).

In the Saanich Peninsula area, three distinct facies are developed within the Saanich member: 1) a crossbedded sandstone facies; 2) a coaly siltstone facies; and 3) a thick bedded massive sandstone facies. The crossbedded sandstone facies consists of thick bedded, coarse grained sandstone exhibiting medium scale planar and trough cross-stratification, interbedded with thin bedded grey shaly siltstone, shale, or thin beds of alternating sandstone and siltstone. Sandstone channels (3 x 10 m in cross-section) with distinct lateral pinch-outs into fine grained beds are present. Indistinct sand filled burrows, and coalified plant debris are common. This facies is well exposed on the shoreline 1 km southeast of Coal Point[27].

The coaly siltstone facies consists of thin bedded laminated siltstone and shale interbedded with thin to medium sandstone beds, which are well exposed at Bryden Bay in Tsehum Harbour[10]. The sandstone interbeds are locally rippled and trough crosslaminated. Coal spars, coalified stumps and roots, and carbonaceous shales are common, as well as rusty weathering concretionary fine grained sandstone and siltstone beds. On Forrest Island[29], this facies contains some thicker coarse grained sandstone lenses bearing robust bivalves, and contains spherical concretions in addition to concretionary beds. Sand filled burrows and bioturbated sediment are common. Coalified tree stumps up to 30 x 60 cm are present. The best exposures of the coaly siltstone facies are on southeastern Coal Island[30] where, in addition to the features described above, there are numerous discontinuous sheared coal seams, one of which is 2 m thick.

The thick bedded massive sandstone facies is well exposed along the Patricia Bay Highway[10] from Tsehum Harbour to the Swartz Bay Ferry Terminal. The section consists of thick to very thick bedded, massive, coarse grained sandstone beds interbedded with thin to medium recessive shale, siltstone and parallel laminated fine grained sandstone. The thick beds show few internal structures and have even, sharp upper and lower contacts. Rare linguoid ripple marks and large-scale load casts and flame structures locally are present. The recessive beds contain much coaly debris, some with thin coal layers up to 2 cm thick; these are probably detrital coal deposits as no root structures are visible. Fine pelecypod shells are present in the recessive beds of the upper part of this section. Gradually, the beds thin upwards, forming a transition to the overlying Haslam Formation turbidites. The thick bedded sandstone facies is well developed on Coal Island[30] and many of the small islands to the east of the Saanich Peninsula.

These three sedimentary facies serve to illustrate end members of the spectrum of facies in this basal sandstone unit of the Nanaimo Group. The base of the Saanich member should be taken to begin above the highest occurrence of Tzuhalem member conglomerate or above the basal unconformity; its top should be taken at the top of the uppermost occurrence of sandstone, 5 m or greater in thickness, beneath the Haslam Formation.

Northumberland Formation

The Northumberland Formation, in its restricted definition as the shales beneath the middle conglomerate member of Clapp's (1914) "Northumberland" Formation, was described by Muller and Jeletzky (1970). The formation overlies the De Courcy Formation and underlies the Galiano Formation. The section at False Narrows[31], originally described by Clapp (1914, p. 48), is a good reference section for the upper two-thirds of the Northumberland Formation. The shales are well exposed at James Bay on Prevost Island[32], on Parker Island[32], and in an outcrop belt running from Village Bay, Mayne Island[14], to Winter Cove[34] on Saturna Island. Reference to a single, completely exposed section in the Nanaimo Basin is not possible, but the outcrop belt described above allows a complete composite section to be constructed. The formation is estimated to be about 200 m thick at Village Bay, increasing to over 350 m thick in the Samuel Island[34] area.

Typically, the Northumberland Formation consists of recessive grey silty shales interbedded with thin very fine grained sandstones and siltstones. Bedding contacts are generally sharp, even, and continuous. Concretions and concretionary layers are common, which locally are rusty weathering. The sandstones and siltstones are massive or planar laminated, and their top surfaces commonly display burrows and grazing trails. Many of the sandstones probably lack internal stratification due to thorough bioturbation. Large fragmented shells of *Inoceramus* and ammonites, as well as coalified plant litter, are locally present. Well developed sandstone dykes are common, as well as some sandstone interbeds with dewatering pipes, sheet structures, and dish structures. In some areas, the sandstone interbeds become coarser grained and increase in thickness to 2-3 m, are graded, with scoured bases and abundant shale rip-up clasts. Locally, larger sandstone bodies are encased in Northumberland shale.

The upper and lower contacts of the Northumberland Formation are generally gradational, but abrupt contacts occur, such as at Welbury Bay[35], Saltspring Island; however, locally, interfingering relationships predominate such as at Winter Cove[34], Saturna Island.

Galiano formation

Galiano replaces the name "Geoffrey" as used by Muller and Jeletzky (1970) to identify the middle coarse grained unit of Clapp's (1914) Northumberland Formation. It overlies the Northumberland Formation and underlies the Mayne formation. The unit is greater than 350 m thick on Mt. Galiano[13] and greater than 550 m thick on northern Saturna Island[34]. In between these two points, rapid facies changes occur such that the Galiano formation can be less than 200 m thick, the remainder of the formation shaling out into Northumberland Formation. The Galiano formation is up to 400 m thick on North Pender Island[36] and Saltspring Island, and thins to only about 150 m on Gabriola Island[37].

The Galiano formation consists of thick bedded, coarse grained sandstone and pebble to cobble conglomerate, and associated finer grained beds. In the sandstone dominant areas, conglomerate forms lenses and channel fills within thick pebbly sandstone and sandstone beds. The sandstones commonly are buff to tan weathering with convolute to crude planar stratification, with planar crossbedding, sheet structures, and dish structures developed locally. The conglomerates display a range of sorting (good to poor) and the clasts are generally subrounded to rounded. In the conglomerate dominant areas, the conglomerates generally are more poorly sorted, containing boulder size clasts and local shale rip-up clasts of very large size. Typically they are clast supported within an unstratified coarse grained sandstone matrix. Associated fine grained beds commonly are graded, thin bedded mudstone and siltstone sequences, interbedded with sandstone. Mudstone rip-up clasts are common in the coarse grained facies.

The upper contact of the formation is sharp on Gabriola Island[37]. The lower contact is sharp but in some areas is more difficult to define because the lower Galiano formation interfingers with the Northumberland Formation. In practice, the base of the Galiano formation should be chosen at the base of the lowest sandstone or conglomerate bed greater than 5 m thick above the Northumberland Formation. Coarse grained bodies encased in upper Northumberland shale should be considered as Northumberland Formation.

Mayne formation

"Mayne" replaces the name "Spray" as used by Muller and Jeletzky (1970) for the upper shale unit of Clapp's (1914) Northumberland Formation. It overlies the Galiano formation and underlies the Gabriola Formation. At Miners Bay and Bennett Bay on Mayne Island[14], the formation is 220 m and 260 m thick, respectively. Between Saturna and Tumbo[38] islands the unit is estimated to be about 280 m thick. In the northwest part of the Nanaimo Basin, the Mayne formation is much thinner. It is measured to be about 100 and 110 m thick at two localities on northern Gabriola Island[37].

The formation consists of thin bedded, brownish-grey siltstone and grey mudstones, with fine grained sandstone and locally coarser grained sandstone interbeds. Contacts generally are sharp, planar, and continuous. The siltstones commonly are finely laminated, containing limonitic bands and small rusty weathering concretions locally. The sandstones are regularly graded or ungraded, may be convolute or planar crosslaminated, and with small-scale ripple marks locally preserved. Bouma BCD, and CD cycles are common. Bioturbation, a variety of trace fossils (including *Thalassinoides* and *Planolites*), coaly branches, and thin-shelled pelecypod shells are present. Large *Inoceramus* and ammonite shells are locally present.

The lower contact of the formation is sharp. The upper contact may be sharp, or, as in the Galiano[13], Mayne[14], Saturna[34] islands area, it may interfinger with or is transitional to the sandstones of the overlying Gabriola Formation. The top of the Mayne formation should be taken at the base of the lowest overlying sandstone bed thicker than 5 m.

COMOX BASIN

In the Comox Basin, the lithostratigraphic nomenclature remains mostly as established by Mackenzie (1922), Williams (1924), and Usher (1952). The tripartite subdivision of the Comox Formation, as described by Bickford et al. (1988), is useful, except that the basal conglomerate member should not be named Benson member, for reasons described earlier. The new informal name selected for the basal conglomerate in the Comox Basin is the Cottam Point member.

Comox Formation, Cottam Point member

The basal conglomerate of the Nanaimo Group in the Comox Basin was described in some detail by Mackenzie (1922). It unconformably overlies older rocks and is overlain by finer grained members of the Comox Formation, or by the Trent River Formation. Mackenzie (1922) noted that the unit infills a paleosurface with considerable relief (> 130 m) and as a result shows rapid but local changes in thickness. The conglomerate is best described as a texturally heterogeneous basal breccia. Muller and Jeletzky (1970) showed that at the Oyster River exposures[39], where the Comox Formation is over 650 m thick, there is more than 125 m of basal conglomerate. Bickford et al. (1988, p. 448) described the member as consisting of up to 300 m of coarse conglomerate interlensed with sandstone, siltstone, and vari-coloured shale, with rare coal seams. In the southern Comox Basin, the member reaches about 120 m in thickness.

Excellent exposures of the member and the basal unconformity occur at Cottam Point[1], east of Parksville[2]. There the member consists of a poorly sorted, clast supported, boulder conglomerate, composed of angular to subangular clasts of metasedimentary rocks, in a greenish-grey gritty sandstone matrix. Relief of up to 2 m is visible on the unconformity. Although the section is thin, it is a spectacular outcrop that is readily accessible. At Englishman River Falls[40], the basal conglomerate member consists of poorly sorted cobble to boulder conglomerate resting on basalts of the Karmutsen Formation. There the clasts are subrounded to well rounded, composed of the basement lithology. Thick-shelled pelecypod fragments are common in the coarse grained sandstone matrix. Stratification in the unit is poor. Muller and Jeletzky (1970) estimated its thickness to be in excess of 120 m at that locality. The conglomerate is thin and discontinuous at Little Qualicum Falls[41], and absent in many boreholes that have been drilled to basement in the Comox Basin.

The upper contact of the member should be taken as the top of the uppermost conglomerate bed, thicker than 5 m, underlying Cumberland member, Dunsmuir member, or Trent River Formation.

Trent River Formation, Parksville member

The Parksville member is a new, informal lithostratigraphic term for the pebble conglomerate and sandstone beds in the Comox Basin that occur within the Trent River Formation shales near Parksville[2]. The most prominent exposure of the conglomerate is at Little Mountain[7], where cliff forming, very thick bedded, massive pebble conglomerate rises 150 m above the surrounding coastal plain. The conglomerate is poor to moderately sorted, generally clast supported, well indurated, and composed of a variety of subrounded clasts in a tan, coarse grained sandstone matrix. The clasts are composed predominantly of chert, granodiorite, and white quartz, with minor sandstone and siltstone. In the Englishman River valley[8] to the east, near the railway bridge, there is at least 40 m of section exposed consisting of 15 m of medium bedded matrix supported pebble conglomerate and interbedded grit, overlain by 25 m of thick bedded, massive, poorly sorted pebble to cobble conglomerate. Outcrops along the lower part of the river valley consist of poorly indurated, medium to thick bedded, poorly sorted, clast supported, chert dominant pebble conglomerate, interbedded with tan to rusty weathering medium sandstone, which is fine to coarse grained, locally containing *Inoceramus* shells and coal clasts. Conglomerates commonly occur as lenses within the sandstones.

To the west, thin sections of conglomerate and sandstone are exposed in French Creek at Coombs[42]. Two folded conglomerate beds occur upstream from the highway bridge, and downstream, medium bedded, well indurated, fine grained carbonaceous sandstone overlies laminated shale. Along the beach east of the mouth of French Creek[43], disorganized, poorly sorted, pebble to cobble conglomerate, and medium grained to granule sandstones are exposed. Medium-scale trough crossbedding is well developed in the sandstones. Coal spars are common.

Overlying Trent River Formation shales at Northwest Bay[1], and exposed at Madrona Point peninsula[1] and on the west side of Cottam Point[1], are extensive outcrops of the Parksville member. About 150 m of section are developed in this area, consisting of about 100 m of light grey to tan weathering, fossiliferous sandstone overlain by 50 m of pebble conglomerate and sandstone. The lower sandstones are medium bedded, fine to medium grained, carbonaceous, and contain abundant brachiopod and pelecypod shells, including *Inoceramus*, and thin coquinas containing some thick shelled bivalves. Concretions, cobbles, and coal pebbles are locally present. The sandstones commonly show

signs of bioturbation. The upper coarse grained section consists of clast supported, poorly sorted pebble and cobble conglomerate occurring as thick beds, some of which are graded, or as lenses intercalated with medium bedded, clean, coarse grained sandstone. The conglomerates contain chert, quartz, granodiorite, and volcanic clasts. Medium to large scale (up to 7 m wide), planar and trough crossbedding is well developed in the uppermost sandstones.

The Parksville member is informally used to describe all of these coarse grained beds in the Parksville[2] area. The beds are obviously discontinuous at outcrop scale and at map scale and are considered to be coarse grained lenses within the Trent River Formation. Thick drift cover, and limited subsurface control hinder detailed definition of individual units. Aside from the probable thrust repeated sections in the Northwest Bay[1] area (Sutherland Brown and Yorath, 1985), they appear to occupy several stratigraphic levels within the shales.

Trent River Formation, Tsable member

The coarse clastic beds in the Tsable River[3] area, north of Trent River[6], and on lower Bloedel Creek[5] are assigned to the informal Tsable member. Muller and Jeletzky (1970, p. 21) described these beds as "lenticular bodies of conglomerate and sandstone, over 1000 ft (305 m) in a few places ... but pinching out within a few miles". They described how conglomerate incised into underlying Comox Formation, completely removing lower Trent River shales on lower Bloedel Creek[5]. The unit is poorly sorted (cobble to boulder size) consisting of well rounded to angular clasts of chert, metasedimentary and granitic lithologies, shales, and calcareous concretions. North of Trent River[6], boreholes have penetrated up to 108 m of coarse grained section within the Trent River Formation (Muller and Atchison, 1971), but on the Trent River only a thin section remains.

Surface mapping in the Tsable River area has revealed that much of the exposures east of Bradley Lake[44] are contiguous with the Comox Formation on upper Bloedel Creek[5] and south of Tsable River[4], and, therefore, cannot be included in the Tsable member as shown by Muller and Jeletzky's (1970) map (their unit 6), and on Bickford et al.'s (1988) map (their unit "E", western block). The beds closer to Langley Lake[3], and on lower Bloedel Creek[5] are considered to be truly intraformational beds of the Trent River Formation and therefore belong to the Tsable member. The beds in question are similar to what Muller and Jeletzky (1970) described as "Extension-Protection Formation" in that area, demonstrating the similarity between certain lithofacies of the Comox Formation and the Tsable member (their "Extension-Protection Formation). Indeed, distinguishing Tsable member from possible tongues of Comox Formation in the lowermost part of the Trent River Formation may be problematical in some areas, such as at the lookout east of Allen Lake[6], north of Trent River[6]. Only where the coarse grained facies can be shown to be within the Trent River shale, or to be laterally continuous to Trent River shale, should it be considered as the Tsable member.

ACKNOWLEDGMENTS

Research and field support by the Geological Survey of Canada and by BP Canada Resources Ltd. is gratefully acknowledged. The ideas in this text have benefitted from discussions with C.J. Yorath of the Pacific Geoscience Centre. Able assistance in the field was provided by G. Linden, L. England, M.V. Yorath, and W. McKittrick.

REFERENCES

American Commission on Stratigraphic Nomenclature
1970: Code of stratigraphic nomenclature; American Association of Petroleum Geologists, Tulsa, 22 p.

Bickford, C. and Kenyon, C.
1988: Coalfield Geology of eastern Vancouver Island (92F); in Geological Fieldwork 1987, British Columbia Ministry of Energy, Mines and Petroleum Resources, Paper 1988-1, p. 441-450.

Clapp, C.H.
1912: Geology of Nanaimo sheet, Nanaimo Coal Field, Vancouver Island, British Columbia; Geological Survey of Canada, Summary Report 1911, p. 91-105.
1914: Geology of the Nanaimo map-area; Geological Survey of Canada, Memoir 51, 135 p.

Clapp, C.H. and Cooke, H.C.
1917: Sooke and Duncan map-areas, Vancouver Island; Geological Survey of Canada, Memoir 96, p. 218-255.

Dickinson, W.R.
1976: Sedimentary basins developed during evolution of Mesozoic-Cenozoic arc-trench system in western North America; Canadian Journal of Earth Sciences, v. 13, p. 1268-1287.

England, T.D.J.
1988: Hydrocarbon potential of the Nanaimo Basin, southwestern British Columbia; *in* Sedimentary Basins of the Canadian Cordillera; Geological Association of Canada, Pacific Section, 1988 Symposium, p. 7.

Hanson, W.
1976: Stratigraphy and sedimentology of the Cretaceous Nanaimo Group, Saltspring Island, British Columbia; unpublished Ph.D. thesis, Oregon State University, 338 p.

McGugan, A.
1979: Biostratigraphy and paleoecology of Upper Cretaceous (Campanian and Maestrichtian) foraminifera from the Upper Lambert, Northumberland, and Spray Formations, Gulf Islands, British Columbia, Canada; Canadian Journal of Earth Sciences, v. 16, p. 2263-2274.

Mackenzie, J.D.
1922: The coal measures of Cumberland and vicinity, Vancouver Island; Canadian Institute of Mining and Metallurgy, Transactions, v. 25, p. 382-411.

McLellan, R.D.
1927: The geology of San Juan Islands; University of Washington Publications in Geology, v. 2, 185 p.

Muller, J.E. and Atchison, M.E.
1971: Geology, history and potential of Vancouver Island coal deposits; Geological Survey of Canada, Paper 70-53, 50 p.

Muller, J.E. and Jeletzky, J.A.
1970: Geology of the Upper Cretaceous Nanaimo Group, Vancouver Island and Gulf Islands, British Columbia; Geological Survey of Canada, Paper 69-25, 77 p.

Sutherland Brown, A. and Yorath C.J.
1985: Lithoprobe profile across southern Vancouver Island: Geology and Tectonics; in Field Guide to Geology and Mineral Deposits in the Southern Canadian Cordillera; Geological Society of America, Cordilleran Section Meeting, Vancouver, B.C., p. 8-1 to 8-23.

Usher, J.L.
1952: Ammonite faunas of the Upper Cretaceous rocks of Vancouver Island, British Columbia; Geological Survey of Canada, Bulletin 21, 182 p.

Ward, P.D.
1978: Revisions to the stratigraphy and biochronology of the Upper Cretaceous Nanaimo Group, British Columbia and Washington State; Canadian Journal of Earth Sciences, v. 15, p. 405-423.

Williams, T.B.
1924: The Comox Coal Basin; unpublished Ph.D. thesis, University of Wisconsin.

Sediment dynamics and implications for submarine landslides at the mouth of the Fraser River, British Columbia

R.A. Kostaschuk[1], B.A. Stephan[1], and J.L. Luternauer
Cordilleran and Pacific Geoscience Division, Vancouver

Kostaschuk, R.A., Stephan, B.A., and Luternauer, J.L., Sediment dynamics and implications for submarine landslides at the mouth of the Fraser River, British Columbia; in Current Research, Part E, Geological Survey of Canada, Paper 89-1E, p. 207-212, 1989.

Abstract

First measurements of sediment movement at and seaward of the mouth of the Fraser River reveal that sediment dynamics are controlled by river and tidal conditions and the position of the salt-wedge. Sediment concentrations and depositional rates are much higher at low tide than at high tide. Rapid deposition at the river mouth produces slope oversteepening and loading, factors that contribute to submarine landslides.

Résumé

Les premières mesures de transport des sédiments dans les limites et au large de l'embouchure du Fraser révèlent que les dynamique des sédiments est contrôlée par l'état du fleuve et des marées et par la position du coin de sel. Les concentrations et les taux de sédimentation sont beaucoup plus élevés à marée basse qu'à marée haute. Une sédimentation rapide à l'embouchure du fleuve produit une accentuation excessive et une surcharge de la pente, facteurs qui contribuent aux glissements de terrain sous-marins.

[1] Geography Department, University of Guelph, Guelph, Ontario, N1G 2W1

INTRODUCTION

In a comprehensive review of sediment survey programs on the Fraser River, Kellerhals (1984) indicated that the most pressing need is a detailed sediment budget of the delta. In response to this, an ongoing project, involving the University of Guelph, Geological Survey of Canada, University of British Columbia, Sediment Survey Section of the Inland Waters Directorate and Public Works Canada, started in 1985 to examine sedimentary processes in the outer Main Channel of the estuary. During 1985-87 the program focused on the factors controlling sediment suspension (Kostaschuk et al., 1986; Kostaschuk and Luternauer 1987, in press), bedform morphology (Kostaschuk and MacDonald, 1988), bed load (Kostaschuk et al., in press a), suspended load (Kostaschuk et al., in press b), salt-wedge related sediment transport and submarine landslides (McKenna and Luternauer, 1987). The results of these programs can be summarized as:

1. sediment transport (bed and suspended loads) varies directly with river discharge and tidal range and inversely with tidal height, although hysteresis complicates these relationships;
2. the salt-wedge affects the erosion, transport and deposition of bed material in the channel and at the mouth;
3. the mouth of the estuary is subject to frequent submarine landslides, during which previously deposited river mouth bar sediments are remobilized and deposited offshore via a delta front canyon-fan system.

These investigations have significantly improved our understanding of sedimentation in the Fraser estuary and have generated a number of related hypotheses requiring testing, the most salient being that rapid sediment deposition at the river mouth is responsible for the initiation of submarine landslides (e.g. McKenna and Luternauer, 1987). The 1988 survey, the preliminary results of which are reported here, was designed to test this hypothesis by examining sediment dynamics at the mouth of the Main Channel.

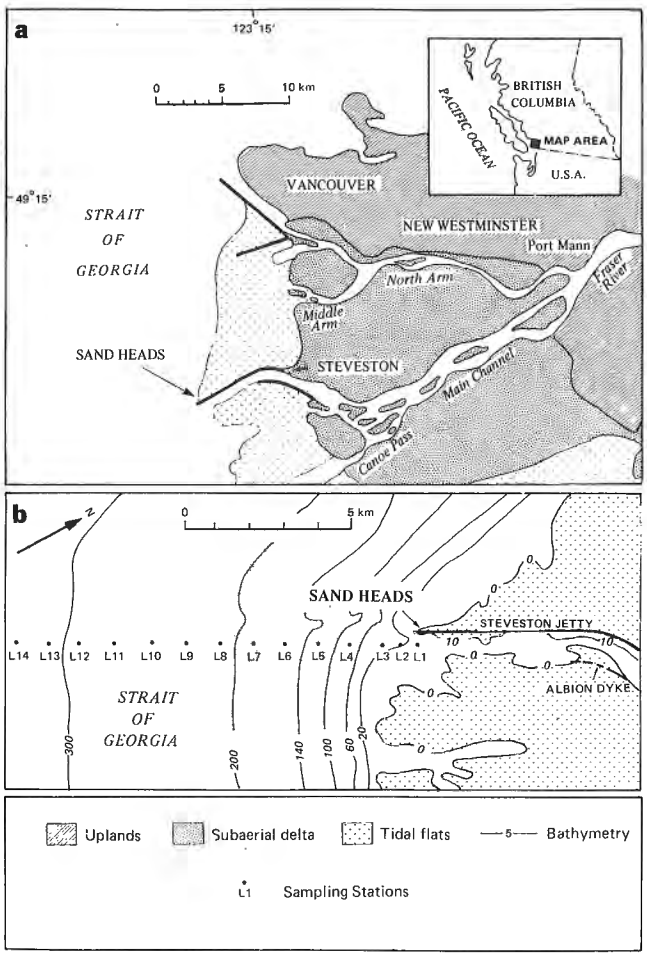

Figure 1. a) Fraser River delta. b) Study area and sampling stations at the mouth of the Main Channel. Note the position of Sand Heads light on a) and b).

SETTING

The Fraser River, the largest river on the Pacific coast of Canada, drains 250 000 km^2 of rugged terrain (Fig. 1). Conditions within the river are characterized in autumn and early spring by low water and low sediment discharge, in late spring and early summer by a snowmelt freshet period with high water and high sediment discharge, and in late summer by high water and low sediment discharge (Milliman, 1980). The 1988 freshet during May and June (Fig. 2) was one of the lowest and earliest on record, consisting of a well-defined peak in late May and several smaller peaks in June.

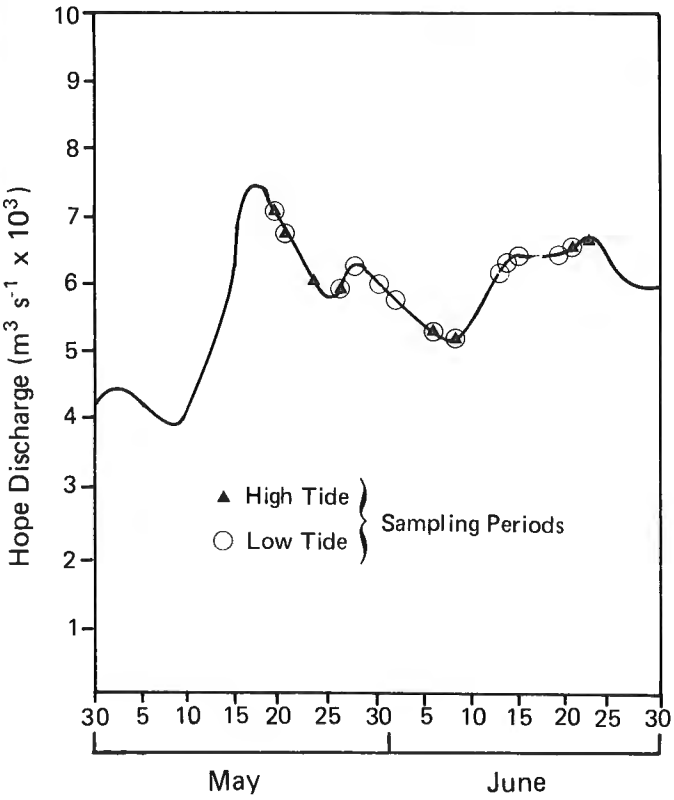

Figure 2. Hydrograph for the Fraser River at Hope during the May-June, 1988, study period. Data courtesy of the Water Survey of Canada.

In the estuary, a strong tidal effect is superimposed on the fluvial regime. Mixed, semi-diurnal tides in the estuary (Fig. 3) have maximum ranges at the river mouth that approach 5 m. Tidal range decreases both upstream and with increasing discharge (Ages and Woolard, 1976). The tide, in concert with river discharge, controls the position of the salt-wedge which in turn affects the mechanisms and rates of sediment transport (Kostaschuk and Luternauer, in press).

METHODS

Nineteen sets (11 at low tide, 8 at high tide) of field data were collected during six one-week cruises between May 16 and June 24, aboard *C.S.L. Jaeger*. Sampling was done during 2 hour time periods surrounding high and low tide (e.g. Fig. 3) in order to minimize temporal variations in conditions related to the tides (e.g. Kostaschuk et al., in press b). The vessel sequentially occupied a series of sampling stations at and seaward of the river mouth (Fig. 1b), finding and maintaining positions with Trisponder fixes. At each station vertical profiles were taken, at 2 m depth intervals, of water temperature and salinity (YSI Model 33 S-C-T meter) and current speed and direction (Marsh-McBirney Model 527 electromagnetic current meter). Suspended sediment samples were also taken at each station (pump sampler), at 2 m depth intervals at the two stations closest to the river mouth and at the surface at stations farther offshore. Suspended sediment samples were collected in 0.5 l containers to determine concentration and in 20 l containers for grain size analysis. Grain size data are not yet available.

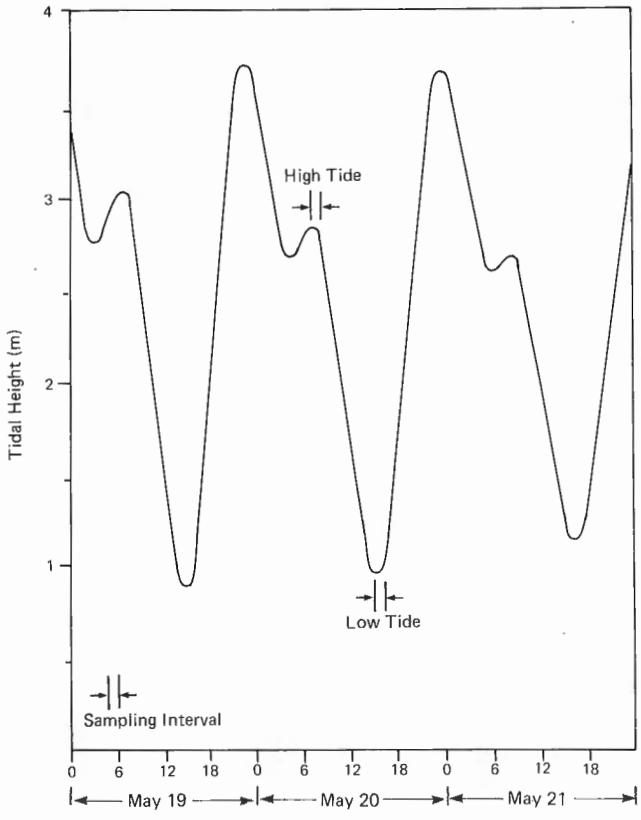

Figure 3. Tidal height at Steveston for 19-21 May, 1988, for a river discharge of 5700 m^3s^{-1} at Hope. Based on the Fraser River numerical model of Ages and Woolard (1976).

SEDIMENT DYNAMICS

The results show that river mouth sedimentary processes are controlled by tidal phase (high or low tide), tidal range and river conditions. In May, when river discharge was rising, sediment concentrations were relatively high as bank sediment in the drainage basin was mobilized (e.g. Kostaschuk et al., in press b). This supply of sediment was quickly exhausted and concentrations for similar discharges were lower in June. Tidal phase and discharge controlled the position of the salt-wedge, density stratification, the speed and direction of currents and suspended sediment concentrations. As a result, profound differences in river mouth sedimentary processes exist between high and low tide stages. Onshore-offshore variations are relatively consistent from tide to tide and can be illustrated by comparing high and low tide results for May 20 (Fig. 4). Comparing measurements from the same date effectively standardizes the influence of river conditions.

May 20 is just after the first freshet peak (Fig. 2) and sediment concentrations in the river were high. This was also a period of large tidal range. The high tide set was taken during lower high water, a stage of 2.75 m, and the low tide set during lower low water at 0.9 m stage (Fig. 3).

High tide

At high tide (Fig. 4a) the salt-wedge has intruded into the channel and flow at the river mouth (station L1) is stratified. Freshwater outflow in the upper layer is strong and there is a moderate upstream flow in the lower saline layer, in response to entrainment of salt-water by the outflow. There is a seaward (L1 to L6) decrease in both the thickness and velocity of the surface layer and the strength of the return flow, characteristics common to all buoyancy-dominated river mouths (Wright, 1977).

Sediment concentrations at the mouth are low, in response to the high tide and the landward intrusion of the salt-wedge in the channel. The rise of the tide in the Fraser results in deceleration of the outflow and deposition of suspended sediment (Kostaschuk et al., in press b). This effect is magnified by the presence of the salt wedge which further reduces sediment concentrations by eliminating the exchange of bed-material between the flow and bed and reducing turbulence in the upper layer (Kostaschuk and Luternauer, in press). There is a consistent, though gradual, seaward decline in concentrations, as sediment settles through the halocline.

Low tide

At low tide the salt-wedge has been flushed out of the channel, with the tip occupying a position near the top of the distributary mouth bar (Fig. 4b). The flow at the mouth (L1) is unstratified, and current speeds are high and directed downstream. Seaward (L3-L11), the flow becomes stratified, accompanied by a decrease in upper layer thickness

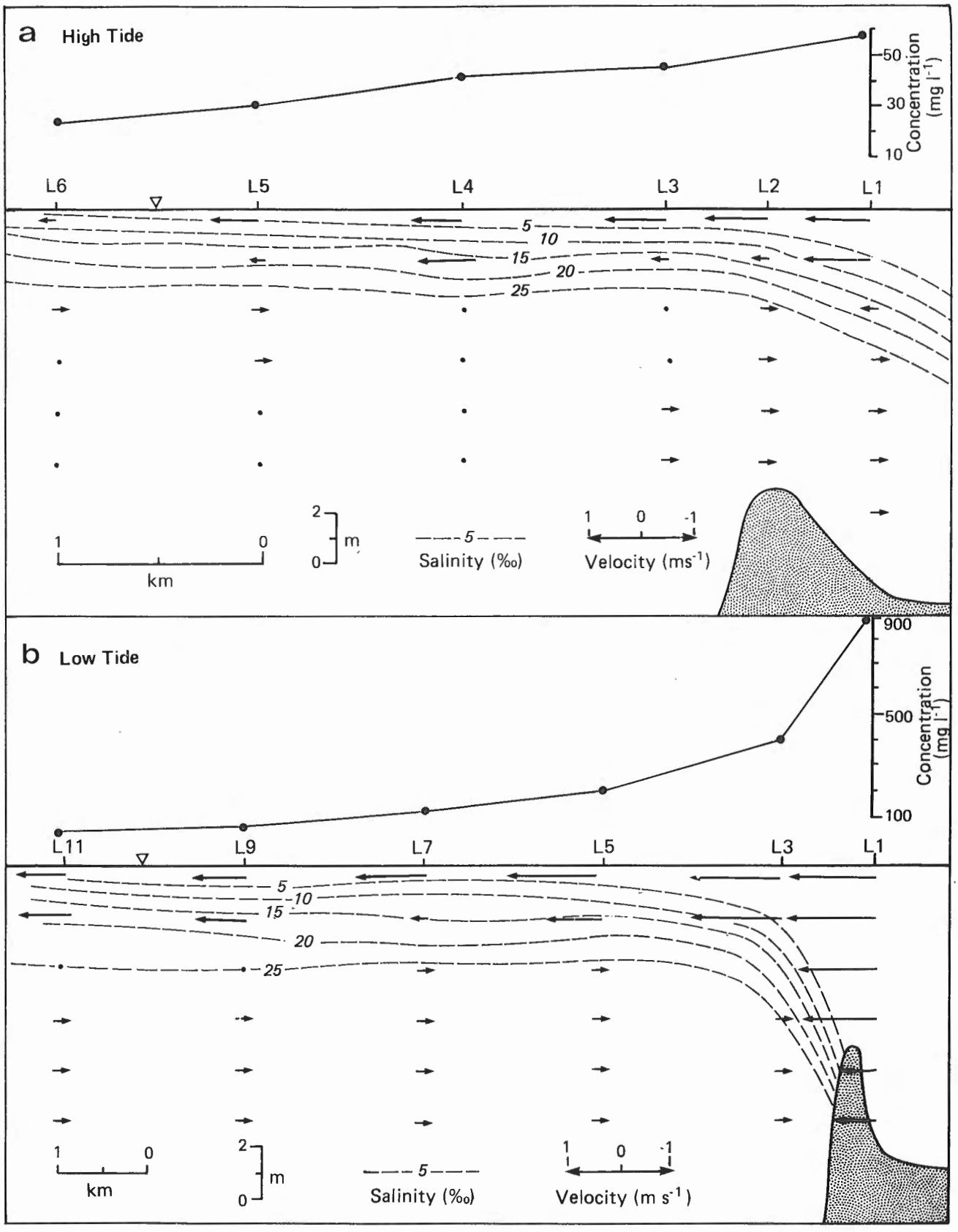

Figure 4. Variations along the centre of the river plume in flow and sediment concentrations, for 20 May, 1988, at: a) high tide, and b) low tide. Note the sampling intervals on Figure 3. River discharge at Hope was 6700 m^3s^{-1}.

and velocity and a weak return flow. Sediment concentrations at the river mouth are extremely high, with near-bed values exceeding 1000 mg l^{-1}, in response to the entrainment and re-suspension of coarse bed-material (e.g. Kostaschuk and Luternauer, in press) by the unstratified flow. Immediately seaward of the mouth (L3) there is a dramatic decline in concentration, due to flow stratification, and then a more gradual decrease offshore (to L11).

IMPLICATIONS FOR THE GENERATION OF SUBMARINE LANDSLIDES

Mass movements are common on the submarine slopes of most deltas (e.g. Kostaschuk and McCann, 1987), including the Fraser. Morphological evidence indicates that failures have occurred in numerous positions on the Fraser delta front, but the zone at the mouth of the Main Channel is most active (Luternauer and Finn, 1983). An extremely large slide occurred at this site in July 1985, having a minimum volume of one million cubic metres and extending to within 100 m of Sand Heads lighthouse (McKenna and Luternauer, 1987). Recent geophysical evidence shows that the distributary mouth bar at Sand Heads is incised by a series of 20-60 m deep gullies that coalesce downslope into a single large canyon (Luternauer et al., 1989). The canyon has a meandering pattern with well defined cut-bank morphology and bedforms on the channel floor. Near the base of the delta front slope, the canyon splits into a series of small distributary channels radiating over a submarine fan. Thus, morphology indicates that slides generated at the river mouth are transformed into debris flows or turbidity currents that transfer sediment downslope within the gullies and canyon, with eventual deposition on the submarine fan.

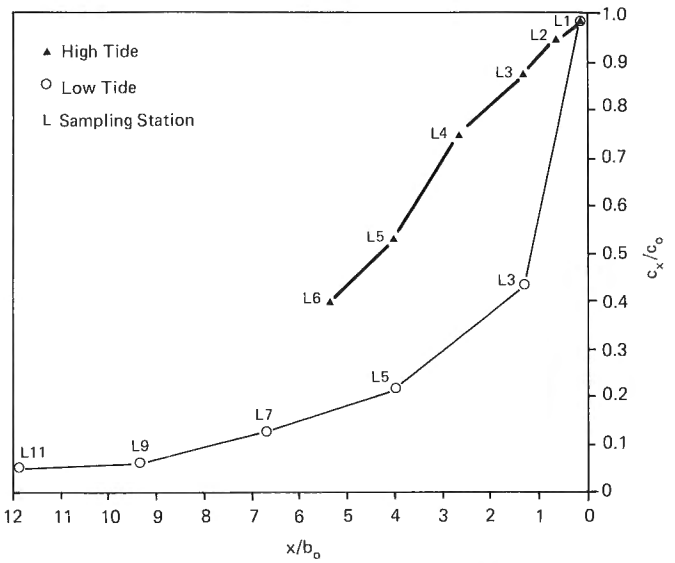

Figure 5. Dimensionless sediment concentration c_x/c_o, where c_x is the concentration at a distance x seaward of the river mouth and c_o is the concentration at the mouth, versus dimensionless distance x/b_o, where b_o is the width of the channel at the mouth. b_o was estimated at 750 m for low tide and 780 m for high tide on May 20, 1988.

Initial failure on the Fraser delta front could result from a number of causes such as earthquakes, waves, slope oversteepening, depositional loading and tidal drawdown according to McKenna and Luternauer (1987). They proposed that a combination of depositional loading and tidal drawdown triggered the 1985 slide. The data from 1988 allow us to examine relative rates and processes of deposition at the river mouth and to make inferences on the causes of slope failure.

It is apparent that large differences exist in depositional rates at the Fraser river mouth between high and low tide conditions (Fig. 4). The relative decline in sediment concentration seaward of the mouth can be considered in dimensionless terms. Figure 5 shows that at high tide there is a gradual, linear decrease in concentration offshore. At low tide the decrease is exponential because of the much coarser nature of the suspended sediment. Thus, for example, 1 km seaward of Sand Heads only 10 % of the sediment in suspension at the mouth has settled out at high tide whereas 55 % has been deposited at low tide. Considering the much higher concentrations at low tide, it is clear that effectively all deposition at the river mouth occurs at low tide.

Rapid deposition at the mouth of the Fraser can affect slope stability in at least two ways. First, the much more rapid sedimentation rates immediately seaward of the mouth relative to offshore will result in increasingly steeper gradients on the upper slope. Slope angles of 23° have been reported in this area (McKenna and Luternauer, 1987) and it seems likely that even steeper angles will result during freshet conditions. In any event, as slope gradients approach the effective friction angle of the sediment (35°; Luternauer and Finn, 1983), the potential for failure will increase. A second effect is the increase in pore-water pressure in underlying sediment caused by rapid depositional loading. Increased pore pressure reduces the strength of the material and consequently reduces the stability of the slope. Both slope oversteepening and depositional loading thus act simultaneously to destabilize the upper delta front. In addition, because most deposition occurs at low tides, tidal drawdown may also be a factor. The rapid fall of the tide produces excess pore pressures in the sediment and a reduction of sediment strength.

To provide a clearer understanding of the morphologies, mechanisms and causes of failure on the Fraser Delta front, a comprehensive form-process investigation is required. Such a program would:

1. map the mass movement morphology of the entire submarine delta;
2. examine the role played by the salt-wedge in the patterns and mechanisms of sediment erosion, transport and deposition;
3. determine the effect of the tidal range on sediment movement;
4. frequently monitor changes in bathymetry at the mouth of the channel.

CONCLUSIONS

The following conclusions can be drawn from this study of sediment dynamics at and seaward of the mouth of the Fraser River:

1. sediment dynamics are controlled by river and tidal conditions and the position of the salt-wedge;
2. sediment transport and deposition rates are much higher at low tide than at high tide;
3. massive deposition will result in slope oversteepening and depositional loading, factors that may produce submarine mass movements.

ACKNOWLEDGMENTS

We thank Randy Smith for piloting the *Jaeger* and M. A. Church and the Department of Geography, University of British Columbia, for technical assistance and the use of laboratory facilities. Financial support was provided by a Natural Sciences and Engineering Research Council Operating Grant to Kostaschuk and by Luternauer's Geological Survey of Canada Project 860022.

REFERENCES

Ages, A. and Woolard, A.
1976: The tides in the Fraser Estuary; Pacific Marine Science Report 76-5, Institute of Ocean Sciences, Sidney, B.C., 100 p.

Kellerhals, R.
1984: Review of sediment survey program; lower Fraser River, British Columbia; Consulting report to Sediment Survey Section, Water Survey of Canada, 36 p.

Kostaschuk, R.A. and Luternauer, J.L.
1987: Large-scale sedimentary processes in a trained, high-energy, sand-rich estuary - Fraser River delta, British Columbia; in Current Research, Part A, Geological Survey of Canada, Paper 87-1A, p. 727-734.

Kostaschuk, R.A. and Luternauer, J.L.
In press: The Role of the salt-wedge in sediment resuspension and deposition - Fraser River estuary, Canada; Journal of Coastal Research.

Kostaschuk, R.A., Luternauer, J.L., and Millard, T.M.
1986: Sediment transport in the outer Main Channel of the Fraser River estuary during the 1985 freshet; in Current Research, Part A, Geological Survey of Canada, Paper 86-1A, p. 565-570.

Kostaschuk, R.A., Church, M.A., and Luternauer, J.L.
In press a: Bed material, bedforms and bed-load in a salt-wedge estuary - Fraser River, British Columbia; Canadian Journal of Earth Sciences.

Kostaschuk, R.A., Luternauer, J.L., and Church, M.A.
In press b: Suspended sediment hysteresis in a salt-wedge estuary - Fraser River, Canada; Marine Geology.

Kostaschuk, R.A. and McCann, S.B.
1987: Subaqueous morphology and slope processes in a fjord delta, Bella Coola, British Columbia: Canadian Journal of Earth Sciences, v.24, p. 52-59.

Luternauer, J.L. and Finn, W.D.L.
1983: Stability of the Fraser River delta front; Canadian Geotechnical Journal, v.20, p. 606-616.

Luternauer, J.L., Dunkley, D., Gunkel, R., and Kostasohuk, R.A.
1989: New base map and computer graphics to help identify failures off the month of the Fraser River, B.C.: in Current Research, Part E, Geological Survey of Canada, Paper 89-1E.

McKenna, G.T. and Luternauer, J.L.
1987: First documented large failure at the Fraser River delta front, British Columbia; in Current Research, Part A, Geological Survey of Canada, Paper 87-1A, p. 919-924.

Milliman, J.O.
1980: Sedimentation in the Fraser River and its estuary, British Columbia; Estuarine and Coastal Marine Science, v.10, p. 609-633.

Wright, L.D.
1977: Sediment transport and deposition at river mouths - a synthesis; Geological Society of America, Bulletin, v.88, p. 857-868.

New base map and computer graphics to help identify failures off the mouth of the Fraser River, British Columbia

J.L. Luternauer, D. Dunkley[1], R. Gunkel[2], and R.A. Kostaschuk[3]
Cordilleran and Pacific Geoscience Division, Vancouver

Luternauer, J.L., Dunkley, D., Gunkel, R., and Kostaschuk, R.A., New base map and computer graphics to help identify failures off the mouth of the Fraser River, British Columbia; in Current Research, Part E, Geological Survey of Canada, Paper 89-1E, p. 213-220, 1989.

Abstract

Detailed bathymetric maps of the largest sea valley on the delta slope, which is the site of a major documented failure, were prepared from high-density-sounding surveys made by the Geological Survey of Canada and Public Works Canada. A hand-contoured bathymetric map which has been digitized, and graphics generated by computer from plotted soundings, offer a precise basis for effectively recognizing and displaying future failures, if a systematic program of revisory surveys is maintained.

Résumé

Les cartes bathymétriques détaillées de la plus vaste vallée marine présente sur le talus du delta, siège d'une importante rupture du terrain étudiée en détail, ont été préparées à partir du relevés réalisés par la Commission géologique du Canada et Travaux Publics Canada à partir de sondages très rapprochés. Les données reportées sur des courbes de niveau tracées manuellement, et numérisées, ainsi que les diagrammes informatiques produits à partir de diagrahies de sondages, nous offrent une façon précise d'identifier et de visualiser les ruptures possibles, à condition que l'on continue un programme systématique de levés d'inspection.

[1] #6-2295 W. 1st Avenue, Vancouver, B.C. V6K 1E9
[2] 2161 E. 20th Avenue, Vancouver, B.C. V5N 2L5
[3] Geography Department, University of Guelph, Guelph, Ontario N1G 2W1

INTRODUCTION

In this project we are investigating sedimentary processes at the lower reaches of the Fraser River and the stability of the delta slope (Fig. 1, 2) in response to: a) concerns raised by Kellerhals (1984) who pointed to the need for a detailed sediment budget of the delta, b) investigations by the Water Resources Branch of Environment Canada in Vancouver that have identified sites of slope retreat, and c) previous studies by the Geological Survey of Canada (eg. Luternauer and Finn, 1983; Hamilton and Luternauer, 1983; Luternauer and Macdonald, 1987; and McKenna and Luternauer, 1987) which have identified potential geohazards to development at the delta front.

Results of surveys of the sediment dynamics at the mouth of the river are discussed by Kostaschuk et al., (1989). This report focuses on our recent investigations of the slope off the Main Channel.

Slope studies have focused on detailed mapping of the Fraser seavalley (named by Shepard and Milliman, 1978) which extends off the Main Channel of the Fraser River (Fig. 2). Failure at this site must be better understood not only because it probably is a major element of the sediment budget of the delta front, but also, because it is a potential hazard (McKenna and Luternauer, 1987).

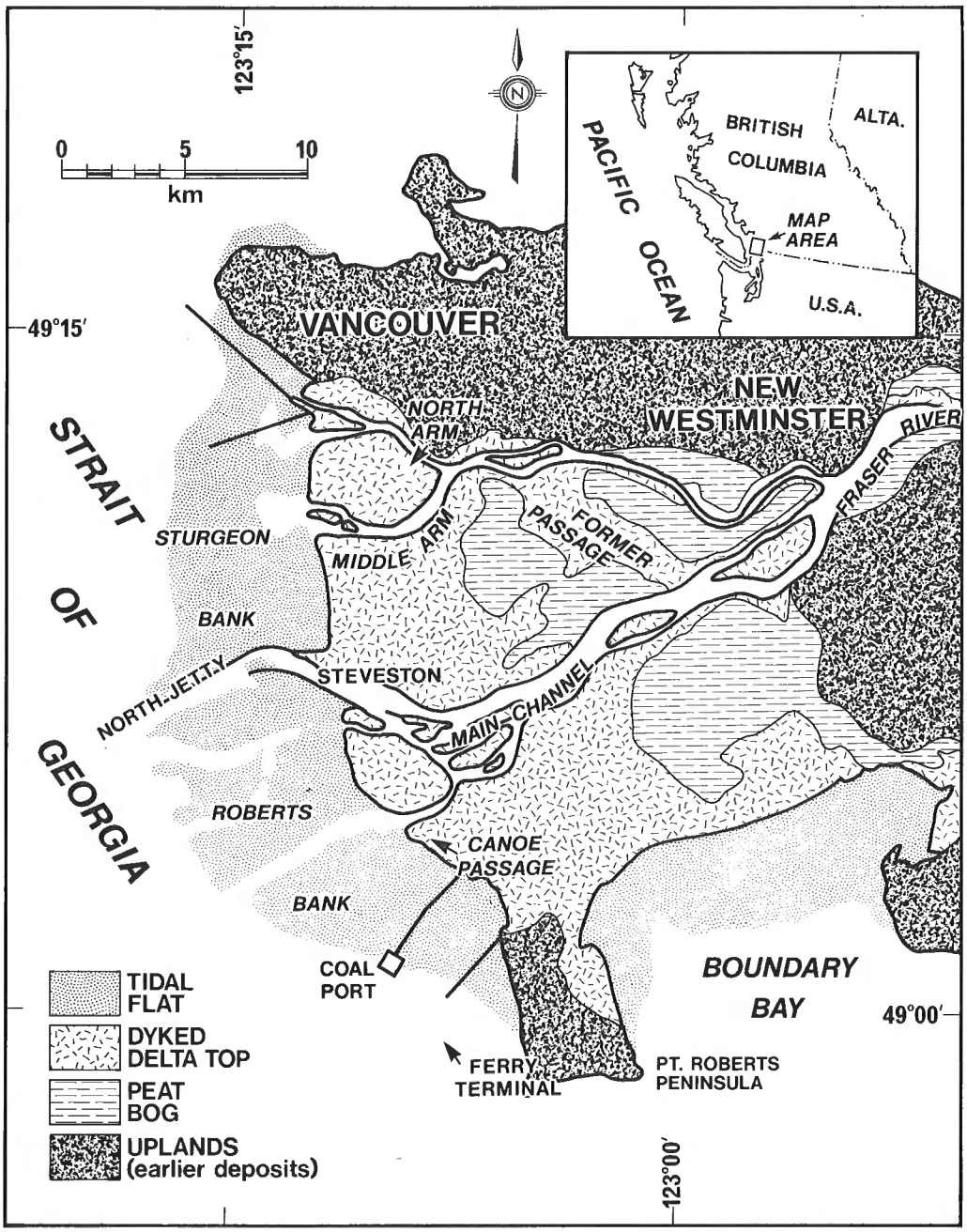

Figure 1. General geographic and sedimentary setting of study area.

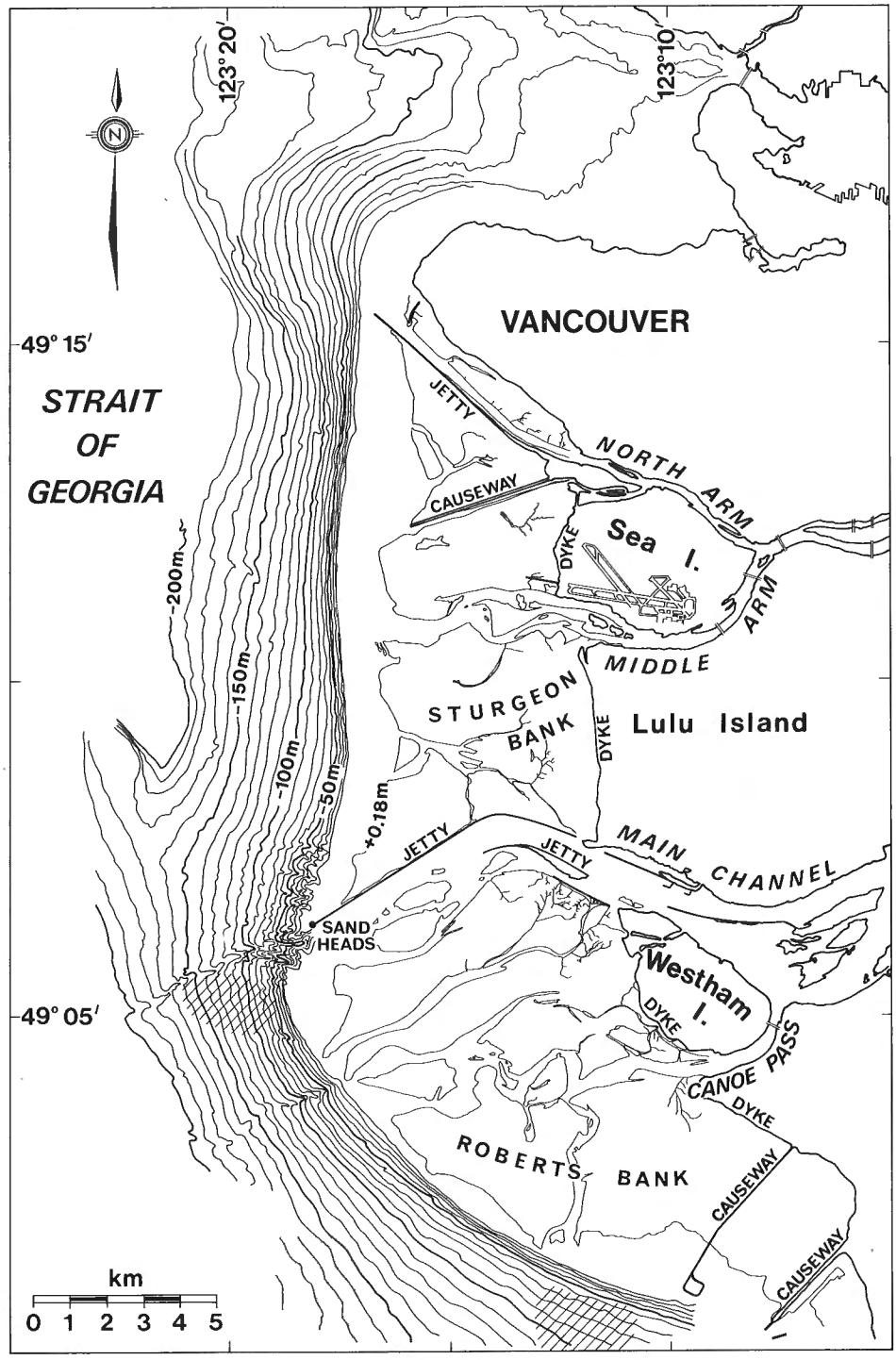

Figure 2. Detailed morphological setting of the Fraser seavalley which extends off the Sand Heads Lighthouse at the mouth of the Main Channel of the Fraser River. Cross-hachured areas on the slope represent areas with anomalous 2-3 m high sandwaves (southern patch) or sedimentary hummocks (northern patch).

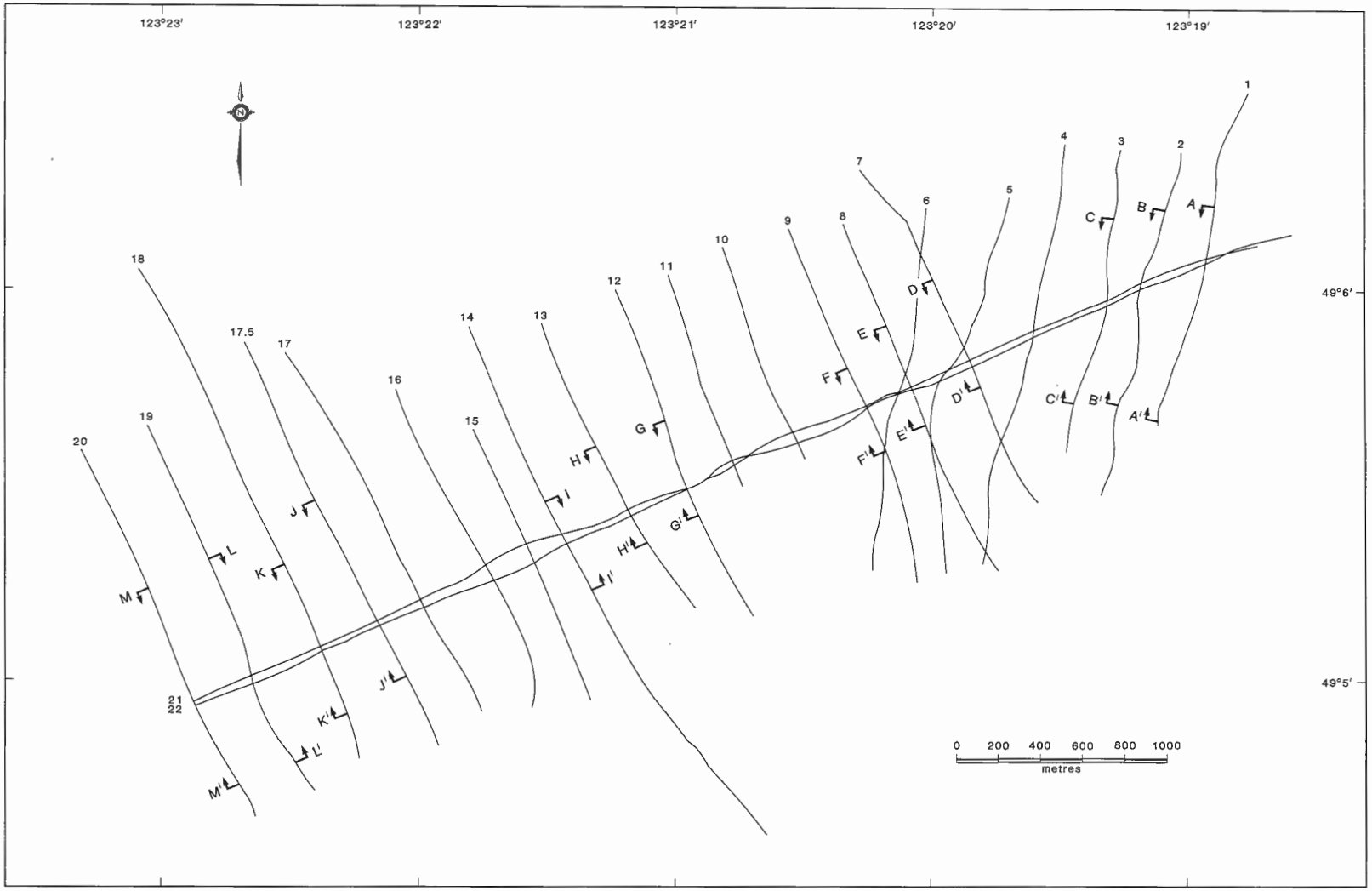

Figure 3. Trackline locations for detailed bathymetric survey of Fraser seavalley. Sections bracketed by lettered arrows indicate locations of profiles in Figure 5 and 6.

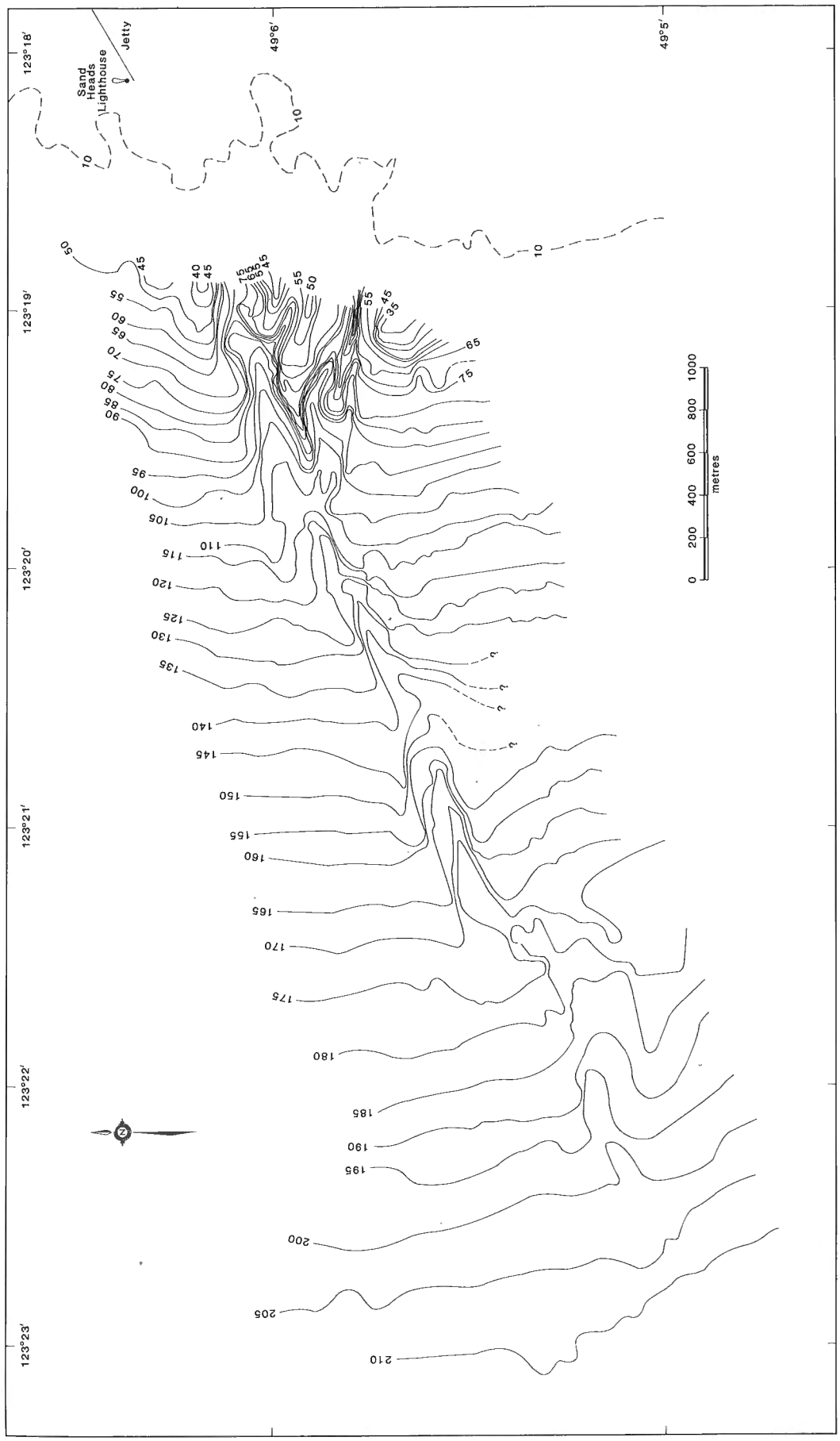

Figure 4. Hand-contoured detailed bathymetry of Fraser seavalley. Contours in metres.

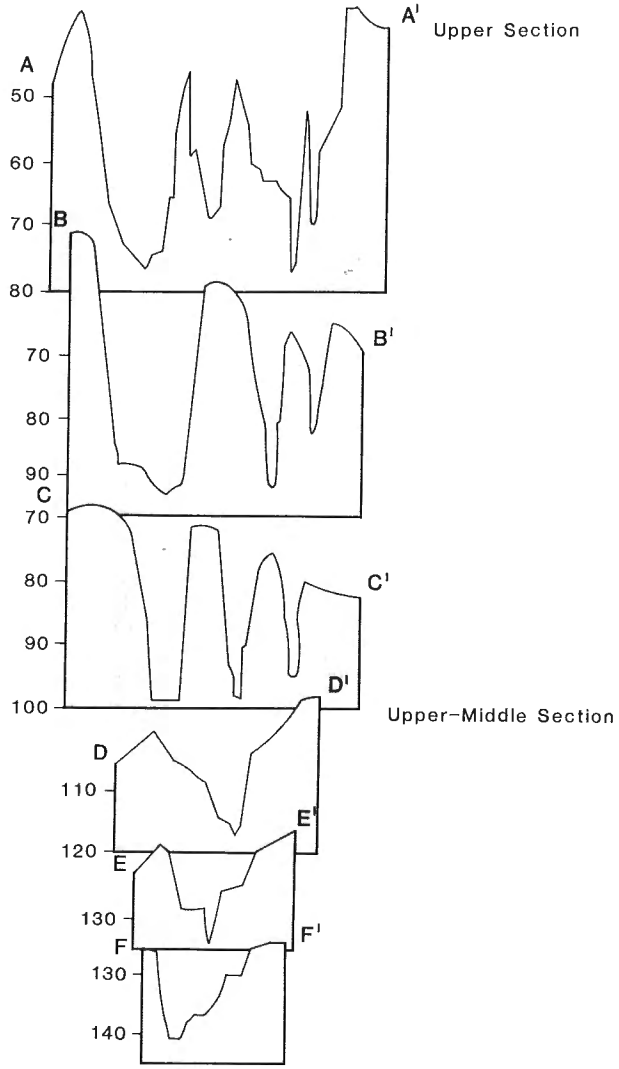

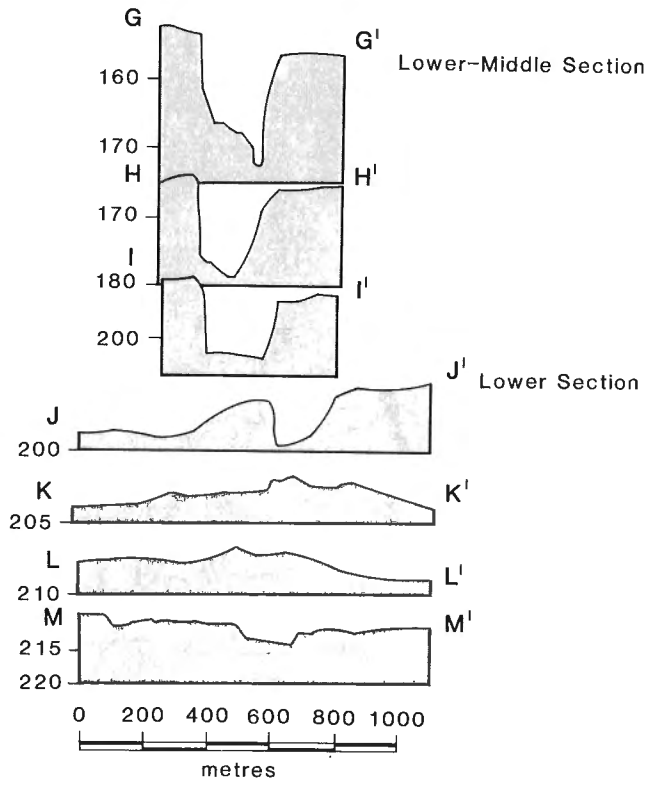

Figure 6. Selected bathymetric profiles of the lower part of the Fraser seavalley. Vertical exaggeration: 20x. Elevations in metres below sea level.

Figure 5. Selected bathymetric profiles of the upper part of the Fraser seavalley. Vertical exaggeration: 20x. Elevations in metres below sea level.

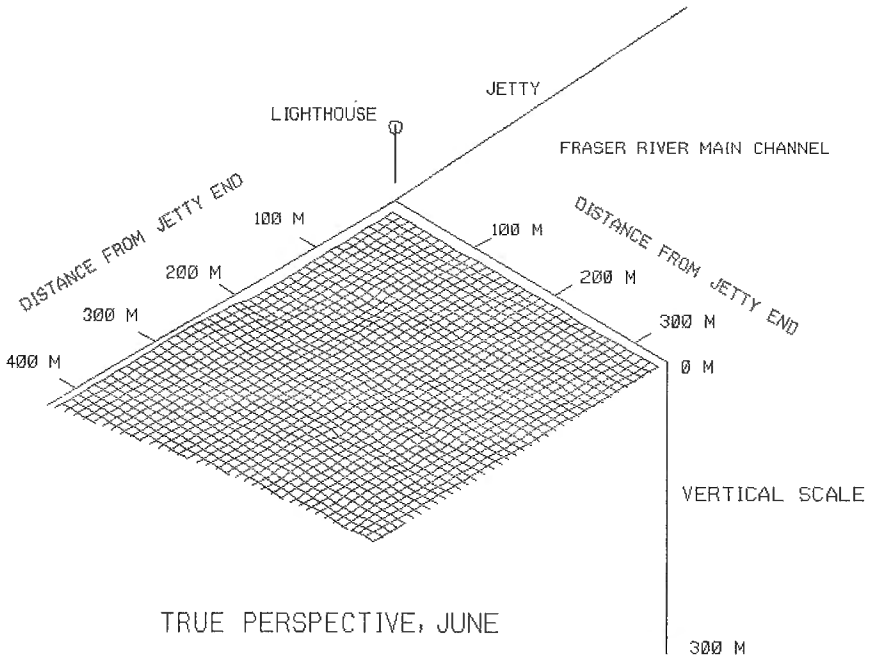

Figure 7. Computer graphic of the relief at the outer channel and upper slope area off Sand Heads Lighthouse on 27 June, 1985, prior to major failure. True scale perspective.

METHODS

The Geological Survey of Canada sounding survey of the seavalley for depths exceeding approximately 50 m below sea level was made from the *C.S.S. VECTOR*, 9-14 February 1987 with a 200 kHz sounder. Navigation was accomplished with a Del Norte Technologies Inc. Trisponder system coupled with the Magnavox 1102 Global Positioning System (Fig. 3). Public Works Canada surveying of the outer channel and upper slope was performed by the Ports and Waterways Engineering Survey Office, also using a 200 kHz sounder. Two sextants were used for navigation.

For the GSC survey, depths of all inflections of the bottom trace on the sounding record were plotted on computer drawn tracklines. The spot depths were hand contoured and contours were digitized for future manipulation.

A contour map of the bathymetric changes resulting from a major failure at the upper part of the seavalley was published earlier (McKenna and Luternauer, 1987). In this report we present computer generated perspective views of the pre-(June, 1985) and post-(July, 1985) failure slope surfaces as an example of the application of this technique to display morphological changes.

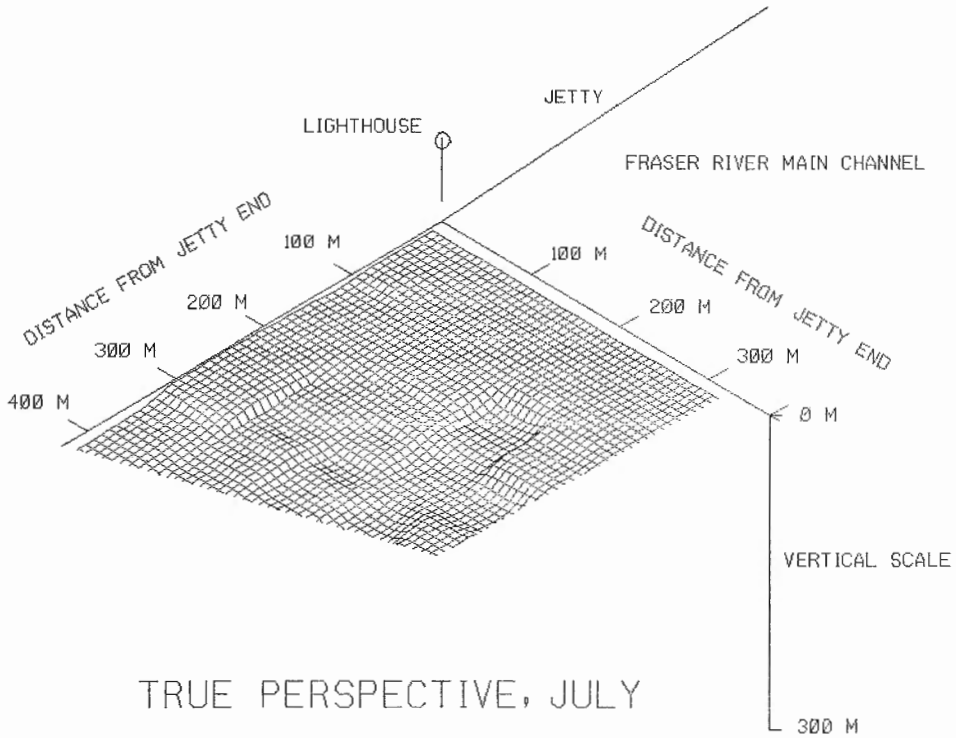

Figure 8. Computer graphic of the relief at the outer channel and upper slope area off Sand Heads Lighthouse on 11 July, 1985, after major failure. True scale perspective.

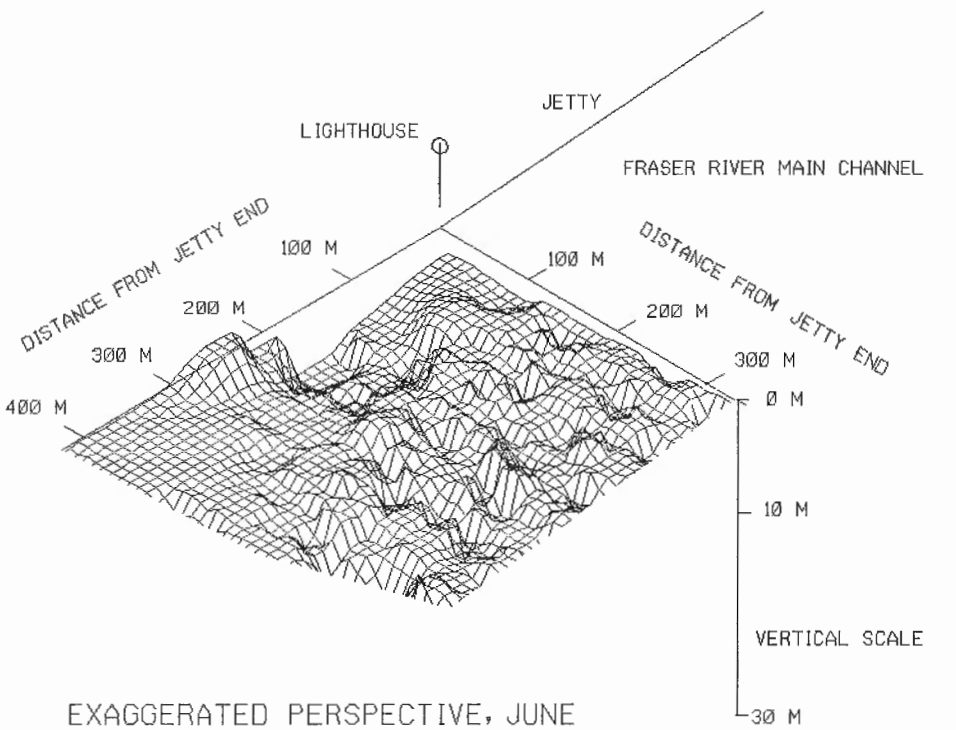

Figure 9. Computer graphic of the relief at the outer channel and upper slope area off Sand Heads Lighthouse on 27 June, 1985. Vertical exaggeration: 10x.

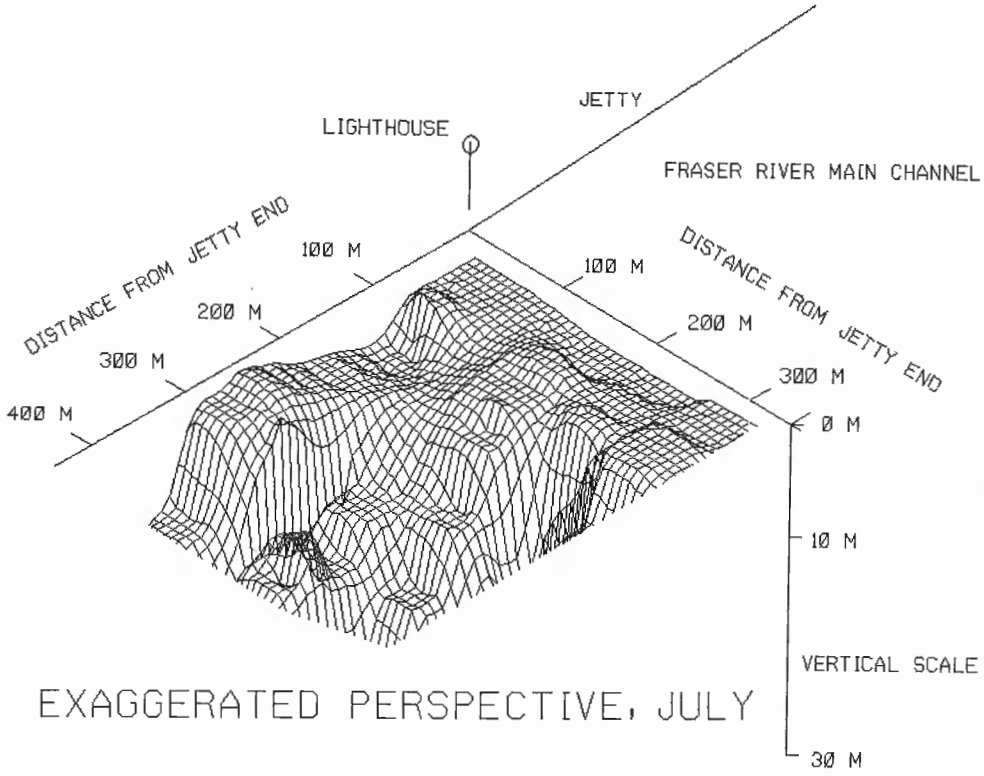

Figure 10. Computer graphic of the relief at the outer channel and upper slope area off Sand Heads Lighthouse on 11 July, 1985. Vertical exaggeration: 10x. McKenna and Luternauer (1987) estimated that about 10^6 m^3 of sediment failed from the area of the major depression shown.

Sounding data from Public Works Canada charts (McKenna and Luternauer, 1987) were digitized and manipulated at Intergraph Corp. workstations at British Columbia Institute of Technology connected to a VAX 750/VMS 4.0 minicomputer. The basic Interactive Graphics Design Software (version 8.8., rev. 2) was supplemented by the Digital Terrain Modelling software package, both provided by Intergraph Corporation.

RESULTS

The detailed bathymetric contour map of the main section of the Fraser seavalley (Fig. 4) coupled with bathymetric cross-sections (Fig. 5, 6) indicates that the many deeply incised tributary valleys at the head of the feature coalesce at about 115 m depth to form the main trunk valley which ends at about 200 m at the head of a muted fan. This fan is crossed by shallow tributary channels.

Well-defined terraces and the subsidiary channel sharply incised into the floor of the middle section of the seavalley suggest that the main valley has been regularly and recently scoured by tractive flows. Such finer morphological texture would rapidly be masked by the rain of finer suspended sediment discharged by the river if the valley floor were not repeatedly eroded. The morphological detail evident on the contoured map and cross-sections offer a precise basis for defining the timing and extent of local submarine landslides even if only a selection of the tracklines run on this first survey are duplicated at regular intervals in the future.

The computer-generated graphics (Fig. 7-10) showing the pre- and post-failure relief at the head of the slope adjacent to the Sand Heads Lighthouse indicate that the sounding data can be effectively manipulated to emphasize significant depositional or erosional events at the delta front. The value of these displays will be enhanced in future if suitable, available programs are applied to the data to calculate volume lost or gained between successive bathymetric surveys.

ACKNOWLEDGMENT

The authors wish to thank C. Davis for final drafting of Figures 3, 4, 5 and 6.

REFERENCES

Hamilton, T.S. and Luternauer, J.L.
1983: Evidence of sea floor instability in the south-central Strait of Georgia, British Columbia: a preliminary compilation; in Current Research, Part A, Geological Survey of Canada, Paper 83-1A, p. 417-421.

Kellerhals, R.
1984: Review of sediment survey program, lower Fraser River, British Columbia; consulting report to Sediment Survey Section, Water Survey of Canada, Environment Canada, 36 p.

Kostaschuk, R.A., Stephan, B.A., and Luternauer, J.L.
1989: Sediment dynamics and implications for submarine landslides at the mouth of the Fraser River, British Columbia; in Current Research, Part E, Geological Survey of Canada, Paper 89-1E.

Luternauer, J.L. and Liam Finn, W.D.
1983: Stability of the Fraser River delta front; Canadian Geotechnical Journal, v. 20, p. 606-616.

Luternauer, J.L. and Macdonald, R.D.
1987: Tractive flows adjacent to site for submarine sewage pipeline, Fraser River delta slope, British Columbia, Canada; in proceedings "Coastal Zone '87", Fifth Symposium on Coastal and Ocean Management (26-29 May, 1987), Seattle, Washington, American Society of Civil Engineers, p. 1862-1873.

McKenna, G.T. and Luternauer, J.L.
1987: First documented large failure at the Fraser River delta front, British Columbia; in Current Research, Part A, Geological Survey of Canada, Paper 87-1A, p. 919-924.

Shepard, F.P. and Milliman, J.D.
1978: Sea-floor currents on the foreset slope of the Fraser River delta, British Columbia (Canada); Marine Geology, v. 28, p. 245-251.

New approaches for assessing liquefaction potential of the Fraser River Delta, British Columbia

W.D.L. Finn[1], D.J. Woeller[2], M.P. Davies[2], J.L. Luternauer, J.A. Hunter[3], and S.E. Pullan[3]
Cordilleran and Pacific Geoscience Division, Vancouver

Finn, W.D.L., Woeller, D.J., Davies, M.P., Luternauer, J.L., Hunter, J.A., and Pullan, S.E., New approaches for assessing liquefaction potential of the Fraser River Delta, British Columbia; in Current Research, Part E, Geological Survey of Canada, Paper 89-1E, p. 221-231, 1989.

Abstract

A field study was conducted in Richmond, B.C. in June 1988 to test procedures and methods proposed for use in a regional assessment of liquefaction potential in the Fraser River Delta. Seismic piezocone tip resistances and shear wave velocities were measured in eight test holes. Sediment samples collected from a 122 m borehole are being processed. Preliminary assessment of the field data suggests that there is the potential for liquefaction during earthquakes of magnitude $M_s > 6.5$ causing peak ground accelerations $a_p > 0.17$ g. It is recommended that data on cone tip resistance, shear wave velocity and subsurface samples be acquired for other areas of the delta.

Résumé

On a réalisé à Richmond en C.-B. au mois de juin 1988 une étude de terrain afin de tester les procédés et méthodes envisagés pour l'évaluation régionale du potentiel thixotrope des terrains du delta du Fraser. On a mesuré dans huit sondages expérimentaux les résistances sismiques mesurées à la pointe d'un piézocône et les vitesses de cisaillement. On a soumis à un traitement en laboratoire des échantillons de sédiments recueillis dans un sondage de 122 m. L'évaluation préliminaire des données de terrain suggère l'existence d'un potentiel thixotrope durant les séismes de magnitude $M_s > 6.5$, qui entraînent au sol des accélérations de pointe > 0.17 g. Il est recommandé que l'on obtienne pour d'autres régions du delta des données sur la résistance mesurée à la pointe d'un cône, sur la vitesse des ondes de cisaillement, et sur les échantillons de subsurface.

[1] Soil Dynamics Group, Department of Civil Engineering University of British Columbia, Vancouver, B.C. V6T 1W5
[2] ConeTec Investigations Ltd., 2447 Beta Avenue, Burnaby, B.C. V5C 5N1
[3] Terrain Sciences Division, Ottawa

INTRODUCTION

The Fraser Delta (Fig. 1) is adjacent to one of the most highly seismic regions of Canada and is therefore exposed to significant seismic hazards (Basham et al., 1982, 1985). There is extensive evidence from past earthquakes that buildings and industrial lifelines, such as transportation arteries and oil and gas lines, on or in saturated loose deltaic sediments are highly vulnerable to damage (Kawasumi, 1968). Consequently, in the Fraser Delta, the effects of seismic loading on structures and foundation soils should be taken into account in the design of structures and the planning of major developments.

One of the most vulnerable areas of the Fraser Delta is the municipality of Richmond because of the relative youth of the sediments underlying this area and the closeness of the water table to the ground surface. A previous study of the liquefaction potential of the area based mainly on standard penetration data (Byrne and Anderson, 1987) suggests liquefiable soils are widespread. A substantial hazard is the possibility of seismically induced damage to the dykes that protect the low-lying lands from flooding.

The most severe threat to the region would probably arise from a "megathrust" earthquake, comparable to the 1985 Mexican earthquake, along the subducting Juan de Fuca Plate (Dragert and Rogers, 1988). Such an earthquake is expected to have a magnitude of $M_s = 8+$. If a megathrust earthquake is possible, then its impact should be considered in any study of seismically induced liquefaction at the Fraser Delta.

BACKGROUND AND PROGRAM OBJECTIVES

The Geological Survey of Canada (GSC) has completed two stages of the multi-stage geophysical and geotechnical program at the Fraser River Delta. The completed stages of the program have included the collection of requisite baseline data in the form of soil samples, seismic cone penetration tests (SCPT), standard penetration tests (SPT) and geophysical logs (Luternauer, 1988). One of the main objectives of the overall program is to make a reliable assessment of the liquefaction potential of this area of the lower mainland of British Columbia by state of the art procedures. Therefore, as a logical third stage, the GSC is planning the collection of additional information which will allow for critical evaluation of the liquefaction potential of near surface sediments within the region of study.

The first step towards this objective is the development of a method of liquefaction assessment which is based on a hierarchy of liquefaction estimators so that complexity is introduced into the assessment only when necessary. The basic procedures to be incorporated into the model for the empirical evaluation of liquefaction potential are: (1) the CPT approach (Seed and deAlba, 1986); (2) the threshold strain approach (Dobry et al., 1981) and (3) the shear wave velocity approach (Stokoe and Nazarian, 1985). These methods give a deterministic assessment of liquefaction potential for a specified earthquake based on the performance of similar sites in past earthquakes.

The Richmond area is unique in that recently much data on near-surface sediments have been obtained using the seismic piezocone penetration test. The seismic cone penetration test provides basic parameters which enable one to evaluate liquefaction potential using three independent procedures.

Over 100 cone penetration tests have been conducted in the Fraser Delta in recent years. About 75 of these tests were made in Richmond and have been submitted to regulatory agencies for permitting purposes. These data are stored in computer files and form the basic framework for a regional assessment of liquefaction. The data can be stored in a data base and then readily manipulated for micro-zoning for liquefaction. An important step in ensuring the continual updating of liquefaction potential is to create a computer database of cone penetration resistances and associated shear wave velocities in which new data can be incorporated.

The proposed method would be applied first using the presently available data to make a preliminary assessment of the regional hazard of liquefaction. This step would expose areas where the data are insufficient or unavailable and should prove useful in optimizing the outlays on future efforts directed towards the goal of determining the liquefaction potential of the Fraser River Delta.

Risk assessments based on the probabilistic occurrence of seismic events need to be developed as an overlay on the basic data base to provide measures of risk to public safety and industrial development (Finn, 1987). In addition, site-specific analyses of dynamic effective stress response should be made for sites that are, or are to be, the locations of critical structures (Finn, 1988).

To demonstrate the field procedures and the operation of the model, a site was selected which incorporates a section of the land protection dykes (Fig. 4). Preliminary field studies were done at this site using seismic piezocone penetration tests. Cone bearing resistance, cone friction, pore pressure response, and shear wave velocities were measured.

The cone penetration tests (CPT) were conducted by Conetec Investigations Ltd., Burnaby, B.C., who were involved in the development of the seismic cone and its application in practice. Data reduction was accomplished automatically using proprietary software developed by Conetec.

LIQUEFACTION POTENTIAL FROM CONE PENETRATION TESTS

The liquefaction resistance of a site is characterized by the tip resistance, Q_t, normalized to a pressure of 100 kPa (= 1 tsf) and designated Q_{tl}. The normalized resistance is given by $Q_{tl} = C_N Q_t$ and C_N may be determined from the charts in Figure 2 (Marcuson and Bieganousky, 1977).

The liquefaction generating power of the earthquake for a given earthquake magnitude is specified by the cyclic stress ratio τ_{eq}/σ_{vo}' given by Seed (1979) as:

$$\tau_{eq}/\sigma_v' = 0.65 \frac{\sigma_v}{\sigma_v'} \cdot Ar_d \qquad (1)$$

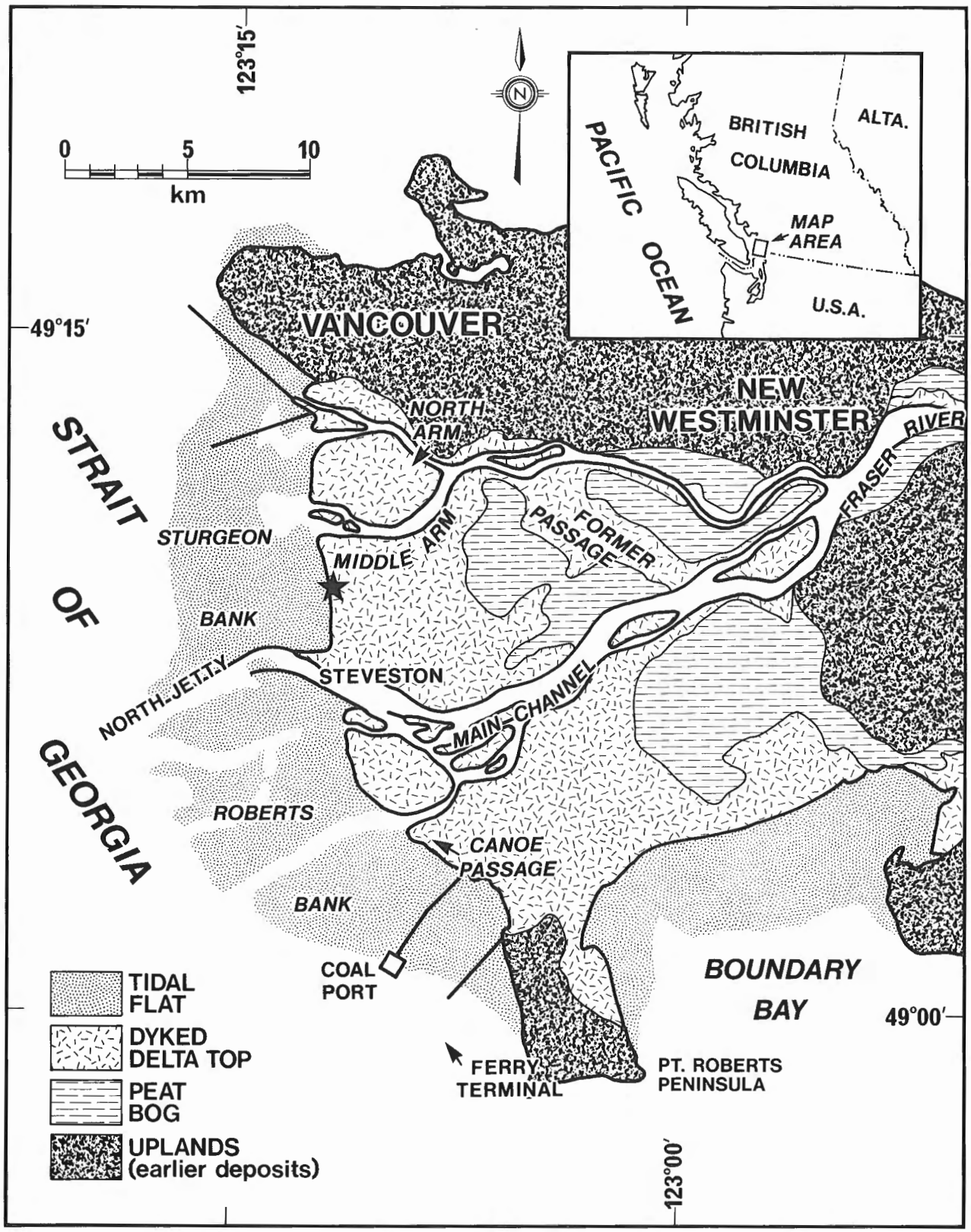

Figure 1. Physiographic subdivisions and surficial deposits, Fraser River delta and environs. Star indicates location of survey site (Fig. 4).

where

σ_v = total overburden stress

σ_v' = effective overburden stress

A = peak ground acceleration as a fraction of the acceleration due to gravity

r_d = a reduction factor to account for soil flexibility (Seed, 1979). It is commonly assumed to vary from 1.0 at ground surface to about 0.9 at a depth of 10 m.

τ_{eq} effective or equivalent average seismically induced shear stress.

Liquefaction potential can be determined on an empirical basis using the chart shown in Figure 3 (Seed and deAlba, 1986). The curves in the chart are lower bounds for separating sites which liquefied in past earthquakes with magnitudes up to M = 7.5 from those which did not liquefy. Therefore, the curves give the critical Q_c value required to prevent liquefaction during earthquakes with magnitudes M_s = 7.5. Lower bound curves for earthquakes of other magnitudes, M_s, may be established by multiplying the critical stress ratios in Figure 3 by the factors given in Table 1.

The potential for liquefaction in a given sand layer during an earthquake of magnitude M_s is determined by plotting the state point (Q_{tl}, τ_{eq}/σ_{vo}') on the chart and noting whether it falls above or below the lower bound curve.

The data base of Figure 3 is limited to sites where liquefaction occurred under effective confining pressures less than 150 kPa (1.5 tsf).

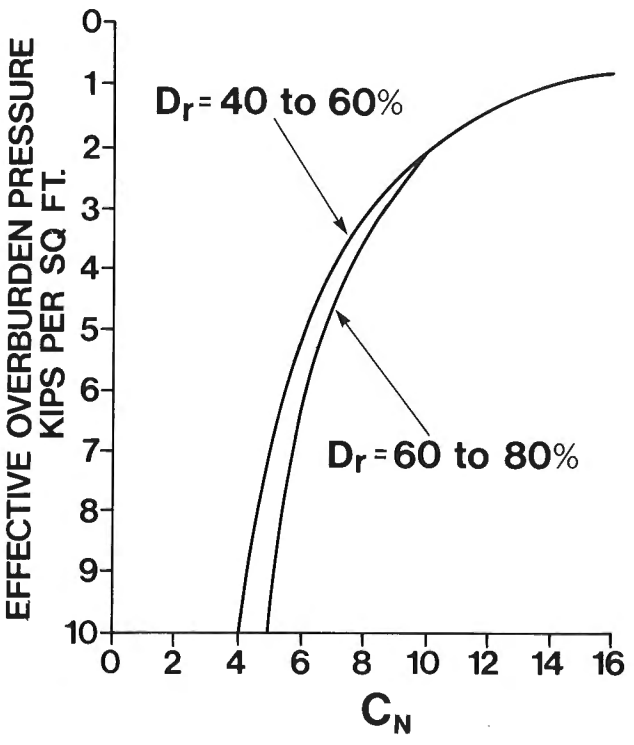

Figure 2. Curves for values of overburden correcting factor C_n. From Seed et al. (1984) based on data and analyses from Marcuson and Bieganousky (1977). 1 KIP = 1000 lbs.

FIELD INVESTIGATIONS IN RICHMOND

The fieldwork was carried out between June 7 and 15, 1988. A total of eight seismic piezocone penetration tests (SCPT) were carried out along the sea protection dyke near the extreme western end of Blundell Road in Richmond (Fig. 4). The SCPTs were advanced to depths varying from 30-45 m below the top of the dyke. During the investigation, the equilibrium water level was, on average, about 1.5 m below ground surface.

Just prior to the seismic cone penetration testing, tests were made to evaluate the potential of using surface shear wave refraction methods to estimate the shear wave velocities as a function of depth. These measurements were carried out on the tidal flats beside the dyke, rather than on the dyke itself, to avoid the disturbed ground associated with the dyke fill.

Table 1. Representative number of cycles and corresponding correction factors (after Seed, 1979)

Earthquake magnitude	No. of representative cycles at 0.65 τ_{max}	Factor to correct abscissa of curve in Figure 3
8.5	26	0.89
7.5	15	1.0
6.75	10	1.13
6.0	5-6	1.32
5.25	2-3	1.5

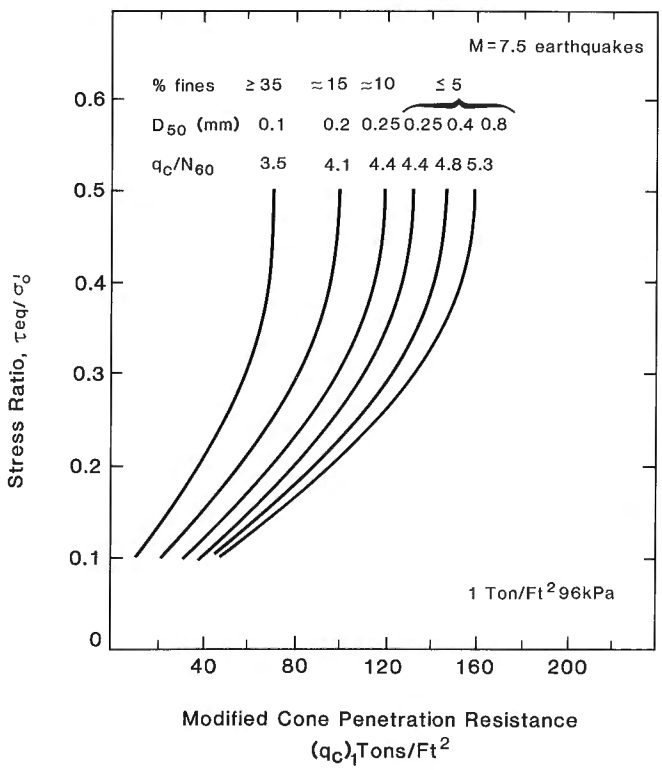

Figure 3. Relationship between stress ratio causing liquefaction and cone tip resistance for sands and silty sands. From Seed and deAlba (1986).

Electric cone testing

A 10 ton subtraction-type cone was used in all the penetration tests. This cone has a tip area of 10 cm^2 and a friction sleeve area of 150 cm^2. The subtraction cone is designed with an equal end area friction sleeve and a tip end area ratio of 0.85. We recorded: tip resistance (Q_t), sleeve friction (F_s), dynamic pore pressure (U_t), temperature (T), cone inclination (i) at scan depth intervals, and shear wave velocity at 1 m $\pm$ 5 cm intervals. These parameters were printed simultaneously on a printer and stored on a bubble cassette cartridge for later transfer to floppy disk for analysis and reference.

Seismic wave velocity measurements

Seismic wave velocity measurements were conducted each time the cone penetration test was stopped to add additional push rods. This corresponds to one metre testing intervals. Before taking wave velocity measurements, the rods were decoupled from the drill rig. An oversized friction reducer was used to facilitate the decoupling of the cone rods from the soils in an effort to ensure both a high quality signal and a high signal to noise ratio.

Shear waves were generated by striking in both longitudinal directions a steel beam which was held down by the rare stabilizers of the drill rig. The centre of the beam was offset 0.92 m horizontally from the cone rods. This offset was accounted for in the velocity calculations.

A contact trigger between the beam and hammer produced precise triggering times and allowed for the accurate timing of the markers of the shear waves.

The wave traces were recorded, inspected and saved on a specially modified microcomputer. The two traces are overlayed on a digital oscilloscope screen and the arrival and first crossover times are determined.

The surface shear wave refraction experiment used a long array of horizontal geophones to record the energy produced by a seismic shotgun source. Source-geophone separations increased in 1 m increments from 1-120 m. The data were recorded on a engineering seismograph and transferred to a microcomputer for processing and display. The onset of shear energy was plotted as a function of time, and inverted using standard refraction techniques to determine the shear wave velocity as a function of depth.

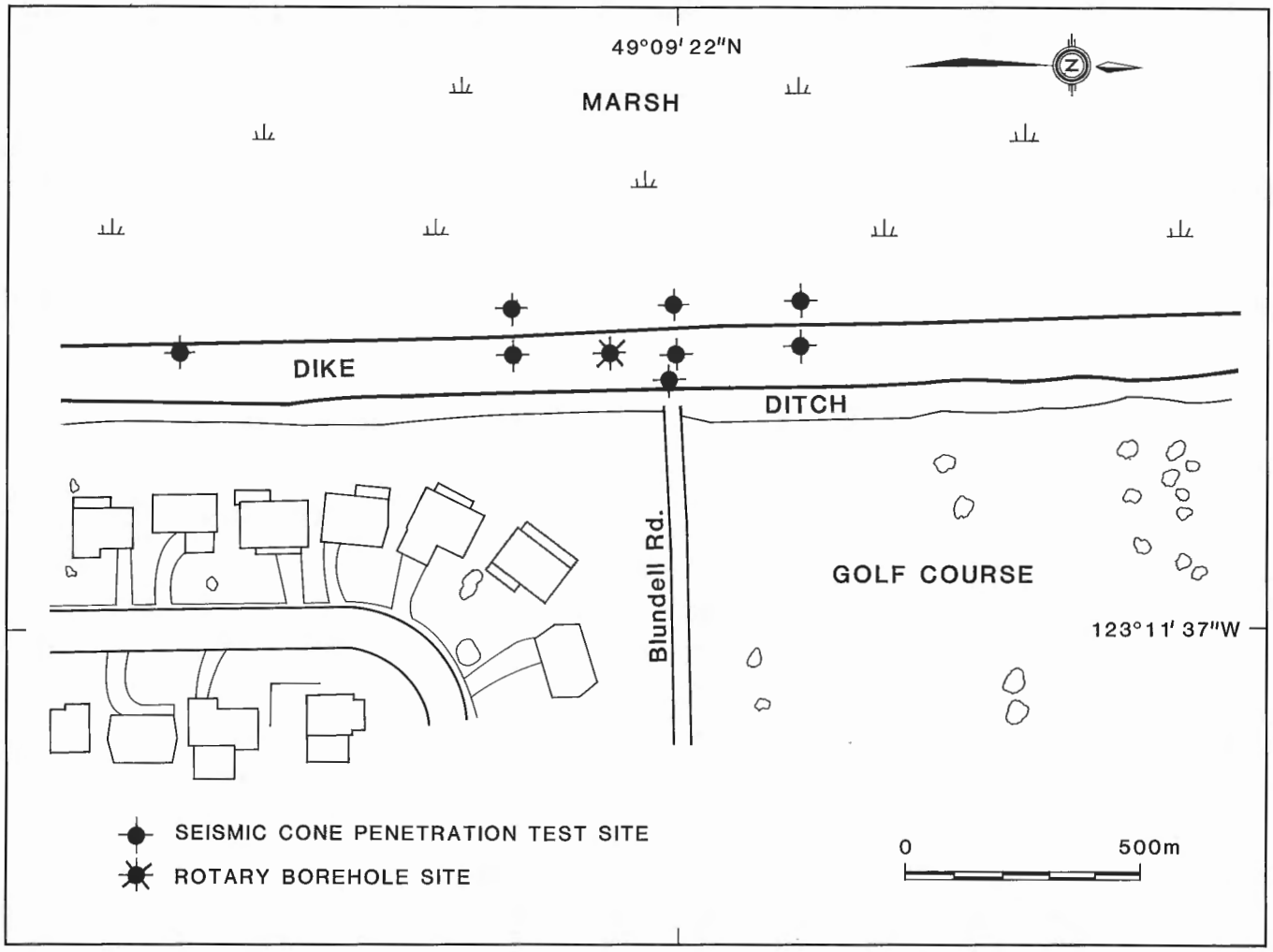

Figure 4. Locations of geotechnical measurements, dyke at foot of Blundell Road, Richmond.

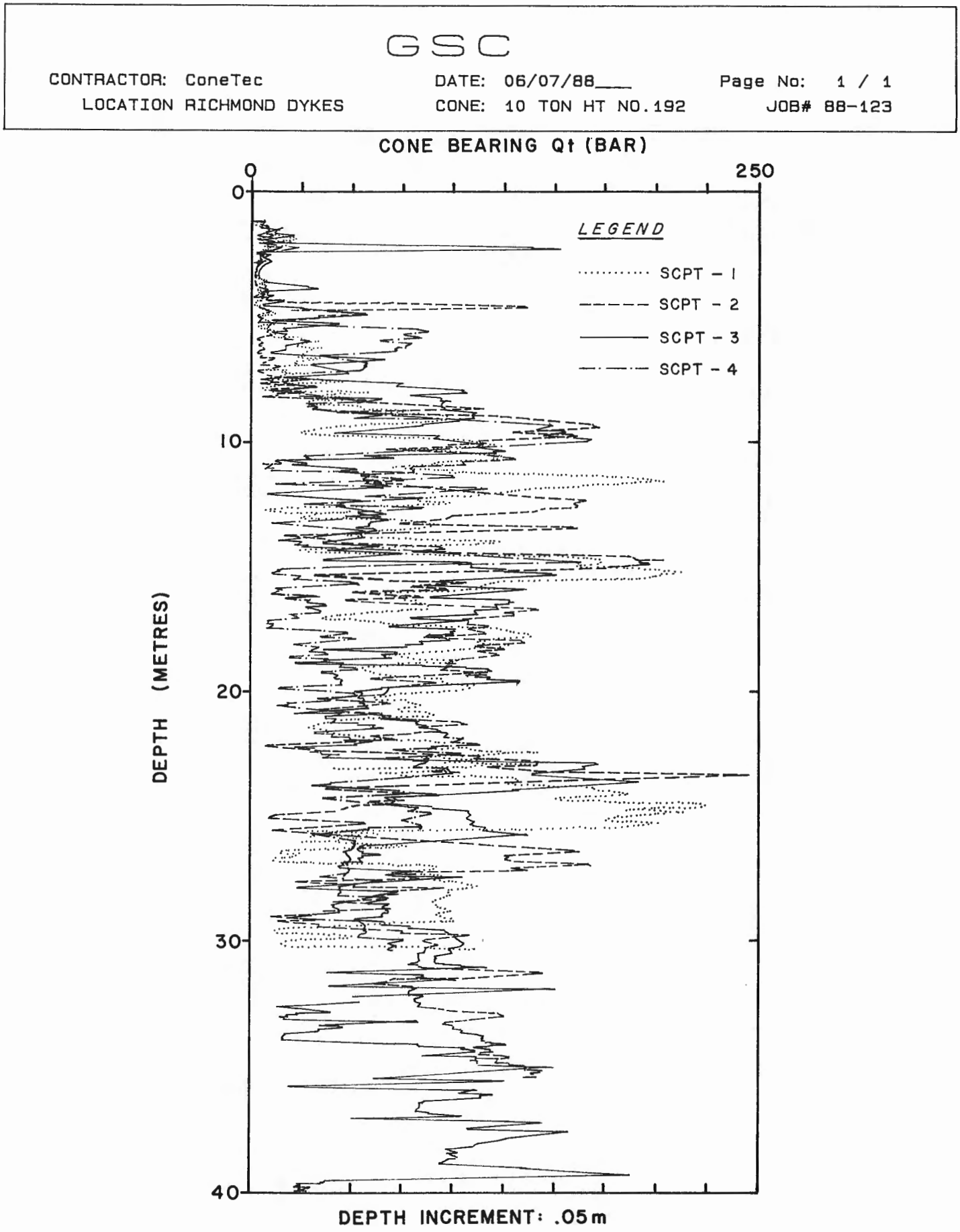

Figure 5. Composite plot of cone bearing (Q_t) for test sites 1 through 4 (Fig. 4).

DATA AND INTERPRETATION

Cone penetration data

Cone penetration data is referenced by depth below existing ground surface. A composite plot of tip resistances (cone bearing), Q_t, for test holes along the dyke, all at the same elevation, is given in Figure 5 and a plot of the average Q_t is shown in Figure 6.

A comparison between normalized cone tip resistances, Q_{tl}, and critical tip resistances Q_c to prevent liquefaction gives a clear indication of the liquefaction potential at a site. Critical tip resistances of Q_c as a function of depth are plotted against the background of the recorded penetration resistances in Figure 7 for two levels of peak ground acceleration and three earthquake magnitudes. Penetration resistances have been standardized to a fines content of less than 5%, the fines content of most samples in previous studies (Seed, 1979). Substantial liquefaction is indicated

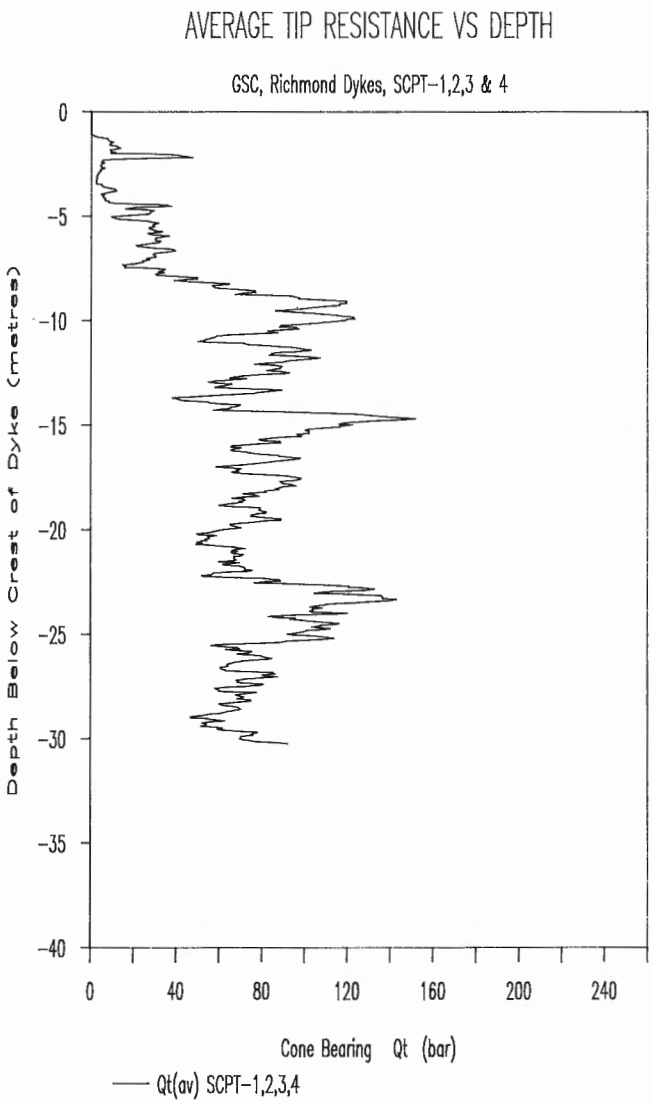

Figure 6. Average cone bearing Q_t for test sites 1 through 4.

where the measured Q_t is less than the critical. However, one further test must be applied. Sediments where $Q_t < Q_c$ must also be saturated and cohesionless to be considered liquefiable. At this site, the sediments in the upper 6 m have been identified as a clayey silt (cohesive) gradually grading to sandy silt and then to a silty sand (cohesionless). Upper parts of this material may not liquefy if it has sufficient plasticity. If parts of the upper 6 m prove not to be liquefiable on the basis of soil plasticity, then the site may be on the borderline between liquefaction and no liquefaction for an earthquake of magnitude $M_s = 6.5$ and a peak acceleration of 0.17 g.

Seismic data

In plots of the shear wave velocity profiles based on crossovers (Fig. 8), the solid vertical line at $V_s = 140$ m/s is the limiting criterion for liquefaction for earthquakes to magnitudes $M_s = 6.5$ causing peak accelerations of about 0.17 g or greater. This criterion is based on data from sites which liquefied in the Imperial Valley, California during the 1979 Imperial Valley and 1981 Westmorland earthquakes (Stokoe and Nazarian, 1985; K.H. Stokoe, pers. comm., 1988) and during the 1987 Superstition Hills earthquake (T.L. Holzer, pers. comm., 1988).

The threshold shear wave velocity necessary to rule out any possibility of developing seismic porewater pressures for different peak surface acceleration levels are shown by the solid curves in Figure 9. A composite plot of wave velocity profiles is also shown. Figure 9 clearly illustrates that any significant earthquake will produce accelerations which will cause sufficient straining within the sediment/soil which will result in the development of some excess porewater pressures. However, the figure does not indicate whether or not the excess pressures will be high enough to actually trigger liquefaction. It is possible to have excess porewater pressures without liquefaction.

The attractive feature of the methods based on shear wave velocity is that approximate velocity profiles may be determined without any drilling or penetration tests using direct measurements of the subsurface velocities by surface techniques. The surface shear wave data collected at this site showed excellent agreement with the downhole seismic cone shear wave velocity results. The surface measurements did not show the high-velocity layer associated with the dyke fill material as these data were recorded off the dyke itself. Because the surface method uses a long horizontal array on the ground, it produces an average measurement for the area, and is not sensitive to reversals in shear wave velocity. The surface refraction method also assumes that velocity increases with depth.

SUMMARY AND CONCLUSIONS

A field study was conducted in Richmond, B.C. in June 1988 to test procedures and methods proposed for use in a regional assessment of liquefaction potential in the Fraser Delta.

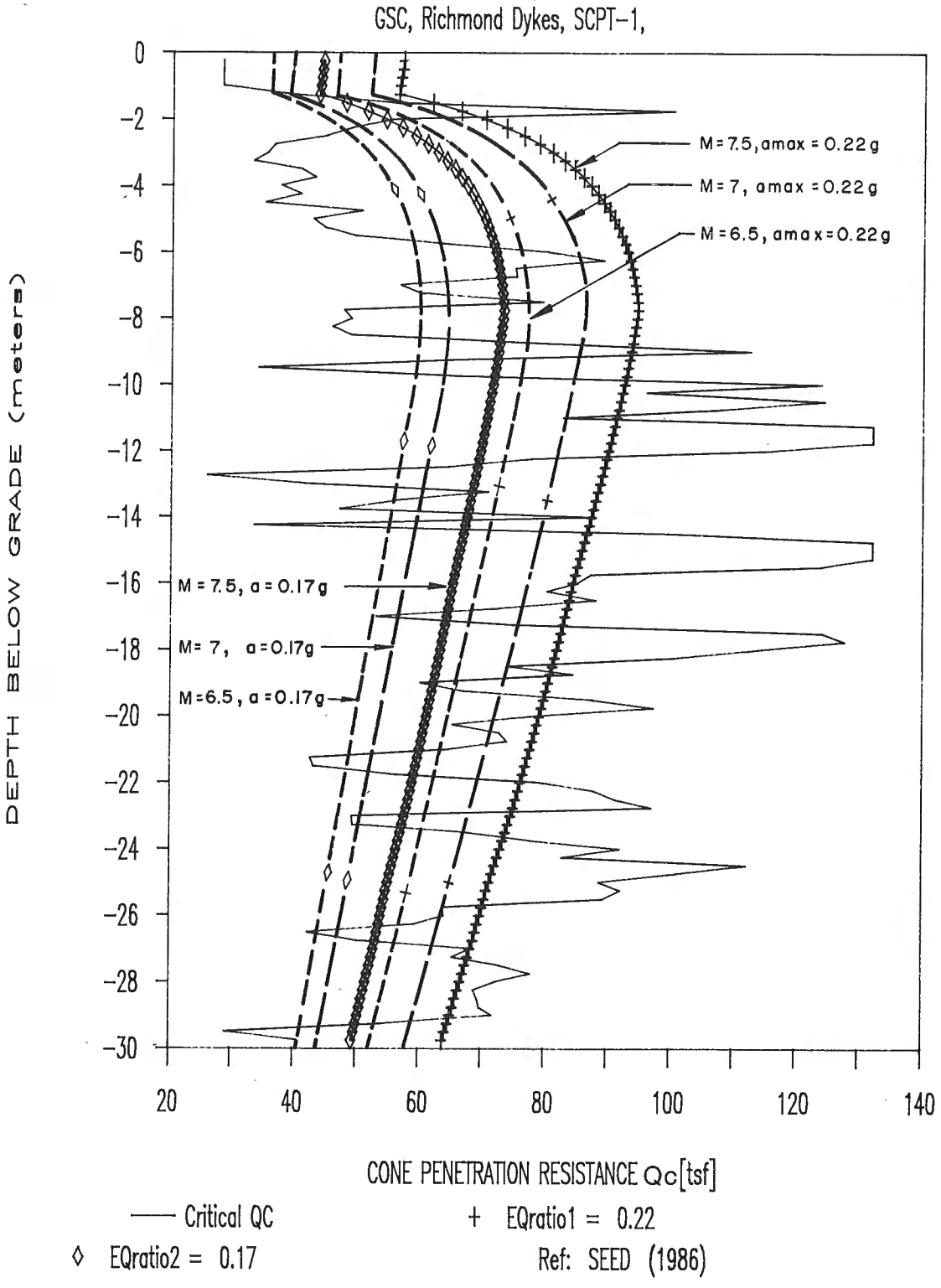

Figure 7. Variation of critical Q_c with earthquake magnitude and peak acceleration for test site 1.

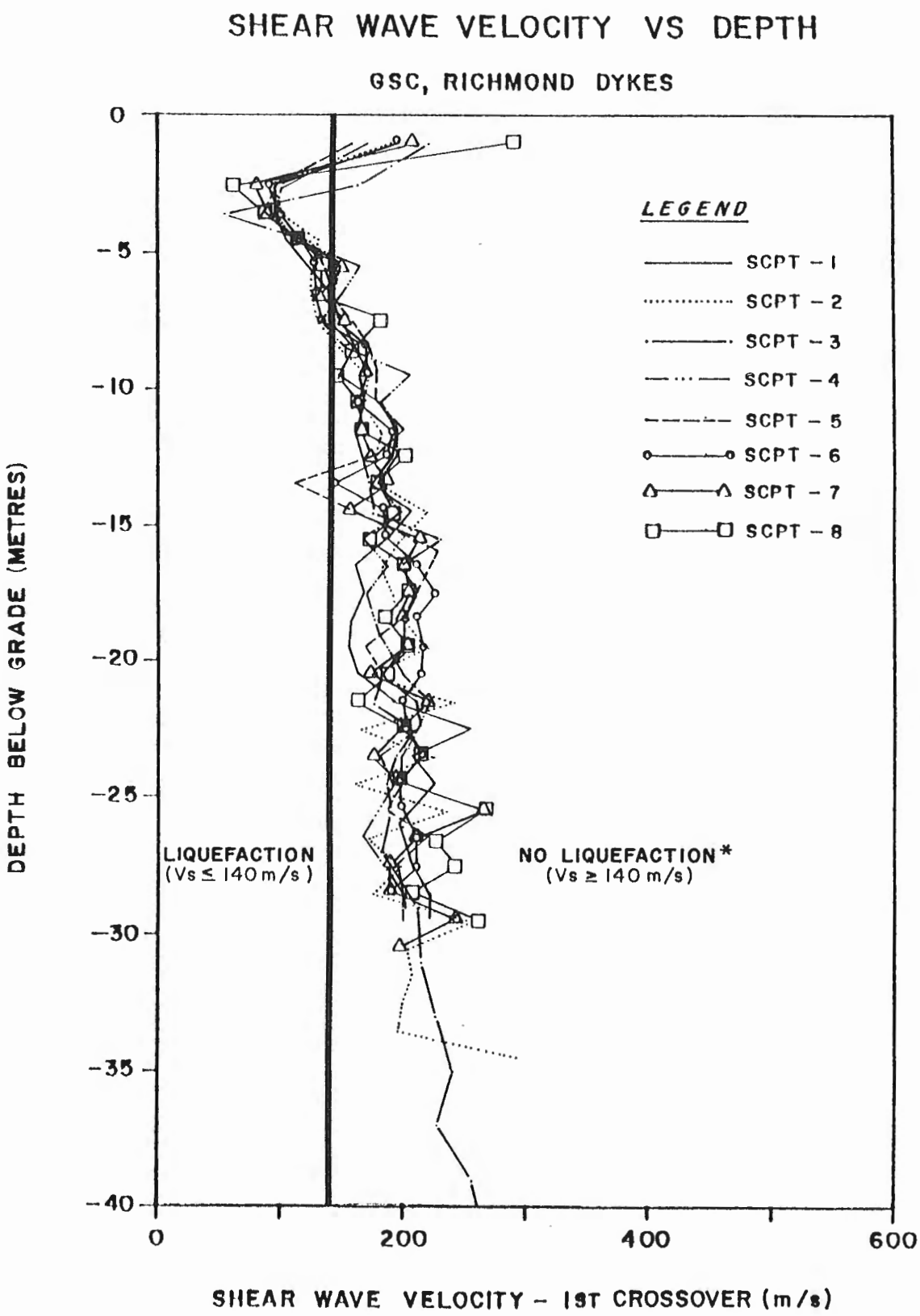

Figure 8. Composite plot of shear wave velocity profiles for all seismic cone penetration test holes.

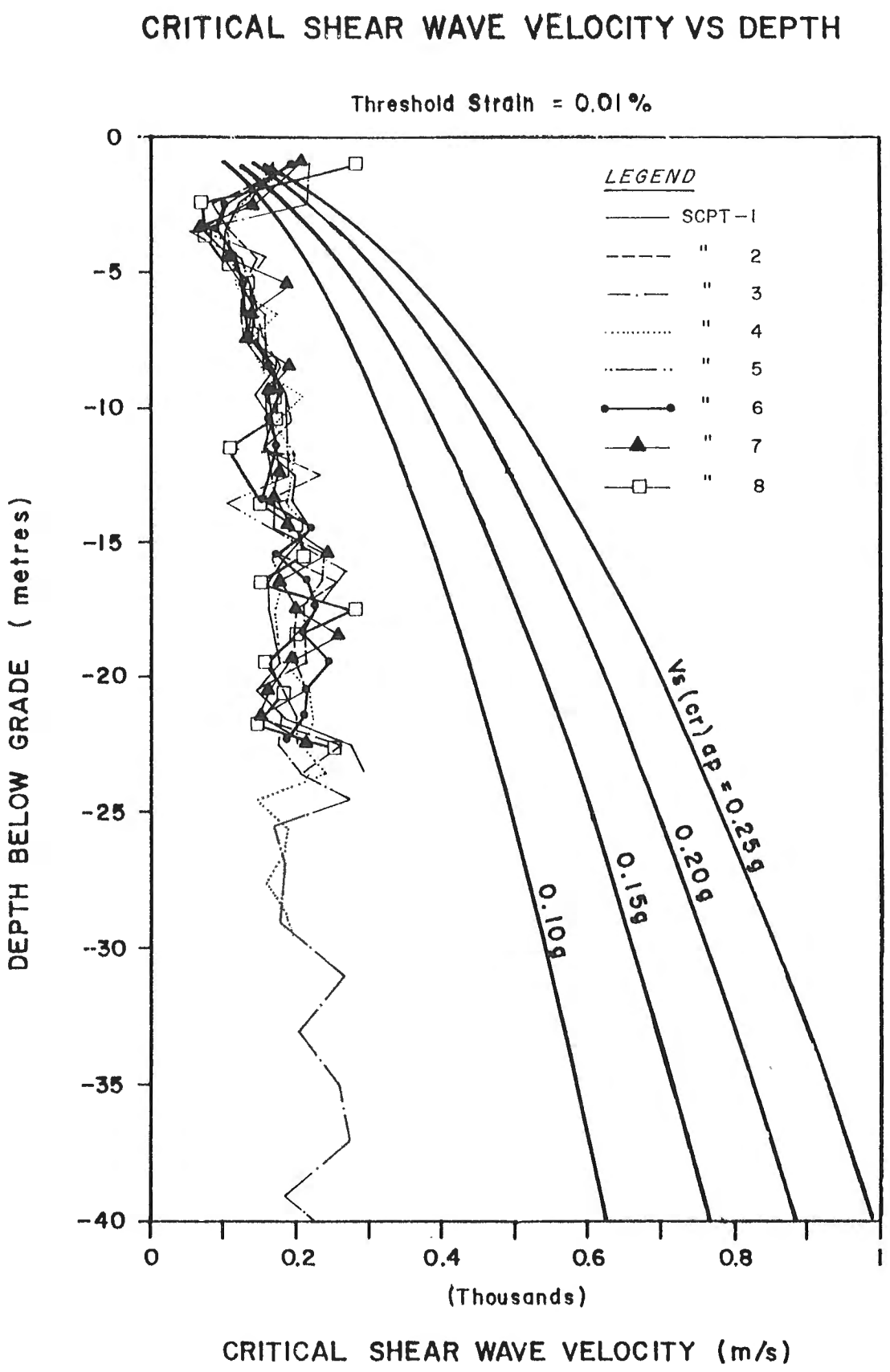

Figure 9. Comparison of threshold shear wave velocities for various peak accelerations compared with measured shear wave velocities for all seismic cone penetration test holes.

Cone tip resistances and shear wave velocities were measured in eight test holes using a state of the art seismic piezocone with automated data acquisition and processing. Liquefaction potential was assessed using three criteria; (1) threshold shear wave velocity; (2) critical shear wave velocity; and (3) critical cone tip resistance Q_c. Preliminary assessment of the field data suggests that the site would undergo some liquefaction during earthquakes of magnitude $M_s > 6.5$ causing peak ground accelerations $a_p = 0.17$ g or greater. Final conclusions for this site depend on the results of laboratory tests to determine whether some of the sediments are of sufficient plasticity to resist liquefaction despite both low Q_c and shear wave velocities.

This project clearly indicates the necessity to create a computer database of tip resistances and shear wave velocities for a regional assessment. This database should allow the inclusion and easy manipulation of cone data already available; it should also allow continual updating as new data became available.

In many areas the threshold shear wave velocity criterion is very useful in quickly ruling out areas where liquefaction is most unlikely. Data from the demonstration study indicate that recorded shear wave velocities are well below those critical values required to preclude significant pore pressure development.

The critical shear wave velocity criterion is limited to earthquakes of magnitudes up to M=6.5 because of a lack of data for the higher magnitudes.

The use of a shear wave velocity criterion is a highly cost-effective method for the preliminary assessment of regional liquefaction potential, if the velocities can be measured reliably using surface techniques. However, the common refraction procedure cannot detect velocity inversion with depth. The special analysis of surface waves technique is now becoming available and appears to have been used successfully in a number of well documented cases. We recommend that this method be tested during the regional assessment program. We also suggest that surface wave methods be confirmed with an adequate number of downhole seismic tests. The seismic piezocone is the preferred tool when a detailed assessment of liquefaction potential is required (K.H. Stokoe, pers. comm., 1988).

ACKNOWLEDGMENTS

The assistance of M. Yogendrakumar in the preparation of this report is gratefully acknowledged. M. Watts assisted in drafting the figures.

REFERENCES

Basham, P.W., Weichert, D.H., Anglin, F.M., and Berry, M.J.
1982: New probabilistic strong seismic ground motion maps of Canada: a compilation of earthquakes source zones, methods and results; Earth Physics Branch, Energy, Mines and Resources Canada, Open File 82-33, 205 p.
1985: New probabilistic strong seismic ground motion maps of Canada; Seismological Society of America, Bulletin, v. 75, p. 563-595.

Byrne, P.M. and Anderson, D.L.
1987: Earthquake design in Richmond, British Columbia (Version II); University of British Columbia, Department of Civil Engineering, Soil Mechanics Series, no. 109, p. 1-90.

Dobry, R., Stokoe, K.H., Ladd, R.S., and Youd, T.L.
1981: Liquefaction susceptibility from S-wave velocity; preprint 81-544, American Society of Civil Engineering, National Convention, St. Louis, Missouri, October, New York, N.Y.

Dragert, H. and Rogers, G.C.
1988: Could a megathrust earthquake strike southwestern British Columbia?; GEOS, v. 17, p. 5-8.

Finn, W.D. L.
1987: Estimating the probability of liquefaction during earthquakes; in Proceedings, Fifth International Conference on Applications of Statistics and Probability in Soil and Structural Engineering, Vancouver, B.C., Canada, May 25-29.
1988: Dynamic analysis in geotechnical engineering; in Earthquake Engineering and Soil Dynamics II, Geotechnical Special Publication, no. 20, American Society of Civil Engineers, New York, N.Y.

Kawasumi, H., (editor)
1968: General report on the Nii gata Earthquake of 1964; Tokyo Electric Engineering Press, Tokyo, Japan.

Luternauer, J.L.
1988: Geoarchitecture, evolution and seismic risk assessment of the southern Fraser River Delta, B.C.; in Current Research, Part E, Geological Survey of Canada, Paper 88-1E, p. 105-109.

Marcuson, W.F., III and Bieganousky, W.A.
1977: SPT and relative density in coarse sands; Journal of the Geotechnical Engineering Division, American Society of Civil Engineers, 103 (GT 11), p. 1295-1309.

Seed, H.B.
1979: Soil liquefaction and cyclic mobility evaluation for level ground during earthquakes; Journal of Geotechnical Engineering Division, ASCE, v. 105, GT2, p. 201-255.

Seed, H.B. and deAlba, P.
1986: Use of SPT and CPT tests for evaluating the liquefaction resistance of soils; Proceedings of the Specialty Conference on the Use of I_n S_{itu} Tests in Geotechnical Engineering, American Society of Civil Engineers, Geotechnical Special Publication, No. 6, June 23-25, Blacksburg, Virginia.

Seed, H.B., Tokimatsu, K., Harder, L.F., and Chung, R.M.
1984: The influence of SPT procedures in soil liquefaction resistance evaluations; Report No. UBC/EERC-84/15, Earthquake Engineering Research Centre, University of California, Berkeley, California.

Stokoe, K.H. and Nazarian, S.
1985: Use of Rayleigh waves in liquefaction studies; in Proceedings, Measurement and Use of Shear Wave Velocity for Evaluating Dynamic Soil Properties, Geotechnical Engineering Division, American Society of Civil Engineers, New York, N.Y.

Late Quaternary sea level change and crustal deformation, southwestern British Columbia

John J. Clague
Terrain Sciences Division, Vancouver

Clague, J.J., Late Quaternary sea level change and crustal deformation, southwestern British Columbia; in Current Research, Part E, Geological Survey of Canada, Paper 89-1E, p. 233-236, 1989.

Abstract

The pattern and timing of Holocene sea level change on southern Vancouver Island is being studied to provide information on recent crustal movements in the region. The study involves the examination and analysis of Holocene sediments at selected coastal sites in the vicinity of Victoria. Cores, backhoe trenches, and pits provide stratigraphic and sedimentological information and samples for paleoecological analysis and radiocarbon dating. Evidence obtained to date indicates that the sea has risen relative to the land on southern Vancouver Island during the late Holocene. At one site near Victoria, a relatively rapid transgression occurred about 2000 radiocarbon years ago. It is not clear, however, if this was caused by crustal subsidence or eustatic sea level rise. There is no evidence at this site for significant sea level change after this event. The pattern of sea level change here may differ from that on parts of the Washington and Oregon coasts where there have been several episodes of rapid subsidence during the late Holocene, each probably associated with a great thrust earthquake on the Cascadia subduction zone.

Résumé

On étudie actuellement la configuration et la chronologie des variations du niveau de la mer à l'Holocène, dans le sud de l'île de Vancouver, pour fournir des données sur les mouvements crustaux survenus récemment dans la région. L'étude porte sur l'examen et l'analyse des sédiments d'âge holocène provenant de localités littorales choisies à proximité de Victoria. Le prélèvement de carottes, le creusement de tranchées avec une pelle excavatrice et le forage de puits ont permis aux auteurs de recueillir de l'information stratigraphique et sédimentologique, ainsi que des échantillons destinés à une analyse paléoécologique et à une datation au carbone radioactif. Les indices obtenus jusqu'à présent indiquent que le niveau de la mer s'est élevé dans le sud de l'île de Vancouver durant l'Holocène supérieur. À un endroit proche de Victoria, se serait produite une transgression relativement rapide il a environ 2000 ans selon les résultats des datations au carbone radioactif. Toutefois, il est difficile de dire si cette transgression a été causée par une subsidence de la croûte ou par une montée eustatique du niveau de la mer. Rien n'indique que dans l'endroit en question, se soit produite une variation importante du niveau de la mer après cet épisode. La configuration des variations du niveau de la mer diffère peut-être à cet endroit de celle observée dans des portions du littoral des états de Washington et de l'Oregon, où se sont déroulés plusieurs épisodes de subsidence rapide durant l'Holocène supérieur, chacun probablement associé à un grand séisme accompagné de failles chevauchantes dans la zone de subduction de Cascadia.

INTRODUCTION

The Geological Survey of Canada has initiated geological studies aimed at determining the character and extent of Quaternary crustal deformation in the western Canadian Cordillera and at relating this deformation to the historical and contemporary stress field. These studies may provide information on the frequency and magnitude of large earthquakes in this region during the Holocene, which in turn can be used to assess the likelihood of comparable earthquakes in the future.

This project involves three types of studies. (1) **Reconstruction of Holocene sea level change**. The pattern and chronology of relative sea level movements during the Holocene are being determined at several places on the British Columbia coast through airphoto interpretation, stratigraphic and sedimentological logging of natural and artificial exposures and cores, paleoecological analysis, and radiocarbon dating of organic material. (2) **Identification of seismically induced mass movements and deformation**. Acoustic subbottom profiles have been obtained in selected lakes on Vancouver Island in order to identify landslides and deformation caused by earthquakes. It is planned to core sediments in these lakes to define and date earthquake-induced disturbances. (3) **Examination of young faults**. Faults and related features suspected of being active during the Quaternary are being examined to determine the character and extent of recent displacements. This involves airphoto interpretation and geological mapping of selected faults, seismic profiling across their offshore extensions, and trenching across faults with known young offsets.

Work in 1988 focussed on the first and second components of this program. This report briefly outlines the methodology and some preliminary results of a study of late Holocene sea level change on southern Vancouver Island. Some results of a subbottom survey of several lakes on Vancouver Island are summarized in a separate report in this volume (Clague et al., 1989).

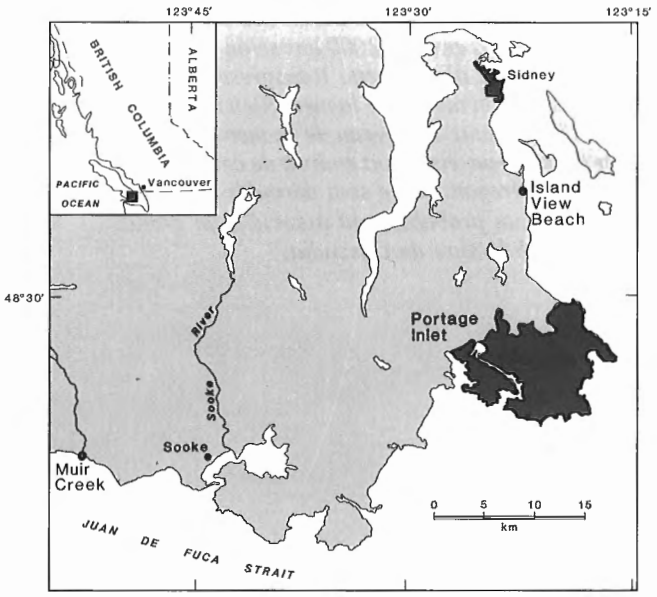

Figure 1. Location map.

AREA OF STUDY

Southern Vancouver Island was chosen for a detailed study of late Holocene sea level change for four reasons. First, it supports a large population and extensive development and thus would be severely affected by a large earthquake. Second, the area is relatively close to the Cascadia subduction zone which many scientists believe has the potential for producing great (M8-9) thrust earthquakes (Heaton and Kanamori, 1984; Rogers, 1988). Geological evidence from the west coast of Washington and Oregon suggests that such earthquakes have occurred on average once every several hundred years during the late Holocene (Atwater, 1987). It might be expected that these events would also have an effect on Vancouver Island. Third, this region is also affected by moderately large (M6-7+) intraplate earthquakes. The most recent of these was a M7.2 event in 1946, centred northwest of Comox on central Vancouver Island (Hodgson, 1946; Rogers and Hasegawa, 1978). Fourth, there are numerous protected coastal embayments and low-elevation sites on southern Vancouver Island that are underlain by Holocene sediments and should preserve a detailed record of recent sea level change.

Previous reconnaissance work at some of these sites has shown that there have, in fact, been changes in sea level on southern Vancouver Island during the Holocene (Mathews et al., 1970; Clague et al., 1982), although their cause remains uncertain. This study was initiated to provide more detailed information on both the pattern and cause of recent sea level change in the region.

METHODS

Stratigraphic and sedimentological information and sediment samples were obtained at Island View Beach, Portage Inlet, and Muir Creek (Fig. 1) by coring, trenching, and the digging of pits. At Island View Beach, late Holocene organic and intertidal sediments have accumulated behind a gravelly spit. Portage Inlet is a restricted embayment that is separated from Victoria Harbour by a shallow, narrow bedrock sill; it contains a relatively thick sequence of Holocene sediments (Foster, 1972). At the mouth of Muir Creek west of Sooke, late Holocene sediments, including a fossil forest bed, are present in the intertidal zone. The Holocene sedimentary sequences at the three sites extend from near the upper limit of tides to below low tide level and comprise interbedded mineral- and organic-rich sediments. The stratigraphy of each core and exposure was logged in detail, with information recorded on texture, colour, sedimentary structures, fossil content, and contact relationships. Samples were collected for radiocarbon dating and for grain-size, pollen, diatom, and foraminiferal analyses.

RESULTS

There is evidence of late Holocene sea level rise at each of the sites examined to date. Only preliminary results can be given, however, because many of the analyses have not been completed and additional field work is scheduled.

In Portage Inlet, a thick terrestrial peat is overlain by marine mud containing foraminifera and a rich molluscan

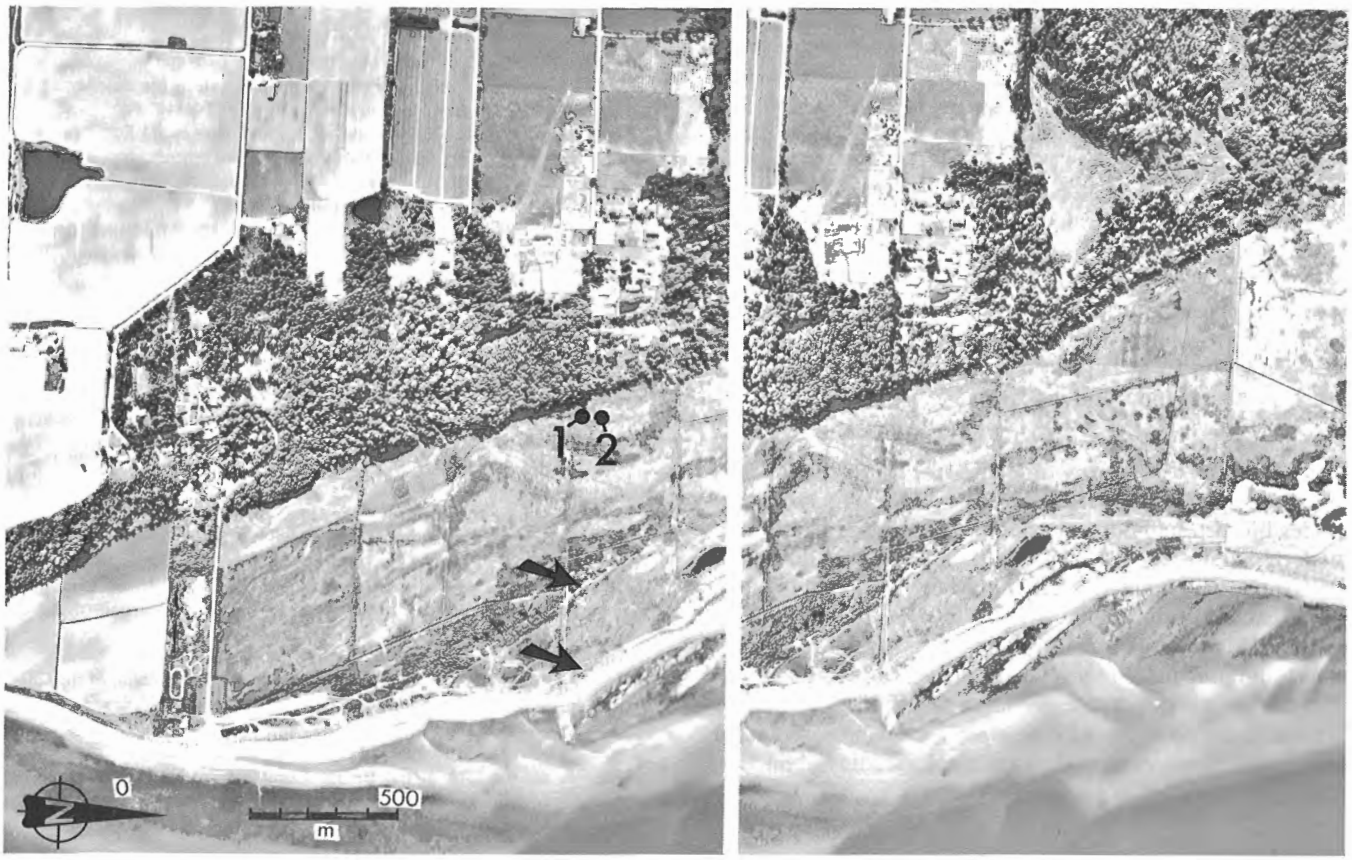

Figure 2. Photostereogram of Island View Beach showing the locations of two stratigraphic sections depicted in Figure 3. A pit was dug at site 1, and a vibrocore taken at site 2. These sites are situated inland of a late Holocene spit (arrows) and are just above high tide level. Province of British Columbia airphotos BC80005-178 and 179.

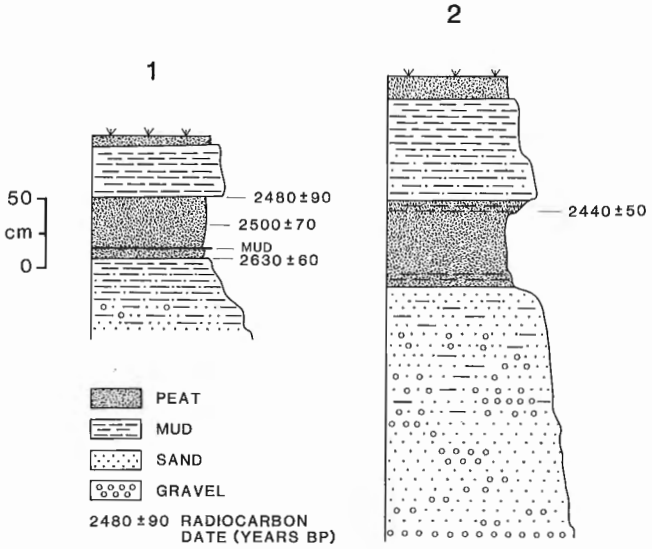

Figure 3. Stratigraphic sections at Island View Beach (see Fig. 2 for locations). Laboratory number for 14C ages are: 2440 ± 50 BP (GSC-4594), 2480 ± 90 BP (GSC-4572), 2500 ± 70 BP (GSC-4593), and 2630 ± 60 BP (GSC-4571).

fauna. The base and top of the peat have yielded radiocarbon ages of 9250 ± 140 and 5470 ± 115 BP (I-3676 and I-3673), respectively (Foster, 1972). There is no evidence for a transgression at this site at any time during deposition of the peat, but there was a transgression some time after 5470 ± 115 BP. This resulted in the termination of peat deposition and in the deposition of mud and sand in a shallow marine embayment. The contact between the peat and the marine sediments is sharp, indicating that the transgression may have been rapid. There is no way of knowing, however, whether the transgression was the result of earthquakes, aseismic subsidence, or eustatic sea level rise. Locally at the edge of Portage Inlet, upper intertidal or supratidal marsh peats interfinger with the marine sediments. This may reflect minor (< 1 m) shifts in sea level during the late Holocene, although it could also record lateral shifts in tidal channels under a stable sea level regime.

In situ fossil stumps occur in the intertidal zone at Island View Beach and Muir Creek. At Island View Beach, one of the stumps, protruding through a peat bed about 1-1.5 m below high tide, has been dated at 2040 ± 130 BP (GSC-252) (Mathews et al., 1970). These stumps provide unequivocal evidence for a relatively rapid rise in sea level on southern Vancouver Island during the late Holocene.

Cores and pits at Island View Beach provide additional evidence for a transgression about 2000 radiocarbon years ago (Fig. 2, 3). Here, fine gravel, sand, and sandy mud of littoral origin are overlain by terrestrial peat which has yielded radiocarbon ages ranging from 2630 ± 60 to 2440 ± 50 BP (GSC-4571 and GSC-4594). The peat, in turn, is overlain by mud which contains a sparse foraminiferal assemblage dominated by the brackish-water species *Trochammina inflata* (P.J. Rauwerda, personal communication, 1988). The contact between the peat and overlying mud is in places sharp and in places gradational. Again, it is not clear whether the transgression recorded by the change from peat to mud is the result of coseismic subsidence or some more gradual process.

There is no evidence at Island View Beach for a significant rise in sea level at any time after the transgression dating to about 2000 BP. Rather, the brackish-water mud grades upward without a sharp break into grass peat of the modern marsh. Any coseismic subsidence at this site during the last two millennia thus may have been too small to leave a noticeable imprint on the Island View Beach sedimentary record. This is in contrast to the situation along the coasts of Washington and Oregon where there are several prominent buried marsh surfaces younger than 2000 BP that are thought to be products of coseismic subsidence associated with great thrust earthquakes on the Cascadia subduction zone (Atwater, 1987).

ACKNOWLEDGMENTS

R.J. Hebda (Royal British Columbia Museum) and D. Dunkley assisted in the field. P.J. Rauwerda performed foraminiferal analyses on sediment samples. C. Davis drafted Figures 1 and 3.

REFERENCES

Atwater, B.F.
1987: Evidence for great Holocene earthquakes along the outer coast of Washington state; Science, v. 236, p. 942-944.

Clague, J., Harper, J.R., Hebda, R.J., and Howes, D.E.
1982: Late Quaternary sea levels and crustal movements, coastal British Columbia; Canadian Journal of Earth Sciences, v. 19, p. 597-618.

Clague, J.J., Shilts, W.W., and Linden, R.H.
1989: Application of subbottom profiling to assessing seismic risk on Vancouver Island, British Columbia; in Current Research, Part E, Geological Survey of Canada, Paper 89-1E.

Foster, H.D.
1972: Geomorphology and water resource management: Portage Inlet, a case study on Vancouver Island; Canadian Geographer, v. 16, p. 128-143.

Heaton, T.H. and Kanamori, H.
1984: Seismic potential associated with subduction in the northwestern United States; Seismological Society of America, Bulletin, v. 74, p. 933-941.

Hodgson, E.A.
1946: British Columbia earthquake, June 23, 1946; Royal Astronomical Society of Canada, Journal, v. 40, p. 285-319.

Mathews, W.H., Fyles, J.G., and Nasmith, H.W.
1970: Postglacial crustal movements in southwestern British Columbia and adjacent Washington state; Canadian Journal of Earth Sciences, v. 7, p. 690-702.

Rogers, G.C.
1988: An assessment of the megathrust earthquake potential of the Cascadia subduction zone; Canadian Journal of Earth Sciences, v. 25, p. 844-852.

Rogers, G.C. and Hasegawa, H.S.
1978: A second look at the British Columbia earthquake of June 23, 1946; Seismological Society of America, Bulletin, v. 68, p. 653-676.

Application of subbottom profiling to assessing seismic risk on Vancouver Island, British Columbia

John J. Clague, W.W. Shilts[1], and R.H. Linden[2]
Terrain Sciences Division, Vancouver

Clague, J.J., Shilts, W.W., and Linden, R.H., Application of subbottom profiling to assessing seismic risk on Vancouver Island, British Columbia; in Current Research, Part E, Geological Survey of Canada, Paper 89-1E, p. 237-242, 1989.

Abstract

Subbottom profiling has been carried out on five lakes on Vancouver Island using a portable 3.5-200 kHz acoustic profiler. The objective of the survey was to document disturbance of late glacial and postglacial lacustrine sediments and, from this, assess paleoseismicity in the region. The acoustic profiles show that there has been widespread subaqueous landsliding in four of the five surveyed lakes. Many of the landslides were triggered by the 1946 Vancouver Island earthquake (M7.2) centered near Comox, but others probably are not related to earthquake activity. Possible earthquake-induced diapirs and tilted and folded sediments were found in two of the lakes.

Résumé

On a établi des profils des couches sous le fond de cinq lacs de l'île de Vancouver, en employant un profileur acoustique de fréquence 3,5-200 kHz. Ce levé avait pour but de fournir des renseignements sur les perturbations des sédiments lacustres d'origine tardiglaciaire et post-glaciaire, à partir desquels il serait alors possible d'évaluer la paléosismicité de la région. Les profils acoustiques montrent qu'il y a eu, en de nombreux endroits, des glissements de terrains subaquatiques dans quatre des cinq lacs explorés. Un grand nombre de glissements de terrain ont été provoqués par le séisme survenu en 1946 dans l'île de Vancouver (M 7,2) et centré près de Comox, mais les autres ne sont probablement pas liés à une activité sismique quelconque. On a rencontré dans deux des lacs des structures qui pourraient être des diapirs d'origine sismique, et des sédiments inclinés et plissés.

[1] Terrain Sciences Division, Ottawa.
[2] Department of Physics, Royal Roads Military College, FMO Victoria, British Columbia, V0S 1B0.

INTRODUCTION

The lakes of the Canadian Cordillera offer opportunities for determining the intensity and character of recent tectonic activity in this seismically active region. Late Quaternary sediment fills in many of these lakes are likely to preserve a record of past earthquakes because they are water saturated and, commonly, fine grained. An understanding of this record is critical to an assessment of seismic risk in the region, which is presently a matter of concern due to the large population and extensive development in some areas. This report briefly describes a new study of sediment fills in selected lakes in western British Columbia and gives some examples of the types of information collected to date (for results of similar studies from other parts of Canada, see Shilts (1984), Shilts and Blais (1989), and references therein).

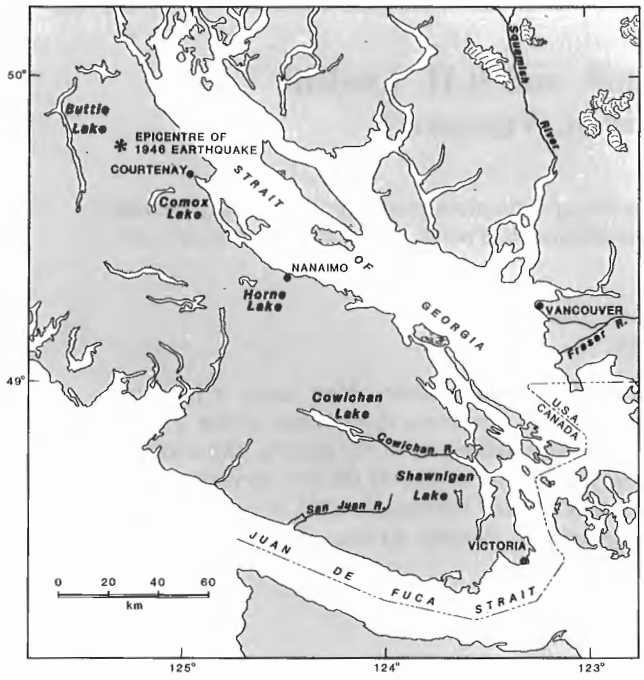

Figure 1. Location map.

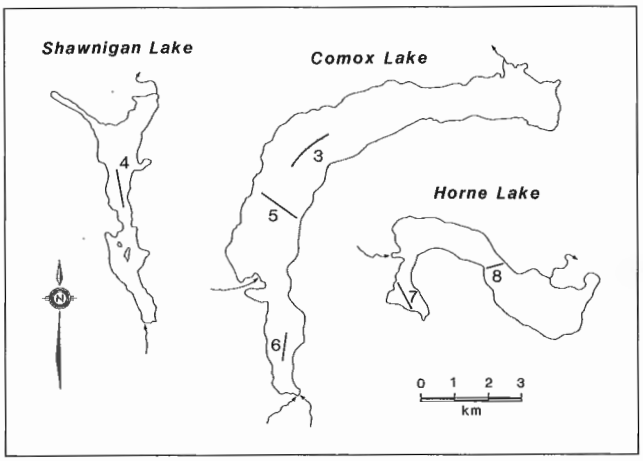

Figure 2. Locations of profiles illustrated in Figures 3-8. The numbers correspond to figure numbers.

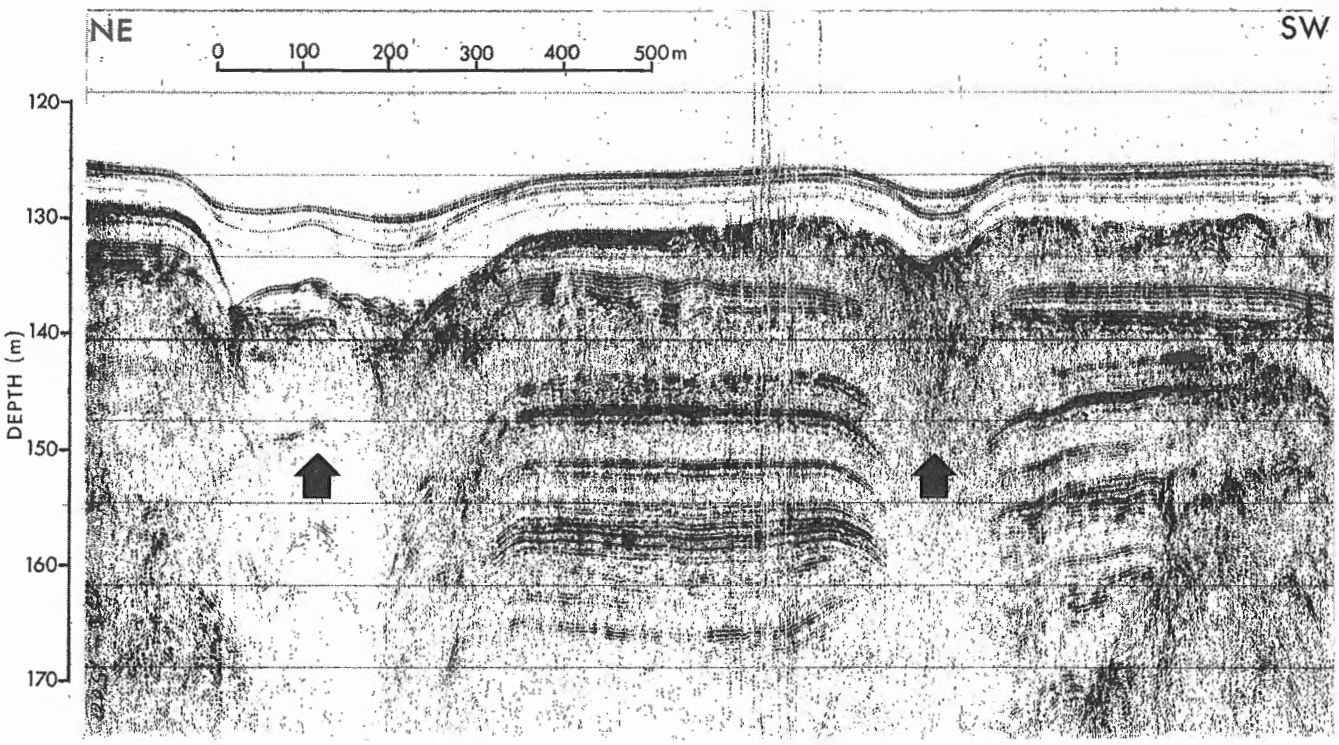

Figure 3. EG&G profile from Comox Lake showing thick, late glacial (?) stratified sediments and overlying thinner Holocene sediments. Possible collapse structures in the late glacial sequence (arrows) may have formed by the melting of buried ice blocks.

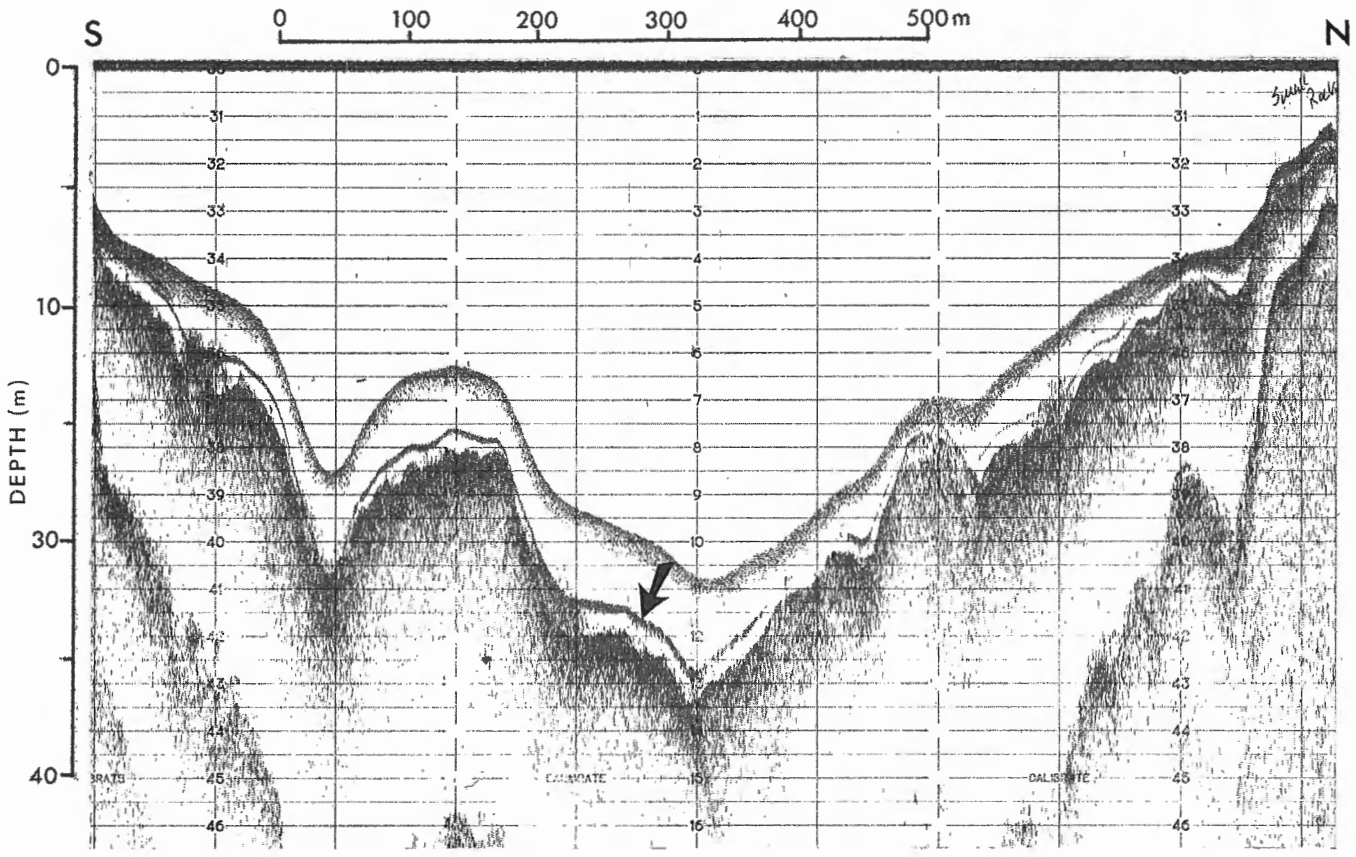

Figure 4. Raytheon profile from Shawnigan Lake. Holocene organic-rich mud passively drapes bedrock and/or till. The conspicuous reflector in the lower part of the mud unit (arrow) may be Mazama tephra, deposited ca. 6800 BP.

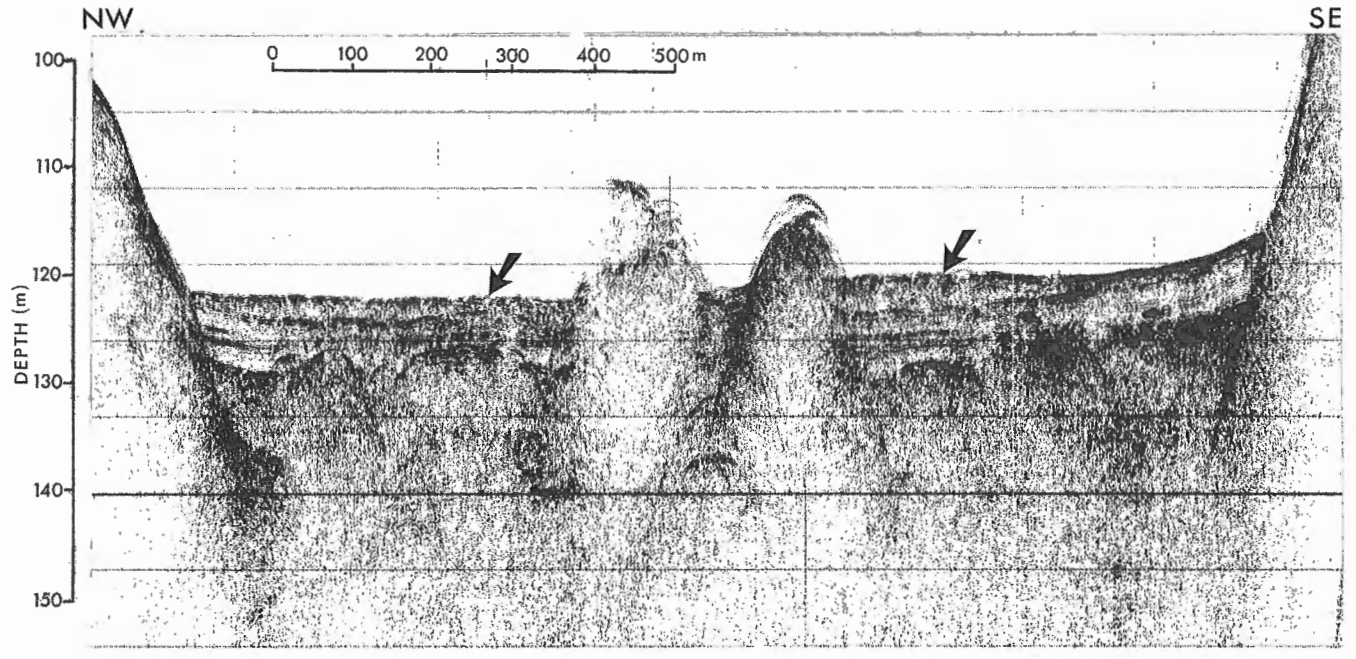

Figure 5. EG&G profile across the floor of Comox Lake north of the mouth of Cruickshank River. Landslide deposits (arrows), which probably were emplaced during the 1946 Vancouver Island earthquake, overlie stratified Holocene prodelta sediments. The two knolls in the centre of the basin are enigmatic, but may be diapirs.

METHODS

Subbottom profiles have been obtained from five lakes on Vancouver Island (Fig. 1) using a portable 3.5-200 kHz acoustic profiler. Vancouver Island was chosen as a study area, because it has high levels of historical seismicity, having last experienced a major earthquake in 1946 (a M7.2 event near Comox; Hodgson, 1946; Rogers and Hasegawa, 1978). Two of the surveyed lakes are within about 20 km of the epicentre of the 1946 earthquake (Fig. 1), which allowed us to assess disturbance caused by a known seismic event. Profiling was done with a Raytheon RTT-1000A-1 "Portable Survey System" with a dual, low frequency (3.5 and 7.0 kHz) transducer coupled with a high frequency (200 kHZ) transducer (Klassen and Shilts, 1982). The power source for the acoustical signal and transceiver-chart

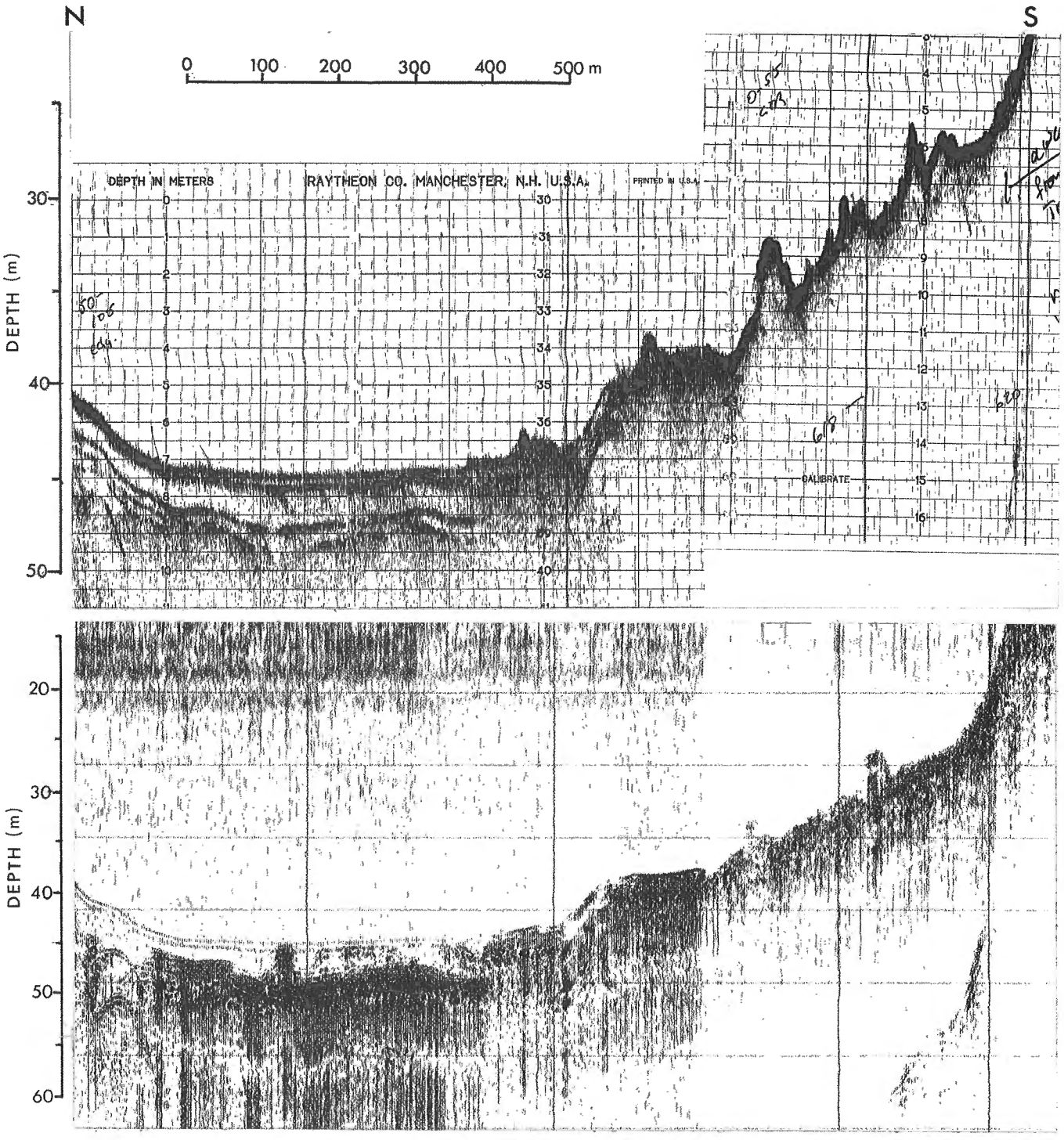

Figure 6. Near-coincident Raytheon (top) and EG&G (bottom) profiles from Comox Lake north of the mouth of Puntledge River, showing hummocky landslide debris (right side of profiles) extending out into a basin underlain by prodelta sediments. The landsliding probably was caused by the 1946 earthquake.

recorder was a standard 12-volt automobile battery. The system was operated from a small aluminum boat powered by a 20-horsepower outboard engine. Navigation was by "dead reckoning" between known points on the shoreline at constant speeds ranging from 3-5 km/h. In 1987 and 1988 265 line kilometres of profiles were obtained: 18 km, 14 lines in Shawnigan Lake; 45 km, 14 lines in Cowichan Lake; 30 km, 30 lines in Horne Lake; 97 km, 60 lines in Comox Lake; and 75 km, 37 lines in Buttle Lake.

The Raytheon survey in Comox Lake was supplemented by a higher energy seismic survey performed with an EG&G model no. 236 boomer, operated at 200 joules. The signal from a 20-element receiver array was amplified and filtered with an Innerspace Technology Model 202 pre-amp filter, operated at 20-1500 Hz. A Del Norte trisponder system was used to locate track lines. About 41 line km of EG&G profiles were obtained, of which 18 km were run in tandem with the Raytheon high-resolution system.

RESULTS

All of the surveyed lakes, except Shawnigan, have local thick fills of late glacial and postglacial sediments, mainly mud, silt, and sand. In the deepest part of Comox Lake, for example, thick horizontally stratified sediments (probably silt or mud) are overlain by fine sediments that have few acoustic reflectors (Fig. 2, 3). The former probably were deposited at the end of the last (Fraser) glaciation, and the latter during the Holocene. In contrast, sediments in Shawnigan Lake are relatively thin and consist mainly of acoustically transparent organic-rich mud of Holocene age (Fig. 4).

Slumps and flows have occurred in all five surveyed lakes, although they are rare in Shawnigan Lake. Many of the landslides have sources on the foreslopes of sand and gravel deltas. Others have resulted from failures of steep underwater slopes far from stream mouths. In Comox and Buttle lakes, landslide deposits are particularly common in

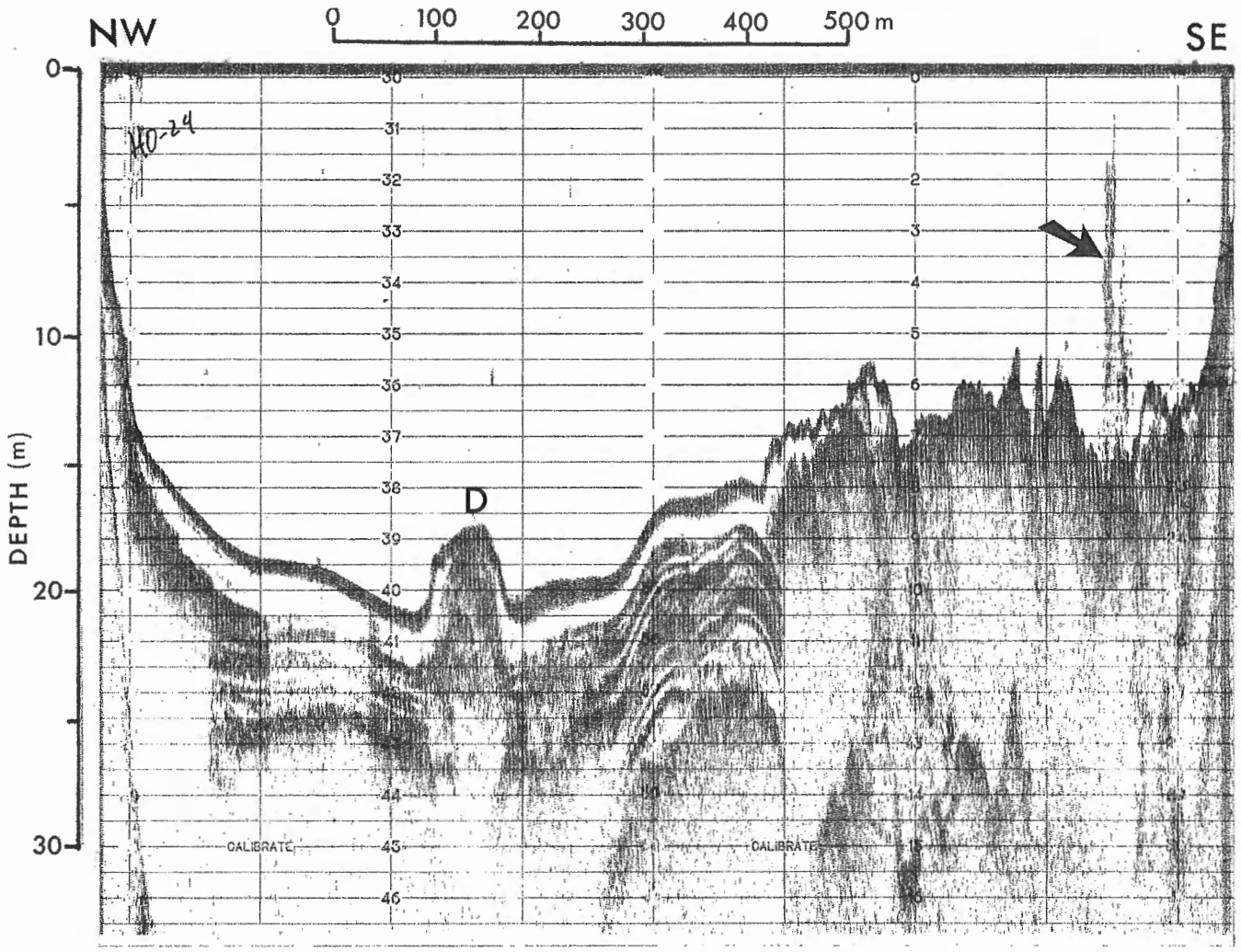

Figure 7. Raytheon profile from Horne Lake, showing slumped sediments and possible diapir (D). The plume of a spring is indicated by an arrow.

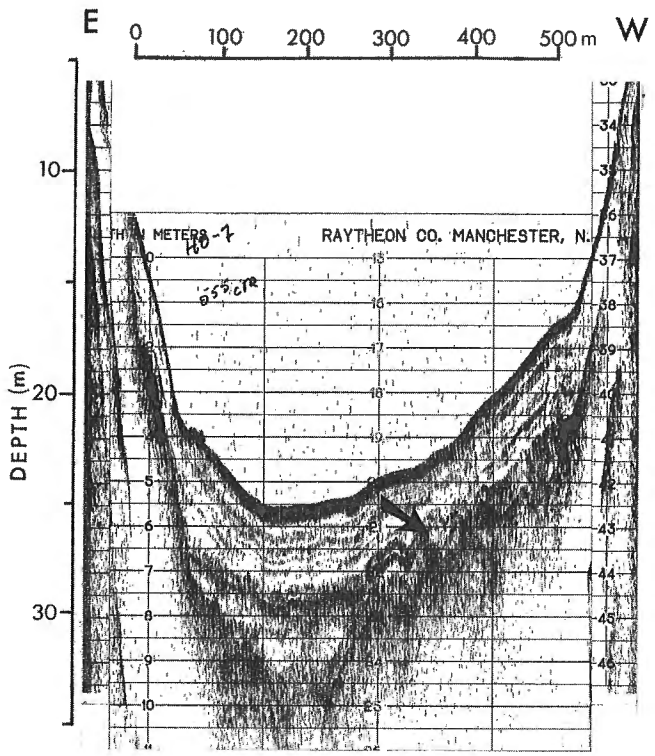

Figure 8. Raytheon profile from Horne Lake, showing old slump deposits (arrow) covered by undisturbed, stratified Holocene sediments.

areas nearest the epicentre of the 1946 earthquake (Fig. 5, 6). From historical evidence, it is known that there was large-scale slumping at the southwest corner of Comox Lake during the 1946 Vancouver Island earthquake (Hodgson, 1946, p. 308-309). Some of the landslide deposits seen in the Raytheon and EG&G records from Comox Lake were probably produced by this shock. These observations indicate that an earthquake of Richter magnitude 7 is likely to trigger large landslides in lakes within at least a few tens of kilometres of its epicentre.

If historical evidence is unavailable, it may be difficult or impossible to discriminate landslides triggered by earthquakes from those caused by other processes, such as depositional oversteepening of delta fronts. This is a problem, for example, in interpreting landslides in Horne Lake, 65 km southeast of the epicentre of the 1946 earthquake. There are numerous slumps, some of large size, on the floor of Horne Lake adjacent to deltas and off steep rocky slopes. Most of these have a very fresh appearance and are not covered by lake-bottom muds; they may have formed during the 1946 earthquake. Others, however, are probably older and not necessarily earthquake-induced.

Features that possibly are products of loading and liquefaction have been observed in a few profiles from Horne and Comox lakes. Sediments at the far southwest end of Horne Lake are tilted and extensively disrupted; at one place, what may be a diapir extends through the sediment column to form a pinnacle or ridge that projects about 3 m above the floor of the lake (Fig. 7). This deformation may have been produced by shaking during an earthquake or by loading of saturated sediments by landslide debris.

Sediments in Shawnigan Lake are little disturbed relative to those in other surveyed lakes. Acoustically transparent mud, the dominant unit in all Shawnigan Lake profiles, forms regular drapes over drift and bedrock (Fig. 4). No significant slumps or flows were observed in these sediments.

The Raytheon profiler, in general, does not penetrate sand, gravel, and slumped sediments. The utility of the system thus is limited in high-energy lakes with coarse or highly disturbed substrates. The EG&G boomer does not give much better results in these materials (Fig. 6), although it provides greater penetration in fine sediments. Consequently, in many lakes in the Cordillera, it may be difficult to obtain the subbottom information necessary to document prehistoric periods of instability. We have, however, identified buried slump deposits in a few Raytheon and EG&G records (Fig. 8); these provide evidence for ancient instability in these lakes.

We plan to continue profiling lakes on Vancouver Island and elsewhere to determine the nature and extent of deformation of late Quaternary lacustrine sediments. If possible, cores will be taken to characterize and date various units and determine their genesis. This may ultimately lead to a better understanding of paleoseismicity in the Canadian Cordillera.

ACKNOWLEDGMENTS

C. Yorath and G. Jewsbury (Geological Survey of Canada) helped with logistical arrangements for field work. C. Davis drafted Figures 1 and 2.

REFERENCES

Hodgson, E.A.
1946: British Columbia earthquake, June 23, 1946; Royal Astronomical Society of Canada, Journal, v. 40, p. 285-319.

Klassen, R.A. and Shilts, W.W.
1982: Subbottom profiling of lakes of the Canadian Shield; in Current Research, Part A, Geological Survey of Canada, Paper 82-1A, p. 375-384.

Rogers, G.C. and Hasegawa, H.S.
1978: A second look at the British Columbia earthquake of June 23, 1946; Seismological Society of America, Bulletin, v. 68, p. 653-676.

Shilts, W.W.
1984: Sonar evidence for postglacial tectonic instability of the Canadian Shield and Appalachians; in Current Research, Part A, Geological Survey of Canada, Paper 84-1A, p. 567-579.

Shilts, W.W., Blais, A., and Adams, J.
1989: Subbottom profiling of Quebec Appalachian lakes and its potential application to assessing seismic hazard; in Current Research, Part B, Geological Survey of Canada, Paper 89-1B.

Placer gold in the Cariboo district, British Columbia

John J. Clague
Terrain Sciences Division, Vancouver

Clague, J.J., Placer gold in the Cariboo district, British Columbia; in Current Research, Part E, Geological Survey of Canada, Paper 89-1E, p. 243-250, 1989.

Abstract

Placer gold in the Cariboo district of central British Columbia is derived from auriferous quartz veins that cut metasedimentary rocks of the Cariboo Group. Most of the gold was released from source rocks during a lengthy period of denudation and weathering that spanned much of the Tertiary. Enrichment both at the source and in some of the placers may have occurred through solution and redeposition of gold. The most important placers occur on the floors of valleys that were cut when the area was uplifted at the end of the Tertiary and, subsequently, during Pleistocene interglaciations and interstades. These placers are drift-covered and have little or no surface expression. Gold also occurs locally in till, glaciofluvial sediments, and postglacial alluvium. The richest placers have been mined one or more times and are now largely exhausted. Significant amounts of gold, however, may be present in late Tertiary (?) and Pleistocene buried valleys that have not yet been discovered. These deposits are likely to be covered by thick nonauriferous drift and thus will be difficult to exploit.

Résumé

L'or alluvionnaire que l'on trouve dans le district de Caribou, au centre de la Colombie-Britannique, provient de filons quartziques aurifères qui traversent les roches métasédimentaires du groupe de Caribou. La majeure partie de l'or a été libérée des roches mères durant une longue période de dénudation et d'altération qui a occupé une grande partie du Tertiaire. L'enrichissement s'est peut-être produit, à la source et dans quelques-uns des placers, par mise en solution et resédimentation de l'or. Les placers les plus importants se trouvent au fond des vallées creusées à l'époque où la région a subi un soulèvement, soit à la fin du Tertiaire, et ensuite durant les interglaciaires et interstades du Pléistocène. Ces placers sont recouverts par des matériaux de transport glaciaires, et n'ont pratiquement pas d'expression en surface. On rencontre aussi par endroits de l'or dans des tills, des sédiments fluvioglaciaires et des alluvions post-glaciaires. Les placers les plus riches ont été exploités une ou plusieurs fois, et sont maintenant en grande partie épuisés. Toutefois, il existe peut-être encore des quantités importantes d'or dans des vallées enfouies datant du Tertiaire supérieur (?) et du Pléistocène que l'on a pas encore découvertes. Il se peut que ces gisements soient recouverts par des matériaux de transport glaciaires non-aurifères, les rendant par conséquent difficiles à exploiter.

INTRODUCTION

The Cariboo is the premier placer gold district in British Columbia, having yielded over 2.5 million ounces of the metal since the first discoveries in 1860 (Johnston and Uglow, 1926; Boyle, 1979). The richest placers are now almost exhausted, but gold continues to be recovered from sediments that have been mined one or more times in the past, as well as from some previously untapped deposits.

The Cariboo gold district lies in the central part of British Columbia at the eastern edge of the Interior Plateau (Fig. 1, 2). It is a deeply dissected region with relatively low rounded hills and upland plateaus and an irregular pattern of streams and gulches. The Cariboo district was glaciated at least twice, and probably many more times, during the Pleistocene, most recently during the Fraser Glaciation from about 20 000 to 10 000 years ago (Fulton, 1971; Clague, 1981, 1987b, in press). The glaciers that covered this part of the province flowed west from the Cariboo Mountains, at times interacting in a complex fashion with easterly flowing ice from the Coast Mountains (Tipper, 1971a,b; Clague, 1987b, in press). These glaciers eroded and redistributed much of the placer gold in the Cariboo, but obviously did not completely remove it from the district.

This report summarizes my observations to date on the origin and distribution of placer gold in the Cariboo, based on field work conducted during the summers of 1985, 1986, and 1987. This work is part of a much larger inventory of the surficial geology of the upper Fraser River basin that

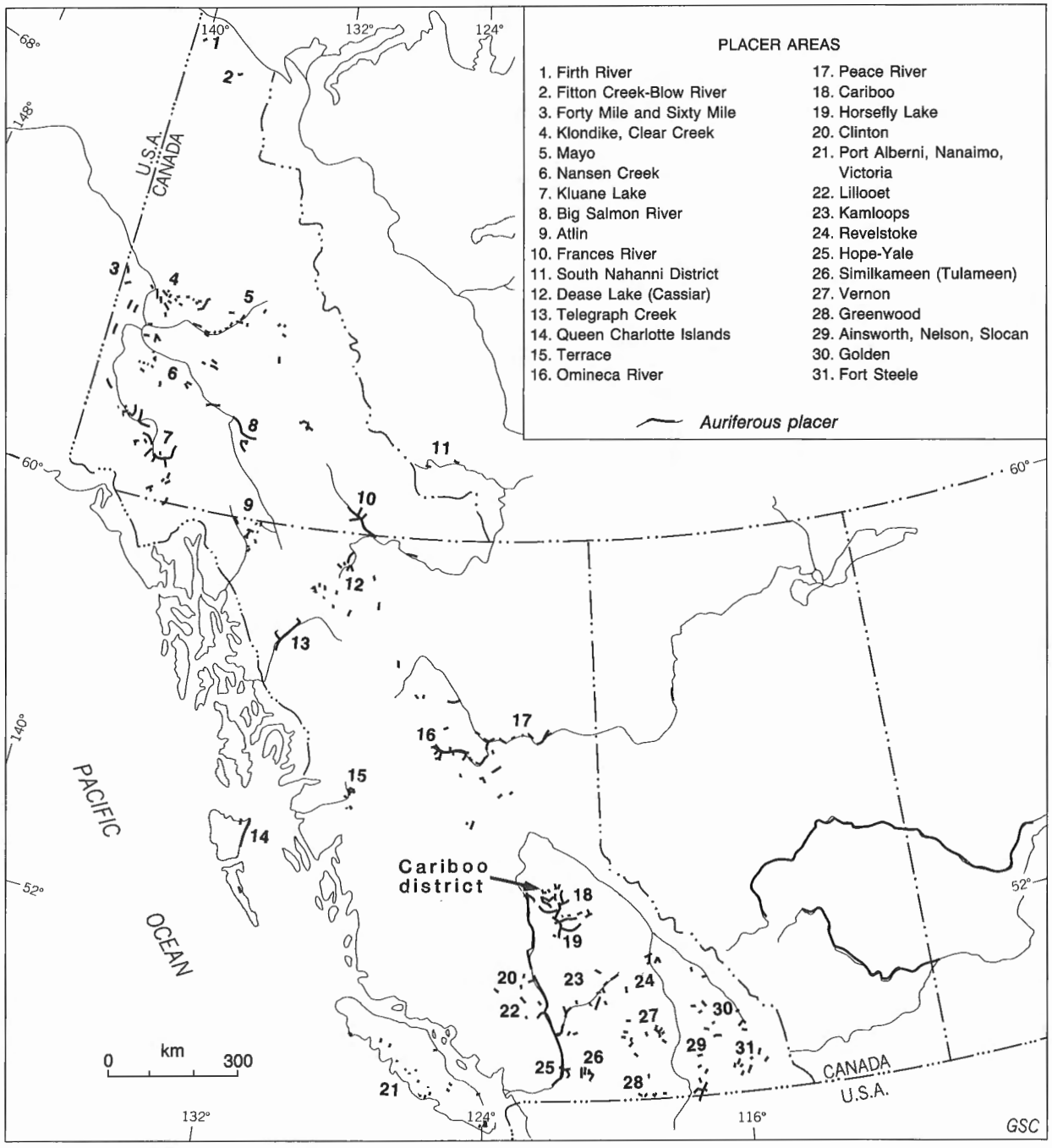

Figure 1. Placer gold deposits in the Canadian Cordillera (adapted from Boyle, 1979, Fig. 79). The Cariboo district has yielded more placer gold than any other area in British Columbia.

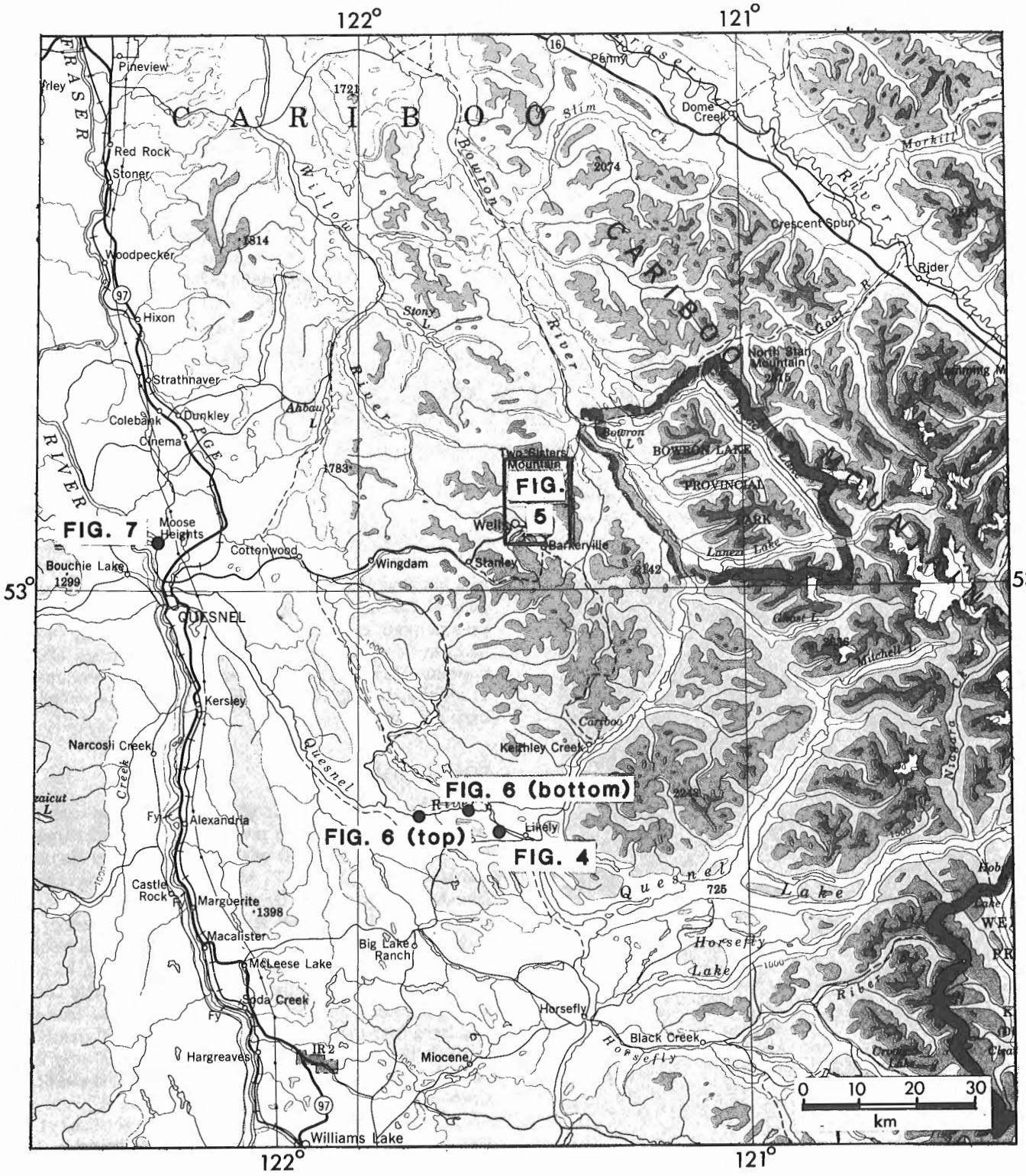

Figure 2. Location and setting of the Cariboo district.

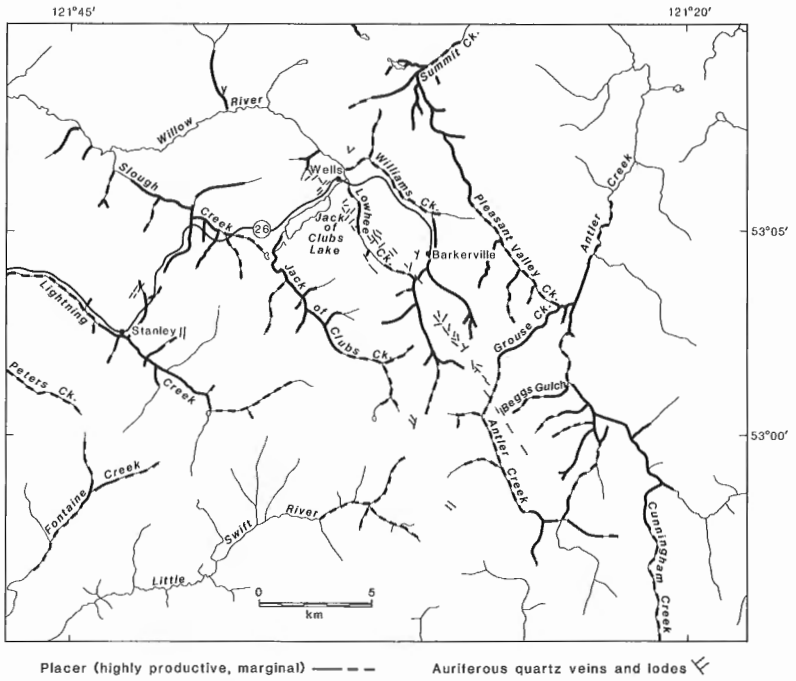

Figure 3. Map of the Wells-Barkerville area showing the relationship of placers to auriferous quartz veins (adapted from Boyle, 1979, Fig. 78).

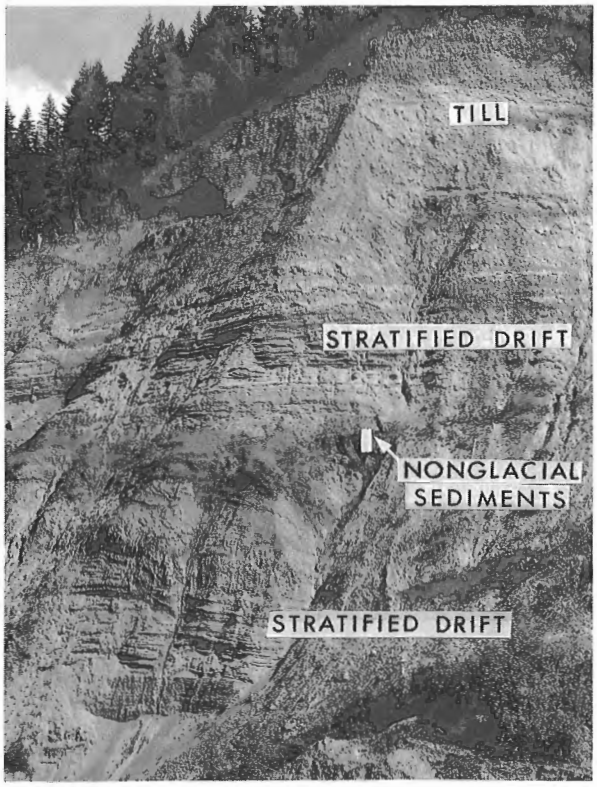

Figure 4. Quaternary sediments at the Bullion placer mine near Likely (see Fig. 2 for location). These sediments contain small amounts of gold. In this exposure, thick till and stratified drift of two glaciations are separated by a thin nonglacial sequence. The exposure is about 70 m high.

was initiated in 1981. The observations reported here are general and somewhat speculative, in part because of the present poor exposure of placer workings and, in part because of the dearth of information on buried alluvial deposits. Hopefully, a more complete picture will emerge as additional work is done, both by myself and other Quaternary geologists.

SOURCE OF GOLD

The main source of placer gold in the Cariboo district is auriferous quartz veins in metasedimentary rocks (mainly phyllite, slate, and schist) of the Cariboo Group (Johnston and Uglow, 1926) (Fig. 3). Most of the gold was released from host rocks during a lengthy period of Tertiary denudation and weathering. Deep weathering under a warmer and perhaps more humid climate during the middle Tertiary (Rouse and Mathews, 1979) permitted oxidation of gold-bearing sulphide minerals and removal of soluble constituents (Johnston and Uglow, 1926). Part of the fine gold thus freed from the sulphides formed enrichments in the oxidized parts of the quartz veins. Gold enrichment may have also taken place by a process of alternate solution and deposition of free gold in the form of crystals, veinlets, and irregular masses in cracks and cavities near the base of the zone of oxidation. These eventually were released to Tertiary streams and concentrated as nuggets in alluvial deposits. Additional solution and redeposition of gold may have occurred within the placers themselves. Gold also is present in late Tertiary and early Quaternary colluvial deposits and soils; it is possible that much of this gold is an in situ chemical precipitate.

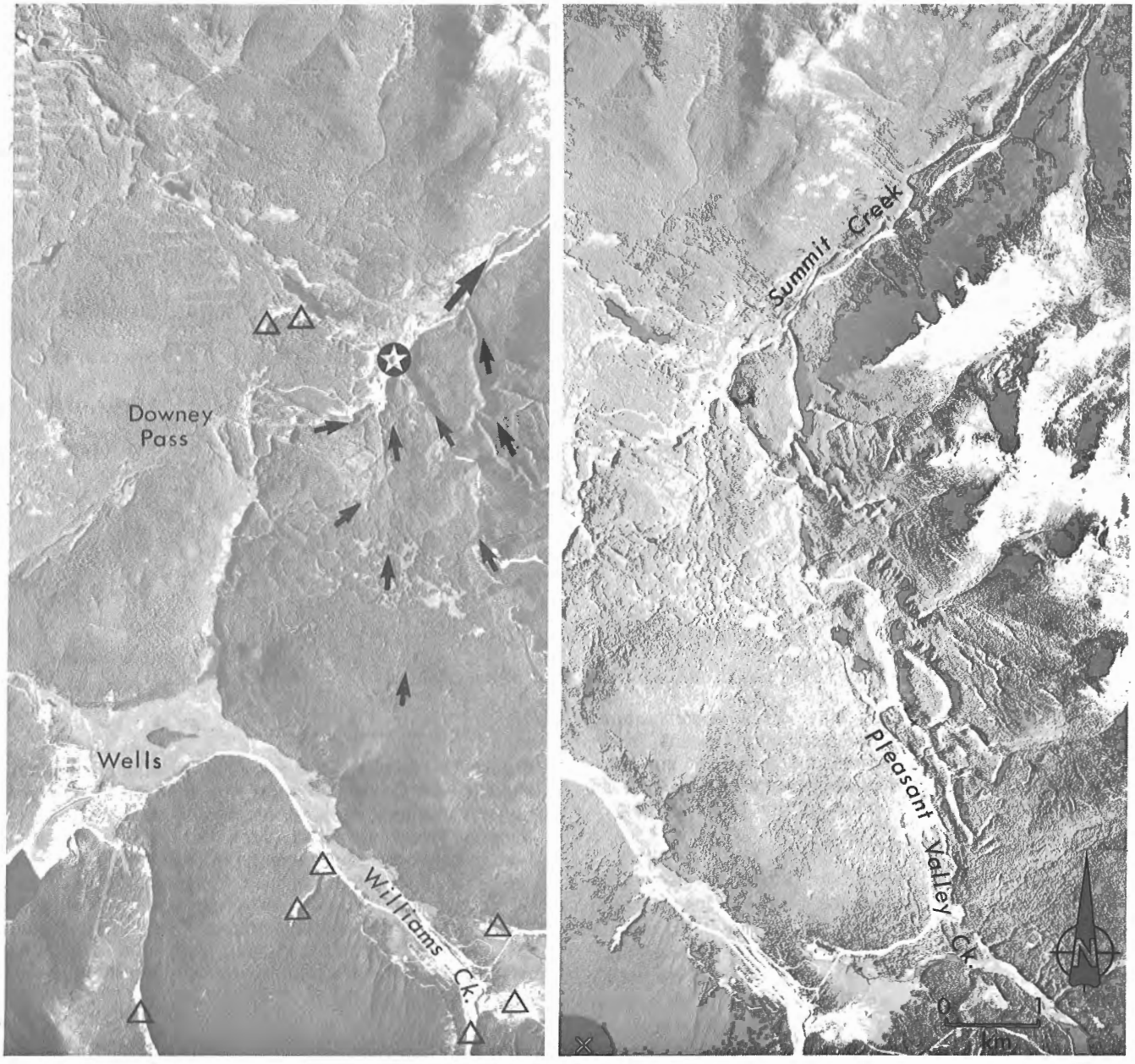

Figure 5. Photostereogram of an area near Wells and Barkerville, showing a complex of meltwater channels eroded in Pleistocene drift and bedrock (see Fig. 2 for location). These channels were cut by meltstreams that flowed from the Cordilleran Ice Sheet as it downwasted and retreated to the southwest about 11 000-12 000 years ago (arrows indicate direction of meltwater flow). Placer gold is present in some of the channels; large amounts were recovered (mainly by dredging) at the starred site. Triangles indicate conspicuous placers in other types of sediments; most of these are now exhausted. NAPL A24756-214 and -215.

TRANSPORT AND DEPOSITION OF GOLD

By the Miocene, relief in the region was considerably less than today. Uplift during late Tertiary time, however, rejuvenated streams and increased relief. Much of the gold that had been released earlier as a result of denudation and weathering became concentrated in valleys cut into the old erosion surface.

Elements of the late Tertiary stream network exist in the present-day physiography. For example, the major rivers in the region, including Fraser, Willow, and Bowron rivers, probably were flowing in something near their present valleys by late Tertiary time, although it is possible that ancestral Fraser River was flowing northward rather than to the south as it does today. Numerous anomalies in the present stream pattern, however, indicate that there have been major changes in drainage in the Cariboo during the Quaternary, probably due to piracy and stream diversion induced by glacier growth and decay. Late Tertiary Willow and Bowron rivers, for example, may have extended farther south than they do today, draining parts of the basins of Lightning Creek and Cariboo River, respectively.

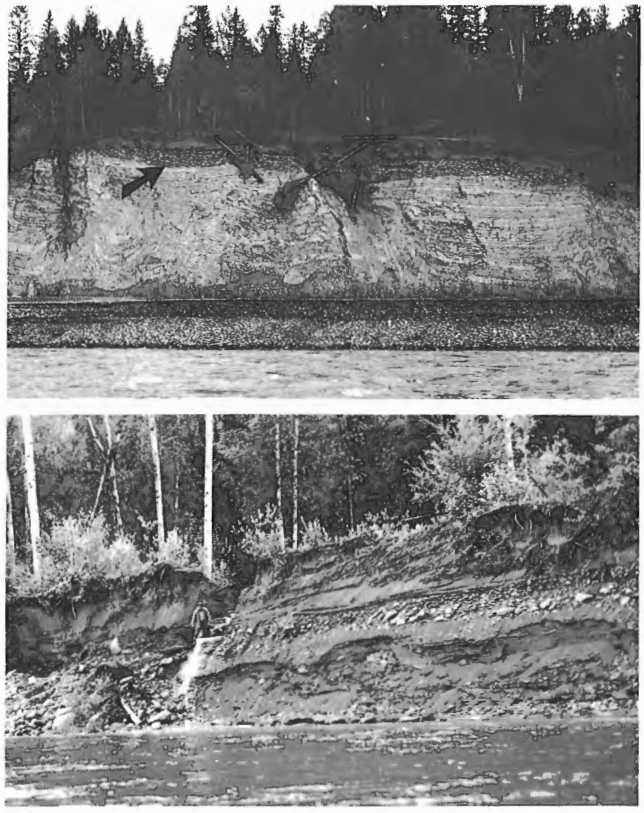

Figure 6. Top: postglacial fluvial gravel unconformably overlying late glacial lacustrine sediments, Quesnel River; placer gold is present on and directly above the unconformity (arrow). Bottom: small placer operation on a low fluvial terrace, Quesnel River. See Figure 2 for photo locations.

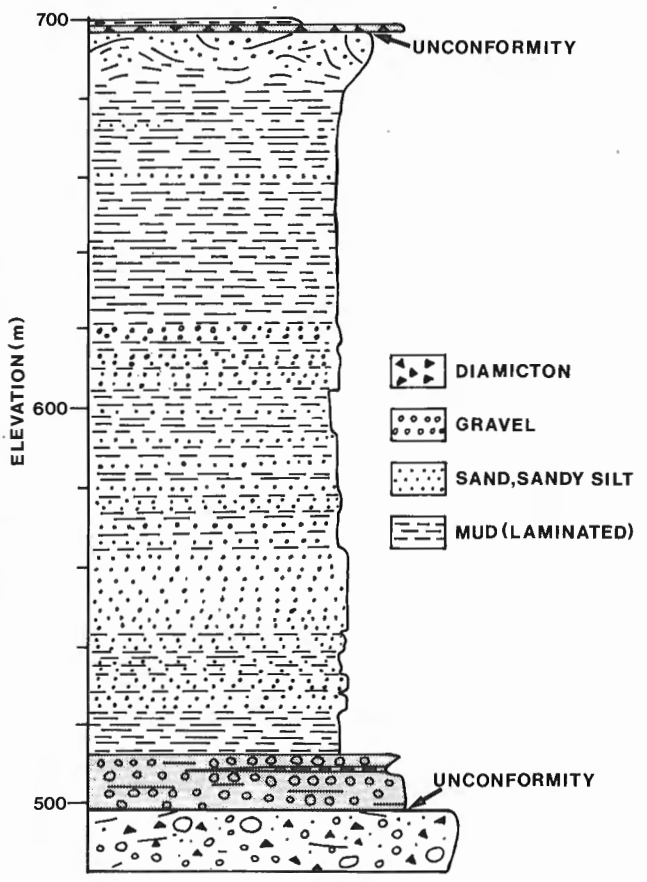

Figure 7. Section of Quaternary sediments at Moose Heights near Quesnel, showing the exposed fill of a large buried valley that predates the last two glaciations (Clague, in press) (see Fig. 2 for location). The gravel unit near the bottom of the sequence was deposited by a stream which eroded the underlying diamicton. Placer gold in the Cariboo commonly is found on the unconformity at the base of this gravel unit. The upper unconformity separates till from glaciolacustrine sand and mud deposited as glaciers advanced into this area during the early part of the Fraser Glaciation.

Remnants of sediments of late Tertiary age have been identified at several sites in the Cariboo (Johnston and Uglow, 1926; Rouse and Mathews, 1979), but it has not been possible to reconstruct the late Tertiary stream network on the basis of the limited outcrop. Such a reconstruction is of fundamental importance in understanding the present distribution of placers in the Cariboo, and can be achieved only through a combination of paleogeomorphic analysis, geophysical profiling and drilling of buried valleys, and sedimentological analysis of valley fills.

During the Quaternary, streams and glaciers removed most Tertiary auriferous gravels. The gold within these gravels, however, was recycled into fluvial and glaciofluvial deposits and tills. Although glaciers, as a rule, are agents of dispersion, gold can be concentrated at the base of the ice by subglacial meltwater and by melt-out of large quantities of debris in the lee of subglacial obstructions. Placer gold has been recovered from till and glaciofluvial sediments in the Cariboo (Fig. 4), but, in most cases, grades have been low and paystreaks of very limited extent.

The most significant Quaternary placers in the Cariboo and elsewhere in British Columbia are products of fluvial deposition during nonglacial periods (interglaciations and interstades). At these times, streams degraded their valleys or were at equilibrium, and gold was washed from Tertiary and Quaternary sediments and concentrated in channels. There undoubtedly were many interglaciations and interstades during the Quaternary, each lasting several thousand to perhaps hundreds of thousands of years, and each separated by glaciations during which placers were eroded and dispersed by ice.

The present interglaciation (Holocene or "postglacial") provides insights on how placers formed in this region during Quaternary nonglacial periods. At the end of the Fraser Glaciation, the ice sheet that enveloped all but the highest peaks in the Cariboo region downwasted and retreated in a generally southwesterly direction towards the centre of the Interior Plateau. Large amounts of meltwater flowed from the melting ice, eroding large quantities of till that had been deposited a short time before (Fig. 5). Glacial deposits also slumped and flowed into valleys from newly deglaciated, unvegetated slopes. As a result of these processes, streams became choked with debris and rapidly aggraded their beds. Colluvial and alluvial fans were built out into trunk valleys by tributary streams, and gravelly deltas prograded into

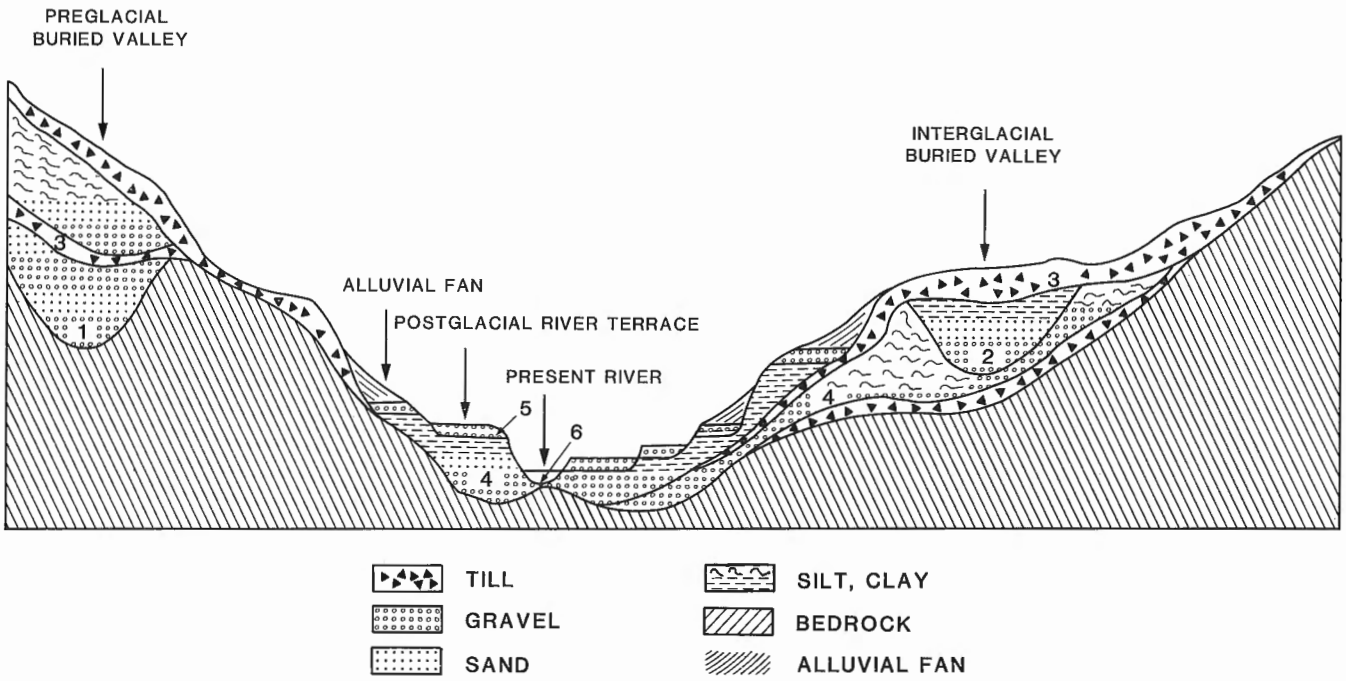

Figure 8. Hypothetical cross-section showing relationships of gold placers to late Tertiary (?) and Quaternary sediments in the Cariboo district. The richest placers are located in preglacial (1) and Pleistocene nonglacial (2) valleys. Smaller amounts of gold are found in some Pleistocene tills (3) and stratified drift (4), in postglacial alluvium (5), and in the present channels of streams (6).

lakes dammed by receding ice. At this time, streams flowed at higher levels than they do today. Gold is dispersed through late glacial and early postglacial valley fills, but concentrations generally are too low to exploit. In a few places, however, these sediments were extensively hydraulicked and dredged during the late 1800s and early 1900s (Fig. 5). As the supply of drift available for erosion and transport decreased and as vegetation became established, streams began to dissect late glacial valleys fills. In some cases, they reoccupied former (pre-Fraser Glaciation) channels, whereas in others they became incised along new courses. As base level fell, gold was washed from late glacial sediments and underlying older Quaternary deposits and concentrated in stream channels. Degradational terraces formed at successively lower levels along some streams as valley fills were progressively dissected. Economic quantities of gold are present at some sites at the base of gravels directly above fluvially eroded substrates (Fig. 6). This process of erosion and concentration continues today, with gold accumulating in the channels of streams such as Quesnel and Cariboo rivers.

Similar valley-fill dissection and placer formation occurred during earlier Quaternary nonglacial periods (Fig. 7). However, all landforms and most sediments produced during these earlier periods were obliterated by subsequent glacial action. Nonglacial sediments, where present, commonly are covered by thick drift. It thus is difficult to identify and follow interglacial and interstadial stream courses. This is unfortunate since large amounts of placer gold are almost certainly present in some of these deposits (Clague, 1987a).

It is not known how many periods of fluvial dissection there have been since the release of gold from source rocks in the Tertiary, although the number is likely large. Some general comments can be made, however, on the potential richness of placers of different ages. Old Quaternary placers, on average, may be richer than young placers. This is because many old placers were concentrated directly from gold-bearing Tertiary sediments before the latter were dispersed by Pleistocene glaciers or buried beneath thick drift. Another important factor is the length of time available for placer formation. Richer, more extensive placers may have developed during long nonglacial periods when large amounts of gold were concentrated by streams flowing in valleys incised into Quaternary sediments. Of course, the gold content of the source sediments is equally important in this respect; brief erosion of sediments rich in gold would produce a richer placer than lengthy erosion of deposits containing little gold.

SUMMARY

Gold placers in the Cariboo district occur in four main groups of sedimentary deposits (Fig. 8).

1. **Preglacial (Tertiary?) fluvial and colluvial sediment and weathered rock.** The gold is associated with fluvial gravels, talus and other forms of colluvium, and weathered bedrock. Large amounts of gold found in the Cariboo in the early years of mining came from these materials. In places, nearly all of the gold lay directly on bedrock or in cracks and crevices within the rock. Some of this gold may be a chemical precipitate.

2. **Pleistocene interglacial and interstadial alluvium**. Paystreaks occur, in places, in gravels deposited by Pleistocene streams. The gravels typically are buried beneath thick till and/or stratified drift deposited during one or more glaciations. Most of the gold is localized at or near the base of the alluvium just above channel floors. The valleys hosting these placers diverge locally from existing valleys and are cut in both bedrock and Quaternary sediments. Most were occupied by streams that flowed at higher levels than present-day streams. There were several periods of valley cutting and filling during the Pleistocene, which gave rise to a complex distribution of valleys and channels of different ages.

3. **Pleistocene glacial sediments**. Gold has been recovered from some tills, from gravel lenses and beds associated with these tills, and from glaciofluvial deposits. In general, the gold is highly disseminated and fine grained, thus most deposits are not economic. Exceptions include some outwash gravels associated with meltwater channels that are conspicuous on airphotos (Fig. 5).

4. **Postglacial alluvium**. Small amounts of gold are present in terrace and fan gravels and on the beds of present-day streams. Most of this gold is fine, and the paystreaks thin and discontinuous.

It is clear from the above that placer gold in the Cariboo occurs in a variety of sediments of different ages. Most surface and near-surface placers have been mined one or more times, although some of these continue to yield gold. Significant new finds probably will be limited to late Tertiary (?) and Pleistocene buried valleys. Although the richest of these were exploited long ago, new finds may be made using various geophysical techniques in conjunction with detailed geomorphic analysis.

ACKNOWLEDGMENTS

B. Ward assisted in the field. C. Davis drafted Figures 2 and 8.

REFERENCES

Boyle, R.W.
1979: The geochemistry of gold and its deposits (together with a chapter on geochemical prospecting for the element); Geological Survey of Canada, Bulletin 280, 584 p.

Clague, J.J.
1981: Late Quaternary geology and geochronology of British Columbia. Part 2: Summary and discussion of radiocarbon-dated Quaternary history; Geological Survey of Canada, Paper 80-35, 41 p.
1987a: A placer gold exploration target in the Cariboo district, British Columbia; in Current Research, Part A, Geological Survey of Canada, Paper 87-1A, p. 177-180.
1987b: Quaternary stratigraphy and history, Williams Lake, British Columbia; Canadian Journal of Earth Sciences, v. 24, p. 147-158.
—: Quaternary stratigraphy and history, Quesnel, British Columbia; Géographie physique et Quaternaire. (in press)

Fulton, R.J.
1971: Radiocarbon geochronology of southern British Columbia; Geological Survey of Canada, Paper 71-37, 28 p.

Johnston, W.A. and Uglow, W.L.
1926: Placer and vein gold deposits of Barkerville, Cariboo district, British Columbia; Geological Survey of Canada, Memoir 149, 246 p.

Rouse, G.E. and Mathews, W.H.
1979: Tertiary geology and palynology of the Quesnel area, British Columbia; Canadian Petroleum Geology, Bulletin, v. 27, p. 418-445.

Tipper, H.W.
1971a: Glacial geomorphology and Pleistocene history of central British Columbia; Geological Survey of Canada, Bulletin 196, 89 p.
1971b: Multiple glaciation in central British Columbia; Canadian Journal of Earth Sciences, v. 8, p. 743-752.

Pleistocene subglacial volcanism near Fort Selkirk, Yukon Territory

Lionel E. Jackson, Jr.
Terrain Sciences Division, Vancouver

Jackson, L.E., Jr., Pleistocene subglacial volcanism near Fort Selkirk, Yukon Territory in Current Research, Part E, Geological Survey of Canada, Paper 89-1E, p. 251-256, 1989.

Abstract

A volcanic edifice near Fort Selkirk, Yukon, is almost entirely composed of hyaloclastite tuffs, breccias, and pillow breccias. Pillow basalt is found near the summit of the mountain. All of these lithologies contain rounded and faceted exotic pebbles. These observations, plus the gentle slopes of the mountain, indicate that it erupted beneath an ice sheet. Since deposits of the Reid Glaciation only reach the base of the mountain, the eruption must have occurred during a pre-Reid glaciation. Faulting may have occurred beneath the north end of the mountain during the Pleistocene.

Résumé

Un édifice volcanique proche de Fort Selkirk au Yukon se compose presque entièrement de tufs de hyaloclastites, de brèches et de brèches basaltiques en coussins. On rencontre les basaltes en coussins près du sommet de la montagne. Toutes ces roches contiennent des galets erratiques arrondis et à facettes. Ces observations, et le fait que la montagne ait des versants en pente douce, indiquent que l'éruption de lave s'est produite sous un inlandsis. Étant donné que les dépôts laissés par la glaciation de Reid n'atteignent que la base de la montagne, l'éruption a dû se produire durant une glaciation antérieure à celle de Reid. Il est possible que des failles se soient formées au-dessous de l'extrêmité nord de la montagne durant le Pléistocène.

INTRODUCTION

An investigation of a small volcanic edifice near Fort Selkirk, Yukon Territory was carried out during the 1988 field season. The investigation was part of surficial geology mapping operations in the Carmacks map area (115 I). The investigation was prompted by Dr. Don Francis, Department of Geology, McGill University who suggested that this volcano may have erupted subglacially. Since the Fort Selkirk area is beyond the limit of the Late Wisconsinan age McConnell Glaciation, detailing such an eruption could be potentially valuable for dating older and more extensive glaciations in the region. This report summarizes preliminary findings based upon field observations.

PREVIOUS WORK

The unnamed volcano, hereafter referred to by its Tutchone name, Ne Ch'e Ddhäwa[1] was given a general description by Sinclair et al. (1978); this report focused on the chemistry and geothermometry of spinel lherzolite nodules found within the tuffs of the mountain rather than on the origin of the edifice itself. Their description consisted of the following main points:

1) Ne Ch'e Ddhäwa is a cinder cone consisting of crudely bedded basaltic tuffs which have been devitrified. These tuffs become increasingly coarse towards the apex of the cone.
2) The tuffs were erupted onto a platform of basalt flows which are constituents of the Pleistocene Fort Selkirk Group (Bostock, 1936).
3) The cone has not been glaciated and postdates the Reid Glaciation.

SETTING

Ne Ch'e Ddhäwa is situated on the east bank of Yukon River 7 km southeast of the ghost town of Fort Selkirk (Fig. 1). It is a circlular, mound-like feature, 1.5 km in diameter and approximately 270 m high, including about 70 m of exposed basalt flows upon which the the mountain has been built (Fig. 2). These basal basalts had a source to the west across Yukon River and are unrelated to the eruption(s) which built the overlying volcanic edifice. Overall slopes on Ne Ch'e Ddhäwa between the top of the basalt flow platform and the summit range from 10 to 15%. Its summit elevation is 712 m. The west margin of the mountain is truncated by the floodplain of Yukon River. Incision by the river along this flank has provided almost continuous exposure. The northern one-third of the volcano is separated from the rest of the mountain by large base to summit ravines on the east and west sides of the mountain (note contours in Fig. 1). This gives the mountain a double summit. The west side ravine is most pronounced — up to 100 m wide and lined with cliffs.

[1] The aboriginal name was supplied by Harry Baum, an elder of the Selkirk Indian Band and transcribed into the Northern Tutchone alphabet by Ruth Gotthardt, consulting archeologist and anthropologist, Whitehorse, Yukon.

METHODS

Exposures of rocks composing Ne Ch'e Ddhäwa are confined to the cliffs along Yukon River, the ravine, and scattered exposures around the south summit; these were traversed, described, and sampled. It was found that part of the edifice was erupted onto stratified Pleistocene sediments. Part of this sequence was exposed in a 1 m by 10 m trench dug into the cliffs along Yukon River. General stratigraphic relationships along the base of the volcano were further documented by observations through field glasses from Yukon River.

STRATIGRAPHY

The stratigraphy and structural relations of Ne Ch'e Ddhäwa are summarized in Figure 3. These units are described and discussed below, from oldest to youngest.

Basalt flow platform (unit 1)

The exposed basalt flows, which form a platform beneath the north and south flanks of Ne Ch'e Ddhäwa, are 70 m and 50 m thick, respectively. Sinclair et al. (1978) reported 9 distinct lava flows or cooling units on the south flank. Four flows of columnar basalt, 3 m thick, outcrop on the north flank and are separated by basaltic tuffs and breccias. The uppermost flow and breccias are best exposed. The flow is dark grey/rusty weathering and vesicular throughout. It overlies a hyaloclastite breccia. Columns range from vertical to horizontal and locally radiate about a central point. Pillows are locally present within the flow.

The flow also shows evidence of lava flow/water interaction, which is not surprising. With a source west of Yukon River, these flows likely dammed the river during their advance, providing ample opportunity for lava and water to interact.

Basal sediments (unit 2)

Along the north end of the Ne Ch'e Ddhäwa, the lowest tuffs are underlain by more than 6 m of diamicton, sands, and clays. Increasing thickness of colluvium downslope prevented the trenching of additional thicknesses of these sediments. The upper 50 cm of the sequence is capped by a stony dark grey diamicton, likely till. Constituent pebbles (Table 1) have rounded and faceted shapes, some of which are striated. Bedding of the basal sediments is inclined or folded. Two fold measurements show fold axial trends 30° to 40° and limbs dipping to the northeast and southwest at 13° to 24°. Two bedding contacts, where no folding is apparent, strike at 30° to 40° and dip to the northeast.

Basal tuffs and pillow basalts (unit 3)

The basal sediments are overlain by 78 m of generally horizontally bedded, cliff-forming to recessive altered tuff to tuff breccia. These range in colour from light grey to orange. Bedding ranges from indistinct and massive to locally well developed and thin to laminated. Cut-and-fill and channel-like features are occur in places along contacts.

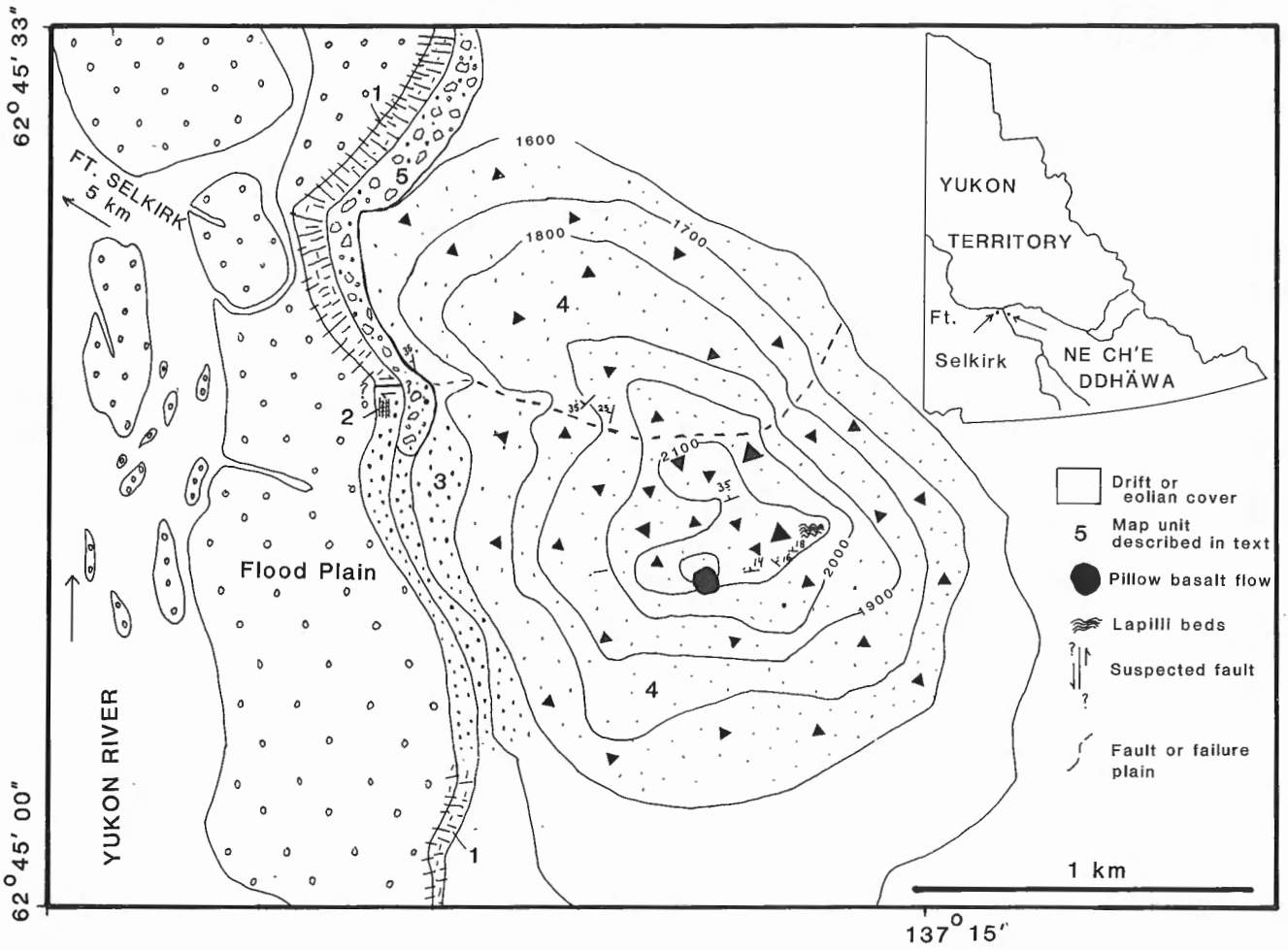

Figure 1. Outcrop map of Ne Ch'e Ddhäwa.

Table 1. Pebble lithologies

Lithology	(percent content) Unit 2[1]	Unit 4[2]	Unit 5[3]
Basalt and tuff	37.5	8.7	60.4
Granitic	0.0	21.7	7.5
Gneiss	10.0	2.9	5.7
Schist and phyllite	12.5	18.8	5.7
Quartzite and sandstone	7.5	21.7	5.7
Siltstone	10.0	1.4	0.0
Chert and cherty sandstone	7.5	13.0	11.3
Quartz	12.5	7.2	3.8
Other	2.5	4.3	0.0
	100.0	99.7	100.11

[1] n=40, pebbles in pre-Reid till at the top of basal sediments.
[2] n=69, pebbles in pillow breccia and pillow basalts.
[3] n=53, pebbles in Reid till.

Figure 2. Oblique view of Ne Ch'e Ddhäwa looking south (up Yukon River valley) from the limit of Reid Glaciation. The confluence of Yukon and Pelly rivers is in the foreground.

Figure 3. Generalized stratigraphy of Ne Ch'e Ddhäwa. Unit 1: basalt flow platform; Unit 2: basal sediments; Unit 3: basal tuffs and pillow basalts; Unit 4: cone complex; Unit 5: till. The fault at the north end of the mountain, could also be a buried erosional scarp.

Figure 4. Horizontally bedded fine breccia at the margin of the cone complex (unit 4). Pick handle length is 100 cm.

Figure 5. Breccia containing black, angular basaltic pillow fragments, scattered granite fragments (g) and cemented gravel (c) near the summit of the cone complex (unit 4).

Foreset beds, which dip at 30o to the northwest away from the centre of the mountain, are present at one location. Constituent clasts are generally finer than 5 mm but some reach clasts up to 5 cm diameter. Scattered fragments of basaltic pillows occur throughout the tuffs and tuff breccias. The tuff also contains scattered pebbles of exotic rock types including quartzite, greenstone, granitics, and chert. Prominent cliff-forming horizons within the tuffs are offset along normal faults which have throws of about 5 m near the northern end of the mountain. These faults are too small to be apparent in Figure 3. Near the middle section of the cliffs, tuff occurs in single beds 4 to 15 m thick. The central part of the cliffs (Fig. 3) is a massive complex of pillows and altered hyaloclastite breccias and tuff breccias.

Cone Complex (unit 4)

The cone complex either overlies or grades upward from the basal tuffs and pillow basalts. It is composed of inclined beds of light grey altered fine breccias and coarse pillow breccias. Alteration products of breccia matrix are dominated by analcime, albite, calcite, and mixed layer and expandable clay minerals. Texture generally coarsens toward the centre and summit of the cone progressing from a fine breccia with constituent clasts 2 to 3 cm in diameter to coarse pillow tuff breccias. This breccia has angular pillow fragments 10 to 20 cm in diameter making up 20 to 30 % of beds. Beds near the base of the cone are horizontally stratified to cross-stratified and are less than 1 cm to 1 m thick. Beds are normally graded or unsorted. Near the centre of the cone, beds are massive and unsorted and are metres in thickness where bedding planes are discernable (Fig. 4, 5). Bedding within the cone complex is generally inclined at angles ranging from 14° to 35°. Exceptions occur near the summit of the cone where near horizontal beds are locally present.

The beccias and pillow breccias of the cone complex contain numerous rounded exotic pebbles (Table 1) and the lherzolite nodules described by Sinclair et al. (1978). In addition, angular blocks of dark grey to olive grey altered tuffs, ranging in size from 10 cm to more than 1 m, are also common (Fig. 6). Most of these clasts are structureless; however, scattered clasts of very light grey laminated silts are present. These clasts may be pieces of tuffs or basal sediments from beneath the cone complex which were carried up to the surface during eruption(s).

Summit pillow basalts and lapilli beds

Pillow basalts discontinuously outcrop over a 17 m vertical distance coming within 1.7 m of the south side of the south summit (Fig. 1). They are interstratified with tuffs near the top of these exposures. Rounded and faceted exotic pebbles are commonly incorporated within the pillows and are visually estimated to make up 3 to 5% of flows by volume (Fig. 7). Black, partly fused lapilli beds occur about 100 m east and 30 m below the summit. Bedding thickness ranges from 1 to 40 cm (Fig. 1, 8). Many individual fragments within the beds have twisted, cable-like appearances. The partial fusing of lapilli indicates eruption and airfall in a partly molten state. These lapilli beds are the only, clearly subaerially erupted volcanic rocks within the mountain.

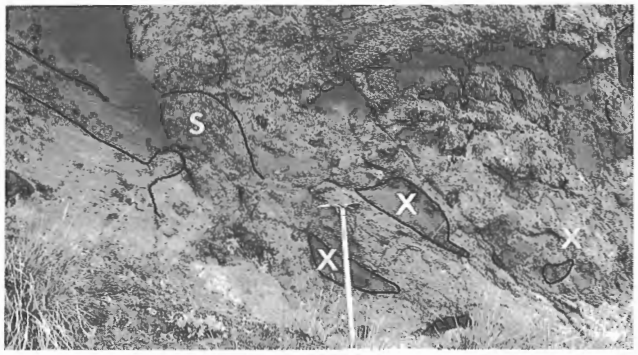

Figure 6. Dark grey angular xenoliths (x) in breccia near the summit of the cone complex. Bedding planes distorted by slumping are outlined near "s".

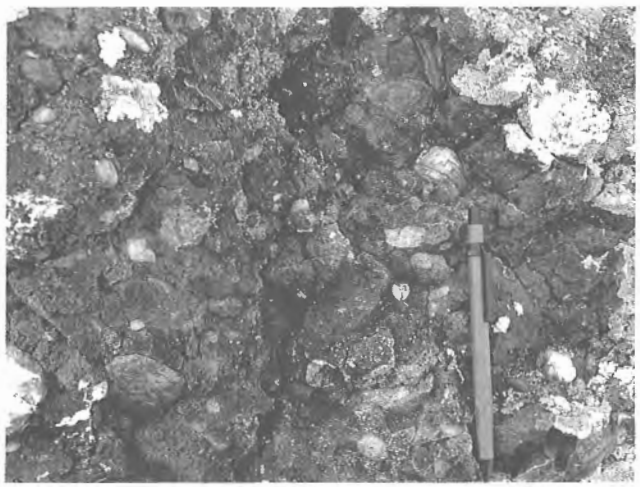

Figure 7. Rounded exotic pebbles in basalt pillows on the summit of the cone complex.

Figure 8. Dark welded scoria beds. The fluting on the surface is the product of sand blasting during the McConnell Glaciation.

Till (unit 5)

Up to 10 m of light grey, sandy, well indurated, and unweathered till overlies both units 1 and 3 along the tops of cliffs above the Yukon River floodplain. The till is stony, fissile, and partly cemented. Till pebbles (Table 1) are commonly faceted and striated. The till does not extend above the base of the cone of Ne Ch'e Ddhäwa (unit 4). The same till is exposed on the west side of Yukon River and can be traced downstream where it can be shown to be laterally bounded by former ice marginal features associated with the penultimate Reid Glaciation (Hughes et al., 1969).

ERUPTIVE ENVIRONMENT OF NE CH'E DDHÄWA

In the preceding description of the units of Ne Ch'e Ddhäwa, many details conflict with the subaerial eruptive origin for the volcano suggested by Sinclair et al. (1978). Cinder cones are usually circular accumulations of subaerially erupted products including scoriaceous blocks, bombs, lapilli, ash, and flows. Slope and bedding angles are close to the angle of repose, approximately 30° (MacDonald, 1972, p. 184-185). Ne Ch'e Ddhäwa differs from a cinder cone in many important ways:

1) Its overall slope angle of 10° to 15° is well below the angle of repose and bedding dips are as low as 14°.
2) Subaerially erupted ejecta accounts for an inconsequential portion of the volcano.
3) Pillow basalts, associated with the interaction of basaltic lava and water, are found at the summit, and pillow fragments are common within the breccias of the cone complex.
4) Exotic (nonvolcanic) pebbles are found throughout the tuffs and breccias and within pillow basalts at the summit of the mountain.

In order to account for the almost complete dominance of hyaloclastite tuffs, breccias, and pillow basalts throughout Ne Ch'e Ddhäwa, water would have to have been in contact with the mountain throughout its eruption(s). Eruption beneath glacial ice, as proposed for volcanic peaks in British Columbia and Iceland by Mathews (1947), Jones (1966, 1969), Allen (1980), Allen et al. (1982), and Hickson (1986), appears to be the only apparent way to provide a continuous subaqueous environment. At least two glacial advances have occurred in the Fort Selkirk area (Bostock, 1966; Hughes et al., 1969).

The exotic pebbles throughout Ne Ch'e Ddhäwa also fit with this model. They were likely continuously melted out from glacial ice during eruption. The pebbles have a smaller basalt percentage than does till in unit 2 and unit 5 and likely reflects the composition of pebbles carried higher in the ice from distant sources (Table 1).

Comparisons with Tuyas

Ne Ch'e Ddhäwa differs from the flat-topped volcanic edifices in northern British Columbia which Mathews (1947) called "tuyas". Tuyas consist of complexes of hyaloclastite tuffs and foreset-bedded hyaloclastite breccias, pillow breccias, and pillows which are capped by extensive

flat-lying flows. They rise within a subglacial water-filled cavity which is melted by the eruptions. Pillow basalt flows form on the hyaloclastite pile once water no longer has access to the eruptive vent. In contrast, Ne Ch'e Ddhäwa lacks all but a small capping of pillow basalt flows and air-fall deposits. Eruption apparently all but ceased before the water level around the mountain dropped below the vent. The lapilli beds represent a last gasp of eruptive activity when the vent was above water level.

The gentle slopes of Ne Ch'e Ddhäwa and the low dips of some beds within it contrast with slopes and bedding angles of tuyas, which are usually steeper than subaerially erupted cinder cones (Hickson, personal communication, 1988). Explanations for these variations are not apparent.

Evidence for contemporaneous faulting

The basal sediments (unit 2) and the overlying tuffs (unit 3) are juxtaposed against the basalt flows and breccias of the flow basalt platform (unit 1) at the north end of the mountain (Fig. 1, 3). The contact between the two units is covered by thick colluvium. This contact is depicted as a normal fault with an estimated throw of at least 60 m in Figures 1 and 3 for the following reasons. (1) The beds in unit 2 dip away from the contact and are folded in a manner compatible with their position in a footwall. (2) Normal faults, too small to depict in Figure 3, cut overlying unit 3; these may be related to faulting between units 1 and units 2 and 3. (3) The large ravine which separates the two summits of Ne Ch'e Ddhäwa likely has been eroded along a planar zone of weakened rock which cuts the northern end of the mountain. The ravine approximately coincides with the contact between unit 1 and units 2 and 3 and may represent an extension of the fault plane.

Alternatively, the contact maybe an erosional scarp. Although sediments in unit 2 are predominantly fine grained, two large, angular basalt boulders were present within this unit below the till. These imply the existence of an adjacent basalt scarp during deposition. Furthermore, the ravine may mark a failure plane caused by postglacial sagging of the north end of the mountain following the loss of mechanical support furnished by glacial ice. The faults in overlying unit 3 may be syndepositional growth faults.

AGE OF ERUPTION

No radiometric or paleomagnetic dating has been carried out on rocks from Ne Ch'e Ddhäwa. However, the eruption can be assigned to one of the known glaciations in the Fort Selkirk area. Ne Ch'e Ddhäwa lies at the down-ice limit of Reid Glaciation. Consequently, it is not likely that ice could have exceeded the height of the mountain during Reid Glaciation. The thick accumulation of till along the base of Ne Ch'e Ddhäwa is likely the remains of a Reid age lateral moraine. Consequently, the mountain erupted during a glaciation predating the Reid. Pre-Reid advance(s) reached more than 900 m elevation in the general area of the mountain and extended more than 20 km beyond Ne Ch'e Ddhäwa down the Yukon River valley (Hughes et al., 1969). An advance of this magnitude would have buried the top of Ne Ch'e Ddhäwa by 180 m. The till which underlies the basal tuffs dates either from this or an older glaciation.

CONCLUSIONS

Ne Ch'e Ddhäwa is almost entirely composed of altered hyaloclastite tuffs, breccias, pillow fragments, and pillow basalts. These units contain rounded and faceted exotic pebbles. These are compatible with eruption beneath an ice sheet during a pre-Reid glaciation. A fault which was active during the Pleistocene prior to or during eruption may exist beneath the north end of the mountain.

ACKNOWLEDGMENTS

The author gratefully acknowledges the critical review of Cathie Hickson. All errors of fact or interpretation, however, are solely the responsibility of the author. The author also acknowledges the field assistance of Brent Ward and Dave Lye and the help of Ruth Gotthardt in interviewing members of the Selkirk Indian Band.

REFERENCES

Allen, C.C.,
1980: Icelandic subglacial volcanism: thermal and physical studies; Journal of Geology, v. 88, p. 108-117.
Allen, C.C., Jercinovic, M., and Allen, J.
1982: Subglacial volcanism in north-central British Columbia and Iceland; Journal of Geology, v. 90, 699-715.
Bostock, H.S.
1936: Carmacks District, Yukon; Geological Survey of Canada, Memoir 189, 67 p.
1966: Notes on glaciation in central Yukon Territory; Geological Survey of Canada, Paper 65-36, 18 p.
Hickson, C.J.
1986: Quaternary volcanism in the Wells Gray-Clearwater area, east central British Columbia; unpublished PhD thesis, Department of Geological Sciences, University of British Columbia, Vancouver, 357 p.
Hughes, O.L., Campbell, R.B., Muller, J.E., and Wheeler, J.O.,
1969: Glacial limits and flow patterns, Yukon Territory, south of 65 degrees north latitude; Geological Survey of Canada, Paper 68-34.
Jones, J.G.
1966: Intraglacial volcanoes of south-west Iceland and their significance in the interpretation of the formation of marine basaltic volcanoes; Nature, v. 212, p. 586-588.
1969: Intraglacial volcanoes of the Laugarvatn region, southwest Iceland, I; Quarterly Journal of the Geological Society of London, v. 124, pt. 3, p. 197-211.
MacDonald, G.A.
1972: Volcanoes; Prentice-Hall, New Jersey, 510 p.
Mathews, W.H.
1947: "Tuyas", flat-topped volcanoes in northern British Columbia; American Journal of Science, v. 245, p. 560-570.
Sinclair, P.D., Templeman-Kluit, D.J., and Medaris, L.G. ,Jr.
1978: Lherzolite nodules from a Pleistocene cinder cone in central Yukon; Canadian Journal of Earth Sciences, v. 15, p. 220-226.

Quaternary stratigraphy along Pelly River in Glenlyon and Carmacks map areas, Yukon Territory

Brent Ward[1]
Terrain Sciences Division

Ward, B., Quaternary stratigraphy along Pelly River in Glenlyon and Carmacks map areas, Yukon Territory; in Current Research, Part E, Geological Survey of Canada, Paper 89-1E, p. 257-264, 1989.

Abstract

This report documents some of the Quaternary stratigraphy along Pelly River, Yukon Territory. The oldest sediments found were at the Bradens Canyon section. There, sands with fine grained organic sediments were overridden by the Cordilleran Ice Sheet during Reid Glaciation. Above this are sediments that record deposition during Reid, McConnell, and Holocene time. Two tills separated by stratified sediment at the Safety Pin Bend section, about 75 km upvalley from Bradens Canyon, indicate two events of the McConnell Glaciation. Section 26, an additional 25 km upvalley, could record two separate glaciations, but the age of the earlier one is unknown. A minimum date for the McConnell Glaciation of 12 590±120 BP, obtained on Pisidium sp., is reported. Sedimentological studies of McConnell sediments confirm that the ice sheet stagnated and downwasted in place.

Résumé

Le présent rapport fait état de la stratigraphie quaternaire le long de la rivière Pelly (territoire du Yukon). Les plus anciens sédiments découverts l'ont été à la coupe du canyon Bradens. À cet endroit, des sables renfermant des sédiments organiques à grain fin ont été chavauchés par l'inlandsis de la Cordillère pendant la glaciation de Reid. Plus haut se trouvent des sédiments déposés pendant les avancées de Reid et McConnell et l'Holocène. Deux tills séparés par des sédiments stratifiés à la coupe de Safety Pin Bend, à environ 75 km en amont de la vallée du canyon Bradens, indiquent deux épisodes de la glaciation de McConnell. La coupe 26, située 25 km encore plus en amont de cette même vallée, pourrait témoigner de deux glaciations distinctes, mais l'âge de la première n'est pas connu. Une date minimum est signalée pour la glaciation de McConnell, soit 12590 ± 120 BP, obtenue avec ***Pisidium sp.*** *Des études sédimentologiques des sédiments de McConnell confirment qu'il y a eu stagnation et fonte de l'inlandsis sur place.*

[1] Department of Geology, University of Alberta, Edmonton, Alberta T6G 2E3

INTRODUCTION

The Glenlyon (105 L) and Carmacks (115 I) map areas lie astride the westernmost limits of the last two glaciations — the McConnell and the Reid (Bostock, 1966) — recognized in the central Yukon (Fig. 1). The younger McConnell Glaciation is generally considered to be Late Wisconsinan, while the older Reid is now considered to be Illinoian (Hughes, 1987). Bostock (1966) defined two older glaciations — the Klaza and the Nansen; however, subsequent workers have been unable to differentiate these two older deposits, so the term pre-Reid was introduced to describe glacial deposits that predate the Reid (Hughes et al., 1969). The Quaternary sediments found in the Glenlyon and Carmacks map areas will be placed in the above framework.

The 1987 and 1988 field seasons were spent in investigations of sediments within Glenlyon map area and along Pelly River within the Carmacks map area (115 I). There are three main objectives of this fieldwork: to produce a detailed surficial geology map of the Glenlyon map area; to determine the Quaternary stratigraphy, tracing it into the Carmacks area along Pelly River (Fig. 1); and to analyze the sedimentology of McConnell age sediments to determine the nature of deglaciation. This report documents some of the stratigraphy that was found along Pelly River and briefly discusses the nature of McConnell deglaciation.

PREVIOUS WORK

Dawson (1888) examined the bedrock and surficial sediments along Pelly River. McConnell (1903) described the geology along MacMillan River and the Pelly downstream from the MacMillan. Campbell (1967) examined the surficial sediments of the Glenlyon map area in conjunction with bedrock mapping in the early 1950s. Combining this with detailed airphoto analysis, he produced a surficial geology map (1222A) that depicts the distribution of lake sediments and geomorphic features such as ice limits, drumlins, and outwash plains. Duk-Rodkin mapped McConnell ice limit features in the area at a scale of 1:50 000. These data were used to construct a profile of the McConnell ice sheet in the area (Duk-Rodkin et al., 1986; Jackson and Duk-Rodkin, in press). Surficial sediments were mapped in the east half of the Carmacks (115 I) map area (Klassen et al., 1987) but stratigraphy along Pelly River was not reported.

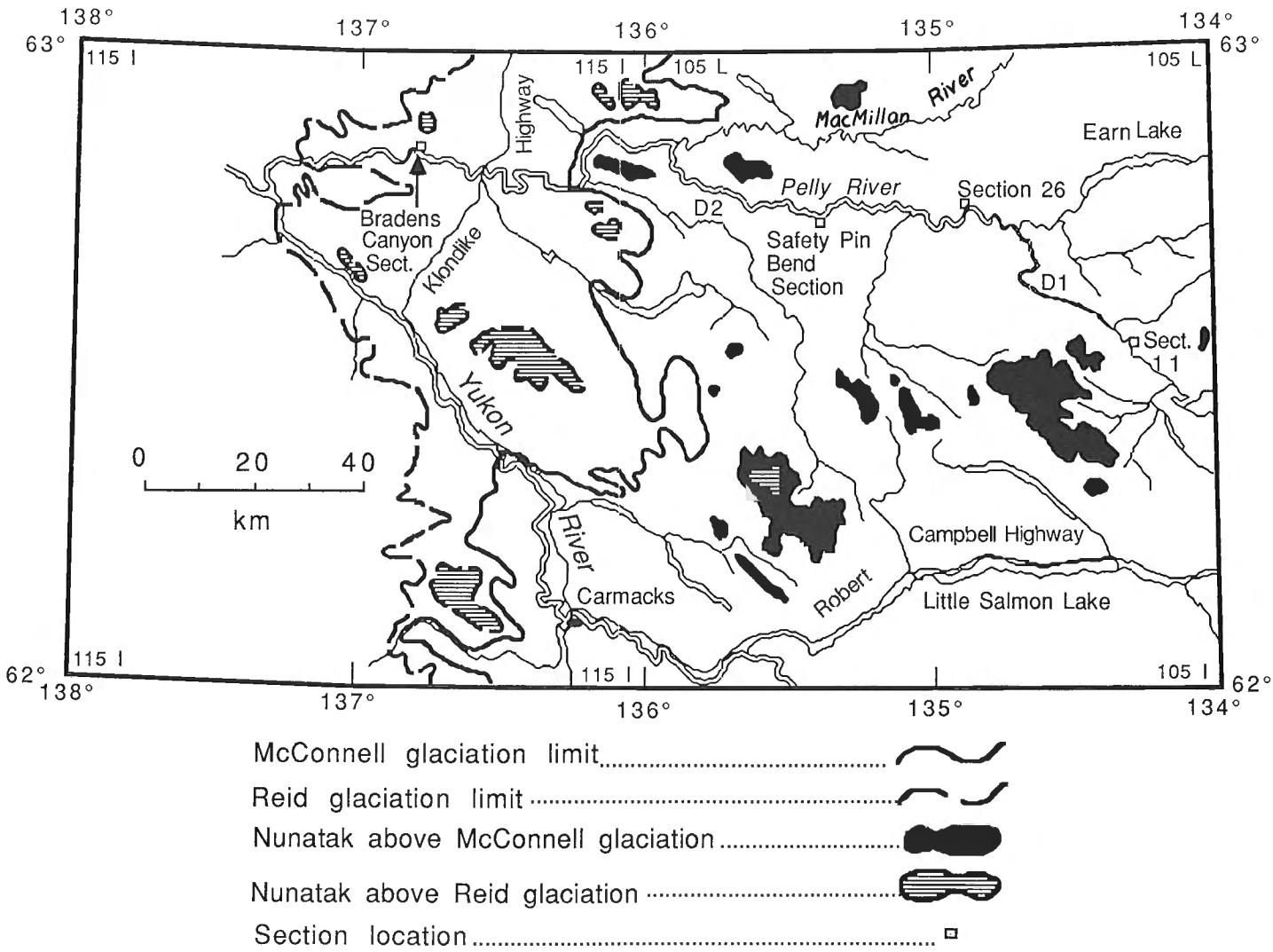

Figure 1. Location map showing the Glenlyon (105 L) and Carmacks (115I) map areas and the limits of the McConnell and Reid glaciations (modified after Duk-Rodkin et al., 1987, Fig. 28.1).

STRATIGRAPHY

Bradens Canyon

The oldest sediments found were at the Bradens Canyon section, located on the north bank of Pelly River within the Carmacks map area (Fig. 1-3). This is west of the McConnell glacial limit but within the Reid glacial limit (Fig. 1). The section is inset into a Reid terrace mapped as a glaciofluvial complex overlying till (Klassen et al., 1987); the terrace is visible in the upper right corner of Figure 2.

Units 1 and 2 of the section consist dominantly of sands (Fig. 3). Unit 1 has several fine grained organic layers in the upper 0.5 to 1 m. These organic layers show evidence of cryoturbation and two structures interpreted as some form of ice wedge cast were found (Fig. 4). A radiocarbon date indicates these organics are >41 000 BP (GSC-4510). The contact between units 1 and 2 is erosive and is marked by a pebble lag. Unit 2 consists mainly of fine to medium sands with no organic material. Units 1 and 2 are interpreted as fluvial sands. Both units are cut by low angle thrust faults (Fig. 5) and at the upstream end of the section organic deposits from unit 1 are thrust over unit 2 (Fig. 6). These thrust faults are interpreted as being produced by an overriding glacier flowing from the east.

Unit 3a has a sharp lower erosive contact which approximately parallels the thrust faults in units 1 and 2 (Fig. 5). A thin (5 to 20 cm) diamicton with striated clasts and incorporated organics overlies this contact. This diamicton is interpreted as basal till. The overlying deposits included in unit 3a are a melange of gravels, sands, silts, and diamictons. Its exact genesis is uncertain but is likely some sort of glaciolacustrine environment. Unit 3b, which is dominantly a boulder to cobble gravel with some areas of ice contact silts and sands, is interpreted as outwash. Both sub-units are not extensively weathered.

The lower contact of unit 4 is erosive and marked by a boulder lag (Fig. 3). Unit 4a is abruptly normally graded from cobble gravels to sands and silts. The elevation of the

Figure 2. View of the Bradens Canyon section looking upstream. The arrow indicates river flow. Section is 33 m high.

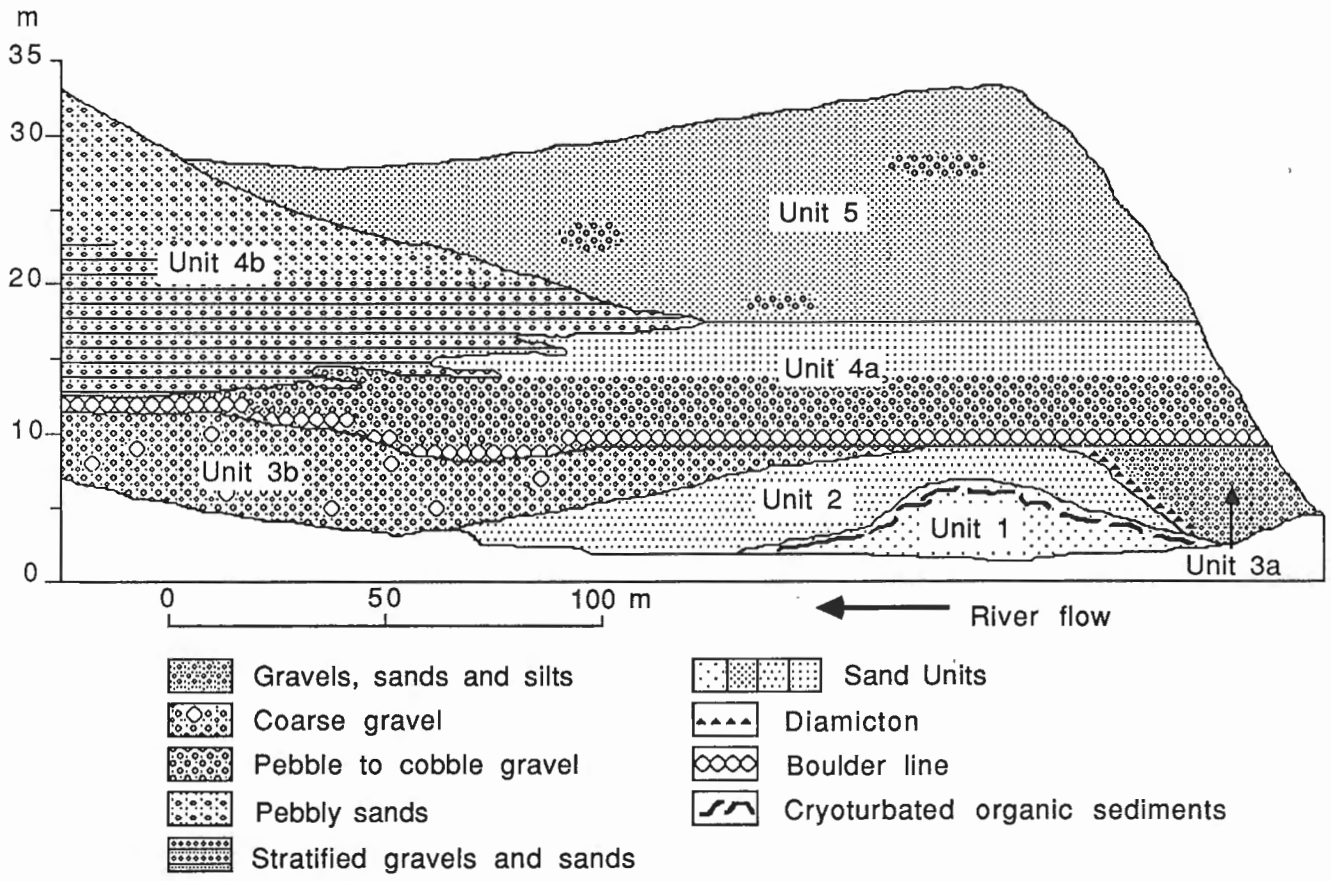

Figure 3. Units present at the Bradens Canyon section; the units are described in the text.

upper contact (17 m above river level) corresponds well to the gradient of McConnell terraces measured between Bradens Canyon and the McConnell limit. The lower part of unit 4b consists of well stratified gravels and sands. The sands contain abundant soft sediment deformation features, climbing ripples, and some dropstones. The stratification becomes less well defined upward and the deposits are more poorly sorted, consisting dominantly of pebbly sands. Unit 4b is interpreted as an alluvial fan sequence that prograded into the river that deposited unit 4a.

The upper contact of unit 4, where overlain by unit 5, is marked by a paleosol. Although the organic matter collected from this paleosol has not yet been dated, it is considered to be early Holocene. Overlying the paleosol, unit 5 consists dominantly of sands with scattered cobble to pebble layers and lenses. The unit is assumed to have been deposited in a minor creek.

Figure 4. One of the possible ice-wedge casts found in unit 1 of Bradens Canyon section. Organic layers present are involuted due to cryoturbation. Visible portion of ice axe is 90 cm long.

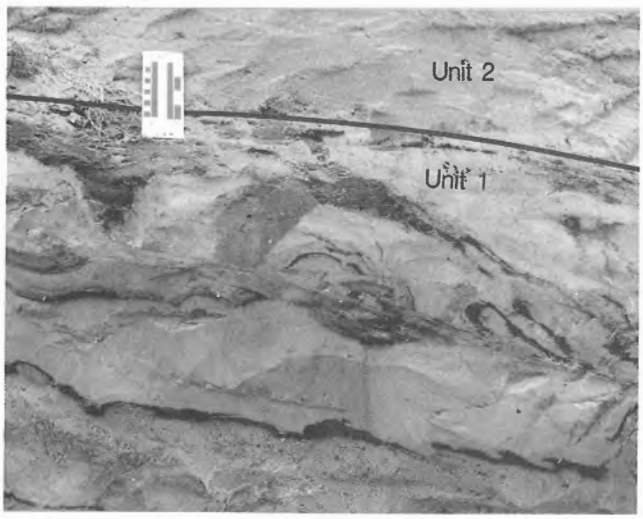

Figure 5. Thrust faults in the organics of unit 1 at the upstream end of the Bradens Canyon section.

Units 1 and 2 are interpreted to predate Reid Glaciation, on the basis of the >41 000 BP ^{14}C date and because both units show evidence of having been overrun by ice. Because of the location of the section in relation to glacial limits (Fig. 1), these units were likely overridden by the Reid or an even older glaciation. Unit 3 is interpreted as a deposit of Reid age because of a lack of extensive weathering and its relative stratigraphic position. Unit 4 is assigned to McConnell time on the basis of relative elevation and relative stratigraphic position. Unit 5 is probably early Holocene, the paleosol indicating a hiatus between deposition of units 4 and 5.

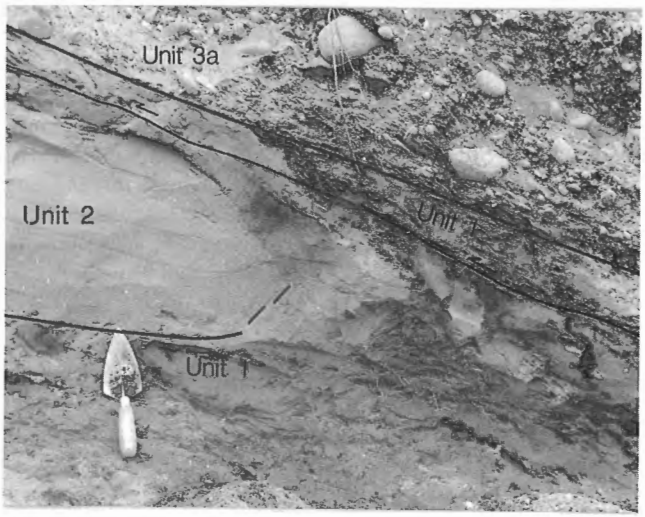

Figure 6. Thrust faulted organic sediments in unit 1 at the upstream end of Bradens Canyon section. These organics have been thrust over unit 2 causing drag folding in the sands, above and to the right of the trowel. A major thrust fault is outlined which parallels the lower contact of Unit 3a. The trowel is 25 cm long.

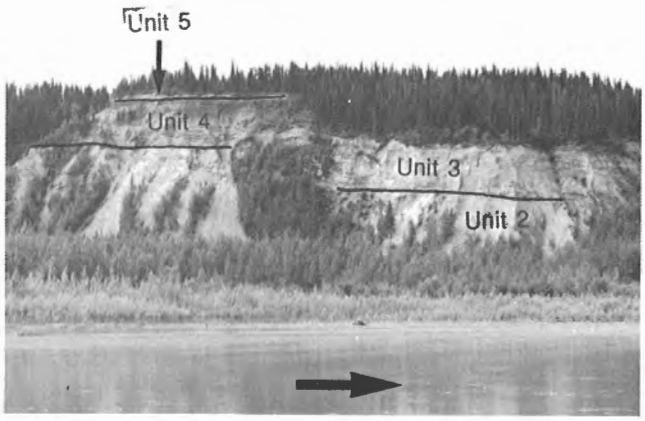

Figure 7. View looking west at Safety Pin Bend section. Units 2 and 5 are diamictons. Unit 3 is a generally fining upward sequence of gravels, sands, and diamictons. Unit 4 is a coarsening upward sequence from sands to gravels. The upper surface is 120 m above the river. Arrow indicates direction of river flow.

Safety Pin Bend section

The Safety Pin Bend section is located on the south bank of Pelly River in the Glenlyon map area (Fig. 1). It is within the limits of both the McConnell and the Reid glaciations. The section has a maximum height of 120 m and has been divided into 5 units, the upper 4 of which are shown in Figure 7. The top of the section forms the topography of the upland surface which is drumlinized.

Unit 1 consists of interstratified sands and gravels of indeterminate age. Unit 2 is a thick (17 m) diamicton with a sharp, approximately planar lower contact. It contains striated and faceted clasts whose lithologies are dominated by igneous and sedimentary rocks, indicating provenance to the north or northeast (Campbell, 1967, Map 1221A). Two pebble fabrics taken from the lower 1 m are strong (E_1 of 0.774 and 0.822) and have principal eigenvectors to the south at a low plunge (183° at 8° and 181° at 12°). Unit 2 is interpretated as a till; it indicates glacier flow from the north along MacMillan River valley (Fig. 1).

Unit 3 is a complex melange of diamictons, gravels, and sands (Fig. 8). Soft sediment deformation structures such as convolute bedding and loading structures are common. The unit generally fines upward. Unit 3 likely represents a deglacial sequence in a proximal lacustrine environment.

Figure 8. Unit 3 at Safety Pin Bend section; visible section is approximately 35 m high.

Unit 4 is a coarsening upward sequence from fine and medium sands to cobble gravels; it has a sharp lower contact. Unit 4 is interpreted as a glacial advance sequence.

Unit 5 is a diamicton that has a sharp, generally planar lower contact that truncates cross-strata in unit 4. It is dense and partially cemented by $CaCO_3$. Clasts are striated and

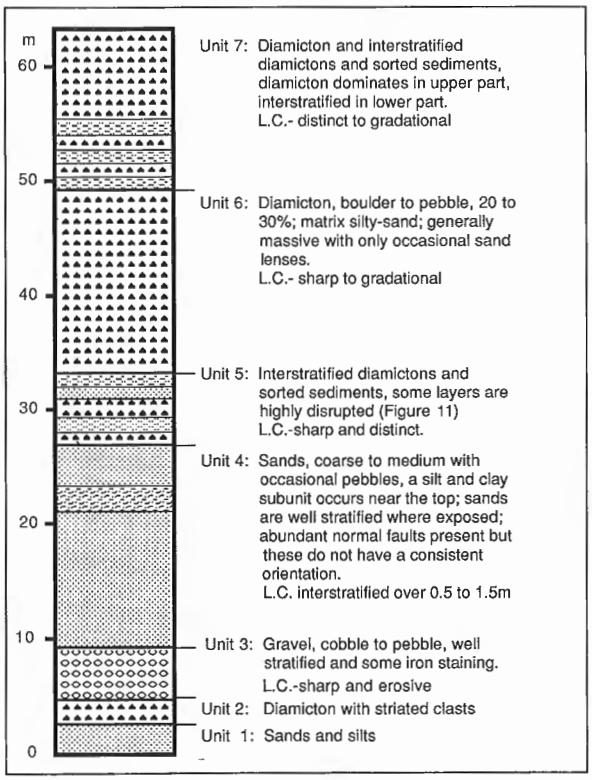

Figure 9. Stratigraphic column for section 26. Datum is river level.

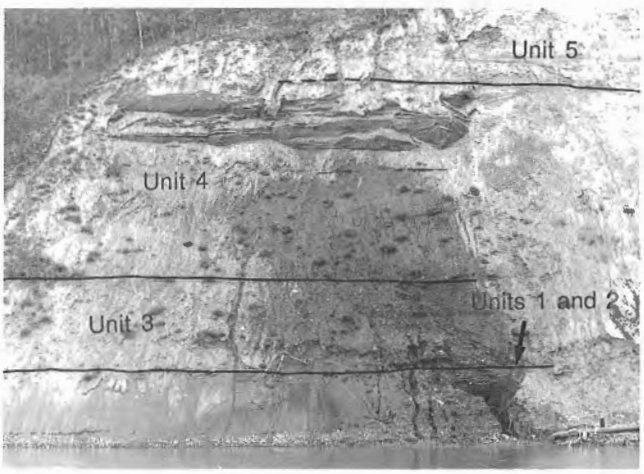

Figure 10. Downstream end of section 26. A brief description of the units is given in Figure 9. The only exposure of units 1 and 2 is in the excavation shown here. Detrital wood was found in the well exposed upper part of unit 4. Base of Unit 5 is 32 m above the river.

faceted and some are flat-iron shaped. Unit 5 is interpreted as a basal till. Drumlins immediately south of the section indiate glacier flow from the northeast (Campbell, 1967, Map 1222A). Pebble lithologies are similar to those of the lower till, thus indicating glacier flow from the MacMillan drainage.

Units 2 to 5 are interpreted as deposits of McConnell age on the basis of stratigraphic position and relationship to geomorphic features. The contact between units 3 and 4 are not thought to represent a major unconformity. Thus, the Safety Pin Bend section indicates two separate events of the McConnell Glaciation.

Section 26

Section 26 is located on the north bank of Pelly River in the Glenlyon map area (Fig. 1, 9, and 10). This section is also within the limits of both the McConnell and the Reid glaciations. The section is more than 1 km long and up to 70 m high. The top of the section forms the upland surface of the valley.

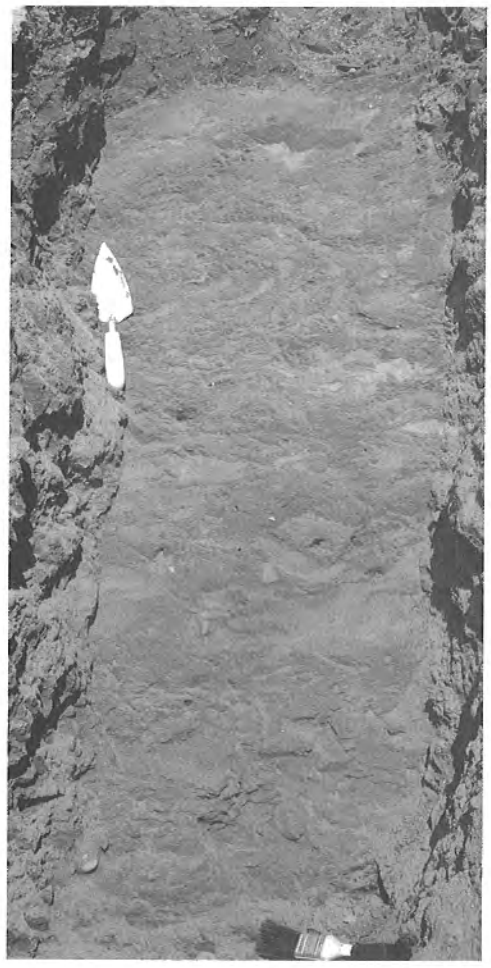

Figure 11. One of the disrupted layers in Unit 5 at section 26. Note the folding to the right of the trowel. Trowel is 25 cm long.

Unit 1 (sand and silt) and Unit 2 (diamicton) were only observed in an exposure at the base of the section (Fig. 10). Unit 2 (Fig. 9) is tentatively identified as a glacial deposit on the basis of striated and far travelled clasts, although these could be reworked from older glacial deposits.

Unit 3 (Fig. 9) is interpreted as a fluvial tractional deposit formed by a river similar to that of the present day Pelly, because of its similarity to Holocene alluvial terraces. The lower part of Unit 4 (Fig. 9) is interpreted as sediments in upper bar deposits, but the large thickness of the unit (18 m) indicates that the river underwent a long period of aggradation. The fine grained beds near the upper part of the unit (Fig. 9) extend across the section and indicate relatively quiet water conditions. Small pieces of wood were found in the upper 5 to 6 m of the unit (Fig. 10), which will help assign an age to the unit.

Unit 5 (Fig. 9) is interpreted as a proximal lacustrine sequence, deposited as the ice advanced into the area. The diamictons are sediment gravity flows, with the silts and sands being interflow deposits. When the ice overran the site it caused the extensive disruption evident in some areas of the unit (Fig. 11). Unit 6 is interpreted as a basal till, with Unit 7 being subsequent deglacial sediment (Fig. 9).

In the absence of firm dating control, the age of glaciation that deposited unit 2 is unknown. Units 3 and 4 are interpreted as interstadial deposits immediately preceding the McConnell based on the relatively conformable nature of the contact with the overlying glacial sediments. The ponding event represented in unit 4 was likely caused by ice advancing down MacMillan Valley. Units 5, 6, and 7 represent the McConnell Glaciation since they form the surface topography. Thus, section 26 could record two separate glacial advances and provide a maximum date for the McConnell event.

Figure 12. Large synclinal structure at section 11. The beds thicken into the depression indicating that melting was penecontemporaneous with deposition. Arrow indicates direction of river flow. Section is 40 m high.

QUATERNARY HISTORY AND CHRONOLOGY

Glacial deposits which correlate with a pre-Reid glaciation were not found at any of the sections. Sediments that contain organic layers showing evidence of having been overrun by the Cordilleran Ice Sheet during Reid Glaciation occur at the Bradens Canyon section. Above this are sediments that record deposition during Reid, McConnell, and Holocene time.

The Safety Pin Bend section has two tills separated by stratified sediment. The two tills are thought to be from the McConnell Glaciation, indicating two distinct advance phases.

Section 26 also records evidence for two glacial advances, but the timing of the older one is unknown. Ice advancing southwest from MacMillan River valley caused damming of the ancestral Pelly River. This advance could have deposited the lower till (unit 2) at Safety Pin Bend. This damming resulted in the deposition of a thick sequence of sands as well as some silts and clays. The upper part of these sands contains organic detritus that could provide a maximum date for McConnell Glaciation.

Two dates aid in the timing of deglaciation in the area. The oldest date comes from an area of ice stagnation topography (D1, Fig. 1). An accelerator ^{14}C date of 12 590±120 BP (TO-931) was obtained on *Pisidium* sp. from the base of a silty marl formed in the bottom of a depression. This date may be too old because of hard water effect, but the magnitude of possible error is difficult to estimate. The second date comes from a paraglacial fan (Ryder, 1971) deposit (D2, Fig. 1). Here wood, cf. *Salix* sp., was ^{14}C dated at 9140±540 BP (AECV-484C). It is unclear how closely this date approximates the time of deglaciation, but it does provide an estimate on the first occurrence of upland vegetation in the area.

LATE WISCONSINAN-HOLOCENE DEGLACIATION

Regional mapping in adjacent map areas indicates that the McConnell ice mass stagnated and downwasted in place (Jackson and Duk-Rodkin, in press); studies of sediments along Pelly River confirm this. Large expanses of glaciolacustrine sediments occur along the valley, as previously reported by Campbell (1967). They are usually associated with ice stagnation topography (Campbell, 1967, Map 1222A). These sediments are commonly tilted and faulted, indicating that the material was deposited onto or adjacent to ice. There are also extensive areas of faulted, folded, and contorted gravels that are also interpreted as ice contact deposits.

Section 11, on the north bank of Pelly River, displays both types of deposits. Figure 12 shows a large synclinal structure developed in gravels and filled with silts and sands, which suggests melting of a large ice block penecontemporaneous with deposition of the sediments. Downstream from the synclinal structure, the deposits consist of a series of normally graded beds in fining-upward sequences (Fig. 13). This trend culminates with rhythmites of clay and silt (marked by arrows in Fig. 13). All these sediments are interpreted as being deposited into standing water. This lacustrine sequence is capped by gravel outwash. The entire sequence is tilted and faulted (Fig. 13), indicating that it was deposited onto ice which melted some time after the lake drained and the gravels were deposited.

Figure 13. Downstream end of section 11. Here a sequence of normally graded beds fines upward to rhythmites of clay and silt (marked by arrows), which is capped by gravelly outwash. The whole sequence is tilted and faulted. Maximum height of section is 35 m.

DISCUSSION

The Bradens Canyon section is important because units 1 and 2 predate Reid Glaciation. Palynological and macrofossil studies of the organic sediments in unit 1 will be used to attempt to reconstruct the paleovegetation. This, combined with the presence of periglacial features, will be used to ascertain the paleoenvironment during deposition.

The Safety Pin Bend section records two advances of the Cordilleran Ice Sheet during McConnell Glaciation, both apparently originating from the MacMillan drainage. This is interesting in terms of paleo ice flow for the area. If the lower till corresponds to the ponding event recorded at section 26, it indicates diachronous advance of McConnell ice along the major valleys of the area. The fact that such good preservation is obtained at section 26 indicates low erosive power of ice in this part of the Pelly River valley. This could have been caused by ice from the MacMillan drainage deflecting ice from the Pelly drainage to the southwest.

Regional stagnation of the McConnell ice mass is suggested by abundant ice contact sediments. These are exemplified by sediments at section 11. Deglaciation occurred some time before 12 590±120 BP (TO-931) and uplands became vegetated in the area some time before 9140±540 BP (AECV-484C).

Further field work and paleoenvironmental studies of organic materials collected are planned.

ACKNOWLEDGMENTS

This study is part of a continuing Ph.D. research project investigating the Quaternary stratigraphy and sedimentology of the Glenlyon map area and adjacent areas. Field work is supported by the Geological Survey of Canada under the supervision of L.E. Jackson, Jr. Assistance in the field was provided by P. Beck and D. Lye. This manuscript benefited from critical review by O.L. Hughes and N. Catto.

REFERENCES

Bostock, H.S.
1966: Notes on glaciation in central Yukon Territory; Geological Survey of Canada, Paper 65-36, 18 p.

Campbell, R.B.
1967: Reconnaissance geology of Glenlyon map-area, Yukon Territory; Geological Survey of Canada, Memoir 352, 92 p., Map 1221A, 1222A.

Dawson, G.M.
1888: Report on an exploration in Yukon district, Northwest Territory, and adjacent portions of British Columbia; Geological Survey of Canada, Annual Report, 1887-1888, vol. 3, pt. B, 183 p.

Duk-Rodkin, A., Jackson, L.E., Jr., and Rodkin, O.
1986: A composite profile of the Cordilleran ice sheet during McConnell Glaciation, Glenlyon and Tay River map areas, Yukon Territory; in Current Research, Part B, Geological Survey of Canada, Paper 86-1B, p. 257-262.

Hughes, O.L.
1987: Quaternary Geology; in Guide book for Quaternary Research in Yukon, S.R. Morison and C.A.S. Smith (ed.); XII INQUA Congress, Ottawa, Canada; National Research Council of Canada, Ottawa, p. 12-16.

Hughes, O.L., Campbell, R.B., Muller, J., and Wheeler, J.D.
1969: Glacial limits and flow patterns, Yukon Territory south of 65°N latitude; Geological Survey of Canada, Paper 68-34, 9 p.

Jackson, L.E., Jr. and Duk-Rodkin, A.
Quaternary stratigraphy and paleoglaciology of the Selwyn Lobe of the Cordilleran ice sheet, east-central, Yukon; USGS circular (in press).

Klassen, R.W., Morison, S.R., and Duk-Rodkin, A.
1987: Surficial geology, Carmacks, Yukon Territory; Geological Survey of Canada, Map 9-1985, scale 1:250 000.

McConnell, R.G.
1903: The Macmillan River district, Yukon; Geological Survey of Canada, Annual Report, 1902, p. 22-38.

Ryder, J.M.
1971: The stratigraphy and morphology of paraglacial alluvial fans in south-central British Columbia; Canadian Journal of Earth Sciences, v. 8, p. 279-298.

Le séisme de mars 1988 de la rivière North Nahanni, T.N.-O. et ses répliques

M. Lamontagne[1], R.B. Horner[2], R.J. Wetmiller[1], D. Monsees[3] et A. Vonk[4]

Lamontagne, M., Horner, R.B., Wetmiller, R.J., Monsees, D., and Vonk, A., Le séisme de mars 1988 de la rivière North Nahanni, T.N.-O., et ses répliques; dans Recherches en cours, partie E, Commission géologique du Canada, Étude 89-1E, p. 265-268, 1989.

Résumé

La région de la rivière North Nahanni dans les T.N.-O. où s'étaient produits deux tremblements de terre majeurs en 1985 (magnitude 6,6 et 6,9), a été le site d'un autre séisme le 25 mars 1988 (magnitude 6,0). Quoique le séisme ait été ressenti sur une grande superficie, aucun dommage n'a été causé par cet événement. Un levé de terrain d'une durée de quatre jours, effectué peu après le choc principal a permis de localiser 150 répliques séismiques de magnitude inférieure à 3,0. Les hypocentres sont localisés à l'intérieur d'une région de 20 × 50 km, et à des profondeurs variant entre 4 et 10km. Le séisme principal représenterait la réactivation d'une faille en profondeur orientée nord-sud à pendage faible vers l'ouest, semblable aux failles de chevauchement de la région. Les répliques semblent se produire suivant plusieurs plans de faille d'orientations diverses, représentant la redistribution de contraintes suite à un grand séisme.

Abstract

The region of the North Nahanni River, N.W.T., where two large earthquakes occurred in 1985 (magnitude 6.6 and 6.9), was shaken by another event on 25 March, 1988 (magnitude 6.0). The shock was felt over a large area, but did not cause damage. A four day field survey was carried out shortly after the main shock, from which 150 aftershocks of magnitude less than 3.0 were located. The hypocentres are located within a 20km × 50km area, with depths varying between 4 and 10 km. The main shock may represent the reactivation of a fault at depth that strikes north-south and dips gently towards the west, similar to mapped thrust faults of the region. The aftershocks appear to be produced along many smaller fault planes of variable orientations, representative of the stress redistribution following a large shock.

[1] Division de la géophysique, 1 Place de l'Observatoire, Ottawa, K1A 0Y3.
[2] Division géoscientifique de la Cordillère et du Pacifique, C.P. 6000, 9860 West Saanich Road, Sidney, C.-B., V8L 4B2.
[3] Division de la géophysique, Observatoire géophysique d'E.M.R., Yellowknife, T.N.-O., X1A 2N1.
[4] Applied Geology Cooperative Student, Faculty of Science, University of Waterloo, Waterloo, Ontario.

INTRODUCTION

Depuis octobre 1985, trois séismes majeurs ont secoué la région de la rivière North Nahanni dans les Territoires du Nord-Ouest. Cette région fait partie de la marge orientale de la Cordillère où se sont produits plusieurs séismes majeurs dans le passé, tels ceux de 1918 (mag. 6), 1940 (mag. 6.2 et mag. 6.5) et 1955 (mag. 6.6). Le 5 octobre 1985, un tremblement de terre de magnitude 6.6 a secoué cette partie des monts Mackenzie (Horner et coll. (1987), Wetmiller et coll. 1988). Ce séisme a été ressenti sur une partie des Territoires du Nord-Ouest, au Yukon, en Alberta et en Colombie-Britannique. Heureusement, ce séisme n'a causé aucun dommage matériel, l'épicentre étant localisé à 150 km du village le plus proche (Fort Simpson). À environ 15 km de l'épicentre cependant, les vibrations ont causé une avalanche de roches d'un volume estimé à 5 millions de m^3. Moins de trois mois plus tard, le 23 décembre 1985, un séisme de magnitude 6.9 s'est produit à moins de quelques kilomètres de l'épicentre d'octobre. Le séisme de décembre a été ressenti sur une région légérement plus étendue que celle du premier choc. Cette fois cependant, seuls des éboulis mineurs furent constatés dans la région épicentrale. Les accélérations du sol produites par ce séisme ont été enregistrés par trois accélérographes installés à proximité de l'épicentre. Ces accélérations sont les plus fortes jamais enregistrées au monde. Tout comme lors du premier séisme, aucun décrochement de surface ne fut observé.

Plusieurs études ont été réalisées sur les séismes majeurs de 1985, sur leurs répliques séismiques, ainsi que sur leurs effets. Ainsi, les deux chocs principaux et leurs répliques enregistrés sur le terrain ont été décrits dans Wetmiller et coll.(1988). Les mouvements forts, dont un a atteint 2g, ont été décrits par Weichert et coll. (1986), et leurs implications analysées par Wetmiller et coll. (1987). L'avalanche de roches a été décrite par Evans et coll. (1987). La géologie structurale telle que révélée par un levé de sismique réflexion a été analysée dans Lamontagne et Milkereit (1988). L'anisotropie et la polarization des ondes séismiques, indicatives des contraintes, sont analysées par Buchbinder (1988). Finalement, un programme de terrain mené en septembre 1986 et les répliques enregistrées par le réseau séismographique canadien est décrit dans Horner et coll. (1988).

Les trois levés de terrain (octobre 1985, janvier et septembre 1986), ont permis de définir la zone active et de mieux comprendre les relations unissant la séismicité et la géologie structurale dans cette région. Les séismes de la Nahanni se sont produits dans la plaine Mackenzie, qui fait partie de la marge est des monts Mackenzie. Les chocs principaux et leurs répliques ne se sont pas produits sur l'une des nombreuses failles de chevauchement cartographiées dans la région. Les séismes principaux se sont probablement produits le long d'une faille de chevauchement en profondeur, dont un anticlinal pourrait représenter la signature en surface. Quant au régime structural actif, il semble que les répliques séismiques de la Nahanni se produisent suivant de nombreux plans de faille. En effet, les répliques séismiques en dépit de leur concentration dans une zone d'environ 50km × 20km montrent des mécanismes au foyer variables. Cette tendance, d'ailleurs remarquée dans d'autres séquences de répliques ailleurs dans le monde, illustre bien la complexité des mécanismes de fracturation après un séisme majeur.

LE SÉISME DU 25 MARS 1988

L'épicentre du séisme du 25 mars 1988 (magnitude 6.0) est localisé à moins de 5 km de ceux des séismes de 1985. Quoique plus faible que les séismes de 1985, celui de mars a été ressenti dans les territoires du Nord-Ouest, au Yukon, en Colombie-Britannique et en Alberta. Cet événement s'inscrit dans une suite de répliques de magnitude supérieure à 5.0 enregistrés depuis octobre 1985. Le tremblement de terre fut enregistré sur tout le réseau séismographique canadien et sur de nombreuses stations internationales. Le mécanisme au foyer du choc principal est semblable aux mécanismes des deux grands séismes de 1985, soit un mouvement inverse le long d'un plan de faille orientée nord-sud. Des deux plans nodaux du mécanisme, le plan à faible pendage vers l'ouest correspond le mieux à notre connaissance de la géologie structurale de la région.

LE LEVÉE DE TERRAIN

Immédiatement après le séisme, une équipe de terrain a été mise sur pied. Des séismologues de la Division de la géophysique basés à Ottawa et à Yellowknife, et de la Division géoscientifique de la Cordillère et du Pacifique basés à Sidney, se sont rendus à Fort Simpson, la localité la plus rapproché de l'épicentre. Tout comme lors des trois levés précédents, les buts étaient d'observer les effets dus au séisme dans la région épicentrale, de localiser précisément les répliques dans la zone active, et finalement de récupérer les films des accélérographes installés dans la région épicentrale. Ces travaux ont été effectués par hélicoptère, en utilisant Fort Simpson comme quartier général des opérations. Malgré la rapidité avec laquelle l'équipe de terrain et son matériel ont pu atteindre Fort Simpson, plusieurs jours se sont passé avant qu'un vol de reconnaissance ait pu être effectué au-dessus de la région épicentrale. Entre temps, plusieurs chutes de neige avaient pu masquer les évidences d'éboulis le long des pentes abruptes. Nous avons cependant la conviction qu'aucune avalanche de roches de dimensions supérieures à une centaine de m^2 auraient pu échapper à notre attention, compte tenu de notre connaissance antérieure de la région épicentrale.

Lors de ce levé de terrain, jusquà 8 appareils analogiques et 5 appareils numériques ont été installés. Le réseau temporaire a donc été comporté jusqu'à huit stations (fig. 1). Pouvant enregistrer pendant 24 heures consécutives, les appareils analogiques permettent d'obtenir une couverture complète de la zone d'activité. Les appareils numériques à trois composantes, quant à eux, permettent de déterminer très précisément les temps d'arrivée des ondes P et S, avec cependant une capacité d'enregistrement limité à environ 6 heures. Le choix des sites s'est effectué en essayant d'entourer la région active avec le réseau de séismographes. Naturellement, l'accessibilité par hélicoptère constituait aussi un facteur déterminant dans ce choix. Malgré la température

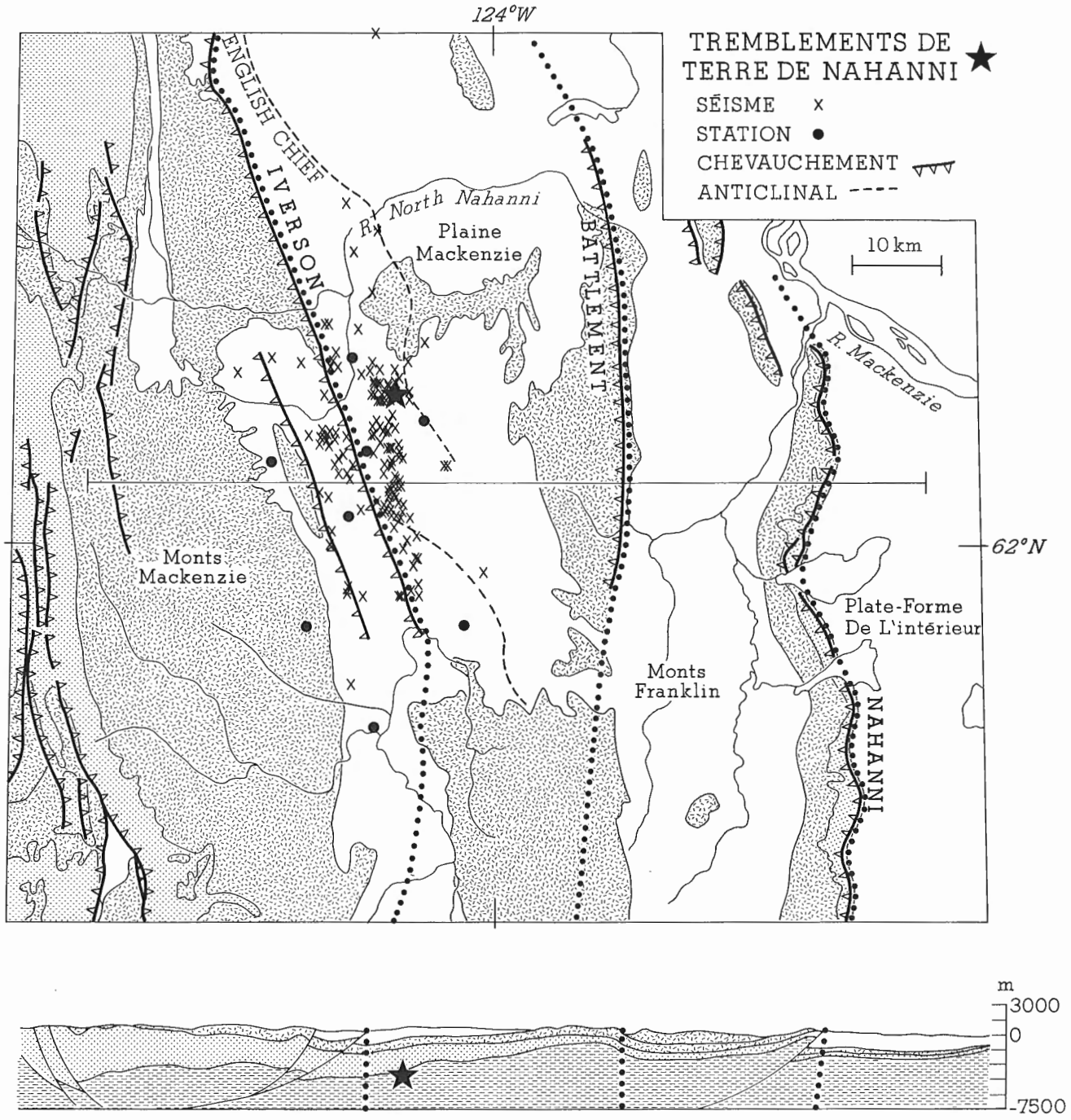

Figure 1. Résultats du levé de terrain suivant le séisme du 25 mars 1988 de magnitude 6.0. Les séismes d'octobre et de décembre 1985 ainsi que celui de mars 1988, ont été localisés avec le réseau séismographique national. D'après ces données, leurs épicentres sont situés à proximité les uns des autres. La carte indique la position des répliques séismiques localisées lors du levé d'avril 1988 et les stations utilisées pour l'enregistrement des répliques. Deux concentrations sont apparentes. La première, dans la partie est de la zone active,regroupe la majorité des épicentres et est d'orientation nord-sud. L'autre concentration est située à l'ouest du chevauchement Iverson. Les unités géologiques sont regroupées en roches sédimentaires friables en blanc, et en carbonates en pointillé.
La figure du bas représente une coupe géologique est-ouest indiquée sur la figure du haut. La position présumée des séismes majeurs y est indiquée.

parfois peu clémente, quatre jours complets d'enregistrement ont été obtenus lors du levé effectué du 2 au 9 avril 1988.

La densité des stations a permis la localisation des foyers de plus de 150 événements séismiques (fig. 1). Un minimum de quatre stations et de cinq phases ont été utilisés pour localiser les foyers séismiques. Un modèle homogène de vitesse des ondes P de 6.2 km/s et des ondes S de 3.57 km/s a été utilisé dans ces calculs. Des corrections de temps ont été appliquées pour corriger les dérives instrumentales des horloges internes.

Les épicentres sont contenus en deux groupes, à l'intérieur d'un rectangle d'environ 50km x 30 km allongé suivant un axe nord-sud. La partie est de ce rectangle est beaucoup plus active, puisqu'elle regroupe plus des trois quarts des événements enregistrés. L'orientation principalement nord-sud de cette concentration est semblable à celles obtenues lors des levés de janvier et septembre 1986. Elle diffère toutefois du levé d'octobre 1985 où la partie nord était la plus active. La concentration d'activité plus à l'ouest, remarqué en janvier et septembre 1986, pourrait représenter la réactivation d'une faille conjuguée de la faille principale. La distribution de l'activité telle que représentée sur la figure 1 est probablement assez juste puisque l'examen des enregistrements analogiques des stations localisées sur le pourtour du réseau n'a révélé que quelques événements isolés à l'extérieur du réseau.

Les foyers séismiques sont contenus majoritairement entre 5 et 9 km de profondeur, donc sous les failles de chevauchement visibles en surface. D'après les informations géologiques dont nous disposons, l'interface entre les roches sédimentaires et cristallines est à environ 8 ou 9 km de profondeur (voir coupe de la figure 1), alors que l'épaisseur des carbonates paléozoïque ne serait que de quelques kilomètres tout au plus. L'activité séismique semble donc localisée surtout à l'intérieur des roches sédimentaires et métasédimentaires du Protérozoïque. Il demeure toutefois extrêmement difficile de connaître exactement les paramètres géologiques existants à ces profondeurs.

Une analyse des longueurs de coda sur les micro-séismes a permis la détermination des magnitudes, et ceci même pour les séismes de magnitude inférieure à 3.0. Pour les données du levé de septembre 1986, une relation mathématique avait été établie entre les longueurs de coda enregistrés par une station du réseau temporaire et la station permanente de Yellowknife (Wetmiller et Plouffe, 1987). La station du réseau temporaire, réoccupée lors du levé d'avril 1988, a donc permis de réutiliser la relation établie et de calculer les valeurs de magnitude pour la majorité des 150 événements localisés. Les valeurs de magnitude varient entre 0.0 et 3.0, donc bien au-dessous du seuil de détection du réseau séismographique canadien permanent (mag. 3.5).

Le levé de terrain a aussi permis d'effectuer l'entretien des accélérographes installés de façon permanente dans la région épicentrale. Malheureusement, un des sites a été trouvé hors d'usage par suite de l'attaque d'un ours, alors que l'autre ne pourra être récupéré que plus tard.

INTERPRÉTATION PRÉLIMINAIRE ET TRAVAUX À VENIR

Plusieurs années après le premier événement de magnitude 6.6 d'octobre 1985,la région de la rivière North Nahanni continue d'être le site d'une activité séismique intense. Il est probable que plusieurs autres répliques seront enregistrées en provenance de cette région dans les années à venir. L'activité des répliques semble être consignée dans un rectangle d'environ 50km × 20km avec deux zones d'activité distinctes. Des mécanismes complexes de faillage semblent intervenir dans la production des répliques. Sous peu, les positions relatives des foyers séismiques seront analysés afin de mettre en évidence les relations avec la géologie structurale. Les mécanismes au foyer devraient aussi permettre de mieux définir ces paramètres. Finalement, la localisation des plus fortes répliques enregistrées par le réseau national permettra d'étudier la distribution spatiale et temporelle des événements précédant et suivant le séisme du 25 mars 1988.

REMERCIEMENTS

Les auteurs tiennent à remercier l'équipe technique des laboratoires de la C.G.C., et en particulier M. R. Schieman qui a participé aux travaux de terrain.

BIBLIOGRAPHIE

Buchbinder, G.G.R.
1988: Shear-wave splitting and anisotropy from the aftershocks of the Nahanni, N.W.T. earthquakes, Soumis au Journal of Geophys. Research.

Evans, S.G., J.D. Aiten, R.J. Wetmiller, et R.B. Horner
1987: A rock avalanche triggered by the october 1985 North Nahanni earthquake, District of Mackenzie, N.W.T., J. Can. Sci. Terre, 24, 176-184.

Horner, R.B., M. Lamontagne et R.J. Wetmiller
1987: Rock and Roll in the N.W.T.,the 1985 Nahanni earthquakes. Geos, 16, no. 2, pp. 3-6. (Disponible en français).

Horner, R.B., R.J. Wetmiller, M. Lamontagne et M. Plouffe
1988: A fault model for the Nahanni earthquakes from aftershock studies. (En préparation).

Lamontagne M. et B. Milkereit
1988: Reprocessing of industry data of the North Nahanni region: Implications for the interpretation of the Nahanni earthquake sequence. Dossier public de la C.G.C. 1728.

Wetmiller, R.J. et M. Plouffe
1988: Duration magnitudes for Nahanni earthquakes recorded by field networks: October 1985; January, 1986; September, 1986. Dossier public de la C.G.C. 1512.

Wetmiller, R.J., P.W. Basham, D.H. Weichert, et S.G. Evans
1987: The 1985 Nahanni earthquakes: problems for seismic hazard estimates in the northeast Canadian Cordillera, dans Communications de la cinquième conférence canadienne sur le génie sismique, Ottawa, juillet 1987 A.A. Balkema, Rotterdams, Pays-Bas, 695-703.

Wetmiller R.J., R.B. Horner, H.S. Hasegawa, R.G. North, M. Lamontagne, D.H. Weichert, et S.G. Evans
1988: An analysis of the 1985 Nahanni earthquakes. Bull. Seismological Soc. of America, 78, No. 2, pp. 590-616.

Earthquakes in western Canada from January 1987 to September 1988

R.B. Horner and R. Kolinsky[1]
Cordilleran and Pacific Geoscience Division, Sidney

Horner, R.B. and Kolinsky, R., Earthquakes in western Canada from January 1987 to September 1988; in Current Research, Part E, Geological Survey of Canada, Paper 89-1E, p. 269-273, 1989.

Abstract

During 1987, more than 1200 earthquakes occurred in western Canada and adjacent areas of the United States. Included are 92 earthquakes with magnitude 4.0 or greater. Eighteen earthquakes were reported felt in western Canada in 1987; 11 have been reported felt in 1988, to the end of September.

Although most of the seismicity continued to occur along the active tectonic zones off the British Columbia coast, significant activity was also observed in the Gulf of Alaska, southeastern Alaska near the Canadian border, the northern Yukon Territory and in the Nahanni region of the Mackenzie Mountains, Northwest Territories. A sequence that began in the Gulf of Alaska on 17 November, 1987, has included one magnitude 6.9 and two magnitude 7.6 earthquakes. In Canada, a magnitude 6.0 earthquake occurred in the Nahanni region on 25 March, 1988. Magnitude 5 events have occurred in the Beaufort Sea and offshore of Vancouver Island.

Résumé

En 1987, plus de 1200 tremblements de terre se sont produits dans l'Ouest canadien et les régions voisines des États-Unis, dont 92 séismes d'amplitude 4,0 ou plus. Dix-huit tremblements de terre ont été signalés dans l'ouest du Canada en 1987 et 11 jusqu'à la fin de septembre de 1988.

Même si les séismes étaient encore concentrés le long des zones tectoniques actives au large de la côte de la Colombie-Britannique, une activité importante a été observée dans le golfe de l'Alaska, dans le sud-est de l'Alaska près de la frontière canadienne, dans le nord du Yukon et dans la région de Nahanni dans les monts Mackenzie, Territoires du Nord-Ouest. Une séquence, qui a débuté dans le golfe de l'Alaska le 17 novembre 1987, renfermait un séisme de magnitude 6,9 et deux de magnitude 7,6. Au Canada, un tremblement de terre d'amplitude 6,2 s'est produit dans la région de Nahanni le 25 mars 1988. Des événements de magnitude 5 se sont produits dans la mer de Beaufort et au large de l'île de Vancouver.

[1] 1438 Mt. Newton X-Rd., Saanichton, B.C. V0S 1M0

INTRODUCTION

Canadian earthquakes are routinely studied by seismologists in the Cordilleran and Pacific Geoscience and the Geophysics divisions of the Geological Survey of Canada. The research centres for the two groups are located at the Pacific Geoscience Centre in Sidney, B.C., and in Ottawa. Earthquake data are routinely published by the Geophysics Division in the form of bi-annual catalogues (annual catalogues prior to 1985) and quarterly reports. A list of catalogues can be found in Drysdale and Horner (1987). All earthquake data are also maintained in a National database at the Geophysics Division.

This paper briefly describes the seismicity in western Canada during 1987, with preliminary results to September, 1988. A more complete discussion will be included in the next catalogue, scheduled for 1989.

SUMMARY OF SEISMIC ACTIVITY FOR 1987

Epicentral and magnitude parameters were determined for 1201 earthquakes in western Canada and adjacent regions of the United States in 1987 (Fig. 1). The largest earthquake, magnitude 7.6, occurred on 30 November as part of an unprecedented sequence in the Gulf of Alaska. The sequence began on 17 November with a magnitude 6.9 event and included 61 other earthquakes with magnitude 4.0 or

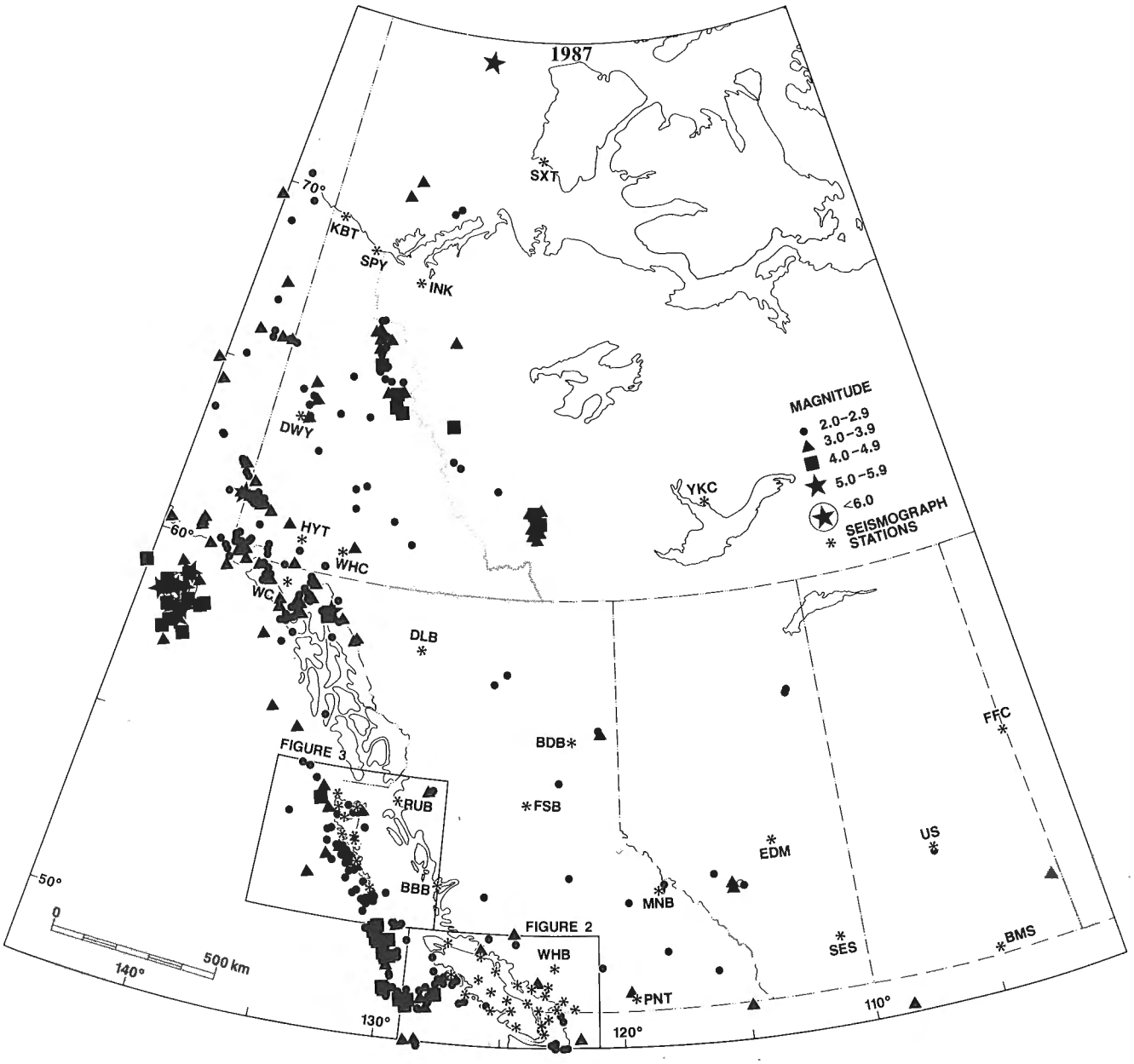

Figure 1. Earthquake epicentres in western Canada and adjacent regions of the United States in 1987 having magnitude 2.0 or greater. Seismograph stations operating in 1987 are also shown. Details of the seismograph network are in Munro et al. (1988).

greater to the end of 1987. In Canada, the largest earthquake occurred in the Beaufort Sea on 30 March, with magnitude 5.5.

Eighteen earthquakes were reported felt during 1987 (Appendix). The most affected region was the southern Yukon Territory where seven earthquakes were felt. Six of these occurred in a 17 day period from 14-30 November. Maximum intensities of V were reported in Whitehorse (WHC in Fig. 1) for the largest Gulf of Alaska earthquake on 30 November. The most widely felt earthquake outside of this region, magnitude 3.9, occurred near Salmon Inlet in the southern Coast Mountains of British Columbia on April 8 (east of SHB in Fig. 2).

Besides the Gulf of Alaska, significant seismicity continued to be observed on the active tectonic zones off the British Columbia coast, in the St. Elias region of the southwestern Yukon Territory and northwestern British Columbia, in the Richardson Mountains in the northern Yukon Territory (south of INK in Fig. 1), and in the Nahanni aftershock zone in the Mackenzie Mountains in the Northwest Territories (west of YKC). The magnitude 5.3 earthquake on 14 November on the east side of Lynn Canal (south of WHC) is the largest ever located in that region of the Coast Mountains. Continuing seismicity was also observed near the IMC potash mine in eastern Saskatchewan; and in the oil and gas fields near Rocky Mountain House, Alberta (southwest of EDM), and Fort St. John, B.C. (east of BDB).

Seismicity in the Vancouver Island - lower mainland and Queen Charlotte Islands areas is shown in more detail in Figures 2 and 3. The closer seismograph spacing allows lower detection thresholds and provides more accurate hypocentral determinations. Four of the seismographs in the Queen Charlotte Islands area (BNAB, MSTB, NDB and PCB), funded by the OERD and FGP programs, were installed in November and December 1987. Only minor seismicity was observed during the year. The largest events occurred offshore and included a magnitude 4.7 earthquake southwest of EDB (Fig. 2) on 7 December, and a magnitude 4.5 earthquake west of LIB (Fig. 3) on 3 July. The seismicity in Hecate Strait and on Graham Island has only been observed the last few years because of the increased number of seismograph stations.

SUMMARY OF SEISMIC ACTIVITY TO SEPTEMBER 1988

Eleven earthquakes were reported to have been felt in western Canada up to September 1988 (Appendix). The earthquake sequence in the Gulf of Alaska has continued and included another magnitude 7.6 event on 6 March. The Nahanni region experienced its third major earthquake since October 1985 (Wetmiller et al., 1988), with a magnitude 6.0 event on March 25. Two large aftershocks with magnitudes of 5.2 and 4.9, occurred on 22 May and 24 June, respectively. A magnitude 5 earthquake also occurred west of Vancouver Island on 26 May.

Preliminary hypocentral determinations in the Vancouver Island - lower mainland region to August 1988, are shown in Figure 4. Minor earthquakes were felt in the Victoria area on September 15 and 26 (Appendix).

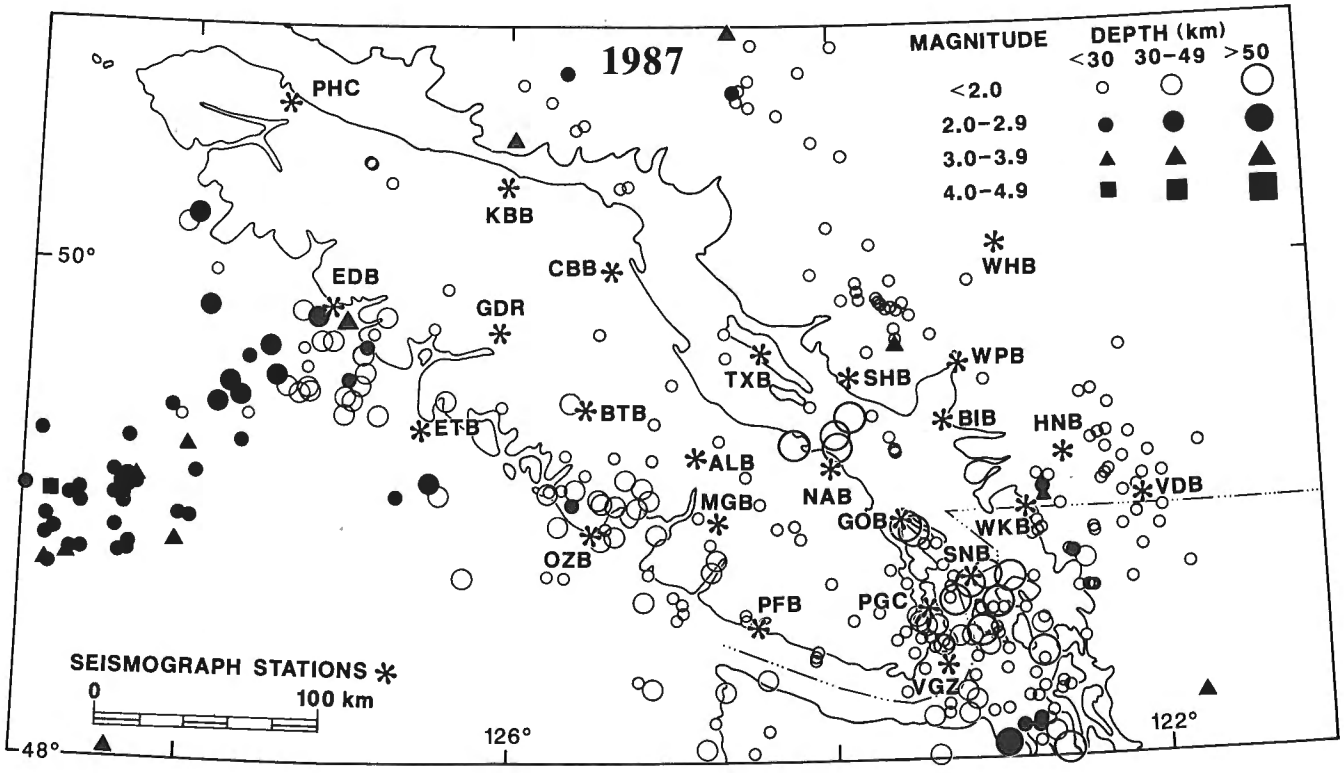

Figure 2. Earthquake hypocentres and seismograph stations in the Vancouver Island - lower mainland region of British Columbia in 1987. Most of the seismograph signals, excluding those from stations on northern Vancouver Island, are telemetered to the Pacific Geoscience Centre (PGC).

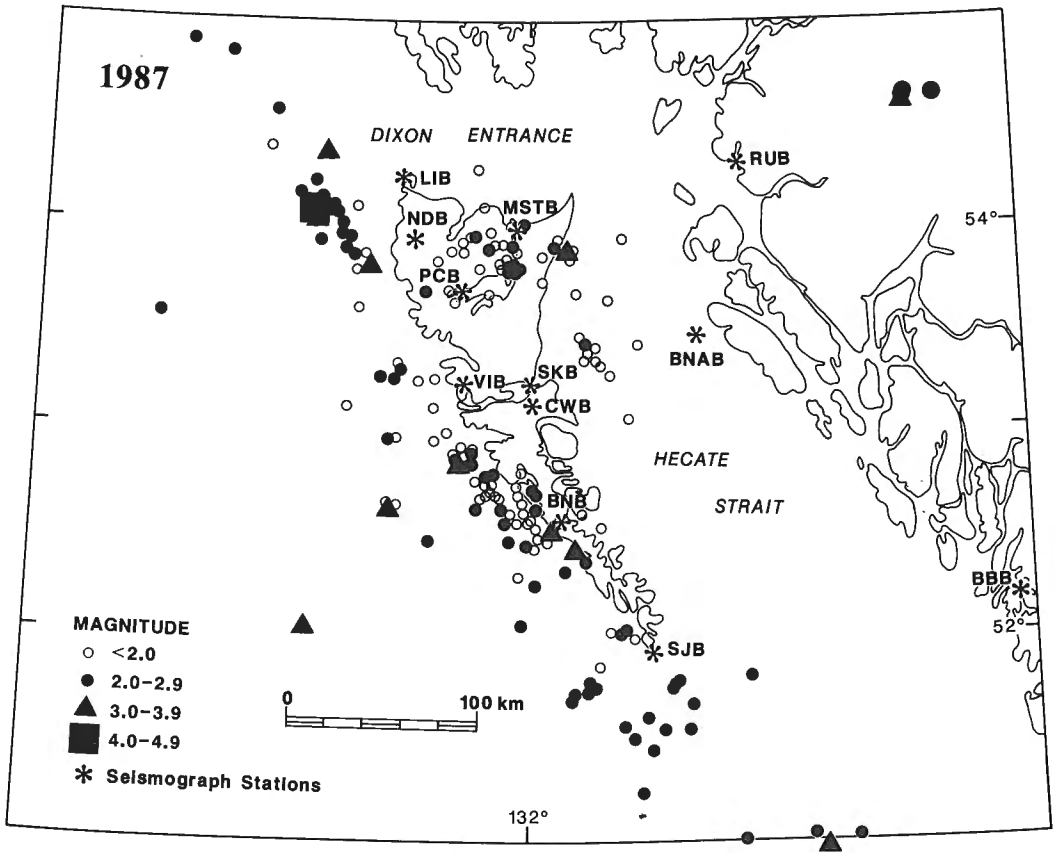

Figure 3. Earthquake epicentres and seismograph stations in the Queen Charlotte Islands region of British Columbia in 1987.

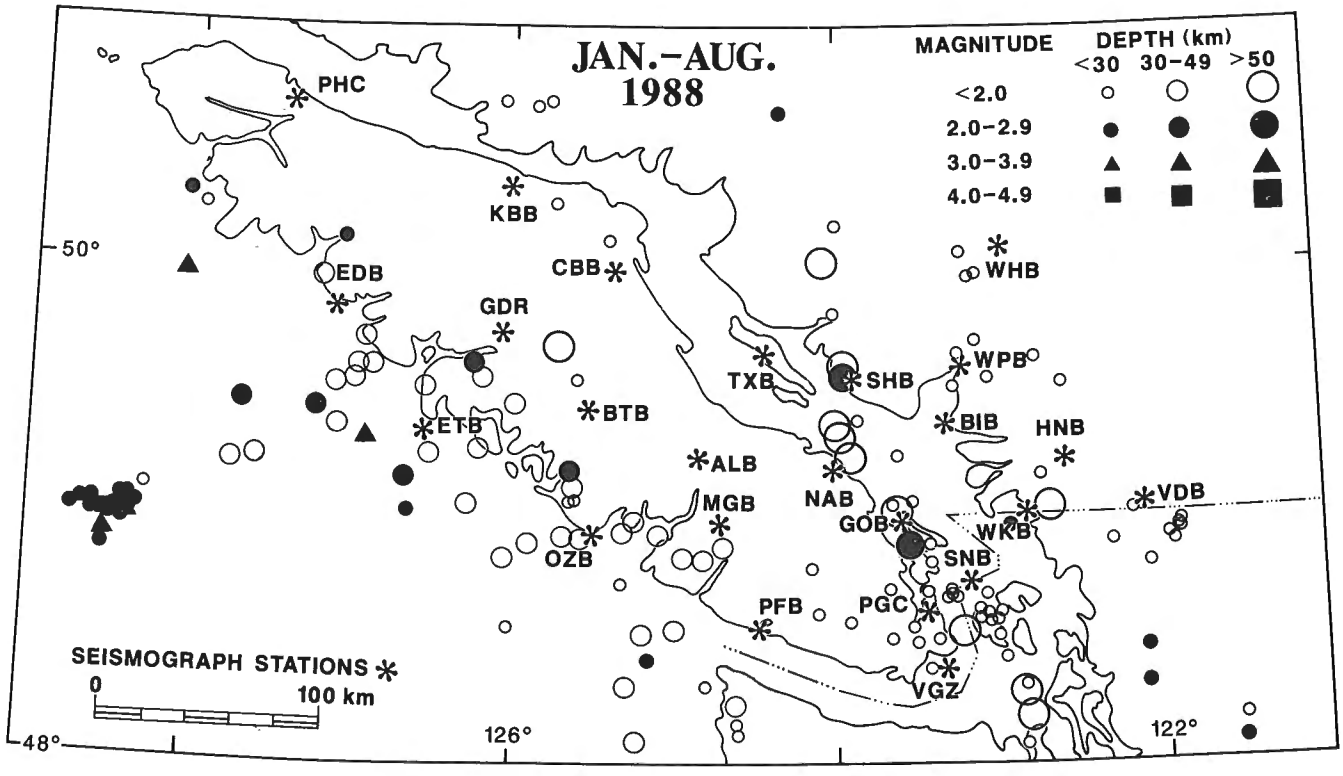

Figure 4. Preliminary earthquake hypocentres in the Vancouver Island - lower mainland region of British Columbia from January to August, 1988.

ACKNOWLEDGMENTS

M. Gregory and M. Wilde assist with data analysis. R. Baldwin provides computer support. We are also very grateful for the support of our colleagues with the Geophysics Division in Ottawa; in particular J. Drysdale, M. Lamontagne and R. Wetmiller. We also thank the USGS in Menlo Park, CA; the University of Washington in Seattle; and the Alaska Tsunami Warning Centre at Palmer, AK, for routinely providing their seismograph data.

REFERENCES

Drysdale, J.A. and Horner, R.B.
1987: Canadian earthquakes - 1984; Geological Survey of Canada, Paper 87-19, 44 p.

Munro, P.S., Halliday, R.J., Shannon, W.E., and Schieman, D.R.J.
1988: Canadian seismograph operations - 1986; Geological Survey of Canada, Paper 88-16, 76 p.

Wetmiller, R.J., Horner, R.B., Hasegawa, H.S., North, R.G., Lamontagne, M., Weichert, D.H., and Evans, S.G.
1988: An analysis of the 1985 Nahanni earthquakes; Bulletin of the Seismological Society of America, v. 78, p. 590-616.

APPENDIX

Summary of earthquakes reported felt in western Canada from January 1987 to September 1988

Date and Time (UT)	Magnitude	Location and Remarks
12 Jan 87 12:17	3.5 ML	Penticton, B.C. Felt from Vernon to Osoyoos.
08 Apr 87 14:33	3.9 ML	Salmon Inlet, B.C. Felt on both sides of the Strait of Georgia from Vancouver to Garibaldi and Courtenay to Nanaimo. Maximum intensity IV at Squamish and Lantzville.
14 Apr 87 10:52	3.1 ML	Coast Mountains, B.C. Felt at Terrace.
07 Jun 87 08:55	3.8 ML	West coast Vancouver Island. Felt on Nootka Island and at Port Eliza, Woss Camp and Port McNeill.
03 Jul 87 01:32	4.5 ML	Queen Charlotte Islands. Felt on Langara Island.
30 Jul 87 14:33	3.3 ML	Eastern Saskatchewan near Esterhazy. Felt at the IMC K2 potash mine.
10 Aug 87 18:43	3.8 ML	Southern Yukon Territory. Felt III-IV at Whitehorse. Also felt at Takini Hot Springs and about 20 km south of Whitehorse.
16 Sep 87 20:10	3.2 ML	Lower mainland, B.C. Felt IV in the White Rock-Cloverdale-Langley area and at Blaine, Washington.
18 Sep 87 18:50	2.3 ML	Lower mainland, B.C. Felt at White Rock and Langley.
22 Oct 87 04:34	3.1 MN	Eastern Saskatchewan near Esterhazy. Felt at the IMC K2 potash mine.
12 Nov 87 05:30	3.4 ML	Northeastern B.C. Felt in the Fort St. John area.
14 Nov 87 15:48	5.3 mb	Lynn Canal, Alaska. Felt at Haines (V) and (IV) at Douglas, Juneau and Skagway, Alaska. Felt strongly at Atlin and Whitehorse.
14 Nov 87 18:38	4.0 mb	Lynn Canal, Alaska. Felt at Whitehorse.
17 Nov 87 08:46	6.9 Ms	Gulf of Alaska. Felt widely in southern Alaska, the southwestern Yukon and northwestern B.C. Maximum observed intensity V.
17 Nov 87 13:26	4.9 mb	Lynn Canal, Alaska. Felt at Haines (V), Skagway (IV), and Juneau (III). Also felt at Atlin and Whitehorse.
23 Nov 87 07:18	5.7 mb	Eastern Alaska. Felt in Alaska at Chitina and Copper Center (IV), and Anchorage and Yakutat. Felt in the southwest Yukon Territory from Beaver Creek to Haines Junction.
30 Nov 87 19:23	7.6 Ms	Gulf of Alaska. Damage (VI) at Yakutat from earthquake and tsunami. Felt widely in Alaska, the southwestern Yukon and northwestern B.C. Some buildings were evacuated in Whitehorse.
19 Dec 87 20:30	2.7 ML	Southern Vancouver Island. Felt in the Victoria area.
07 Jan 88 09:57	3.2 MN	Eastern Saskatchewan near Esterhazy. Felt at the IMC K2 potash mine.
06 Mar 88 22:35	7.6 Ms	Gulf of Alaska. Some damage to ships in the epicentral region. Felt widely in Alaska, southwestern Yukon and northwestern B.C. Maximum intensity V.
25 Mar 88 19:36	6.0 Ms	Nahanni region of the Mackenzie Mountains. Felt strongly at Fort Simpson, Wrigley, Nahanni Butte and Fort Liard. Also felt in the Yukon, northern B.C. and northern Alberta.
05 Apr 88 16:49	3.8 ML	Queen Charlotte Islands. Felt on Langara Island.
29 Apr 88 01:45	3.5 ML	Brooks Peninsula, Vancouver Island. Felt at Port Alice and Port Hardy.
22 May 88 19:18	5.2 mb	Nahanni region, N.W.T. Felt at Fort Simpson.
26 May 88 19:01	5.1 mb	West of Vancouver Island. Felt at Port McNeill.
06 Jun 88 15:01	5.0 mb	Southeastern Alaska. Felt (IV) at Elfin Cove, Haines, Juneau, Skagway and Yakutat. Also felt at Windy Craggy, B.C., and Whitehorse.
24 Jun 88 15:37	4.9 mb	Nahanni region. Felt at Fort Simpson.
15 Sep 88 06:18	2.2 ML	Southern Vancouver Island. Felt in Victoria and on Saanich Peninsula.
26 Sep 88 00:28	2.9 ML	Near Anacortes, Washington. Felt mildly in the Victoria area.

Low-level seismic monitoring at the Windy Craggy deposit in northwestern British Columbia

R.B. Horner
Cordilleran and Pacific Geoscience Division, Sidney

Horner, R.B., Low-level seismic monitoring at the Windy Craggy deposit in northwestern British Columbia; in Current Research, Part E, Geological Survey of Canada, Paper 89-1E, p. 275-278, 1989.

Abstract

The Windy Craggy deposit in the Saint Elias Mountains is in an area of extreme seismic hazard. The region is bounded by the Fairweather fault to the west, the Denali fault to the east and north, and a significant seismicity trend in the Glacier Bay area to the south. To improve the regional seismograph coverage and monitor low-level seismicity near the mine, a seismograph was operated at Windy Craggy from 30 June to 3 August 1987 and again since 10 June 1988. During the 1987 period, 27 earthquakes were located within 200 km of Windy Craggy; the closest was within 15 km. Magnitudes ranged from about 1.0 to 2.5.

Résumé

Le gisement d'un Windy Craggy situé dans le massif de Saint-Élie est une région d'extrême risque sismique. La région est limitée par la faille de Fairweather à l'ouest, par la faille de Denali à l'est et au nord, et par une importante ligne de sismicité dans la région de Glacier Bay au sud. Pour améliorer la couverture sismographique régionale et surveiller la sismicité de faible niveau à proximité de la mine on a utilisé à Windy Craggy un sismographe du 30 juin au 3 août 1987 et après le 10 juin 1988. Pendant la période d'observation de 1987, on a localisé 27 séismes à moins de 200 km de Windy Craggy; le plus proche a eu lieu à 15 km de cette localité. Les magnitudes étaient de l'ordre de 1,0 à 2,5.

INTRODUCTION

The Windy Craggy deposit in northwestern British Columbia lies in an extremely complex and active tectonic zone caused by the interaction of the North American and Pacific plates (Perez and Jacob, 1980; Plafker et al., 1978). The plate interaction is reflected by a history of large and damaging earthquakes (Fig. 1). Over the last century several major earthquakes within about 150 km of Windy Craggy have ruptured most of the plate boundary. The list includes three earthquakes near magnitude 8 in the Yakutat Bay-Icy Bay area in 1899, and a magnitude 7.9 earthquake on the Fair-

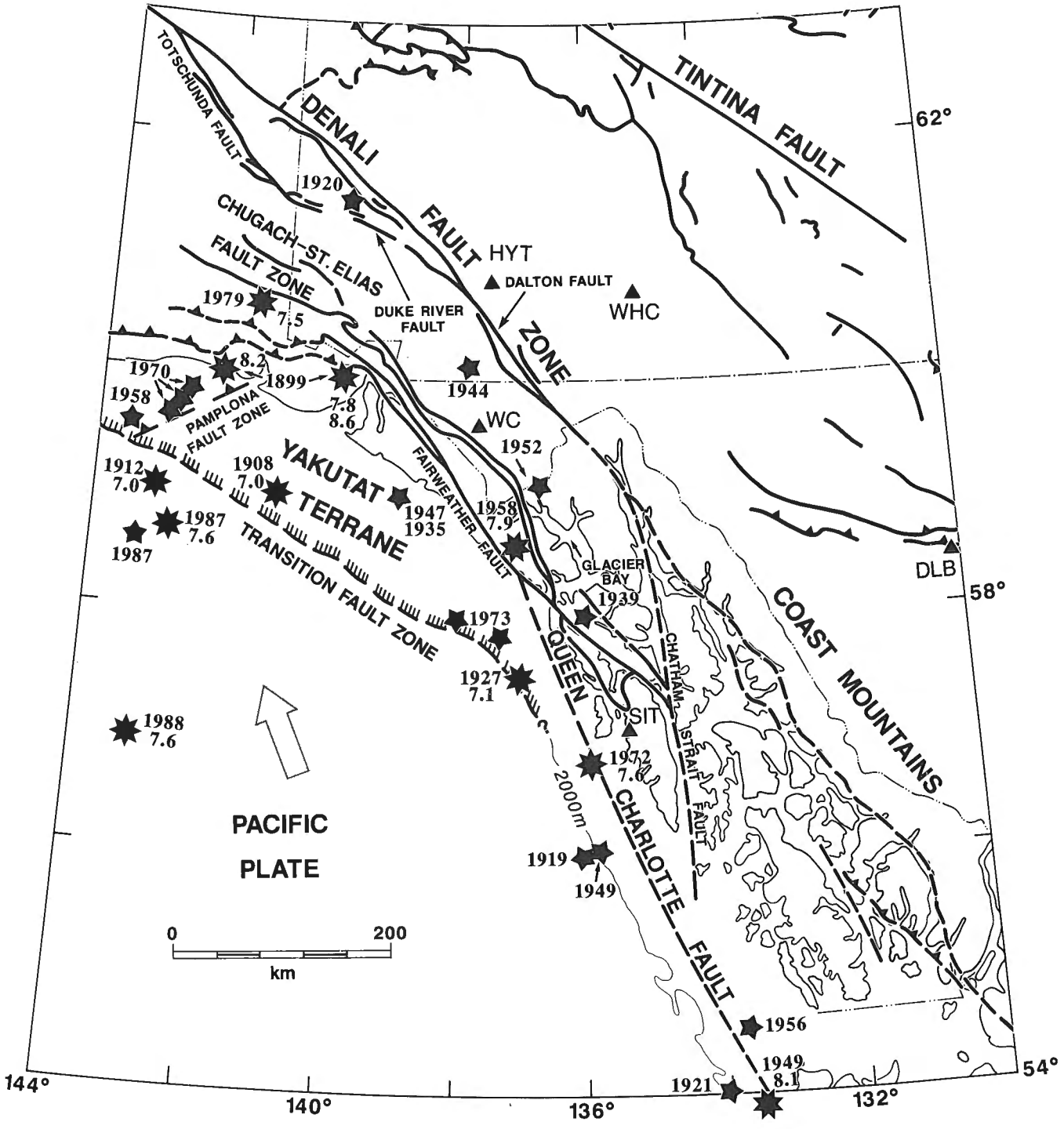

Figure 1. Historical seismicity, magnitude 6, in southeastern Alaska and adjacent areas of British Columbia and the Yukon Territory, superimposed on the major tectonic features (after Plafker et al. 1978). Magnitude 6 events are shown with only their year of occurrence. Arrow indicates relative motion between the Pacific and North American plates. Also shown are the seismographs (triangles) currently operating in Canada, plus the station at Sitka (SIT). WC is Windy Craggy.

weather fault near Lituya Bay (Fig. 2) in 1958. Although most of the relative motion in this region is accommodated on the Queen Charlotte-Fairweather transform boundary, there is about 10-20 mm/yr convergence across the Fairweather fault (Lisowski et al., 1987) that may be responsible for the seismicity inland from the plate margin (Horner, 1983). The largest earthquakes inland have occurred north of Windy Craggy, just across the Yukon border in 1944 (magnitude 6.5) and northeast of Tarr Inlet near the B.C.-Alaska border in 1952 (magnitude 6.0).

A seismograph was installed at Windy Craggy to monitor seismicity close to the mine and to improve overall network location capability. The present seismograph network can locate most earthquakes about magnitude 2.5 and greater (Fig. 2). Because there are no permanent seismograph stations within about 150 km of most of these events (Fig. 1), epicentres may be uncertain by as much as 20 km. The wide station spacing also prevents focal depth determinations.

RESULTS FROM 1987

On 30 June 1987, a portable MEQ 800 seismograph was installed at the Windy Craggy main camp. Seismometer coordinates are 59.6278° N, 137.7160° W, at an elevation of 750 m. The station ran for about 23 of the next 34 days and was closed for the remainder of the year on 3 August 1987. During this period 27 earthquakes were located within 200 km of Windy Craggy. Magnitudes ranged from about 1.0 to 2.5. The distribution of epicentres coincided with the patterns shown in Figure 2. The closest earthquake, magnitude 0.7, occurred within 15 km of the seismograph site but could not be accurately located because of its low magnitude.

The seismograph was re-installed at Windy Craggy on 10 June 1988, and is planned to operate to the end of the year.

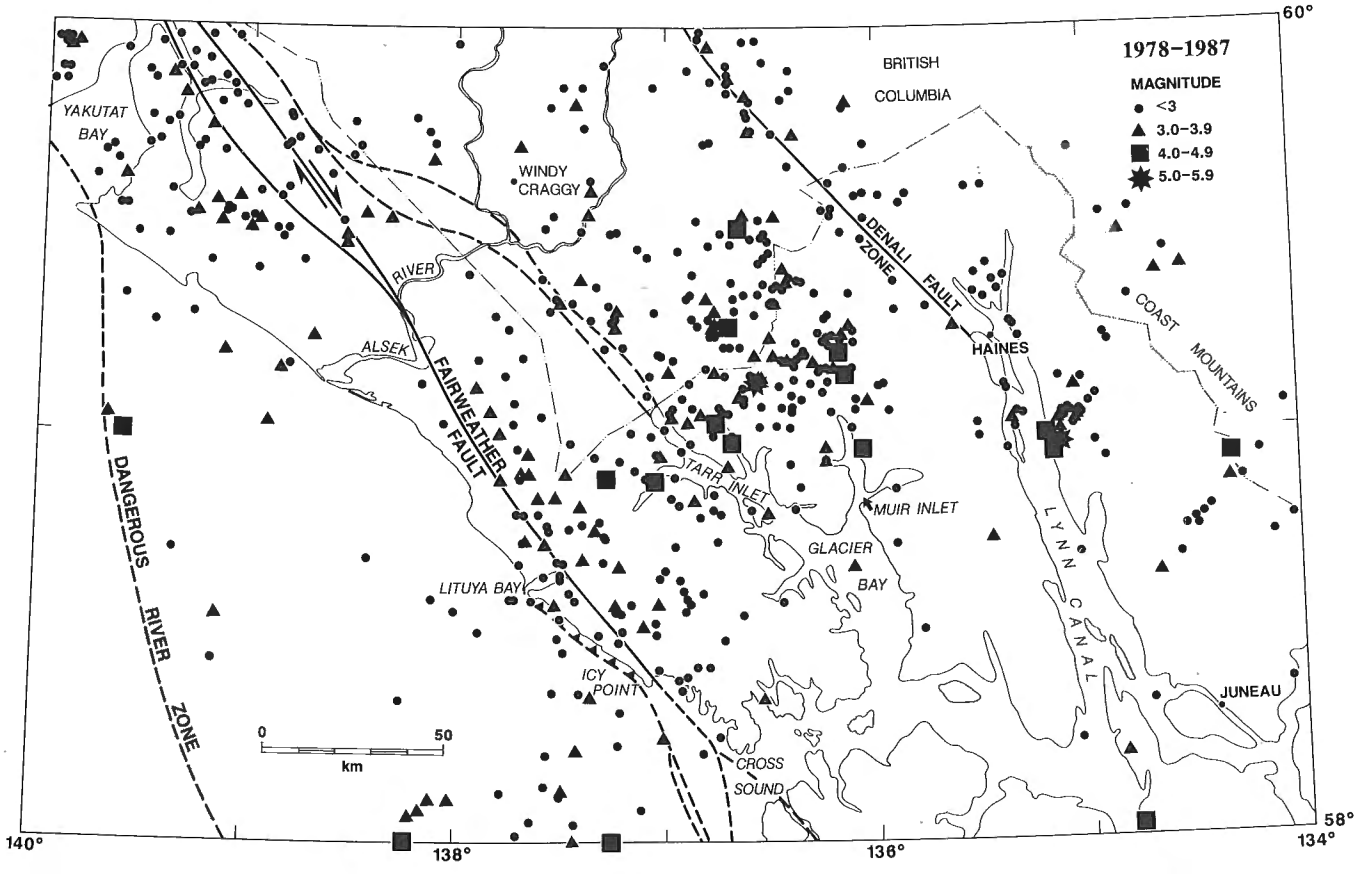

Figure 2. Seismicity in northwestern British Columbia and adjacent areas of Alaska, from 1978 to 1987. A temporary seismograph is currently operating (fall of 1988) at Windy Craggy.

ACKNOWLEDGMENTS

The author gratefully acknowledges the extensive support and assistance of Doug Little and Mary Webster of Geddes Resources Limited. Dennis Monsees, Geophysics Division, Yellowknife, N.W.T., assisted with the seismograph installation.

REFERENCES

Horner, R.B.
1983: Seismicity in the St. Elias region of northwestern Canada and southeastern Alaska; Bulletin of the Seismological Society of America, v. 73, p. 1117-1137.

Lisowski, M., Savage, J.C., and Burford, R.O.
1987: Strain accumulation across the Fairweather and Totschunda faults, Alaska; Journal of Geophysical Research, v. 92, p. 11552-11560.

Perez, O.J. and Jacob, K.H.
1980: Tectonic model and seismic potential of the eastern Gulf of Alaska and Yakataga seismic gap; Journal of Geophysical Research, v. 85, p. 7132-7150.

Plafker, G., Hudson, T., Burns, T., and Rubin, M.
1978: Late Quaternary offsets along the Fairweather fault and crustal plate interactions in southern Alaska; Canadian Journal of Earth Sciences, v. 15, p. 805-816.

AUTHOR INDEX

Geological Survey of Canada, Paper 89-1, Current Research is published as eight parts, listed below, that can be purchased separately.

Recherches en cours, une publication de la Commission géologique du Canada, classée Étude 89-1, est publiée en huit parties, énumérées ci-dessous; chaque partie est vendu séparément.

Part A, Abstracts
Partie A, Résumés

Part B, Eastern and Atlantic Canada
Partie B, Est et région atlantique du Canada

Part C, Canadian Shield
Partie C, Bouclier Canadien

Part D, Interior Plains and Arctic Canada
Partie D, Plaines intérieures et région arctique du Canada

Part E, Cordillera and Pacific Margin
Partie E, Cordillère et marge du Pacifique

Part F, National and general programs
Partie F, Programmes nationaux et généraux

Part G, Frontier Geoscience Program, Arctic Canada
Partie G, Programme géoscientifique des régions pionnières, région arctique du Canada

Part H, Frontier Geoscience Program, Queen Charlotte Islands, British Columbia
Partie H, Programme géoscientifique des régions pionnières, îles de la Reine-Charlotte, Colombie-Britannique

Energy, Mines and Resources Canada
Énergie, Mines et Ressources Canada